Final Report

Rejection of Pharmaceuticals by Reverse Osmosis Membranes: Quantitative Structure Activity Relationship (QSAR) Analysis

Submitted by:

Grisel Rodriguez, Sarah Buonora, Tom Knoell, Don Phipps, Jr.
Orange County Water District

Dr. Harry Ridgway
AquaMem

Submitted to:

The National Water Research Institute (NWRI)

West Basin Municipal Water District (WBMWD)

Orange County Water District (OCWD)

Orange County Sanitation District (OCSD)

U.S. Bureau of Reclamation

NWRI Project 01-EC-002

October 2004

Acknowledgements

The authors of this report wish to thank the National Water Research Institute (NWRI), the West Basin Municipal Water District (WBMWD), the Orange County Sanitation District (OCSD) and the Unites States Bureau of Reclamation (US BuREC) for providing funding for this research project. Furthermore, the authors would like to thank the management and Board of Directors of the Orange County Water District (OCWD) for supporting this research effort. Special thanks are also extended to Dr. Harry F. Ridgway of AquaMem for his contributions to this study.

Table of Contents

List of Figures

List of Tables

Executive Summary

- Quantitative Structure Activity Relationship (QSAR) molecular descriptors were calculated for over 200 organic compounds, mostly of public health concern.
- Using cluster analysis methods, 51 surrogate compounds were identified from this master compound list representing a wide range of molecular properties.
- The compound-membrane interactions between these 51 surrogates with four commercial polyamide (PA) membranes and one commercial cellulose acetate (CA) reverse osmosis (RO) membrane were determined using radiolabeled forms of the surrogate compounds and a small radiometric membrane performance (RMP) assay pressure cell.
- Use of radiolabeled tracers allowed quantification of three basic compound-membrane interactions: 1) passage of the compound through the membrane (P-Flux), 2) adsorption or absorption of the compound to the membrane (M-Flux) and 3) reflection of the compound back to the feed side of the membrane (R-Flux).
- The PA membranes generally interacted with the test compounds in a similar fashion.
- Using the measured flux data for all the membranes and the calculated QSAR molecular descriptors, a successful empirical model was constructed describing each compound-membrane interaction for each of the test membranes using a genetic algorithm (GA) to select specific molecular descriptors affecting the interaction and an artificial neural network (ANN) to describe the specific relationship between the descriptor set and the interaction.
- A set of "Universal" PA ANN models were successfully constructed by combining data from each of the individual PA ANN models. Although several specific membrane parameters (specific water flux, zeta potential, contact angle, indices of crosslinking) were included as potential inputs to this model, the GA did not select any of them, suggesting the variations between compound structures were more predictive than the variations in these membrane parameters.

- Behavior of the "Universal" PA models in general mirrored the behavior of the individual PA membrane models.
- Molecular descriptors included by the ANN models included those describing molecular charge/polarity, molecular complexity, hydrogen bonding and hydrophobicity.
- There was variation in the exact descriptors included in each of the models across membrane types; CA differed from PA, and within the four PA membranes (and with the "Universal" models), inputs differed.
- However, there were some commonly included descriptors in the models between membranes and between interactions. Notably, descriptors related to electrophilic interactions (Gmin), molecular dipole and quadripole moments (P, Py and Q), hydrogen bonding (numHBa) and hydrophobicity (LogP) were used by multiple models.
- Behavior of all 202 compounds in the master compound list was modeled; predictions passing a "virtual mass balance" criterion based on the summation of mass fluxes achieving ±25% of the original feed flux was used to validate predictions. Based on this criterion, behavior of between 57% and 70% of the master list compounds were successfully predicted by the ANN models.
- The "Universal" PA models were able to describe ~76% of the compounds within this criterion.
- Percent rejection was estimated based on the predicted P-Flux and R-Flux values. Many pharmaceutically active compounds (PhACs) and disinfection byproducts (DBPs) were predicted to be highly rejected, especially by PA membranes. However, in many cases, a significant component of rejection involved adsorption/absorption to the RO membrane material. Tables of rejection data are presented for each membrane, and for the "Universal" PA models.
- Percent rejection determined from the P-Flux predictions of theANN models agreed favorably with values published in the literature or observed in the field.
- Failures of the models were associated with specific compounds; an iterative gap analysis process was suggested that could converge on a more robust set of models by choosing additional surrogates from the failed compounds

- A computer program was written to automatically build fully-atomistic, geometry-optimized models of a polyamide (PA) reverse osmosis membrane useful for molecular dynamics (MD) simulation of the free diffusion behavior of 1,1,2,2-tetrachloroethylene (PCE) and nitrosodimethylamine (NDMA).
- Although the simulations were of relatively short duration, typically 200 picoseconds (ps), differences were evident in the behavior of the two organics; NDMA exhibited two "jump" events involving rapid long-range (~7Å) excursions from the origin at t = 0 ps whereas PCE did not in the time period.
- Calculated solute fluxes based on root mean square (RMS) displacements of local diffusion were much greater than experimental values, although calculated water fluxes agreed with those expected for PA membranes.
- Two factors contributed to overestimation of organic fluxes: (i) inability to account for solute jump frequencies in the short duration simulations, and (ii) likely overestimation of solute partition coefficients.
- Although NDMA and PCE diffusivities were nearly identical in pure-water simulations, there was a 4-fold reduction of PCE diffusion in the membrane system relative to NDMA, suggesting greater interaction of PCE with the membrane. The results agreed relatively with the laboratory observations in this study for these two compounds and PA membranes.
- Analysis of simulation playbacks revealed NDMA associated more with water and polymer atoms than did PCE. The relative lack of a hydration field around PCE may contribute to stronger long-range electrostatic interactions with membrane atoms resulting in lower diffusivity and higher rejection for this compound.
- An idealized PA membrane pore model is proposed that may be able to rapidly estimate and compare solute-membrane interaction potentials.

Abstract

In this study, 51 radiolabeled surrogate compounds selected from an initial compound list of over 200 organic compounds, mostly of public health concern, were used to construct a series of quantitative structure activity relationship (QSAR) based empirical multivariate models describing the interaction of the compounds with several commercial polyamide (PA) and cellulose acetate (CA) reverse osmosis (RO) membranes. Models were constructed using artificial neural networks (ANNs) based on data obtained from calculated QSAR molecular descriptors and direct measurements of compound-membrane associations. The penetration of molecules through the membranes, the adsorption/absorption of molecules on/in the membranes and the rejection of molecules at the feed/membrane interface were associated with molecular properties that included charge/polarity, structural complexity, hydrogen bonding and hydrophobicity. Percent rejection, calculated from the ANN model predictions, compared favorably with published values. Models developed in this study were capable of predicting the compound-membrane interactions of 57% to 70% of the organics in the initial compound list. In addition to the individual membrane models, a "Universal" PA model was constructed from individual PA membrane performance data capable of predicting the compound-membrane interactions for 76% of the compounds. A gap analysis that could improve model performance was discussed. A fully-atomistic geometry-optimized model of a PA membrane was created and used to study the free diffusion behavior of 1,1,2,2-tetrachloroethylene (PCE) and N-nitrosodimethylabine (NDMA). Predicted PCE diffusion was 4-fold less than NDMA. This result agreed in general with the relationship between PCE and NDMA relative membrane fluxes; however, absolute values were much overestimated compared to laboratory results, although water flux measurements were not. Movement of compounds through the membrane by low-frequency, longer-range "jumps" as opposed to local diffusion and underestimation of the solute partition coefficients may account for the discrepancies. A simplified membrane model system using a single PA membrane "pore" to speed investigation of compound-membrane interactions is proposed.

1 INTRODUCTION

1.1 Background

Ultra-low-pressure reverse osmosis (RO) and nanofiltration (NF) membrane processes are arguably the most cost-effective modern technologies for removing trace organic and inorganic constituents from water. Because of their favorable energy efficiencies, flexible engineering design and scale-up, and ability to remove a wide range of low-molecular-weight (LMW) organics, membrane processes are increasingly being employed in drinking water purification and water reuse applications worldwide. Whereas their overall performance can be modeled with considerable precision, the mechanisms by which organics and other substances are transported across or rejected by these semi-permeable membranes are still incompletely understood (Weisner and Buckley, 1996).

The ability of RO membranes to remove organic contaminants such as pharmaceutically active compounds (PhACs) and endocrine disrupting compounds (EDCs) from drinking water supplies is very desirable because of the potential health risk posed by these substances. This issue has been widely reported in the literature (Drewes et al., 2002; Hileman, 2001; Kolpin et al., 2002; Schafer et al., 2003). It is currently recognized that molecular mass and size of organic compounds are perhaps among the most significant factors in determining how well they are rejected by any given RO membrane. In general, compounds exceeding a molecular-weight cutoff (MWCO) value of about 300 Daltons are rejected well by most RO membranes regardless of their other inherent molecular properties. Almost all of the compounds categorized as EDCs or PhACs have molecular weights of >200 Da. (Kimura et al., 2003), although some EDCs with molecular weight near 300 such as 17β-estradiol (MW = 279g/mol) may be detected in RO permeate at very low concentrations (Salveson et al., 2000). For compounds that lie below the MWCO value for a particular membrane type, rejection and transport behaviors are based on a host of other compound molecular properties. Together, these molecular properties determine the nature of the compound's interaction with the solvent phase (typically water), dissolved salts and other organics, and the polymer membrane

matrix, which in turn determines the diffusion rate and transport behavior of the organic compound. Some of the molecular properties (also referred to as attributes or descriptors) that may affect a compound's transport across RO or NF membranes include shape, hydrophobicity, partial atomic charges and their distribution, molecular orbital shapes, reactive centers and locations of electron and recipient donor atoms, bonding arrangements, atom types, dipole moment, ionization potentials, *etc.*

A few efforts have been made to identify relationships between molecular structure and the ability of an organic compound to pass through modern RO or NF membrane materials. Huang and Negishi (1993) examined the transport behaviors of aliphatic acids, alcohols, and amines for a series of experimental cellulose acetate derivative RO membrane materials. It was found that for *n*-alkyl organics, solute rejections firstly increased with alkyl chain length, reaching a maximum at about three carbons atoms, and then decreased thereafter or remained stable. Branched compounds were rejected best, presumably due to steric hindrances as they interacted with the polymer matrix. According to Matsuura and Sourirajan (1971) for a given membrane material and structure, polar effects constitute one of the most important physicochemical criteria governing reverse osmosis separation of organic solutes. They developed and confirmed a method for estimating Taft numbers for polyhydric alcohols, and used this technique to predict solute transport of alcohols, aldehydes, and carbohydrates in porous cellulose acetate membranes. Several investigators have reported that organic removal from membranes depends highly on the degree of compound ionization. It has been found that formic acid removal by the NS-100 membrane varied from ~ 6% when partially undissociated to 98% when dissociated completely (Fang and Chian, 1975).

The nature of the membrane material itself greatly influences the types and the degree to which organic compounds are rejected. For example, Reinhard and coworkers (1986) reported that both polyamide thin-film composite (TFC) membranes as well as blend cellulose acetate membranes tended to reject branched complex organic molecules including neutrals, bases, acids, and phenols. However, various halogenated DBPs and chlorinated solvents were only rejected significantly by the TFC membranes. Membrane

properties that affect compound rejection include surface charge and charge distribution, degree of polymer crosslinking and polymer mobility, overall thickness, hydrophobicity, density, surface morphology, hydration energy, and other factors. The trend in recent years to make membranes with lower operating pressures has generally resulted in somewhat poorer organics rejection. Lipp et al. (1994) showed that when using FT-30 membranes, the transmembrane pressure drop, ion composition, ion concentration and pH have an influence on the solute and salt rejection. An increase in pH increases the solute rejection and an increase in the ion concentration decreases the solute rejection.

The rejection exhibited by membranes is also strongly influenced by the nature of the fouling layer that develops. Schafer and coworkers (2000) recently reported that the rejection of LMW organic acids by a series of microfiltration, ultrafiltration, and NF membranes was dependent on the type of deposit on the membrane surface. Positively charged ferric chloride precipitates on the membrane surfaces were found to improve the rejection of cationic species but reduced the rejection of LMW organic acids present in natural organic matter (NOM).

Given the effects of natural fouling layers on rejection, it is not surprising that purposeful modification of membrane surfaces also has met with some success in terms of improving the rejection of organics. For example, Kilduff et al. (2000) reported recently that ultraviolet (UV)-assisted graft polymerization of N-vinyl-2-pyrrolidinone onto sulfonated polyethersulfone NF membranes not only helped to mitigate NOM fouling, but also could under certain circumstances leave NOM rejection and water flux relatively unaffected. On the other hand, when the same membranes were simply UV irradiated in the absence of graft polymerization to increase surface hydrophilicity and wettability, the degree of NOM rejection was diminished significantly.

The foregoing examples suggest it is theoretically possible to predict the membrane transport or rejection behavior of organic compounds from a knowledge of their fundamental molecular attributes. However, since more than one molecular attribute may influence a compound's ability to penetrate a semi-permeable membrane barrier and

diffuse through it, multivariate statistical procedures such as multiple linear regression analyses or artificial neural network (ANN) analyses are required to accurately model the phenomenon. Such a multivariate statistical approach which seeks to correlate some minimum set of independent molecular descriptors with molecular activity or function (*i.e.*, membrane transport or rejection) is referred to as quantitative structure-activity relationship (QSAR) analysis. The predictive statistical model developed from this analytical approach is referred to as a QSAR model. Because of the multitude of interacting solute-membrane factors, QSAR models describing organics rejection by membranes will very likely turn out to be specific to a particular membrane type. Thus, multiple models will be needed for a series of membrane materials.

In recent years, QSAR models have been successfully developed for a variety of experimental systems involving complex bio-organic interactions. For example, Carroll et al. (1994) developed QSAR models for predicting the potency of dopamine binding inhibitors by various natural cocaine derivatives (*e.g.*, 3*B*-(substituted phenyl)tropane-2*B*-carboxylic acids). Many physical and chemical material properties of natural and synthetic polymers can be predicted with reasonable accuracy (typically >85%) using QSAR type models based on molecular group contribution and topological (graph theory) techniques (Bicerano, 1996). More recently, Campbell et al. (1999) working at OCWD's Water Factory 21, developed regression-based QSAR models to predict the effectiveness of charged and neutral surfactants for inhibiting the attachment of fouling bacteria to TFC and cellulose acetate RO membranes. Because the surfactants examined interacted differently with each membrane chemistry, separate QSAR models were developed for polyamide TFC and cellulose acetate membranes.

We proposed to apply multivariate (ANN-based) techniques to create QSAR models that could accurately describe and predict the rejection of organic compounds by several modern commercial TFC membranes. The project focused on those compounds that exhibit a potential for negatively impacting human health or the environment. The compounds of most interest include a host of endocrine disruptors, human and animal antibiotics, DBPs, insecticides and herbicides, and various neuroactive drugs (e.g.,

aspirin, anticancer agents, etc.). Many of these compounds have been found in recent years to enter natural ecosystems at still bioactive concentrations by way of sewage outfalls and urban runoff.

Although research on RO membrane performance is extensive, the majority of studies have relied upon empirical observations to formulate and bolster theoretical precepts of membrane structure and function. Indeed, until very recently, membranes were treated as structurally and chemically homogeneous "black boxes." However, recent ultrastructural studies of PA membranes have revealed that they are chemically and structurally asymmetric (Figs. 27 and 28; Freger, 2003). The observed chemical and structural asymmetry of PA membranes is believed to result from differential rates of diffusion of the reactive monomers into the incipient membrane during the interfacial polymerization reaction. Because of the morphological complexity of TFC membranes, compelling ultrastructural or experimental evidence is lacking as to the exact location of the solute-water separation layer. Other unknowns concerning the PA membranes include the surface and bulk charge distribution, polymer density as a function of membrane depth, and water content. Such uncertainties have hindered our efforts to fully validate atomistic models of PA membrane materials and underscore a strong need to better characterize the membranes experimentally. Unfortunately, apart from microscopy, there are few analytic techniques able to effectively probe PA membrane substructure at the nanoscale, a consideration that has in recent years prompted efforts to model the structure and functionality of the PA separation layer.

Atomistic modeling of small-molecule sorption and diffusion in the PA layer is complex. In contrast to simulations of simple gas solutes where solute-solute and polymer-solute interactions can be often neglected, RO simulations must account for specific interactions, such as water-water, water-solute, water-polymer and solute-polymer interactions (Kotelyanskii *et al.*, 1998). In addition, models need to accurately describe the physical and chemical characteristics of the aromatic crosslinked PA thin film of current RO membranes. Key properties include density, hydrogen bonding and water sorption capacities, and concentrations of crosslinks and functional groups (*e.g.*,

unreacted free amine and carboxylic acid). Due to insufficient experimental data, it is not surprising that the literature on atomistic modeling of RO membranes and water sorption in polyamides is limited. Important studies in this field are those by Knopp and Suter (1997a, 1997b) and by Kotelyanskii *et al.* (1998, 1999).

Knopp and Suter (1997a) developed a method based on atomistic models to calculate the excess chemical potential of a solute in dense polymer microstructures. The technique consists of combining two well-established procedures for determining excess chemical potentials such that the shortcomings associated with each individual method are minimized. Consequently, the technique can then be applied to a wider range of solute-polymer systems. This hybrid method was successfully tested in separate studies using water as the solute and polyamides (Knopp and Suter, 1997b), bisphenol-A-polycarbonate and polyvinyl alcohol (Nick and Suter, 2001), as the polymers. The difference between the calculated excess chemical potential of water in a given polymer and the excess value of pure water can be used to give an initial prediction of the equilibrium water sorption capability of that polymer.

In simulations of PA films, information on the water content within the polymeric matrix is crucial for the success of the atomistic model. Although Knopp and Suter (1997a, 1997b) evaluated their method on PAs unlike the typical crosslinked aromatic PA used in RO membranes, valuable insight can be still obtained about the accuracy of the technique and its potential in simulations of RO systems. In comparison to experimental data, this method was able to reasonably predict the variation in sorption values between two linear PAs that differ from each other only in the number of amide bonds. However, it failed to recognize sorption differences between two PAs with the same number of amide bonds, but different chemical structure. The authors concluded that the force field used in the simulation must correctly model chemical structure differences such that they will be reflected in the estimated sorption values. It was also found that equilibrium sorption of water cannot be described by a simple function of the concentration of amide groups.

Kotelyanskii *et al.* (1998, 1999) performed atomistic simulations of water and salt transport in the aromatic polyamide film of an FT-30 RO membrane in order to obtain information about diffusion and rejection mechanisms. Specific objectives of these studies included the investigation of crosslinking effects on density and solute transport, ion mobility (Na^+ and Cl^-), estimation of water diffusion coefficients and water structure and interactions within the polyamide. The polyamide structure modeled was designed based on data for density, equilibrium water content and number of crosslinks obtained from the industry, but not available elsewhere (Kotelyanskii *et al., 1*998). These properties are essential to the outcome of the simulations, and it is therefore critical to generate more accurate and reliable experimental data to support the models.

Simulation results show, as expected, that a higher concentration of crosslinks increased the density of the polyamide and reduced the mobility of water molecules. The authors found that water diffusion in the hydrated polyamide occurred by "jumps" between localized sites (Kotelyanskii *et al.,* 1998). These sites may be described as void spaces arising from the dynamic structure of the polymer chains. Water molecules oscillate in these sites until thermal fluctuations or local structure rearrangements of the polymer permit another "jump". The estimated "jump" length was approximately 3Å, which was independent of the simulation conditions. The frequency of these "jump" events, on the other hand, decreased with higher polymer densities. In other words, the mobility of water molecules was reduced due to the decrease in the dynamics of the polymer chain caused by more crosslinks (*i.e.*, higher density; Kotelyanskii *et al.,* 1999). The authors concluded that about 90% of the water molecules within the polymer matrix are interconnected by hydrogen bonds, forming a large network. Water mobility (*i.e.*, "jump" frequency) decreased as the concentration of hydrogen bonds increased. With respect to salt transport in the polyamide, it was found that salt ions were partially hydrated with some water interactions replaced by ion-polymer interactions. The mobility of the salt molecule was significantly lower than that of water and was limited by the chloride ion, which is consistent with the observed permselectivity of PA membranes.

Although atomistic simulations may be powerful tools for the investigation of transport and rejection mechanisms within the PA film of RO membranes, modeling predictions must be verified by experimental data since simulation results may be strongly influenced by PA characteristics. Experimental data will allow the construction of more consistent PA models and help validate conclusions extracted from simulations.

1.2 Project Objective

The primary goal of this project was to develop robust solute rejection QSAR models for a series of commercial RO membranes challenged with a structurally diverse suite of organic compounds of immediate interest to water utilities and regulatory agencies. Compounds of special interest included endocrine disruptors, antibiotic agents, neuroactive drugs, insecticides, and DBPs. To accomplish this goal, a radiometric membrane performance (RMP) assay was developed which permited rapid determination of the interactions of radiolabeled organic substances (rejection, association) with RO membrane materials. QSAR models enabling prediction of compound rejection for each membrane type evaluated were developed using the RMP assay dataset and calculated compound molecular properties (descriptors).

Specific project objectives included (1) validation and calibration of the RMP assay (described in further detail below), (2) use of the RMP assay to quantify the rejection behaviors of a wide range of endocrine disruptors, antibiotics, and DBPs by commercial low-pressure TFC membranes, and (3) development of QSAR models (one model for each membrane type investigated) based on the mass transport/rejection data for the compounds examined. Compound transport data derived from RMP experiments were also compared with the results of molecular dynamics (MD) simulations.

A second objective of this study was to evaluate the usefulness and accuracy of MD simulations for determining RO membrane fluxes and rejections of trace organic compounds of public health concern. Examples of compounds of particular interest include disinfection by-products such as N-nitrosodimethylamine (NDMA) and 1,1,2,2-tetrachloroethylene (PCE), as well as the endocrine disruptor 17a estradiol. The initial

focus was on polyamide RO membranes since they are widely used in water treatment and organic compound rejections are generally superior for this class of membranes. If successful, MD simulations could provide an approach that may be generalized for predicting the organic rejection properties of any membrane material that can be modeled.

2 TECHNICAL DESCRIPTION

2.1 Creation of Empirical (QSAR) Models Describing Organic Compound Rejection

The experimental approach involved application of the RMP assay to build a database of membrane interactions between the test membranes and organic compounds which have special relevance for water utilities and regulatory agencies, and then to relate the membrane interactions with molecular properties (defined by QSAR molecular descriptors).

2.1.1 Organic Compound Master List

A master list of 190 compounds was compiled based on a search of the following governmental databases: U.S. Geological Survey Toxic Substances Hydrology Program, U.S. Environmental Protection Agency Unregulated Contaminant Monitoring Rule and Drinking Water Contaminant Candidate List, April, 1999 and the California Department of Health Services Unregulated Chemicals Requiring Monitoring, May, 2001. The compound list included many endocrine disruptors, antibiotics, neuroactive drugs, insecticides, and DBPs. Additional compounds (amino acids, marine toxins) were added to increase the breadth of molecular properties variations. The final master list of 202 compounds with brief descriptions of their regulatory or environmental relevance is shown in Tables 1a-1e.

2.1.2 Selection of QSAR Molecular Descriptors

Compounds were constructed using molecular modeling computer software and initially more than 370 molecular descriptors were calculated for each of the compounds in the master list using QSARis software (SciVision, Inc., Lexington, MA). The descriptors were organized into eight general categories, each of which contained numerous sub-categories, as indicated below:

- Molecular Connectivity Chi indices (3 descriptors total)
- Kappa Shape indices (2 descriptors total)
- Electrotopological State (E-State) indices (6 descriptors total)

- Information indices (7 descriptors total)
- Subgraph Count indices (22 descriptors total)
- Total Topological descriptors (11 descriptors total)
- Molecular Properties (17 descriptors total)
- Other descriptors (4 descriptors total)

Due to software limitations that restricted the total number of independent-variable (descriptor) inputs that could be used for the development of QSAR models, a strategy was devised to reduce the total number of descriptors to be used in model development. This approach involved performing a series of cluster analyses (nearest neighbor, squared Euclidian method) on each major descriptor category using a statistical analysis package (Statgraphics, Manugistics, Rockville, MD) to reveal any highly cross-correlated descriptors in that particular group. For example, the seven descriptors in the information indices category were observed to form four independent clusters (*i.e.*, non-correlated subgroups). One or more information index from each of the four subgroups was subsequently selected for candidate membership in the final (master) descriptor list. Selection of descriptors from within cluster subgroups was based on the perceived relevance of the descriptor based on its definition (*e.g.*, simple descriptors were generally favored over more complex derivative descriptors) and done in a conservative manner, *i.e.*, often more than one member of a subgroup was chosen for inclusion in the master descriptor list. Following this protocol for each of the eight major descriptor categories resulted in a master list of 73 molecular descriptors for each organic compound used in the study (Table 2).

2.1.3 Clustering Compounds by Similar QSAR Descriptor Properties

Cluster analyses were similarly employed to break the list of compounds of interest into subgroups of compounds having similar descriptor values. Such statistically-based grouping was necessary because most of the compounds were known to be unavailable in a radiolabeled form. Therefore, the simplifying assumption was made that compounds having similar descriptor-set values would exhibit similar rejection behaviors across the

different RO membranes used in the study, and *vice versa*. A single cluster analysis was performed using Statgraphics (Ward's squared Euclidian method). In this case, truncation of the master descriptor list was necessary in this step since Statgraphics would accept a maximum of 64 independent variables as inputs for clustering analyses. In this case, a Pearson's R correlation matrix was used to eliminate the most highly cross-correlated descriptors. A subsequent dendritic analysis of the remaining descriptors resulted in creation of 20 subgroups (QSAR molecular property clusters) (Fig. 7). A complete listing of all master database compounds with their properties, QSAR descriptor values and QSAR descriptor clusters is presented in Appendix 3.

2.1.4 Selection of Surrogate Compounds for Analysis

From the contents of each of these 20 clusters, one or more compounds were identified as surrogates to represent the molecular behavior of the members of the cluster for determination of actual compound interactions with the five different RO membranes. A total of 51 compounds were obtained as surrogates for this study (Table 4). Not all clusters were represented, but in many cases more than one member of a cluster was included in the surrogate list. Compounds used in the study were obtained from American Radiolabeled Chemicals, Inc., St. Louis, MO; Amersham, Piscataway, NJ; ICN, Irvine, CA; Perkin Elmer Life Sciences, Inc., Boston, MA; Moravek Biochemicals, Inc., Brea, CA and Sigma, St. Louis, MO. Purity of the compounds was >99% and all compounds were stored either at 4 C or –20 C (depending on the compound) for a minimal period of time (typically less than one week) prior to assay to lessen the opportunity for post-manufacture chemical changes. Compounds labeled with ^{14}C were chosen preferentially over compounds labeled with ^{3}H to reduce the possibility of radiolysis during storage and to avoid the possibility of the ^{3}H proton exchanging with water during interaction with the membrane (Riley et. al., 1988). Only four compounds labeled with ^{3}H were used in the study. Complete surrogate compound information is presented in Appendix 2.

2.1.5 Membranes Used In Study

Four commercial polyamide (PA) RO membranes and one cellulose acetate (CA) RO membrane were selected for this project (Table 5). Due to the high solute rejection and throughput, PA membranes have become the commercial membranes of choice utilized in the water and wastewater treatment industry today. However, CA membranes are still extensively used in the industry and one was included for comparative purposes.

2.1.6 Membrane Preparation and Coupon Fabrication

Swatches (4" x 6') were randomly obtained from sheets of each of the membranes (to avoid the potential for regional variations in the membrane material) and preconditioned under crossflow conditions in a stainless steel cell designed at OCWD (Fig. 4) at a pressure of 150 PSIG for 16 hrs using 1 μohm-cm deionized water. This process was necessary to hydrate the membrane material and to extract unreacted monomers (e.g., trimesoyl chloride and *m*-phenylenediamine) or other chemical substances (e.g., certain surfactants and possibly biocides) that could remain associated with the membranes following their manufacture.

Following preconditioning, circular 12.5-mm diameter coupons of membrane were cut from the swatches using a circular punch. As with the swatches, coupons were randomly harvested from the swatch surface to help eliminate effects of short order inhomogenieties in the membrane material. The coupons thus obtained were stored in 17 Mohm-cm ASTM I ultrapure water at 4 C for no more than one week before use.

2.1.7 Determination of Membrane-Compound Interactions

2.1.7.1 Radiometric Membrane Performance (RMP) Assay

The Radiometric Membrane Performance (RMP) assay (Figs. 2 and 3) was performed using a small stainless-steel/Teflon pressure cell (VWR, Bristol, CN), which supported the membrane coupon on a perforated stainless steel disk with the feed surface gasketed

with a Teflon O-ring. The pressure cell was screwed together to a constant torque of 15 inch-lb with a torque wrench. Care was taken to apply sufficient torque to avoid leaks, but not so much as to crush or damage the permselective membrane surface.

The feed side of the pressure cell was filled with a feed solution consisting of 17 Mohm-cm ASTM I ultrapure water containing typically 100,000 – 1,000,000 disintegrations per minute (DPM) of radiolabeled (^{14}C or ^{3}H) test compound (typically approximately 9 μM concentration of feed compound) adjusted to pH 7 as needed (using extremely small amounts of HCl or NaOH). At this concentration, the effects of concentration polarization was expected to be relatively low in spite of a lack of cross-flow.

A 10 μL sample of the feed solution was recovered and placed in 10 mL of scintillation cocktail (Optifluor, Packard Instrument Company, Meriden, CT) prior to filling a 5 mL glass and Teflon gas-tight syringe (Hamilton Company, Reno, NV) with 2 mL of feed solution. The pressure cell was connected to the syringe such that all air bubbles were excluded. The pressure cell and syringe were then placed in a polyvinyl chloride (PVC) housing equipped with a 50 mL glass and Teflon Hamilton syringe designed such that the plungers of both, it and the feed syringe, were brought into contact. When regulated 15 PSI compressed air was supplied to the larger syringe, the 10:1 area ratio of the pistons generated 150 PSI of hydraulic pressure at 24 C in the smaller feed solution syringe.

Product expressed through the membrane coupon under pressure was collected through a 18 gauge (GA) hypodermic needle attached to the pressure cell product side. As soon as product was observed at the needle tip, the tip was submerged below the surface of 10 mL of scintillation cocktail in a 22 mm scintillation vial and a stopwatch was started to record the time required for collection of the product sample. Collection of the product in this manner avoided significant loss of the more volatile surrogate compounds during product collection.

A product volume of approximately 0.5 mL was collected; the volume was gravimetrically determined using a 2-place digital balance (Sartorius Model PT-120,

Sartorius Corp., Bohemia, NY; error ±-0.005 g). The time required for collection of the product was noted during each assay and varied from 10 to 40 min depending on the membrane in use.

After product collection, the pressure cell was recovered and detached from the pressure apparatus. A second 10 μL feed sample was obtained from the chamber reservoir and placed in 10 mL of scintillation cocktail as was previously described. This second sample was used to determine whether or not significant loss of feed concentration occurred (by adsorption to the apparatus, e.g.) during the course of the experiment. No significant differences were observed between the initial and final feed samples during the study.

Following sampling, the residual feed and product solutions remaining in the pressure cell were removed using a thin pipette tip (Ranin Instrument Corporation, Woburn, MA). The pressure cell was carefully unscrewed and the membrane coupon recovered using clean forceps. The coupon was rinsed by sequentially dipping and swishing six times in three 400-mL beakers containing 350 mL of 17 Mohm ASTM I grade ultrapure water. The coupon was then blotted by gently touching the front and back surfaces to adsorbent paper to wick away any adhering water and placed into 10 mL of scintillation cocktail in a 22 mL scintillation vial. Membrane coupons in scintillation cocktail were incubated overnight (roughly 12 hr) in order to facilitate permeation of the cocktail into the membrane material. Tests performed in the laboratory indicated that this procedure yielded the most complete recovery of membrane-associated compound.

Scintillation vials containing feed samples, product samples and membrane coupons were placed in a scintillation counter (Wallac LKB 1219 Rackbeta Liquid Scintillation Counter, Perkin-Elmer, Shelton, CT) and counted for 1min. Quench and counting efficiency were corrected using the external sample channel ratio method with ^{226}Ra as the external standard to yield a measurement of DPM. Background correction was applied by subtracting DPM obtained by counting 10 mL of scintillation cocktail with no sample.

A minimum of 5 replicate measurements were performed with each combination of membrane and solute compound in order to define noise due to variations in the membrane coupons, counting error, assay errors (pippetting errors), etc. The numbers of replicates were occasionally greater for certain compounds or membrane materials.

Statistical outliers were defined as having values >3 interquartile ranges below the first or above the third quartile, and may have been caused by defective membrane coupons or leaky seals in the RMP assay apparatus. Outliers were detected in sets of 5 or more replicates using Statgraphics and eliminated from the data set if discovered. In cases where outliers were eliminated, additional replicates were acquired to replace them such that the total number of replicates remained consistent.

All pressure cell components, needles and glass syringes were thoroughly decontaminated by placing in a stainless steel tray and spraying with a radiodecontamination solution (Radiacwash #005-400, Biodex Medical Systems, Inc., Shirley, MA) followed by laboratory detergent to remove organic contaminants (Micro-90, International Products Corporation, Burlington, NJ). After spraying, deionized water (1 μohm-cm deionized water) was added to cover the treated parts and they were soaked for a minimum of one hr. Parts were then scrubbed thoroughly with a nylon bristle brush and rinsed with deionized water followed by 70% laboratory grade denatured ethanol (squirt bottles were used to insure chamber and needle lumens were thoroughly cleaned). Following a final thorough rinsing with deionized water, components were air-dried on the bench. Experiments performed in the laboratory demonstrated that this procedure reduced background activity (contamination) by the apparatus to below 50 DPM in the product.

As 100,000 to 1,000,000 DPM were typically used in experiments, the RMP assay dynamic range of measurable attenuation was typically on the order of 3 to 4 logs removal (99.9% to 99.99% rejection).

2.1.7.2 Membrane-Compound Interactions: Relative Solute Fluxes

There are three basic mechanisms by which the incoming flux of solute in the feed may interact with a membrane. The solute can be rejected at the membrane surface, showing no interaction with the membrane and remaining feed. For purposes of this study we term this flux of mass the "R-Flux", where "R" indicates rejection at the membrane surface (the membrane acts as a mechanical barrier). The solute can be adsorbed onto or absorbed into the membrane, which we define in this study as the "M-Flux", where "M" indicates "membrane". Finally, the solute mass can pass through the membrane and into the product, an interaction we term the "P-Flux", where "P" means "product"). These fluxes may be normalized by considering the flux of solute impinging on the membrane ("F-Flux") as 100 (%); thus the other values represent a mass distribution amongst the three membrane interactions (Fig. 1).

2.1.7.3 Determining Relative P-, M- and R-Fluxes from the RMP Assay Results

Using the RMP assay, the solute mass entering the product and the membrane were directly determined by measuring the amount of radioactivity accumulated in the total recovered product volume and in the membrane coupon. From the concentration of radioactivity in the feed solution and knowledge of the total feed volume recovered, relative values for the P-Flux and M-Flux may be obtained using the following expressions:

$$\textbf{Relative P-Flux} = [\text{Total DPM}_{\text{Product}}/((\text{DMP}_{\text{Feed}}/\text{ml})(\text{Volume}_{\text{Product}}))] \times 100$$

$$\textbf{Relative M-Flux} = [\text{DPM}_{\text{Membrane}}/((\text{DMP}_{\text{Feed}}/\text{ml})(\text{Volume}_{\text{Product}}))] \times 100$$

The relative F-Flux = 100 by definition; therefore the relative R-Flux could be calculated from the following expression:

$$\textbf{Relative R-Flux} = \textbf{F-Flux} - (\textbf{P-Flux} + \textbf{M-Flux})$$

These expressions represent the distribution of solute mass during membrane interactions such that the sum of the relative P-, M- and R-Fluxes should equal 100 (which affords a simple means to evaluate the results of predictions of the models created independently from these data as described below). Actual fluxes of compounds (in terms of mass per unit area per unit time) may be calculated from the relative fluxes by treating them as a proportion of the actual feed flux. Actual specific feed flux may be obtained by calculating the mass of solute per unit area per unit time impinging on the membrane based on a knowledge of the recovered product volume, the area of the membrane coupon, and the concentration of solute in the feed. At 9 μM solute concentration, an average water flux of 28.11 GFD for PA membranes and a coupon area of 6.58×10^{-5} m^2, the average specific feed flux observed in RMP assay experiments typically was on the order of 0.54 μM of compound • m^{-2} membrane • min^{-1} per μM solute in the feed.

2.1.8 Comparison of RMP Assay Results to Crossflow Membrane Test Unit

The RMP assay lacked the crossflow component present in RO systems, which is required for prevention of significant formation of a polarization layer on the membrane. Formation of this layer seriously degrades RO performance by increasing osmotic backpressure and by increasing compound concentration at the membrane surface, which increases overall mass flux of compound through to the product side. The concentration of substances capable of influencing the osmotic pressure of an aqueous solution was far lower in the experimental feedstock that would be typically present in an operational RO system; nonetheless, it was desired to compare the behavior of the RMP assay with that of a standard crossflow RO unit to determine the similarity in performance, and to confirm that behavior of the assay was at least reasonably consistent with what could be expected of membrane performance under nominal operating conditions.

Four test compounds, urea, N-nitrosodimethylamine, caffeine, and sulfate, were chosen for this comparison based on their disparate rejection behavior and their relative ease of analysis by traditional methods. The test compounds were obtained in both radiolabeled (^{14}C for the organic compounds and ^{35}S for sulfate) and cold forms.

For the RMP assay, the test compounds were present in the feedstock at approximately 9 μM for NDMA and caffeine, 20 μM for urea and 10^{-5} μM for sulfate. Relative P-Fluxes for each of these compounds were determined for each of the test membranes (n = 5) using the RMP assay methods described above, and from this value a percent rejection was calculated for these test compounds from:

% Rejection = 100 – P-Flux.

Rejection for each of the test compounds by each of the test membranes (n = 2 to 3) was also determined using a 4" x 6" rectangular crossflow block tester unit (Fig. 4). For this assay, the membranes were conditioned with 1 μohm-cm deionized water as previously described. Following conditioning, a feedstock was introduced containing either 9 μM caffeine, 2,800 μM sulfate, 10,000 μM urea or 0.0054 μM NDMA. The block tester was operated with a crossflow velocity of 0.3 m/sec at 150 PSI (approximating nominal RO operating conditions). Operating temperature was 22 – 27 C, (rejection was corrected to 25 C), and membranes were operated for 5 to 7 hrs before the product stream and feedstock were sampled. Concentration of solute in the feed and product was immediately analyzed by the following protocols:

Sulfate: Concentration in the feed and product was estimated by conductivity using a field conductivity meter (Model 115A + Orion Research Inc. Beverly, MA). Two meters were used; one to measure the higher feed conductivity and the other to measure the lower product conductivity to enhance accuracy. Meter was temperature-compensated.

Urea: Concentration was analyzed spectrophotometrically (OD_{200}) (Spectral Instruments, Inc., Tuscon, AZ). Concentration of urea was determined by correlation with a standard curve generated using duplicate standards prepared in 17 Mohm ASTM I ultrapure water.

NDMA: Concentration was determined by gas chromatography (3800 Varian gas chromatograph with DB-VRX column, Varian Corp., Walnut Creek, CA).

Caffeine: Concentration was determined using EPA Method 507 (Varian 3500 gas chromatograph with dual columns and an NPD detector, Varian Corp., Walnut Creek, CA).

Rejection was determined using the following expression:

(([Solute feed] – [Solute Product])/[Solute feed]) x 100

The performance of the crossflow block tester and RMP assay were compared using a standard linear regression model for each of the RO membranes used in the study (Fig. 5).

2.1.9 Construction of Artificial Neural Network Models Describing Association of Organic Compounds with RO Membranes

Figure 6 presents a schematic illustrating the methods used to select molecular descriptor input parameters using a genetic algorithm (GA) and to construct artificial neural network (ANN) models of compound/membrane interactions.

2.1.9.1 Selection of QSAR Descriptors Best Correlating with Organic Compound Membrane Association

The three compound-membrane interactions (the relative P-Flux, M-Flux and R-Flux) described above were modeled in this study for each of the five study membranes. In addition, data were pooled for the PA membranes and used to construct "'Universal" PA models for P- M- and R-Flux (a total of 18 models in all).

The initial set of 73 QSAR molecular descriptors originally identified (Table 2) was chosen without regard for their relationship to specific organic compound/membrane interactions. Thus, for each membrane and for each interaction, an initial selection process was required to identify the subset of molecular descriptors best correlated with each compound-membrane interaction prior to model construction.

2.1.9.1.1 Choice of Exemplars and Randomization of Order.

All numerical operations were carried out using Microsoft Excel (Microsoft Corp., Redmond, WA). For all the individual membrane models, data spreadsheets were created containing a line of data for each individual exemplar. Exemplars were constructed for each surrogate compound by combining the originally identified 73 molecular descriptors (independent input parameters) with the measured relative compound flux (either P, M, or R; dependent output parameter). The original laboratory replicates were used in this process rather than averages of the data. Each of the 51 surrogate compounds was typically represented by 5 or more laboratory replicates, raising the total number of exemplars used in the individual models to 255 or more. This was done because there was a relatively small number of surrogates for multivariate analysis, and this approach increased the number of available exemplars for modeling as well as captured the full range of statistical variation present in the laboratory measurements which otherwise would have been lost in the averaging process.

For the "Universal" PA membrane models, in addition to the molecular descriptors, numerical measurements related to specific PA membrane properties (Table 3) were also included in the input parameter set, the *a priori* assumption being that one or more of

these membrane properties could prove as influential on compound-membrane interactions as the QSAR molecular descriptors.

In all cases, the order of the exemplars was randomized prior to any input winnowing or modeling efforts. This was achieved by first creating random numbers using the Excel randomization function and assigning these numbers to each of line of exemplar data, then sorting the exemplars using these random numbers. This resulted in a complete randomization of the order of the exemplars in the data spreadsheet. Randomization of the order of the exemplars was performed before each input selection or modeling effort as an additional precaution to insure that the order in which data were presented did not influence the final results.

2.1.9.1.2 Identification of Subsets of Influential Descriptors Using a Genetic Algorithm (GA)

Reduction of input data by determination of inputs salient to the process being modeled is the first step in any modeling process. There are a number of possible methods by which this may be achieved, but with the advent of more powerful desktop computer systems, genetic algorithms (GA) are now commonly being used to find a set of parameters that optimize a complex multiparameter function (Mitchell, 1998), especially when there is a large number of potential input parameters and a restricted number of exemplars to analyze. Evolutionary computation theory is too complex to thoroughly explain in this report; however, in a simple sense genetic algorithms operate by using the rules of genetic recombination and evolution to select the “fittest” set of input parameters to describe the behavior of a chosen output parameter. They all have in common populations of “chromosomes”, “crossover” to produce new "offspring", and "random mutation" (Mitchell, 1998). In this case, “chromosomes” refer to a set of input parameters (initially randomly chosen), “crossover” is the process of randomly exchanging inputs between “chromosomes”, and “mutation” refers to the occasional random inclusion of lost inputs back into the population. The algorithm operates by sequentially performing “crossover” functions and “mutation” functions to produce a new combination of input variables, and then tests this new combination to determine whether

or not it better describes observed variations in the output parameter (using some testing protocol such as linear regression) than the original combinations. If so, net new combination becomes the "parent" for a subsequent "generation". Thus, by iterative processing using evolutionary theory, the algorithm converges upon a "fittest" subset of input parameters.

Selection of input parameters for this study was achieved using a GA provided as part of the NeuralWorks Predict package (NeuralWorks Predict, Neuralware, Carnegie, PA). This program utilized a logistic multiple linear regression fitness evaluation. In addition to the normal GA selection criteria, an additional "Cascaded Variable Selection" was employed to rapidly eliminate inputs with a low probability of inclusion in the optimum input set (a function especially useful with large input arrays). Inclusion of inputs by the GA was detected by construction of a single neural network and performing a sensitivity analysis to detect influential inputs (methods described below). The GA eliminated descriptors that did not predict compound-membrane interactions, and typically reduced the initial 73 molecular descriptor set down to subsets of from 7 to 21 descriptors each.

2.1.9.1.3 Identification of Most Common Influential Descriptors.

The GA converges on an optimum fit between the input parameters and the output parameter, but it does not necessarily predict a globally optimum input set. More than one combination of inputs may lead to an acceptable solution, especially if the inputs are partially intercorrelated, as are many of the molecular descriptors (even though efforts were taken to reduce intercorrelation, some still persisted). Therefore, some randomness exists in the selection of inputs by the GA. However, it was expected that statistically the GA should choose the most highly influential inputs most frequently. Thus, a histogram constructed from multiple, independent GA selections should reveal the most influential input parameters for subsequent modeling. This histogram was constructed for each model by operating the GA on each data set for 10 iterations. For each iteration, the order of exemplars in the data spreadsheet was re-randomized, ensuring that the GA started with a completely different and randomized seed population each time. Inputs selected by the GA were detected as described above and recorded to produce a

histogram. "Influential" inputs were retained using a simple filter based on inclusion of the input in ≥ 50% of the input sets by the GA. This method typically resulted in selection of from 4 to 10 of the inputs per spreadsheet for inclusion in the artificial neural network (ANN) models.

2.1.9.2 Construction of Artificial Neural Network (ANN) Models

Multivariate analysis methods based on standard statistical approaches are capable of predicting the behavior of reasonably complex systems provided the systems are well-behaved and that the input functions describing the system are statistically independent of each other. In the case of organic compound interactions with RO membranes, the literature suggests that there may be reasonably smooth relationships within the scope of the interactions that could model well by traditional techniques. However, the molecular descriptors are by nature not entirely independent of one another. For example, it is difficult to design a molecule in which the molecular weight increases very much without a concomitant increase in molecular complexity. Thus, existence of intercorrelations between molecular descriptor inputs makes modeling compound-membrane interactions more difficult. However, neural network computing is less susceptible to these issues than are more traditional modeling methods. Moreover, neural computing methods are capable of describing the behavior of highly complex, nonlinear systems in which the exclusive rules of the interaction are either unknown or difficult to quantify. Although, as with GAs, the details regarding how ANNs are designed and constructed is outside the scope of this report (Bharath and Drosen, 1994, provides a good review), ANNs may be simply described as virtual models of biological brains.

An ANN is composed of a network of virtual neurons ("perceptrons"). Information enters each perceptron via "synapses"; each feeding a simple function with a weighting factor that can emphasize or de-emphasize the overall influence of the function. The effects of all the input functions are summed in the perceptron, then fed to an output function (often sigmoidal) by which the perceptron passes information to units further down in the network. The neural net is constructed by interconnecting layers of these perceptrons. Although highly complex multlayered networks are possible, the design

adopted for this study was a three-layered network consisting of an input layer, a "hidden" processing layer and an output layer (a single output perceptron in this case). The relationship between inputs and the outputs of a complex system are embossed upon the network by "training" it using concrete exemplars from the real world. During the training process, perceptrons are added and the values of the weighting factors are adjusted until the behavior of the network converges on the behavior of the real system as determined by one or more correlative comparisons. At this point, the network has "learned" to recognize patterns in the input data that predict the output data. As with any empirical mathematical modeling method, challenging the network with a "test" set of exemplars evaluates the predictive ability of the network. Test data typically consist of 10% to 20% of the exemplars that were not present during training. A well-trained network will predict behavior of the test exemplars as well as it did the training exemplars.

2.1.9.2.1 Randomization of Exemplars Prior to Model Construction

As before, the order of exemplars was randomized prior to GA selection and ANN model construction. This ensured that any ordering of the exemplars would not influence selection of inputs by the GA or training of the ANN.

2.1.9.2.2 Construction of ANN Models

ANN models were constructed from the surviving input parameters using NeuralWorks Predict v2.41 (Neuralware, Carnegie, PA).

2.1.9.2.2.1 Assigning a Data Noise Level

Although the input data were theoretically "clean", the output data were considered to be "moderately noisy". The software settings were was adjusted accordingly to help prevent model over fitting (modeling variations caused by noise).

2.1.9.2.2.2 Assignment of I/O Transformation Functions

Input data entering and leaving the network had to be transformed from real world values to the relative input values required by the ANN. This was accomplished by use of one or more transformation functions. Whereas during selection of salient inputs the choice of transforms was limited to one, in this case up to three transforms could be assigned per input (thus, there could be up to three input perceptrons per descriptor in the ANN). Transformation functions could either be linear (scaling only), or nonlinear (log, ln, exponential, power, inverse, inverse power or hyperbolic tangent) expressions. The software automatically optimized the choice of functions by regression analysis.

2.1.9.2.2.3 Selection of Model Inputs Using the GA

The method used was more extensive than that for identification of salient input parameters described above in an attempt to further reduce the number of input parameters per ANN model. Once again a multiple logistic linear regression routine was employed with the cascade variable selection activated.

2.1.9.2.2.4 Selecting Training and Test Exemplar Pools

Input data were divided into two sets using a round robin selection criterion that eliminated every fifth exemplar from the training pool and used these eliminated exemplars to create a testing pool. As the data were previously randomized, this process yielded a random selection of 20% of the exemplars for testing. This process did not specifically remove entire surrogate compounds from the training pool. The number of surrogates was so small and the variation in chemical structures so great that elimination of any compound from the exemplar database would have seriously affected the experience of the ANN. Thus, the model was tested for its ability to predict around noise variations in the exemplar data, and an approach combining the behavior of all three models describing compound-membrane interactions (P-, M- and R-Flux models) was employed to evaluate the overall prediction performance of the ANN models (see below).

2.1.9.2.2.5 Training and Selecting the Best ANN Model

Three networks were constructed using the training data. Construction and training the networks proceeded using an adaptive gradient learning rule in which back-propagated gradient information was used to guide an iterative search algorithm. Back-propagation involves determining the difference between the desired output (the actual laboratory result) and the network prediction, then adjusting the output layer (perceptron) weighting factors in proportion to the difference. The calculations involved in this correction are then used as a basis for making correction to weights in the hidden layer and finally in the input layer (Bharath and Drosen, 1994).

Performance of the networks was evaluated by comparison of the linear correlation (R) between the predicted outputs and the actual laboratory flux data, and the best of the three ANNs chosen. Correlation values were found to be in excess of 0.95 in most cases for these models.

2.1.9.2.2.6 Testing the Selected Network

The test exemplar set previously described was used to determine the ability of the network to model behavior of the surrogates. Comparison of the correlation coefficient was used as a measure of overall performance. Close matches between training and test data sets were taken as an indication of a good model. Typically, training and test R values were within 0.05 - 0.07 for these models. Additional measures of good model behavior included tight predicted 95% confidence limits. The number of molecular descriptors per model at this point was 4 to 10.

2.1.9.2.3 Using Sensitivity Analysis to Eliminate Non-Influential ANN Inputs

Due to the more stringent GA settings and the ability to employ more than one transformation function during ANN model construction, the possibility existed that not all of the descriptors provided to the model would be chosen for inclusion in the model. In order to eliminate inputs that had been rejected by the ANN, a sensitivity analysis was

performed on the entire data set. This analysis generally indicates the degree and direction of influence that each input in the ANN model has on the model output. If the sensitivity analysis is zero, the input likely has no significant effect on the model and may be eliminated without a significant change in model fitness.

Inputs discovered with null sensitivity indices were eliminated from the input data set and a new ANN model was then constructed using the above methods. This process was continued until all inputs demonstrated influence in the model. It typically took 2 to 3 iterations to achieve this. This served to simplify each flux model by eliminating one or two inputs without significantly sacrificing model predictability. The final ANN models contained from 4 to 10 input descriptors.

2.1.9.3 Characterization and Validation of the ANN Models

2.1.9.3.1 Determining Basic Model Attributes

For each ANN model, the predicted output was graphically compared with the actual measured flux data, the correlation coefficients between predicted and actual flux data were determined, and the 95% confidence intervals were calculated (Figs 14a through 19c; Tables 9a through 14c).

2.1.9.3.2 Determining the Overall Influence of Model Inputs on Organic Compound Fluxes

A final sensitivity analysis was performed to evaluate the relative influence of each of the molecular descriptors included in the model on compound P-, M- and R-Fluxes (Tables 15a through 15c).

2.1.9.3.3 Predicting Behavior of the Remaining Compounds in the Database

The P-, M- and R-Fluxes of all 202 compounds in the organic compound database were predicted for each membrane and for the “Universal” PA model.

2.1.10 Validating the ANN Models

2.1.10.1 "Virtual Mass Balance" Method

The relative mass fluxes of organic compounds are related by:

$$\textit{P-Flux + M-Flux + R-Flux = F-Flux}$$

where the F-Flux equals the initial flux of compound in the feed interacting with the membrane, defined as 100%. As all three flux models were derived independently from each other, the ability to predict the behavior of a compound interacting with a membrane by summing the fluxes predicted by all three models and determining their ability to close a "virtual mass balance" is a good test of all three models. Using this technique and allowing for a 25% noise band, the number of compounds in the original database that could be successfully modeled was determined for each membrane and for the "Universal" PA membrane model (Tables 16a through 21c).

2.1.10.2 Comparison of Model Results with Rejection Values Reported for Organic Compounds in the Literature

Traditional percent rejection of compounds by RO membranes may be determined by either the P-Flux or R-Flux measurements. The P-Flux yields the traditional rejection measurements based on penetration of compounds through the membrane. Because the P-Flux has been determined as percent of the total feed flux, the percent rejection may be directly determined from:

$$\textit{100 – (P-Flux)}$$

Comparisons were made between rejection estimated by this method and data obtained from a number of observations in the literature (Table 23).

2.1.11 Producing Excel-Enabled Exportable ANN Models Describing Organic Compound Interactions with RO Membranes

Each of the ANN compound flux models were converted to Visual Basic (VB) source code using a Visual Basic compiler provided with NeuralWorks Predict. For each of the test membranes and for the "Universal" PA model, the relevant P-, M- and R-Flux models were imported as macro functions into an Excel spreadsheet. This spreadsheet was designed to include input cells allowing the user to manually enter relevant molecular descriptor data for any compound of interest, after which the embedded ANN VB programs calculate the predicted P-, M- and R-Fluxes, and percent rejection based on both P- and R-Fluxes. Further user inputs regarding compound feed concentration and membrane water flux are provided so that the user may project absolute compound fluxes as well as concentration of compound expected in the RO product. An F-Flux calculator and a residual comparator allows testing of the prediction results using the "virtual mass balance" method so that the user may determine whether or not the model predictions are acceptable for the particular test compound.

These exportable models are capable of running under Windows on any PC computer running a macro enabled version of Excel (version for Office 2000 or later) and are available upon request.

2.2 Molecular Modeling Method Simulation of Compound-Membrane Interactions

2.2.1 PA Modeling Methods and Simulation Conditions

The steps carried out to achieve the above objective included (i) preparation and optimization of fully atomistic molecular models of PA membranes, (ii) preparation of specific compound molecular models, (iii) introduction of a selected compound into the hydrated PA membrane system, (iv) running the MD simulation, and (v) analysis of the results.

2.2.2 Building the Membrane Models

The membrane modeling (MM) software used to build the PA membrane models has evolved steadily over the past several years. It is custom written in the Tool Command and Tool Kit (Tcl/Tk) language, a freeware, string-based, cross-platform dialect similar to Javascript. Tcl/Tk has been ported to HyperChem, a commercial molecular modeling package containing more than 600 commands and state variables that can be addressed and logically controlled by Tcl. A complete description of Tcl/Tk may be found at www.scriptics.com. The version of software available before this project began had a number of limitations and bugs that needed to be overcome at the project inception.

A screen capture of the variable setup page for the MM program is shown in Fig 29. The software automatically constructs models of randomly crosslinked PA membranes using optimized models of *meta*-phenylenediamine (MPD) and trimesoyl chloride (TMC) as monomer building blocks. This program involves several key steps which are outlined in Fig. 30, including:

Step1. Laying down non-bonded alternating MPD and TMC monomers at the vertices of a 3D cubic lattice.

Step 2. Bonding of the monomers into a nascent linear "backbone" chain by creating an amide bond at each step of a "random walk" through the 3D lattice. This method ensures a randomly folded chain is produced, which is in accordance with X-ray crystallographic data indicating a chaotic polymer arrangement in PA membranes.

Step 3. Initiation of random crosslinking between TMC residues in adjacent regions of the folded backbone structure. This is carried out by forming amide bonds from the two TMC residues to a mutually-shared and neighboring MPD monomer. Crosslinking effectively establishes membrane "pores", as illustrated in Figs. 31 and 32. The size, number, location, and dynamic behavior of such pores is a factor in controlling water and solute transport in the membrane.

Step 4. Elimination of remaining non-bonded MPD and TMC monomers followed by proportional scaling of partial atom charges to achieve the correct net membrane charge. Charge is based on the number of free non-protonated carboxylate groups. The membrane concentration of these groups can exceed 1 M.

Step 5. Geometry optimization of the model followed by iteration of the program to build additional models. At each iteration cycle, certain variables, such as the probability of crosslinking, can be incremented by some amount or randomly varied across a predetermined range. In this way, a diverse population of membrane models can be prepared. Models having the most suitable properties (e.g., globular shape, higher charge, etc.) can then be selected for a particular modeling task.

The nascent membranes constitute a latticework of alternating TMC and MPD monomers connected by a random series of elongated amide bonds (Fig. 32). The bonds rapidly shorten to realistic lengths and angles when the system is geometry optimized using a suitable classical force field, such as AMBER. The "pores" remain distinctly visible,

however, as void spaces even in the final geometry-optimized structures. The software monitors the number and location along the initial chain of crosslinks. It should therefore be possible to calculate the number of pores in a membrane based on this information, but the relationship between crosslink number and location is not simple due to the occurrence of nested and overlapping crosslinks. Efforts to resolve this relationship are underway.

2.2.3 Modeling the Organic Solutes

Software was developed to automatically call up and geometry-optimize any set of organic compounds using tandem classical and semi-empirical force fields. This software was used to create the master compound list used for this study (previously described). Final molecular structure optimizations were carried out using the PM3 semi-empirical force field.

Based on the results of the RMP assay (previously described), two compounds were chosen as surrogates for this modeling subtask; NDMA, which is poorly rejected by PA membranes (~50%) and 1,1,2,2-tetrachloroethylene (PCE) which is well rejected (>99.9%). The disinfection by-products NDMA and PCE are of particular interest because they both are uncharged, low-molecular-weight organics, yet one passes through the PA membrane well while the other is retarded. The orbital structures and electrostatic configurations of NDMA and PCE are presented in Fig. 33.

2.2.4 MD Simulation Setup & Run Conditions

The basic conditions of the MD simulations are given in Table 25. Four relatively short duration (~200 ps) simulations have been conducted, two each for NDMA and PCE in either a hydrated membrane system of in water. The simulations are preliminary in nature because of the brief simulation times and the need to explore the effects of key variables in future simulations, e.g., membrane charge, density, crosslinking, pressure, etc.

The densities of the initial optimized model membranes are generally about 0.1 g/cm^3, i.e., more than 10-fold less than the value of 1.3 g/cm^3 for actual PA membranes that has been reported in the literature (Kotelyanskii et al., 1998). The membranes do not spontaneously undergo contraction and densification on their own in MD simulations due to strong electrostatic charge repulsion between the non-protonated carboxylate groups. Because pKa values for organic acid carboxyl groups generally range from about 3-4, these groups were left non-protonated in the membrane models. This assumption seems reasonable given that many water treatment membranes are operated at ~pH 6-7 and sometimes higher. However, this point may be contested and therefore should be explored more carefully in future work.

The membranes undergo spontaneous contraction ("densification") if monovalent or divalent cations (e.g., Na+ or Ca++) are placed in the system (data not shown) resulting in shielding and neutralization of the carboxylate charges by the cations. However, this was not done in this study because the ion concentrations needed to achieve significant membrane contraction were unrealistically high (>1M). Instead, densification was accomplished by "packing" the hydrated membrane into a cubic periodic cell of appropriate volume (30 Å per side), as illustrated in Fig. 34. Packing occurs by shortening and bending bonds resulting in a strained molecular conformation with some bad contacts and increased potential energy. However, much of the strain is relieved by geometry optimizations and by running 100 ps of MD prior to introduction of the organic solute. It is unknown whether real PA membranes are as highly packed and strained as the models seem to indicate, but this possibility is plausible in view of the extremely rapid nature of the interfacial polycondensation reaction between MPD and TMC. The insoluble polymer network could rapidly precipitate in a strained conformation before it had time to fully relax. Reliable surface energy measurements of PA membranes might shed light on the conformational stability of this polymer and such data could be useful in model verification and refinement of model structural details.

Membrane hydration was performed by random addition of 200 TIP3P water models to the membrane prior to packing, yielding a water concentration of about 19 wt%. These

are flexible water molecules with partial charges of -0.834e on oxygen and +0.417e on hydrogens. The "packed" hydrated membrane system (with a density of ~1.19 g/cm^3) was relaxed for 100 ps of MD simulation (300^{o}K) before adding either NDMA or PCE to the system's center. The resulting system for NDMA is shown in Fig. 35, but water molecules have been removed to facilitate visual localization of the organic molecule. Note that membrane void spaces resembling membrane "pores" can still be observed even at the higher system density.

3 PROJECT RESULTS

3.1 QSAR ANN Modeling Results

3.1.1 Comparison of RMP Assay with a Crossflow RO System

Although the absolute value of rejection determined by the RMP assay and the block tester were not equal (Fig. 5), there was an overall agreement in the comparative behavior of the two systems (e.g., compounds rejecting well in the RMP assay were observed to reject well with the crossflow block tester and vice-versa.). The lack of the crossflow in the RMP assay, and subsequent increase in membrane concentration of solute at the membrane surface likely explains the reason why the rejection results deviate from ideal values (the dotted line in the figure). However, the difference between the RMP assay and the cross-flow block tester is greatest where rejection is poor, and the results tend to converge as rejection improves (with the exception of the CA membrane). Thus, for the most part, predictions of high rejection by the RMP assay (at least for PA membranes) should tend to reflect high rejection values observed in a standard RO unit.

3.1.2 Determination of Compound-Membrane Interactions

In the RMP assay, use of radioactively tagged compounds allows the mass of compound in the product, the feed, and in the membrane to be directly measured, and fluxes of compound through the membrane (P-Flux) and into the membrane (M-Flux) to be directly determined. By difference, it was possible to estimate the flux of compound that remained in the feed. Thus, the fate of surrogate compounds could be accurately tracked and their behavior could be determined.

Figures 8a, 9a, 10a, 11a, 12a and 13a represent performance diagrams that illustrate compound behaviors determined for each membrane. In these representations, the X-axis shows the relative M-Flux (values 0 – 100) representing increasing membrane association from the left to the right of the graph. The Y-axis shows the relative P-Flux (values 100 – 0) decreasing membrane penetration (increasing rejection) from bottom to top of the graph. Each of the numbers on the graphs represent the identity of a surrogate

compound. A list of these compounds with their respective ID numbers and relative compound fluxes (P-, M- and R-Fluxes) are presented in Figs. 8b, 8c, 9b, 9c, 10b, 10c, 11b, 11c, 12b, 12c, 13b and 13c. The QSAR descriptor cluster numbers correspond to the compounds' molecular properties categories.

The graphs representing compound fate are divided into four quadrants. Compounds in quadrant "A" interact poorly with the membrane; they neither associate with the membrane nor do they pass through it. This can be confirmed by their relatively low P-Flux and M-Flux values, but relatively high R-Flux values (high rejection at the membrane surface). Compounds in quadrant "A" are well rejected by the membrane acting as a mechanical barrier. Some examples of compounds in this category include the pharmaceuticals ibuprofen, ciprofloxacin, the endocrine disruptor bisphenol, and the herbicide alachlor. These compounds are very well rejected by all the PA membranes.

Compounds in quadrant "B" do not associate with the membrane well, but pass through it relatively easily. These compounds are poorly rejected, as the membrane provides a poor barrier to them. Urea and NDMA are the only two surrogate compounds that fell in this category in for the PA membranes, while the CA membrane had several others, including caffeine and t-butyl alcohol.

Compounds in quadrant "C" pass through the membrane poorly; however, they strongly associate with the membrane so their apparently high rejection is largely due to membrane absorption or adsorption. In this case the membrane acts as an affinity filter. Although these compounds are initially well rejected, if the membrane reaches saturation (may occur if compound is constantly in the feed), these compounds may eventually break through, especially if they are absorbed into the membrane and not adsorbed on the membrane surface. Examples of compounds that fall in this category for all the PA membranes are the endocrine hormones 17a-estradiol and estrone, the aromatic hydrocarbons toluene, benzene and the aromatic alcohol phenol.

The CA membrane behaved somewhat differently than PA membranes. In general, there were less surrogate compounds associated with quadrant "A" and there were more compounds that fell in quadrant "B", indicating that the CA membrane was not as successful as the PA membranes in rejecting organic compounds.

A direct performance comparison between membranes for P-, M- and R-Flux for each surrogate compound is presented in Tables 6, 7 and 8.

3.1.3 ANN Models Describing Organic Compound-Membrane Interactions

3.1.3.1 Overall Performance of ANN Membrane Models

Results of ANN modeling for P-, M- and R-Fluxes for all membranes (and for the "Universal" PA model) are summarized in Figs. 14a through 19c and Tables 9a through 14c. In each of Figs. 14a through 19c, a scatter plot comparing actual surrogate compound behavior with that predicted by the ANN model visually indicates model performance. The diagonal line in this plot indicates perfect agreement between the model and real world values. Error bars represent one standard deviation about the mean for the actual behavior data (n = 4 to 7). ANN model statistics are presented beneath the scatter plot, including the R correlation values (linear correlation between predicted and actual values), the average absolute error values (average absolute error between the predicted and actual values) the root mean squared (RMS) error values (root mean square error between the predicted and actual values), the 95% confidence interval for the model and the number of exemplar records used to create the model. The identity of the QSAR molecular descriptors used in model construction is indicated below the statistics panel. For each input, a value representing a sensitivity index calculation relating the direction and degree of influence of each of the input parameters to the model is presented (explained in more detail below). Tables 9a through 14c present the predicted and actual behavior results for P-, M- and R-Fluxes for each of the surrogate compounds for all the membrane models (in the case of the "Universal" PA membrane, the actual values reported are the averages of results for all the PA membranes combined).

Performance of the ANN models was evaluated by comparing the linear correlation (R) coefficients between the predicted model outputs and the actual laboratory flux data. Correlation values were typically in excess of 0.95 in most cases. Moreover, the closeness of matching between training and test data sets indicated a predictive model. Reasonably close ranges for the predicted 95% confidence limits also indicated good model behavior. The P- and M-Fluxes tended to model better than the R-Flux, primarily due to the fact that the R-Flux was a calculated value made up of data from the other fluxes, and therefore contained the sum of their statistical noise. For a like reason, the "Universal" PA membrane model was also noisier than the individual PA membrane models (but still possesse a relatively high R value). Because of an increase in internal noise, this model is more flexible than the individual PA models, and tended to be somewhat more applicable to compound behavior prediction (see below).

3.1.3.1.1 ANN Model Sensitivity Analysis Results

Because the models in this study were constructed using QSAR molecular descriptors (for a detailed listing see Appendix 1) linked to fundamental molecular properties, it was hoped that the nature of the individual inputs to the models and the degree to which they influenced the predicted behavior of the surrogate compounds would provide insights as to the molecular mechanisms defining compound-membrane interactions. One goal of the study was, therefore, a search for "universal behaviors" in a broad sense between membrane models with regard to the basic molecular properties.

By considering the inputs selected by the GA during model construction, it was possible to gain insight as to which input parameter proved influential in a given compound-membrane interaction. However, the direction and magnitude of that influence was not revealed. In the case of multivariate linear models, it is possible to gain this insight by analysis of the magnitude and direction of the slopes of the individual linear equations from which the model was assembled. In the case of the ANN models, this is not possible. However, it is possible with the ANN models to compute a "sensitivity index" for each of the input parameters. The sensitivity index is a measure of the overall magnitude and direction of influence that each of the model input parameters has on the

model output. If this index is calculated over the entire range of the input data set (for all the surrogate compounds), then it tends to represent the overall strength and direction the input parameter has on the model output. However, it may not entirely indicate a long-range output response. For example, the sensitivity index for a constantly increasing function would be positive and one for a constantly decreasing function would be negative, and the magnitude of the index would be a relative index of slope. If, on the other hand, the function contained a number of hills and valleys (a sine wave parallel to the X-axis would be an extreme example of this), the sensitivity index could be large because of short-range influences, but would not well indicate the long-range relationships in the function.

A summary of the sensitivity indices for all the membranes with regard to each of the compound-membrane interactions (P-, M- and R-Fluxes) is presented in Tables 15a through 15c. Of the original 73 molecular descriptors used in the modeling, a total of 33 survived as inputs used in the ANN models (See Appendix 2). In these tables, the molecular descriptors were broadly grouped into five categories to aid comparison. The five groupings include descriptors related to molecular charge or polarity (ABSQ, MaxQp, MaxNeg, P, Py, Pz, Q, SsCH3, SdssC, SaaCH, SdO, Gmax, Gmin, Hmin), descriptors related to molecular size or complexity (Ovality, Surface, xpc4, xv1, xvpc4, nxp5, nxch6, k1, k2, k3, Iy, fw, idcbar, sumdelI, Wt), descriptors related to molecular hydrophobicity (Log P), descriptors related to hydrophobicity/charge (Qs, Qsv), and descriptors related to the extent of molecular hydrogen bonding (numHBa). (For a detailed explanation of these descriptors, see Appendix 1.)

3.1.3.1.1.1 Relative P-Flux Sensitivity Index Analysis: Molecular Descriptors Associated with Penetration of Organic Compounds through the RO Membranes

In the case of the relative P-Flux (solute passing through the membrane, Table 15a), it was observed that, depending on the membrane, this compound-membrane interaction was associated with all five molecular descriptor groups, although models contained varying numbers of inputs (a minimum of 4 inputs for LFC1 to a maximum of 8 inputs for ESPA-2 and for the CA model). Thus, ability of compounds to pass through the membranes were related to molecular charge and charge distribution, molecular size and complexity, hydrophobicity and to the hydrogen bonding. However, the magnitude and direction of influence for many of these properties varied from membrane to membrane.

In general, for the polyamide membranes, influential molecular descriptors included MaxQp (the largest positive charge over the atoms in the compound), Py (the magnitude of charge separation along the compound's inertial Y-axis), P (the magnitude of the compound's dipole moment), SsCH3 (the sum of the E-state values for all the methyl groups in the compound), SdssC (the sum of the E-states for all the aromatic carbon atoms in the molecule), and Hmin (the smallest hydrogen atom E-state in the compound). The CA membrane model included the same descriptors as the PA models (P and SdssC). There was a general variation in the direction and magnitude of the influences of the inputs related to molecular charge and polarity. However, in general, Py (component of the dipole moment along the inertial Y-axis) tended to show agreement across three of the four PA models. An increase in this descriptor was related to an increase in P-Flux. The CA model did not contain unique charge/polarity related inputs (some were also shared by one more PA models).

Molecular complexity descriptors included in the models were Ovality (the deviation of the compound's shape from a perfect sphere), Surface (the molecular surface area), the chi indices xpc4 (5 atom chi index encoding patterns of adjacency), xv1 (2 atom chi index encoding degree of branching) and xvpc4 (5 atom chi index encoding patterns of

adjacency), nxp5 (the number of paths in the molecule with 5 edges), Iy (the principal moment of inertia along the compound's Y-axis), and fw (the compound's molecular weight). The relationship between molecular complexity and P-Flux was also mixed. It would be generally expected that as molecular size and complexity increased that P-Flux should decrease. In many cases (9 of 13 involving molecular complexity parameters), this was observed. The CA membrane model emphasized the chi indices more than did the PA models, but the chi index descriptor xvpc4, though not included in the CA model, occurred in 3 out of 4 PA models. Sensitivity indices for the chi indices tended to be negative, suggesting that ability to transverse the RO membrane matrix was in general inversely proportional to molecular complexity.

Qsv (the average molecular group polarity descriptor) was only included in the CA model, and was positively associated with P-Flux.

Hydrophobicity was almost universally important in models predicting P-Flux, evident by the nearly universal inclusion of LogP in both PA and CA models (with the exception of the TFC-HR model). This input universally exhibited a negative relationship with the P-Flux. As LogP increases, compound hydrophobicity increases. This means that as compound hydrophobicity increased, there was a fairly universal tendency for the compound to be retained by the membrane.

There was also a generally positive relationship between numHBa (the number of hydrogen bond acceptors in the compound) and the P-Flux (in three of the four PA membranes). This indicates that as the number of hydrogen bond acceptors on the molecule increase, there is a greater tendency for the molecule to pass through the membrane.

The "Universal" PA model exhibited general overall agreement with the nature and direction of influence of the parameters included in the other models. More interesting was the fact that, although the membrane properties (Table 3) were included in construction of the P-Flux model, none of them survived during the evolution of the

inputs by the GA. This suggests that compound molecular properties were more influential than the measured membrane properties with regard to penetration of compounds through the PA membranes.

The CA membrane model included many of the same descriptors appearing in the PA models, although there were some unique inputs (Qsv, xv1, xpc4) which did not appear in any of the PA models.

3.1.3.1.1.2 Relative M-Flux Sensitivity Index Analysis: Molecular Descriptors Associated with the Adsorbtion/Absorption of Organic Compounds to the RO Membranes

ANN models describing the interaction of the compounds with the membranes (M-Flux) once again included representative molecular descriptors from all the five basic descriptor groups, and as with the P-Flux models there were differences in the descriptors emphasized by each membrane model (Table 15b). Some descriptors included in the P-Flux models also appeared in the M-Flux models (specifically MaxQp, P, SdssC, nxch6, LogP and NumHBa). Once again, there was a range in the number of descriptors included in each membrane model (from as few as 4 with BW-30 and CA to as many as 10 with LFC-1).

With regard to the charge/polarity-related descriptors, besides MaxQp, P and SdssC, the M-Flux models included Q (the magnitude of the principal quadripole moment), SaaCH (the average E-state value for all aromatic carbon-hydride groups in the compound), Gmax (the largest atom E-state in the compound) and Gmin (the smallest atom E-state in the compound). Once again, there was variation in the direction and magnitude of influence amongst the various membrane models for these inputs, though all of the models did include an input indicating that molecular charge and/or polarity played an important role in the association of the compounds with the membranes. Gmin (the smallest atom E-state in the molecule (the most electrophilic atom in the molecule) was universally included in this category, and its sensitivity index was universally positive

and relatively strong. This suggested that the association of compounds with the membranes might involve electrophilic interactions. Likewise, P (the magnitude of charge separation along the whole molecule) was universally included in all models. In the case of 3 of the 4 PA models (and in the case of the "Universal" PA model), the sensitivity indices for P were negative, indicating that as the magnitude of the charge separation decreased, the association of the compound with the membrane increased. This relationship reversed in the case of CA and TFC-HR, however, but remained a strong relationship.

Of the indices related to molecular complexity, only fw (formula weight) appeared in the P-Flux models. Additional complexity descriptors related to M-Flux included nxch6 (the number of 6-membered rings in the compound), k1 (kappa shape index related to the degree of cyclicity in the compound) and idcbar (the Bonchev-Trinajsti mean information content). The contribution of molecular descriptors related to molecular complexity to the M-Flux varied. In some cases, (BW-30, TFC-HR and CA), complexity did not seem to be important in the models at all, and in the case of LFC-1 and ESPA-2, the models exhibited strong but inconsistent directions of influence with regards to formula weight (mass) and indicators related to molecular structural complexity (idcbar and k1).

The number of hydrogen bond acceptors (numHBa) was once again included in the M-Flux models, at least in 3 of the 4 PA models as well as in the "Universal" PA model. It is universally positive, indicating that the presence of more hydrogen bonding acceptors in the compound is associated with increased tendencies to associate with the membrane (either adsorption or absorption).

Log P is not as prevalent with regard to membrane association, (it was included in just two of the PA membrane models, the "Universal" membrane model and the CA model). It also exhibits some variation in response, but in the case of BW-30, the "Universal" PA and CA, it was positively associated with M-Flux, suggesting that in these cases increasing hydrophobicity may increase compound association with the membranes.

As with P-Flux, there was general agreement between the "Universal" PA model inputs and direction of influence as the individual PA models. Once again, none of the membrane parameters were included in the final model, although they were present during model construction. As with the P-Flux, this indicates that none of the membrane parameters included in the modeling were more influential than the compound molecular descriptors in predicting the interaction of the compounds with PA membranes.

The CA model describing M-Flux differed from the PA models in the direction of influence the charge/polarity-related descriptors, possibly indicating a difference in mechanism of interaction between the compounds and the CA membrane.

3.1.3.1.1.3 Relative R-Flux Sensitivity Index Analysis: Molecular Descriptors Associated with the Ability of RO Membranes to Repel Compounds at the Membrane Surface

Molecular descriptors and their sensitivity indices are shown for the R-Flux models in Table 15c. There are molecular descriptors in these models which appear in both the P-Flux and/or M-Flux models, including Py, Q, SaaCH, SdssC, Gmax, Gmin, nxch6, idcbar, LogP and numHBa. Again, as with the other compound flux models, responses of the individual membrane models varied with respect to the individual molecular descriptors included in the R-Flux models. Also, as with the other compound flux models, the molecular descriptors are related to charge/polarity, molecular complexity, hydrophobicity or hydrogen bonding, although not all membrane models contain descriptors from all of these groups. The complexity of the models covers a range similar to that seen with the other flux models (from 4 inputs for BW-30 to 10 inputs for TFC-HR). There was a general tendency for the sensitivity indices for R-Flux to be opposite those noted for the M-Flux, and as R-Flux is a measure of the tendency of compounds not to associate with the membranes, this is not a wholly unexpected result.

Charge/polarity descriptors serving as inputs for the R-Flux models that were not included in other flux models include ABSQ (the sum of the absolute value of the

charges on all atoms in the compound), MaxNeg (the largest negative charge over the atoms in the compound), Pz (the component of the dipole moment along the compound's inertial Z-axis) and SdO (the sum of all E-state values for the doubly bonded oxygen atom in the compound). There was in general a negative relationship noted between charge-related inputs and R-Flux in most of the models. The most commonly represented molecular descriptor related to compound charge was Gmin, which was also strongly represented here as it was in the M-Flux models, except that its direction of influence is reversed. Q (the magnitude of the principal quadripole moment) was contained in three of four PA models and Gmin was contained in all PA models.

Regarding molecular complexity, nxch6 and idcbar were shared with other flux models, but sumdelI (the sum of the delta intrinsic states of atoms in the compound), Wt (the total Weiner number) and the kappa shape indices k2 (encoding the degree of central branching in the compound) and k3 (encoding the degree of separated branching in the compound) were unique to the R-Flux models. The direction of influence of molecular complexity indices tended to vary; however, they were on the overall positive, indicating that for the most part, R-Flux tended to increase with increases in molecular complexity.

Where models included LogP (BW-30 and TFC-HR), as an input parameter, its sensitivity index was negative, indicating that compounds with lower hydrophobicity tended to remain unassociated with the membrane. In the case of BW-30, this effect was opposite that for M-Flux and similar to that for P-Flux, consistent with a model in which hydrophobic association with the membrane removed compounds from solution on the feed side and also prevented them from passing to the product side.

The number of hydrogen bond acceptors (numHBa) was again included in three of the four PA models, as well as in the "Universal" PA model. In this case, the sensitivity analysis indicated a negative relationship between the number of hydrogen bond acceptors in the solute molecules and the ability of the molecule to remain free in the feed. This is consistent with the results for the M-Flux, which indicated an opposite role for this parameter, and for the P-Flux models as well. This suggests that hydrogen

bonding may facilitate the attachment of compounds to the membrane as well as facilitate their transport through the membrane matrix.

Once again, there was general agreement between the "Universal" PA model and the individual PA models with regard to the inputs emphasized and the direction of their influence. In this case, as with the other "Universal" PA models, no membrane input parameters survived in the final evolution of input parameters, indicating that the measured membrane parameters were far less predictive of the ability of the membranes to reject compounds at membrane-feedwater surface than were the molecular descriptors.

The CA model was also in general agreement with respect to the type and direction of influence of the molecular descriptors. The CA model tended to emphasize the charge/polarity descriptors, and included the absolute molecular charge (ABSQ) as one of the more influential inputs. The sensitivity index suggested that the R-Flux was positively related to compound absolute charge.

3.1.3.2 Validation of the "Universal" PA ANN Models – Comparison with the Individual PA Models

The success of prediction of the "Universal" PA ANN model was evaluated by comparing it to the outputs of each individual PA membrane models. These comparisons were determined for P-, M- and R-Fluxes (Figs. 20a through 23c). In these figures, the closed circles represent the specific PA membrane models while open circles represent the "Universal" PA model. All the "Universal" models agreed reasonably well with the individual membrane models. The "Universal" PA models generally exhibited more noise, which is an expected result of them containing the combined statistical noise of all of the other PA membrane models. It was also noted that, as with the individual membrane models, the R-Flux model was the noisiest.

3.1.4 Application of the ANN Models to the Master Compound List – Prediction of Compound Interactions with RO Membranes

3.1.4.1 Prediction of Compound-Membrane Interactions; Determination of Prediction Success Using the "Virtual Mass Balance" Method

The ANN models were applied to all 202 compounds in the master compound list to predict relative P, M and R-Fluxes for each of the 5 membranes used in the study as well as for the "Universal" PA model. Following prediction of relative fluxes, the F-Flux was calculated from the predicted values by summation of the individual relative mass fluxes. This F-Flux represents the estimated total relative compound flux impinging on the membrane in the RMP assay, and by definition should have equaled 100 in all cases. As each of the ANN models was developed independently of the other, this combination of their data to provide a "virtual mass balance" should have amounted to a conservative performance evaluation. Based in the confidence intervals observed in the individual models, a somewhat subjective criterion was used to establish a noise band of ± 25% as the cutoff for the study. Compounds whose predicted F-Flux values were outside this range were culled from the database for each membrane

The final list of compounds, in alphabetical order, that were successfully modeled in the study is presented, for each membrane used in Tables 16a through 21c. In these tables, the compounds appearing in boldfaced type represent the surrogates that were used to construct the predictive models. The predicted values for the relative P-Flux, the relative M-Flux, the relative R-Flux and the summation of these values (the F-Flux) are presented to the right of each of the compounds..

Based on the above criterion, success in prediction of the interactions between the organic compounds with the test membranes varied with membrane type. With CA, the ANN models were capable of predicting the behavior of 58% of the compounds. The PA models could describe the behavior of between 57% and 70% of the compounds. The

"Universal" PA model was the most flexible, and was able to predict the behavior of 76% of the compounds in the master compound list.

3.1.4.2 Interpretation of the Relative Flux Table Data

The relative fluxes presented in Tables 16a through 21c may be used to gain insight as to the expected performance of the membranes on a given compound. In general, compounds exhibiting a low relative P-Flux and a low relative M-Flux (and a concomitantly high relative R-Flux) will be rejected well by the membrane in question (they would fall in quadrant "A" in a quadrant diagram such that presented in Figure 8a). Because the membrane interaction is predicted as being low, rejection should be relatively insensitive to mechanisms such as compound binding and saturation of the membrane material.

If a compound presents a high value for the relative P-Flux and a low value for the relative M-Flux (also a low value for the relative R-Flux), then the compound is passing through the membrane with little interaction. The membrane is providing neither a mechanical or adsorptive/absorptive barrier to the compound in this case. Compounds in this category are not well susceptible to removal from the feed by reverse osmosis using the particular membrane in question.

Finally, in situations where the P-Flux is high and the M-Flux is high (but the R-Flux is low), the compound is being removed by the membrane by a largely adsorbtive/absorptive mechanism. Compounds exhibiting this behavior are initially blocked from the product water effectively, but as the membrane begins loading with bound material, removal may begin to suffer, especially should the compound be removed by absorption into the membrane structure (or the support materials). Compounds exhibiting this sort of behavior could eventually prove problematic if provided to the RO system in low concentrations over long time periods as opposed to spikes with long periods in between.

3.1.4.3 Estimation of Membrane Percent Rejection from the Relative Compound Flux Data

It is possible to convert the relative flux data provided by the RMP assay into a percent rejection value. Two mass fluxes can provide the basis for this sort of conversion; the relative P-Flux or the relative R-Flux (as described in the methods section).

Rejection calculated by relative P-Flux is based on two principal mechanisms: mechanical exclusion and adsorptive/adsorptive compound-membrane interactions. This is the "classical" method of determining RO membrane rejection. In the field, as with the RMP assay, rejection does not take into account association of the compound with the membrane at all (e.g., a high rejection doesn't indicate *a priori* that the compound is being physically rejected at the feed/membrane interface).

On the other hand, percent rejection determined by the relative R-Flux value is based solely on the interaction (or lack of interaction) at the membrane surface. It is indeed "rejection" directly into the feed; thus the relative R-Flux value (as defined in this study) directly represents a "percent rejection."

Percent rejection values predicted by all of the ANN models, determined by both P-Flux and R-Flux methods, are presented for each membrane used in the study as well as for the "Universal" PA membrane model in Tables 22a through 22e. All of the compounds used in the study were included in these tables in alphabetical order. Blank cells in these tables indicate compounds whose behavior could not be predicted by a particular membrane model.

Compounds exhibiting large percent rejection values determined by both P-Flux and R-Flux (such as Diazinon, Disulfoton, Lincomycin, Mestranol, and Triphenyl Phosphate) suggest very good rejection, as the compounds are not only poorly able to pass through the membrane but are also poorly able to associate with the membrane material (similar to the situation of compounds in the "A" quadrant of Fig. 8a). In the case of compounds

in which the rejection as determined by P-Flux and R-Flux is both nearly equal and moderate to low (such as Bromochloromethane, NDMA, and Urea), the compound passes through the membrane without interacting with it. RO in this instance provides a relatively poor barrier to the compound (similar to the situation with compounds in the "B" quadrant of Fig. 8a). Finally, when the rejection based on P-Flux is high but rejection based on the R-Flux is low, (such as with TCE, PCE, 4,6 Dichlorophenol, Acetaminophen, Benzene, Dibromoacetonitrile, 17a Estradiol, and Estrone), the compound is being removed mainly by adsorption/absorption to the membrane. In this case, the compound's rejection may initially be very good, and remain good so long as the compound is present in short spikes. However, if the compound is chronically present in the feed, as the membrane begins to saturate with the compound, rejection may significantly degrade. Therefore, compounds with high P-Flux rejection but poor R-Flux should be regarded as potentially problematic.

3.1.5 Comparison of Rejection Predicted by the ANN Model to Rejection Reported in the Literature and Field

The rejection results predicted by the RMP assay data and the ANN models for P-Flux were compared to results reported in the literature and from the field (Table 23). Data were compiled for 18 compounds, including pharmaceuticals, disinfection byproducts, pesticides, endocrine disruptors, low molecular weight aromatic hydrocarbons, and others. In general, rejection predicted by the ANN models for PA and CA membranes exhibit very good agreement with that reported in the literature or from the field.

3.1.6 Instances where Models Failed to Predict Compound Behavior: Gap Analysis and Suggestion for Further Study

Even though a reasonably large proportion of the master compound list (~25%) was included as surrogates for model construction and some care was taken to insure that the molecular properties of the surrogates were diverse, the resultant ANN models were still

unable to predict the behavior of many compounds. The failure rate varied somewhat depending on the membrane being modeled; however, in a many cases the same compounds were observed to fail prediction in multiple membrane models.

Table 24 shows a listing of compounds that failed in 75% or more (3 or more) of the polyamide models, and includes 45 compounds (slightly less than 25% of the total number of compounds examined). These compounds possessed molecular properties outside of the experience of the ANN models, and thus the models were unable to predict their behavior.

Failure of the models could be due to two reasons: either there were insufficient surrogates chosen to define one or more of the original QSAR molecular descriptor groups initially identified in the study, resulting in too narrow a variation of molecular properties, or else the original QSAR molecular descriptor groupings were not appropriately related to the compound-membrane interactions that were modeled. The very small number of total exemplars used in ANN model construction may have been problematic; only 51 surrogates were used in the study whereas often hundreds or thousands of exemplars are typically employed in constructing ANN models. For a small number of surrogates as was employed in this study to yield a highly predictive model requires the system under study to be very well-behaved and relatively simple so that it may be adequately defined with a limited number of points scattered in n-dimensional space. Clearly, the failures observed in this case indicate that this system is more complex than can be adequately defined by only 51 different input patterns.

Figure 24 shows the fraction of compounds in the QSAR descriptor clusters that were represented by surrogates (the density of information defining the cluster) plotted against the percent of cluster compounds failing to model (compound failure defined as the F-Flux failing to be predicted by at least 3 of the 4 PA ANN models within ± 25%). The numbers on the chart represent each of the QSAR descriptor clusters identified in the study. The general expectation is that failure of the ANN models will be inversely proportional to model experience; that is, the greater the representation of a cluster by

surrogates, the greater the ability to predict behavior of the cluster compounds. Where surrogates representing a cluster were sparse (clusters 11, 17, 9 10, 2) model failure rates were relatively high and generally increased in proportion to lack of exemplars. In this case, clearly the model experience is lacking, creating significant information gaps. More surrogate compounds representing these clusters should materially improve prediction of the models. The negative slope of the trend line supports this general hypothesis, but the trend is relatively weak, indicating that other factors influence failure other than simply the absence of sufficient exemplars for each cluster.

The original QSAR molecular descriptor clusters were chosen based on a suite of molecular descriptors not necessarily related to compound-membrane interactions. Thus, compounds may have been grouped on the basis of properties not germane to these interactions. The data presented in Fig. 24 suggest this might have been the case. For example, compounds in clusters 3, 4, 16 and especially 6, 15, 18, 19 and 20 could be adequately predicted by the ANN models ("adequate" meaning failure rate $\leq$ ~15%) using data provided by the surrogate compounds chosen for the study in spite of relatively poor surrogate representation. On the other hand, compounds in clusters 1, 5, 12, 13 and especially 8 failed to model even when they were relatively well represented by surrogates.

In order to close the "gaps" in the ANN models, additional surrogates are needed that address the lack of information currently limiting predictive ability of the models. Moreover, the choice of compounds for this purpose may now be based on a smaller universe of molecular descriptors known to be related to compound-membrane interactions, as these descriptors were identified in the current study.

Figure 25 represents a dendritic analysis of the 45 poorly modeled compounds. As before, the intent of this analysis was to identify compounds with similar properties so that they may be clustered for purposes of surrogate identification. A somewhat arbitrary criterion was adopted for separating clusters; a distance of 300 was chosen because, in general, it isolated like compounds well. In addition to this criterion, a fine-tuning was

performed to separate clusters that appeared to have larger numbers of compounds, so that cluster size was reduced to no more than 7 compounds. A total of 16 clusters were identified containing from 1 to 7 compounds.

Addition of surrogate compounds chosen from these clusters should substantially improve predictability of the current models. This approach should be considered as a future area of study.

3.2 Analysis of MD Simulations

3.2.1 System Energies

Data presented in Fig. 36 indicates system potential energy fluctuations for the NDMA membrane simulation. PCE data (not shown) were similar and, in each case, system potential energies initially increased, followed by a gradual decline to steady state. The initial increase in potential energy was due to early interactions as the system temperature was raised from 0^{o}K to 300^{o}K in the first 0.1 ps of simulation. Once the specified simulation temperature was reached, both systems drifted toward more relaxed conformations with lower overall potential energies.

3.2.2 Diffusion Behaviors of NDMA and PCE

Using center-of-mass (COM) positional data to dampen the effects of single-atom motions, NDMA and PCE trajectories were monitored over the course of the membrane simulations. The data revealed that both compounds exhibited continuous, small-scale translocations (usually on the order of ~1Å) primarily centered in the local region of the membrane into which the compound had been first introduced. Preliminary efforts to compute diffusion coefficients for NDMA and PCE were based on these small-scale translations (see below), but other types of longer-range excursions were also observed, particularly for NDMA. It is these irregular long-range translocations that must be more fully documented and statistically described in terms of their magnitudes and frequencies of occurrence before accurate diffusion kinetics can be obtained. For example, NDMA was observed to make two abrupt translocations beginning at about 20 ps of elapsed

simulation time. These translocations can be observed in the COM trajectory paths shown in Fig. 37. In the first "outbound" translocation, occurring at about 20 ps, NDMA traveled nearly 7Å away from its point of origin at t = 0 ps. This was followed approximately 8-10 ps later by an equally abrupt "inbound" translocation and return to the immediate vicinity of the molecule origin (Fig. 38). Following the inbound movement, NDMA was observed to resume small-scale excursions, but superimposed on this was a gradual drift away from the origin over the next 60 ps. In contrast, PCE did not exhibit any large-scale translocations of the magnitude exhibited by NDMA. Moreover, PCE tended to reside within a fairly restricted region, traveling not more than ~1-2 Å from its point of origin for the duration of the 200-ps simulation. However, larger-scale movements of PCE might have been observed if simulation times were extended.

The type of rapid translocation behavior in which a solute such as NDMA moves from one "vacancy" or void space in the polymer matrix to an adjoining void is referred to as a "jump" or "hop" (Fig. 39). This motif of solute transport has been well documented for dilute gas molecules diffusing in amorphous polymers, such as carbon dioxide or methane in polyethylene or polypropylene (Takeuchi, 1990; Gusev et al., 1994; Takeuchi and Okazaki, 1996; Mueller-Plathe, 1994). Such a jump mechanism has also been recently reported for water diffusion in PA membrane networks (Kotelyanskii et al., 1998); and, in that study, it was demonstrated that the accuracy of water diffusion coefficients were critically dependent on the jump frequencies. The jumps occur when the solute and membrane undergo conformational changes such that the solute can suddenly squeeze into and through a passage or channel that is temporarily formed between two adjoining void spaces in the membrane. The probability of this happening depends on numerous variables including (i) the flexibility of the membrane and solute, i.e., how readily they can undergo conformational rearrangements by overcoming torsional barriers, (ii) the solute size and shape, and (iii) short- and long-range interactions with water and membrane atoms (i.e., electrostatic and van der Waals interactions).

Conventional calculation methods for solute diffusion coefficients (**D**) based on root-mean-square (RMS) molecule displacements ($\mathbf{\langle x^2 \rangle = q_i Dt}$, where $\mathbf{\langle x^2 \rangle}$ is RMS displacement, $\mathbf{q_i}$ is the dimensionality factor, **t** is the displacement time step) are generally suitable for substances that demonstrate continuous localized diffusion behavior, i.e., diffusion that is unmarked by jumps. However, as illustrated in Fig. 39, if abrupt and large translocations occur, it is necessary to compute diffusion coefficients based on the magnitude and frequency of such translocations.

3.2.3 Calculation of Water and Solute Diffusivities and Theoretical Fluxes

In spite of the limitations discussed above regarding the lack of information on solute jump frequencies, apparent diffusion coefficients for water (D_{BM}) and the organic solutes (D_{AM}) were nevertheless computed from the time-resolved RMS displacements of the compounds during selected periods of the MD simulations. The RMS displacements were computed from molecule COM coordinates to dampen the effects of single atom motions. The results of a typical diffusion coefficient calculation for five randomly selected water molecules and the NDMA solute are given in Fig. 40. Diffusion coefficients and theoretical solute fluxes are presented in Table 26. At this stage, the diffusion coefficients should be regarded as *providing only relative* indications of transport kinetics. As expected, the organics diffused relatively more slowly than water within the membrane matrix. It should be noted that whereas the diffusion coefficients for NDMA and PCE were nearly indistinguishable in pure water simulations (~7.82×10^{-6} cm^2/s), PCE diffusion in the hydrated membrane system (1.92×10^{-6} cm^2/s) was nearly four-fold less than that of NDMA (7.25×10^{-6} cm^2/s). The similarity of NDMA diffusivities in the water and membrane systems reflects the fact that calculations for D_{AM} were based on local molecule excursions rather than on discontinuous jump frequencies.

Theoretical fluxes ($\mathbf{J_A}$) for NDMA and PCE were calculated based on the modeled diffusivities ($\mathbf{D_{AM}}$) and experimental values for $\mathbf{K_A}$, the water-membrane equilibrium partition coefficient: $\mathbf{J_A = -D_{AM} K_A (\Delta C_A / \sigma)}$, where $\mathbf{\Delta C_A}$ is the solute concentration gradient and $\boldsymbol{\sigma}$ is the thickness of the PA discriminating layer (~10^{-5} cm). Water flux, $\mathbf{J_B}$,

was calculated from the expression: $\mathbf{J_B = -C_{BM}D_{BM}V_{BM}(\Delta P - \Delta\pi)/(RT\sigma)}$, where $\mathbf{C_{BM}}$ is the membrane solvent concentration (12.3 M), $\mathbf{D_{BM}}$ is the modeled diffusivity (Table 26), $\mathbf{V_{BM}}$ is the solvent molar volume, $\mathbf{\Delta P - \Delta\pi}$ is the net pressure, **R** is the gas constant, and **T** is the temperature (300°K). The solute partition coefficient, $\mathbf{K_A}$, is perhaps the most critical factor and at this time can only be crudely estimated from experiment. Values for K_A were determined by rinsing membranes in ultrapure water following laboratory rejection tests using radiolabeled compounds. It was assumed that the 30-minute rejection test provided sufficient time for equilibration between feed and membrane solute concentrations, although this has not been experimentally verified. It was also assumed that the water rinse was adequate to extract unbound compound from the fabric backing and that remaining label was evenly distributed throughout the polysulfone support and the much thinner PA layer. Given the inherent weaknesses of the method and underlying assumptions, the K_A values must be viewed as conservative and very likely too high, possibly by orders of magnitude. It is perhaps noteworthy that K_A for PCE was ~24-fold higher than NDMA which is consistent with the lower water solubility (higher LogP) of PCE. Actual feed and permeate solute concentrations were used to calculate the solute gradient, ΔC_A, and a net driving pressure of 100 psi was assumed. Poor agreement was observed between theoretical and experimental fluxes, with modeled fluxes for NDMA and PCE ranging from ~4-6 logs higher than experimental values (Table 26). However, good agreement was observed between calculated water flux and that expected for a PA membrane. The principal reasons for overestimation of the solute fluxes are likely that (i) the modeled diffusion coefficients for the organics were too large since jump frequencies have not yet been determined, (ii) the K_A values were grossly overestimated, or (iii) both of the above.

3.2.4 Water and Membrane Interactions with the Organics

Although the mass of PCE (~165 amu) is greater than that of NDMA (~74 amu), this difference alone is insufficient to explain the discrepancy in their relative motilities in the PA membrane. Perhaps the simplest explanation for retarded PCE transport is that it interacts more with the membrane polymer. In order to determine if PCE was interacting

more strongly than NDMA with the membrane, a Tcl script was developed to extract the energy of interaction (i.e., "energy of association" or "binding energy") of the organic species with the *hydrated* membrane, i.e., with the water-membrane complex, at each step of the simulation playback. As illustrated in Fig. 41, the binding energies were computed by subtracting the component energies for (i) the water-membrane complex and (ii) the organic species from the geometry-optimized total system energy at specified simulation intervals (e.g., every 10 ps). The results, which are shown in Fig. 42, indicate that on average PCE was more strongly associated with the hydrated membrane complex than was NDMA, i.e., the association of PCE with the membrane-water complex was energetically more favorable. The greater binding of PCE to PA membranes observed in the laboratory RMP assay lends support to this hypothesis.

Based on these data, it was hypothesized that PCE should spend a larger proportion of time in closer proximity to PA membrane atoms than NDMA. Moreover, simulation playbacks suggested water molecules tended to associate more closely with NDMA than PCE, an observation that was not entirely unexpected given the ability of NDMA to hydrogen bond with water. To confirm this observation, a Tcl script was written to monitor the association of NDMA and PCE with nearby water molecules, as well as with membrane atoms. The method invoked a virtual sphere or "shell" around the organic solute. The shell radius was set at 4.0Å because it was felt this distance was a reasonable compromise between too few water molecules or membrane atoms to analyze and so many that subtle proximity effects (such as hydrogen bonding) would be averaged out by more distant molecules or atoms. Water molecules (COM coordinates) or polymer atoms (point coordinates) that penetrated the shell at each step of the simulation were monitored during playbacks. Data were collected for both of the membrane simulations discussed above, as well as for MD simulations in which the organic solutes were immersed in pure water (no membrane). The results of these analyses are summarized in Fig. 43 and Table 27, respectively. On average, over the course of the 200 ps membrane simulations, more than four times (4X) the number of water molecules entered the 4Å NDMA shell (ave=1.68±0.80, N=200) as compared to the PCE shell (ave=0.40±0.62, N=200). The mean distances to shell water molecules was nearly equal for both organic solutes.

Because the association energy of PCE for the hydrated membrane was lower than for NDMA (Fig. 40), it was anticipated that a correspondingly greater number of membrane atoms should be found within the PCE shell. However, the opposite situation was observed with >6X membrane atoms falling within the NDMA shell than the PCE shell. Compared to the membrane systems, greater numbers of water molecules associated with both NDMA and PCE in the pure-water simulations, presumably a result of higher water concentrations (55 M vs.12.3 M). However, in the pure-water simulations, there was a disproportionate increase in the number of water molecules associating with PCE (Table 27). Evidently both organic solutes compete for water and membrane interactions; however, the disproportionate increase in water association with PCE in the pure-water simulations argues for a greater interaction of PCE with membrane atoms. The relative lack of a hydration field around PCE might contribute to stronger long-range electrostatic interactions with membrane atoms. Since the membrane is essentially a condensed immobile phase, an increase in reactivity or affinity of an organic with the membrane would result in reduced transmigration (and thus higher observed rejection).

3.2.5 Idealized PA Membrane Pore Model to Estimate Solute-Membrane Interactions

According to the solution-diffusion theory (Lonsdale et. al., 1965), a first-principals calculation of organic solute fluxes requires knowledge of the solute diffusion (D) and membrane partition coefficients (K_a). The diffusion coefficient can be directly obtained from MD simulations from RMS displacement measurements of solute motions. However, computing the partition coefficient K_a is more problematic. A useful hypothesis is that solute partitioning into the PA film depends on the interaction potential of the solute with membrane and water atoms. Thus, stronger solute-membrane and weaker solute-water interactions should result in greater membrane partitioning. An idealized PA membrane pore model (as illustrated in Fig. 44) should allow rapid estimation and comparison of relative solute-membrane interaction potentials. The solute-membrane potential may be computed for different solutes introduced into the

hydrated pore space. Using this approach, modeled potentials were compared to experimental measurements of solute-membrane associations obtained by the RMP assay for NDMA, PCE and 17a-Estradiol (Fig. 45). Although these are limited results, they suggest a possible correlation between modeled compound-membrane potentials and experimental determinations of solute-membrane association. The database developed from the RMP assay and ANN modeling could provide a significant database of low molecular weight compounds with which to further test this approach.

.

4 CONCLUSIONS AND RECOMMENDATIONS

4.1 QSAR ANN Model Predictions of Compound-Membrane Interactions

4.1.1 Interaction of Organic Compounds with RO Membranes

According to the solution-diffusion theory (Wiesner et. al., 1996) solutes passing through RO membranes do so by entering the membrane matrix from the feed side, then driven by diffusive forces pass through the membrane matrix to the product side, and finally enter the product. The primary association with the membrane surface, the rate of passage through the membrane and final release from the product side of the membrane is governed by the intrinsic rate of diffusion of the solute through the membrane, plus the kinetics of adsorption and desorption to and from the membrane surfaces. These factors are in turn dependent on the nature of the solute and membrane chemistry; specifically on the molecular skeletal structure, distribution of electron density, nature of chemical constituents, chemical reactivity, and other physicochemical parameters.

The nature of solute chemistry is for the most part well understood; however, the nature of the membrane chemistry is more of a mystery. Although the basic composition of both CA and PA membrane polymers are known, fine details of molecular structure (degree of internal cross-linking, ionization, etc.) of membrane polymers *in situ* still are elusive. Measurements of zeta potential indicate that both PA and CA membranes surfaces carry negative charges at lightly acidic to neutral pH (5.5 – 7.5). Some of these negative charges are due to the presence of deprotonated carboxylate groups. However, because commercial RO membranes are often surface-modified by proprietary means, the precise nature of the surface chemistry of these negative groups remains largely unknown. These groups may significantly affect solute adsorption. Moreover, the precise chemical structure of the internal membrane matrix is almost a complete mystery. PA membranes are perhaps more enigmatic than CA membranes. The location of the permselective layer in the PA membranes remains controversial. These membranes

typically present a blebbed and convoluted surface in cross-section by electron microscopy (Fig. 28), and whether or not the thin (often <20 nanometer) membrane surface of the blebs or the PA-polysulfone interface is principally responsible for permselectivity is not known. The density of the permselective layer, therefore, is unclear. Also, the nature of the internal membrane chemistry is also largely unknown. In the case of PA membranes, the free carboxylate groups (those not involved in crosslinking) may or may not be protonated, a condition that materially affects the internal chemical milieu of the membrane.

Lack of complete understanding of the nature of the chemistry of RO membranes makes prediction of compound-membrane interactions by first principals difficult. For this reason, an empirical approach was undertaken in this study. In this project, organic compounds with disparate molecular properties served as "probes" to delineate the nature and extent of organic compound-membrane interactions. The results of these interactions served as exemplars that were used to train a neural network, which then could act as a silicon analog of the membrane system. From this model, compound chemical properties affecting compound-membrane interactions could be elucidated, and the behavior of other organic compounds predicted.

During membrane operations, compounds are transported to the feed side of the membrane by a combination of convective transport and diffusion. The vector of convective transport into the membrane, at 28 GFD water flux (nominal for PA membranes at 150 PSI in the study), was on the order of 13 microns sec^{-1}. It was presumed that convective flux was the dominant transport mechanism conveying solute molecules to the membrane surface during RO membrane operation.

The mass of solute compound transported to the membrane per unit area per unit time was defined as the feed flux (F-Flux). Molecules comprising the F-Flux were presumed to interact with the membrane in one of three ways (Fig. 1): they could fail to interact with the membrane and remain in the feed solution (R-Flux), they could bind onto or into the membrane (M-Flux), or they could pass completely through the membrane and enter

the product (P-Flux). The three membrane solute fluxes may be expressed as percentages of the feed flux. In this case, they represent the proportions of compound that interact with the membrane.

Rejection, in the classical sense, may be expressed as the difference between the relative mass of compound impinging on the membrane and that passing through the membrane, divided by the mass impinging on the membrane. This expression represents a combination of compound removal by rejection at the membrane surface and compound removal as a function of interaction with the membrane matrix, either by adsorption or absorption. Although initially nearly constant, rate of removal by adsorption or absorption mechanisms are expected to exhibit decay, such that as the membrane saturates it eventually offers no significant compound retardation. Thus, spike studies may show large percent rejections (based on P-Flux or traditional means of determining solute rejection), but tests involving longer exposures of the membrane that allow equilibration with the solute may ultimately result in poorer membrane performance. Rejection estimated by R-Flux, on the other hand, measures direct interaction of solutes with the membrane-water interface, and is expressed in relative proportion to the feed flux as described above. This is another means by which percent rejection may be estimated. In this case, a large value for rejection is indicative of poor interaction with or penetration through the membrane material, and likely provides a good indication of longer term membrane performance (apart from properties of the membrane surface or internal matrix changing significantly with time).

4.1.2 Use of QSAR Molecular Descriptors to Explain Compound Behavior

A QSAR analysis using basic molecular descriptors defining basic molecular structural and electronic features forms a powerful basis for predictive modeling because the fundamental nature of these numerical factors tends to reflect simpler molecular issues. Physicochemical properties of molecules (solubility, vapor pressure, melting point, solubility, etc.) are based on combinations of these more basic descriptors. Models using descriptors of molecular structure as a basis for predicting RO membrane performance

provide a means of analyzing the compound-membrane interactions in terms of fundamental molecular interactions. Such QSAR molecular descriptors have recently been used to evaluate molecular chemistry responsible for compound toxicity (Votano et. al., 2004 in press).

4.1.3 Use of Radiolabeled Tracers and the RMP Assay as a Rapid Method to Evaluate Compound Fate

The use of radiolabeled compounds in this study provided a means by which solutes could be traced as they interacted with RO membrane materials, and has been successfully been used by others to examine the fate of organic compounds interacting with RO and NF membranes (Schaffer et. al., 2003). Detection of the label is simple using liquid scintillation counting. Evaluation of organic compound mass in the product was completely straightforward, involving direct counting of recovered product. Determination of mass in the membrane was more challenging, but was achievable.

Measuring uptake of compounds by the membrane materials was complicated by the fact that it was impossible to determine the location of bound compound. RO membranes used in the study were commercial membranes, and therefore consisted of several different layers of dissimilar materials. In the case of the CA membrane, in addition to the permselective layer there was the support backing. The PA membrane consisted of a more complex sandwich, with the permselective PA layer resting on a microporous polysulfone layer, which in turn was supported on a polyester backing. Labeled compound could have bound entirely on the feed surface of the membrane, entirely inside the permselective PA layer, or if it penetrated this layer could have bound up in the polysulfone layer or the backing material. Therefore, for purposes of this study, the term "membrane" actually refers to the whole commercial product and not solely to the permselective layer.

Holdup of labeled compound in the bulk product water contained in the interstices of the polysulfone and backing layer was another potential source of experimental error. The thorough washing steps were meant to address at least some of this potential error.

Although it was not possible to directly evaluate the degree of holdup for all compounds, it was possible, (using urea) to indirectly determine that for the most part holdup error was probably small. This compound exhibited poor binding to the membrane even though a large amount passed into the product, and presumably would have filled the interstices along with the bulk water. In the case of the ESPA-2 membrane sample, the pore volume of the entire membrane coupon was estimated at ~3.9 μL (by gravimetric determination of dry and hydrated coupons). In this case, the product contained ~2,479,000 DPM/mL. If the washing steps removed none of this activity from the pore water in the coupon, the total counts remaining in the coupon due to product in the pore space would have amounted to ~9,700 DPM. The membrane activity recorded for ESPA-2 and urea was actually ~25,800 DPM, therefore the pore water holdup could only have accounted for ~38% or less of the observed mass in the membrane. As urea bound poorly to the membrane and was present at the highest concentration in the feed, this would have been a worst-case scenario. For compounds with far lower product concentrations and far higher membrane binding, the error due to pore water holdup was likely negligible.

The RMP pressure cell provided a convenient means for determination of compound-membrane interactions. The cell was easy to assemble, operate and clean, and up to 10 units could be set up on the bench in parallel. The small size of the test coupon presented a potential challenge, but randomization applied during swatch and coupon harvesting, replicate assay measurements and statistical filtering of results sufficiently addressed this issue. The study was somewhat hampered, however, by lack of availability of many of the organic compounds in radiolabeled form, and especially in ^{14}C radiolabeled form. Lack of the crossflow component typically resulted in underestimation of rejection compared with an RO block test unit, especially with the CA membrane, but the membrane performance with respect to the order of rejection (poor to good) of compounds observed in the block tester was paralleled by the RMP assay.

4.1.4 Application of ANN Modeling to Determine Salient Parameters Related to Compound Interactions with RO Membranes

Artificial neural networks (ANNs) are useful for providing explanatory models for myriad and diverse systems, from industrial processes control to stock market forecasting. Quite recently, ANN models have been constructed capable of successfully predicting organic compound toxicity (Votano et.al., 2004, in press).

In the last few years, commercial software packages combining ANN construction kits with GAs and providing a highly user-friendly interface (such as Neuralware's Neuralworks Predict) have been made available to the scientific community. The advent of faster algorithms and faster computer platforms have greatly facilitated application of these advanced mathematical tools to perform data mining and to model complex processes.

For their usefulness, ANN models do have some shortcomings. They depend, for accuracy, on sufficient exemplars being provided to adequately define the nature of the system being modeled. When the system being explained is relatively simple (may be explained by a small collection of continuous functions, e.g.), a small number of exemplars may be used to construct an adequate model, provided the exemplars represent well the vertices of the system. Often this is not the case; it is typical to employ hundreds to thousands of exemplars to construct ANN models describing natural systems. ANN models, while they may predict behavior of the system very well within the range of input parameters provided by the exemplars used in their construction, often are poorly able to extrapolate beyond the range of the exemplars (especially in complex systems). Therefore, it is important to define the input data well before attempting to construct predictive models using this technique.

4.1.5 Successful Construction of ANN Models Describing Compound-Membrane Interactions

In this study, there were at the outset a relatively large number of potential input parameters (QSAR descriptors) and a relatively small number of exemplars (QSAR descriptors linked to observed compound-membrane interactions) with which to build the models. Like many multivariate methods, choice of the input data set can be one of the most important steps in constructing a successful ANN model. Inclusion of a large number of weakly influential or non-influential inputs can greatly weaken the effectiveness of a multivariate model. However, the fact that only a limited number of exemplars were available with which to select inputs required a slightly modified approach in winnowing the input set prior to model construction.

Cluster analysis (dendrogram) was initially employed to reduce the number of QSAR descriptors. In this case, compound-membrane interactions were not considered; rather, the full set of compound data were used. QSAR descriptors were divided by type and clustered. From each of these clusters, a descriptor was chosen as a surrogate to represent the cluster. In this fashion, the original input set was winnowed down to 73 QSAR descriptors. From this point, compound-membrane interactions were considered in further winnowing the input set. A GA was used to reduce the QSAR descriptor set to a minimum of 33 inputs descriptive of compound-membrane interactions. ANN models were constructed from this pool of descriptors. In this fashion, a set of salient inputs was detected using the limited number of laboratory data available for the study.

The input sets converged upon by this construction technique present a good solution to describe each compound-membrane interaction problem; however, it may not be the sole solution. It should be noted that GAs and the algorithms used to construct the ANN models rely on random seeds, and thus there is a possibility that more than one set of inputs may adequately be employed. In order to help select the most “global” set of inputs, iterative applications of the GA were employed during the initial input screening

to identify and select the most commonly influential input parameters prior to ANN model construction.

The ANN models constructed in the study to describe P-, M- and R-Flux values determined by the RMP assay were in general fairly robust. They were able to explain with reasonable accuracy the variations in behavior observed amongst the surrogate compounds selected for the study.

It was possible to construct a reasonable "Universal" PA model by incorporating all of the data for each of the 4 PA membranes and adding PA membrane parameters to the potential input list. This model exhibited more noise than did the individual PA models, which is not unexpected as it represents the sum of the experimental noise in all 4 PA membrane models as well as incorporates the intrinsic differences in performance that occurred between membranes. It is notable that, for many compounds, it predicts the nature of compound-membrane interactions nearly as well as the individual PA models, and thus may at least serve as a "first cut" prediction of general PA membrane performance.

Interestingly, none of the membrane parameters survived in the final "Universal" PA models for P-Flux, M-Flux or R-Flux, even though some of these parameters represented several fold changes in value between membranes (Table 3). This does not at all indicate that membrane differences do not play a role in the variations observed in membrane performance; indeed, all of the individual PA membrane models exhibit differences in inclusion of molecular descriptors. However, it does indicate that the particular membrane properties selected for inclusion in the models were not nearly as influential as the compound molecular descriptors in predicting compound-membrane interactions.

4.1.6 QSAR Analysis – Relating Descriptors to Compound-Membrane Interactions

Figure 26 shows a composite of the QSAR molecular descriptors that the ANN models associated with each of the basic compound-membrane interactions (P-Flux, M-Flux and R-Flux) defined in the study.

Analysis of the parameters included in each of the models and the direction and magnitude of their influence (sensitivity analysis) gives some general insight as to the possible molecular mechanisms involved in the compound-membrane interactions observed in the study. It would be expected that differences would be seen between membrane types with completely disparate chemistries (PA vs CA), and indeed this was observed. Although none of the PA membrane models utilized exactly the same QSAR descriptor input set, some themes could be noted amongst the descriptors associated with each type of compound-membrane interaction (P-, M- or R-Flux).

If the molecular descriptors are considered in broader categories related to charge/polarity issues, molecular complexity, hydrophobicity and hydrogen bonding, then some similarities may be noted amongst the different membrane models. In many cases, the direction of relationships commonly occurring in the R-Flux and M-Flux models show reversed signs, indicating the inverse relationship possible between these interactions (molecular mechanisms favoring strong membrane surface binding, for example, would also favor reduced release of compounds from the membrane surface to the feed).

Charge and polarity descriptors were very much represented as inputs in all of the models, indicating that these molecular parameters were very much involved in compound-membrane interactions. This is not at all an unexpected result, as the literature already suggests that this should indeed be the case (Kosutic et. al., 2002; Fang et. al., 1976; Koyama et. al., 1982; Schafer et. al., 2003). In the case of the M-Flux and R-Flux, the Gmin was commonly selected as by the PA membranes (and the "Universal"

PA models). This molecular descriptor indicates the minimum atom E-state in the compounds. This value is related to how electrophilic the atom is. Electrophilic atoms participate in chemical bonding interactions, including hydrogen bonding. In this case, the M-Flux (membrane association) was relatively strongly positively associated with Gmin values, while the R-Flux was strongly negatively associated with Gmin. This suggests that compounds bearing more reactive atoms tended to interact more strongly with PA membranes (were less likely to be rejected into the feed).

Descriptors of electrical dipole magnitude (P, Py and Q) were observed in several of the PA models. In general, indications were that the greater the separation of charge across the molecule, the less likely the compound was found to associate with the PA membranes (and found to remain in the feed). Compounds passing through the PA membranes were favored by increased dipole separation in the direction of the molecular Y-axis. The CA membrane model presented a more confusing relationship, however. The Q sensitivity index was negative for R-Flux (increased charge separation, increased R-Flux), but P was strongly positive for the M-Flux, indicating that as dipole magnitude increased, the compounds associated more strongly with CA (which indicates increased polarity should favor *decreased* R-Flux).

Hydrogen bonding acceptor density (numHBa) was also commonly related to compound-membrane interactions in the PA membranes (included in 3 of 4 models). The number of hydrogen bond acceptors in compounds was typically positively associated with M-Flux (and inversely associated with R-Flux) in the PA membranes. The "Universal" PA models also shared this relationship. In addition, this descriptor also appeared as an input in the P-Flux models for PA. Hydrogen bonding may well facilitate interactions between compounds and the membrane (at least with PA), and in addition, facilitate transport through the membrane as well.

Hydrophobic/hydrophilic interactions (LogP) appeared to be important in determining P-Flux for compounds (noted both for PA and CA membranes, but stronger with CA), but was only included in a few of the M-Flux models. The direction of the sensitivity

index suggests that overall the more hydrophilic the compound, the more likely it will traverse the membrane. It may be that the hydrophobic compounds interact with the membrane, but the interaction is swamped by the magnitude of the charge interactions, and thus didn't appear in many of the M-Flux models. Where it does appear most strongly (the BW-30 model and "Universal PA" model), the sensitivity index is positive, suggesting PA membranes favor binding of the more hydrophobic compounds.

Molecular complexity, especially formula weight (fw) has been suggested as a key factor in determining rejection by RO membranes, and may be expected to be a major factor in determining membrane permeability (Schutte, 2003; Fang et. al., 1976; Kosutic et. al., 2002; Wiesner et. al., 1996; Ozaki et. al., 2002; Slater et. al., 1983). Complexity descriptors indeed appeared more often in the P-Flux models, but as a rule were not as universally represented as were the charge/polarity descriptors in the M- and R-Flux models. Most notably, the chi index xvpc4 appeared in 3 of the 4 PA models, as well as in the "Universal" PA model, and the sensitivity index analysis indicated moderate to strong (but variable) influence. With BW-30, ESPA-2 and the "Universal" PA models there was an overall negative influence between this descriptor and P-Flux, suggesting that as the complexity of the compounds increased (measured by patterns of adjacently amongst 5 atom groups, sensitive to heteroatom type), they were less able to pass through these membranes. However, effects of other descriptors related to molecular complexity were more variable. In general, though, it was suggested that the more complex molecules were less likely to pass through both PA and CA membranes. Formula weight did appear in the P-Flux model for the TFC-HR membrane; in this case, as expected, flux through the membrane was favored by less massive molecules.

4.1.7 Prediction of Compound-Membrane Interactions for Compounds in the Master Compound List

Outputs of the ANN models of P-, M- and R-Flux values for each of the 5 membranes and for the "Universal" PA model (Tables 16a through 21c) suggest that predictions of compound behavior were possible in over half to three-quarters of the cases (depending

on the membrane). Given the relatively small number of surrogate compounds available as exemplars, and the wide range of potential compound structures represented in the master compound list, this result is very encouraging. That the sum of the membrane fluxes in these cases closes a "virtual mass balance" and the ability to match rejection with at least a handful of laboratory experiments and field observations (Table 23) is also very encouraging. However, as the matrix employed in this study was relatively simple compared to field applications, much more data from the field will be needed to determine just how much the compound-membrane interactions elucidated in this study may be extrapolated to the field.

It is possible, within the context of the conditions established in the study, to make comparisons between performance of the RO membranes and to assess the relative ability of the membranes to deal with classes of organic compounds of public health concern presented in the master compound list (Tables 22a through 22e). The differences in rejection values based on the P-Flux and the R-Flux are especially illuminating, as instances where the R-Flux predictions of rejection are significantly lower than P-Flux predictions of rejection may signify compound removal by association with the membrane materials as opposed to a barrier mechanism. It should be noted that the ANN models may predict negative values of rejection based on R-Flux as a consequence of noise in the models; in these instances extremely strong association between the compound and the membrane may be inferred, and observed removal based on P-Flux is predicted to almost entirely be due to adsorptive or absorptive mechanisms.

The ANN predictions indicate that PA membranes, for the most part, appear to perform nearly equally well with respect to compound removal, although some exceptions may be found (dichloroacetic acid, molinate, methylene bromide, e.g.). Most of the pharmaceutical compounds were predicted to be very well rejected by P-Flux; however in many cases a part of compound removal may be attributed to membrane association (rejection based on R-Flux < rejection based on P-Flux). The steroid hormones (estrone and the estradiols, e.g.) are examples. The ANN models also predicted that many of the disinfection byproducts (DBPs) should be removed well based on P-Flux rejection;

however, as with the pharmaceuticals, in many cases a large part of their removal may be due to membrane association (dibromoacetonitrile, bromochloroacetonitrile, 1,1, dichloropropanone, e.g.). Metformin was predicted to be the most poorly rejected of the pharmaceuticals, and amongst the DBPs, bromochloromethane was predicted to be most poorly rejected.

Compounds associating strongly with the RO membranes may bind to the membrane surface, enter into and bind within the polymer matrix, or pass through to the product side of the permselective layer and bind to the polysulfone or to the nonwoven support layer. The location and intrinsic ability of the molecule to penetrate the membrane is unclear based solely on data provided by the RMP assay. For compounds poorly able to penetrate the membrane polymer matrix, surface binding may not lead to a serious deterioration in longer term rejection providing the compound does not significantly alter rejection properties of the permselective layer . Desorption and penetration of such a compound would be expected to be relatively slow. On the other hand, for compounds able to absorb into the membrane polymer matrix with facility, once the membrane concentration increases to saturation, desorption and subsequent penetration may result in a significant release of material into the product. Thus, although it is unclear from this study which specific mechanism is responsible for compound binding, any organics the study revealed were exhibiting rejection based largely on affinity to the RO membrane should be treated with some caution with regard to the ability of the membranes to exclude them over longer periods of time (Schafer et. al., 2003).

That “Universal” PA ANN flux models generally mirror performance of the individual PA models for a wide variety of compounds, may suggest commonness of mechanism with respect to compound-membrane interactions. Providing the PA membranes selected for this study are fairly representative of the range of membrane chemistries defining the commercial market, the “Universal” models can serve as generic surrogates to predict the gross ability of a PA RO membrane to reject specific organic compounds.

It was noted that the CA models generally predicted poorer rejection performance than the PA models; however, this result may have been somewhat artifactual, as comparisons between the performance of the RMP assay and actual membrane performance in the block tester indicated that the RMP assay may have significantly underestimated CA rejection. However, compounds exhibiting high rejection in the RMP assay are expected, for the most part, also to be rejected well in the field.

4.1.8 Improving the ANN QSAR Models

A number of gaps exist in the ANN models, presumably due to a lack of exemplars covering specific novel patterns of molecular properties that affect interactions between the compounds and RO membranes. Although model failure frequency was somewhat dependent on the membrane being emulated, the ANN models were completely unable to predict 15 compounds, most notably many of the N-nitroso compounds. In this case, the mechanism responsible for compound-membrane interactions were most likely significantly different from those exemplified by the surrogate compounds chosen for the study.

One way to improve the predictive ability of the ANN models would be to include one or more of these compounds in the surrogate database and reconstruct the models de novo. The use of QSAR descriptors known to be related to compound-membrane interactions may greatly enhance the ability to detect appropriate surrogates in this case. By taking an iterative approach from this point, the models may be developed in an "evolutionary" fashion, converging on a broadly predictive solution using a minimal set of exemplars. Future work would proceed in this direction.

4.1.9 Extending QSAR ANN Model Results to the Real World

Although some comparisons with laboratory and field data suggest that the predictions of these ANN models may have a good deal of merit, validation by more widespread comparisons between the model predictions and experience under field conditions is desirable. It is hoped that dissemination of the ANN models as well as data presented in

this study (tables of predicted performance data for the 5 membranes used in the study, and also of the "Universal" models for PA) to agencies possessing or collecting specific information regarding removal of these compounds by RO membranes will aid in model validation.

This study focused on fundamental relationships between several organic compounds of public health concern and several commercial RO membranes within the context of a simple experimental matrix. Actual matrices defining commercial RO feed water are far more complex, and certainly are capable of modifying the behavior of organic compounds and RO membranes (Chen et. al., 1997; Koops et. al., 2001). The temperature, pH, salinity and nature of the organic constituents in the feed may vary considerably from one plant location to another. Moreover, throughout the length of an RO purification plant from the feed inlet to the brine outlet, concentration of salts and organics may increase as much as 5-fold, so that membranes in different locations of the plant are exposed to different feed conditions. An understanding of how these changing conditions may modulate the interaction of organic compounds with the membranes would be a valuable modulation factor to include in membrane performance models. Future work is planned to help achieve this goal.

4.2 Description of Compound-Membrane Interactions Using Molecular Dynamics (MD) Simulations

Software has been successfully developed that automatically builds, geometry optimizes, analyzes, and stores fully-atomistic models of randomly crosslinked PA membranes using MPD and TMC monomers as building blocks. The program allows control over all membrane structural parameters including the membrane mass, degree of intra-chain crosslinking, and the net membrane charge. The program also provides the ability to automatically create a diverse population of PA membrane models whose properties vary incrementally or randomly over user-specified ranges. The models can be used in studies of membrane structure and dynamics and to gain insight into theoretical motifs of solute transport and surface biomolecular fouling.

Compared to experimental data, the calculated fluxes of NDMA and PCE through a model PA membrane proportionally represented laboratory observations (NDMA > PCE), though absolute values were overestimated by several logs. Short simulation times (200 ps) resulting in the inability to account for low-frequency solute jumps is likely to have contributed to the overestimation of compound diffusivities and fluxes. In addition, the water-membrane partition coefficients for the organics, K_A, which were derived from experimental data, were likely to have been overestimated as well, further compounding errors in the modeled diffusivities.

In spite of the problems outlined above regarding calculations of absolute solute fluxes, a comparison of the *relative* diffusivities of the organic solutes in the pure-water and membrane simulations suggested that PCE interacts more strongly than NDMA with the hydrated PA membrane, a factor which should retard its mobility in the membrane and increase its rejection compared to NDMA. In addition, both water and membrane atoms were found to generally associate more with NDMA than PCE. The reduced hydration sphere around PCE may result in less shielding of long-range electrostatic interactions with membrane atoms leading to diminished mobility compared to NDMA.

Future work, which may be carried out in collaboration with the recently established NSF "Center for Advanced Materials for Water Purification with Systems" at UIUC, could pursue several key issues that were not possible to address in this project. Key objectives undertaken in such future work would include:

1. Implementation of MD simulations up to 10 nanoseconds (ns) with larger membrane systems to better document and quantify solute diffusion behaviors, such as jump frequencies and magnitudes, under a variety of conditions. It is anticipated that a range of organic solutes would be explored in these studies along with a host of other variables, including the membrane density, degree of hydration, ion and pH effects, temperature, and pressure.

2. Establishment of a predictive relationship between one or more organic molecular descriptors and K_A, the equilibrium water-membrane partition coefficient. Reliable estimates of K_A are required to calculate solute fluxes in RO membranes from first principles. An attempt could be made to correlate a limited number of experimental K_A values with one or more easily determined molecular descriptors, such as LogP, solvation energies, or other parameters that can be readily computed from molecular simulations.

3. More detailed simulations and analyses of water interactions with the organic solutes and membrane atoms could be performed. Similarly, more in-depth analyses of organic compound interactions with membrane atoms are also required. Such interactions are critical to an explanation of differences in organic compound flux (and rejection) by RO membranes. Moreover, greater insights into these processes will enable more accurate and reliable predictions of the transport behaviors of unknown trace organic compounds and facilitate the design of novel molecular architectures to enhance rejection.

5 LITERATURE CITED

Bharath, R.and Drosen, J. 1994. *Neural Network Computing*. Windcrest/McGraw-Hill, New York, New York.

Bicerano, J. 1996. *Prediction of Polymer Properties*. 528 pp. Marcel Dekker, Inc., New York.

Campbell, P., Srinivasan, R., Knoell, T., Phipps, D., Ishida, K., Safarik, J., Cormack, T. and H. Ridgway. 1999. Quantitative structure activity relationship (QSAR) analysis of surfactants influencing attachment of a *Mycobacterium* species to cellulose acetate and aromatic polyamide reverse osmosis membranes. Biotechnology and Bioengineering 64, 527-544.

Carroll, F. I., Mascarella, S.W., Kuzemko, M.A., Gao, Y., Abraham, P., Lewin, A.H., Boja, J.W. and M.J. Kuhar. 1994. Synthesis, ligand binding, and QSAR (CoMFA and Classical) study of 3.beta.-(3'-substituted phenyl) tropane-2.beta.-carboxylic acid methyl esters. Journal of Medicinal Chemistry. 37: 2865-2873.

Chen, S-S, Taylor, J.S., Norris, C.D. and J.A.M.H. Hofman. Flat sheet for pesticide removal by varying RO/NF membrane. Membrane Technology Conference Proceedings, American Water Works Association, New Orleans, LA. 1997.

Drewes, J.E., Heberer, T. and K. Reddersen. 2002. Removal of pharmaceuticals during conventional wastewater treatment, advanced membrane treatment and soil-aquifer treatment. ACWA Xenobiotics Workshop. Sept. 19, 2002.

Fang, H.H.P. and E.S.K. Chian. 1975. Removal of alcohols, amines and aliphatic acids in aqueous solution by NS-100 membrane. Journal of Applied Polymer Science. 19(5):1347-1358.

Fang, H.H.P. and E.S.K. Chian. 1976. Reverse Osmosis Separation of Polar Organic Compounds in Aqueous Solution. Environmental Science and Technology. 10(4):364-369.

Freger, V. 2003. Nano-scale heterogeneity of polyamide membrane formed by interfacial polymerization. Langmuir 19:4791-4797.

Gusev, A.A., Mueller-Plathe, F., van Gunsteren, W.F. and U.W. Suter. 1994. Dynamics of small molecules in bulk polymers. Advances in Polymer Science. 209-246.

Hileman, B. 2001. Troubled Waters: EPA, USGS try to quantify prevalence, risks of compounds from drugs, personal care products. Chemical and Engineering Technology. 79:31-33.

Huang, J., Haruhiko, O., and Y. Negishi. 1993. Studies on reverse osmosis separation of aqueous solutions of low molecular weight organics by cellulose acetate derivative membranes. Membrane 18:285-292.

Kilduff, J. E., Mattaraj, S., Pieracci, J. P. and G. Belfort. 2000. Photochemical modification of poly(ether sulfone) and sulfonated poly(sulfone) nanofiltration membranes for control of fouling by natural organic matter. Desalination 132:133-142.

Kimura, K., Amy, G., Drewes, J. and Y. Watanabe. 2003. Adsorption of hydrophobic compounds onto NF/RO membranes: an artifact leading to overestimation of rejection. Journal of Membrane Science. 221:89-101.

Knopp, B. and U.W. Suter. 1997a. Atomistically modeling the chemical potential of small molecules in dense polymer microstructures. 1. Method. Macromolecules. 30:6107-6113.

Knopp, B. and U.W. Suter. 1997b. Atomistically modeling the chemical potential of small molecules in dense polymer microstructures. 2. Water sorption by polyamides. Macromolecules. 30:6114-6119.

Kolpin, D.W., Furlong, E.T., Meyer, M.T., Thurman, E.M., Zaugg, S.D., Barber, L.B. and H.T. Buxton. 2002. Pharmaceuticals, hormones, and other organic wastewater contaminants in U.S. streams, 1999-2000: A National Reconnaissance. Environmental Science and Technology. 36:1202-1211.

Koops, G.H., Yamada, S. and S.-I. Nakao. 2001. Separation of linear hydrocarbons and carboxylic acids from ethanol and hexane solutions by RO. Journal of Membrane Science. 189:241-254.

Kosutic, K. and B. Kunst. 2002. Removal of organics from aqueous solutions by commercial RO and NF membranes of characterized porosities. Desalination. 142:47-56.

Kotelyanskii, M.J., Wagner, N.J. and M.E. Paulaitis. 1998. Atomistic simulation of water and salt transport in the reverse osmosis membrane FT-30. Journal of Membrane Science 139:1-16.

Kotelyanskii, M. J., Wagner, N. J. and M.E. Paulaitis. 1999. Molecular dynamics simulation study of the mechanisms of water diffusion in a hydrated, amorphous polyamide. Computational and Theoretical Polymer Science. 9:301-306.

Koyama, K., Nishi, T., Hashida, I. and M. Nishimura. 1982. The rejection of polar organic solutes in aqueous solution by an interpolymer anionic composite RO membrane. Journal of Applied Polymer Science. 27:2845-2855.

Lipp, P., Gimbel, R. and F.H. Frimmel. 1994. Parameters influencing the rejection properties of FT30 membranes. Journal of Membrane Science. 95:185-197.

Lonsdale, H., Merten, U. and R. Riley. 1965. Journal of Applied Polymer Science. 9:1341-1362.

Matsuura, T. and S. Sourirajan. 1971. Physicochemical criteria for reverse osmosis separation of alcohols, phenols, and monocarboxylic acid in aqueous solutions using porous cellulose acetate membranes. Journal of Applied Polymer Science. 15(12):2905-2927.

Mitchell, M. 1998. *An Introduction to Genetic Algorithms*. The MIT Press, Cambridge, Massachusetts.

Mueller-Plathe, F. 1994. Permeation of polymers – a computational approach. Acta Polymerica. 45:259-293.

Nick, B. and U.W. Suter. 2001. Solubility of water in polymers - atomistic simulations. Computational and Theoretical Polymer Science. 11:49-55.

Ozaki, H. and L. Huafang. 2002. Rejection of organic compounds by ultra-low pressure reverse osmosis membrane. Water Research. 36:123-130.

Reinhard, M., Goodman, N. L., McCarty, P., and D. G. Argo. 1986. Removing trace organics by reverse osmosis using cellulose acetate and polyamide membranes. Journal of the American Water Works Association 78:163-174.

Riley, R.T., Kemppainen, B.W. and W.P. Norred. 1988. Quantitative tritium exchange of (/sup 3/H) aflatoxin B1 during penetration through isolated human skin. Biochemical and Biophysical Research Communications. 153(1).

Salveson, A.T., Requa, D.A., Whitley, R.D. and G. Tchobanoglous. 2000. Potable versus reclaimed water quality, regulatory issues, emerging concerns, in: Proceedings of the Annual Conference of Water Environment Federation, WEFTEC, Anaheim, CA

Schafer, A., Fane, A. G. and T. D. Waite. 2000. Fouling effects on rejection in the membrane filtration of natural waters. Desalination 131, 215-224.

Schafer, A.I., Nghiem, L.D. and T.D. Waite. 2003. Removal of the natural hormone estrone from aqueous solutions using nanofiltration and reverse osmosis. Environmental Science and Technology. 37:182-188.

Schutte, C.F. 2003. The rejection of specific organic compounds by reverse osmosis membranes. Desalination. 158:285-294.

Slater, C.S., Ahlert, R.C. and C.G. Uchrin. 1983. Applications of RO to complex industrial wastewater treatment. Desalination. 48:171-187.

Takeuchi, H. 1990. A jump motion of small molecules in glassy polymers: a molecular dynamics simulation. Journal of Chemical Physics. 93:2062-2067.

Takeuchi, H. and K. Okazaki. 1996. Dynamics of small molecules in a dense polymer matrix: molecular dynamics studies. Molecular Simulations 16:59-74.

Votano, J.R., Parham, M., Hall, L.H., Kier, L.B., Oloff, S., Tropsha, A., Xie, Q. and W. Tong. Three New Consensus QSAR Models for the Prediction of Ames Genotoxicity. Reprint Submitted to Mutagenesis, 2004.

Weisner, M. R. and C. A. Buckley. 1996. Principles of rejection in pressure-driven membrane processes. In Mallevialle, J., Odendaal, P. E. and M. R. Weisner (Eds.), *Water Treatment Membrane Processes*. pp. 5.1-5.17. McGraw-Hill, New York.

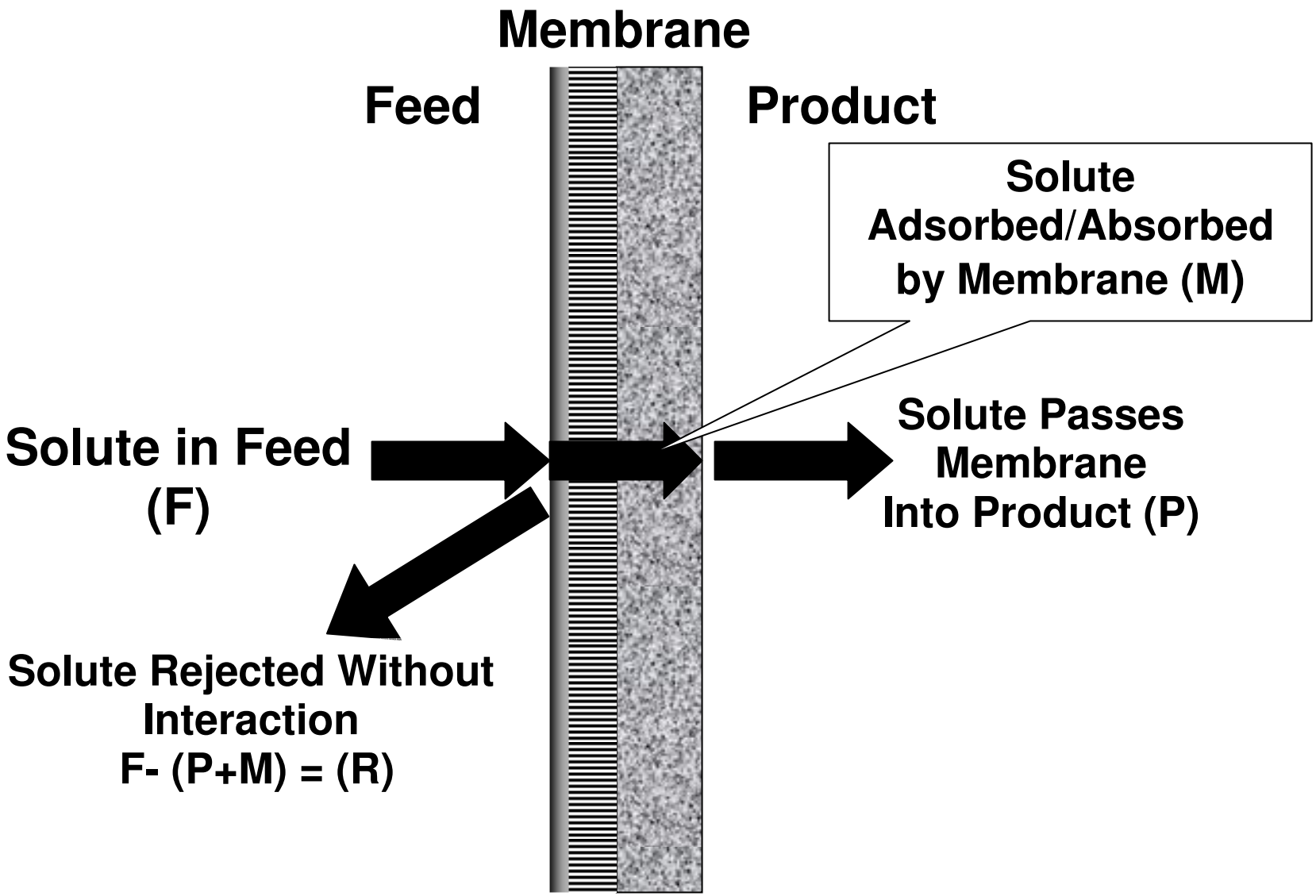

Figure 1. Interaction of a Compound (Solute) with a Membrane
A compound transported from the membrane surface from the feed can interact with the membrane in three different ways: it can adsorb or absorb into the membrane (M-Flux), it can pass entirely through the membrane into the product (P-Flux), or it can fail to interact with the membrane and remain in the feed (R-Flux).

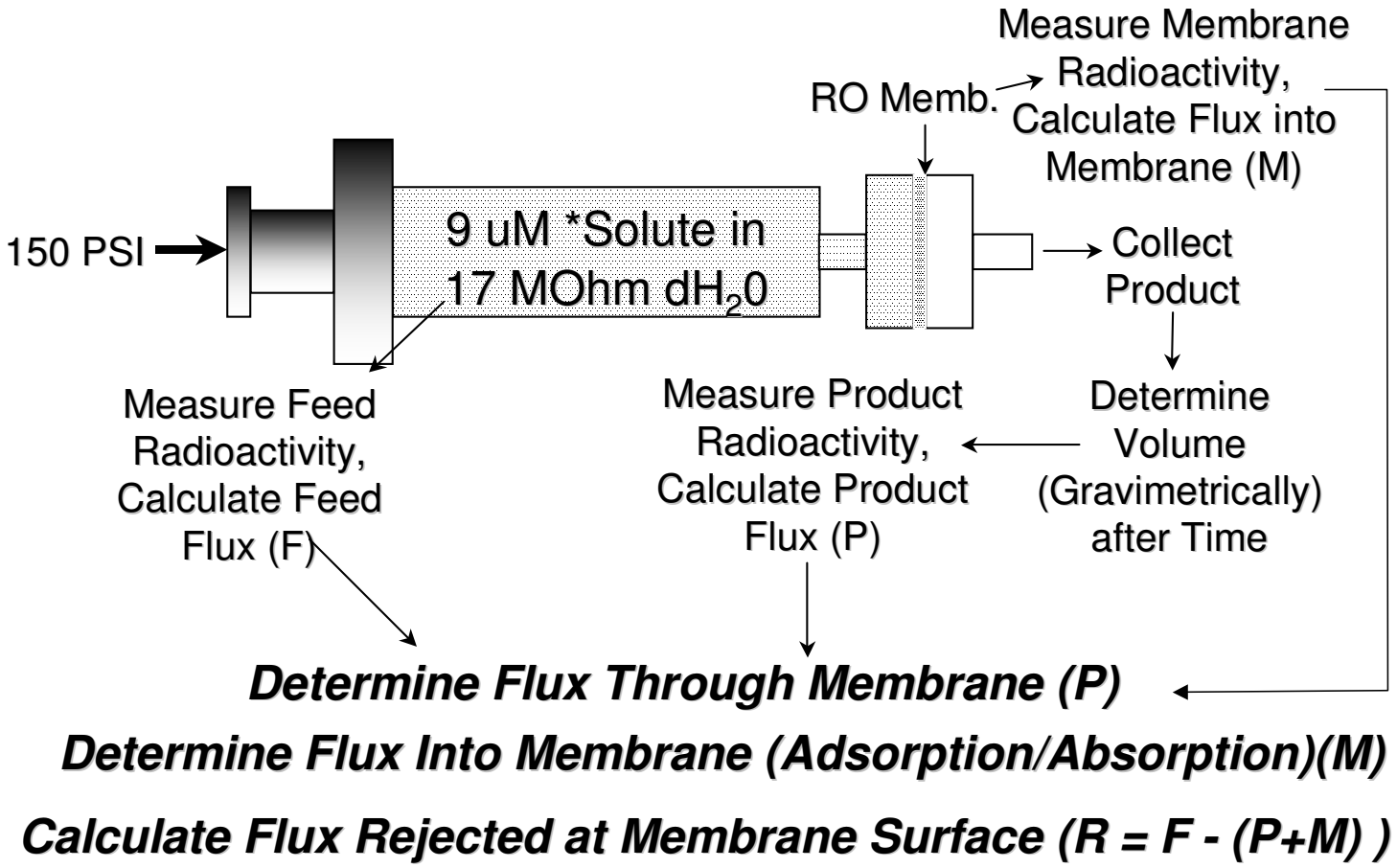

Figure 2. RMP Assay Diagram and Flux Determinations
The radiolabeled compound consisted of either ^{14}C or ^{3}H isotope. Radioactivity was measured using a scintillation counter. Feed activity of 100,000 to 1,000,000 DPM provided 2-4 logs of dynamic range (99 – 99.99% rejection).

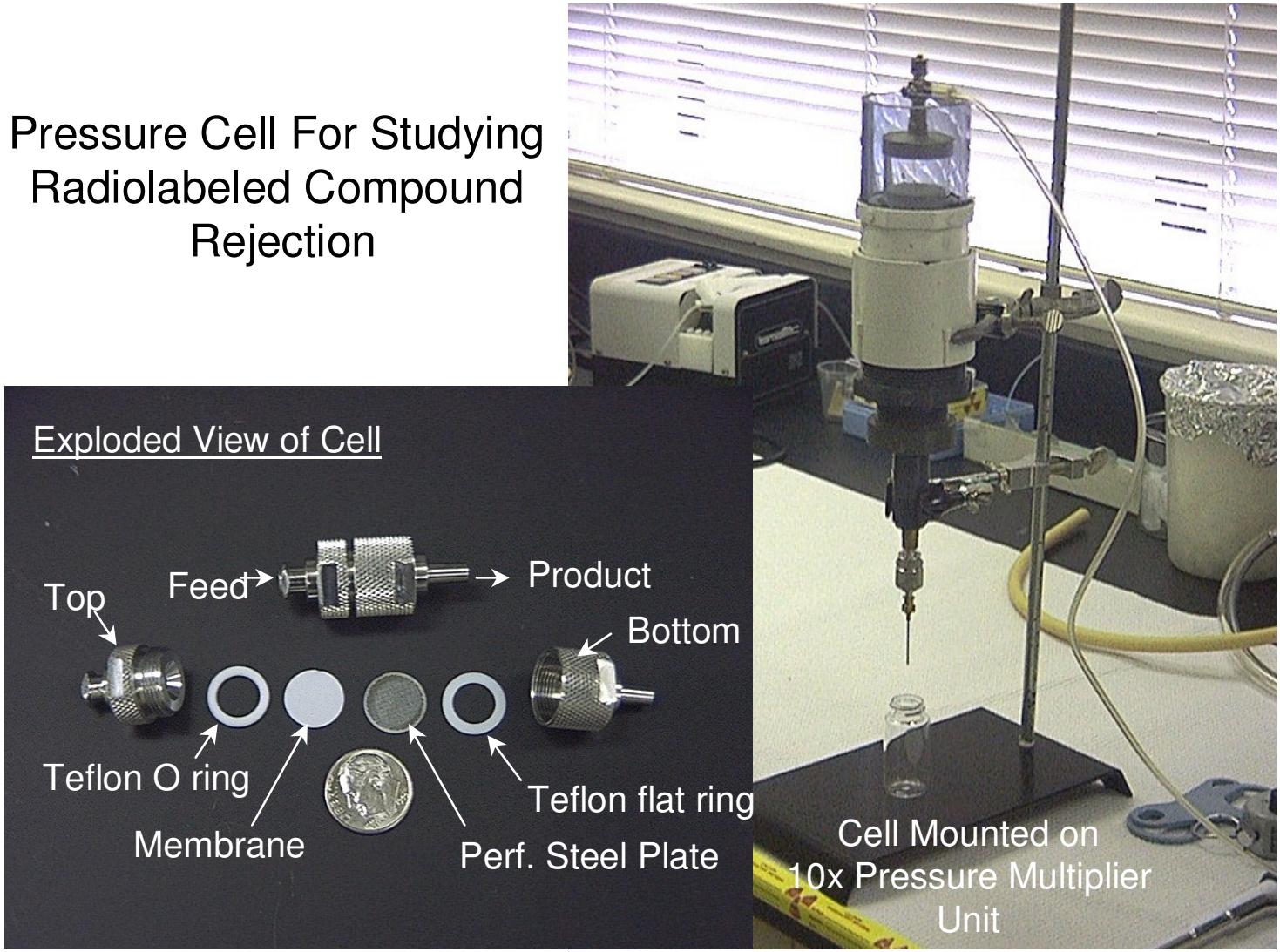

Figure 3. Apparatus used for the RMP Assay Method
The assembled stainless steel pressure cell is shown at the top of the left panel and in the right panel attached to the lower part of the syringe housing. A gas-tight syringe is used to generate the 150 psi of pressure needed to force water through the membrane.

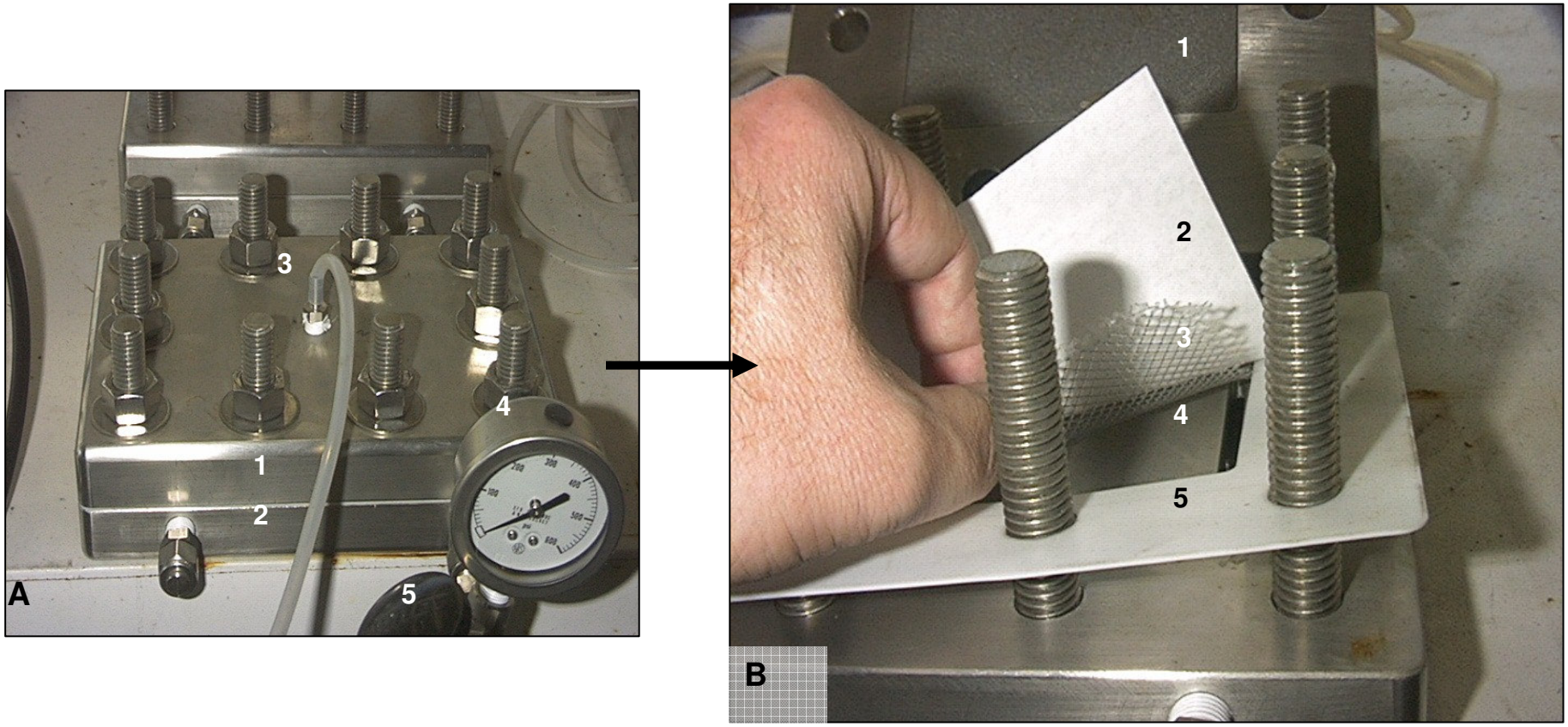

Figure 4. Cross-Flow Membrane Test Unit
This unit is used for membrane preparation (hydration under pressure) and validation of the RMP Assay. The assembled test unit is illustrated in (A) above and consists of a top plate (A1), bottom plate (A2), permeate tube with attached flexible tubing (A3), pressure gauge (A4) and a concentrate flow valve (A5). The disassembled test unit is illustrated in (B) and consists of a stainless steel permeate carrier (B1), membrane material (B2), feed spacer (B3), feed flow channel (B4) and teflon shim/gasket (B5).

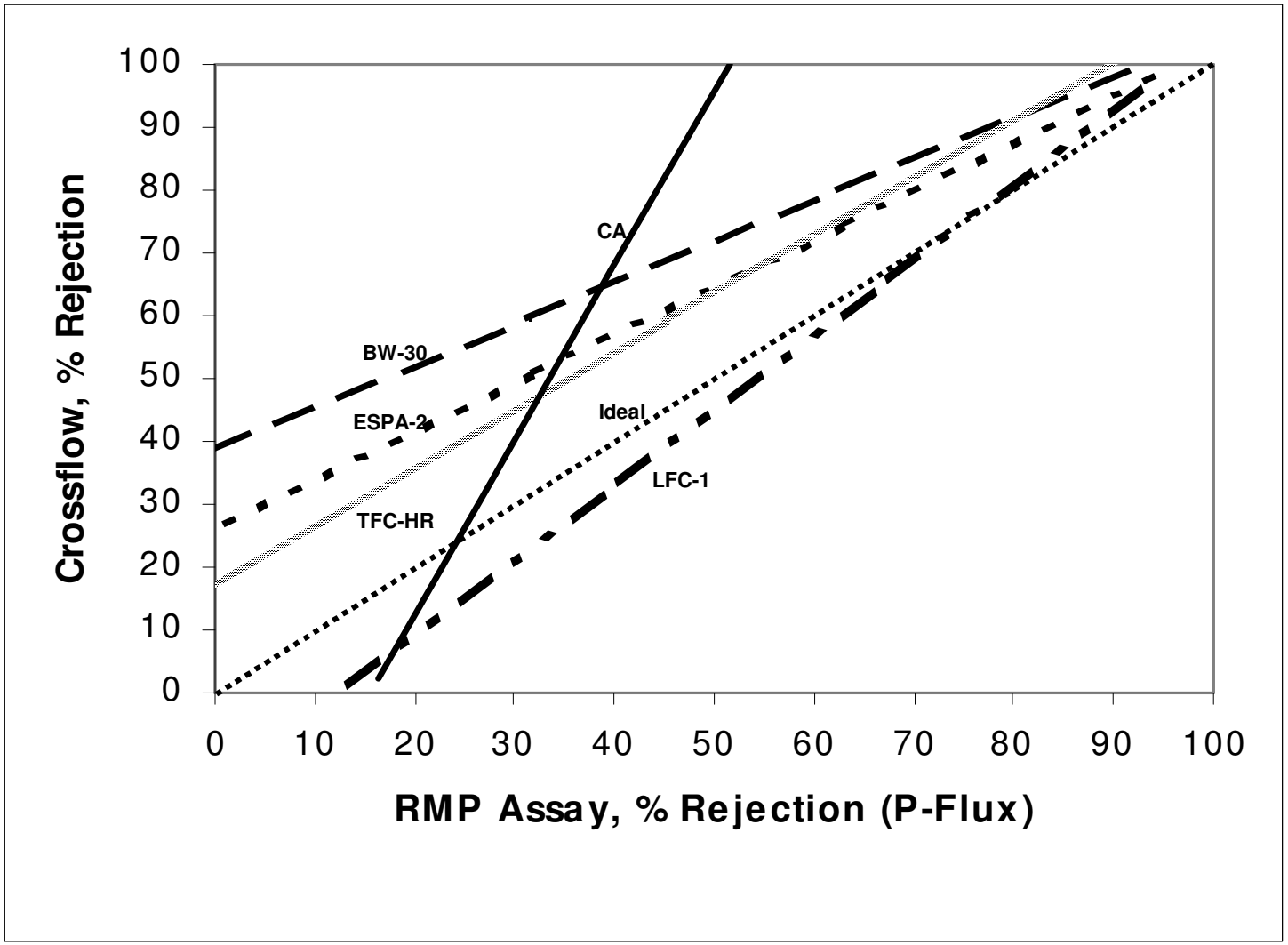

Figure 5. Comparison of RMP Assay to Crossflow Block Tester Performance
A standard linear regression model was performed for each RO membrane used in the study. There was an overall agreement in the comparative behavior of the two systems.

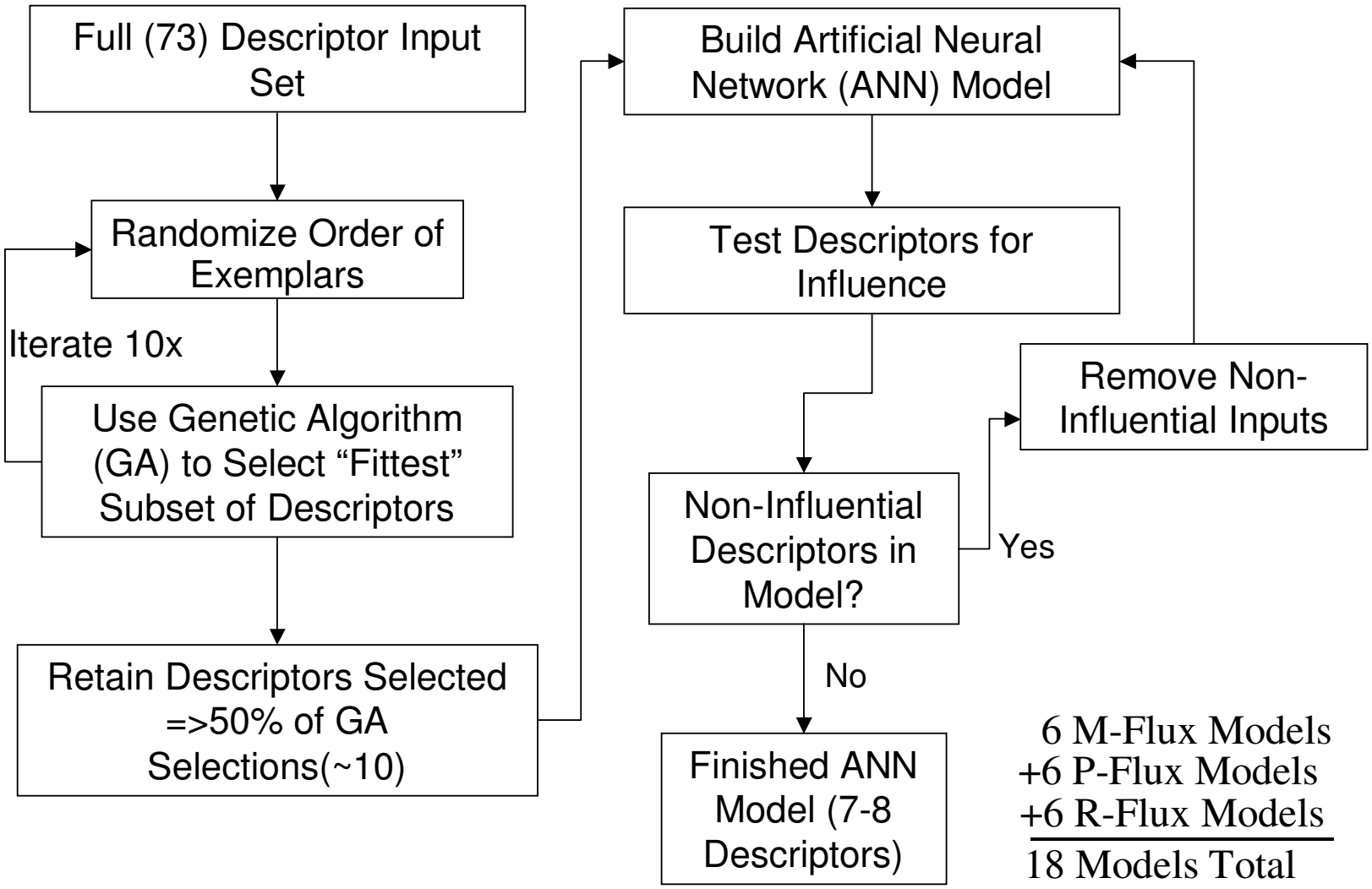

Figure 6. Selection of Molecular Descriptor Inputs and Construction of Artificial Neural Network (ANN) Models

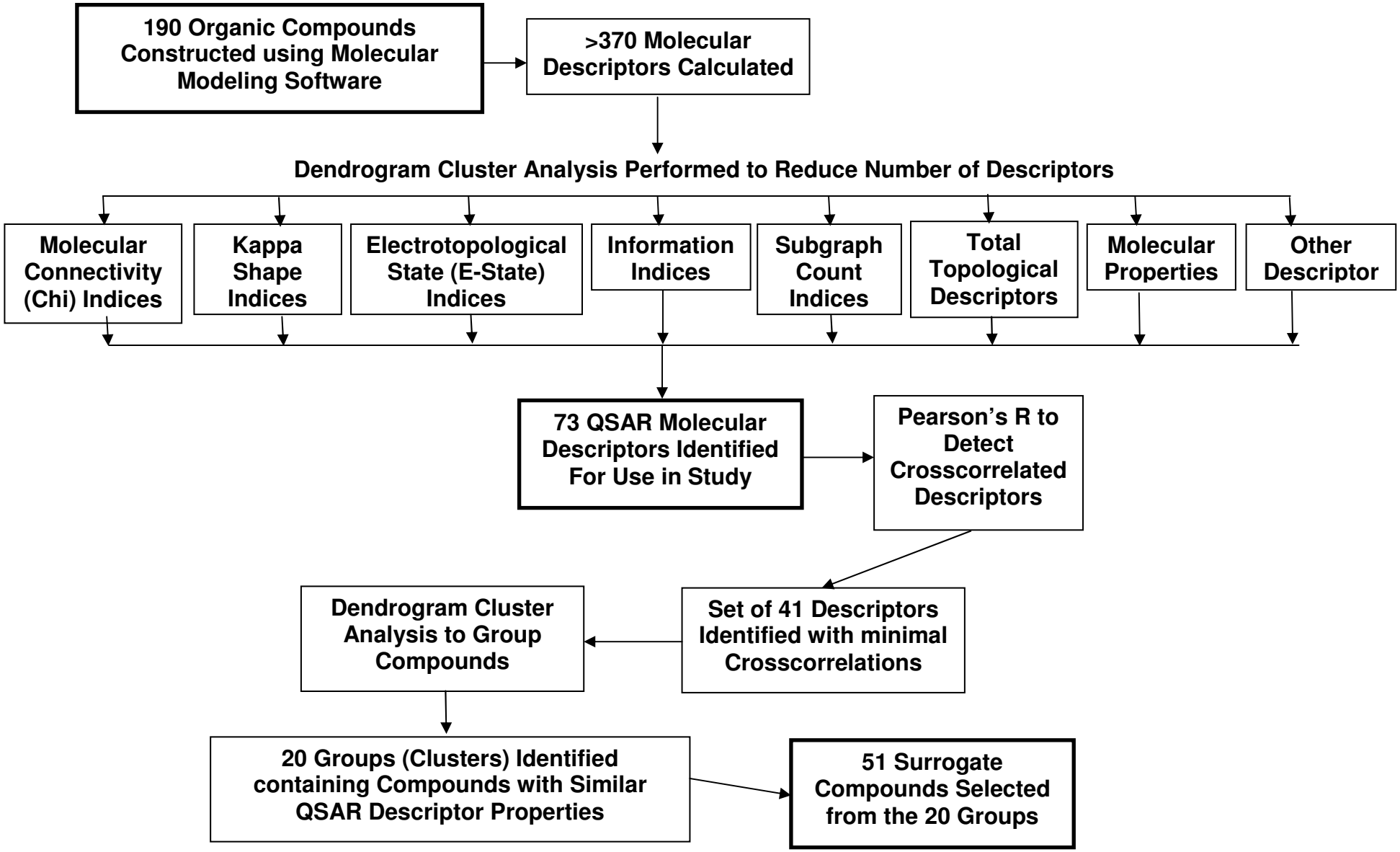

Figure 7. Selection of QSAR Molecular Descriptors and Surrogate Compounds

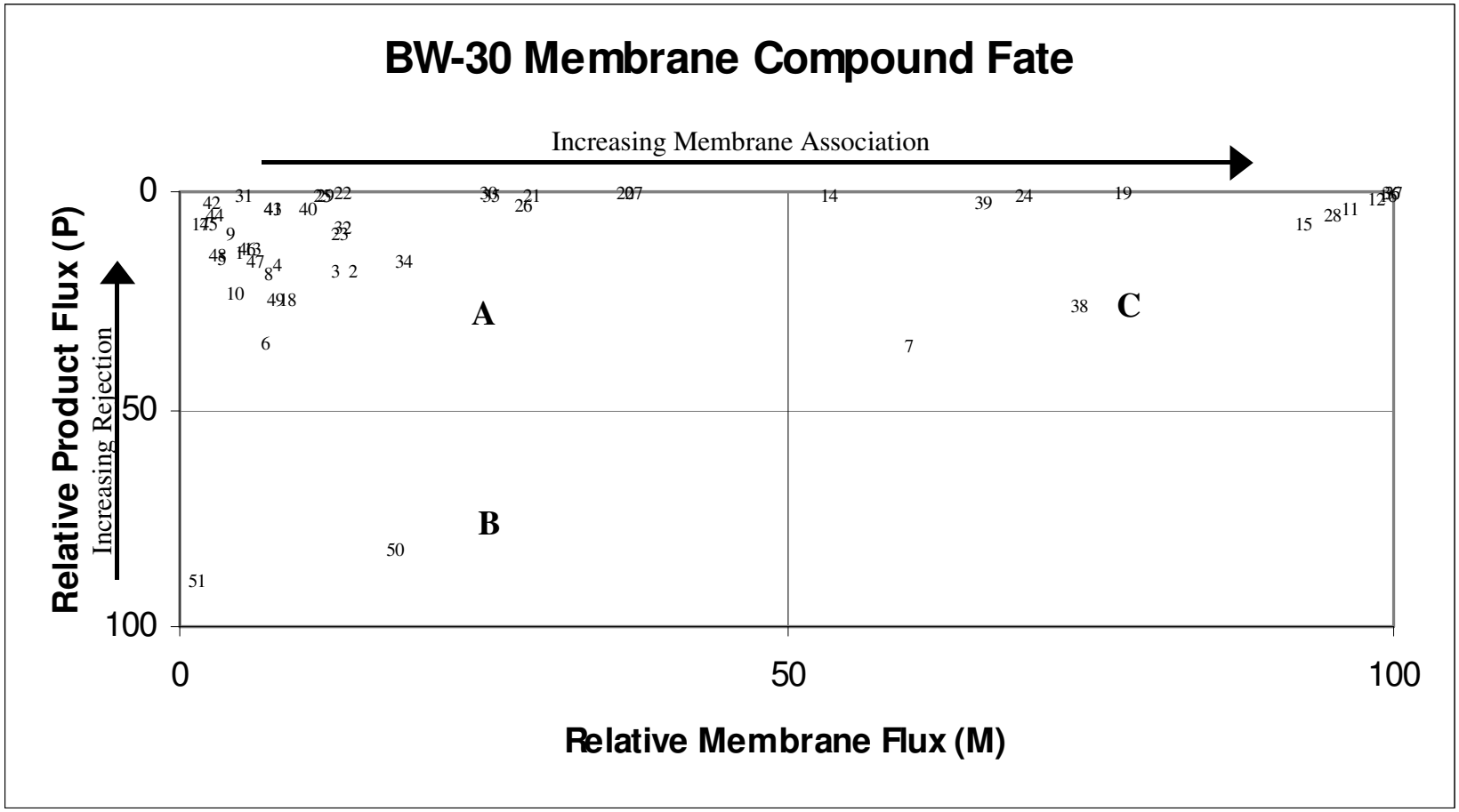

Figure 8a. Surrogate Compound Fate in BW-30 Membrane
Compounds in Quadrant "A" are well rejected; they neither associate with the membrane nor they pass through it. Compounds in Quadrant "B" are poorly rejected and do not interact well with the membrane. Compounds in Quadrant "C" are initially well rejected; however, they strongly associate with the membrane, so their rejection is largely due to membrane uptake. Numbers in the graph correspond to compounds listed in Figs. 8b and 8c.

ID Number	Compound	QSAR Cluster	M-Flux	P-Flux	R-Flux
1	Alanine	1	4.84	13.62	81.54
2	Caffeine	1	14.07	17.86	68.07
3	Cysteine	1	12.61	17.78	69.61
4	Dichloroacetic Acid	1	7.83	16.48	75.70
5	Glycine	1	3.37	14.88	81.74
6	N-dimethylamine	1	6.88	34.73	58.38
7	Phenol	1	59.99	35.43	4.58
8	t Butyl Alcohol	1	7.11	18.40	74.48
9	Threonine	1	4.04	9.23	86.74
10	Valine	1	4.58	22.95	72.46
11	Ethylbenzene	2	96.45	3.55	0.00
12	Toluene	2	98.49	1.51	0.00
13	1,4 Dichlorophenoxyacetic Acid	3	5.99	13.26	80.76
14	2,3,4,5,6 Pentachlorophenol	3	53.42	0.43	46.15
15	4,6 Dichlorophenol	3	92.59	7.41	0.00
16	Nitrobenzene	3	99.62	0.38	0.00
17	Phthalic Anhydride	3	1.68	6.84	91.48
18	Trichloroacetic Acid	3	8.83	24.37	66.80
19	17a Estradiol	4	77.59	0.19	22.22
20	4 Nonylphenol	4	36.64	0.30	63.06
21	beta Sitostanol n Hydrate	4	28.93	0.47	70.59
22	Cholesterol	4	13.39	0.07	86.54
23	Codeine	4	13.11	9.43	77.46
24	Estrone	4	69.61	0.62	29.77
25	Testosterone	4	11.65	0.94	87.41

Figure 8b. Surrogate Compound Fate in BW-30 Membrane
The ID number corresponds to numbers in Fig. 8a. Relative P, M, R fluxes for surrogate compounds are shown. Cluster numbers indicate compounds with similar molecular properties based on QSAR molecular descriptors.

ID Number	Compound	QSAR Cluster	M-Flux	P-Flux	R-Flux
26	Bisphenol	5	28.34	3.11	68.55
27	Diethylstilbestrol	5	37.33	0.09	62.58
28	2,4 Dinitrotoluene	6	94.94	5.06	0.00
29	methyl parathion	8	12.00	0.97	87.03
30	Progesterone	8	25.33	0.04	74.64
31	2-chloro-2'-6'-diethyl-N-methoxymethyl-acetanilide (Alachlor)	9	5.20	0.42	94.38
32	Cimetidine	9	13.37	7.75	78.88
33	Diethylphthalate	9	37.02	6.81	56.16
34	Ibuprofen	9	18.36	16.15	65.49
35	Chlorpyrifos	10	25.68	0.81	73.50
36	Phenanthrene	12	99.71	0.28	0.00
37	1,1,2,2, Tetrachloroethylene (PCE)	13	99.95	0.05	0.00
38	Benzene	13	74.01	25.99	0.00
39	Lindane	13	66.26	2.36	31.38
40	Doxycycline	15	10.54	3.26	86.21
41	Tetracycline	15	7.69	3.43	88.88
42	Ciprofloxacin	16	2.67	2.08	95.24
43	Erythromycin	16	7.66	3.77	88.56
44	Ethylenediaminetetraacetic Acid (EDTA)	18	2.98	5.31	91.72
45	Asparagine	N/A	2.37	6.93	90.70
46	Aspartic Acid	N/A	5.54	12.60	81.86
47	Histidine	N/A	6.22	16.17	77.61
48	Lysine	N/A	3.11	14.04	82.85
49	Methionine	N/A	7.93	24.13	67.94
50	N-nitroso dimethyl amine (NDMA)	N/A	17.66	82.34	0.00
51	Urea	N/A	1.40	89.37	9.23

Figure 8c. Surrogate Compound Fate in BW-30 Membrane. (Continued – See Fig. 8b)

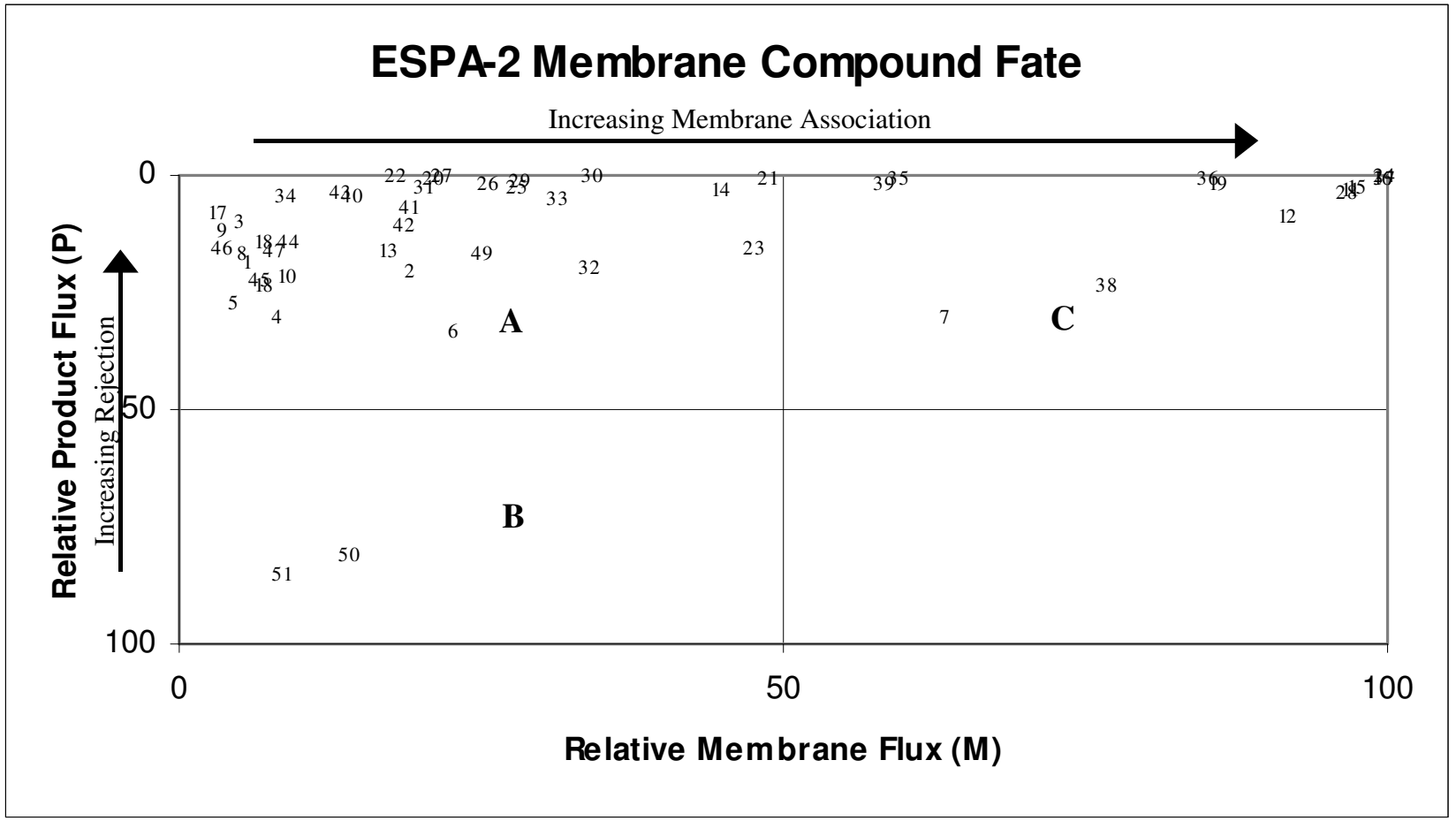

Figure 9a. Surrogate Compound Fate in ESPA-2 Membrane
Compounds in Quadrant "A" are well rejected; they neither associate with the membrane nor they pass through it. Compounds in Quadrant "B" are poorly rejected and do not interact well with the membrane. Compounds in Quadrant "C" are initially well rejected; however, they strongly associate with the membrane, so their rejection is largely due to membrane uptake. Numbers in the graph correspond to compounds listed in Figs. 9b and 9c.

ID Number	Compound	QSAR Cluster	M-Flux	P-Flux	R-Flux
1	Alanine	1	5.61	18.54	75.85
2	Caffeine	1	19.13	20.62	60.25
3	Cysteine	1	4.98	10.06	84.96
4	Dichloroacetic Acid	1	8.16	30.30	61.55
5	Glycine	1	4.57	26.92	68.52
6	N-dimethylamine	1	22.79	33.12	44.09
7	Phenol	1	63.34	30.36	6.30
8	t Butyl Alcohol	1	5.17	16.96	77.86
9	Threonine	1	3.57	11.80	84.62
10	Valine	1	8.78	21.48	69.74
11	Ethylbenzene	2	96.81	3.19	0.00
12	Toluene	2	91.63	8.37	0.00
13	1,4 Dichlorophenoxyacetic Acid	3	17.28	15.84	66.87
14	2,3,4,5,6 Pentachlorophenol	3	44.66	2.87	52.48
15	4,6 Dichlorophenol	3	97.35	2.65	0.00
16	Nitrobenzene	3	99.50	0.50	0.00
17	Phthalic Anhydride	3	3.05	8.02	88.93
18	Trichloroacetic Acid	3	6.90	23.32	69.78
19	17a Estradiol	4	85.93	1.65	12.42
20	4 Nonylphenol	4	21.02	0.33	78.65
21	beta Sitostanol n Hydrate	4	48.57	0.53	50.90
22	Cholesterol	4	17.87	0.06	82.06
23	Codeine	4	47.68	15.42	36.90
24	Estrone	4	99.78	0.22	0.00
25	Testosterone	4	27.93	2.34	69.73

Figure 9b. Surrogate Compound Fate in ESPA-2 Membrane
The ID number corresponds to numbers in Fig. 9a. Relative P, M, R fluxes for surrogate compounds are shown. Cluster numbers indicate compounds with similar molecular properties based on QSAR molecular descriptors.

ID Number	Compound	QSAR Cluster	M-Flux	P-Flux	R-Flux
26	Bisphenol	5	25.50	1.88	72.62
27	Diethylstilbestrol	5	21.66	0.09	78.25
28	2,4 Dinitrotoluene	6	96.55	3.45	0.00
29	methyl parathion	8	28.17	1.54	70.29
30	Progesterone	8	34.21	0.25	65.54
31	2-chloro-2'-6'-diethyl-N-methoxymethyl-acetanilide (Alachlor)	9	19.99	2.33	77.67
32	Cimetidine	9	34.06	19.61	46.33
33	Diethylphthalate	9	31.46	4.93	63.62
34	Ibuprofen	9	8.89	4.45	86.66
35	Chlorpyrifos	10	59.64	0.66	39.70
36	Phenanthrene	12	85.27	0.45	14.28
37	1,1,2,2, Tetrachloroethylene (PCE)	13	99.67	0.33	0.00
38	Benzene	13	76.68	23.32	0.00
39	Lindane	13	58.30	2.13	39.57
40	Doxycycline	15	14.46	4.37	81.17
41	Tetracycline	15	18.89	7.08	74.02
42	Ciprofloxacin	16	18.68	10.57	70.76
43	Erythromycin	16	13.32	3.86	82.82
44	Ethylenediaminetetraacetic Acid (EDTA)	18	9.07	14.29	76.64
45	Asparagine	N/A	6.72	22.01	71.27
46	Aspartic Acid	N/A	3.54	15.69	80.77
47	Histidine	N/A	7.91	16.02	76.07
48	Lysine	N/A	6.90	14.23	78.87
49	Methionine	N/A	25.10	16.74	58.17
50	N-nitroso dimethyl amine (NDMA)	N/A	14.08	80.76	5.16
51	Urea	N/A	8.29	85.11	6.59

Figure 9c. Surrogate Compound Fate in ESPA-2 Membrane. (Continued – See Fig. 9b)

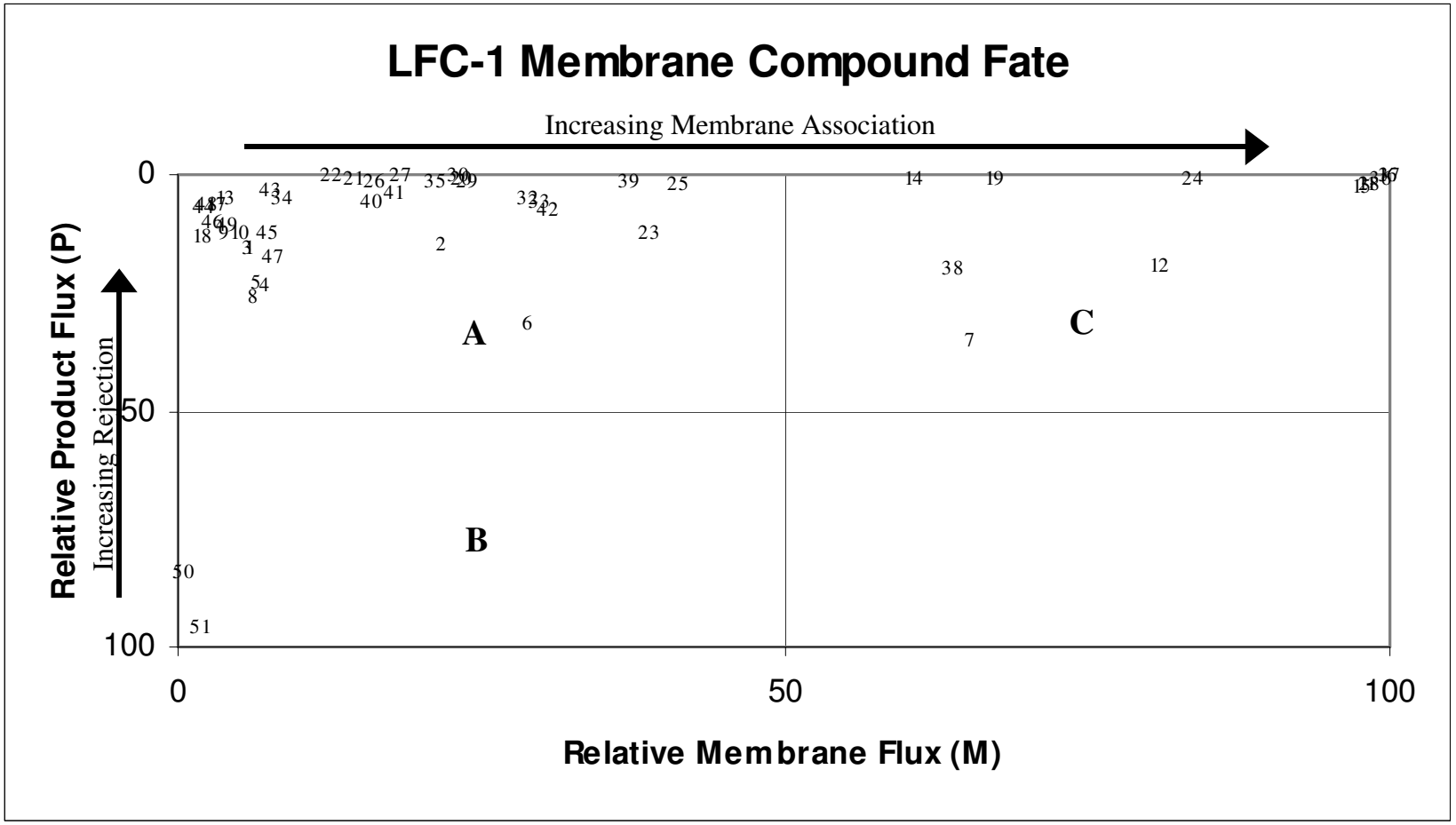

Figure 10a. Surrogate Compound Fate in LFC-1 Membrane
Compounds in Quadrant "A" are well rejected; they neither associate with the membrane nor they pass through it. Compounds in Quadrant "B" are poorly rejected and do not interact well with the membrane. Compounds in Quadrant "C" are initially well rejected; however, they strongly associate with the membrane, so their rejection is largely due to membrane uptake. Numbers in the graph correspond to compounds listed in Figs. 10b and 10c.

ID Number	Compound	QSAR Cluster	M-Flux	P-Flux	R-Flux
1	Alanine	1	5.77	15.45	78.77
2	Caffeine	1	21.78	14.62	63.61
3	Cysteine	1	5.77	15.45	78.77
4	Dichloroacetic Acid	1	7.12	23.43	69.45
5	Glycine	1	6.45	22.85	70.70
6	N-dimethylamine	1	28.80	31.30	39.90
7	Phenol	1	65.33	34.67	0.00
8	t Butyl Alcohol	1	6.18	25.89	67.93
9	Threonine	1	3.88	12.00	84.12
10	Valine	1	4.89	12.18	82.92
11	Ethylbenzene	2	98.09	1.91	0.00
12	Toluene	2	80.97	19.03	0.00
13	1,4 Dichlorophenoxyacetic Acid	3	3.92	4.76	91.32
14	2,3,4,5,6 Pentachlorophenol	3	60.72	0.69	38.59
15	4,6 Dichlorophenol	3	97.65	2.35	0.00
16	Nitrobenzene	3	99.71	0.29	0.00
17	Phthalic Anhydride	3	3.06	6.06	90.88
18	Trichloroacetic Acid	3	1.99	12.80	85.21
19	17a Estradiol	4	67.29	0.67	32.04
20	4 Nonylphenol	4	23.36	0.31	76.32
21	beta Sitostanol n Hydrate	4	14.30	0.47	85.23
22	Cholesterol	4	12.56	0.27	87.17
23	Codeine	4	38.88	12.07	49.06
24	Estrone	4	83.66	0.92	15.42
25	Testosterone	4	41.21	1.65	57.14

Figure 10b. Surrogate Compound Fate in LFC-1 Membrane
The ID number corresponds to numbers in Fig. 10a. Relative P, M, R fluxes for surrogate compounds are shown. Cluster numbers indicate compounds with similar molecular properties based on QSAR molecular descriptors.

ID Number	Compound	QSAR Cluster	M-Flux	P-Flux	R-Flux
26	Bisphenol	5	16.12	1.08	82.80
27	Diethylstilbestrol	5	18.39	0.19	81.42
28	2,4 Dinitrotoluene	6	98.31	1.69	0.00
29	methyl parathion	8	23.85	1.32	74.82
30	Progesterone	8	23.25	0.03	76.73
32	Cimetidine	9	28.99	5.19	65.82
33	Diethylphthalate	9	29.88	5.48	64.65
34	Ibuprofen	9	8.62	5.20	86.18
35	Chlorpyrifos	10	21.23	1.08	77.70
36	Phenanthrene	12	99.34	0.66	0.00
37	1,1,2,2, Tetrachloroethylene (PCE)	13	99.93	0.07	0.00
38	Benzene	13	64.01	19.46	16.54
39	Lindane	13	37.32	1.07	61.61
40	Doxycycline	15	15.95	5.33	78.71
41	Tetracycline	15	17.59	3.52	78.89
42	Ciprofloxacin	16	30.45	7.61	61.94
43	Erythromycin	16	7.58	2.99	89.43
44	Ethylenediaminetetraacetic Acid (EDTA)	18	2.12	6.69	91.20
45	Asparagine	N/A	7.41	12.01	80.58
46	Aspartic Acid	N/A	2.81	9.68	87.52
47	Histidine	N/A	7.98	17.34	74.68
48	Lysine	N/A	2.35	6.21	91.44
49	Methionine	N/A	4.14	10.25	85.60
50	N-nitroso dimethyl amine (NDMA)	N/A	0.53	84.23	15.25
51	Urea	N/A	1.66	95.48	2.86

Figure 10c. Surrogate Compound Fate in LFC-1 Membrane. (Continued – See Fig. 10b)

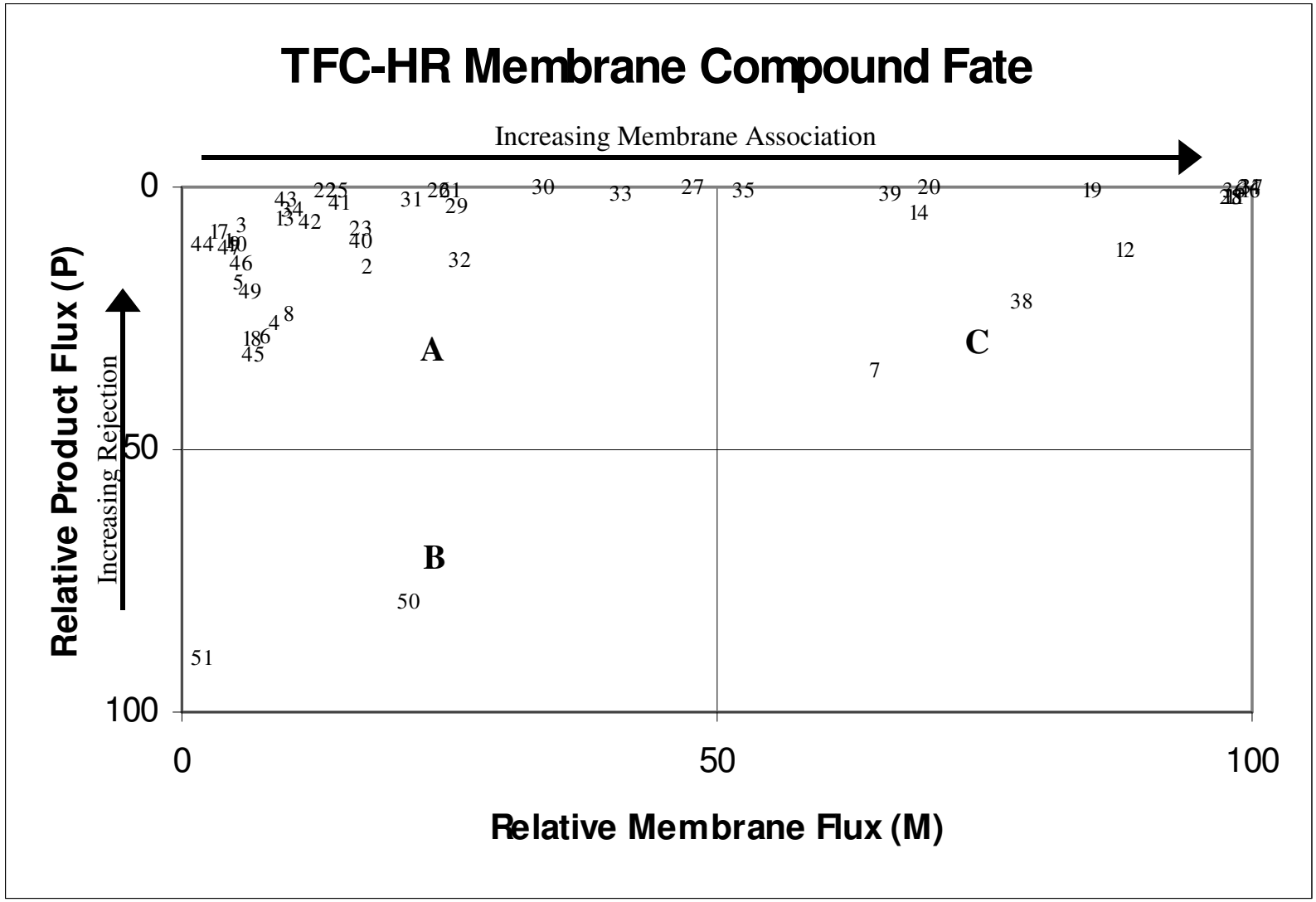

Figure 11a. Surrogate Compound Fate in TFC-HR Membrane
Compounds in Quadrant "A" are well rejected; they neither associate with the membrane nor they pass through it. Compounds in Quadrant "B" are poorly rejected and do not interact well with the membrane. Compounds in Quadrant "C" are initially well rejected; however, they strongly associate with the membrane, so their rejection is largely due to membrane uptake. Numbers in the graph correspond to compounds listed in Figs. 11b and 11c.

ID Number	Compound	QSAR Cluster	M-Flux	P-Flux	R-Flux
1	Alanine	1	4.16	10.20	85.64
2	Caffeine	1	17.38	14.78	67.84
3	Cysteine	1	5.68	7.02	87.30
4	Dichloroacetic Acid	1	8.78	25.82	65.41
5	Glycine	1	5.36	18.03	76.61
6	N-dimethylamine	1	7.89	28.58	63.53
7	Phenol	1	64.67	35.10	0.23
8	t Butyl Alcohol	1	10.10	23.94	65.95
9	Threonine	1	4.89	10.63	84.48
10	Valine	1	5.07	11.10	83.82
11	Ethylbenzene	2	98.39	1.61	0.00
12	Toluene	2	88.09	11.91	0.00
13	1,4 Dichlorophenoxyacetic Acid	3	9.60	5.97	84.43
14	2,3,4,5,6 Pentachlorophenol	3	68.69	5.08	26.23
15	4,6 Dichlorophenol	3	97.98	2.02	0.00
16	Nitrobenzene	3	99.64	0.36	0.00
17	Phthalic Anhydride	3	3.45	8.14	88.41
18	Trichloroacetic Acid	3	6.50	29.05	64.46
19	17a Estradiol	4	84.92	0.46	14.61
20	4 Nonylphenol	4	69.90	0.29	29.81
21	beta Sitostanol n Hydrate	4	24.75	0.43	74.82
22	Cholesterol	4	13.33	0.38	86.30
23	Codeine	4	16.76	7.66	75.59
24	Estrone	4	99.84	0.16	0.00
25	Testosterone	4	14.54	0.51	84.95

Figure 11b. Surrogate Compound Fate in TFC-HR Membrane
The ID number corresponds to numbers in Fig. 11a. Relative P, M, R fluxes for surrogate compounds are shown. Cluster numbers indicate compounds with similar molecular properties based on QSAR molecular descriptors.

ID Number	Compound	QSAR Cluster	M-Flux	P-Flux	R-Flux
26	Bisphenol	5	24.01	0.60	75.39
27	Diethylstilbestrol	5	47.75	0.12	52.14
28	2,4 Dinitrotoluene	6	98.06	1.94	0.00
29	methyl parathion	8	25.57	3.52	70.91
30	Progesterone	8	33.90	0.04	66.06
31	2-chloro-2'-6'-diethyl-N-methoxymethyl-acetanilide (Alachlor)	9	21.19	2.43	76.39
32	Cimetidine	9	26.06	13.96	59.98
33	Diethylphthalate	9	41.18	1.47	57.35
34	Ibuprofen	9	10.36	3.97	85.67
35	Chlorpyrifos	10	52.56	0.73	46.71
36	Phenanthrene	12	98.28	0.46	1.26
37	1,1,2,2, Tetrachloroethylene (PCE)	13	99.98	0.02	0.00
38	Benzene	13	78.59	21.41	0.00
39	Lindane	13	66.34	0.94	32.72
40	Doxycycline	15	16.74	10.24	73.03
41	Tetracycline	15	14.45	2.93	82.62
42	Ciprofloxacin	16	12.11	6.61	81.28
43	Erythromycin	16	9.85	2.53	87.61
44	Ethylenediaminetetraacetic Acid (EDTA)	18	2.03	11.10	86.87
45	Asparagine	N/A	6.59	31.86	61.55
46	Aspartic Acid	N/A	5.54	14.67	79.79
47	Histidine	N/A	4.57	11.68	83.76
48	Lysine	N/A	3.82	10.72	85.46
49	Methionine	N/A	6.49	19.96	73.55
50	N-nitroso dimethyl amine (NDMA)	N/A	21.33	78.67	0.00
51	Urea	N/A	1.74	90.01	8.25

Figure 11c. Surrogate Compound Fate in TFC-HR Membrane. (Continued – See Fig. 11b)

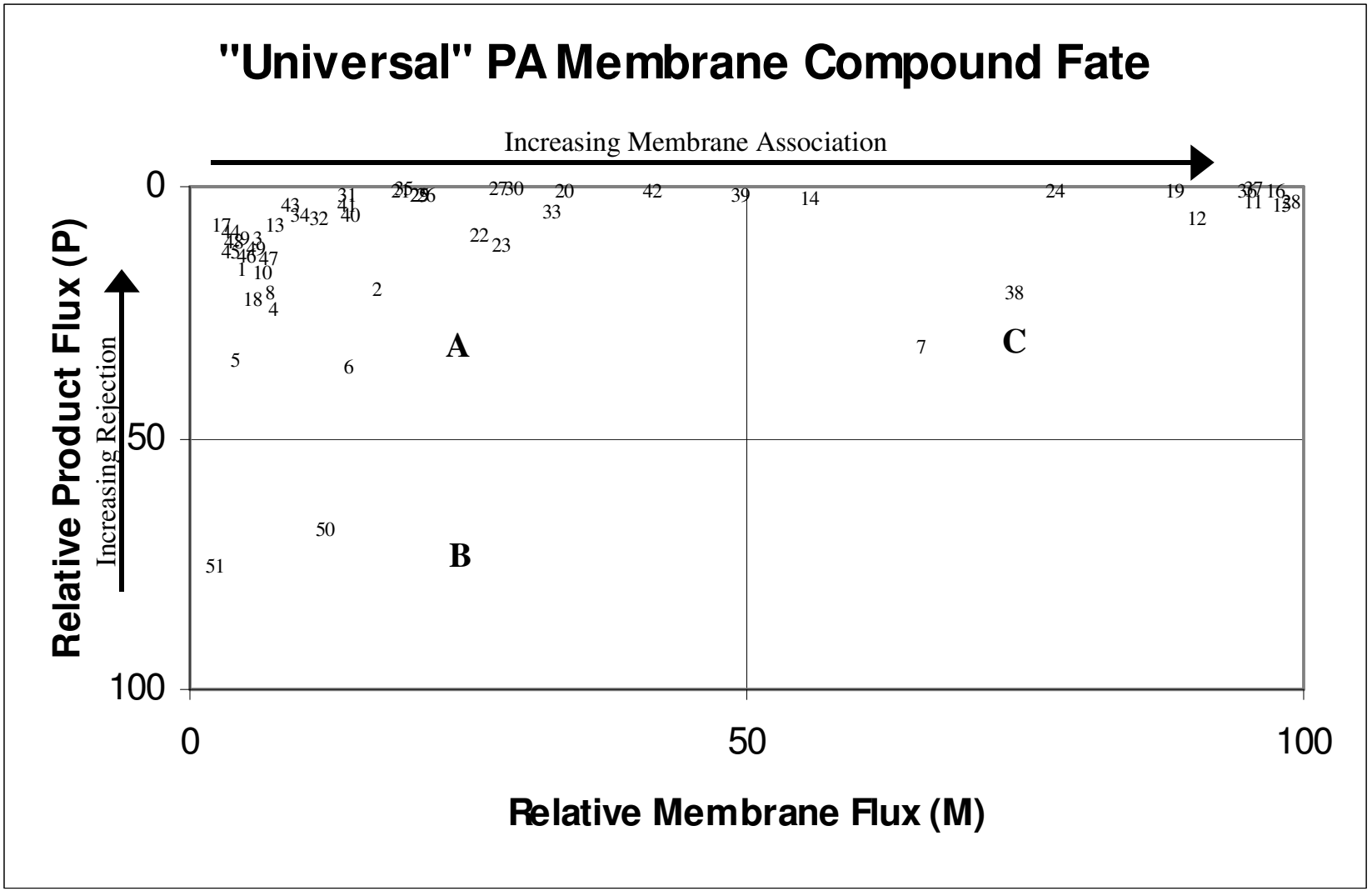

Figure 12a. Surrogate Compound Fate in "Universal" PA Membrane
Compounds in Quadrant "A" are well rejected; they neither associate with the membrane nor they pass through it. Compounds in Quadrant "B" are poorly rejected and do not interact well with the membrane. Compounds in Quadrant "C" are initially well rejected; however, they strongly associate with the membrane, so their rejection is largely due to membrane uptake. Numbers in the graph correspond to compounds listed in Figs. 12b and 12c.

ID Number	Compound	QSAR Cluster	M-Flux	P-Flux	R-Flux
1	Alanine	1	4.40	16.43	80.97
2	Caffeine	1	16.70	20.08	64.92
3	Cysteine	1	6.06	9.99	82.35
4	Dichloroacetic Acid	1	7.46	23.83	66.72
5	Glycine	1	3.93	33.98	86.59
6	N-dimethylamine	1	14.10	35.30	51.93
7	Phenol	1	65.52	31.55	3.93
8	t Butyl Alcohol	1	7.08	20.79	71.30
9	Threonine	1	4.86	10.38	82.90
10	Valine	1	6.39	16.93	76.44
11	Ethylbenzene	2	95.58	2.61	-4.95
12	Toluene	2	90.38	5.76	-4.88
13	1,4 Dichlorophenoxyacetic Acid	3	7.65	7.33	80.77
14	2,3,4,5,6 Pentachlorophenol	3	55.61	1.72	39.53
15	4,6 Dichlorophenol	3	97.88	3.30	-3.38
16	Nitrobenzene	3	97.53	0.37	-6.95
17	Phthalic Anhydride	3	2.90	7.53	89.95
18	Trichloroacetic Acid	3	5.51	22.09	73.92
19	17a Estradiol	4	88.30	0.58	24.93
20	4 Nonylphenol	4	33.54	0.45	68.02
21	beta Sitostanol n Hydrate	4	18.84	0.54	70.10
22	Cholesterol	4	25.86	9.39	85.63
23	Codeine	4	28.03	11.13	61.67
24	Estrone	4	77.69	0.42	32.56
25	Testosterone	4	20.57	1.04	75.39

Figure 12b. Surrogate Compound Fate in “Universal” PA Membrane
The ID number corresponds to numbers in Fig. 12a. Relative P, M, R fluxes for surrogate compounds are shown. Cluster numbers indicate compounds with similar molecular properties based on QSAR molecular descriptors.

ID Number	Compound	QSAR Cluster	M-Flux	P-Flux	R-Flux
26	Bisphenol	5	21.31	1.18	74.46
27	Diethylstilbestrol	5	27.74	0.14	69.13
28	2,4 Dinitrotoluene	6	98.89	2.76	-2.48
29	methyl parathion	8	20.55	1.45	78.87
30	Progesterone	8	28.97	0.21	70.12
31	2-chloro-2'-6'-diethyl-N-methoxymethyl-acetanilide (Alachlor)	9	14.15	1.51	85.37
32	Cimetidine	9	11.68	6.24	67.54
33	Diethylphthalate	9	32.62	4.88	61.30
34	Ibuprofen	9	9.92	5.07	82.17
35	Chlorpyrifos	10	19.07	0.21	62.81
36	Phenanthrene	12	94.79	0.47	7.52
37	1,1,2,2, Tetrachloroethylene (PCE)	13	95.55	0.12	-3.28
38	Benzene	13	74.11	20.79	8.13
39	Lindane	13	49.52	1.51	47.32
40	Doxycycline	15	14.48	5.08	78.59
41	Tetracycline	15	14.16	3.40	83.29
42	Ciprofloxacin	16	41.47	0.71	80.62
43	Erythromycin	16	9.15	3.33	88.25
44	Ethylenediaminetetraacetic Acid (EDTA)	18	3.56	8.77	85.89
45	Asparagine	N/A	3.78	12.98	79.02
46	Aspartic Acid	N/A	5.04	13.22	80.64
47	Histidine	N/A	6.98	14.13	78.75
48	Lysine	N/A	3.88	10.41	84.69
49	Methionine	N/A	6.01	12.22	75.75
50	N-nitroso dimethyl amine (NDMA)	N/A	12.02	67.55	3.63
51	Urea	N/A	2.21	75.25	4.50

Figure 12c. Surrogate Compound Fate in “Universal” PA Membrane. (Continued – See Fig. 12b)

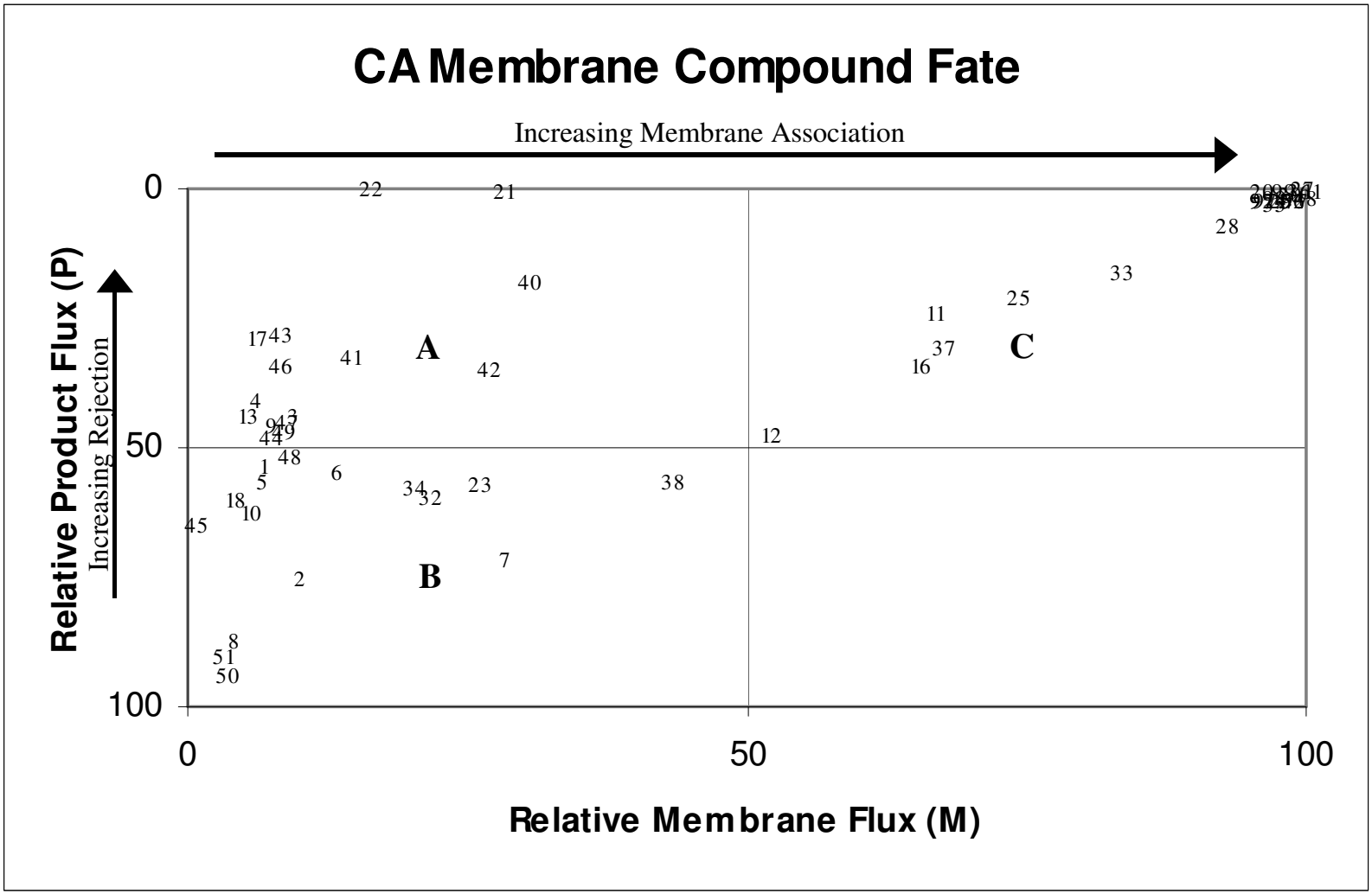

Figure 13a. Surrogate Compound Fate in CA Membrane
Compounds in Quadrant "A" are well rejected; they neither associate with the membrane nor they pass through it. Compounds in Quadrant "B" are poorly rejected and do not interact well with the membrane. Compounds in Quadrant "C" are initially well rejected; however, they strongly associate with the membrane, so their rejection is largely due to membrane uptake. Numbers in the graph correspond to compounds listed in Figs. 13b and 13c.

ID Number	Compound	QSAR Cluster	M-Flux	P-Flux	R-Flux
1	Alanine	1	6.78	53.89	39.33
2	Caffeine	1	10.09	75.53	14.37
3	Cysteine	1	9.37	43.88	46.75
4	Dichloroacetic Acid	1	6.23	41.26	52.51
5	Glycine	1	6.72	56.36	36.92
6	N-dimethylamine	1	13.25	54.91	31.84
7	Phenol	1	28.33	71.67	0.00
8	t Butyl Alcohol	1	4.04	87.42	8.53
9	Threonine	1	7.52	45.73	46.75
10	Valine	1	5.64	62.72	31.64
11	Ethylbenzene	2	66.72	24.15	9.13
12	Toluene	2	52.21	47.79	0.00
13	1,4 Dichlorophenoxyacetic Acid	3	5.30	43.74	50.96
14	2,3,4,5,6 Pentachlorophenol	3	97.77	2.23	0.00
15	4,6 Dichlorophenol	3	97.56	2.44	0.00
16	Nitrobenzene	3	65.54	34.46	0.00
17	Phthalic Anhydride	3	6.22	29.08	64.70
18	Trichloroacetic Acid	3	4.19	60.12	35.70
19	17a Estradiol	4	97.52	2.48	0.00
20	4 Nonylphenol	4	95.98	0.73	3.29
21	beta Sitostanol n Hydrate	4	28.23	0.67	71.10
22	Cholesterol	4	16.48	0.25	83.27
23	Codeine	4	26.16	57.34	16.50
24	Estrone	4	97.32	2.68	0.00
25	Testosterone	4	74.38	20.97	4.65

Figure 13b. Surrogate Compound Fate in CA Membrane
The ID number corresponds to numbers in Fig. 13a. Relative P, M, R fluxes for surrogate compounds are shown. Cluster numbers indicate compounds with similar molecular properties based on QSAR molecular descriptors.

ID Number	Compound	QSAR Cluster	M-Flux	P-Flux	R-Flux
26	Bisphenol	5	99.11	0.89	0.00
27	Diethylstilbestrol	5	99.74	0.26	0.00
28	2,4 Dinitrotoluene	6	92.94	7.06	0.00
29	methyl parathion	8	97.82	2.18	0.00
30	Progesterone	8	98.51	1.49	0.00
32	Cimetidine	9	21.67	59.89	18.44
33	Diethylphthalate	9	83.52	16.48	0.00
34	Ibuprofen	9	20.45	57.98	21.57
35	Chlorpyrifos	10	97.09	2.91	0.00
36	Phenanthrene	12	99.57	0.43	0.00
37	1,1,2,2, Tetrachloroethylene (PCE)	13	67.77	30.80	1.44
38	Benzene	13	43.42	56.58	0.00
39	Lindane	13	98.48	1.52	0.00
40	Doxycycline	15	30.61	18.03	51.36
41	Tetracycline	15	14.42	32.26	53.32
42	Ciprofloxacin	16	27.03	35.12	37.85
43	Erythromycin	16	8.28	28.32	63.41
44	Ethylenediaminetetraacetic Acid (EDTA)	18	7.52	48.06	44.42
45	Asparagine	N/A	0.73	64.97	34.30
46	Aspartic Acid	N/A	8.48	34.23	57.29
47	Histidine	N/A	8.82	45.29	45.89
48	Lysine	N/A	9.30	51.85	38.85
49	Methionine	N/A	8.58	46.93	44.49
50	N-nitroso dimethyl amine (NDMA)	N/A	3.51	94.06	2.44
51	Urea	N/A	3.08	90.58	6.34

Figure 13c. Surrogate Compound Fate in CA Membrane. (Continued – See Fig. 13b)

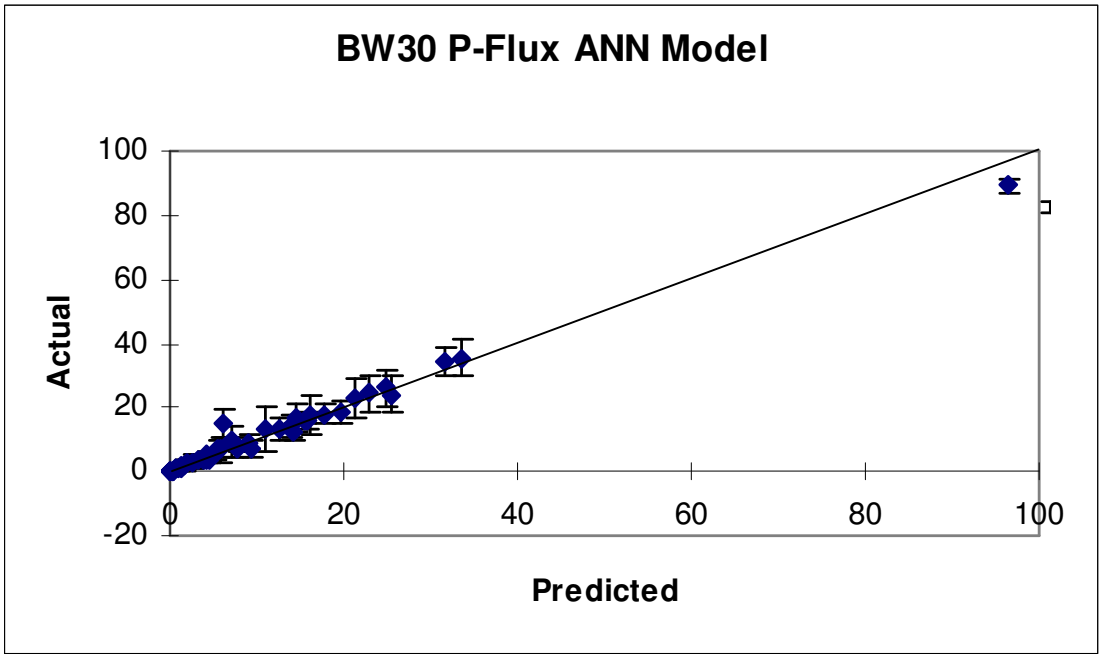

Norm P Flux (%)	R	Avg. Abs.	RMS	Conf. Interval (95%)	Records
All	0.9821	2.3256	4.0927	8.0013	255
Train	0.9829	2.3317	4.1521	8.1379	178
Test	0.9805	2.3114	3.9518	7.8298	77

Sensitivity Index

Ovality	xvpc4	Py	LogP	SsCH3	numHBa
-0.1699	-0.7242	0.2610	-0.0119	0.6658	1.3186

Figure 14a. ANN Model Results for BW-30 – P-Flux

The graph shows the accuracy of prediction. The overall R values are high and there is a good agreement between the test and the train values. The line indicates a perfect model. The bar represents one standard deviation above the mean based on n=4-7. R=Linear correlation between predicted and actual, Avg.Abs.=Average absolute error between predicted and actual, RMS=mean root square error between predicted and actual, Conf.Interval (95%)=Represents 95% confidence interval, Records=Represents number of exemplars used. The sensitivity index lists the inputs to the model and indicates how sensitive the model output is to small changes in each input.

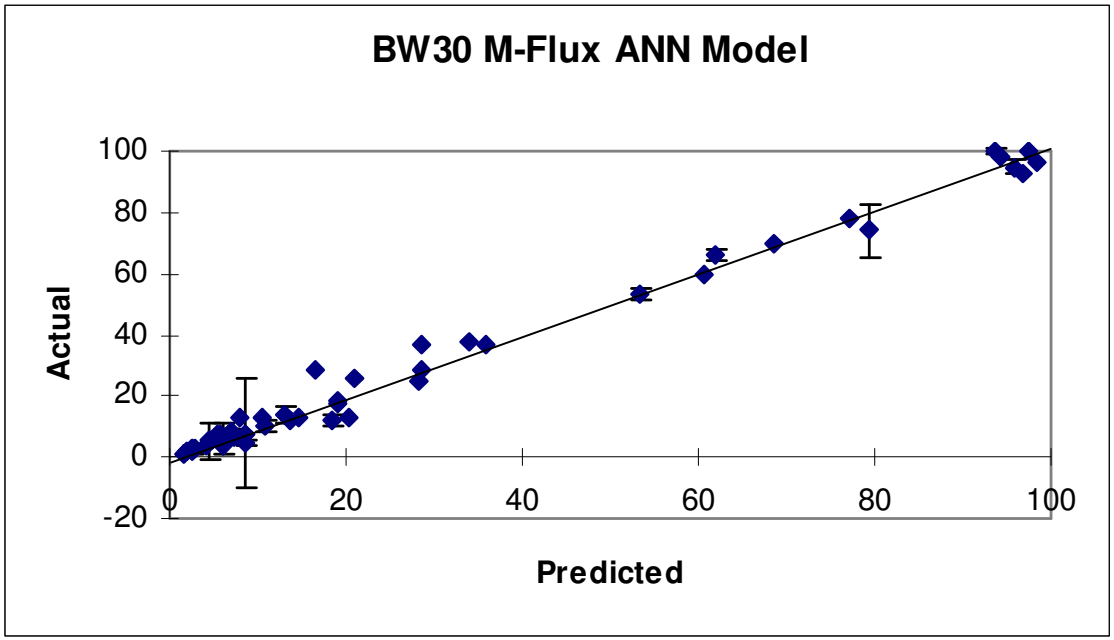

Norm. M Flux (%)	R	Avg. Abs.	RMS	Conf. Interval (95%)	Records
All	0.9839	3.6830	5.9178	11.5696	255
Train	0.9860	3.4998	5.5314	10.8412	178
Test	0.9793	4.1064	6.7266	13.3277	77

Sensitivity Index

P	LogP	Gmax	Gmin
-0.6355	0.3669	0.0131	0.7941

Figure 14b. ANN Model Results for BW-30 – M-Flux

The graph shows the accuracy of prediction. The overall R values are high and there is a good agreement between the test and the train values. The line indicates a perfect model. The bar represents one standard deviation above the mean based on n=4-7. R=Linear correlation between predicted and actual, Avg.Abs.=Average absolute error between predicted and actual, RMS=mean root square error between predicted and actual, Conf.Interval (95%)=Represents 95% confidence interval, Records=Represents number of exemplars used. The sensitivity index lists the inputs to the model and indicates how sensitive the model output is to small changes in each input.

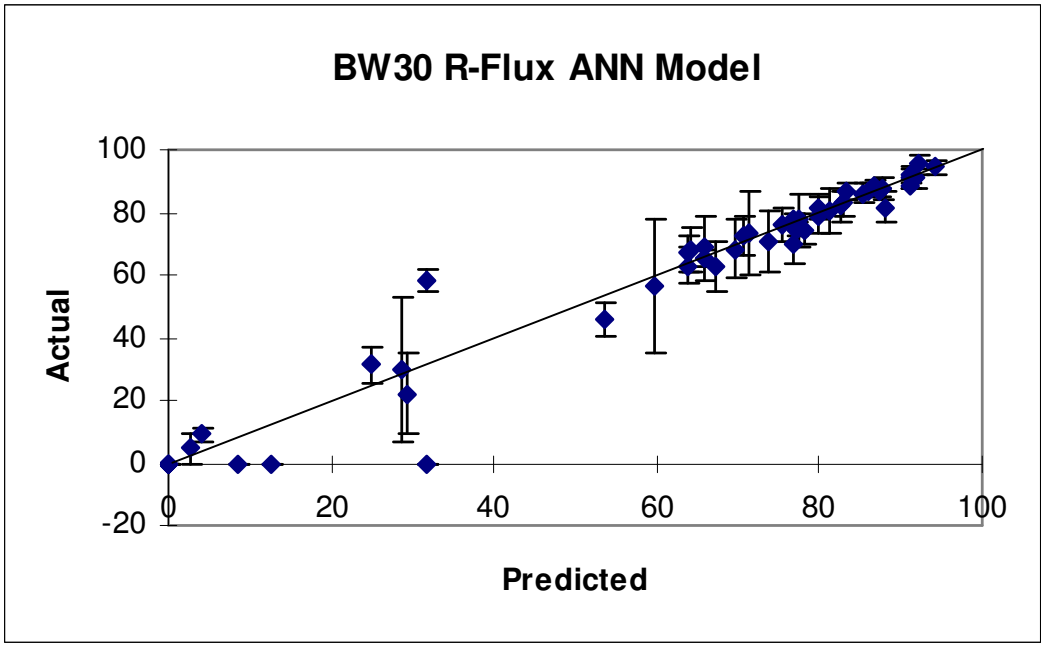

Norm R Flux (%)	R	Avg. Abs.	RMS	Conf. Interval (95%)	Records
All	0.9608	6.0026	9.4015	18.3803	255
Train	0.9569	6.2819	9.9020	19.4073	178
Test	0.9705	5.3567	8.1272	16.1028	77

Sensitivity Index

Pz	Wt	LogP	Gmin
-0.4680	-6.1063	-1.0190	-2.1272

Figure 14c. ANN Model Results for BW-30 – R-Flux

The graph shows the accuracy of prediction. The overall R values are high and there is a good agreement between the test and the train values. The line indicates a perfect model. The bar represents one standard deviation above the mean based on n=4-7. R=Linear correlation between predicted and actual, Avg.Abs.=Average absolute error between predicted and actual, RMS=mean root square error between predicted and actual, Conf.Interval (95%)=Represents 95% confidence interval, Records=Represents number of exemplars used. The sensitivity index lists the inputs to the model and indicates how sensitive the model output is to small changes in each input.

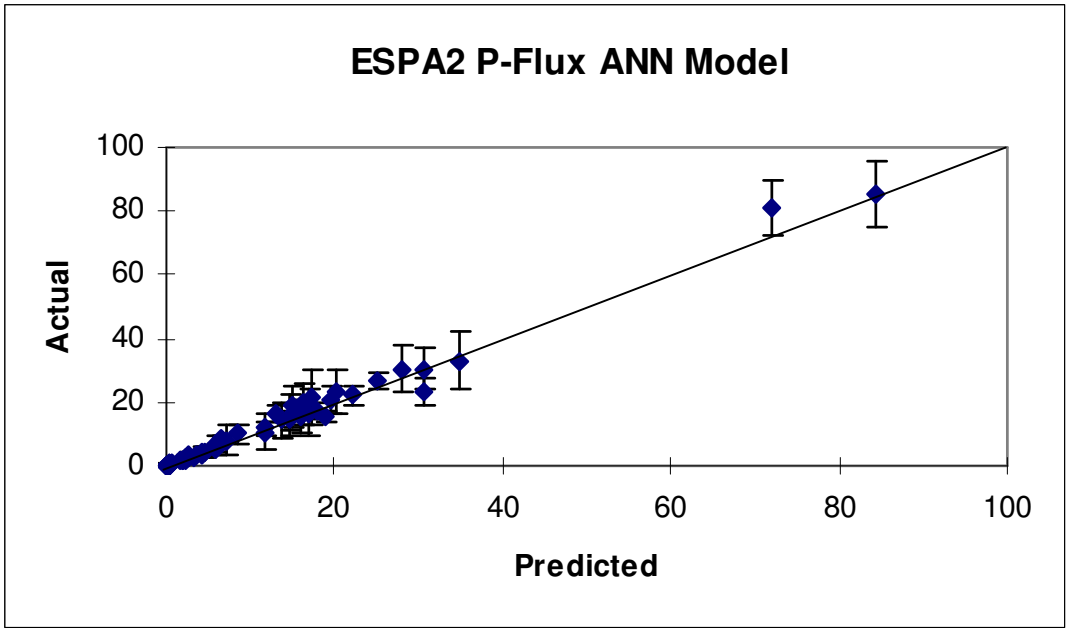

Norm P Flux (%)	R	Avg. Abs.	RMS	Conf. Interval (95%)	Records
All	0.9644	2.8041	4.7706	9.3254	261
Train	0.9704	2.6084	4.3232	8.4717	182
Test	0.9521	3.2551	5.6683	11.2254	79

Sensitivity Index

MaxQp	xvpc4	Iy	Py	LogP	SsCH3	Hmin	numHBa
-0.3767	-0.4996	-1.0265	0.1432	-0.3241	0.1174	0.3817	0.3934

Figure 15a. ANN Model Results for ESPA-2 – P-Flux
The graph shows the accuracy of prediction. The overall R values are high and there is a good agreement between the test and the train values. The line indicates a perfect model. The bar represents one standard deviation above the mean based on n=4-7. R=Linear correlation between predicted and actual, Avg.Abs.=Average absolute error between predicted and actual, RMS=mean root square error between predicted and actual, Conf.Interval (95%)=Represents 95% confidence interval, Records=Represents number of exemplars used. The sensitivity index lists the inputs to the model and indicates how sensitive the model output is to small changes in each input.

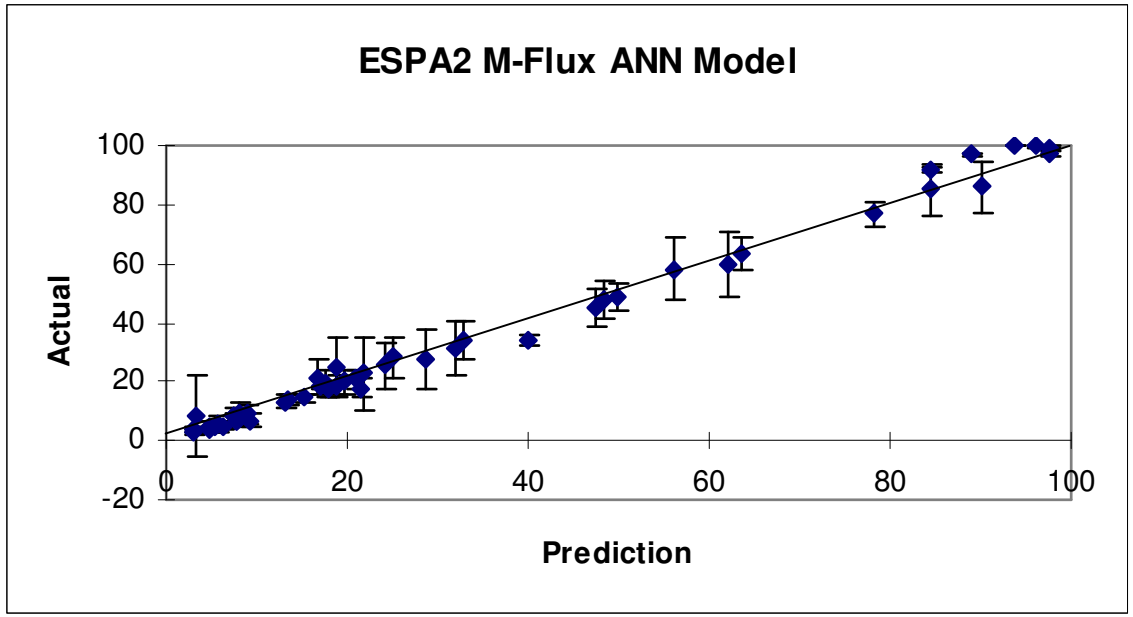

Norm. M Flux (%)	R	Avg. Abs.	RMS	Conf. Interval (95%)	Records
All	0.9853	3.8561	5.5805	10.9087	261
Train	0.9860	3.8111	5.4474	10.6747	182
Test	0.9838	3.9597	5.8756	11.6360	79

Sensitivity Index

P	k1	SdssC	Gmin	fw	numHBa	Qs
-0.2011	-1.6738	-0.3071	0.5616	1.2028	0.2102	1.3982

Figure 15b. ANN Model Results for ESPA-2 – M-Flux

The graph shows the accuracy of prediction. The overall R values are high and there is a good agreement between the test and the train values. The line indicates a perfect model. The bar represents one standard deviation above the mean based on n=4-7. R=Linear correlation between predicted and actual, Avg.Abs.=Average absolute error between predicted and actual, RMS=mean root square error between predicted and actual, Conf.Interval (95%)=Represents 95% confidence interval, Records=Represents number of exemplars used. The sensitivity index lists the inputs to the model and indicates how sensitive the model output is to small changes in each input.

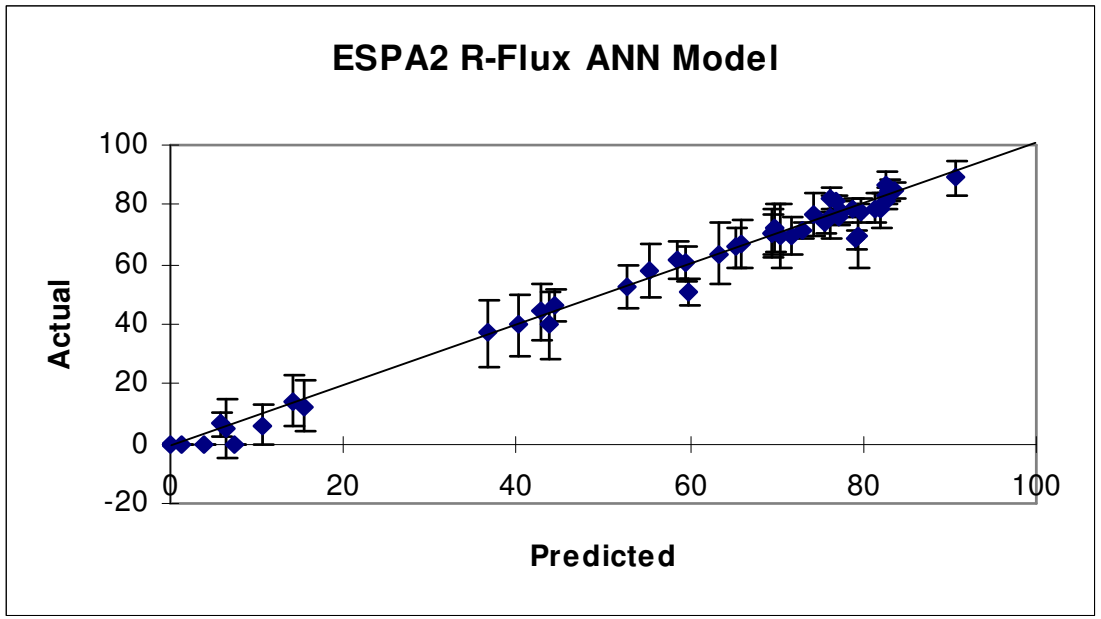

Norm R Flux (%)	R	Avg. Abs.	RMS	Conf. Interval (95%)	Records
All	0.9791	4.9779	6.3888	12.4887	261
Train	0.9824	4.5969	5.8686	11.4999	182
Test	0.9729	5.8556	7.4503	14.7544	79

Sensitivity Index

MaxNeg	nxch6	Q	k2	Gmax	Gmin	numHBa
0.0384	0.2095	-1.6123	0.3314	-0.5237	-2.1458	-1.4751

Figure 15c. ANN Model Results for ESPA-2 – R-Flux

The graph shows the accuracy of prediction. The overall R values are high and there is a good agreement between the test and the train values. The line indicates a perfect model. The bar represents one standard deviation above the mean based on n=4-7. R=Linear correlation between predicted and actual, Avg.Abs.=Average absolute error between predicted and actual, RMS=mean root square error between predicted and actual, Conf.Interval (95%)=Represents 95% confidence interval, Records=Represents number of exemplars used. The sensitivity index lists the inputs to the model and indicates how sensitive the model output is to small changes in each input.

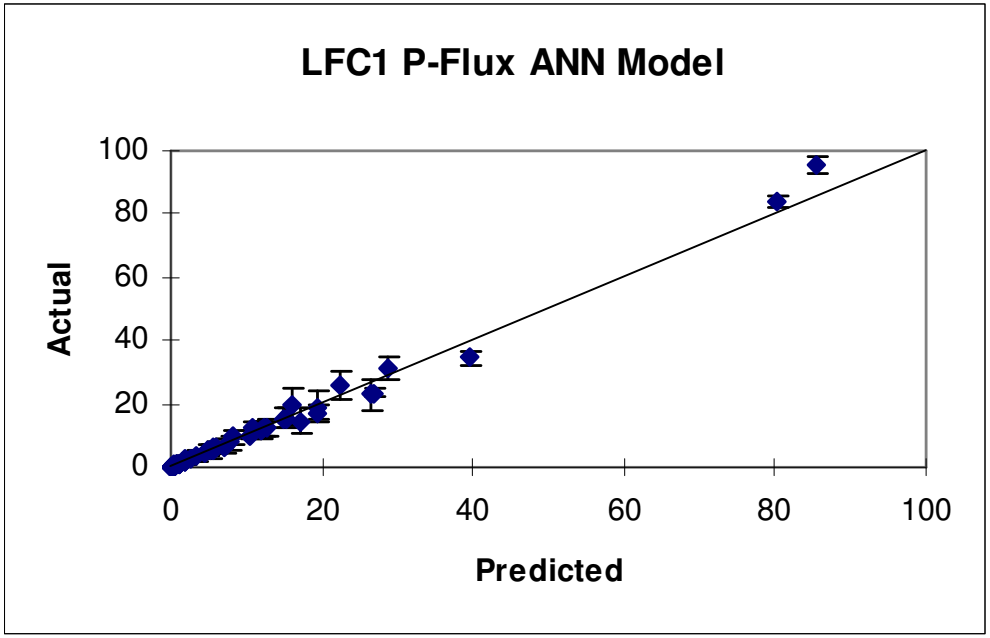

Norm P Flux (%)	R	Avg. Abs.	RMS	Conf. Interval (95%)	Records
All	0.9914	1.7375	2.9206	5.7102	252
Train	0.9913	1.7245	2.9384	5.7596	176
Test	0.9918	1.7675	2.8789	5.7055	76

Sensitivity Index

Iy	Py	LogP	SdssC
0.4935	0.7729	-0.3455	-0.0801

Figure 16a. ANN Model Results for LFC-1 – P-Flux

The graph shows the accuracy of prediction. The overall R values are high and there is a good agreement between the test and the train values. The line indicates a perfect model. The bar represents one standard deviation above the mean based on n=4-7. R=Linear correlation between predicted and actual, Avg.Abs.=Average absolute error between predicted and actual, RMS=mean root square error between predicted and actual, Conf.Interval (95%)=Represents 95% confidence interval, Records=Represents number of exemplars used. The sensitivity index lists the inputs to the model and indicates how sensitive the model output is to small changes in each input.

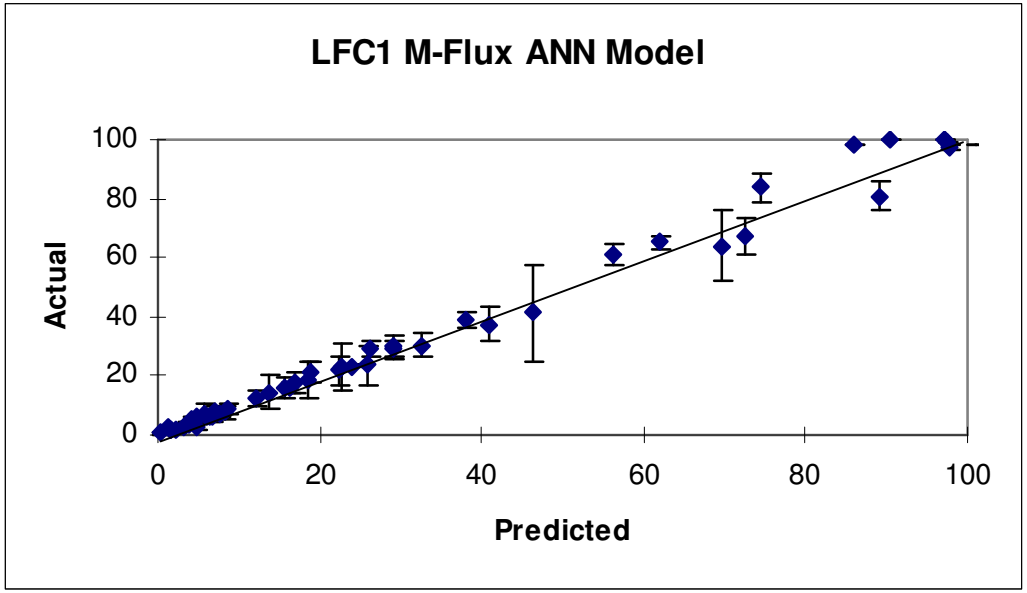

Norm. M Flux (%)	R	Avg. Abs.	RMS	Conf. Interval (95%)	Records
All	0.9887	3.0407	4.9548	9.6876	252
Train	0.9926	2.7627	4.1714	8.1765	176
Test	0.9807	3.6845	6.4115	12.7066	76

Sensitivity Index

MaxQp	P	Q	SaaCH	SdssC	Gmin	idcbar	fw	numHBa	Qs
2.1870	-0.6448	0.4650	0.4792	-0.3696	1.3010	-1.2797	0.6555	0.7628	1.9183

Figure 16b. ANN Model Results for LFC-1 – M-Flux

The graph shows the accuracy of prediction. The overall R values are high and there is a good agreement between the test and the train values. The line indicates a perfect model. The bar represents one standard deviation above the mean based on n=4-7. R=Linear correlation between predicted and actual, Avg.Abs.=Average absolute error between predicted and actual, RMS=mean root square error between predicted and actual, Conf.Interval (95%)=Represents 95% confidence interval, Records=Represents number of exemplars used. The sensitivity index lists the inputs to the model and indicates how sensitive the model output is to small changes in each input.

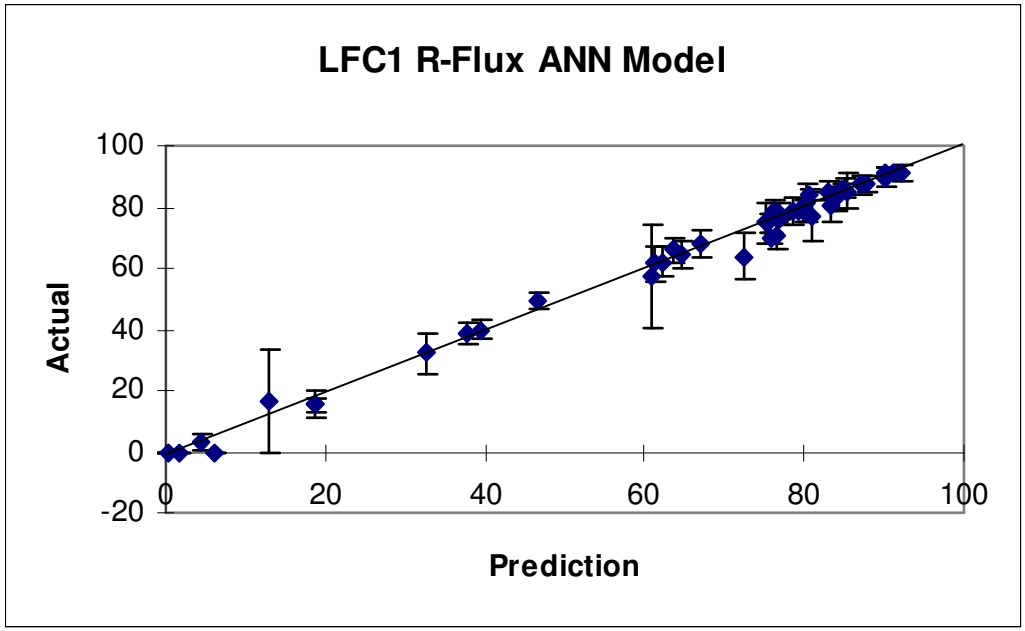

Norm R Flux (%)	R	Avg. Abs.	RMS	Conf. Interval (95%)	Records
All	0.9879	3.5841	5.1401	10.0498	252
Train	0.9897	3.5236	4.7465	9.3037	176
Test	0.9841	3.7242	5.9525	11.7969	76

Sensitivity Index

nxch6	Q	sumdell	k2	SdssC	Gmin	numHBa
0.8560	-0.3335	-0.3209	1.5810	-3.1102	-0.3399	-0.6827

Figure 16c. ANN Model Results for LFC-1 – R-Flux

The graph shows the accuracy of prediction. The overall R values are high and there is a good agreement between the test and the train values. The line indicates a perfect model. The bar represents one standard deviation above the mean based on n=4-7. R=Linear correlation between predicted and actual, Avg.Abs.=Average absolute error between predicted and actual, RMS=mean root square error between predicted and actual, Conf.Interval (95%)=Represents 95% confidence interval, Records=Represents number of exemplars used. The sensitivity index lists the inputs to the model and indicates how sensitive the model output is to small changes in each input.

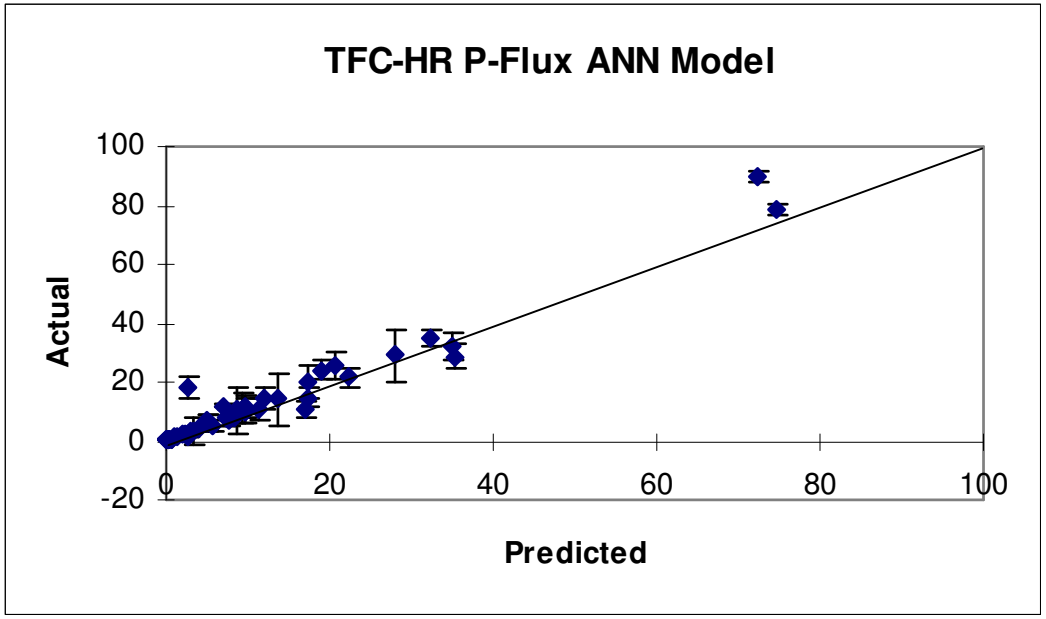

Norm P Flux (%)	R	Avg. Abs.	RMS	Conf. Interval (95%)	Records
All	0.9691	2.6487	4.4316	8.6630	260
Train	0.9713	2.5938	4.4266	8.6746	181
Test	0.9667	2.7745	4.4430	8.7989	79

Sensitivity Index

MaxQp	xvpc4	nxp5	P	Hmin	fw	numHBa
-1.5199	0.3931	0.0100	0.6744	0.2301	-0.5962	0.2296

Figure 17a. ANN Model Results for TFC-HR – P-Flux

The graph shows the accuracy of prediction. The overall R values are high and there is a good agreement between the test and the train values. The line indicates a perfect model. The bar represents one standard deviation above the mean based on n=4-7. R=Linear correlation between predicted and actual, Avg.Abs.=Average absolute error between predicted and actual, RMS=mean root square error between predicted and actual, Conf.Interval (95%)=Represents 95% confidence interval, Records=Represents number of exemplars used. The sensitivity index lists the inputs to the model and indicates how sensitive the model output is to small changes in each input.

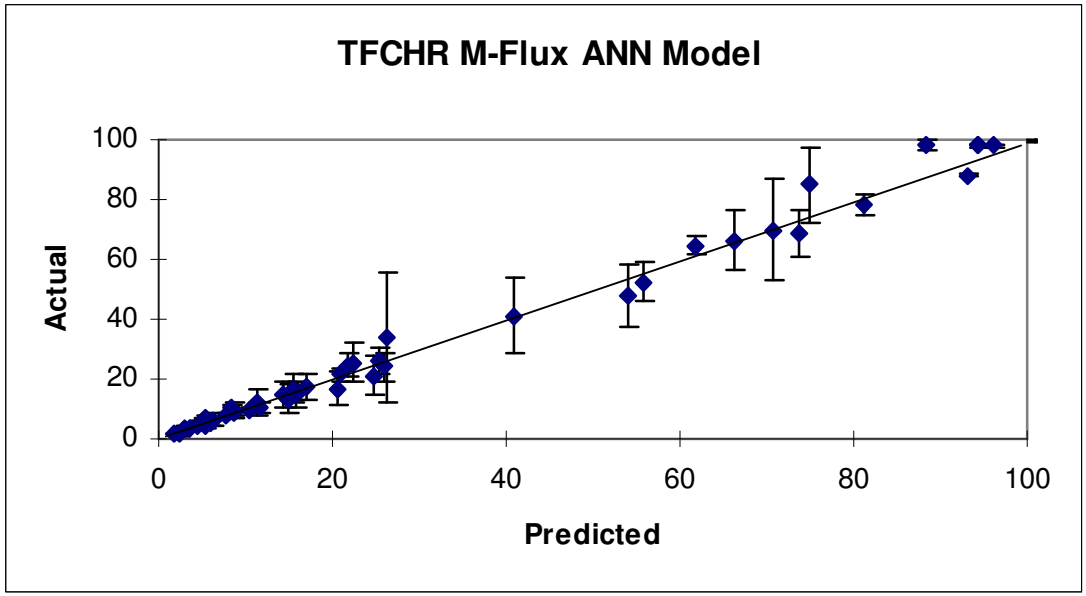

Norm. M Flux (%)	R	Avg. Abs.	RMS	Conf. Interval (95%)	Records
All	0.9844	3.7152	6.0456	11.8181	260
Train	0.9891	3.3200	5.0634	9.9226	181
Test	0.9736	4.6208	7.8452	15.5365	79

Sensitivity Index

P	LogP	SaaCH	Gmin	numHBa
0.4421	-0.1036	3.3047	1.5067	0.1772

Figure 17b. ANN Model Results for TFC-HR – M-Flux

The graph shows the accuracy of prediction. The overall R values are high and there is a good agreement between the test and the train values. The line indicates a perfect model. The bar represents one standard deviation above the mean based on n=4-7. R=Linear correlation between predicted and actual, Avg.Abs.=Average absolute error between predicted and actual, RMS=mean root square error between predicted and actual, Conf.Interval (95%)=Represents 95% confidence interval, Records=Represents number of exemplars used. The sensitivity index lists the inputs to the model and indicates how sensitive the model output is to small changes in each input.

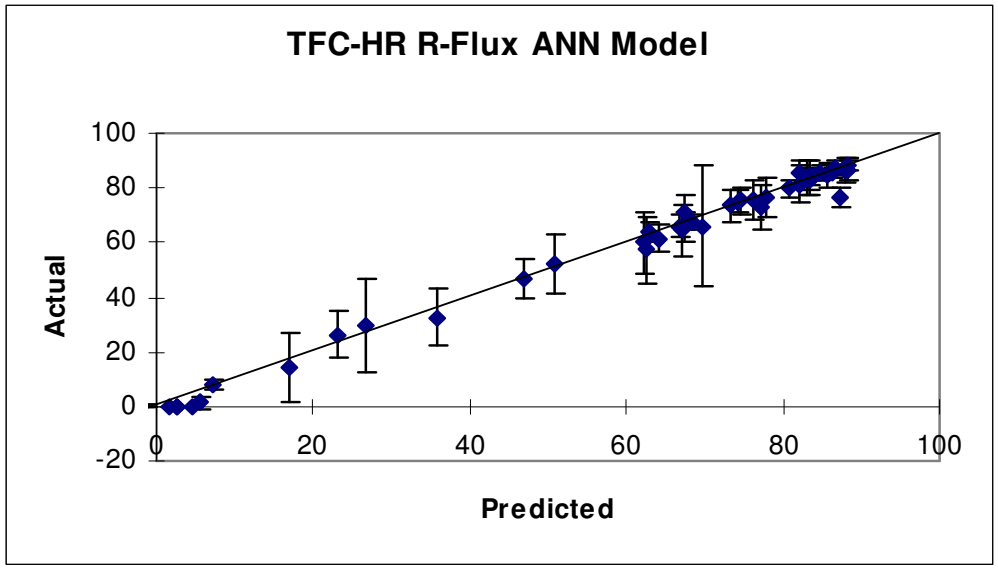

Norm R Flux (%)	R	Avg. Abs.	RMS	Conf. Interval (95%)	Records
All	0.9803	4.5211	6.5732	12.8495	260
Train	0.9818	4.2638	6.3169	12.3789	181
Test	0.9769	5.1107	7.1259	14.1121	79

Sensitivity Index

Py	Q	LogP	SaaCH	SdssC	SdO	Gmax	Gmin	idcbar	numHBa
-0.8254	-1.6494	-0.5547	-2.7032	-0.4940	0.0280	0.0117	-1.3812	1.3378	-1.4252

Figure 17c. ANN Model Results for TFC-HR – R-Flux
The graph shows the accuracy of prediction. The overall R values are high and there is a good agreement between the test and the train values. The line indicates a perfect model. The bar represents one standard deviation above the mean based on n=4-7. R=Linear correlation between predicted and actual, Avg.Abs.=Average absolute error between predicted and actual, RMS=mean root square error between predicted and actual, Conf.Interval (95%)=Represents 95% confidence interval, Records=Represents number of exemplars used. The sensitivity index lists the inputs to the model and indicates how sensitive the model output is to small changes in each input.

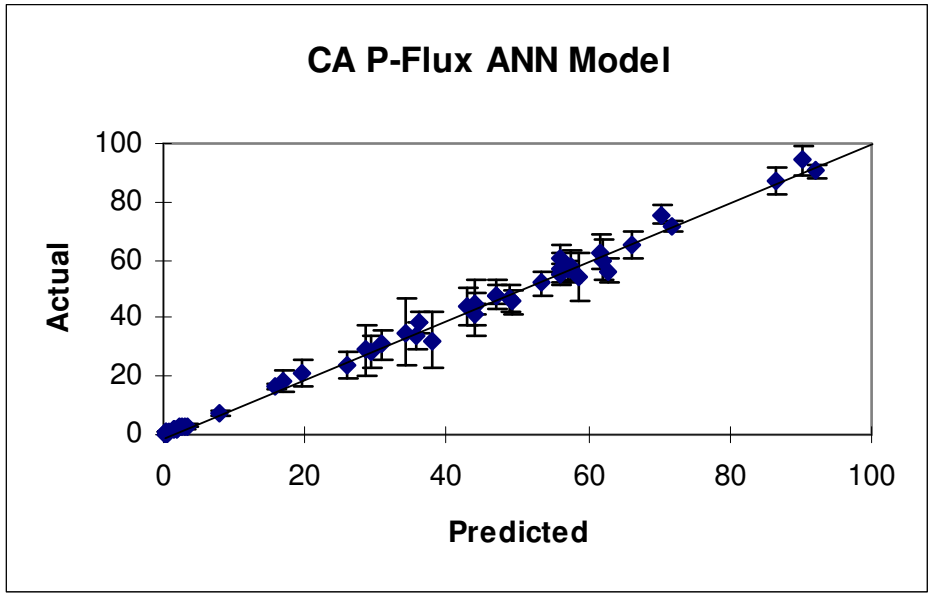

Norm P Flux (%)	R	Avg. Abs.	RMS	Conf. Interval (95%)	Records
All	0.9853	3.0996	4.6515	9.0943	253
Train	0.9858	3.0948	4.5760	8.9690	177
Test	0.9842	3.1107	4.8229	9.5582	76

Sensitivity Index

Surface	xpc4	xv1	P	LogP	SdssC	numHBa	Qsv
-0.6895	0.4585	-1.4028	1.0620	-0.9874	-0.6083	0.0015	0.7710

Figure 18a. ANN Model Results for CA – P-Flux

The graph shows the accuracy of prediction. The overall R values are high and there is a good agreement between the test and the train values. The line indicates a perfect model. The bar represents one standard deviation above the mean based on n=4-7. R=Linear correlation between predicted and actual, Avg.Abs.=Average absolute error between predicted and actual, RMS=mean root square error between predicted and actual, Conf.Interval (95%)=Represents 95% confidence interval, Records=Represents number of exemplars used. The sensitivity index lists the inputs to the model and indicates how sensitive the model output is to small changes in each input.

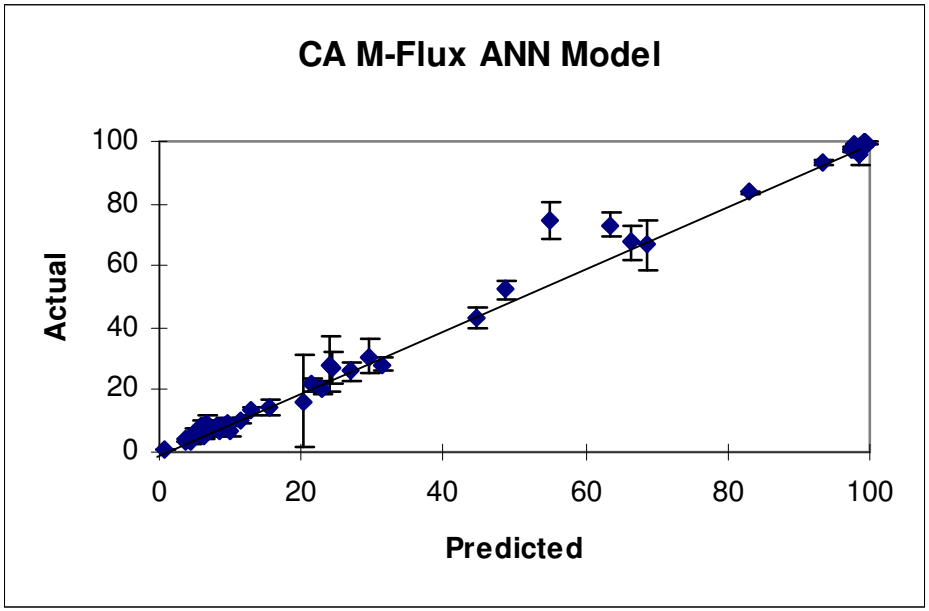

Norm. M Flux (%)	R	Avg. Abs.	RMS	Conf. Interval (95%)	Records
All	0.9900	2.4784	5.4600	10.6748	254
Train	0.9883	2.5333	5.9050	11.5740	177
Test	0.9939	2.3520	4.2644	8.4493	77

Sensitivity Index

P	Q	LogP	SdssC
2.0098	0.9829	1.2532	1.2304

Figure 18b. ANN Model Results for CA – M-Flux

The graph shows the accuracy of prediction. The overall R values are high and there is a good agreement between the test and the train values. The line indicates a perfect model. The bar represents one standard deviation above the mean based on n=4-7. R=Linear correlation between predicted and actual, Avg.Abs.=Average absolute error between predicted and actual, RMS=mean root square error between predicted and actual, Conf.Interval (95%)=Represents 95% confidence interval, Records=Represents number of exemplars used. The sensitivity index lists the inputs to the model and indicates how sensitive the model output is to small changes in each input.

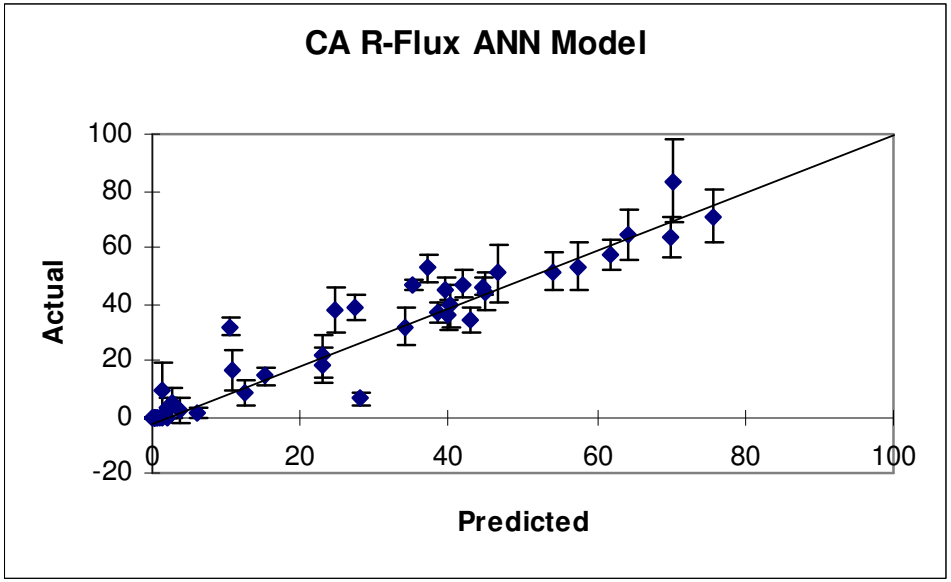

Norm R Flux (%)	R	Avg. Abs.	RMS	Conf. Interval (95%)	Records
All	0.9435	5.4438	8.2063	16.0441	254
Train	0.9427	5.4063	8.2350	16.1408	177
Test	0.9464	5.5302	8.1400	16.1282	77

Sensitivity Index

ABSQ	Q	sumdell	SaaCH	SdssC
0.7603	-0.8255	-0.2971	-0.3784	-0.7532

Figure 18c. ANN Model Results for CA – R-Flux

The graph shows the accuracy of prediction. The overall R values are high and there is a good agreement between the test and the train values. The line indicates a perfect model. The bar represents one standard deviation above the mean based on n=4-7. R=Linear correlation between predicted and actual, Avg.Abs.=Average absolute error between predicted and actual, RMS=mean root square error between predicted and actual, Conf.Interval (95%)=Represents 95% confidence interval, Records=Represents number of exemplars used. The sensitivity index lists the inputs to the model and indicates how sensitive the model output is to small changes in each input.

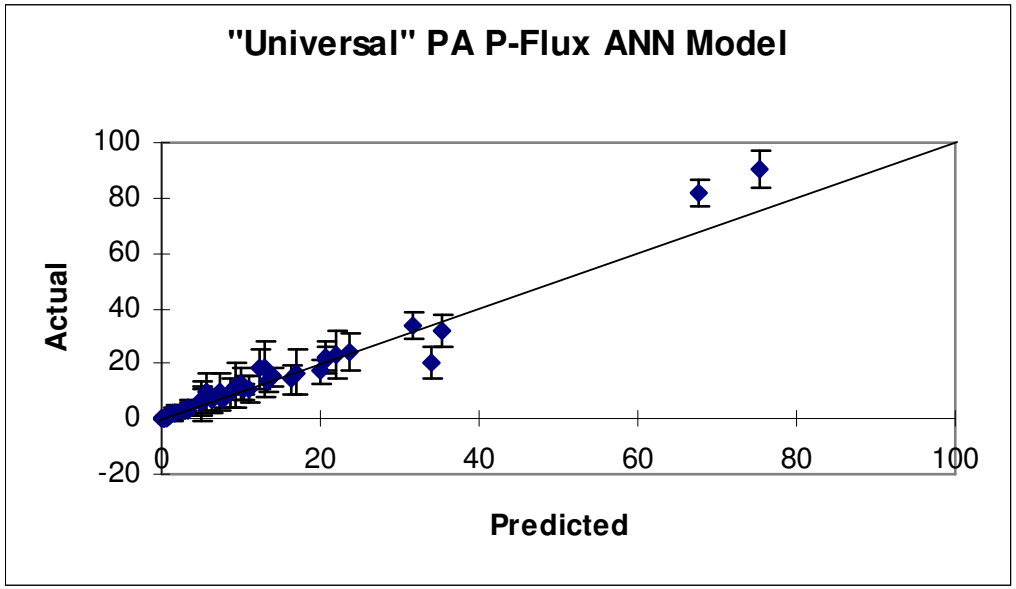

Norm P Flux (%)	R	Avg. Abs.	RMS	Conf. Interval (95%)	Records
All	0.9617	3.3033	5.6340	10.9670	1028
Train	0.9644	3.1853	5.5692	10.8476	719
Test	0.9559	3.5779	5.7818	11.2923	309

Sensitivity Index

Average	Surface	xvpc4	Py	LogP	SsCH3	SdssC	Hmin
NetOut01	-0.1755	-0.6933	-0.0110	-0.2393	0.1387	-0.0178	0.2539

Figure 19a. ANN Model Results for "Universal" PA – P-Flux
The graph shows the accuracy of prediction. The overall R values are high and there is a good agreement between the test and the train values. The line indicates a perfect model. The bar represents one standard deviation above the mean based on n=4-7. R=Linear correlation between predicted and actual, Avg.Abs.=Average absolute error between predicted and actual, RMS=mean root square error between predicted and actual, Conf.Interval (95%)=Represents 95% confidence interval, Records=Represents number of exemplars used. The sensitivity index lists the inputs to the model and indicates how sensitive the model output is to small changes in each input.

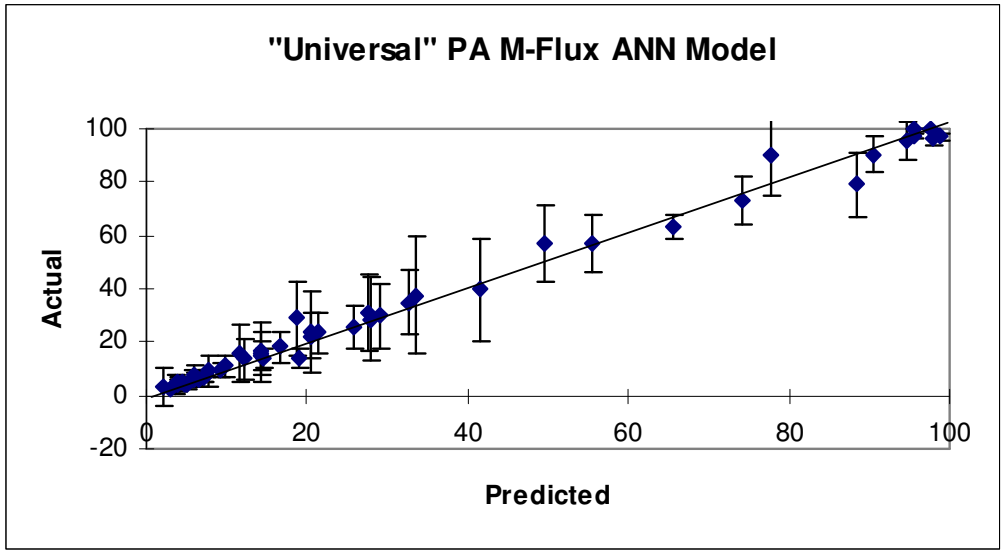

Norm. M Flux (%)	R	Avg. Abs.	RMS	Conf. Interval (95%)	Records
All	0.9646	5.6114	8.8493	17.2259	1027
Train	0.9634	5.6258	8.9931	17.5167	718
Test	0.9674	5.5779	8.5057	16.6123	309

Sensitivity Index

Average	Surface	xvpc4	Py	LogP	SsCH3	SdssC	Hmin
NetOut01	-0.1755	-0.6933	-0.0110	-0.2393	0.1387	-0.0178	0.2539

Figure 19b. ANN Model Results for "Universal" PA – M-Flux

The graph shows the accuracy of prediction. The overall R values are high and there is a good agreement between the test and the train values. The line indicates a perfect model. The bar represents one standard deviation above the mean based on n=4-7. R=Linear correlation between predicted and actual, Avg.Abs.=Average absolute error between predicted and actual, RMS=mean root square error between predicted and actual, Conf.Interval (95%)=Represents 95% confidence interval, Records=Represents number of exemplars used. The sensitivity index lists the inputs to the model and indicates how sensitive the model output is to small changes in each input.

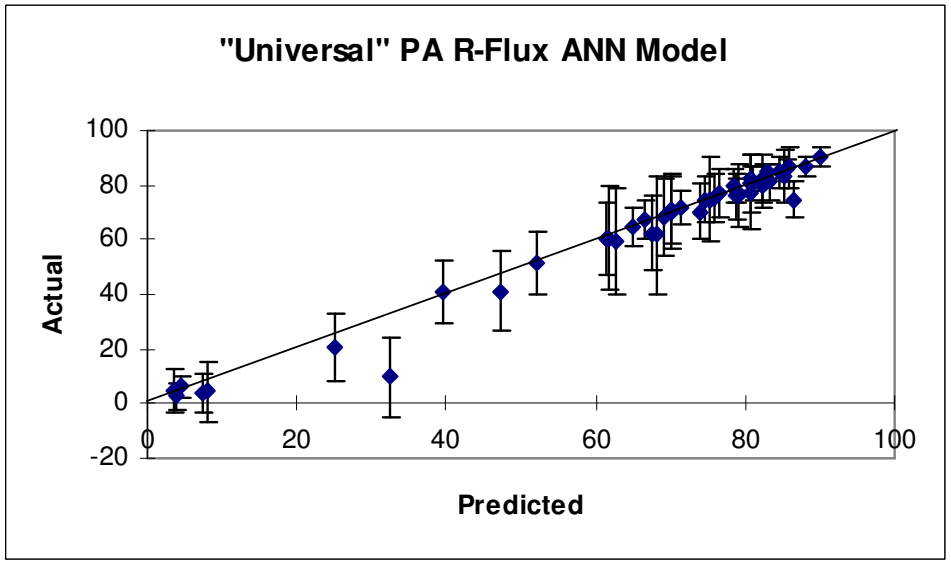

Norm R Flux (%)	R	Avg. Abs.	RMS	Conf. Interval (95%)	Records
All	0.9487	7.7847	10.4720	20.3846	1029
Train	0.9463	7.8690	10.7083	20.8573	720
Test	0.9543	7.5883	9.8997	19.3348	309

Sensitivity Index

Q	Wt	k3	LogP	Gmax	Gmin	numHBa
-1.2360	22.6983	-0.0397	-0.6264	-0.4501	-0.0899	-0.8011

Figure 19c. ANN Model Results for "Universal" PA – R-Flux
The graph shows the accuracy of prediction. The overall R values are high and there is a good agreement between the test and the train values. The line indicates a perfect model. The bar represents one standard deviation above the mean based on n=4-7. R=Linear correlation between predicted and actual, Avg.Abs.=Average absolute error between predicted and actual, RMS=mean root square error between predicted and actual, Conf.Interval (95%)=Represents 95% confidence interval, Records=Represents number of exemplars used. The sensitivity index lists the inputs to the model and indicates how sensitive the model output is to small changes in each input.

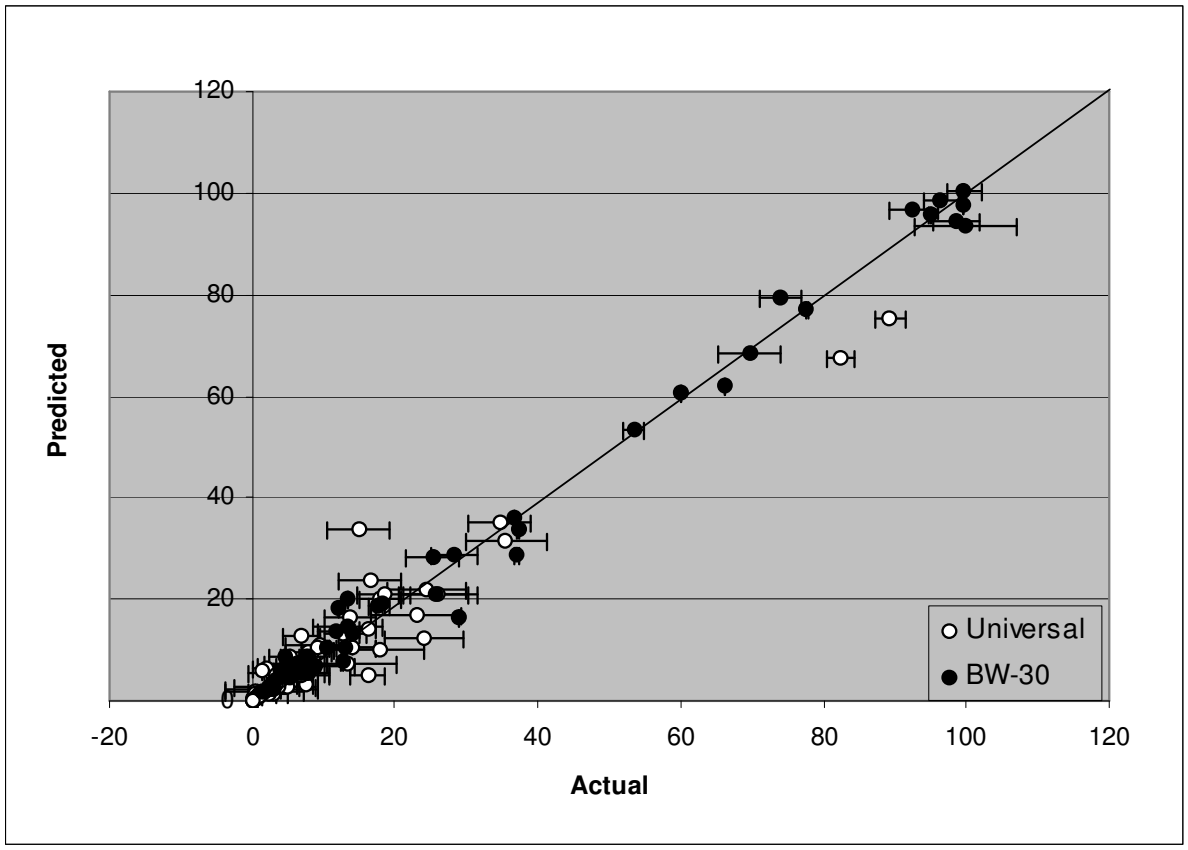

Figure 20a. Comparison of "Universal" PA Model Output to BW-30 – P-Flux
The closed circles represent the specific PA membrane model and the opened circles represent the "Universal" PA model. The "Universal" PA model agrees reasonably well with the BW-30 model.

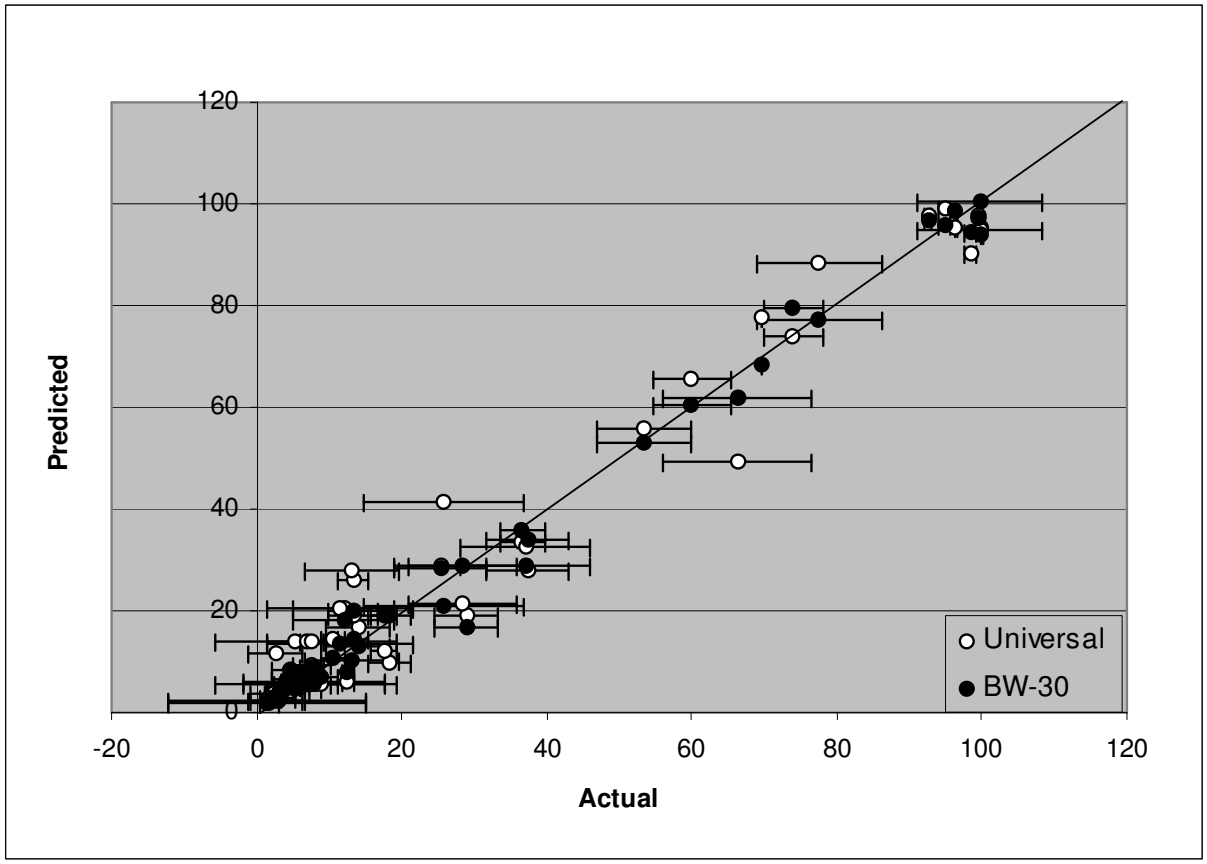

Figure 20b. Comparison of "Universal" PA Model Output to BW-30 – M-Flux
The closed circles represent the specific PA membrane model and the opened circles represent the "Universal" PA model. The "Universal" PA model agrees reasonably well with the BW-30 model.

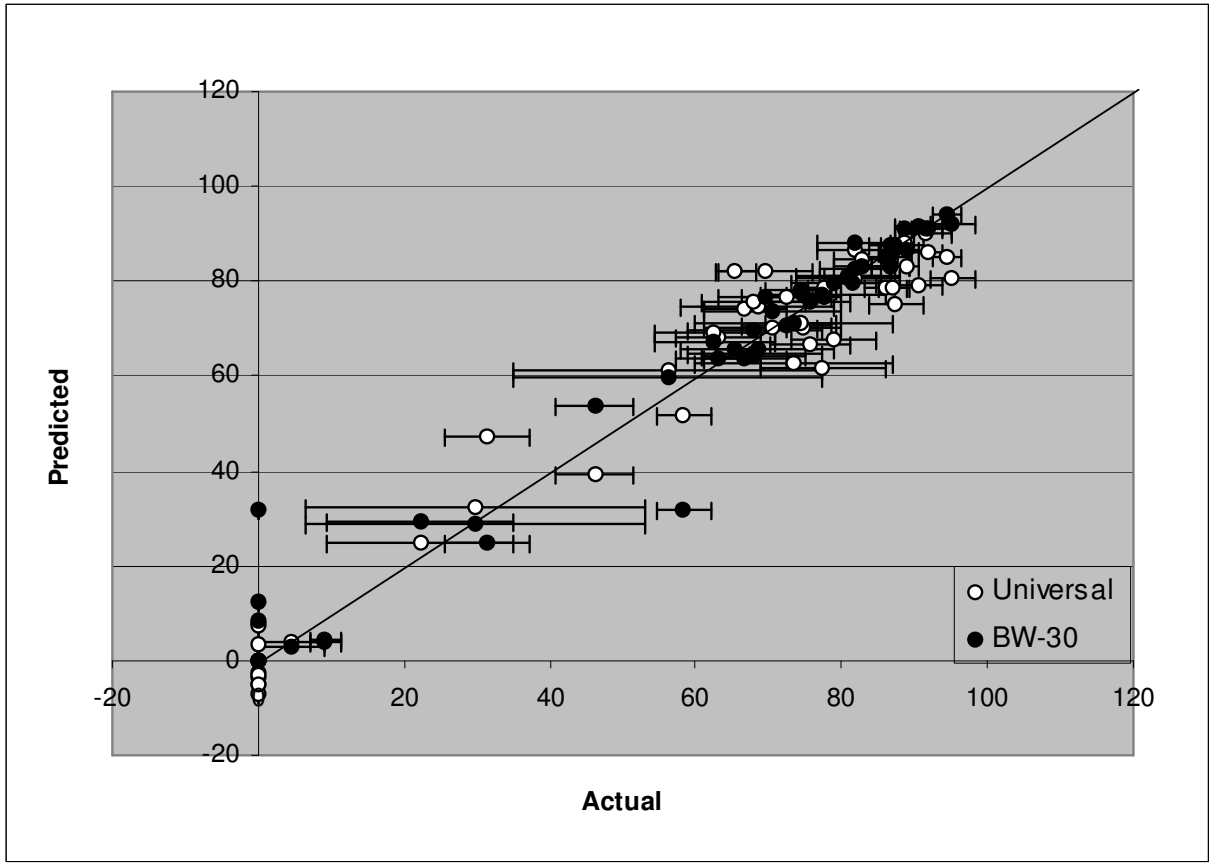

Figure 20c. Comparison of "Universal" PA Model Output to BW-30 – R-Flux
The closed circles represent the specific PA membrane model and the opened circles represent the "Universal" PA model. The "Universal" PA model agrees reasonably well with the BW-30 model.

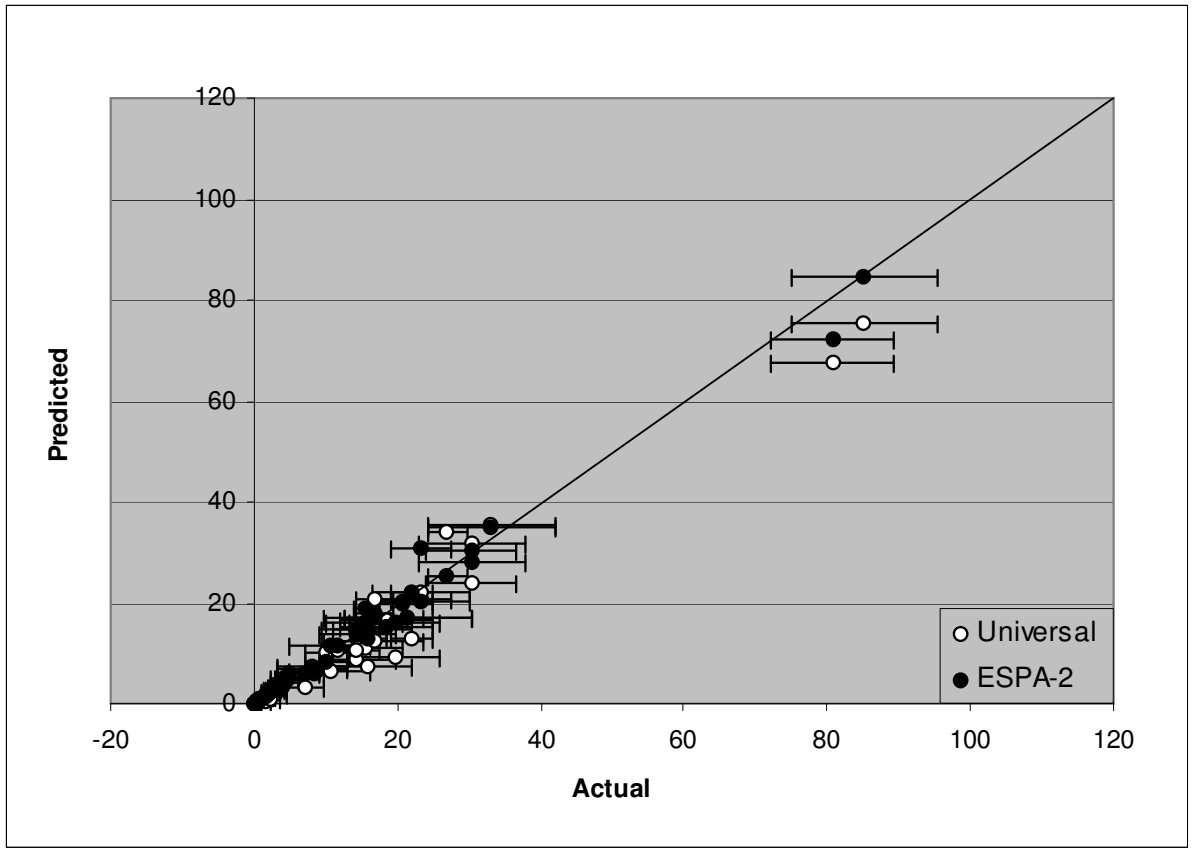

Figure 21a. Comparison of "Universal" PA Model Output to ESPA-2 – P-Flux
The closed circles represent the specific PA membrane model and the opened circles represent the "Universal" PA model. The "Universal" PA model agrees reasonably well with the ESPA-2 model.

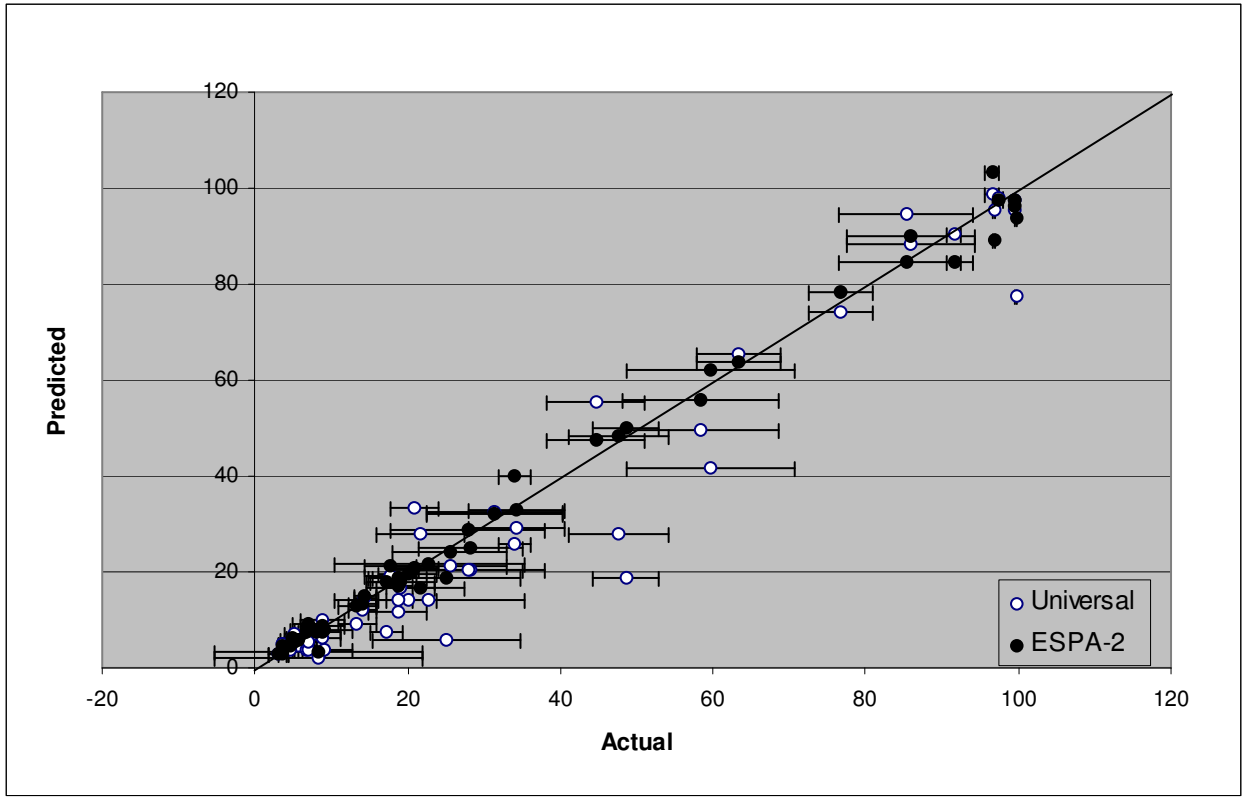

Figure 21b. Comparison of "Universal" PA Model Output to ESPA-2 – M-Flux
The closed circles represent the specific PA membrane model and the opened circles represent the "Universal" PA model. The "Universal" PA model agrees reasonably well with the ESPA-2 model.

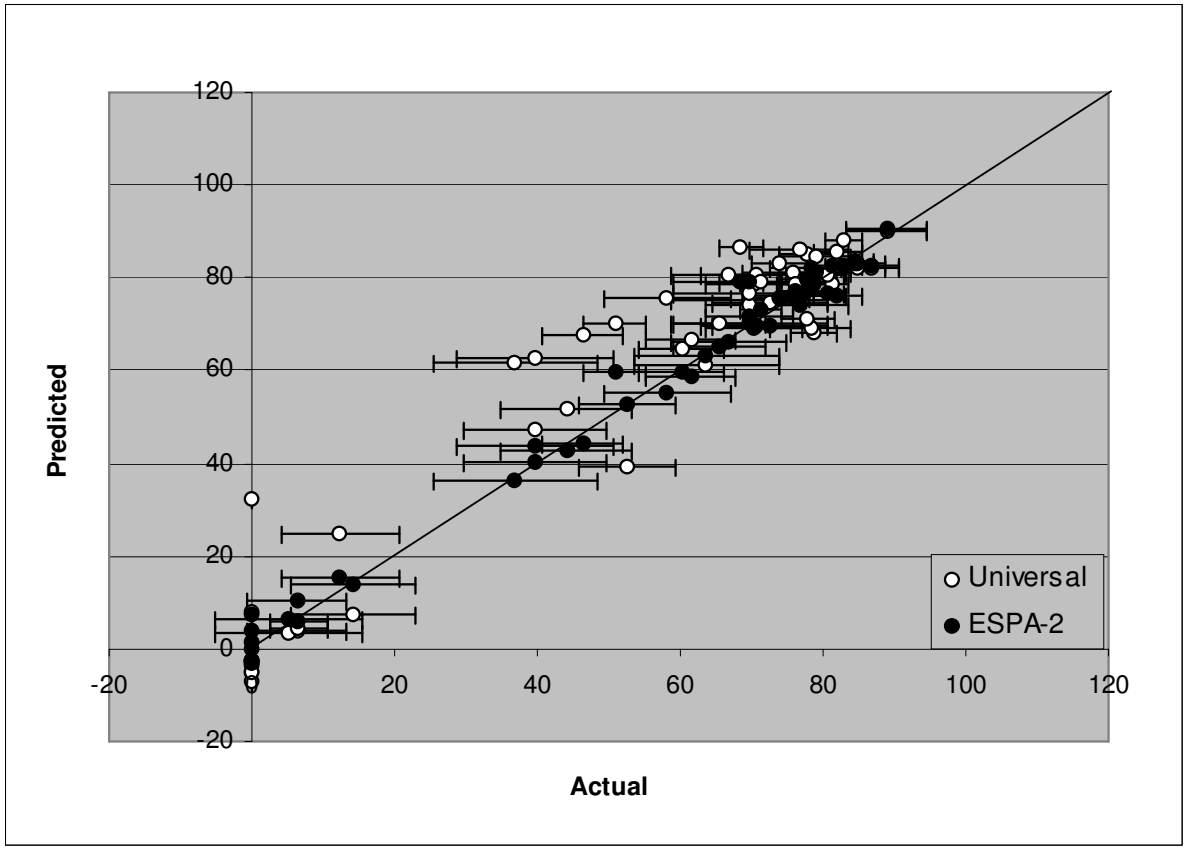

Figure 21c. Comparison of "Universal" PA Model Output to ESPA-2 – R-Flux
The closed circles represent the specific PA membrane model and the opened circles represent the "Universal" PA model. The "Universal" PA model agrees reasonably well with the ESPA-2 model.

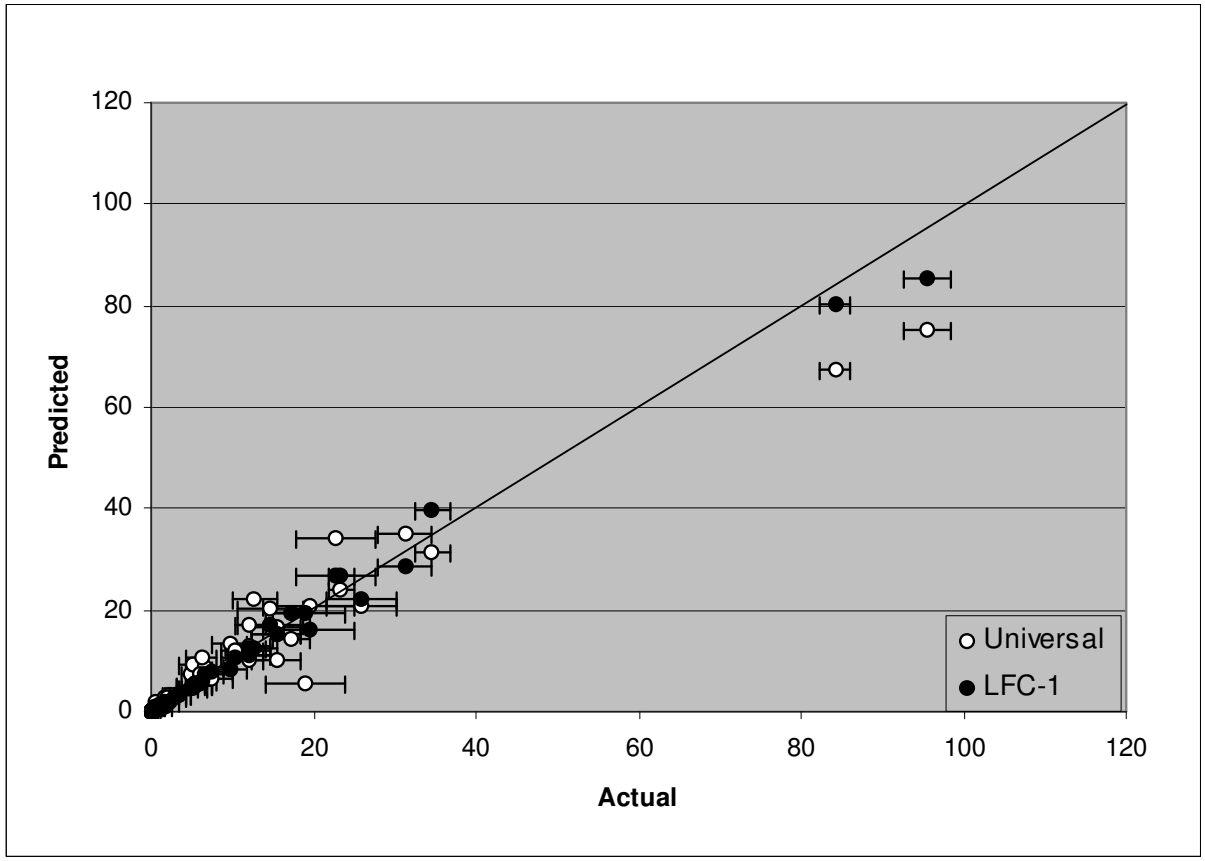

Figure 22a. Comparison of "Universal" PA Model Output to LFC-1 – P-Flux
The closed circles represent the specific PA membrane model and the opened circles represent the "Universal" PA model. The "Universal" PA model agrees reasonably well with the LFC-1 model.

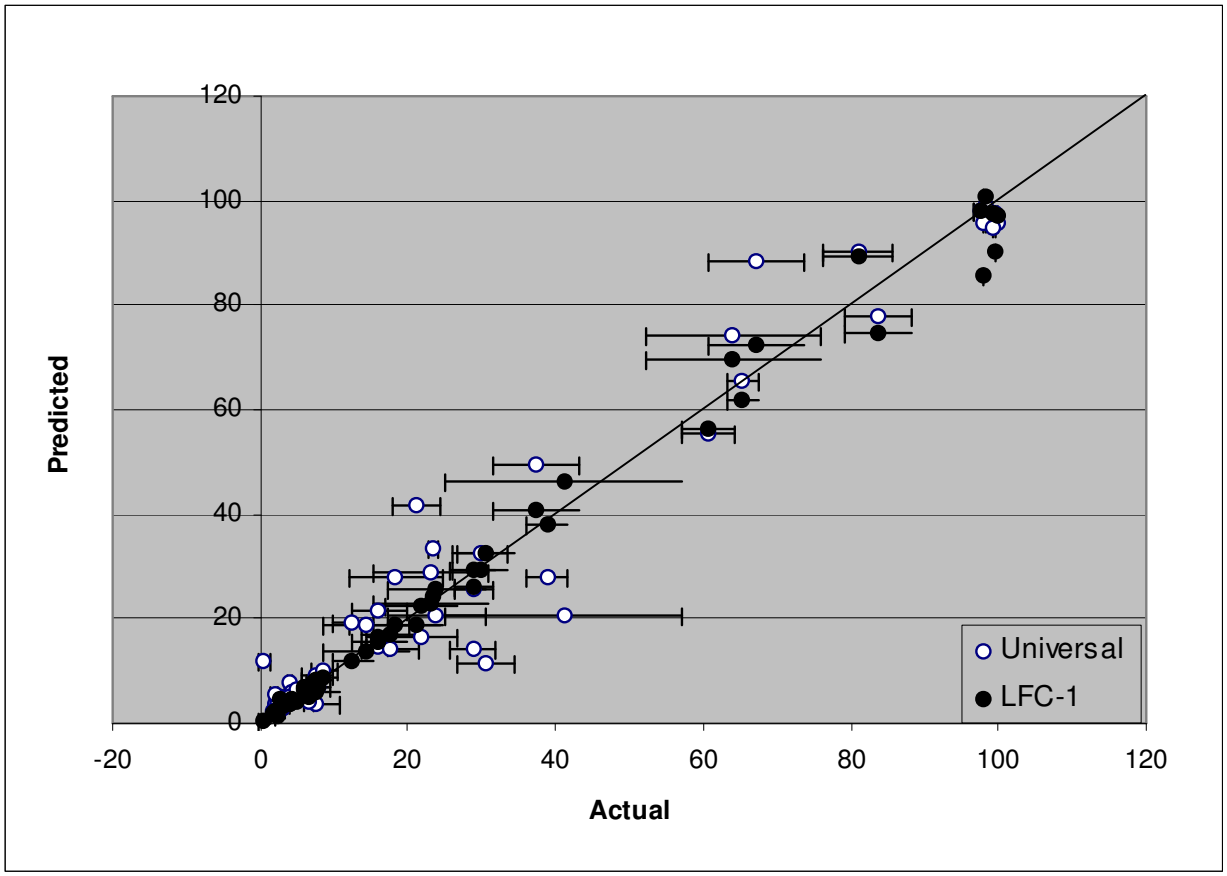

Figure 22b. Comparison of "Universal" PA Model Output to LFC-1 – M-Flux
The closed circles represent the specific PA membrane model and the opened circles represent the "Universal" PA model. The "Universal" PA model agrees reasonably well with the LFC-1 model.

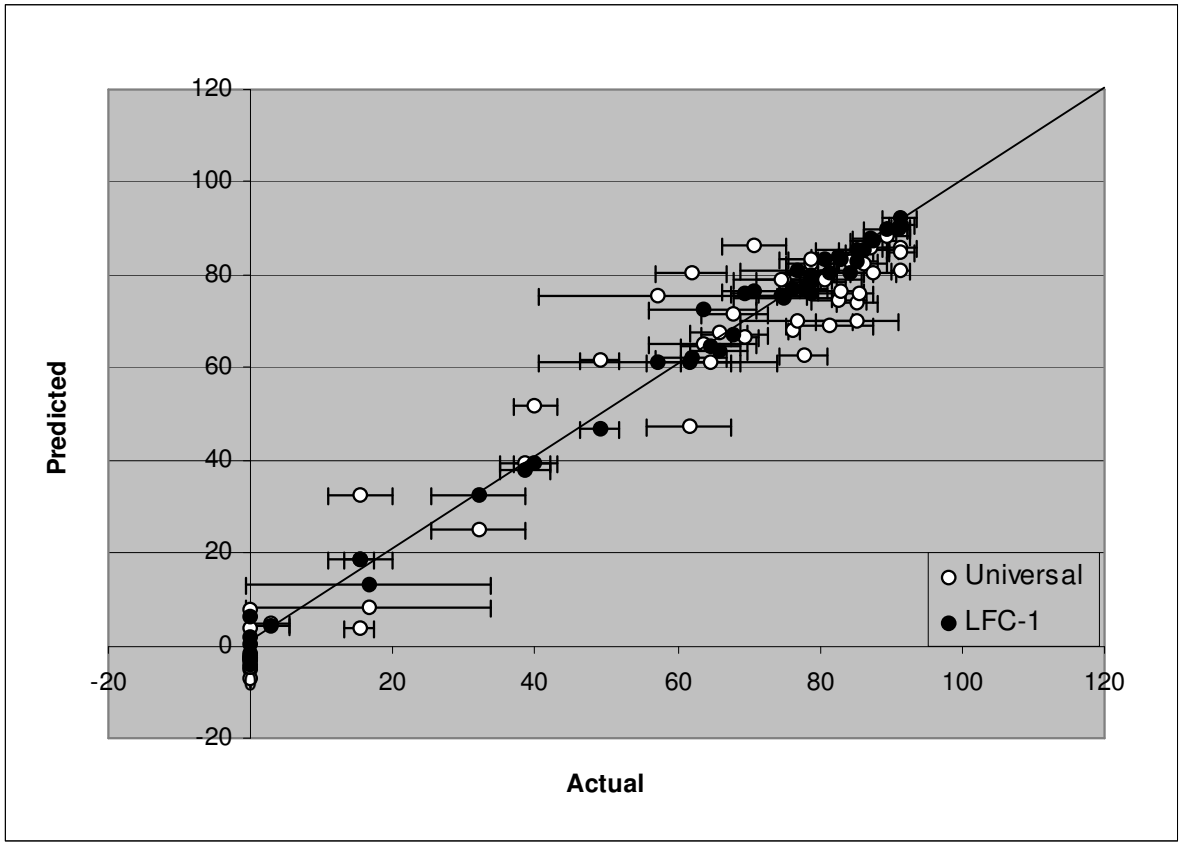

Figure 22c. Comparison of "Universal" PA Model Output to LFC-1 – R-Flux
The closed circles represent the specific PA membrane model and the opened circles represent the "Universal" PA model. The "Universal" PA model agrees reasonably well with the LFC-1 model.

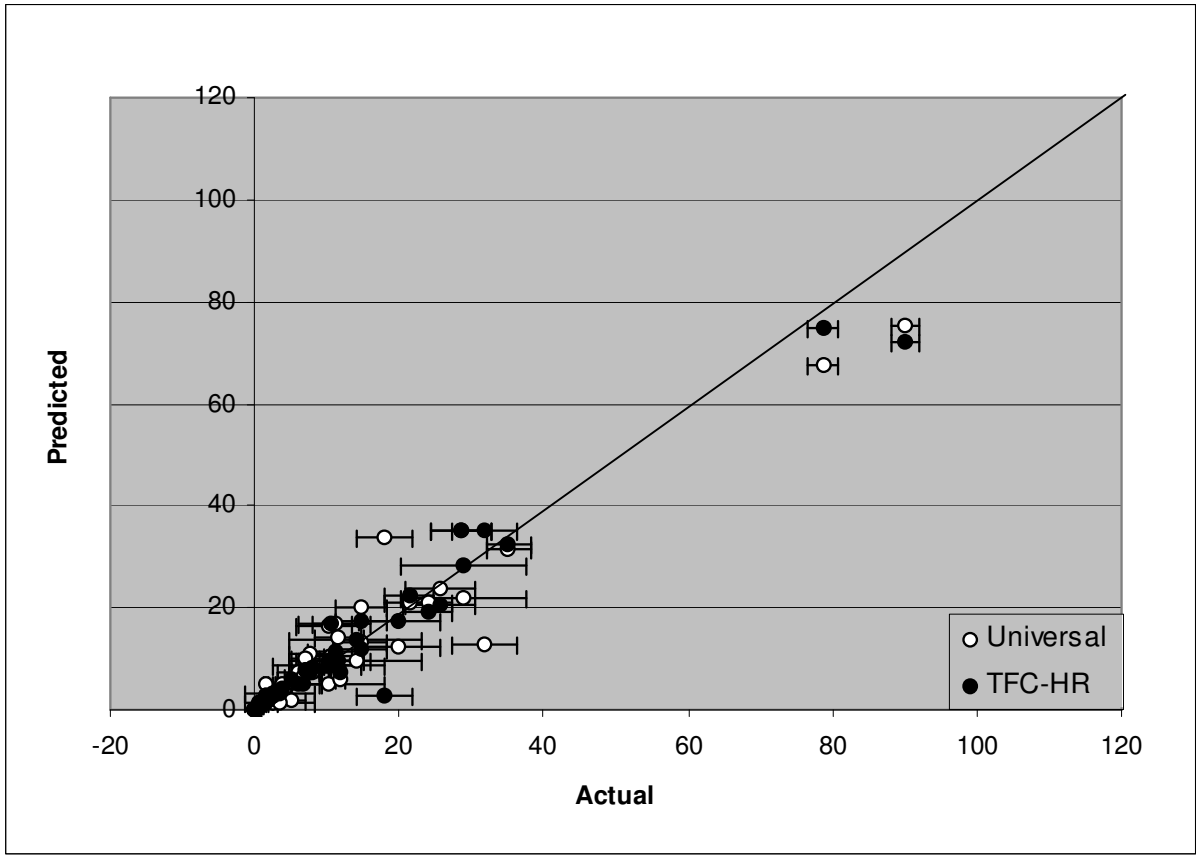

Figure 23a. Comparison of "Universal" PA Model Output to TFC-HR – P-Flux
The closed circles represent the specific PA membrane model and the opened circles represent the "Universal" PA model. The "Universal" PA model agrees reasonably well with the TFC-HR model.

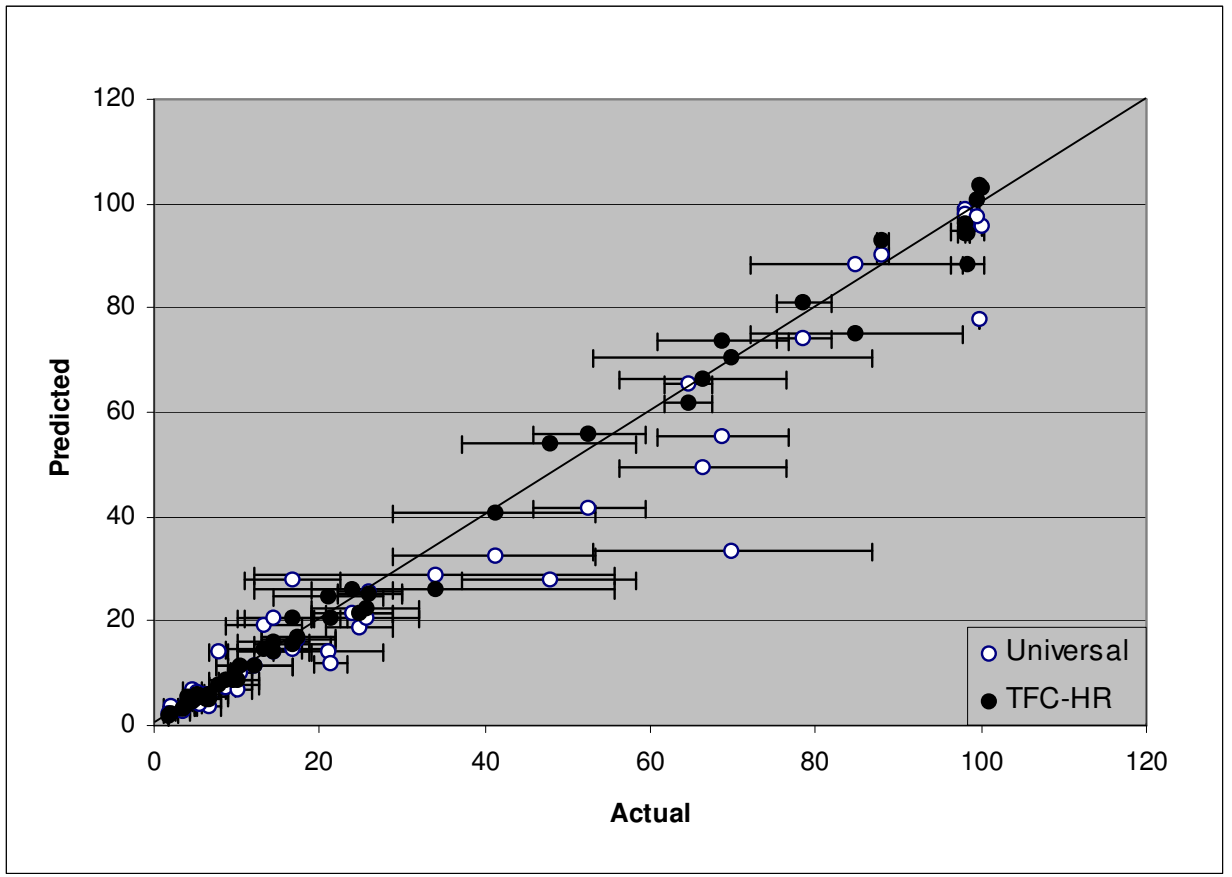

Figure 23b. Comparison of "Universal" PA Model Output to TFC-HR – M-Flux
The closed circles represent the specific PA membrane model and the opened circles represent the "Universal" PA model. The "Universal" PA model agrees reasonably well with the TFC-HR model.

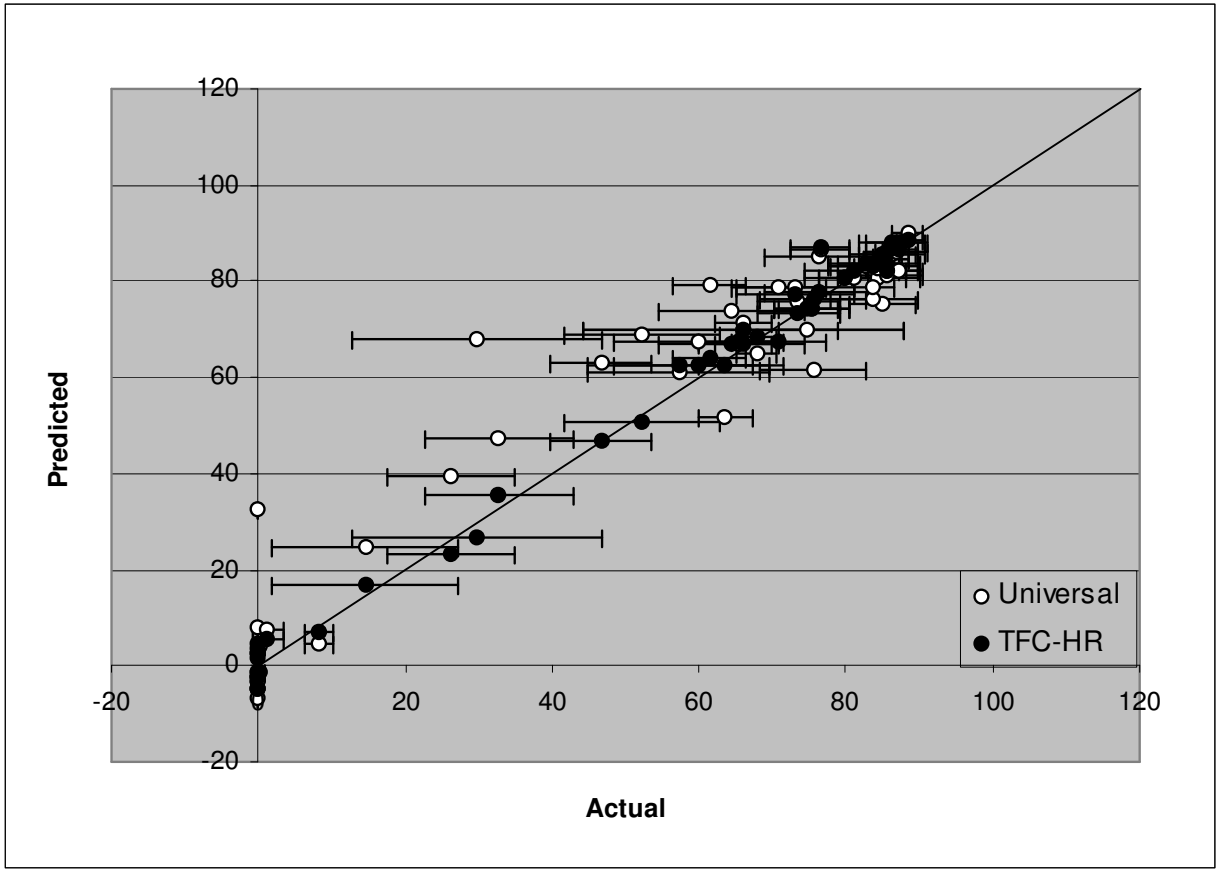

Figure 23c. Comparison of "Universal" PA Model Output to TFC-HR – R-Flux
The closed circles represent the specific PA membrane model and the opened circles represent the "Universal" PA model. The "Universal" PA model agrees reasonably well with the TFC-HR model.

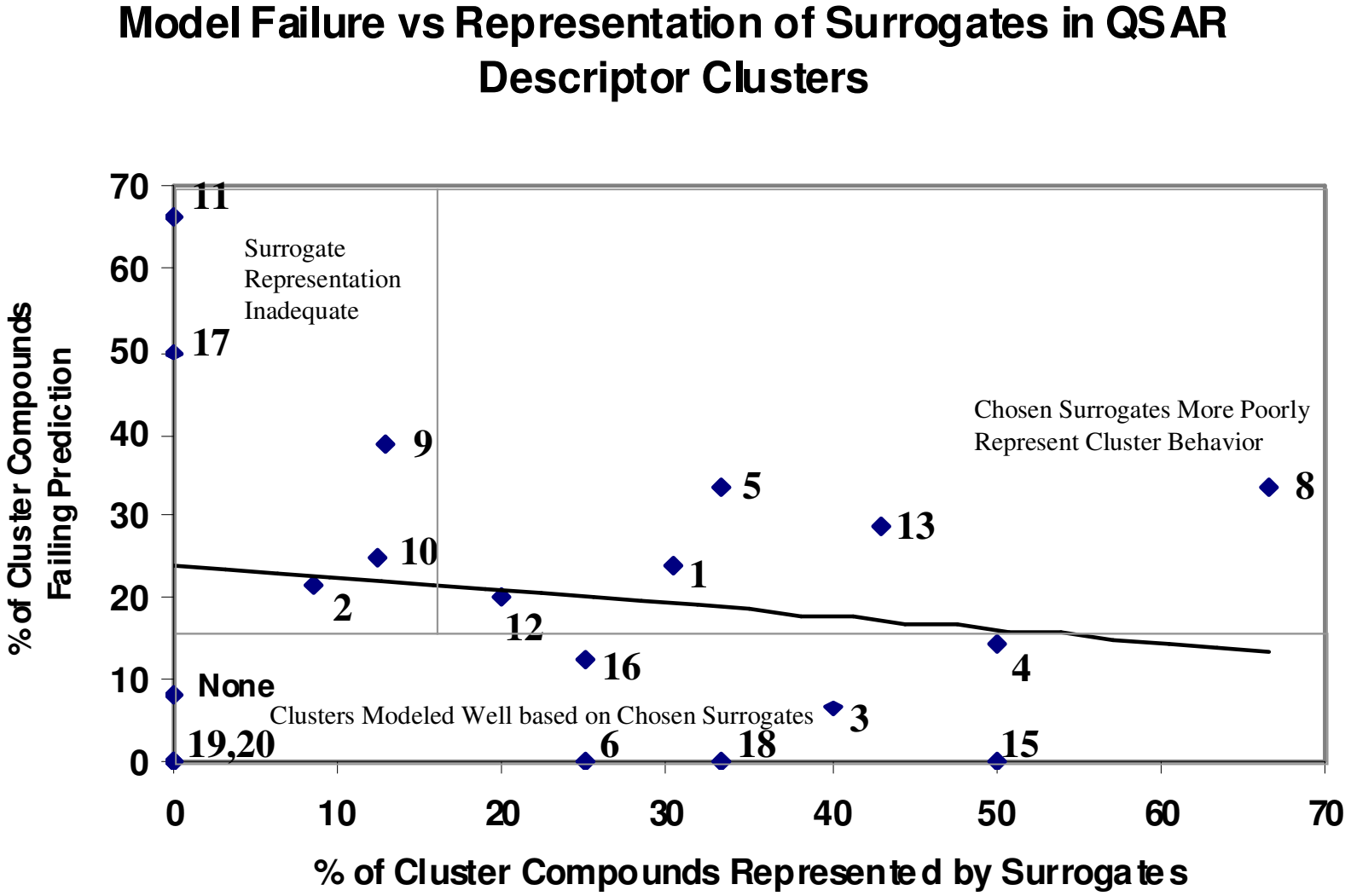

Figure 24. Model Failure vs Representation of Surrogates in QSAR Descriptor Clusters
This figure shows the relationship between the percentage of the cluster compounds represented by surrogate compounds and the percentage of compounds in each QSAR descriptor cluster that failed model prediction. Each QSAR descriptor cluster is indicated on the chart by numbers.

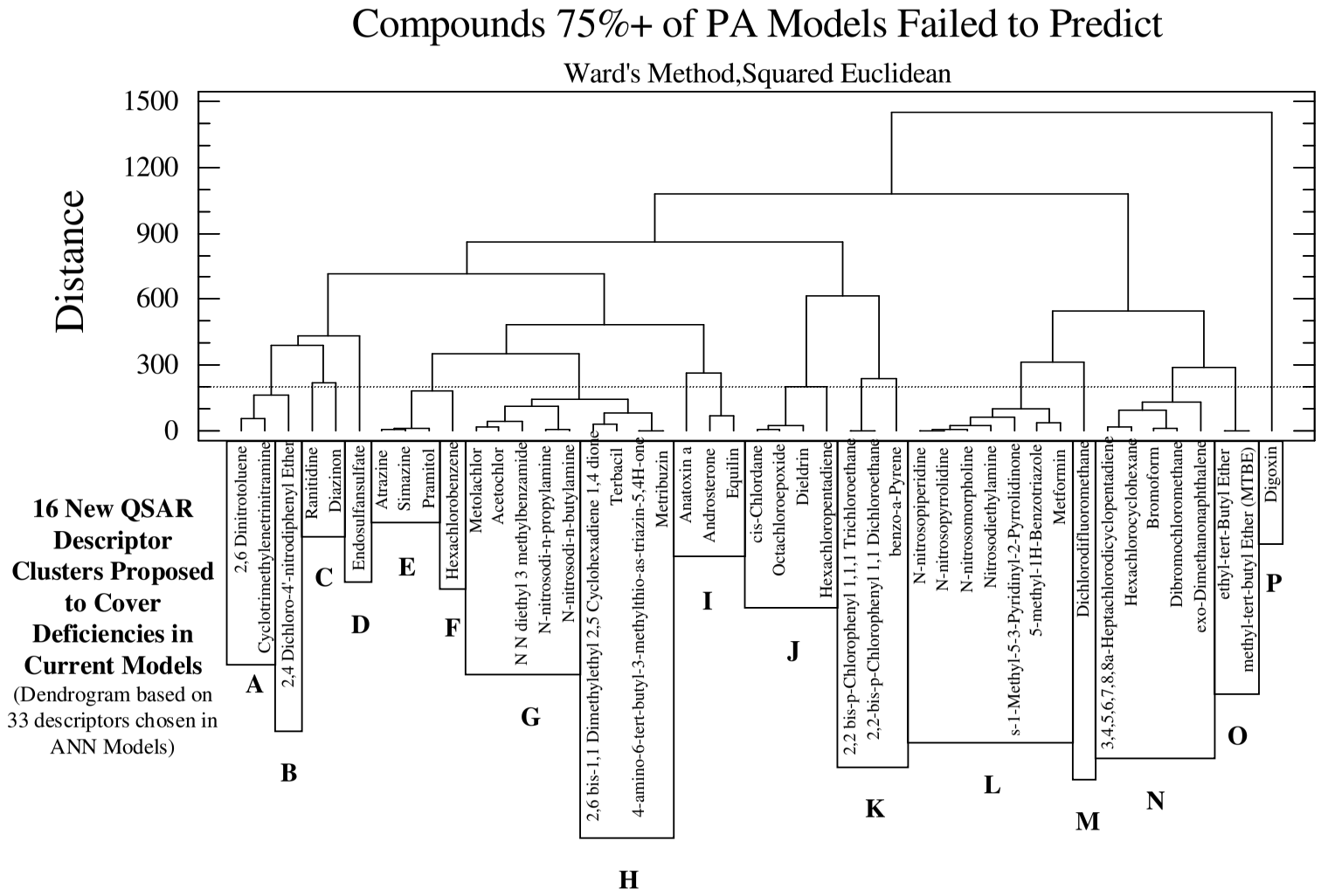

Figure 25. Dendrogram illustrating compounds that 75% or more of the PA Models Failed to Predict
The compounds that were identified in Fig. 24 are in this figure, clustered by similar QSAR molecular descriptor properties using dendritic analysis. The identified clusters are shown in the figure in boxes. These clusters represent compounds whose properties were in general poorly represented in the original models. Inclusion of one or more surrogates from these clusters in the surrogate list should substantially improve predictability of the current models.

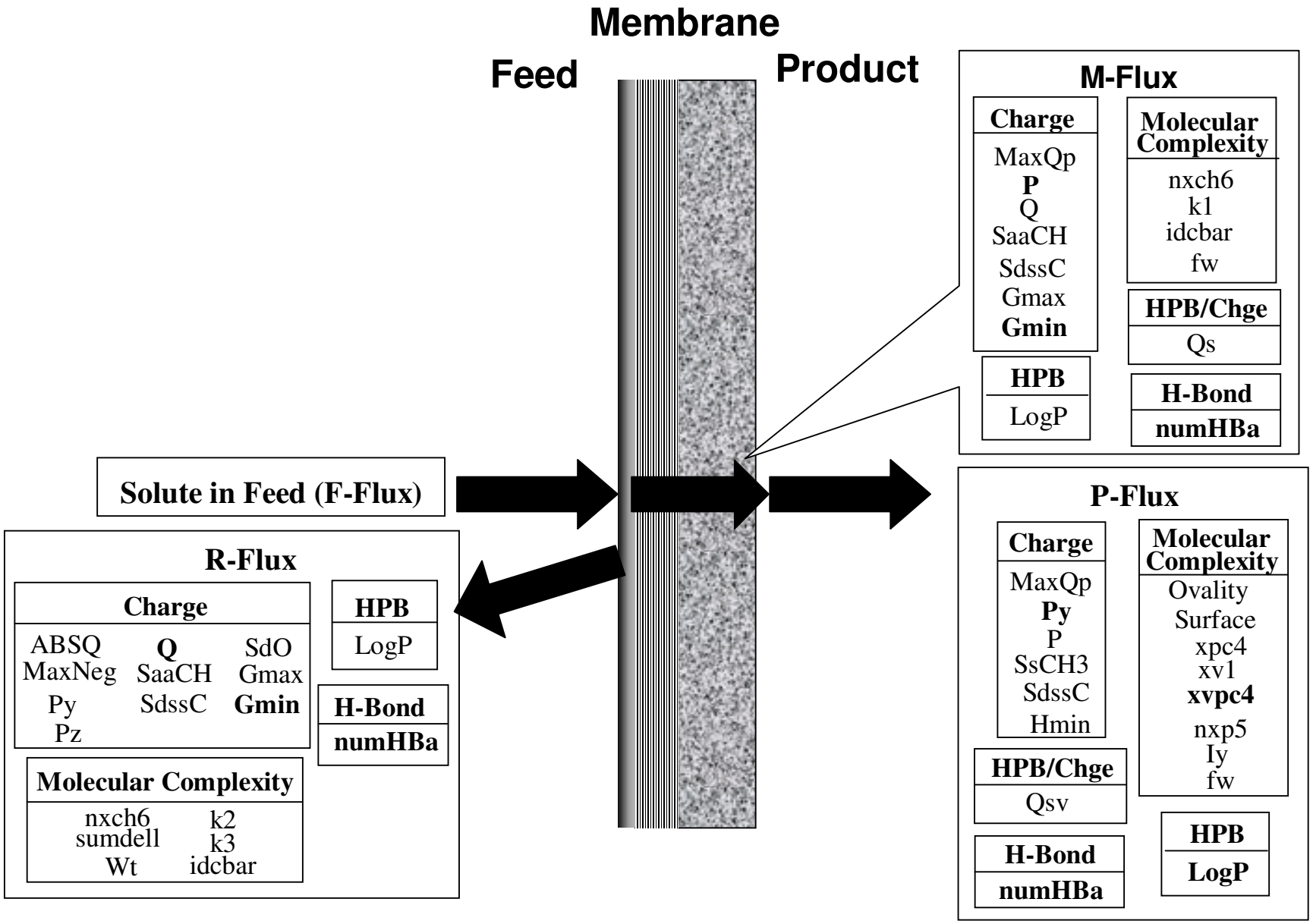

Figure 26. QSAR Molecular Descriptors Relating to Compound Transport
Bolded QSAR molecular descriptors indicate those that were common and most influential amongst the PA membranes

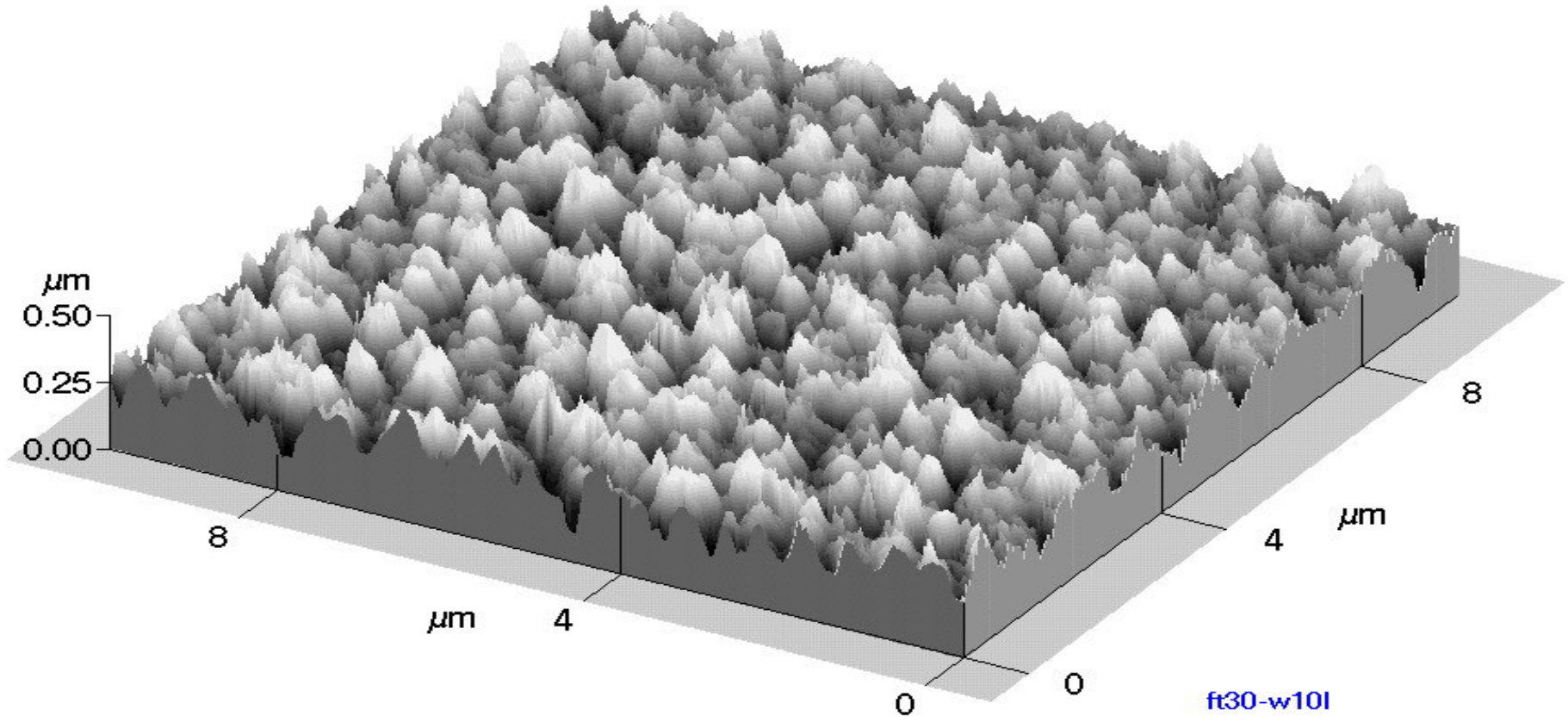

Figure 27. Atomic force microscope image of a polyamide TFC membrane showing rough feedwater surface. (Image courtesy of J Safarik, Orange County Water District).

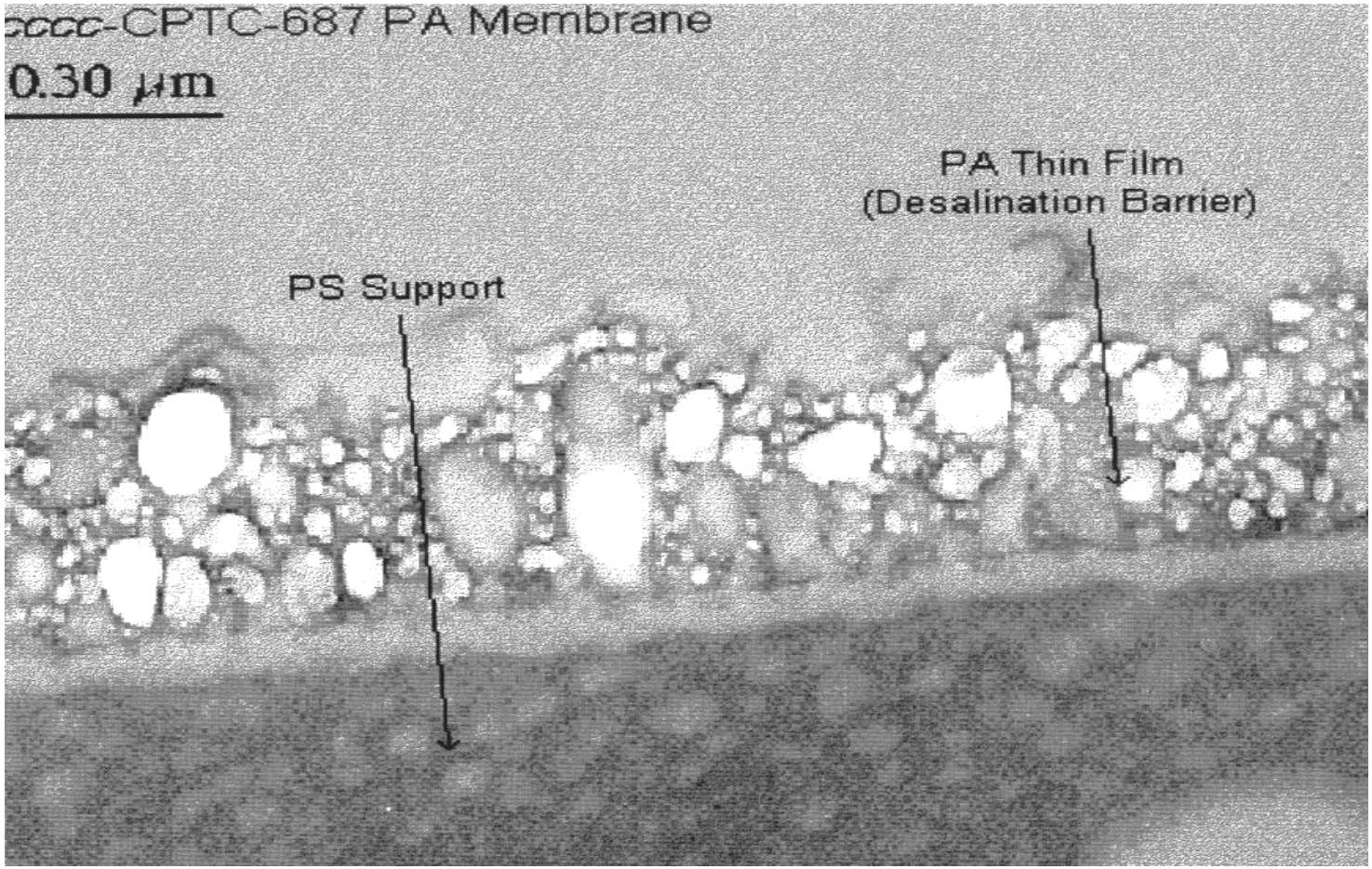

Figure 28. Transmission electron micrograph of an experimental polyamide TFC membrane showing spatial asymmetry and structural heterogeneity. Image courtesy of R. Riley, Separation Systems Technology.

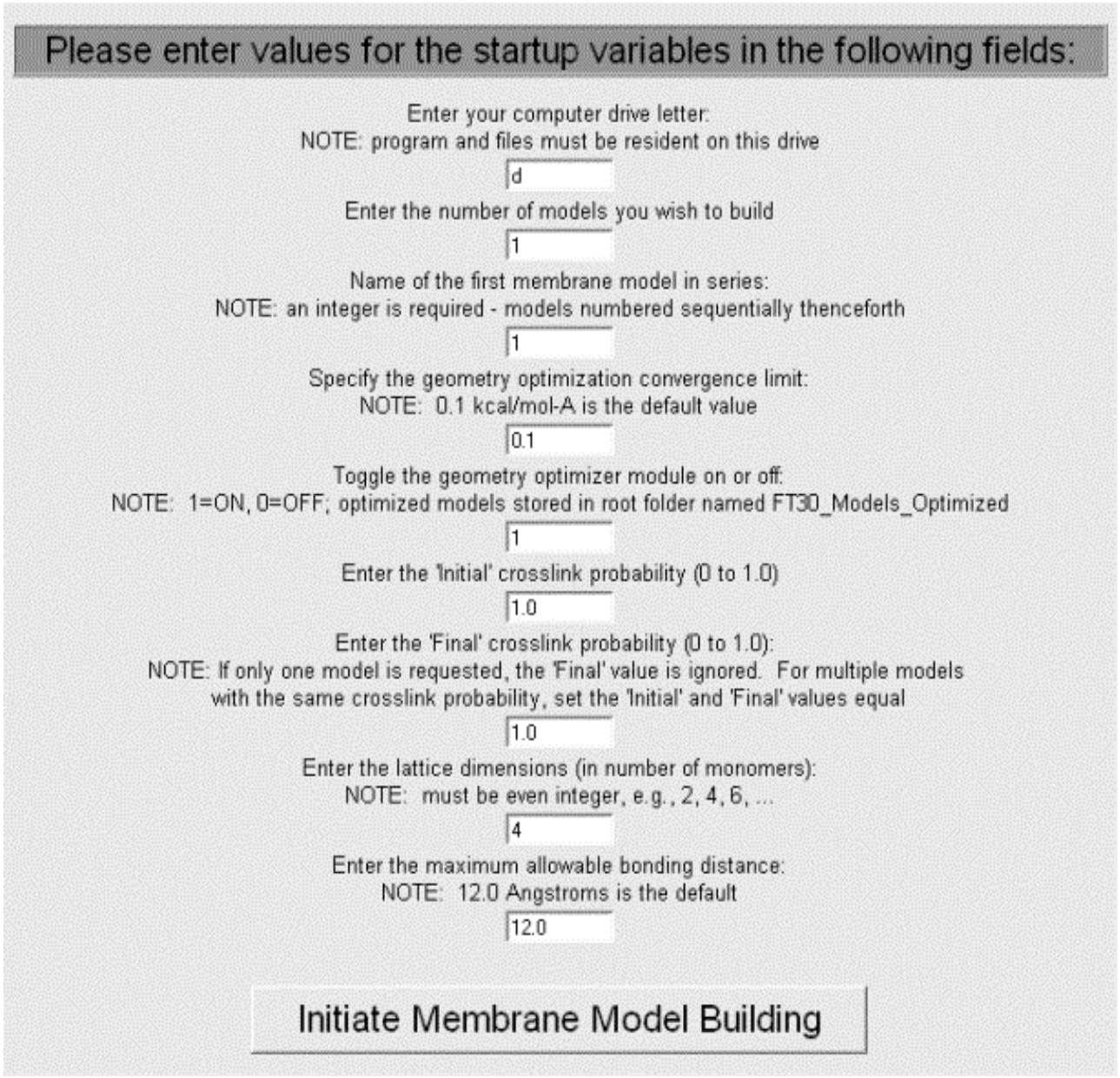

Figure 29. Screen capture of membrane build software. Note provisions for setting the degree of membrane crosslinking.

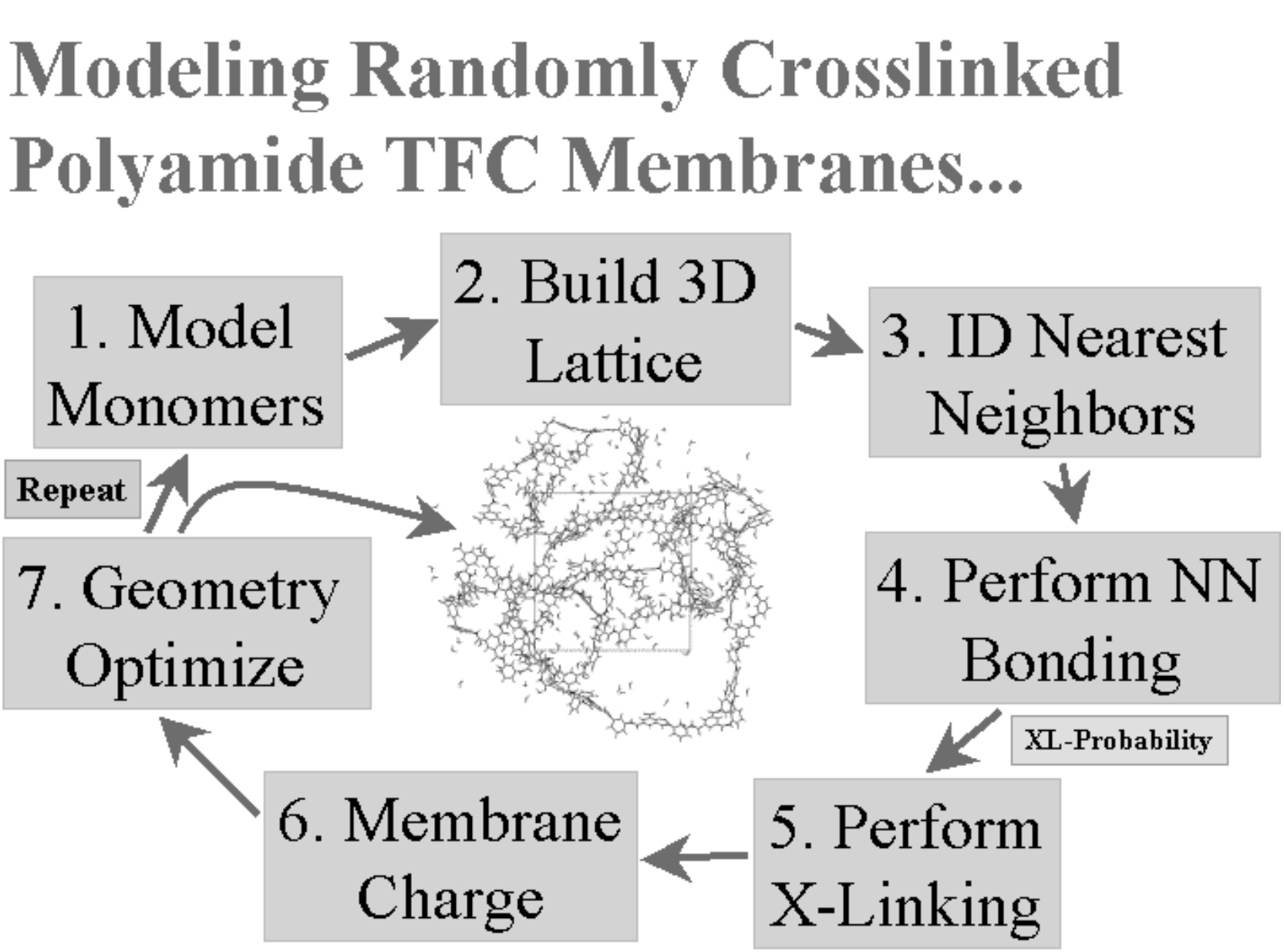

Figure 30. Main steps used in building crosslinked PA membrane models. NN = nearest neighbor.

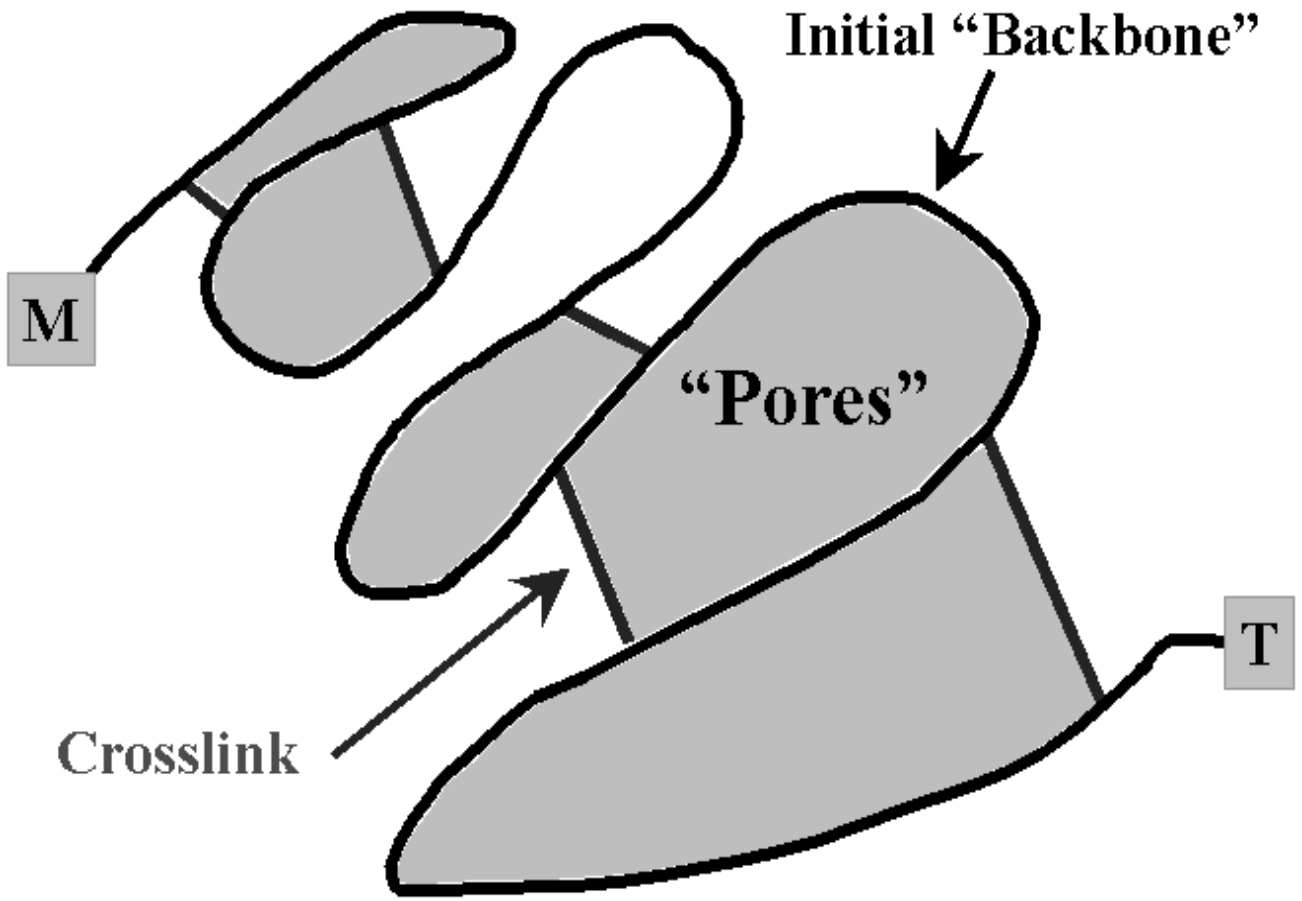

Figure 31 . Schematic illustrating the role of internal crosslinks in establishing membrane "pores" or void spaces.

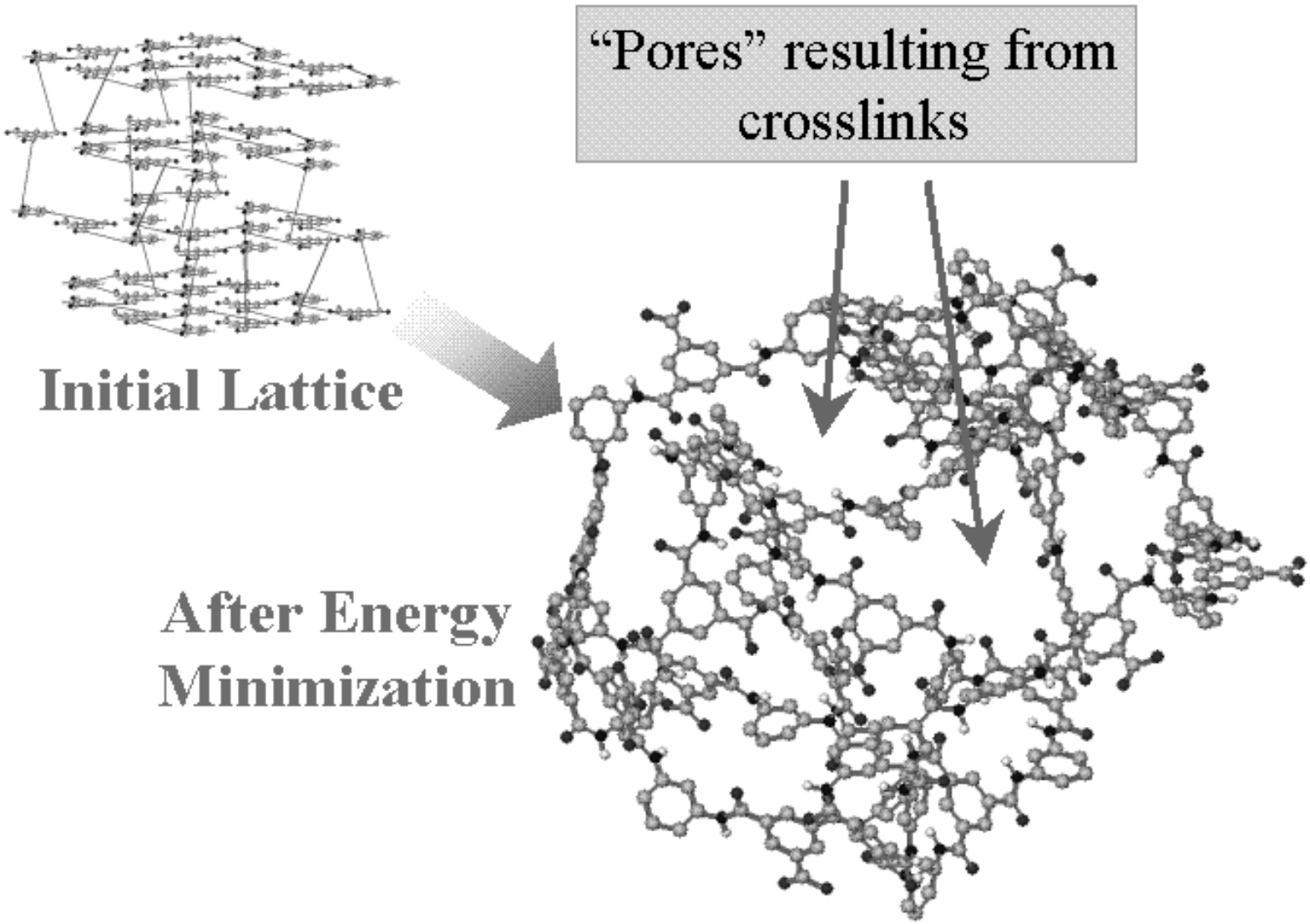

Figure 32. A PA membrane model before and after geometry optimization using the AMBER force field.

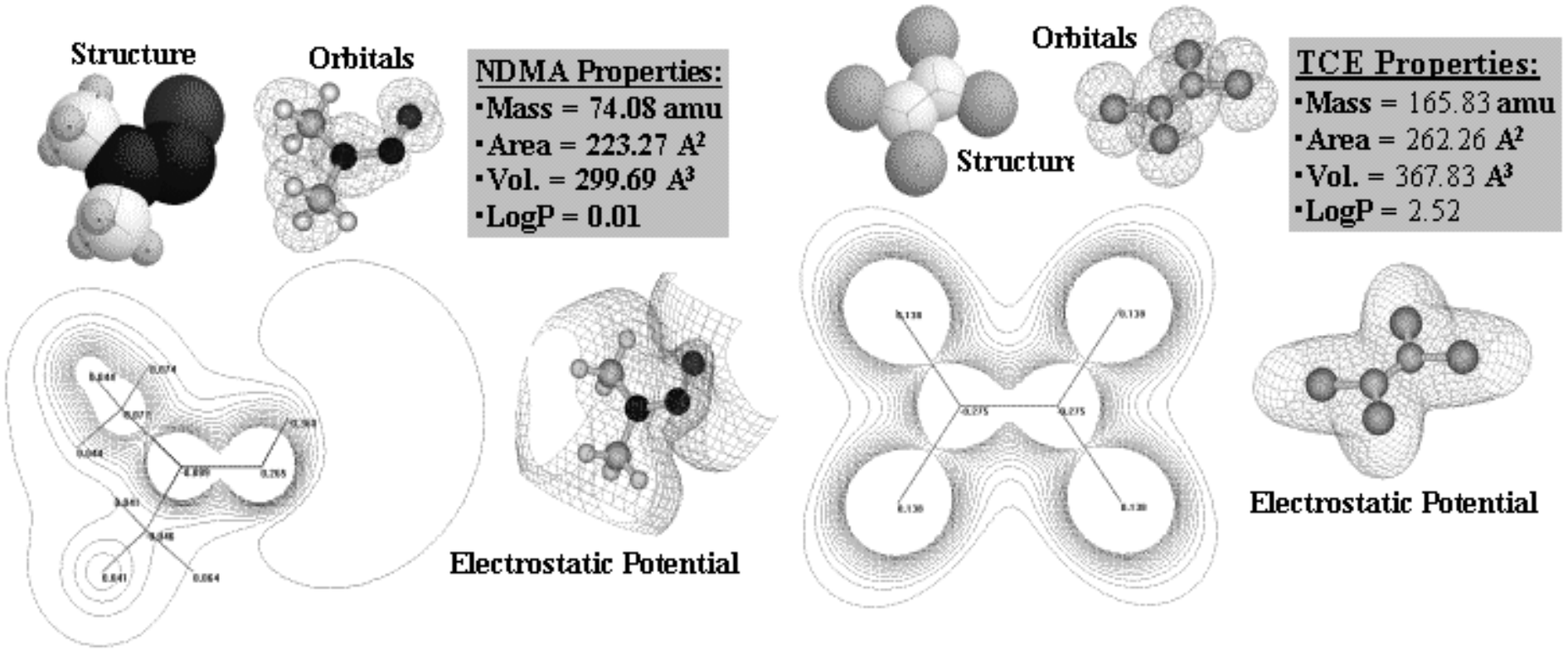

Figure 33. Model properties and atom partial charges for NDMA and PCE (mislabeled TCE in figure).

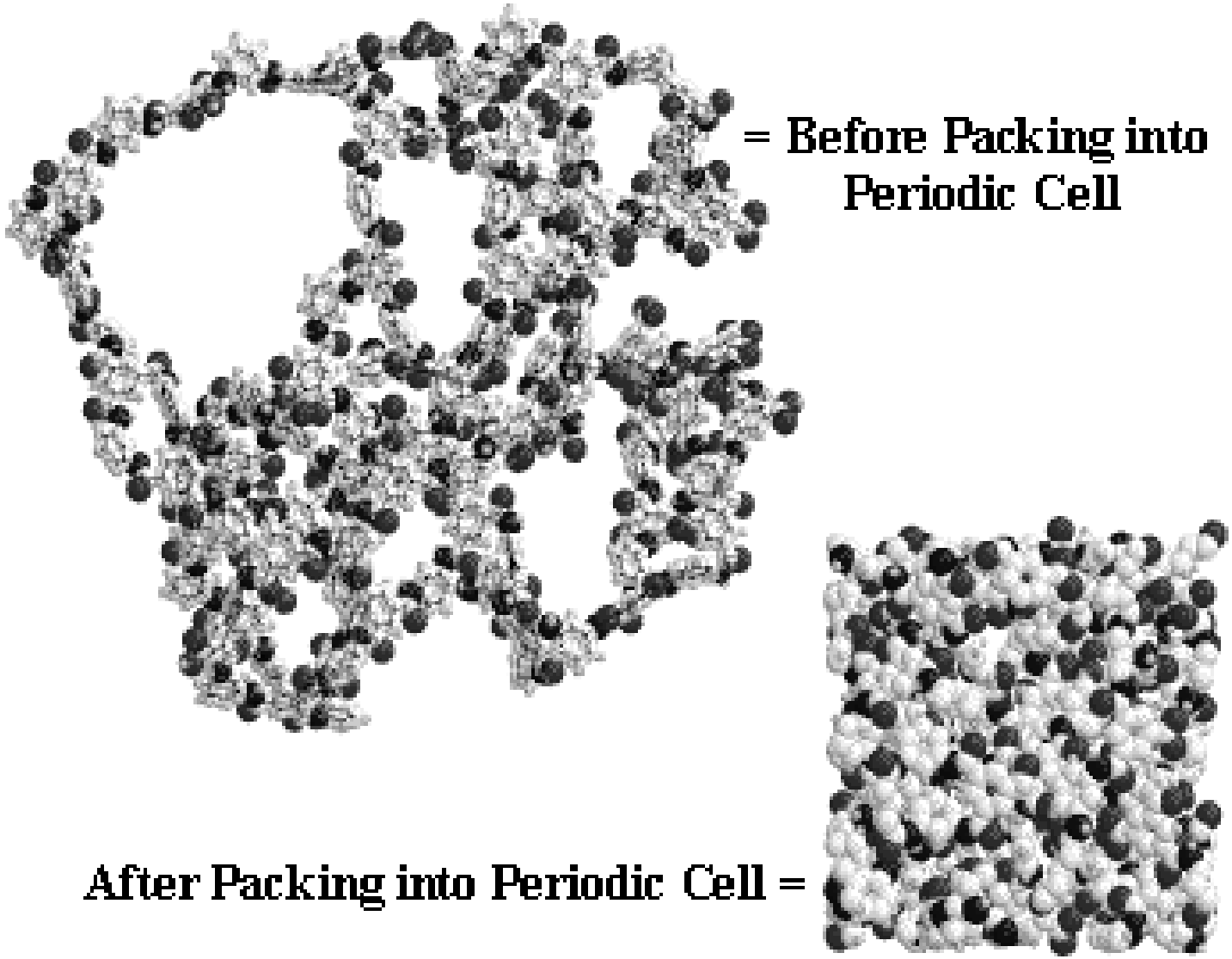

Figure 34. Structure of the FT30 membrane model before and after imposing periodic boundary conditions.

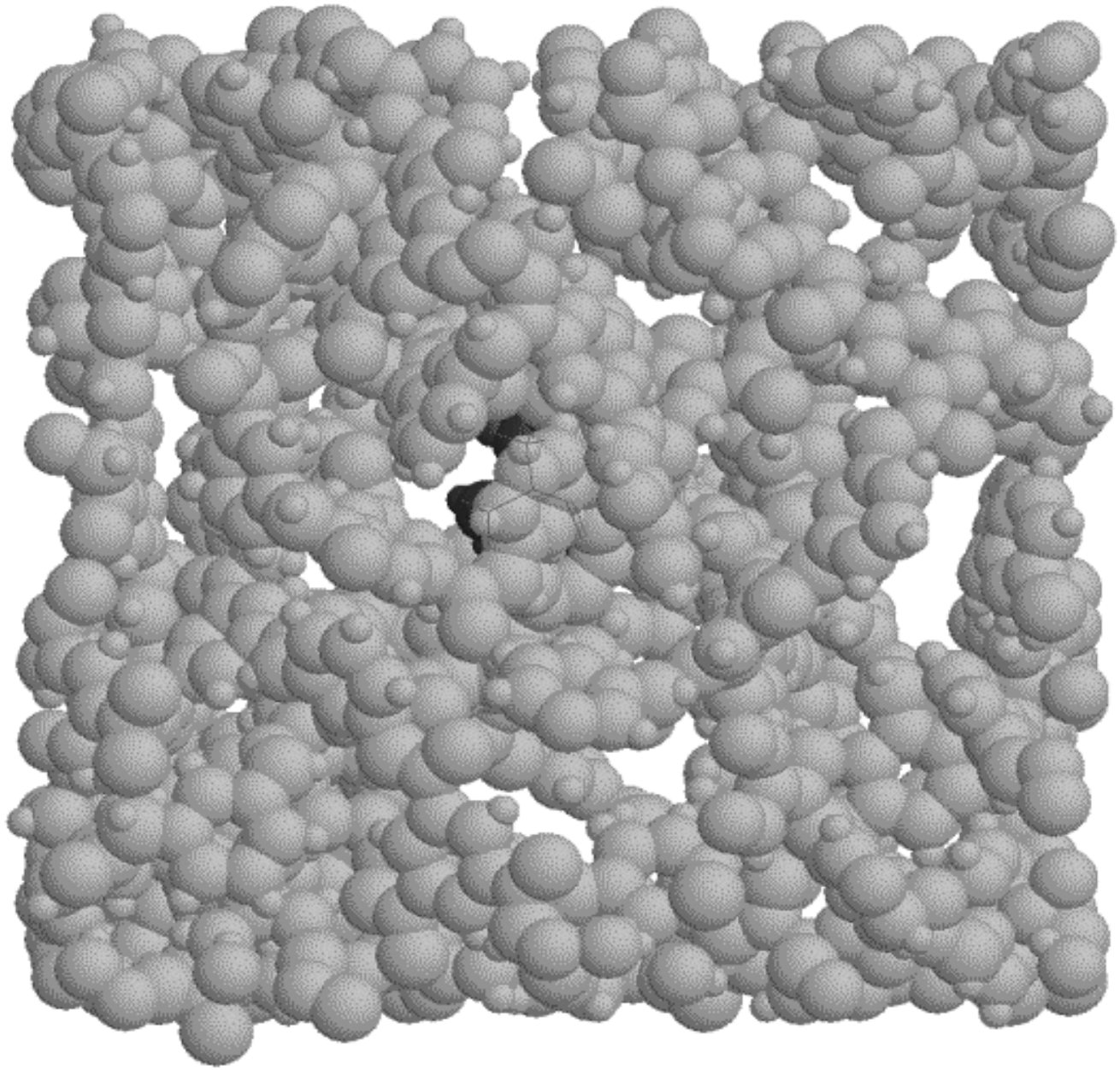

Figure 35. Compacted membrane with water removed. NDMA=dark gray; polymer=light gray.

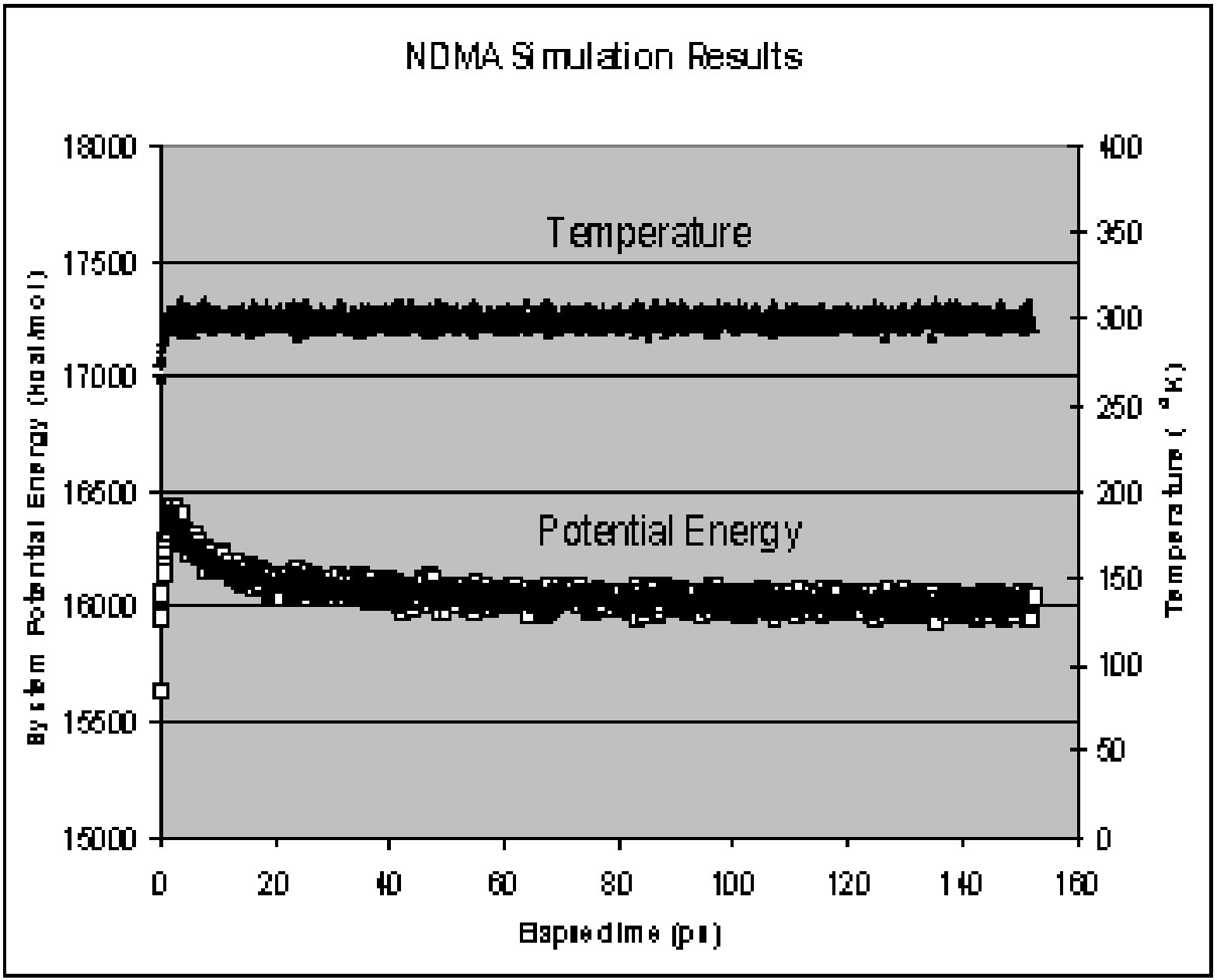

Figure 36. System potential energy and temperature for the NDMA simulation.

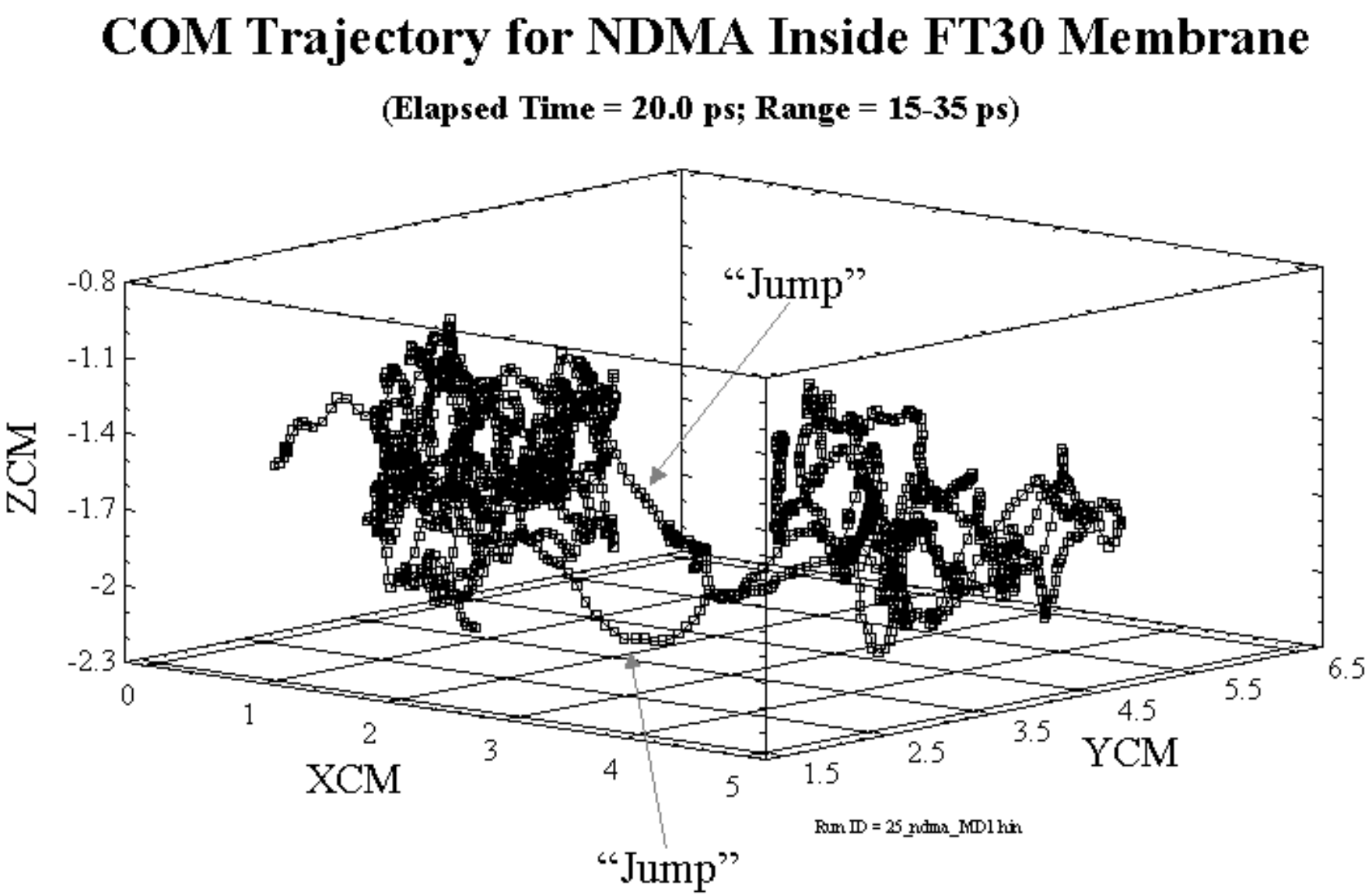

Figure 37. Three-axis plot showing trajectory of NDMA in membrane system between 15 and 35 ps.

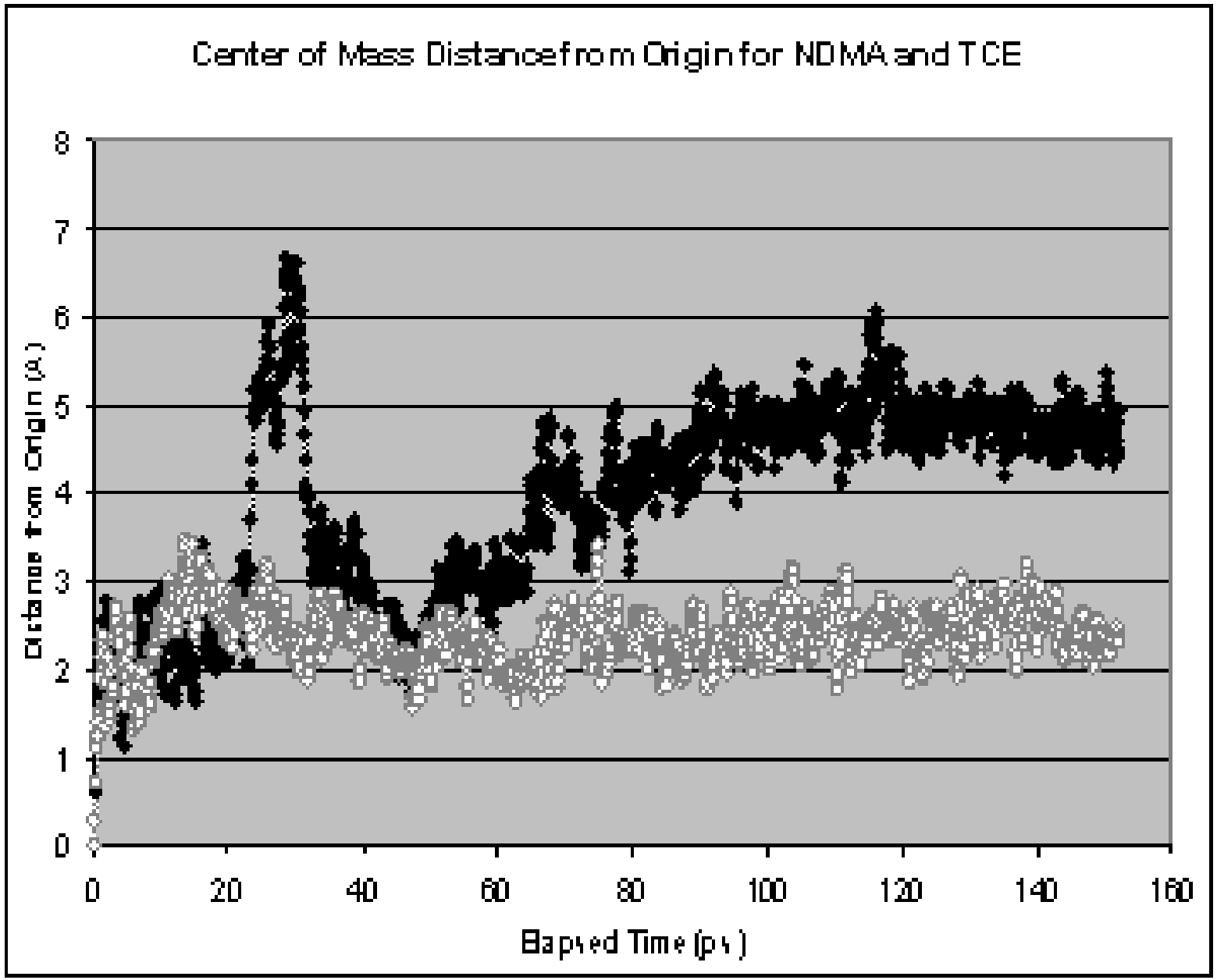

Figure 38. COM distances from the origin at t=0 ps for NDMA and PCE (mislabeled TCE in figure). Note that NDMA underwent two "jumps", a outbound jump beginning at about 20 ps and a return (inbound) jump at about 30 ps.

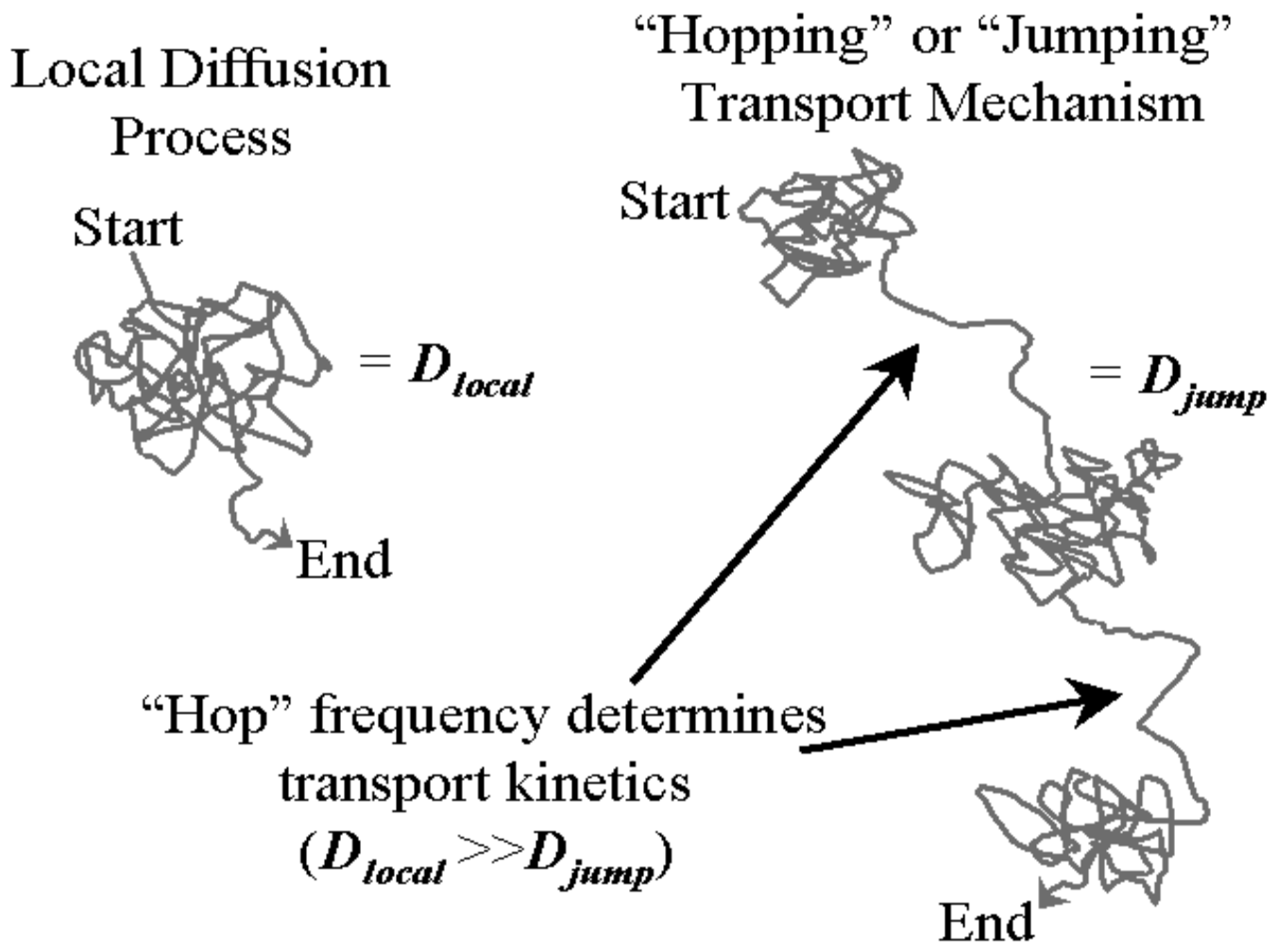

Figure 39. Schematic illustrating the concept of diffusional jumps or hops. A separate "diffusion coefficient" may be computed based on jump magnitude and frequency while ignoring local free diffusion.

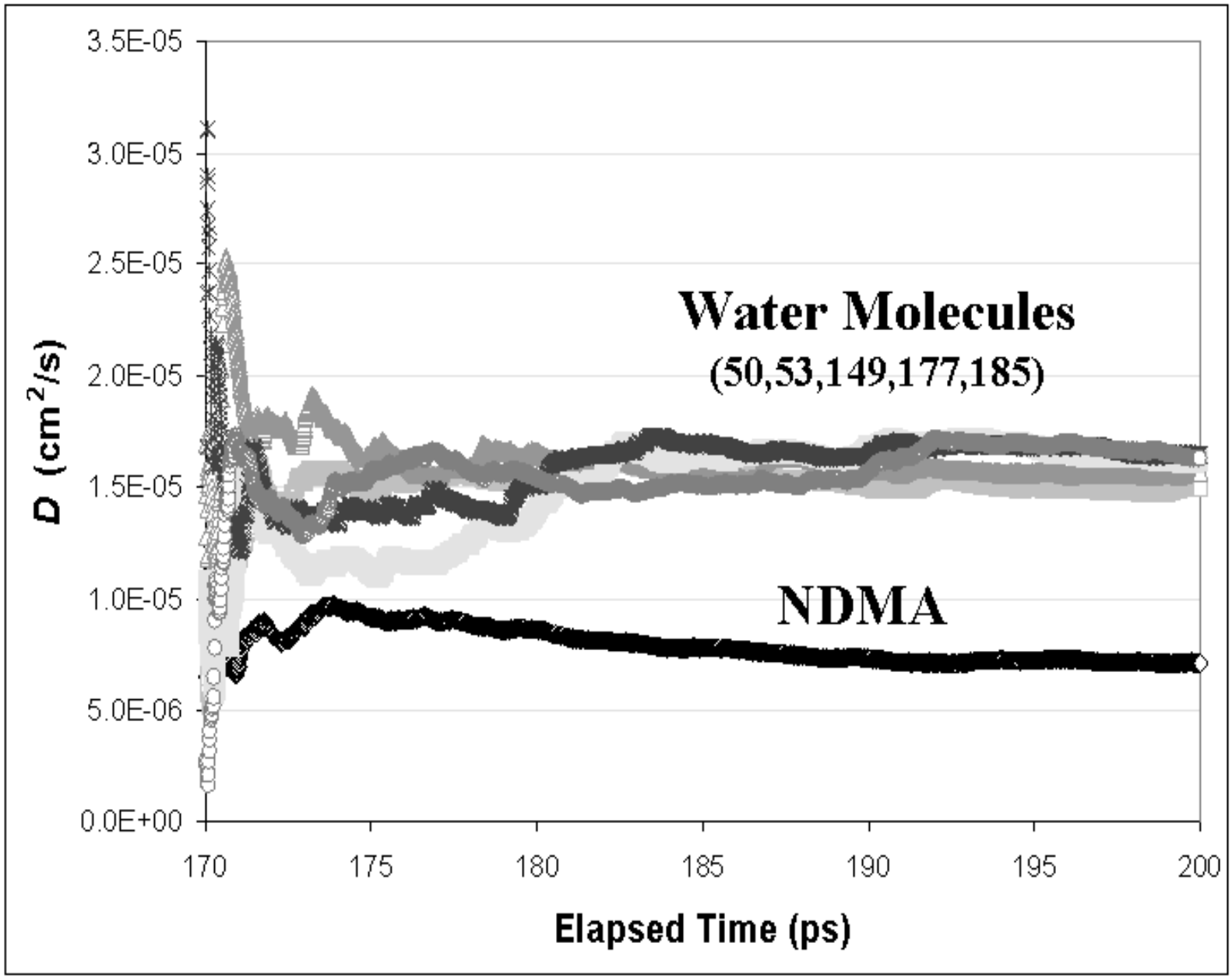

Figure 40. Calculated diffusion coefficients for five randomly chosen water molecules and NDMA.

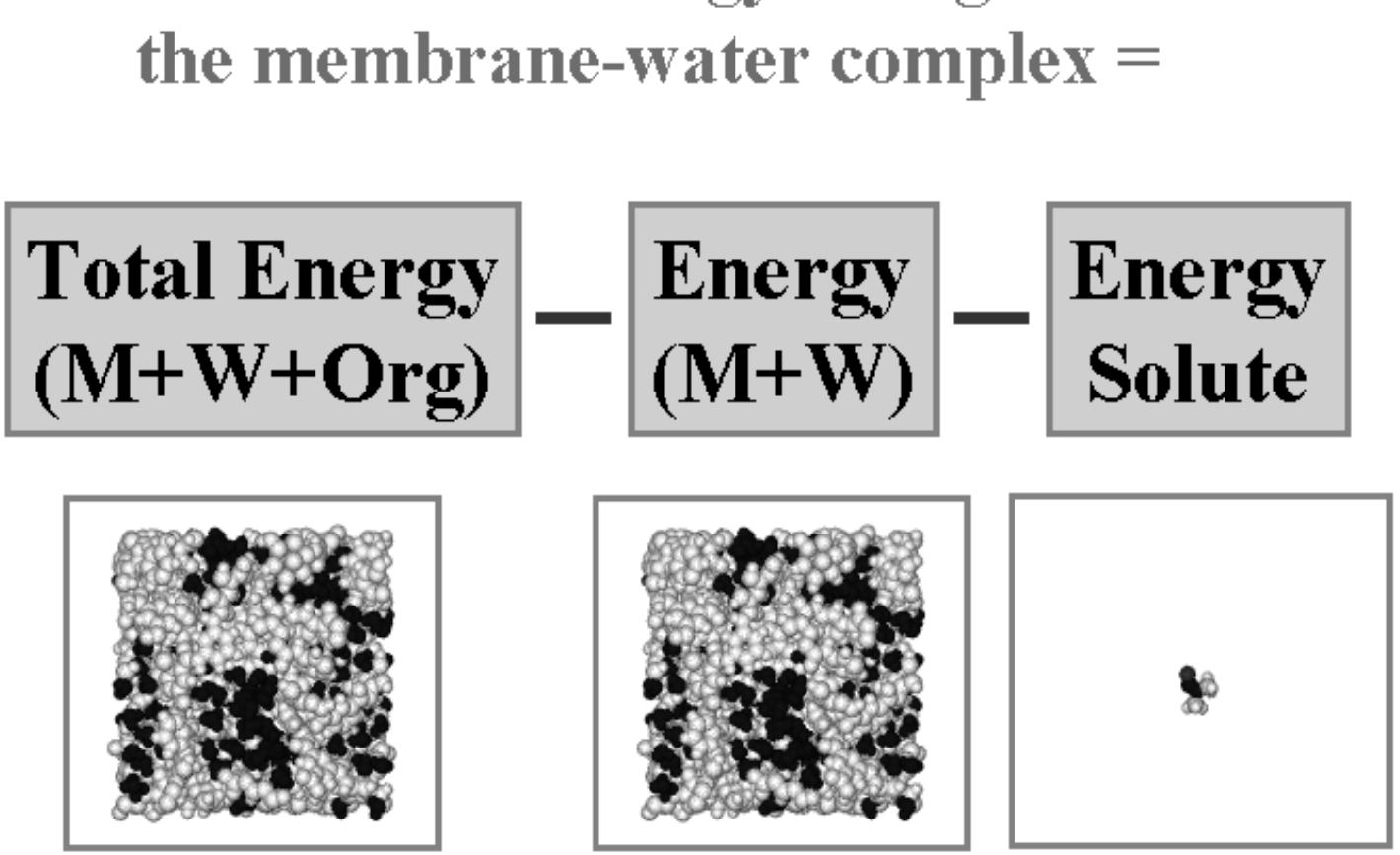

Figure 41. Schematic showing method for estimating the energy of association ("interaction energy") of the organic solute with the membrane-water complex.

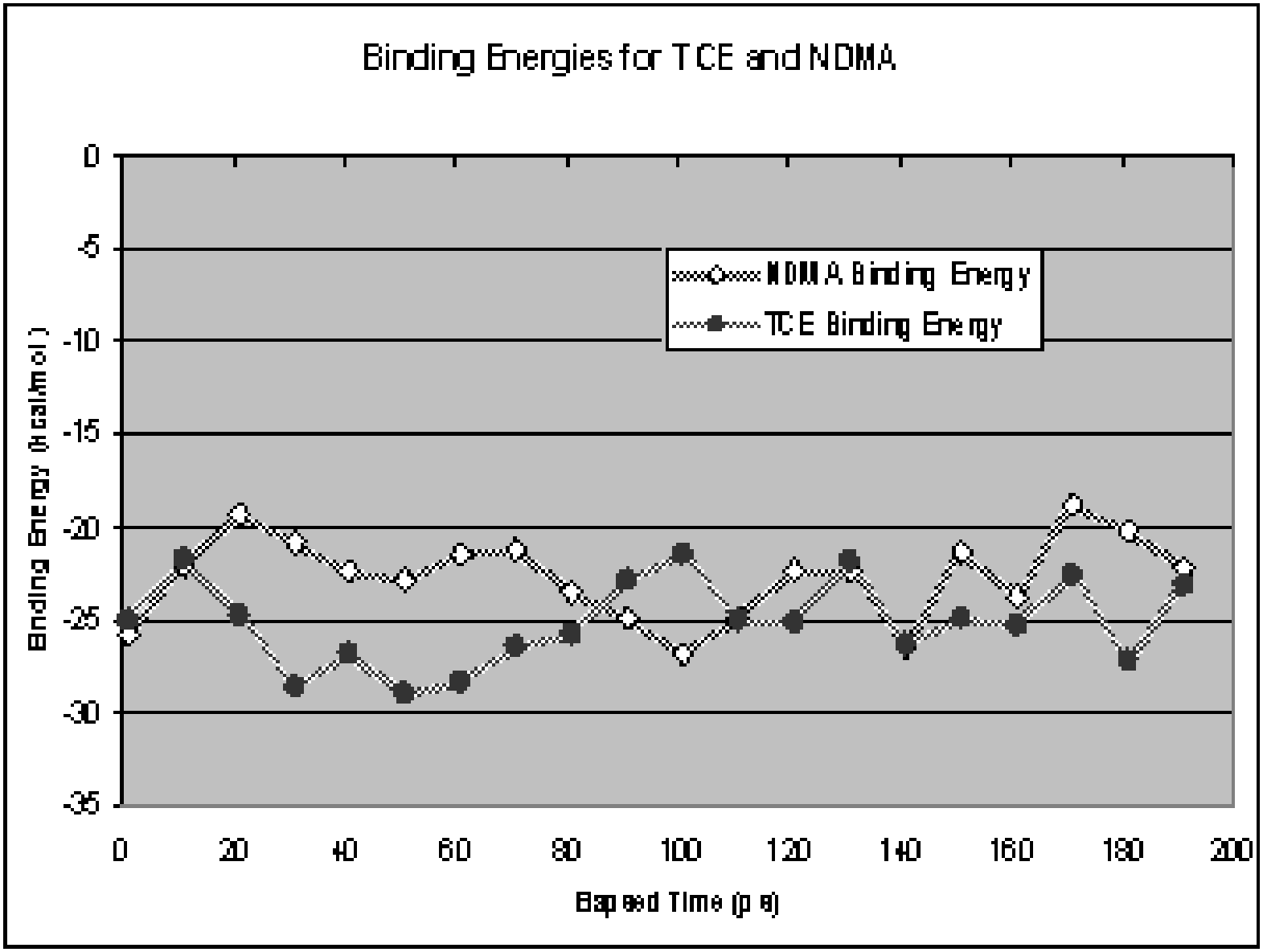

Figure 42. Estimated energies of interaction (binding energies) of NDMA and PCE (mislabeled TCE in figure) within the hydrated membrane system.

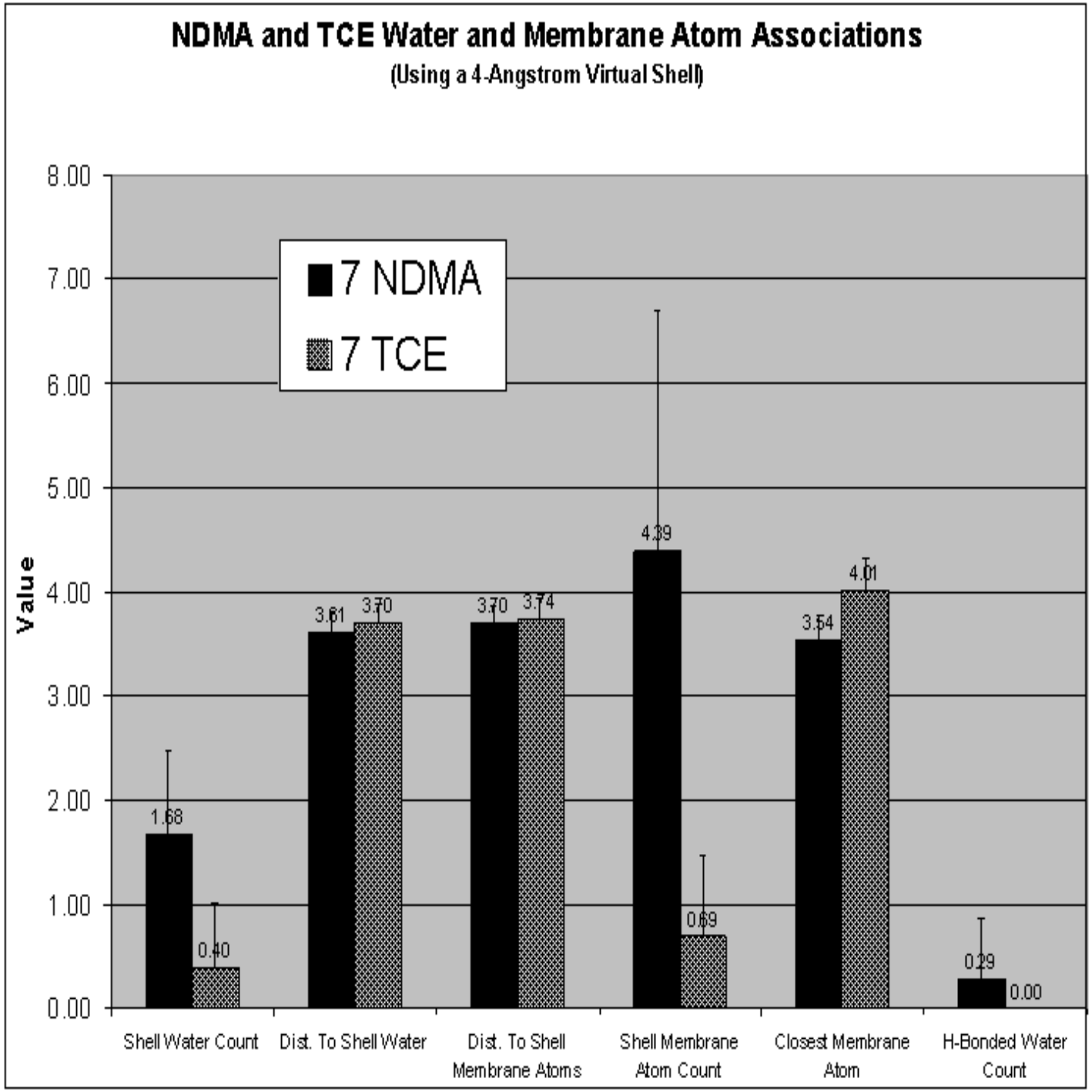

Figure 43. NDMA and PCE (mislabeled TCE in figure) interactions with water and membrane atoms. Distances are in Å.

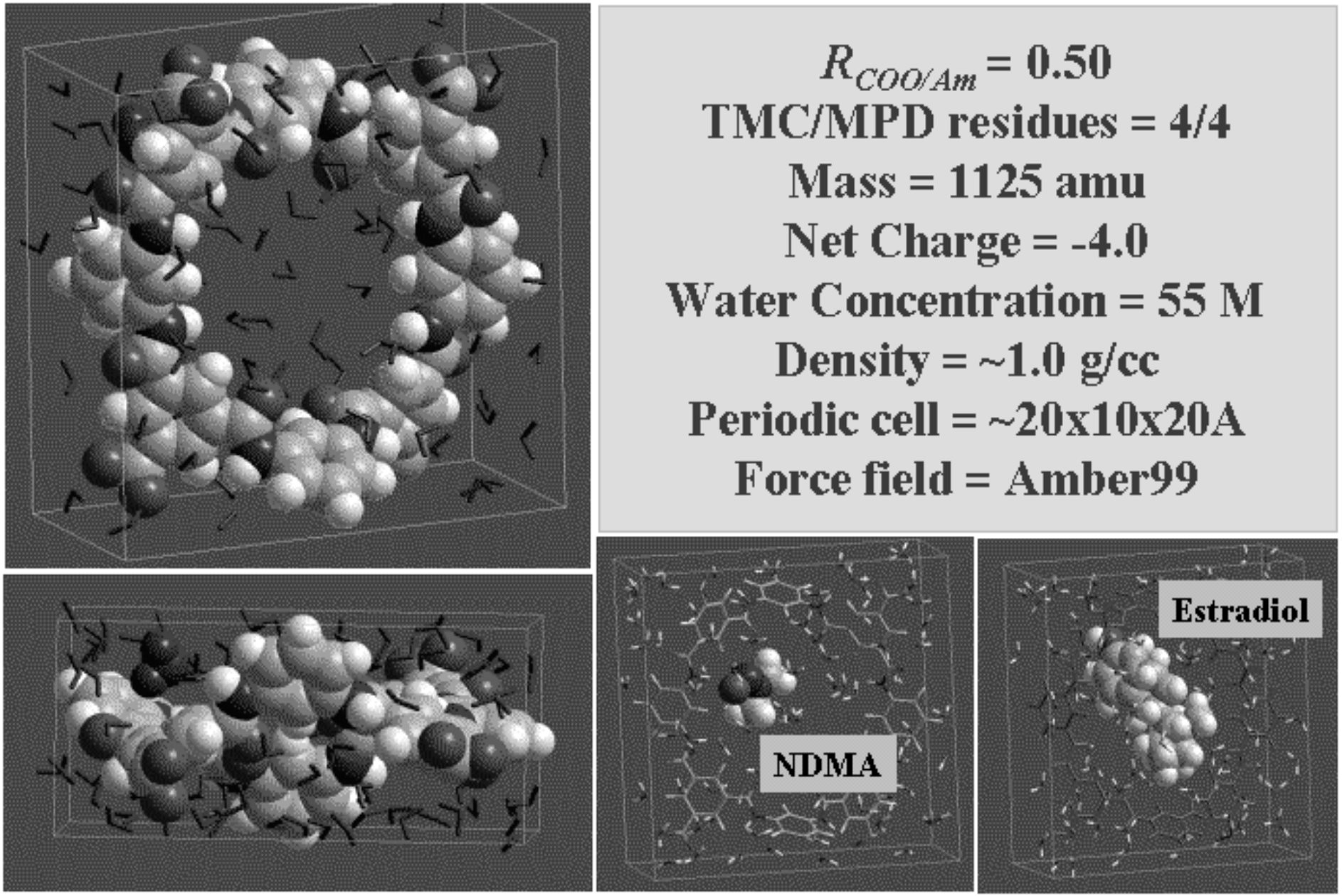

Figure 44. Idealized model PA membrane pores.

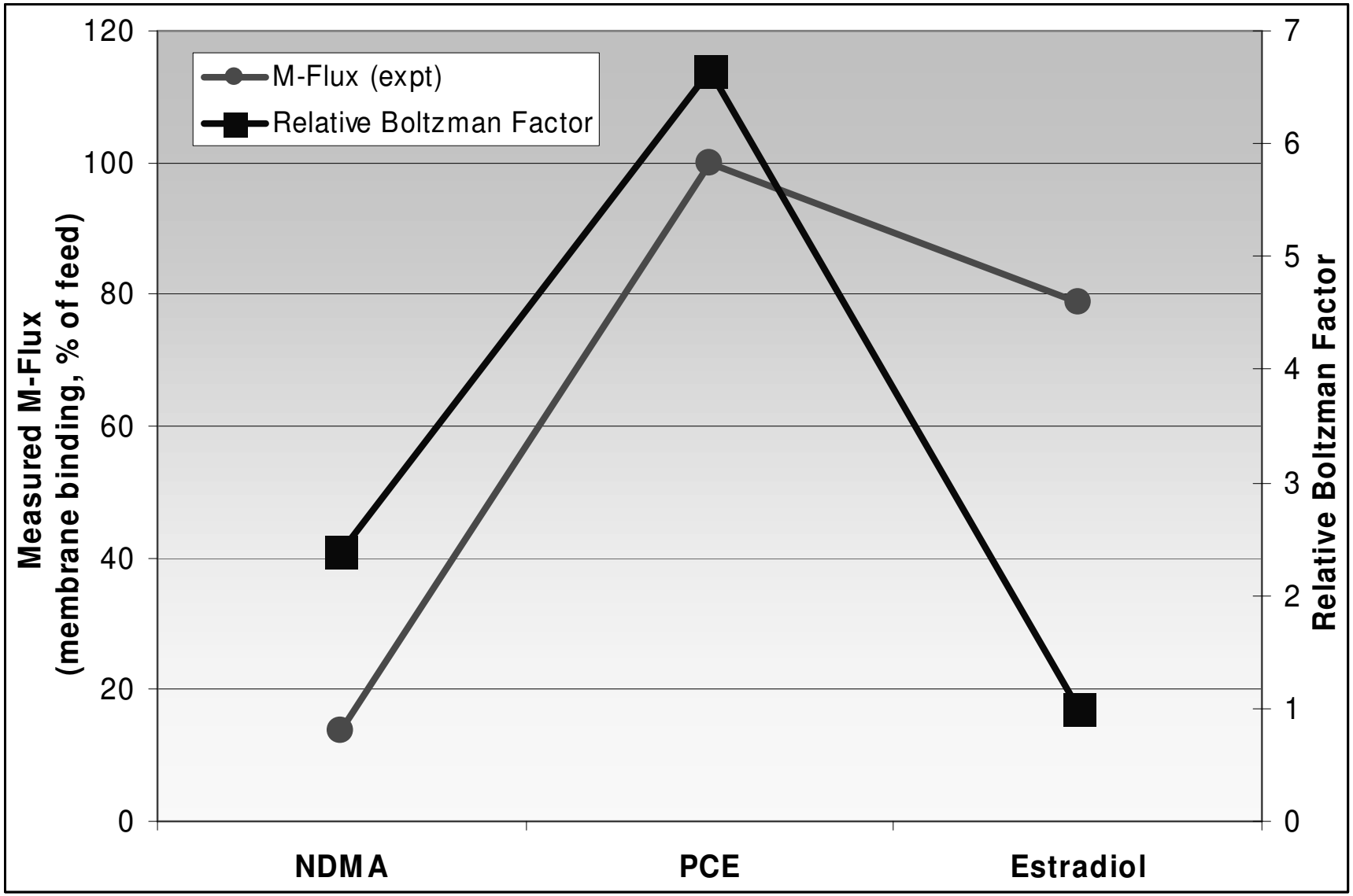

Figure 45. Solute-membrane interaction potentials (Relative Boltzman Factors) as a function of compound type and measured solute-membrane binding activity.

Table 1a. Description of Compounds Considered in the Study

The table shows a comprehensive list of 202 compounds, mostly obtained from the USGS Toxic Substances Hydrology (Toxics) Program, USEPA Drinking Water Contaminant Candidate List (March, 1995), USEPA Unregulated Contaminant Monitoring Rule (April, 1999), California Department of Health Services (May, 2001). "QSAR clusters" represent grouping of compounds based on their molecular descriptors.

QSAR Cluster	Compound	Compound Properties
1	1,1 Dichloropropanone	Disinfection Byproduct
1	3-amino-1H-1,2,4 Triazole	Endocrine Disruptor
1	Alanine	Amino Acid
1	benzo-e-1,3,2 Dioxathiepin-3-oxide	Endocrine Disruptor
1	Bromochloroacetic Acid	Disinfection Byproduct
1	Bromochloroacetonitrile	Disinfection Byproduct
1	Caffeine	Pharmaceutical-Human Drug
1	Chloralhydrate	Disinfection Byproduct
1	Cyclotrimethylenetrinitramine	Carcinogen
1	Cysteine	Amino Acid
1	Dibromoacetatic Acid	Disinfection Byproduct
1	Dibromoacetonitrile	Disinfection Byproduct
1	Dichloroacetic Acid	Disinfection Byproduct
1	Dichloroacetonitrile	Disinfection Byproduct
1	Dichlorodifluoromethane	Refrigerant Gas
1	Dichloropropane	Chemical intermediate of perchloroethylene and other chlorinated chemicals
1	Glycine	Amino Acid
1	Leucine	Amino Acid
1	Metformin	Pharmaceutical-Human Drug
1	N-Dimethylamine	used as a raw material of solvent /used to make organic chemicals
1	Nitrosodiethylamine	Carcinogen
1	N-nitrosomorpholine	Carcinogen
1	N-nitrosopiperidine	Carcinogen
1	N-nitrosopyrrolidine	Carcinogen
1	o-Cresol	Intermediate for production of pesticides, pharmaceuticals
1	Paraxanthine	Caffeine metabolite
1	p-Cresol	Wood preservative-Industrial/Household w astew ater product
1	Phenol	Disinfectant-Industrial/Household w astew ater product
1	s-1-Methyl-5-3-Pyridinyl-2-Pyrrolidinone	
1	Serine	Amino Acid
1	t Butyl Alcohol	Alcohol
1	Threonine	Amino Acid
1	Valine	Amino Acid
2	1,1,2 Trichloroethene (TCE)	Solvent/Carcinogen
2	1,2 Dichlorobenzene	Fumigant
2	1,2 Dimethylbenzene	Fuel Hydrocarbon-Carcinogen

Table 1b. Description of Compounds Considered in the Study
(Continued – See Table 1a)

QSAR Cluster	Compound	Compound Properties
2	1,2,4 Trimethylbenzene	Fuel Hydrocarbon
2	1,3,5 Trimethylbenzene	Fuel Hydrocarbon
2	1,4 Dichlorobenzene	Fumigant-Carcinogen/Industrial-Household w astew ater product
2	3,4,5,6,7,8,8a-Heptachlorodicyclopentadiene	Endocrine Disruptor
2	5-methyl-1H-Benzotriazole	Antioxidant-Industrial/Household w astew ater product
2	Bromochloromethane	Disinfection Byproduct
2	Bromodichloromethane	Disinfection Byproduct
2	Bromoform	Disinfection Byproduct-Carcinogen
2	Bromomethane	Fumigant/Solvent
2	Chloroform	Disinfection Byproduct-Carcinogen
2	Cymene	Manufacture of synthetic resins
2	Dibromochloromethane	Disinfection Byproduct
2	Dibromochloropropane	Carcinogen
2	Ethylbenzene	Fuel Hydrocarbon
2	exo-Dimethanonaphthalene	Endocrine Disruptor
2	Methylene Bromide	Solvent; intermediate in production of herbicides
2	Methylene Chloride	Solvent/found in aerosol and pesticide products, photographic film
2	Monobromobenzene	Solvent
2	p-Dichlorobenzene	Carcinogen
2	Toluene	Fuel Hydrocarbon-Carcinogen
3	1,4 Dichlorophenoxyacetic Acid	Endocrine Disruptor
3	2,3 Naphthalenedicarboxylic Acid	Plasticizer
3	2,3,4,5,6 Pentachlorophenol	Endocrine Disruptor
3	2,3,5,6 Tetrachloroterephthalic Acid	Herbicide
3	2,4 Dichloro-4'-nitrodiphenyl Ether	Endocrine Disruptor
3	2,4 Dinitrophenol	Released from mines, metals, petroleum and dye plants
3	2,4,5 Trichlorophenoxyacetic Acid	Endocrine Disruptor
3	2,6 Naphthalenedicarboxylic Acid	Manufacture polyethylenenaphthalate and polyethylenephthalate polymers
3	4,6 Dichlorophenol	Algicide, antihelmintic, bactericide, agricultural fungicide
3	Acetaminophen	Pharmaceutical-Analgesic-Human Drug
3	Dichlorodiphenyldichloroethylene	Pesticide-Carcinogen
3	Nitrobenzene	production of aniline, used to make drugs, dyes, herbicides
3	Phthalic Anhydride	Plasticizer-Industrial/Household w astew ater product
3	Trichloroacetic Acid	Disinfection Byproduct
3	Triclosan	Antimicrobial-Industrial/Household w astew ater product
4	17a Estradiol	Pharmaceutical-Estrogen-Sex/Steroid hormone
4	4 Nonylphenol	Surfactant/Wastew ater product-Endocrine Disruptor
4	Androsterone	Pharmaceutical-Sex/Steroid hormone
4	beta Sitostanol n Hydrate	Plant Sterol-Endocrine Disruptor
4	beta-Estradiol	Pharmaceutical-Estrogen-Sex/Steroid hormone
4	Cholesterol	Pharmaceutical-Sex/Steroid hormone-Fecal indicator

Table 1c. Description of Compounds Considered in the Study
(Continued – See Table 1b)

QSAR Cluster	Compound	Compound Properties
4	Codeine	Pharmaceutical-Human Drug
4	Digoxigenin	Pharmaceutical-Human Drug
4	Equilenin	Pharmaceutical-Sex/Steroid hormone
4	Equilin	Pharmaceutical-Sex/Steroid hormone
4	Estrone	Pharmaceutical-Sex/Steroid hormone
4	Mestranol	Pharmaceutical-Sex/Steroid hormone
4	Norethindrone	Form of progesterone
4	Testosterone	Pharmaceutical-Sex/Steroid hormone
5	2,2 bis-p-Chlorophenyl 1,1,1 Trichloroethane	Endocrine Disruptor
5	2,2 bis-p-Methoxyphenyl 1,1,1 Trichloroethane	Endocrine Disruptor
5	2,2,2 Trichloro 1,1-bis-4-chlorophenyl Ethanol	Endocrine Disruptor
5	2,2-bis-p-Chlorophenyl 1,1 Dichloroethane	Endocrine Disruptor
5	Bisphenol	Oestrogenic/Antiandrogen-Household/Wastew ater product
5	Diethylstilbestrol	Pharmaceutical-Estrogen-Carcinogen
6	2,4 Dinitrotoluene	Production of isocyanate and explosives-Carcinogen
6	d--n-Butylphthalate	Plasticizer
6	Estriol	Pharmaceutical-Sex/Steroid hormone
6	Thio-N-methyl-carbamoyl-oxy-methylester	Endocrine Disruptor
7	2,6 bis-1,1 Dimethylethyl 2,5 Cyclohexadiene 1,4 dione	
7	2,6 bis-1,1 Dimethylethyl Phenol	Intermediate for preparation of antioxidants and UV stabilizers
7	2,6 di-tert-butyl-p-Cresol	Antioxidant/Antiskimming agent
7	ethyl-tert-Butyl Ether	Fuel oxygenate-Carcinogen
7	methyl-tert-butyl Ether (MTBE)	Fuel Hydrocarbon-Carcinogen
7	tert amyl methyl Ether	Solvent
8	2,6 Dinitrotoluene	Production of polyurethane foams; ammunition and explosives
8	methyl Parathion	Insecticide
8	Progesterone	Pharmaceutical-Sex/Steroid hormone
9	2-chloro-2'-6'-diethyl-N-methoxymethyl-acetanilide (Alachlor)	Endocrine Disruptor
9	3-Hydroxycarbofuran	Pesticide
9	4-amino-6-tert-butyl-3-methylthio-as-triazin-5,4H-one	Endocrine Disruptor
9	6-chloro-N-ethyl-N'-isopropyl-1,3,5 Triazine-2,4-diamine	Endocrine Disruptor
9	Acetochlor	Herbicide
9	alpha-naphthyl-N-Methylcarbamate	Endocrine Disruptor
9	Atrazine	Carcinogen
9	Butylated-Hydroxyanisole	Antioxidant-Industrial/Household w astew ater product
9	Carbadox	Pharmaceutical-Human/Veterinary Antibiotic
9	Cimetidine	Pharmaceutical-Human Drug
9	Diethylphthalate	Plasticizer-Industrial/Household w astew ater product
9	Dipropylthiocarbamic Acid-s-ethylester	
9	Diuron	Herbicide
9	Fluoxetine	Pharmaceutical-Human Drug

Table 1d. Description of Compounds Considered in the Study
(Continued – See Table 1c)

QSAR Cluster	Compound	Compound Properties
9	Fonofos	Insecticide
9	Gemfibrozil	Pharmaceutical-Human Drug
9	Ibuprofen	Pharmaceutical-Human Drug
9	Linuron	Herbicide
9	Metolachlor	Pesticide
9	Metribuzin	Pesticide
9	Molinate	Herbicide
9	N N diethyl 3 methylbenzamide	Insecticide
9	Nitrosodibutylamine	Carcinogen
9	N-nitrosodi-n-butylamine	Carcinogen
9	N-nitrosodi-n-propylamine	Carcinogen
9	Paroxetine	Pharmaceutical-Human Drug
9	Pramitol	Herbicide
9	Salbutamol	Pharmaceutical-Human Drug
9	Simazine	Carcinogen
9	Terbacil	Herbicide
9	Trimethoprim	Pharmaceutical-Human/Veterinary Antibiotic
10	Aldicarbsulfone	Agricultural product residue
10	Clorpyrifos	Insecticide-Industrial/Household w astew ater product
10	Diazinon	Insecticide
10	Disulfoton	Insecticide
10	Endosulfansulfate	Pesticide
10	Terbufos	Insecticide
10	triphenyl Phosphate	Plasticizer-Industrial/Household w astew ater product
10	tris 2 Chloroethyl Phosphate	Plasticizer/Flame retardant-Industrial/Household w astew ater product
11	Aldrin	Insecticide
11	cis-Chlordane	Insecticide
11	Dieldrin	Insecticide-Industrial/Household w astew ater product
11	Hexachloropentadiene	Endocrine Disruptor
11	Octachloro-4-7-methanotetrahydroindane	Endocrine Disruptor
11	Octachloroepoxide	Endocrine Disruptor
12	Anthracene	Polycyclic aromatic Hydrocarbon
12	benzo-a-Pyrene	Polycyclic aromatic Hydrocarbon
12	Fluoranthrene	Polycyclic aromatic Hydrocarbon
12	Phenanthrene	Polycyclic aromatic Hydrocarbon
12	Pyrene	Polycyclic aromatic Hydrocarbon
13	1,1,2,2 Tetrachloroethane	Solvent
13	1,1,2,2, Tetrachloroethylene (PCE)	Industrial Solvent
13	Benzene	Fuel Hydrocarbon-Carcinogen
13	Hexachlorobenzene	Endocrine Disruptor
13	Hexachlorobutadiene	Used to make rubber compounds/solvent
13	Hexachlorocyclohexane	Carcinogen

Table 1e. Description of Compounds Considered in the Study
(Continued – See Table 1d)

QSAR Cluster	Compound	Compound Properties
13	Lindane	Insecticide-Industrial/Household w astew ater product
14	bis-2-Ethylhexyl-adipate	Plasticizer-Industrial/Household w astew ater product
14	di-sec-Octylphthalate	Carcinogen
14	d--n-Octylphthalate	Plasticizer
15	Chlorotetracycline	Pharmaceutical-Human/Veterinary Antibiotic
15	Doxycycline	Pharmaceutical-Human/Veterinary Antibiotic
15	Terramycin	Antibiotic
15	Tetracycline	Pharmaceutical-Human/Veterinary Antibiotic
16	Ciprofloxacin	Pharmaceutical-Human/Veterinary Antibiotic
16	Diltiazem	Pharmaceutical-Human Drug
16	Enalaprilat	Pharmaceutical-Human Drug
16	Enrofloxacin	Antibiotic-Industrial/Household w astew ater product
16	Erythromycin	Pharmaceutical-Human/Veterinary Antibiotic
16	Lincomycin	Pharmaceutical-Human/Veterinary Antibiotic
16	Norfloxacin	Pharmaceutical-Human/Veterinary Antibiotic
16	Ranitidine	Pharmaceutical-Human Drug
17	Digoxin	Pharmaceutical-Human Drug
17	Tylosin	Pharmaceutical-Human/Veterinary Antibiotic
18	Ethylenediaminetetraacetic Acid (EDTA)	Chelating agent
18	Nitrilotriacetic Acid	Carcinogen
18	N-triacetic Acid	
19	Perchloric Acid	Used to prepare perchlorate, produce films, oxidant-Carcinogen
19	Sulfachlorpyridazine	Pharmaceutical-Human/Veterinary Antibiotic
19	Sulfadimethoxine	Pharmaceutical-Human/Veterinary Antibiotic
19	Sulfamerazine	Pharmaceutical-Human/Veterinary Antibiotic
19	Sulfamethazine	Pharmaceutical-Human/Veterinary Antibiotic
19	Sulfamethizole	Pharmaceutical-Human/Veterinary Antibiotic
19	Sulfamethoxazole	Pharmaceutical-Human/Veterinary Antibiotic
19	Sulfathiazole	Pharmaceutical-Human/Veterinary Antibiotic
20	Tributyl Tin	Estrogen
N/A	Anatoxin a	Algal toxin
N/A	Asparagine	Amino Acid
N/A	Aspartic Acid	Amino Acid
N/A	Cylindrospermopsin	Algal toxin
N/A	Histidine	Amino Acid
N/A	Lysine	Amino Acid
N/A	Methionine	Amino Acid
N/A	Microcystin LR	Algal toxin
N/A	N-nitroso dimethyl amine (NDMA)	Carcinogen
N/A	Phenylalanine	Amino Acid
N/A	Saxitoxin	Algal toxin
N/A	Urea	Fertilizer

Table 2. Molecular Descriptors Used in Models
(For detailed description refer to Appendix 1)

Charge/Polarity Properties
3D Descriptors of Entire Molecule
ABSQ
Dipole
MaxHp
MaxNeg
MaxQp
Polarizability
3D Descriptors for CoMMA
Py
Pz
P
Q
Dx
Dy
Dz
Qxx
Qyy
Atom Type E-State Descriptors
SsCH3
SssCH2
SaaCH
SdssC
SdO
SsCl
Hydrogen Atom Type E-State Descriptors
SssOH
Shother
Hmax
Gmax
Hmin
Gmin
Molecular Properties
Qs
Qsv

Hydrogen Bonding Properties
Molecular Properties
numHBa
SHHbd

Hydrophobicity Properties
LogP

Other
LD50

Molecular Complexity Properties
3D Descriptors of Entire Molecule
Ovality
Surface
Chi Indices
x1
xp4
xc3
xpc4
xv1
xvp4
xvp7
xvp10
xvc3
xvpc4
xvch6
Subgraph Count Indices
nxp5
nxc3
nxch6
3D Descriptors for CoMMA
Ix
Iy
Total Topological Descriptors
W
Pf
sumdell
tets2
totop
Wt
nclass
Traditional Kappa Shape Indices
k0
k1
k2
k3
Information Indices
si
IC
R
idc
idcbar
Molecular Properties
fw
nelem
nrings
ncirc
phia
knotp

Table 3. Polyamide (PA) Reverse Osmosis Membrane Properties
These were used as inputs in development of the "Universal" PA model. BW-30 shows a higher OH/Amide I Ratio, meaning it is a less cross-linked membrane. Largest differences were observed with OH/Amide I Ratio (measure of cross-linking), Roughness, relative Polyamide Thickness and Zeta Potential. Other properties exhibited less variation. (For detailed definitions refer to Appendix 1)

Membrane Properties	BW-30	ESPA-2	LFC-1	TFC-HR
Contact Angle (degrees)	61.48	61.33	61.68	61.47
Zeta Potential (mV)	-12.82	-26.03	-17.33	-16.27
Zeta Potential Slope (pH 5-7)	-2.67	-5.00	-1.03	-1.61
COO/Amide I Ratio	0.46	0.31	0.43	0.33
COO/Amide II Ratio	0.42	0.27	0.42	0.33
OH/Amide I Ratio	2.09	0.53	1.37	0.80
Polyamide Thickness	1.30	1.31	1.19	0.69
Roughness (nm)	82.90	90.86	111.50	48.64
Specific Water Flux (GFD/PSI)	0.15	0.21	0.21	0.18

Table 4. Surrogate Compounds Chosen for the Study
The table shows that QSAR cluster the compounds fall into, the commercial source and the radioisotope used in the study.

QSAR Cluster	Compound	Commercial Source	Isotope
1	Alanine	American Radiolabeled Chemicals	^{14}C
1	Caffeine	American Radiolabeled Chemicals	^{14}C
1	Cysteine	American Radiolabeled Chemicals	^{14}C
1	Dichloroacetic Acid	American Radiolabeled Chemicals	^{14}C
1	Glycine	American Radiolabeled Chemicals	^{14}C
1	N-dimethylamine	American Radiolabeled Chemicals	^{14}C
1	Phenol	Moravek	^{14}C
1	t Butyl Alcohol	Moravek	^{14}C
1	Threonine	American Radiolabeled Chemicals	^{14}C
1	Valine	American Radiolabeled Chemicals	^{14}C
2	Ethylbenzene	Sigma	^{14}C
2	Toluene	Sigma	^{14}C
3	1,4 Dichlorophenoxyacetic Acid	American Radiolabeled Chemicals	^{14}C
3	2,3,4,5,6 Pentachlorophenol	American Radiolabeled Chemicals	^{14}C
3	4,6 Dichlorophenol	American Radiolabeled Chemicals	^{14}C
3	Nitrobenzene	American Radiolabeled Chemicals	^{14}C
3	Phthalic Anhydride	American Radiolabeled Chemicals	^{14}C
3	Trichloroacetic Acid	American Radiolabeled Chemicals	^{14}C
4	17a Estradiol	American Radiolabeled Chemicals	^{14}C
4	4 Nonylphenol	American Radiolabeled Chemicals	^{14}C
4	beta Sitostanol n Hydrate	American Radiolabeled Chemicals	^{3}H
4	Cholesterol	American Radiolabeled Chemicals	^{14}C
4	Codeine	American Radiolabeled Chemicals	^{14}C
4	Estrone	American Radiolabeled Chemicals	^{14}C
4	Testosterone	American Radiolabeled Chemicals	^{14}C
5	Bisphenol	Moravek	^{14}C
5	Diethylstilbestrol	American Radiolabeled Chemicals	^{14}C
6	2,4 Dinitrotoluene	American Radiolabeled Chemicals	^{14}C
8	methyl parathion	American Radiolabeled Chemicals	^{14}C
8	Progesterone	American Radiolabeled Chemicals	^{14}C
9	2-chloro-2'-6'-diethyl-N-methoxymethyl-acetanilide (Alachlor)	Sigma	^{14}C
9	Cimetidine	Amersham	^{3}H
9	Diethylphthalate	American Radiolabeled Chemicals	^{14}C
9	Ibuprofen	American Radiolabeled Chemicals	^{14}C
10	Chlorpyrifos	American Radiolabeled Chemicals	^{14}C
12	Phenanthrene	Moravek	^{14}C
13	1,1,2,2, Tetrachloroethylene (PCE)	American Radiolabeled Chemicals	^{14}C
13	Benzene	Moravek	^{14}C
13	Lindane	American Radiolabeled Chemicals	^{14}C
15	Doxycycline	American Radiolabeled Chemicals	^{3}H
15	Tetracycline	Moravek	^{3}H
16	Ciprofloxacin	Moravek	^{14}C
16	Erythromycin	American Radiolabeled Chemicals	^{14}C
18	Ethylenediaminetetraacetic Acid (EDTA)	Sigma	^{14}C
N/A	Asparaginine	American Radiolabeled Chemicals	^{14}C
N/A	Aspartic Acid	American Radiolabeled Chemicals	^{14}C
N/A	Histidine	American Radiolabeled Chemicals	^{14}C
N/A	Lysine	American Radiolabeled Chemicals	^{14}C
N/A	Methionine	American Radiolabeled Chemicals	^{14}C
N/A	N-nitroso dimethyl amine (NDMA)	American Radiolabeled Chemicals	^{14}C
N/A	Urea	American Radiolabeled Chemicals	^{14}C

Table 5. Membranes Used in the Study
The table shows the membranes source and their fundamental classification.

Membranes Used in the Study		
Membrane	**Manufacturer**	**Classification**
BW-30	DOW / Filmtec	TFC Brackish Water RO
TFC-HR	Koch / Fluid Systems	TFC High Rejectin RO
ESPA-2	Hydranautics	TFC Brackish Water RO
LFC-1	Hydranautics	TFC Low Fouling Brackish Water RO
CA	Osmonics	CA Brackish Water RO

Table 6. Comparison of Membrane Performance – Relative P-Flux
Measured results (raw data) from RMP assay. Averaged Relative fluxes are based on F-Flux of 100% and mean based on n = 4-7. For the most part the values are very similar among the PA membranes.

Compound	BW-30	ESPA-2	LFC-1	TFC-HR	CA
1,1,2,2-Tetrachloroethylene	0.05	0.33	0.07	0.02	30.80
17a Estradiol	0.19	1.65	0.67	0.46	2.48
2,3,4,5,6 Pentachlorophenol	0.43	2.87	0.69	5.08	2.23
2,4-Dichlorophenol	7.41	2.65	2.35	2.02	2.44
2,4-Dichlorophenoxyacetic Acid	13.26	15.84	4.76	5.97	43.74
2,4-Dinitrotoluene	5.06	3.45	1.69	1.94	7.06
2-chloro-2'-6'-diethyl-N-methoxymethyl-acetanilide (Alachlor)	0.42	2.33	N/A	2.43	N/A
4-Nonylphenol	0.30	0.33	0.31	0.29	0.73
Alanine	13.62	18.54	15.45	10.20	53.89
Asparagine	6.93	22.01	12.01	31.86	64.97
Aspartic Acid	12.60	15.69	9.68	14.67	34.23
Benzene	25.99	23.32	19.46	21.41	56.58
beta Sitostanol n Hydrate	0.47	0.53	0.47	0.43	0.67
Bisphenol-A	3.11	1.88	1.08	0.60	0.89
Caffeine	17.86	20.62	14.62	14.78	75.53
Chlorpyrifos	0.81	0.66	1.08	0.73	2.91
Cholesterol	0.07	0.06	0.27	0.38	0.25
Cimetidine	7.75	19.61	5.19	13.96	59.89
Ciprofloxacin	2.08	10.57	7.61	6.61	35.12
Codeine	9.43	15.42	12.07	7.66	57.34
Cysteine	17.78	10.06	15.45	7.02	43.88
Dichloroacetic Acid	16.48	30.30	23.43	25.82	41.26
Diethylphthalate	6.81	4.93	5.48	1.47	16.48
Diethylstilbestrol	0.09	0.09	0.19	0.12	0.26
Doxycycline	3.26	4.37	5.33	10.24	18.03
Erythromycin	3.77	3.86	2.99	2.53	28.32
Estrone	0.62	0.22	0.92	0.16	2.68
Ethylbenzene	3.55	3.19	1.91	1.61	24.15
Ethylenediaminetetraacetic Acid (EDTA)	5.31	14.29	6.69	11.10	48.06
Glycine	14.88	26.92	22.85	18.03	56.36
Histidine	16.17	16.02	17.34	11.68	45.29
Ibuprofen	16.15	4.45	5.20	3.97	57.98
Lindane	2.36	2.13	1.07	0.94	1.52
Lysine	14.04	14.23	6.21	10.72	51.85
Methionine	24.13	16.74	10.25	19.96	46.93
methyl Parathion	0.97	1.54	1.32	3.52	2.18
N-dimethylamine	34.73	33.12	31.30	28.58	54.91
Nitrobenzene	0.38	0.50	0.29	0.36	34.46
N-nitroso dimethyl amine (NDMA)	82.34	80.76	84.23	78.67	94.06
Phenanthrene	0.28	0.45	0.66	0.46	0.43
Phenol	35.43	30.36	34.67	35.10	71.67
Phthalic Anhydride	6.84	8.02	6.06	8.14	29.08
Progesterone	0.04	0.25	0.03	0.04	1.49
t Butyl Alcohol	18.40	16.96	25.89	23.94	87.42
Testosterone	0.94	2.34	1.65	0.51	20.97
Tetracycline	3.43	7.08	3.52	2.93	32.26
Threonine	9.23	11.80	12.00	10.63	45.73
Toluene	1.51	8.37	19.03	11.91	47.79
Trichloroacetic Acid	24.37	23.32	12.80	29.05	60.12
Urea	89.37	85.11	95.48	90.01	90.58
Valine	22.95	21.48	12.18	11.10	62.72

Table 7. Comparison of Membrane Performance – Relative M-Flux
Measured results (raw data) from RMP assay. Averaged Relative fluxes are based on F-Flux of 100% and mean based on n = 4-7. For the most part the values are very similar among the PA membranes.

Compound	BW-30	ESPA-2	LFC-1	TFC-HR	CA
1,1,2,2-Tetrachloroethylene	99.95	99.67	99.93	99.98	67.77
17a Estradiol	77.59	85.93	67.29	84.92	97.52
2,3,4,5,6 Pentachlorophenol	53.42	44.66	60.72	68.69	97.77
2,4-Dichlorophenol	92.59	97.35	97.65	97.98	97.56
2,4-Dichlorophenoxyacetic Acid	5.99	17.28	3.92	9.60	5.30
2,4-Dinitrotoluene	94.94	96.55	98.31	98.06	92.94
2-chloro-2'-6'-diethyl-N-methoxymethyl-acetanilide (Alachlor)	5.20	19.99	N/A	21.19	N/A
4-Nonylphenol	36.64	21.02	23.36	69.90	95.98
Alanine	4.84	5.61	5.77	4.16	6.78
Asparagine	2.37	6.72	7.41	6.59	0.73
Aspartic Acid	5.54	3.54	2.81	5.54	8.48
Benzene	74.01	76.68	64.01	78.59	43.42
beta Sitostanol n Hydrate	28.93	48.57	14.30	24.75	28.23
Bisphenol-A	28.34	25.50	16.12	24.01	99.11
Caffeine	14.07	19.13	21.78	17.38	10.09
Chlorpyrifos	25.68	59.64	21.23	52.56	97.09
Cholesterol	13.39	17.87	12.56	13.33	16.48
Cimetidine	13.37	34.06	28.99	26.06	21.67
Ciprofloxacin	2.67	18.68	30.45	12.11	27.03
Codeine	13.11	47.68	38.88	16.76	26.16
Cysteine	12.61	4.98	5.77	5.68	9.37
Dichloroacetic Acid	7.83	8.16	7.12	8.78	6.23
Diethylphthalate	37.02	31.46	29.88	41.18	83.52
Diethylstilbestrol	37.33	21.66	18.39	47.75	99.74
Doxycycline	10.54	14.46	15.95	16.74	30.61
Erythromycin	7.66	13.32	7.58	9.85	8.28
Estrone	69.61	99.78	83.66	99.84	97.32
Ethylbenzene	96.45	96.81	98.09	98.39	66.72
Ethylenediaminetetraacetic Acid (EDTA)	2.98	9.07	2.12	2.03	7.52
Glycine	3.37	4.57	6.45	5.36	6.72
Histidine	6.22	7.91	7.98	4.57	8.82
Ibuprofen	18.36	8.89	8.62	10.36	20.45
Lindane	66.26	58.30	37.32	66.34	98.48
Lysine	3.11	6.90	2.35	3.82	9.30
Methionine	7.93	25.10	4.14	6.49	8.58
methyl Parathion	12.00	28.17	23.85	25.57	97.82
N-dimethylamine	6.88	22.79	28.80	7.89	13.25
Nitrobenzene	99.62	99.50	99.71	99.64	65.54
N-nitroso dimethyl amine (NDMA)	17.66	14.08	0.53	21.33	3.51
Phenanthrene	99.71	85.27	99.34	98.28	99.57
Phenol	59.99	63.34	65.33	64.67	28.33
Phthalic Anhydride	1.68	3.05	3.06	3.45	6.22
Progesterone	25.33	34.21	23.25	33.90	98.51
t Butyl Alcohol	7.11	5.17	6.18	10.10	4.04
Testosterone	11.65	27.93	41.21	14.54	74.38
Tetracycline	7.69	18.89	17.59	14.45	14.42
Threonine	4.04	3.57	3.88	4.89	7.52
Toluene	98.49	91.63	80.97	88.09	52.21
Trichloroacetic Acid	8.83	6.90	1.99	6.50	4.19
Urea	1.40	8.29	1.66	1.74	3.08
Valine	4.58	8.78	4.89	5.07	5.64

Table 8. Comparison of Membrane Performance – Relative R-Flux
Measured results (raw data) from RMP assay. Averaged Relative fluxes are based on F-Flux of 100% and mean based on n = 4-7. For the most part the values are very similar among the PA membranes.

Compound	BW-30	ESPA-2	LFC-1	TFC-HR	CA
1,1,2,2-Tetrachloroethylene	0.00	0.00	0.00	0.00	1.44
17a Estradiol	22.22	12.42	32.04	14.61	0.00
2,3,4,5,6 Pentachlorophenol	46.15	52.48	38.59	26.23	0.00
2,4-Dichlorophenol	0.00	0.00	0.00	0.00	0.00
2,4-Dichlorophenoxyacetic Acid	80.76	66.87	91.32	84.43	50.96
2,4-Dinitrotoluene	0.00	0.00	0.00	0.00	0.00
2-chloro-2'-6'-diethyl-N-methoxymethyl-acetanilide (Alachlor)	94.38	77.67	N/A	76.39	N/A
4-Nonylphenol	63.06	78.65	76.32	29.81	3.29
Alanine	81.54	75.85	78.77	85.64	39.33
Asparagine	90.70	71.27	80.58	61.55	34.30
Aspartic Acid	81.86	80.77	87.52	79.79	57.29
Benzene	0.00	0.00	16.54	0.00	0.00
beta Sitostanol n Hydrate	70.59	50.90	85.23	74.82	71.10
Bisphenol-A	68.55	72.62	82.80	75.39	0.00
Caffeine	68.07	60.25	63.61	67.84	14.37
Chlorpyrifos	73.50	39.70	77.70	46.71	0.00
Cholesterol	86.54	82.06	87.17	86.30	83.27
Cimetidine	78.88	46.33	65.82	59.98	18.44
Ciprofloxacin	95.24	70.76	61.94	81.28	37.85
Codeine	77.46	36.90	49.06	75.59	16.50
Cysteine	69.61	84.96	78.77	87.30	46.75
Dichloroacetic Acid	75.70	61.55	69.45	65.41	52.51
Diethylphthalate	56.16	63.62	64.65	57.35	0.00
Diethylstilbestrol	62.58	78.25	81.42	52.14	0.00
Doxycycline	86.21	81.17	78.71	73.03	51.36
Erythromycin	88.56	82.82	89.43	87.61	63.41
Estrone	29.77	0.00	15.42	0.00	0.00
Ethylbenzene	0.00	0.00	0.00	0.00	9.13
Ethylenediaminetetraacetic Acid (EDTA)	91.72	76.64	91.20	86.87	44.42
Glycine	81.74	68.52	70.70	76.61	36.92
Histidine	77.61	76.07	74.68	83.76	45.89
Ibuprofen	65.49	86.66	86.18	85.67	21.57
Lindane	31.38	39.57	61.61	32.72	0.00
Lysine	82.85	78.87	91.44	85.46	38.85
Methionine	67.94	58.17	85.60	73.55	44.49
methyl Parathion	87.03	70.29	74.82	70.91	0.00
N-dimethylamine	58.38	44.09	39.90	63.53	31.84
Nitrobenzene	0.00	0.00	0.00	0.00	0.00
N-nitroso dimethyl amine (NDMA)	0.00	5.16	15.25	0.00	2.44
Phenanthrene	0.00	14.28	0.00	1.26	0.00
Phenol	4.58	6.30	0.00	0.23	0.00
Phthalic Anhydride	91.48	88.93	90.88	88.41	64.70
Progesterone	74.64	65.54	76.73	66.06	0.00
t Butyl Alcohol	74.48	77.86	67.93	65.95	8.53
Testosterone	87.41	69.73	57.14	84.95	4.65
Tetracycline	88.88	74.02	78.89	82.62	53.32
Threonine	86.74	84.62	84.12	84.48	46.75
Toluene	0.00	0.00	0.00	0.00	0.00
Trichloroacetic Acid	66.80	69.78	85.21	64.46	35.70
Urea	9.23	6.59	2.86	8.25	6.34
Valine	72.46	69.74	82.92	83.82	31.64

Table 9a. BW-30 Performance Based on Individual Compounds – Relative P-Flux
The table shows how well compound behavior could be predicted by the ANN model. In most cases, the model accurately predicted behavior.
Actual = laboratory determination
Predicted = ANN model prediction

Compound	P-Flux		
	Actual (Avg)	(StDev)	Predicted
1,1,2,2, Tetrachloroethylene (PCE)	0.05	0.03	0.09
1,4 Dichlorophenoxyacetic Acid	13.26	7.08	11.12
17a Estradiol	0.19	0.06	0.18
2,3,4,5,6 Pentachlorophenol	0.43	0.15	0.37
2,4 Dinitrotoluene	5.06	1.52	4.06
2-chloro-2'-6'-diethyl-N-methoxymethyl-acetanilide (Alachlor)	0.42	0.10	0.44
4 Nonylphenol	0.30	0.08	0.25
4,6 Dichlorophenol	7.41	1.27	7.63
Alanine	13.62	3.53	12.74
Asparagine	6.93	2.61	9.47
Aspartic Acid	12.60	2.52	14.32
Benzene	25.99	5.45	24.97
beta Sitostanol n Hydrate	0.47	0.06	0.45
Bisphenol	3.11	1.95	2.69
Caffeine	17.86	2.91	17.61
Cholesterol	0.07	0.01	0.09
Cimetidine	7.75	3.26	7.80
Ciprofloxacin	2.08	1.98	1.51
Clorpyrifos	0.81	0.05	0.80
Codeine	9.43	4.74	7.15
Cysteine	17.78	6.42	16.20
Dichloroacetic Acid	16.48	4.42	14.65
Diethylphthalate	6.81	4.04	5.76
Diethylstilbestrol	0.09	0.11	0.10
Doxycycline	3.26	0.84	4.14
Erythromycin	3.77	0.38	3.72
Estrone	0.62	0.16	0.59
Ethylbenzene	3.55	0.36	4.50
Ethylenediaminetetraacetic Acid (EDTA)	5.31	1.49	5.09
Glycine	14.88	4.37	6.12
Histidine	16.17	1.01	15.61
Ibuprofen	16.15	2.48	15.83
Lindane	2.36	0.89	1.93
Lysine	14.04	3.25	13.88
Methionine	24.13	5.48	25.39
methyl Parathion	0.97	0.15	1.19
N-Dimethylamine	34.73	4.38	31.62
Nitrobenzene	0.38	0.10	0.39
N-nitroso dimethyl amine (NDMA)	82.34	1.87	101.35
Phenanthrene	0.28	0.01	0.27
Phenol	35.43	5.68	33.46
Phthalic Anhydride	6.84	2.73	5.58
Progesterone	0.04	0.01	0.06
t Butyl Alcohol	18.40	3.76	19.63
Testosterone	0.94	0.50	0.87
Tetracycline	3.43	1.48	3.32
Threonine	9.23	2.48	9.01
Toluene	1.51	0.04	1.41
Trichloroacetic Acid	24.37	5.41	22.80
Urea	89.37	2.10	96.32
Valine	22.95	6.43	21.39

Table 9b. BW-30 Performance Based on Individual Compounds – Relative M-Flux
The table shows how well compound behavior could be predicted by the ANN model. In most cases, the model accurately predicted behavior.
Actual = laboratory determination
Predicted = ANN model prediction

Compound	M-Flux		
	Actual (Avg)	(StDev)	Predicted
1,1,2,2, Tetrachloroethylene (PCE)	99.95	0.03	93.76
1,4 Dichlorophenoxyacetic Acid	5.99	1.51	6.07
17a Estradiol	77.59	12.82	77.02
2,3,4,5,6 Pentachlorophenol	53.42	5.33	53.23
2,4 Dinitrotoluene	94.94	1.52	95.97
2-chloro-2'-6'-diethyl-N-methoxymethyl-acetanilide (Alachlor)	5.20	1.87	4.47
4 Nonylphenol	36.64	5.83	35.99
4,6 Dichlorophenol	92.59	1.27	96.83
Alanine	4.84	0.73	5.57
Asparagine	2.37	0.72	2.66
Aspartic Acid	5.54	2.61	4.90
Benzene	74.01	5.45	79.34
beta Sitostanol n Hydrate	28.93	9.38	16.59
Bisphenol	28.34	8.87	28.63
Caffeine	14.07	6.54	13.06
Cholesterol	13.39	1.26	20.17
Cimetidine	13.37	2.91	14.46
Ciprofloxacin	2.67	1.36	2.41
Clorpyrifos	25.68	13.53	20.83
Codeine	13.11	4.08	10.35
Cysteine	12.61	1.31	7.82
Dichloroacetic Acid	7.83	1.06	8.62
Diethylphthalate	37.02	17.76	28.67
Diethylstilbestrol	37.33	8.08	33.85
Doxycycline	10.54	2.52	10.67
Erythromycin	7.66	1.69	5.36
Estrone	69.61	23.30	68.57
Ethylbenzene	96.45	0.36	98.43
Ethylenediaminetetraacetic Acid (EDTA)	2.98	0.94	2.46
Glycine	3.37	0.81	4.19
Histidine	6.22	1.75	7.29
Ibuprofen	18.36	0.69	19.16
Lindane	66.26	5.63	62.01
Lysine	3.11	0.78	2.96
Methionine	7.93	2.68	5.60
methyl Parathion	12.00	1.86	18.28
N-Dimethylamine	6.88	1.79	5.49
Nitrobenzene	99.62	0.10	97.42
N-nitroso dimethyl amine (NDMA)	17.66	1.87	18.90
Phenanthrene	99.71	0.02	100.45
Phenol	59.99	5.06	60.66
Phthalic Anhydride	1.68	0.99	1.96
Progesterone	25.33	2.14	28.41
t Butyl Alcohol	7.11	1.80	6.80
Testosterone	11.65	3.45	13.49
Tetracycline	7.69	0.94	8.63
Threonine	4.04	0.62	5.92
Toluene	98.49	0.04	94.23
Trichloroacetic Acid	8.83	1.23	7.05
Urea	1.40	0.06	1.68
Valine	4.58	1.41	8.57

Table 9c. BW-30 Performance Based on Individual Compounds – Relative R-Flux
The table shows how well compound behavior could be predicted by the ANN model. In most cases, the model accurately predicted behavior.
Actual = laboratory determination
Predicted = ANN model prediction

Compound	R-Flux		
	Actual (Avg)	(StDev)	Predicted
1,1,2,2, Tetrachloroethylene (PCE)	0.00	0.00	0.00
1,4 Dichlorophenoxyacetic Acid	80.76	7.08	81.08
17a Estradiol	22.22	12.81	29.32
2,3,4,5,6 Pentachlorophenol	46.15	5.30	53.52
2,4 Dinitrotoluene	0.00	0.00	8.41
2-chloro-2'-6'-diethyl-N-methoxymethyl-acetanilide (Alachlor)	94.38	1.95	94.03
4 Nonylphenol	63.06	5.88	63.88
4,6 Dichlorophenol	0.00	0.00	0.00
Alanine	81.54	3.84	79.84
Asparagine	90.70	3.26	91.74
Aspartic Acid	81.86	4.84	82.57
Benzene	0.00	0.00	0.00
beta Sitostanol n Hydrate	70.59	9.41	73.77
Bisphenol	68.55	10.53	65.81
Caffeine	68.07	9.29	69.59
Cholesterol	86.54	1.25	87.46
Cimetidine	78.88	5.83	79.85
Ciprofloxacin	95.24	3.15	92.20
Clorpyrifos	73.50	13.49	71.33
Codeine	77.46	8.49	77.34
Cysteine	69.61	6.37	76.79
Dichloroacetic Acid	75.70	5.45	75.43
Diethylphthalate	56.16	21.24	59.64
Diethylstilbestrol	62.58	8.14	67.32
Doxycycline	86.21	2.96	85.33
Erythromycin	88.56	1.33	91.16
Estrone	29.77	23.40	28.69
Ethylbenzene	0.00	0.00	0.00
Ethylenediaminetetraacetic Acid (EDTA)	91.72	2.07	91.11
Glycine	81.74	5.07	87.92
Histidine	77.61	2.19	76.70
Ibuprofen	65.49	2.77	65.88
Lindane	31.38	5.85	24.78
Lysine	82.85	3.88	82.97
Methionine	67.94	7.21	64.32
methyl Parathion	87.03	1.95	86.03
N-Dimethylamine	58.38	3.73	31.81
Nitrobenzene	0.00	0.00	0.00
N-nitroso dimethyl amine (NDMA)	0.00	0.00	31.79
Phenanthrene	0.00	0.00	12.63
Phenol	4.58	4.66	2.68
Phthalic Anhydride	91.48	3.59	91.30
Progesterone	74.64	2.15	77.15
t Butyl Alcohol	74.48	4.76	78.13
Testosterone	87.41	3.72	87.55
Tetracycline	88.88	1.63	86.62
Threonine	86.74	2.64	83.13
Toluene	0.00	0.00	0.00
Trichloroacetic Acid	66.80	5.79	63.68
Urea	9.23	2.16	4.12
Valine	72.46	6.12	70.71

Table 10a. ESPA-2 Performance Based on Individual Compounds – Relative P-Flux
The table shows how well compound behavior could be predicted by the ANN model. In most cases, the model accurately predicted behavior.
Actual = laboratory determination
Predicted = ANN model prediction

Compound	P-Flux		
	Actual (Avg)	(StDev)	Predicted
1,1,2,2, Tetrachloroethylene (PCE)	0.33	0.22	0.29
1,4 Dichlorophenoxyacetic Acid	15.84	6.32	14.64
17a Estradiol	1.65	0.62	1.84
2,3,4,5,6 Pentachlorophenol	2.87	1.55	2.60
2,4 Dinitrotoluene	3.45	0.83	3.44
2-chloro-2'-6'-diethyl-N-methoxymethyl-acetanilide (Alachlor)	2.33	0.64	2.55
4 Nonylphenol	0.33	0.13	0.13
4,6 Dichlorophenol	2.65	0.59	3.31
Alanine	18.54	6.46	14.96
Asparagine	22.01	2.99	22.17
Aspartic Acid	15.69	1.87	18.82
Benzene	23.32	4.14	30.72
beta Sitostanol n Hydrate	0.53	0.02	0.47
Bisphenol	1.88	0.69	2.00
Caffeine	20.62	4.20	19.64
Cholesterol	0.06	0.01	0.03
Cimetidine	19.61	6.43	16.21
Ciprofloxacin	10.57	5.74	11.67
Clorpyrifos	0.66	0.05	0.71
Codeine	15.42	5.20	15.88
Cysteine	10.06	2.99	8.36
Dichloroacetic Acid	30.30	6.42	30.56
Diethylphthalate	4.93	1.62	5.91
Diethylstilbestrol	0.09	0.10	0.15
Doxycycline	4.37	2.02	4.09
Erythromycin	3.86	0.53	4.24
Estrone	0.22	0.11	0.28
Ethylbenzene	3.19	0.15	2.63
Ethylenediaminetetraacetic Acid (EDTA)	14.29	5.34	13.69
Glycine	26.92	2.75	25.22
Histidine	16.02	2.53	13.00
Ibuprofen	4.45	1.60	4.51
Lindane	2.13	0.48	2.34
Lysine	14.23	3.33	14.75
Methionine	16.74	7.04	16.95
methyl Parathion	1.54	0.18	1.54
N-Dimethylamine	33.12	8.90	34.94
Nitrobenzene	0.50	0.06	0.47
N-nitroso dimethyl amine (NDMA)	80.76	8.57	71.97
Phenanthrene	0.45	0.06	0.55
Phenol	30.36	7.40	27.89
Phthalic Anhydride	8.02	4.82	7.08
Progesterone	0.25	0.13	0.21
t Butyl Alcohol	16.96	2.64	17.89
Testosterone	2.34	1.22	2.31
Tetracycline	7.08	2.56	5.82
Threonine	11.80	2.29	11.59
Toluene	8.37	0.88	6.60
Trichloroacetic Acid	23.32	6.68	20.20
Urea	85.11	10.20	84.52
Valine	21.48	8.84	17.16

Table 10b. ESPA-2 Performance Based on Individual Compounds – Relative M-Flux
The table shows how well compound behavior could be predicted by the ANN model. In most cases, the model accurately predicted behavior.
Actual = laboratory determination
Predicted = ANN model prediction

Compound	M-Flux		
	Actual (Avg)	(StDev)	Predicted
1,1,2,2, Tetrachloroethylene (PCE)	99.67	0.22	96.26
1,4 Dichlorophenoxyacetic Acid	17.28	2.14	18.06
17a Estradiol	85.93	8.50	90.12
2,3,4,5,6 Pentachlorophenol	44.66	6.42	47.44
2,4 Dinitrotoluene	96.55	0.83	103.20
2-chloro-2'-6'-diethyl-N-methoxymethyl-acetanilide (Alachlor)	19.99	3.86	19.66
4 Nonylphenol	21.02	3.14	20.79
4,6 Dichlorophenol	97.35	0.59	97.69
Alanine	5.61	2.38	5.69
Asparagine	6.72	1.02	7.64
Aspartic Acid	3.54	0.56	3.05
Benzene	76.68	4.14	78.22
beta Sitostanol n Hydrate	48.57	4.34	49.82
Bisphenol	25.50	7.50	24.05
Caffeine	19.13	4.41	17.74
Cholesterol	17.87	3.42	21.43
Cimetidine	34.06	2.06	40.06
Ciprofloxacin	18.68	3.78	18.84
Clorpyrifos	59.64	11.05	61.97
Codeine	47.68	6.58	48.31
Cysteine	4.98	0.86	6.21
Dichloroacetic Acid	8.16	1.21	7.60
Diethylphthalate	31.46	8.92	31.95
Diethylstilbestrol	21.66	5.69	16.59
Doxycycline	14.46	1.48	15.10
Erythromycin	13.32	2.50	13.02
Estrone	99.78	0.11	93.84
Ethylbenzene	96.81	0.15	88.96
Ethylenediaminetetraacetic Acid (EDTA)	9.07	3.78	8.02
Glycine	4.57	1.59	4.69
Histidine	7.91	0.71	8.12
Ibuprofen	8.89	2.87	8.84
Lindane	58.30	10.23	56.03
Lysine	6.90	2.10	9.25
Methionine	25.10	9.80	18.83
methyl Parathion	28.17	6.83	25.00
N-Dimethylamine	22.79	12.44	21.84
Nitrobenzene	99.50	0.06	97.58
N-nitroso dimethyl amine (NDMA)	14.08	1.78	13.32
Phenanthrene	85.27	8.74	84.54
Phenol	63.34	5.43	63.55
Phthalic Anhydride	3.05	1.23	3.11
Progesterone	34.21	6.30	32.75
t Butyl Alcohol	5.17	1.23	5.50
Testosterone	27.93	10.07	28.66
Tetracycline	18.89	1.65	17.15
Threonine	3.57	0.50	4.77
Toluene	91.63	0.88	84.41
Trichloroacetic Acid	6.90	2.31	7.78
Urea	8.29	13.68	3.22
Valine	8.78	2.44	7.46

Table 10b. ESPA-2 Performance Based on Individual Compounds – Relative M-Flux
The table shows how well compound behavior could be predicted by the ANN model. In most cases, the model accurately predicted behavior.
Actual = laboratory determination
Predicted = ANN model prediction

Compound	M-Flux		
	Actual (Avg)	(StDev)	Predicted
1,1,2,2, Tetrachloroethylene (PCE)	99.67	0.22	96.26
1,4 Dichlorophenoxyacetic Acid	17.28	2.14	18.06
17a Estradiol	85.93	8.50	90.12
2,3,4,5,6 Pentachlorophenol	44.66	6.42	47.44
2,4 Dinitrotoluene	96.55	0.83	103.20
2-chloro-2'-6'-diethyl-N-methoxymethyl-acetanilide (Alachlor)	19.99	3.86	19.66
4 Nonylphenol	21.02	3.14	20.79
4,6 Dichlorophenol	97.35	0.59	97.69
Alanine	5.61	2.38	5.69
Asparagine	6.72	1.02	7.64
Aspartic Acid	3.54	0.56	3.05
Benzene	76.68	4.14	78.22
beta Sitostanol n Hydrate	48.57	4.34	49.82
Bisphenol	25.50	7.50	24.05
Caffeine	19.13	4.41	17.74
Cholesterol	17.87	3.42	21.43
Cimetidine	34.06	2.06	40.06
Ciprofloxacin	18.68	3.78	18.84
Clorpyrifos	59.64	11.05	61.97
Codeine	47.68	6.58	48.31
Cysteine	4.98	0.86	6.21
Dichloroacetic Acid	8.16	1.21	7.60
Diethylphthalate	31.46	8.92	31.95
Diethylstilbestrol	21.66	5.69	16.59
Doxycycline	14.46	1.48	15.10
Erythromycin	13.32	2.50	13.02
Estrone	99.78	0.11	93.84
Ethylbenzene	96.81	0.15	88.96
Ethylenediaminetetraacetic Acid (EDTA)	9.07	3.78	8.02
Glycine	4.57	1.59	4.69
Histidine	7.91	0.71	8.12
Ibuprofen	8.89	2.87	8.84
Lindane	58.30	10.23	56.03
Lysine	6.90	2.10	9.25
Methionine	25.10	9.80	18.83
methyl Parathion	28.17	6.83	25.00
N-Dimethylamine	22.79	12.44	21.84
Nitrobenzene	99.50	0.06	97.58
N-nitroso dimethyl amine (NDMA)	14.08	1.78	13.32
Phenanthrene	85.27	8.74	84.54
Phenol	63.34	5.43	63.55
Phthalic Anhydride	3.05	1.23	3.11
Progesterone	34.21	6.30	32.75
t Butyl Alcohol	5.17	1.23	5.50
Testosterone	27.93	10.07	28.66
Tetracycline	18.89	1.65	17.15
Threonine	3.57	0.50	4.77
Toluene	91.63	0.88	84.41
Trichloroacetic Acid	6.90	2.31	7.78
Urea	8.29	13.68	3.22
Valine	8.78	2.44	7.46

Table 11a. LFC-1 Performance Based on Individual Compounds – Relative P-Flux
The table shows how well compound behavior could be predicted by the ANN model. In most cases, the model accurately predicted behavior.
Actual = laboratory determination
Predicted = ANN model prediction

Compound	P-Flux		
	Actual (Avg)	(StDev)	Predicted
1,1,2,2, Tetrachloroethylene (PCE)	0.07	0.02	0.11
1,4 Dichlorophenoxyacetic Acid	4.76	1.02	4.52
17a Estradiol	0.67	0.14	0.89
2,3,4,5,6 Pentachlorophenol	0.69	0.11	0.82
2,4 Dinitrotoluene	1.69	0.27	1.89
2-chloro-2'-6'-diethyl-N-methoxymethyl-acetanilide (Alachlor)	N/A	N/A	N/A
4 Nonylphenol	0.31	0.03	0.37
4,6 Dichlorophenol	2.35	1.01	1.72
Alanine	15.45	3.00	15.11
Asparagine	12.01	2.70	12.06
Aspartic Acid	9.68	2.24	8.31
Benzene	19.46	5.64	16.21
beta Sitostanol n Hydrate	0.47	0.20	0.31
Bisphenol	1.08	0.52	0.96
Caffeine	14.62	4.08	17.01
Cholesterol	0.27	0.08	0.24
Cimetidine	5.19	1.70	4.78
Ciprofloxacin	7.61	2.33	7.97
Clorpyrifos	1.08	0.13	1.12
Codeine	12.07	2.56	10.85
Cysteine	15.45	3.00	15.33
Dichloroacetic Acid	23.43	1.51	26.75
Diethylphthalate	5.48	1.21	5.50
Diethylstilbestrol	0.19	0.07	0.15
Doxycycline	5.33	0.38	5.74
Erythromycin	2.99	1.23	2.78
Estrone	0.92	0.13	0.90
Ethylbenzene	1.91	0.12	1.95
Ethylenediaminetetraacetic Acid (EDTA)	6.69	2.28	7.21
Glycine	22.85	4.86	26.60
Histidine	17.34	2.30	19.26
Ibuprofen	5.20	2.16	5.25
Lindane	1.07	0.29	1.09
Lysine	6.21	1.84	5.85
Methionine	10.25	1.63	10.56
methyl Parathion	1.32	0.21	1.14
N-Dimethylamine	31.30	3.35	28.76
Nitrobenzene	0.29	0.06	0.29
N-nitroso dimethyl amine (NDMA)	84.23	1.81	80.37
Phenanthrene	0.66	0.17	0.72
Phenol	34.67	2.19	39.54
Phthalic Anhydride	6.06	1.29	5.59
Progesterone	0.03	0.00	0.01
t Butyl Alcohol	25.89	4.19	22.32
Testosterone	1.65	0.94	1.77
Tetracycline	3.52	1.45	3.33
Threonine	12.00	1.84	11.86
Toluene	19.03	4.79	19.51
Trichloroacetic Acid	12.80	2.73	12.65
Urea	95.48	2.81	85.33
Valine	12.18	1.96	12.29

Table 11b. LFC-1 Performance Based on Individual Compounds – Relative M-Flux
The table shows how well compound behavior could be predicted by the ANN model. In most cases, the model accurately predicted behavior.
Actual = laboratory determination
Predicted = ANN model prediction

Compound	M-Flux		
	Actual (Avg)	(StDev)	Predicted
1,1,2,2, Tetrachloroethylene (PCE)	99.93	0.02	96.99
1,4 Dichlorophenoxyacetic Acid	3.92	0.40	3.68
17a Estradiol	67.29	6.49	72.51
2,3,4,5,6 Pentachlorophenol	60.72	3.58	56.12
2,4 Dinitrotoluene	98.31	0.27	100.87
2-chloro-2'-6'-diethyl-N-methoxymethyl-acetanilide (Alachlor)	N/A	N/A	N/A
4 Nonylphenol	23.36	0.75	24.07
4,6 Dichlorophenol	97.65	1.01	97.84
Alanine	5.77	1.15	6.50
Asparagine	7.41	3.29	5.73
Aspartic Acid	2.81	1.19	4.63
Benzene	64.01	11.87	69.75
beta Sitostanol n Hydrate	14.30	5.73	13.78
Bisphenol	16.12	3.63	15.61
Caffeine	21.78	4.86	22.36
Cholesterol	12.56	2.75	12.00
Cimetidine	28.99	2.69	26.25
Ciprofloxacin	30.45	3.94	32.59
Clorpyrifos	21.23	3.31	18.88
Codeine	38.88	2.76	37.98
Cysteine	5.77	1.15	6.74
Dichloroacetic Acid	7.12	0.71	7.57
Diethylphthalate	29.88	3.73	29.19
Diethylstilbestrol	18.39	6.18	18.62
Doxycycline	15.95	1.44	16.43
Erythromycin	7.58	2.07	8.30
Estrone	83.66	4.56	74.58
Ethylbenzene	98.09	0.12	85.79
Ethylenediaminetetraacetic Acid (EDTA)	2.12	0.20	2.12
Glycine	6.45	0.63	4.91
Histidine	7.98	1.38	7.09
Ibuprofen	8.62	1.85	8.78
Lindane	37.32	5.83	40.88
Lysine	2.35	0.29	1.40
Methionine	4.14	0.78	4.53
methyl Parathion	23.85	6.68	25.75
N-Dimethylamine	28.80	2.96	29.10
Nitrobenzene	99.71	0.06	90.41
N-nitroso dimethyl amine (NDMA)	0.53	0.72	0.46
Phenanthrene	99.34	0.17	97.55
Phenol	65.33	2.19	61.98
Phthalic Anhydride	3.06	0.36	3.16
Progesterone	23.25	7.77	22.68
t Butyl Alcohol	6.18	0.64	5.96
Testosterone	41.21	16.05	46.42
Tetracycline	17.59	3.78	16.99
Threonine	3.88	0.43	3.54
Toluene	80.97	4.79	89.27
Trichloroacetic Acid	1.99	0.48	1.68
Urea	1.66	0.32	1.70
Valine	4.89	1.67	4.21

Table 11c. LFC-1 Performance Based on Individual Compounds – Relative R-Flux
The table shows how well compound behavior could be predicted by the ANN model. In most cases, the model accurately predicted behavior.
Actual = laboratory determination
Predicted = ANN model prediction

Compound	R-Flux		
	Actual (Avg)	(StDev)	Predicted
1,1,2,2, Tetrachloroethylene (PCE)	0.00	0.00	-2.58
1,4 Dichlorophenoxyacetic Acid	91.32	1.28	90.28
17a Estradiol	32.04	6.62	32.61
2,3,4,5,6 Pentachlorophenol	38.59	3.47	37.65
2,4 Dinitrotoluene	0.00	0.00	1.75
2-chloro-2'-6'-diethyl-N-methoxymethyl-acetanilide (Alachlor)	N/A	N/A	N/A
4 Nonylphenol	76.32	0.74	76.99
4,6 Dichlorophenol	0.00	0.00	6.22
Alanine	78.77	3.45	76.08
Asparagine	80.58	5.15	83.17
Aspartic Acid	87.52	3.12	87.17
Benzene	16.54	17.15	12.98
beta Sitostanol n Hydrate	85.23	5.90	85.52
Bisphenol	82.80	3.87	84.03
Caffeine	63.61	7.55	72.39
Cholesterol	87.17	2.70	87.83
Cimetidine	65.82	3.99	63.65
Ciprofloxacin	61.94	4.99	62.14
Clorpyrifos	77.70	3.34	76.80
Codeine	49.06	2.68	46.74
Cysteine	78.77	3.45	80.05
Dichloroacetic Acid	69.45	1.88	75.94
Diethylphthalate	64.65	4.23	64.57
Diethylstilbestrol	81.42	6.14	80.44
Doxycycline	78.71	1.51	79.40
Erythromycin	89.43	3.19	90.00
Estrone	15.42	4.62	18.65
Ethylbenzene	0.00	0.00	-2.06
Ethylenediaminetetraacetic Acid (EDTA)	91.20	2.34	92.16
Glycine	70.70	4.57	76.65
Histidine	74.68	3.51	75.48
Ibuprofen	86.18	3.37	85.14
Lindane	61.61	5.90	61.22
Lysine	91.44	1.83	91.00
Methionine	85.60	1.85	84.79
methyl Parathion	74.82	6.87	75.01
N-Dimethylamine	39.90	3.06	39.43
Nitrobenzene	0.00	0.00	-2.69
N-nitroso dimethyl amine (NDMA)	15.25	2.23	18.60
Phenanthrene	0.00	0.00	-4.09
Phenol	0.00	0.00	-1.45
Phthalic Anhydride	90.88	1.60	90.03
Progesterone	76.73	7.78	80.95
t Butyl Alcohol	67.93	4.71	66.91
Testosterone	57.14	16.70	61.03
Tetracycline	78.89	4.60	78.49
Threonine	84.12	2.09	80.51
Toluene	0.00	0.00	0.23
Trichloroacetic Acid	85.21	2.86	82.86
Urea	2.86	2.58	4.38
Valine	82.92	3.18	83.59

Table 12a. TFC-HR Performance Based on Individual Compounds – Relative P-Flux
The table shows how well compound behavior could be predicted by the ANN model. In most cases, the model accurately predicted behavior.
Actual = laboratory determination
Predicted = ANN model prediction

Compound	P-Flux		
	Actual (Avg)	(StDev)	Predicted
1,1,2,2, Tetrachloroethylene (PCE)	0.02	0.01	0.08
1,4 Dichlorophenoxyacetic Acid	5.97	2.93	5.04
17a Estradiol	0.46	0.15	0.37
2,3,4,5,6 Pentachlorophenol	5.08	1.82	5.74
2,4 Dinitrotoluene	1.94	0.54	1.96
2-chloro-2'-6'-diethyl-N-methoxymethyl-acetanilide (Alachlor)	2.43	0.79	2.65
4 Nonylphenol	0.29	0.08	0.22
4,6 Dichlorophenol	2.02	0.65	2.18
Alanine	10.20	4.43	9.73
Asparagine	31.86	4.44	34.91
Aspartic Acid	14.67	3.69	12.00
Benzene	21.41	3.41	22.21
beta Sitostanol n Hydrate	0.43	0.03	0.40
Bisphenol	0.60	0.21	0.24
Caffeine	14.78	3.54	17.20
Cholesterol	0.38	0.05	0.34
Cimetidine	13.96	9.19	13.54
Ciprofloxacin	6.61	2.60	4.89
Clorpyrifos	0.73	0.24	0.75
Codeine	7.66	2.93	7.39
Cysteine	7.02	1.85	7.75
Dichloroacetic Acid	25.82	4.86	20.67
Diethylphthalate	1.47	0.32	1.42
Diethylstilbestrol	0.12	0.03	0.15
Doxycycline	10.24	7.79	8.58
Erythromycin	2.53	0.50	2.54
Estrone	0.16	0.02	0.20
Ethylbenzene	1.61	0.23	2.83
Ethylenediaminetetraacetic Acid (EDTA)	11.10	3.67	11.30
Glycine	18.03	3.90	2.68
Histidine	11.68	3.38	9.64
Ibuprofen	3.97	1.12	3.91
Lindane	0.94	0.22	1.00
Lysine	10.72	2.79	16.85
Methionine	19.96	5.59	17.45
methyl Parathion	3.52	4.74	3.28
N-Dimethylamine	28.58	4.20	35.24
Nitrobenzene	0.36	0.08	0.34
N-nitroso dimethyl amine (NDMA)	78.67	2.07	74.72
Phenanthrene	0.46	0.04	0.51
Phenol	35.10	2.99	32.48
Phthalic Anhydride	8.14	2.18	8.20
Progesterone	0.04	0.02	0.17
t Butyl Alcohol	23.94	3.32	19.14
Testosterone	0.51	0.22	0.33
Tetracycline	2.93	0.93	2.98
Threonine	10.63	0.98	8.68
Toluene	11.91	0.64	7.12
Trichloroacetic Acid	29.05	8.69	28.16
Urea	90.01	1.84	72.31
Valine	11.10	5.00	9.41

Table 12b. TFC-HR Performance Based on Individual Compounds – Relative M-Flux
The table shows how well compound behavior could be predicted by the ANN model. In most cases, the model accurately predicted behavior.
Actual = laboratory determination
Predicted = ANN model prediction

Compound	M-Flux		
	Actual (Avg)	(StDev)	Predicted
1,1,2,2, Tetrachloroethylene (PCE)	99.98	0.01	103.08
1,4 Dichlorophenoxyacetic Acid	9.60	2.96	8.58
17a Estradiol	84.92	12.73	75.07
2,3,4,5,6 Pentachlorophenol	68.69	7.92	73.84
2,4 Dinitrotoluene	98.06	0.54	96.01
2-chloro-2'-6'-diethyl-N-methoxymethyl-acetanilide (Alachlor)	21.19	6.62	24.66
4 Nonylphenol	69.90	16.95	70.73
4,6 Dichlorophenol	97.98	0.65	94.19
Alanine	4.16	0.60	5.41
Asparagine	6.59	1.40	5.26
Aspartic Acid	5.54	0.49	5.32
Benzene	78.59	3.41	81.24
beta Sitostanol n Hydrate	24.75	4.01	21.71
Bisphenol	24.01	4.96	25.91
Caffeine	17.38	4.49	17.06
Cholesterol	13.33	4.58	14.79
Cimetidine	26.06	3.97	25.32
Ciprofloxacin	12.11	4.52	11.23
Clorpyrifos	52.56	6.78	55.86
Codeine	16.76	5.82	20.50
Cysteine	5.68	1.21	5.58
Dichloroacetic Acid	8.78	1.06	8.61
Diethylphthalate	41.18	12.30	40.75
Diethylstilbestrol	47.75	10.61	54.06
Doxycycline	16.74	4.68	15.54
Erythromycin	9.85	0.53	10.48
Estrone	99.84	0.02	103.33
Ethylbenzene	98.39	0.23	94.23
Ethylenediaminetetraacetic Acid (EDTA)	2.03	0.79	2.28
Glycine	5.36	0.46	5.51
Histidine	4.57	1.24	4.59
Ibuprofen	10.36	1.54	11.54
Lindane	66.34	10.00	66.21
Lysine	3.82	0.98	3.48
Methionine	6.49	0.69	5.07
methyl Parathion	25.57	6.43	22.48
N-Dimethylamine	7.89	1.18	7.62
Nitrobenzene	99.64	0.08	100.87
N-nitroso dimethyl amine (NDMA)	21.33	2.07	20.80
Phenanthrene	98.28	2.07	88.47
Phenol	64.67	2.85	61.87
Phthalic Anhydride	3.45	0.86	3.06
Progesterone	33.90	21.76	26.30
t Butyl Alcohol	10.10	1.59	8.47
Testosterone	14.54	4.44	14.39
Tetracycline	14.45	4.32	15.89
Threonine	4.89	1.02	5.22
Toluene	88.09	0.64	93.08
Trichloroacetic Acid	6.50	2.51	6.18
Urea	1.74	0.13	1.76
Valine	5.07	1.05	6.05

Table 12c. TFC-HR Performance Based on Individual Compounds – Relative R-Flux
The table shows how well compound behavior could be predicted by the ANN model. In most cases, the model accurately predicted behavior.
Actual = laboratory determination
Predicted = ANN model prediction

Compound	R-Flux		
	Actual (Avg)	(StDev)	Predicted
1,1,2,2, Tetrachloroethylene (PCE)	0.00	0.00	-2.44
1,4 Dichlorophenoxyacetic Acid	84.43	5.57	83.49
17a Estradiol	14.61	12.71	16.91
2,3,4,5,6 Pentachlorophenol	26.23	8.79	23.23
2,4 Dinitrotoluene	0.00	0.00	1.68
2-chloro-2'-6'-diethyl-N-methoxymethyl-acetanilide (Alachlor)	76.39	7.29	77.77
4 Nonylphenol	29.81	16.92	26.83
4,6 Dichlorophenol	0.00	0.00	4.68
Alanine	85.64	4.72	82.22
Asparagine	61.55	4.97	64.01
Aspartic Acid	79.79	3.38	80.79
Benzene	0.00	0.00	2.46
beta Sitostanol n Hydrate	74.82	4.03	74.20
Bisphenol	75.39	5.14	74.45
Caffeine	67.84	2.79	68.49
Cholesterol	86.30	4.57	88.03
Cimetidine	59.98	11.52	62.29
Ciprofloxacin	81.28	6.81	82.21
Clorpyrifos	46.71	6.91	46.84
Codeine	75.59	7.17	76.11
Cysteine	87.30	2.36	86.50
Dichloroacetic Acid	65.41	5.54	67.59
Diethylphthalate	57.35	12.37	62.42
Diethylstilbestrol	52.14	10.64	50.95
Doxycycline	73.03	8.00	77.12
Erythromycin	87.61	0.82	87.94
Estrone	0.00	0.00	-1.54
Ethylbenzene	0.00	0.00	-4.96
Ethylenediaminetetraacetic Acid (EDTA)	86.87	4.09	88.17
Glycine	76.61	3.98	87.17
Histidine	83.76	2.77	83.38
Ibuprofen	85.67	1.55	86.27
Lindane	32.72	10.06	35.69
Lysine	85.46	2.94	84.53
Methionine	73.55	5.68	73.18
methyl Parathion	70.91	6.40	67.29
N-Dimethylamine	63.53	3.66	62.76
Nitrobenzene	0.00	0.00	-2.19
N-nitroso dimethyl amine (NDMA)	0.00	0.00	2.72
Phenanthrene	1.26	2.05	5.46
Phenol	0.23	0.51	-1.19
Phthalic Anhydride	88.41	2.09	88.36
Progesterone	66.06	21.78	69.81
t Butyl Alcohol	65.95	3.88	66.84
Testosterone	84.95	4.49	85.55
Tetracycline	82.62	5.08	83.45
Threonine	84.48	1.80	84.04
Toluene	0.00	0.00	-1.25
Trichloroacetic Acid	64.46	9.81	67.17
Urea	8.25	1.87	7.26
Valine	83.82	5.94	82.94

Table 13a. CA Performance Based on Individual Compounds – Relative P-Flux
The table shows how well compound behavior could be predicted by the ANN model. In most cases, the model accurately predicted behavior.
Actual = laboratory determination
Predicted = ANN model prediction

Compound	P-Flux		
	Actual (Avg)	(StDev)	Predicted
1,1,2,2, Tetrachloroethylene (PCE)	0.12	0.16	0.12
1,4 Dichlorophenoxyacetic Acid	9.96	6.65	7.33
17a Estradiol	0.77	0.65	0.58
2,3,4,5,6 Pentachlorophenol	2.27	2.22	1.72
2,4 Dinitrotoluene	3.03	1.62	2.76
2-chloro-2'-6'-diethyl-N-methoxymethyl-acetanilide (Alachlor)	1.77	1.09	1.51
4 Nonylphenol	0.31	0.08	0.45
4,6 Dichlorophenol	3.61	2.42	3.30
Alanine	14.25	5.25	16.43
Asparagine	18.20	10.27	12.98
Aspartic Acid	13.23	3.43	13.22
Benzene	22.60	5.08	20.79
beta Sitostanol n Hydrate	0.48	0.11	0.54
Bisphenol	1.67	1.39	1.18
Caffeine	16.97	4.25	20.08
Cholesterol	0.20	0.14	0.21
Cimetidine	11.84	8.06	9.39
Ciprofloxacin	6.72	4.48	6.24
Clorpyrifos	0.82	0.21	0.71
Codeine	10.98	4.74	11.13
Cysteine	12.83	5.83	9.99
Dichloroacetic Acid	24.44	6.66	23.83
Diethylphthalate	6.23	7.42	4.88
Diethylstilbestrol	0.12	0.09	0.14
Doxycycline	5.80	4.61	5.08
Erythromycin	3.29	0.92	3.33
Estrone	0.48	0.35	0.42
Ethylbenzene	2.57	0.87	2.61
Ethylenediaminetetraacetic Acid (EDTA)	9.35	4.88	8.77
Glycine	20.39	6.06	33.98
Histidine	15.30	3.16	14.13
Ibuprofen	6.78	4.99	5.07
Lindane	1.62	0.81	1.51
Lysine	11.43	4.25	10.41
Methionine	18.16	7.14	12.22
methyl Parathion	1.84	2.41	1.45
N-Dimethylamine	31.93	5.68	35.30
Nitrobenzene	0.38	0.10	0.37
N-nitroso dimethyl amine (NDMA)	81.54	4.79	67.55
Phenanthrene	0.46	0.16	0.47
Phenol	33.89	5.07	31.55
Phthalic Anhydride	7.27	2.93	7.53
Progesterone	0.09	0.11	0.21
t Butyl Alcohol	21.30	5.00	20.79
Testosterone	1.36	1.03	1.04
Tetracycline	4.24	2.31	3.40
Threonine	10.91	2.15	10.38
Toluene	9.62	6.58	5.76
Trichloroacetic Acid	23.30	8.47	22.09
Urea	90.57	6.53	75.25
Valine	16.93	7.82	16.93

Table 13b. CA Performance Based on Individual Compounds – Relative M-Flux
The table shows how well compound behavior could be predicted by the ANN model. In most cases, the model accurately predicted behavior.
Actual = laboratory determination
Predicted = ANN model prediction

Compound	M-Flux		
	Actual (Avg)	(StDev)	Predicted
1,1,2,2, Tetrachloroethylene (PCE)	67.77	5.49	66.34
1,4 Dichlorophenoxyacetic Acid	5.30	1.07	6.40
17a Estradiol	97.52	0.53	97.45
2,3,4,5,6 Pentachlorophenol	97.77	0.30	97.69
2,4 Dinitrotoluene	92.94	0.85	93.28
2-chloro-2'-6'-diethyl-N-methoxymethyl-acetanilide (Alachlor)	N/A	N/A	N/A
4 Nonylphenol	95.98	3.64	98.57
4,6 Dichlorophenol	97.56	0.36	97.54
Alanine	6.78	1.42	8.33
Asparagine	0.73	0.19	0.64
Aspartic Acid	8.48	2.33	9.24
Benzene	43.42	3.24	44.79
beta Sitostanol n Hydrate	28.23	8.99	24.04
Bisphenol	99.11	0.07	97.96
Caffeine	10.09	0.58	11.46
Cholesterol	16.48	14.86	20.11
Cimetidine	21.67	2.42	21.54
Ciprofloxacin	27.03	5.33	24.20
Clorpyrifos	97.09	0.48	97.63
Codeine	26.16	3.05	27.10
Cysteine	9.37	2.37	6.61
Dichloroacetic Acid	6.23	1.02	5.87
Diethylphthalate	83.52	0.56	82.97
Diethylstilbestrol	99.74	0.06	99.37
Doxycycline	30.61	5.57	29.48
Erythromycin	8.28	1.56	6.06
Estrone	97.32	0.33	97.30
Ethylbenzene	66.72	8.20	68.70
Ethylenediaminetetraacetic Acid (EDTA)	7.52	1.90	7.05
Glycine	6.72	1.67	9.95
Histidine	8.82	0.95	8.06
Ibuprofen	20.45	2.15	23.00
Lindane	98.48	0.42	98.80
Lysine	9.30	1.02	9.55
Methionine	8.58	1.95	8.93
methyl Parathion	97.82	0.18	97.86
N-Dimethylamine	13.25	1.31	12.92
Nitrobenzene	73.09	3.84	63.65
N-nitroso dimethyl amine (NDMA)	3.51	0.11	3.67
Phenanthrene	99.57	0.05	99.65
Phenol	28.33	1.84	31.30
Phthalic Anhydride	6.22	1.19	5.34
Progesterone	98.51	0.21	98.63
t Butyl Alcohol	4.04	0.43	3.69
Testosterone	74.38	5.94	55.06
Tetracycline	14.42	2.76	15.49
Threonine	7.52	2.55	7.53
Toluene	52.21	3.16	48.83
Trichloroacetic Acid	4.19	0.43	4.60
Urea	3.08	0.35	4.59
Valine	5.64	1.67	4.93

Table 13c. CA Performance Based on Individual Compounds – Relative R-Flux
The table shows how well compound behavior could be predicted by the ANN model. In most cases, the model accurately predicted behavior.
Actual = laboratory determination
Predicted = ANN model prediction

Compound	R-Flux		
	Actual (Avg)	(StDev)	Predicted
1,1,2,2, Tetrachloroethylene (PCE)	1.44	1.99	6.04
1,4 Dichlorophenoxyacetic Acid	50.96	10.26	46.61
17a Estradiol	0.00	0.00	0.84
2,3,4,5,6 Pentachlorophenol	0.00	0.00	0.35
2,4 Dinitrotoluene	0.00	0.00	0.47
2-chloro-2'-6'-diethyl-N-methoxymethyl-acetanilide (Alachlor)	N/A	N/A	N/A
4 Nonylphenol	3.29	3.71	1.88
4,6 Dichlorophenol	0.00	0.00	-0.80
Alanine	39.33	7.76	40.05
Asparagine	34.30	4.39	42.86
Aspartic Acid	57.29	4.94	61.70
Benzene	0.00	0.00	1.48
beta Sitostanol n Hydrate	71.10	8.98	75.84
Bisphenol	0.00	0.00	0.21
Caffeine	14.37	3.17	15.14
Cholesterol	83.27	14.80	70.30
Cimetidine	18.44	6.38	22.86
Ciprofloxacin	37.85	7.65	24.76
Clorpyrifos	0.00	0.00	-0.19
Codeine	16.50	6.97	10.66
Cysteine	46.75	4.94	42.02
Dichloroacetic Acid	52.51	4.75	37.16
Diethylphthalate	0.00	0.00	0.22
Diethylstilbestrol	0.00	0.00	0.43
Doxycycline	51.36	6.91	53.97
Erythromycin	63.41	6.88	70.00
Estrone	0.00	0.00	-0.39
Ethylbenzene	9.13	10.19	1.42
Ethylenediaminetetraacetic Acid (EDTA)	44.42	6.49	45.09
Glycine	36.92	3.71	38.56
Histidine	45.89	3.20	44.55
Ibuprofen	21.57	7.70	22.96
Lindane	0.00	0.00	-0.22
Lysine	38.85	4.23	27.34
Methionine	44.49	4.88	39.66
methyl Parathion	0.00	0.00	-0.10
N-Dimethylamine	31.84	2.92	10.38
Nitrobenzene	0.00	0.00	0.80
N-nitroso dimethyl amine (NDMA)	2.44	4.67	3.67
Phenanthrene	0.00	0.00	0.97
Phenol	0.00	0.00	-0.34
Phthalic Anhydride	64.70	8.85	64.35
Progesterone	0.00	0.00	-0.28
t Butyl Alcohol	8.53	4.42	12.52
Testosterone	4.65	5.50	2.77
Tetracycline	53.32	8.11	57.31
Threonine	46.75	1.96	35.08
Toluene	0.00	0.00	2.04
Trichloroacetic Acid	35.70	5.25	39.79
Urea	6.34	2.36	28.21
Valine	31.64	6.68	34.09

Table 14a. "Universal" PA Performance Based on Individual Compounds – Relative P-Flux
The table shows how well compound behavior could be predicted by the ANN model. In most cases, the model accurately predicted behavior.
Actual = laboratory determination
Predicted = ANN model prediction

Compound	P-Flux		
	Actual (Avg)	(StDev)	Predicted
1,1,2,2, Tetrachloroethylene (PCE)	0.12	0.16	0.12
1,4 Dichlorophenoxyacetic Acid	9.96	6.65	7.33
17a Estradiol	0.77	0.65	0.58
2,3,4,5,6 Pentachlorophenol	2.27	2.22	1.72
2,4 Dinitrotoluene	3.03	1.62	2.76
2-chloro-2'-6'-diethyl-N-methoxymethyl-acetanilide (Alachlor)	1.77	1.09	1.51
4 Nonylphenol	0.31	0.08	0.45
4,6 Dichlorophenol	3.61	2.42	3.30
Alanine	14.25	5.25	16.43
Asparagine	18.20	10.27	12.98
Aspartic Acid	13.23	3.43	13.22
Benzene	22.60	5.08	20.79
beta Sitostanol n Hydrate	0.48	0.11	0.54
Bisphenol	1.67	1.39	1.18
Caffeine	16.97	4.25	20.08
Cholesterol	0.20	0.14	0.21
Cimetidine	11.84	8.06	9.39
Ciprofloxacin	6.72	4.48	6.24
Clorpyrifos	0.82	0.21	0.71
Codeine	10.98	4.74	11.13
Cysteine	12.83	5.83	9.99
Dichloroacetic Acid	24.44	6.66	23.83
Diethylphthalate	6.23	7.42	4.88
Diethylstilbestrol	0.12	0.09	0.14
Doxycycline	5.80	4.61	5.08
Erythromycin	3.29	0.92	3.33
Estrone	0.48	0.35	0.42
Ethylbenzene	2.57	0.87	2.61
Ethylenediaminetetraacetic Acid (EDTA)	9.35	4.88	8.77
Glycine	20.39	6.06	33.98
Histidine	15.30	3.16	14.13
Ibuprofen	6.78	4.99	5.07
Lindane	1.62	0.81	1.51
Lysine	11.43	4.25	10.41
Methionine	18.16	7.14	12.22
methyl Parathion	1.84	2.41	1.45
N-Dimethylamine	31.93	5.68	35.30
Nitrobenzene	0.38	0.10	0.37
N-nitroso dimethyl amine (NDMA)	81.54	4.79	67.55
Phenanthrene	0.46	0.16	0.47
Phenol	33.89	5.07	31.55
Phthalic Anhydride	7.27	2.93	7.53
Progesterone	0.09	0.11	0.21
t Butyl Alcohol	21.30	5.00	20.79
Testosterone	1.36	1.03	1.04
Tetracycline	4.24	2.31	3.40
Threonine	10.91	2.15	10.38
Toluene	9.62	6.58	5.76
Trichloroacetic Acid	23.30	8.47	22.09
Urea	90.57	6.53	75.25
Valine	16.93	7.82	16.93

Table 14b. "Universal" PA Performance Based on Individual Compounds – Relative M-Flux
The table shows how well compound behavior could be predicted by the ANN model. In most cases, the model accurately predicted behavior.
Actual = laboratory determination
Predicted = ANN model prediction

Compound	M-Flux		
	Actual (Avg)	(StDev)	Predicted
1,1,2,2, Tetrachloroethylene (PCE)	99.88	0.16	95.55
1,4 Dichlorophenoxyacetic Acid	9.20	5.53	7.65
17a Estradiol	79.01	12.26	88.30
2,3,4,5,6 Pentachlorophenol	56.87	10.66	55.61
2,4 Dinitrotoluene	96.97	1.62	98.89
2-chloro-2'-6'-diethyl-N-methoxymethyl-acetanilide (Alachlor)	15.81	8.44	14.15
4 Nonylphenol	37.73	21.69	33.54
4,6 Dichlorophenol	96.39	2.42	97.88
Alanine	5.05	1.43	4.40
Asparagine	4.62	2.33	3.78
Aspartic Acid	4.41	1.82	5.04
Benzene	73.05	8.78	74.11
beta Sitostanol n Hydrate	29.14	13.97	18.84
Bisphenol	23.49	7.61	21.31
Caffeine	18.09	5.53	16.70
Cholesterol	14.29	3.66	19.07
Cimetidine	25.66	7.99	25.86
Ciprofloxacin	15.98	10.89	11.68
Clorpyrifos	39.78	19.13	41.47
Codeine	28.52	15.54	28.03
Cysteine	7.52	3.48	6.06
Dichloroacetic Acid	8.05	1.15	7.46
Diethylphthalate	34.99	12.18	32.62
Diethylstilbestrol	31.28	14.19	27.74
Doxycycline	14.42	3.59	14.48
Erythromycin	9.59	3.02	9.15
Estrone	89.73	14.75	77.69
Ethylbenzene	97.43	0.87	95.58
Ethylenediaminetetraacetic Acid (EDTA)	4.05	3.51	3.56
Glycine	4.86	1.47	3.93
Histidine	6.67	1.88	6.98
Ibuprofen	10.97	4.17	9.92
Lindane	57.06	14.31	49.52
Lysine	4.00	2.07	3.88
Methionine	6.34	2.00	6.01
methyl Parathion	22.40	8.31	20.55
N-Dimethylamine	16.27	11.18	14.10
Nitrobenzene	99.62	0.10	97.53
N-nitroso dimethyl amine (NDMA)	13.80	7.76	12.02
Phenanthrene	95.65	7.42	94.79
Phenol	63.33	4.33	65.52
Phthalic Anhydride	2.81	1.09	2.90
Progesterone	29.83	12.10	28.97
t Butyl Alcohol	7.14	2.28	7.08
Testosterone	23.83	15.10	20.57
Tetracycline	14.66	5.24	14.16
Threonine	4.10	0.80	4.86
Toluene	90.38	6.58	90.38
Trichloroacetic Acid	6.28	2.96	5.51
Urea	3.28	6.95	2.21
Valine	5.83	2.36	6.39

Table 14c. "Universal" PA Performance Based on Individual Compounds – Relative R-Flux
The table shows how well compound behavior could be predicted by the ANN model. In most cases, the model accurately predicted behavior.
Actual = laboratory determination
Predicted = ANN model prediction

Compound	R-Flux		
	Actual (Avg)	(StDev)	Predicted
1,1,2,2, Tetrachloroethylene (PCE)	0.00	0.00	-3.28
1,4 Dichlorophenoxyacetic Acid	80.84	10.71	80.77
17a Estradiol	20.22	12.40	24.93
2,3,4,5,6 Pentachlorophenol	40.86	11.62	39.53
2,4 Dinitrotoluene	0.00	0.00	-2.48
2-chloro-2'-6'-diethyl-N-methoxymethyl-acetanilide (Alachlor)	83.40	9.75	85.37
4 Nonylphenol	61.96	21.67	68.02
4,6 Dichlorophenol	0.00	0.00	-3.38
Alanine	80.70	5.98	80.97
Asparagine	76.02	11.75	79.02
Aspartic Acid	82.35	4.43	80.64
Benzene	4.35	11.02	8.13
beta Sitostanol n Hydrate	70.39	14.02	70.10
Bisphenol	74.84	8.62	74.46
Caffeine	64.94	7.09	64.92
Cholesterol	85.52	3.61	85.63
Cimetidine	62.50	13.58	67.54
Ciprofloxacin	77.30	13.89	80.62
Clorpyrifos	59.40	19.01	62.81
Codeine	60.51	19.16	61.67
Cysteine	79.66	8.28	82.35
Dichloroacetic Acid	67.52	7.11	66.72
Diethylphthalate	59.93	13.26	61.30
Diethylstilbestrol	68.59	14.18	69.13
Doxycycline	79.78	6.37	78.59
Erythromycin	87.13	3.47	88.25
Estrone	9.79	14.57	32.56
Ethylbenzene	0.00	0.00	-4.95
Ethylenediaminetetraacetic Acid (EDTA)	86.60	7.35	85.89
Glycine	74.74	6.71	86.59
Histidine	78.03	4.39	78.75
Ibuprofen	82.25	8.85	82.17
Lindane	41.32	14.54	47.32
Lysine	84.57	5.68	84.69
Methionine	75.50	8.61	75.75
methyl Parathion	75.76	8.77	78.87
N-Dimethylamine	51.48	11.21	51.93
Nitrobenzene	0.00	0.00	-6.95
N-nitroso dimethyl amine (NDMA)	4.66	7.87	3.63
Phenanthrene	3.88	7.42	7.52
Phenol	2.78	4.75	3.93
Phthalic Anhydride	89.92	3.52	89.95
Progesterone	70.74	12.19	70.12
t Butyl Alcohol	71.56	6.33	71.30
Testosterone	74.81	15.77	75.39
Tetracycline	81.10	6.69	83.29
Threonine	84.99	2.32	82.90
Toluene	0.00	0.00	-4.88
Trichloroacetic Acid	70.42	10.12	73.92
Urea	6.15	3.74	4.50
Valine	77.24	9.08	76.44

Table 15a. Analysis of Influence – Sensitivity Index for Relative P-Flux
The table represents a summary of input parameters that were influential in the model. The index represents the magnitude and direction of strength of influence of each input on the model output.

Sensitivity Index P-Flux							
		BW-30	ESPA-2	LFC-1	TFC-HR	"Univ" PA	CA
Charge	MaxQp		-0.38		-1.52		
	Py	0.26	0.14	0.77		-0.01	
	P				0.67		1.06
	SsCH3	0.67	0.12			0.14	
	SdssC			-0.08		-0.02	-0.61
	Hmin		0.38		0.23	0.25	
Molecular Complexity	Ovality	-0.17					
	Surface					-0.18	-0.69
	xpc4						0.46
	xv1						-1.40
	xvpc4	-0.72	-0.50		0.39	-0.69	
	nxp5				0.01		
	Iy		-1.03	0.49			
	fw				-0.60		
HPB/CHGE	Qsv						0.77
HPB	LogP	-0.01	-0.32	-0.35		-0.24	-0.99
H-Bond	numHBa	1.32	0.39		0.23		0.00

HPB/CHGE = Hydrophobicity/Charge
HPB = Hydrophobicity
H-Bond = Hydrogen Bonding

Table 15b. Analysis of Influence – Sensitivity Index for Relative M-Flux
The table represents a summary of input parameters that were influential in the model. The index represents the magnitude and direction of strength of influence of each input on the model output.

Sensitivity Index M-Flux							
		BW-30	ESPA-2	LFC-1	TFC-HR	"Univ" PA	CA
Charge	MaxQp			2.19			
	P	-0.64	-0.20	-0.64	0.44	-0.24	2.01
	Q			0.47			0.98
	SaaCH			0.48	3.30		
	SdssC		-0.31	-0.37			1.23
	Gmax	0.01					
	Gmin	0.79	0.56	1.30	1.51	0.52	
Molecular Complexity	nxch6					0.76	
	k1		-1.67				
	idcbar			-1.28			
	fw		1.20	0.66		-0.65	
HPB/CHGE	Qs		1.40	1.92			
HPB	LogP	0.37			-0.10	0.70	1.25
H-Bond	numHBa		0.21	0.76	0.18	1.20	

HPB/CHGE = Hydrophobicity/Charge
HPB = Hydrophobicity
H-Bond = Hydrogen Bonding

Table 15c. Analysis of Influence – Sensitivity Index for Relative R-Flux
The table represents a summary of input parameters that were influential in the model. The index represents the magnitude and direction of strength of influence of each input on the model output.

Sensitivity Index R-Flux							
		BW-30	ESPA-2	LFC-1	TFC-HR	"Univ" PA	CA
Charge	ABSQ						0.76
	MaxNeg		0.04				
	Py				-0.83		
	Pz	-0.47					
	Q		-1.61	-0.33	-1.65	-1.24	-0.83
	SaaCH				-2.70		-0.38
	SdssC			-3.11	-0.49		-0.75
	SdO				0.03		
	Gmax		-0.52		0.01	-0.45	
	Gmin	-2.13	-2.15	-0.34	-1.38	-0.09	
Molecular Complexity	nxch6		0.21	0.86			
	sumdeII			-0.32			-0.30
	Wt	-6.11				22.70	
	k2		0.33	1.58			
	k3					-0.04	
	idcbar				1.34		
HPB	LogP	-1.02			-0.55	-0.63	
H-Bond	numHBa		-1.48	-0.68	-1.43	-0.80	

HPB/CHGE = Hydrophobicity/Charge
HPB = Hydrophobicity
H-Bond = Hydrogen Bonding

Table 16a. Final Relative Flux Model Outputs for BW-30
The predicted values represent a 25% noise-band criteria. Bolded compounds represent surrogates used to build the models

Compound Name	P-Flux	M-Flux	R-Flux	F-Flux
1,1,2 Trichloroethene (TCE)	4.04	92.54	21.20	117.78
1,1,2,2 Tetrachloroethane	0.09	92.35	0.00	92.44
1,1,2,2, Tetrachloroethylene (PCE)	**0.09**	**93.76**	**0.00**	**93.85**
1,2 Dichlorobenzene	1.23	94.17	2.00	97.41
1,2 Dimethylbenzene	3.96	97.75	0.00	101.70
1,2,4 Trimethylbenzene	0.12	100.84	0.00	100.96
1,3,5 Trimethylbenzene	1.00	100.27	0.00	101.28
1,4 Dichlorobenzene	1.93	100.11	0.52	102.56
1,4 Dichlorophenoxyacetic Acid	**11.12**	**6.07**	**81.08**	**98.27**
17a Estradiol	**0.18**	**77.02**	**29.32**	**106.52**
2,2 bis-p-Chlorophenyl 1,1 Dichloroethane	0.51	21.66	71.86	94.03
2,2 bis-p-Chlorophenyl 1,1,1 Trichloroethane	3.26	45.96	72.46	121.69
2,2 bis-p-Methoxyphenyl 1,1,1 Trichloroethane	9.64	34.09	72.19	115.92
2,2,2 Trichloro 1,1-bis-4-chlorophenyl Ethanol	0.85	37.13	71.60	109.58
2,3 Naphthalenedicarboxylic Acid	15.65	9.68	90.42	115.74
2,3,4,5,6 Pentachlorophenol	**0.37**	**53.23**	**53.52**	**107.13**
2,3,5,6 Tetrachloroterephthalic Acid	0.92	17.68	68.40	87.00
2,4 Dichloro-4'-nitrodiphenyl Ether	10.54	37.38	75.16	123.08
2,4 Dinitrotoluene	**4.06**	**95.97**	**8.41**	**108.44**
2,4,5 Trichlorophenoxyacetic Acid	6.57	16.63	73.24	96.44
2,6 bis-1,1 Dimethylethyl 2,5 Cyclohexadiene 1,4 dione	22.48	21.72	54.10	98.29
2,6 bis-1,1 Dimethylethyl Phenol	0.42	31.03	70.31	101.76
2,6 di-tert-butyl-p-Cresol	1.84	30.17	74.91	106.91
2-chloro-2'-6'-diethyl-N-methoxymethyl-acetanilide (Alachlor)	**0.44**	**4.47**	**94.03**	**98.93**
3 Hydroxycarbofuran	0.77	95.32	94.98	113.40
3,4,5,6,7,8,8a-Heptachlorodicyclopentadiene	0.30	2.69	19.81	115.43
3-amino-1H-1,2,4 Triazole	6.97	17.65	81.25	90.91
4 Nonylphenol	**0.25**	**35.99**	**63.88**	**100.12**
4,6 Dichlorophenol	**7.63**	**96.83**	**0.00**	**104.46**
5-methyl-1H-Benzotriazole	6.29	71.15	33.56	111.01
Acetaminophen	6.44	66.99	3.34	76.78
Alanine	**12.74**	**5.57**	**79.84**	**98.15**
Aldicarbsulfone	21.63	8.85	86.28	116.76
alpha-naphthyl-N-Methylcarbamate	8.14	4.99	81.67	94.80
Androsterone	0.24	18.06	95.88	114.18
Anthracene	0.09	99.68	12.48	112.25
Asparagine	**9.47**	**2.66**	**91.74**	**103.87**
Aspartic Acid	**14.32**	**4.90**	**82.57**	**101.80**
Atrazine	3.59	110.61	34.50	148.70
Benzene	**24.97**	**79.34**	**0.00**	**104.32**
benzo-e-1,3,2 Dioxathiepin-3-oxide	4.45	4.47	94.70	103.61
beta Sitostanol n Hydrate	**0.45**	**16.59**	**73.77**	**90.80**
beta-Estradiol	0.24	72.30	33.22	105.76
bis-2-Ethylhexyl-adipate	53.38	49.91	0.00	103.29
Bisphenol	**2.69**	**28.63**	**65.81**	**97.14**
Bromochloroacetic Acid	5.26	15.70	87.76	108.72
Bromochloromethane	89.81	10.36	15.85	116.02
Caffeine	**17.61**	**13.06**	**69.59**	**100.26**
Chloralhydrate	0.53	6.99	71.24	78.76

Table 16b. Final Relative Flux Model Outputs for BW-30
(Continued – See Table 16a)

Compound Name	P-Flux	M-Flux	R-Flux	F-Flux
Chlorotetracycline	0.46	4.76	86.21	91.44
Chlorpyrifos	**0.80**	**20.17**	**71.33**	**92.96**
Cholesterol	**0.09**	**14.46**	**87.46**	**107.72**
Cimetidine	**7.80**	**2.41**	**79.85**	**102.11**
Ciprofloxacin	**1.51**	**52.82**	**92.20**	**96.12**
Codeine	**7.15**	**10.35**	**77.34**	**94.83**
Cylindrospermopsin	6.63	3.83	91.02	101.48
Cymene	0.68	102.20	0.00	102.88
Cysteine	**16.20**	**7.82**	**76.79**	**100.81**
Diazinon	4.40	20.69	96.52	121.60
Dibromoacetatic Acid	1.72	10.36	78.09	90.17
Dibromoacetonitrile	9.57	96.12	0.00	105.69
Dibromochloropropane	0.43	113.67	0.00	114.10
Dichloroacetic Acid	**14.65**	**8.62**	**75.43**	**98.71**
Dichlorodiphenyldichloroethylene	2.55	15.64	79.24	97.43
Dieldrin	0.04	11.34	94.96	106.34
Diethylphthalate	**5.76**	**28.67**	**59.64**	**94.07**
Diethylstilbestrol	**0.10**	**33.85**	**67.32**	**101.27**
Digoxigenin	0.91	2.58	81.64	85.14
Digoxin	4.00	2.15	73.73	79.88
Disulfoton	0.19	3.89	96.58	100.66
Diuron	63.78	14.05	2.64	80.48
d--n-Butylphthalate	0.40	42.25	67.47	110.13
d--n-Octylphthalate				
Doxycycline	**4.14**	**10.67**	**85.33**	**100.14**
Enalaprilat	0.44	8.32	92.11	100.86
Endosulfansulfate	0.06	29.66	93.66	123.37
Enrofloxacin	3.18	3.81	89.40	96.39
Equilenin	0.23	37.29	42.95	80.48
Erythromycin	**3.72**	**5.36**	**91.16**	**100.24**
Estriol	0.03	23.38	94.26	117.68
Estrone	**0.59**	**68.57**	**28.69**	**97.85**
Ethylbenzene	**4.50**	**98.43**	**0.00**	**102.94**
Ethylenediaminetetraacetic Acid (EDTA)	**5.09**	**2.46**	**91.11**	**98.66**
Fluoranthrene	0.08	67.44	19.06	86.58
Fluoxetine	0.37	30.42	90.00	120.78
Fonofos	0.22	8.93	72.71	81.86
Gemfibrozil	14.06	24.82	72.36	111.25
Glycine	**6.12**	**4.19**	**87.92**	**98.23**
Hexachlorobutadiene	10.41	70.90	39.32	120.63
Histidine	**15.61**	**7.29**	**76.70**	**99.60**
Ibuprofen	**15.83**	**19.16**	**65.88**	**100.87**
Lincomycin	3.13	3.87	91.88	98.89
Lindane	**1.93**	**62.01**	**24.78**	**88.72**
Linuron	42.07	16.36	26.34	84.76
Lysine	**13.88**	**2.96**	**82.97**	**99.82**
Mestranol	0.18	21.97	83.41	105.56
Methionine	**25.39**	**5.60**	**64.32**	**95.32**
methyl Parathion	**1.19**	**18.28**	**86.03**	**105.49**

Table 16c. Final Relative Flux Model Outputs for BW-30
(Continued – See Table 16b)

Compound Name	P-Flux	M-Flux	R-Flux	F-Flux
Microcystin LR	13.43	5.68	79.75	98.86
Molinate	24.63	36.94	31.17	92.74
Monobromobenzene	1.47	91.80	0.00	93.27
Nitrobenzene	**0.39**	**97.42**	**0.00**	**97.81**
Nitrosodibutylamine	12.51	73.14	1.88	87.52
N-nitroso dimethyl amine (NDMA)	**101.35**	**18.90**	**31.79**	**152.04**
Norethindrone	0.10	55.90	25.64	81.64
Norfloxacin	1.87	2.59	92.71	97.17
N-triacetic Acid	27.30	3.61	85.39	116.30
o-Cresol	11.18	83.52	13.24	107.94
Octachloro-4-7-methanotetrahydroindane	0.07	24.70	91.90	116.67
Octachloroepoxide	0.42	25.49	86.70	112.60
Paraxanthine	22.33	10.62	79.02	111.97
Paroxetine	0.64	23.25	83.20	107.09
p-Cresol	2.68	67.97	8.39	79.03
p-Dichlorobenzene	2.00	100.11	0.52	102.62
Perchloric Acid	11.35	8.47	74.43	94.25
Phenanthrene	**0.27**	**100.45**	**12.63**	**113.35**
Phenol	**33.46**	**60.66**	**2.68**	**96.79**
Phenylalanine	34.59	11.75	40.71	87.06
Phthalic Anhydride	**5.58**	**1.96**	**91.30**	**98.84**
Progesterone	**0.06**	**28.41**	**77.15**	**105.61**
Pyrene	0.14	92.92	18.31	111.37
Saxitoxin	3.32	1.37	92.84	97.54
Serine	28.23	2.31	85.65	116.18
Sulfachlorpyridazine	1.85	8.38	79.70	89.94
Sulfadimethoxine	4.12	10.76	83.37	98.25
Sulfamerazine	0.58	9.08	84.60	94.26
Sulfamethazine	2.28	11.91	82.96	97.16
Sulfamethizole	2.36	8.53	88.97	99.86
Sulfamethoxazole	2.52	7.29	82.42	92.23
Sulfathiazole	1.25	7.13	82.91	91.29
t Butyl Alcohol	**19.63**	**6.80**	**78.13**	**104.56**
Terbufos	2.58	15.06	74.10	91.74
Terramycin	4.33	12.58	86.59	103.50
tert amyl methyl Ether	0.65	112.67	0.00	113.32
Testosterone	**0.87**	**13.49**	**87.55**	**101.91**
Tetracycline	**3.32**	**8.63**	**86.62**	**98.57**
Threonine	**9.01**	**5.92**	**83.13**	**98.06**
Toluene	**1.41**	**94.23**	**0.00**	**95.63**
Tributyl Tin	0.15	64.74	54.28	119.17
Trichloroacetic Acid	**22.80**	**7.05**	**63.68**	**93.52**
Trimethoprim	7.36	18.51	95.68	121.55
triphenyl Phosphate	1.96	13.45	91.86	107.27
tris 2 Chloroethyl Phosphate	4.05	2.93	95.96	102.95
Tylosin	7.75	16.17	97.15	121.06
Urea	**96.32**	**1.68**	**4.12**	**102.13**
Valine	**21.39**	**8.57**	**70.71**	**100.67**

Table 17a. Final Model Output for ESPA-2
The predicted values represent a 25% noise-band criteria. Bolded compounds represent surrogates used to build the models

Compound Name	P-Flux	M-Flux	R-Flux	F-Flux
1,1 Dichloropropanone	14.82	42.67	33.24	90.73
1,1,2 Trichloroethene (TCE)	19.57	93.57	11.14	124.28
1,1,2,2, Tetrachloroethylene (PCE)	**0.29**	**96.26**	**-2.36**	**94.19**
1,2 Dichlorobenzene	6.24	89.24	-1.78	93.70
1,2 Dimethylbenzene	2.98	87.66	-5.39	85.25
1,2,4 Trimethylbenzene	0.86	92.70	-6.13	87.43
1,3,5 Trimethylbenzene	1.63	95.86	-5.02	92.47
1,4 Dichlorobenzene	5.38	90.75	-4.85	91.28
1,4 Dichlorophenoxyacetic Acid	**14.64**	**18.06**	**66.00**	**98.69**
17a Estradiol	**1.84**	**90.12**	**15.35**	**107.31**
2,3 Naphthalenedicarboxylic Acid	2.93	2.68	79.80	85.40
2,3,4,5,6 Pentachlorophenol	**2.60**	**47.44**	**52.89**	**102.93**
2,3,5,6 Tetrachloroterephthalic Acid	3.24	14.28	75.26	92.78
2,4 Dinitrotoluene	**3.44**	**103.20**	**3.88**	**110.52**
2,4,5 Trichlorophenoxyacetic Acid	10.13	13.95	56.28	80.36
2,6 Naphthalenedicarboxylic Acid	2.20	3.68	74.88	80.76
2-chloro-2'-6'-diethyl-N-methoxymethyl-acetanilide (Alachlor)	**2.55**	**19.66**	**77.40**	**99.62**
3 Hydroxycarbofuran	1.57	102.82	60.74	77.06
4 Nonylphenol	**0.13**	**20.79**	**78.85**	**99.77**
4,6 Dichlorophenol	**3.31**	**97.69**	**0.07**	**101.06**
4-amino-6-tert-butyl-3-methylthio-as-triazin-5,4H-one	20.88	6.13	70.65	97.66
Acetochlor	8.09	12.85	80.83	101.77
Alanine	**14.96**	**5.69**	**76.28**	**96.93**
Aldicarbsulfone	2.74	5.16	69.22	77.12
alpha-naphthyl-N-Methylcarbamate	0.84	27.61	77.57	106.01
Anthracene	0.45	86.36	14.71	101.52
Asparagine	**22.17**	**7.64**	**73.00**	**102.81**
Aspartic Acid	**18.82**	**3.05**	**76.75**	**98.62**
Benzene	**30.72**	**78.22**	**-2.55**	**106.39**
benzo-a-Pyrene	0.01	74.12	18.06	92.20
benzo-e-1,3,2 Dioxathiepin-3-oxide	18.74	9.10	81.43	109.28
beta Sitostanol n Hydrate	**0.47**	**49.82**	**59.95**	**110.24**
beta-Estradiol	1.99	88.94	30.65	121.58
bis-2-Ethylhexyl-adipate	3.55	6.77	79.05	89.37
Bisphenol	**2.00**	**24.05**	**69.88**	**95.93**
Bromochloroacetonitrile	24.65	63.98	32.48	121.10
Bromochloromethane	11.43	27.47	63.48	102.38
Bromomethane	17.41	9.35	49.51	76.27
Butylated-Hydroxyanisole	0.25	50.09	31.89	82.24
Caffeine	**19.64**	**17.74**	**59.49**	**96.87**
Chloralhydrate	6.97	8.47	89.52	104.96
Chlorpyrifos	**0.71**	**21.43**	**43.86**	**106.55**
Cholesterol	**0.03**	**40.06**	**76.24**	**97.70**

Table 17b. Final Model Output for ESPA-2
(Continued – See Table 17a)

Compound Name	P-Flux	M-Flux	R-Flux	F-Flux
Cimetidine	**16.21**	**18.84**	**44.47**	**100.74**
Ciprofloxacin	**11.67**	**96.98**	**69.51**	**100.02**
Codeine	**15.88**	**48.31**	**36.50**	**100.70**
Cymene	0.24	96.65	14.69	111.58
Cysteine	**8.36**	**6.21**	**83.09**	**97.66**
Dibromoacetatic Acid	32.76	8.99	66.79	108.54
Dichloroacetic Acid	**30.56**	**7.60**	**58.63**	**96.78**
Dichloroacetonitrile	19.15	42.16	39.77	101.08
Dichlorodiphenyldichloroethylene	0.61	38.09	78.66	117.36
Dichloropropane	4.02	47.19	33.88	85.09
Diethylphthalate	**5.91**	**31.95**	**63.20**	**101.06**
Diethylstilbestrol	**0.15**	**16.59**	**81.93**	**98.68**
Digoxigenin	1.35	29.53	89.12	120.00
Diltiazem	7.35	13.54	72.69	93.58
Dipropylthiocarbamic Acid-s-ethylester	5.68	11.30	91.28	108.25
di-sec-Octylphthalate	1.54	8.82	70.20	80.56
Diuron	3.96	16.08	60.35	80.39
d--n-Butylphthalate	3.70	33.82	71.57	109.08
d--n-Octylphthalate	0.06	9.29	74.83	84.17
Doxycycline	**4.09**	**15.10**	**82.58**	**101.77**
Enrofloxacin	2.61	18.73	69.09	90.44
Erythromycin	**4.24**	**13.02**	**82.74**	**100.00**
Estriol	8.38	68.32	26.36	103.06
Estrone	**0.28**	**93.84**	**1.39**	**95.50**
Ethylbenzene	**2.63**	**88.96**	**-2.72**	**88.87**
Ethylenediaminetetraacetic Acid (EDTA)	**13.69**	**8.02**	**74.29**	**96.01**
Fluoranthrene	0.15	87.71	13.32	101.17
Fonofos	0.16	10.20	108.88	119.24
Gemfibrozil	6.21	11.45	83.44	101.09
Glycine	**25.22**	**4.69**	**79.11**	**109.01**
Hexachlorobenzene	0.01	89.30	18.07	107.38
Histidine	**13.00**	**8.12**	**77.22**	**98.33**
Ibuprofen	**4.51**	**8.84**	**82.48**	**95.83**
Leucine	4.53	7.56	77.42	89.52
Lindane	**2.34**	**56.03**	**40.32**	**98.68**
Lysine	**14.75**	**9.25**	**81.25**	**105.25**
Mestranol	0.82	16.83	106.34	123.99
Methionine	**16.95**	**18.83**	**55.26**	**91.04**
methyl Parathion	**1.54**	**25.00**	**69.41**	**95.94**
Methylene Bromide	6.78	72.64	45.07	124.48
Metribuzin	20.87	6.12	70.58	97.58
Molinate	1.31	47.26	71.99	120.55

Table 17c. Final Model Output for ESPA-2
(Continued – See Table 17b)

Compound Name	P-Flux	M-Flux	R-Flux	F-Flux
Monobromobenzene	6.24	76.75	11.34	94.32
N-Dimethylamine	**34.94**	**21.84**	**42.84**	**99.62**
Nitrobenzene	**0.47**	**97.58**	**-3.05**	**95.00**
Nitrosodibutylamine	2.73	36.12	63.27	102.12
N-nitroso dimethyl amine (NDMA)	**71.97**	**13.32**	**6.45**	**91.73**
N-nitrosodi-n-butylamine	3.81	41.82	59.18	104.81
Norfloxacin	6.39	11.60	67.80	85.79
o-Cresol	5.70	75.39	10.57	91.66
Paraxanthine	17.18	12.20	60.94	90.32
p-Cresol	4.92	71.71	7.43	84.06
p-Dichlorobenzene	5.38	90.75	-4.85	91.28
Phenanthrene	**0.55**	**84.54**	**14.04**	**99.12**
Phenol	**27.89**	**63.55**	**10.55**	**102.00**
Phthalic Anhydride	**7.08**	**3.11**	**90.53**	**100.72**
Progesterone	**0.21**	**32.75**	**65.15**	**98.11**
Pyrene	0.27	89.48	22.23	111.98
s-1-Methyl-5-3-Pyridinyl-2-Pyrrolidinone	3.96	39.80	62.09	105.85
Salbutamol	10.84	5.46	68.81	85.12
Saxitoxin	8.25	48.12	65.29	121.66
Serine	21.86	5.80	85.84	113.50
Sulfachlorpyridazine	2.11	42.31	70.01	114.43
Sulfadimethoxine	2.89	46.65	58.41	107.95
Sulfamerazine	1.37	26.22	74.61	102.20
Sulfamethazine	2.60	26.69	77.32	106.62
Sulfamethoxazole	1.35	31.30	73.11	105.76
Sulfathiazole	2.42	35.22	74.96	112.60
t Butyl Alcohol	**17.89**	**5.50**	**79.67**	**103.06**
Terbufos	1.40	18.53	73.79	93.71
Terramycin	8.95	18.08	74.69	101.72
Testosterone	**2.31**	**28.66**	**70.40**	**101.37**
Tetracycline	**5.82**	**17.15**	**75.41**	**98.39**
Thio-N-methyl-carbamoyl-oxy-methylester	18.75	4.64	66.30	89.68
Threonine	**11.59**	**4.77**	**83.70**	**100.06**
Toluene	**6.60**	**84.41**	**7.43**	**98.44**
Trichloroacetic Acid	**20.20**	**7.78**	**71.78**	**99.77**
Triclosan	1.00	25.09	72.65	98.74
Trimethoprim	5.57	50.05	56.41	112.03
triphenyl Phosphate	0.78	10.68	90.90	102.35
tris 2 Chloroethyl Phosphate	1.24	33.95	53.03	88.21
Tylosin	5.45	11.28	72.09	88.82
Urea	**84.52**	**3.22**	**5.69**	**93.44**
Valine	**17.16**	**7.46**	**79.31**	**103.93**

Table 18a. Final Model Output for LFC-1
The predicted values represent a 25% noise-band criteria. Bolded compounds represent surrogates used to build the models

Compound Name	P-Flux	M-Flux	R-Flux	F-Flux
1,1 Dichloropropanone	19.68	21.24	61.57	102.49
1,1,2 Trichloroethene (TCE)	6.54	69.36	34.08	109.98
1,1,2,2 Tetrachloroethane	0.11	92.52	16.02	108.65
1,1,2,2, Tetrachloroethylene (PCE)	**0.11**	**96.99**	**-2.58**	**94.52**
1,2 Dimethylbenzene	1.46	93.81	-19.89	75.37
1,2,4 Trimethylbenzene	1.04	102.38	-16.39	87.04
1,3,5 Trimethylbenzene	0.24	105.35	-19.54	86.06
1,4 Dichlorophenoxyacetic Acid	**4.52**	**3.68**	**90.28**	**98.48**
17a Estradiol	**0.89**	**72.51**	**32.61**	**106.01**
2,3 Naphthalenedicarboxylic Acid	11.25	4.01	81.66	96.93
2,3,4,5,6 Pentachlorophenol	**0.82**	**56.12**	**37.65**	**94.59**
2,3,5,6 Tetrachloroterephthalic Acid	13.53	6.07	99.68	119.28
2,4 Dinitrophenol	2.46	56.64	44.18	103.28
2,4 Dinitrotoluene	**1.89**	**100.87**	**1.75**	**104.51**
2,4,5 Trichlorophenoxyacetic Acid	3.27	3.47	82.31	89.05
2,6 Naphthalenedicarboxylic Acid	3.89	5.49	82.51	91.89
3 Hydroxycarbofuran	5.37	101.27	74.71	94.32
3-amino-1H-1,2,4 Triazole	23.60	14.25	0.29	120.03
4 Nonylphenol	**0.37**	**24.07**	**76.99**	**101.44**
4,6 Dichlorophenol	**1.72**	**97.84**	**6.22**	**105.77**
Alanine	**15.11**	**6.50**	**76.08**	**97.69**
Aldicarbsulfone	12.54	1.53	75.89	89.97
Aldrin	0.98	6.86	67.59	75.43
Anthracene	0.55	96.14	-10.69	85.99
Asparagine	**12.06**	**5.73**	**83.17**	**100.97**
Aspartic Acid	**8.31**	**4.63**	**87.17**	**100.11**
Benzene	**16.21**	**69.75**	**12.98**	**98.95**
benzo-e-1,3,2 Dioxathiepin-3-oxide	0.11	24.62	81.18	105.90
beta Sitostanol n Hydrate	**0.31**	**13.78**	**85.52**	**99.61**
Bisphenol	**0.96**	**15.61**	**84.03**	**100.60**
Bromochloroacetonitrile	46.44	10.58	67.87	124.90
Bromodichloromethane	5.39	26.54	72.32	104.25
Bromomethane	13.86	5.33	75.90	95.10
Caffeine	**17.01**	**22.36**	**72.39**	**111.75**
Carbadox	1.87	29.58	73.90	105.36
Chloroform	11.08	30.80	56.31	98.19
Chlorotetracycline	0.96	19.34	100.87	121.17
Chlorpyrifos	**1.12**	**12.00**	**76.80**	**96.80**
Cholesterol	**0.24**	**26.25**	**87.83**	**100.07**

Table 18b. Final Model Output for LFC-1
(Continued – See Table 18a)

Compound Name	P-Flux	M-Flux	R-Flux	F-Flux
Cimetidine	**4.78**	**32.59**	**63.65**	**94.68**
Ciprofloxacin	**7.97**	**12.26**	**62.14**	**102.70**
Codeine	**10.85**	**37.98**	**46.74**	**95.57**
Cylindrospermopsin	9.11	0.60	84.36	94.07
Cymene	0.78	96.22	26.58	123.58
Cysteine	**15.33**	**6.74**	**80.05**	**102.12**
Dibromoacetatic Acid	18.00	6.18	80.90	105.08
Dibromochloropropane	1.20	28.54	50.91	80.65
Dichloroacetic Acid	**26.75**	**7.57**	**75.94**	**110.26**
Dichloroacetonitrile	8.21	1.44	71.71	81.36
Dichloropropane	8.76	18.13	66.38	93.27
Diethylphthalate	**5.50**	**29.19**	**64.57**	**99.26**
Diethylstilbestrol	**0.15**	**18.62**	**80.44**	**99.21**
Dipropylthiocarbamic Acid-s-ethylester	2.85	9.86	87.52	100.23
Disulfoton	1.09	11.59	93.07	105.75
Doxycycline	**5.74**	**16.43**	**79.40**	**101.58**
Enalaprilat	0.88	26.36	74.00	101.23
Enrofloxacin	3.38	32.41	54.77	90.56
Equilenin	0.84	56.31	56.24	113.39
Equilin	0.24	55.91	27.29	83.45
Erythromycin	**2.78**	**8.30**	**90.00**	**101.08**
Estrone	**0.90**	**74.58**	**18.65**	**94.13**
Ethylbenzene	**1.95**	**85.79**	**-2.06**	**85.68**
Ethylenediaminetetraacetic Acid (EDTA)	**7.21**	**2.12**	**92.16**	**101.50**
Gemfibrozil	1.61	16.78	94.10	112.48
Glycine	**26.60**	**4.91**	**76.65**	**108.15**
Hexachlorobutadiene	6.90	32.88	69.69	109.46
Histidine	**19.26**	**7.09**	**75.48**	**101.83**
Ibuprofen	**5.25**	**8.78**	**85.14**	**99.18**
Lincomycin	0.11	0.85	87.68	88.65
Lindane	**1.09**	**40.88**	**61.22**	**103.19**
Linuron	2.00	12.19	78.01	92.20
Lysine	**5.85**	**1.40**	**91.00**	**98.26**
Methionine	**10.56**	**4.53**	**84.79**	**99.88**
methyl Parathion	**1.14**	**25.75**	**75.01**	**101.90**
Methylene Bromide	20.15	33.44	70.36	123.95
Methylene Chloride	14.91	7.64	70.67	93.22
Microcystin LR	3.08	13.72	105.68	122.48
N-Dimethylamine	**28.76**	**29.10**	**39.43**	**97.29**

Table 18c. Final Model Output for LFC-1
(Continued – See Table 18b)

Compound Name	P-Flux	M-Flux	R-Flux	F-Flux
Nitrilotriacetic Acid	3.44	6.34	102.92	112.70
Nitrobenzene	**0.29**	**90.41**	**-2.69**	**88.00**
N-nitroso dimethyl amine (NDMA)	**80.37**	**0.46**	**18.60**	**99.43**
Norethindrone	0.17	53.32	63.79	117.28
Norfloxacin	8.38	25.64	51.13	85.15
N-triacetic Acid	0.43	5.85	96.32	102.61
o-Cresol	14.48	95.55	-0.03	110.00
Paraxanthine	10.37	17.39	77.01	104.77
Paroxetine	0.64	17.64	78.53	96.81
p-Cresol	34.87	72.70	-3.43	104.14
Phenanthrene	**0.72**	**97.55**	**-4.09**	**94.18**
Phenol	**39.54**	**61.98**	**-1.45**	**100.07**
Phenylalanine	34.30	3.56	58.11	95.97
Phthalic Anhydride	**5.59**	**3.16**	**90.03**	**98.78**
Progesterone	**0.01**	**22.68**	**80.95**	**103.63**
Pyrene	0.57	102.02	-26.66	75.92
Saxitoxin	2.09	9.52	82.08	93.69
Serine	34.22	2.72	80.40	117.35
Sulfachlorpyridazine	3.51	17.56	51.27	72.33
Sulfadimethoxine	3.42	26.49	62.32	92.23
Sulfamethazine	2.35	28.12	48.85	79.31
Sulfamethizole	15.24	13.65	84.93	113.82
Sulfamethoxazole	6.40	18.53	60.94	85.86
Sulfathiazole	4.56	20.90	80.74	106.19
t Butyl Alcohol	**22.32**	**5.96**	**66.91**	**95.19**
Terbacil	1.56	25.49	65.34	92.38
Terbufos	0.63	51.00	70.40	122.04
Terramycin	4.58	18.67	80.61	103.86
Testosterone	**1.77**	**46.42**	**61.03**	**109.22**
Tetracycline	**3.33**	**16.99**	**78.49**	**98.81**
Thio-N-methyl-carbamoyl-oxy-methylester	1.55	0.68	75.62	77.85
Threonine	**11.86**	**3.54**	**80.51**	**95.91**
Toluene	**19.51**	**89.27**	**0.23**	**109.01**
Tributyl Tin	0.78	2.31	96.50	99.59
Trichloroacetic Acid	**12.65**	**1.68**	**82.86**	**97.20**
tris 2 Chloroethyl Phosphate	2.52	19.73	92.71	114.96
Tylosin	0.71	38.11	68.20	107.02
Urea	**85.33**	**1.70**	**4.38**	**91.41**
Valine	**12.29**	**4.21**	**83.59**	**100.09**

Table 19a. Final Model Output for TFC-HR
The predicted values represent a 25% noise-band criteria. Bolded compounds represent surrogates used to build the models

Compound Name	P-Flux	M-Flux	R-Flux	F-Flux
1,1 Dichloropropanone	15.34	32.71	58.21	106.26
1,1,2,2 Tetrachloroethane	0.09	102.96	0.12	103.17
1,1,2,2, Tetrachloroethylene (PCE)	**0.08**	**103.08**	**-2.44**	**100.72**
1,3,5 Trimethylbenzene	0.10	86.66	-7.06	79.70
1,4 Dichlorophenoxyacetic Acid	**5.04**	**8.58**	**83.49**	**97.11**
17a Estradiol	**0.37**	**75.07**	**16.91**	**92.35**
2,2 bis-p-Chlorophenyl 1,1,1 Trichloroethane	0.48	9.53	77.47	87.48
2,2 bis-p-Methoxyphenyl 1,1,1 Trichloroethane	1.20	13.39	98.03	112.62
2,2,2 Trichloro 1,1-bis-4-chlorophenyl Ethanol	0.37	14.88	58.85	74.10
2,3 Naphthalenedicarboxylic Acid	2.52	4.00	78.47	85.00
2,3,4,5,6 Pentachlorophenol	**5.74**	**73.84**	**23.23**	**102.82**
2,4 Dinitrophenol	10.10	39.33	36.53	85.97
2,4 Dinitrotoluene	**1.96**	**96.01**	**1.68**	**99.65**
2,4,5 Trichlorophenoxyacetic Acid	9.33	9.15	74.91	93.39
2,6 bis-1,1 Dimethylethyl Phenol	0.09	26.31	52.45	78.85
2,6 di-tert-butyl-p-Cresol	0.12	35.36	40.35	75.82
2,6 Naphthalenedicarboxylic Acid	3.19	8.30	76.20	87.69
2-chloro-2'-6'-diethyl-N-methoxymethyl-acetanilide (Alachlor)	**2.65**	**24.66**	**77.77**	**105.08**
3 Hydroxycarbofuran	0.22	87.93	42.92	121.72
3-amino-1H-1,2,4 Triazole	12.35	78.57	1.20	119.60
4 Nonylphenol	**0.22**	**70.73**	**26.83**	**97.78**
4,6 Dichlorophenol	**2.18**	**94.19**	**4.68**	**101.05**
Acetaminophen	21.02	36.51	31.71	89.24
Alanine	**9.73**	**5.41**	**82.22**	**97.35**
Aldicarbsulfone	1.42	3.29	77.50	82.21
Aldrin	8.01	29.67	84.69	122.37
Anthracene	0.49	87.50	16.93	104.92
Asparagine	**34.91**	**5.26**	**64.01**	**104.17**
Aspartic Acid	**12.00**	**5.32**	**80.79**	**98.11**
Benzene	**22.21**	**81.24**	**2.46**	**105.92**
benzo-e-1,3,2 Dioxathiepin-3-oxide	9.17	24.11	83.96	117.23
beta Sitostanol n Hydrate	**0.40**	**21.71**	**74.20**	**96.31**
beta-Estradiol	0.38	62.55	17.25	80.19
Bisphenol	**0.24**	**25.91**	**74.45**	**100.59**
Bromochloroacetic Acid	9.97	14.08	69.30	93.35
Bromochloroacetonitrile	26.04	12.94	74.57	113.55
Bromochloromethane	21.17	11.48	62.77	95.42
Bromodichloromethane	18.55	9.18	59.89	87.61
Bromoform	0.28	45.88	51.00	97.17
Bromomethane	19.70	11.08	52.96	83.74
Butylated-Hydroxyanisole	0.19	37.37	39.50	77.06
Caffeine	**17.20**	**17.06**	**68.49**	**102.75**
Carbadox	9.71	40.91	71.49	122.11
Chloroform	26.18	19.04	56.20	101.42
Chlorpyrifos	**0.75**	**14.79**	**46.84**	**103.46**

Table 19b. Final Model Output for TFC-HR
(Continued – See Table 19a)

Compound Name	P-Flux	M-Flux	R-Flux	F-Flux
Cholesterol	**0.34**	**25.32**	**88.03**	**103.17**
Cimetidine	**13.54**	**11.23**	**62.29**	**101.15**
Ciprofloxacin	**4.89**	**82.57**	**82.21**	**98.33**
Codeine	**7.39**	**20.50**	**76.11**	**104.00**
Cyclotrimethylenetrinitramine	70.17	97.78	-54.30	113.65
Cylindrospermopsin	13.00	2.71	73.06	88.78
Cymene	0.08	74.55	35.94	110.57
Cysteine	**7.75**	**5.58**	**86.50**	**99.83**
Dibromoacetatic Acid	3.15	18.59	80.56	102.29
Dibromoacetonitrile	9.10	6.43	75.88	91.40
Dibromochloromethane	7.53	6.72	67.86	82.11
Dichloroacetic Acid	**20.67**	**8.61**	**67.59**	**96.87**
Dichlorodifluoromethane	21.72	13.90	61.43	97.06
Dichlorodiphenyldichloroethylene	16.63	58.94	36.15	111.71
Dichloropropane	15.01	28.69	76.99	120.69
Diethylphthalate	**1.42**	**40.75**	**62.42**	**104.58**
Diethylstilbestrol	**0.15**	**54.06**	**50.95**	**105.16**
Digoxigenin	0.57	47.26	58.85	106.68
Diltiazem	0.28	20.93	73.85	95.06
di-sec-Octylphthalate	0.18	23.09	82.66	105.93
Disulfoton	0.22	12.58	103.16	115.96
d--n-Octylphthalate	0.04	22.76	93.84	116.64
Doxycycline	**8.58**	**15.54**	**77.12**	**101.24**
Enalaprilat	0.33	15.50	76.88	92.70
Enrofloxacin	8.75	4.70	81.74	95.19
Erythromycin	**2.54**	**10.48**	**87.94**	**100.95**
Estrone	**0.20**	**103.33**	**-1.54**	**101.99**
Ethylbenzene	**2.83**	**94.23**	**-4.96**	**92.10**
Ethylenediaminetetraacetic Acid (EDTA)	**11.30**	**2.28**	**88.17**	**101.76**
ethyl-tert-Butyl Ether	18.66	10.21	84.91	113.77
exo-Dimethanonaphthalene	1.27	54.06	57.89	113.22
Fluoranthrene	1.85	87.29	-0.87	88.26
Fluoxetine	4.52	4.43	66.67	75.62
Fonofos	0.11	4.29	75.24	79.64
Gemfibrozil	4.17	9.43	84.61	98.21
Glycine	**2.68**	**5.51**	**87.17**	**95.36**
Hexachlorocyclohexane	0.40	77.22	10.65	88.27
Histidine	**9.64**	**4.59**	**83.38**	**97.62**
Ibuprofen	**3.91**	**11.54**	**86.27**	**101.72**
Leucine	6.54	7.22	94.32	108.07
Lincomycin	0.97	21.24	98.72	120.93
Lindane	**1.00**	**66.21**	**35.69**	**102.91**
Lysine	**16.85**	**3.48**	**84.53**	**104.86**
Metformin	63.82	31.44	13.44	108.71

Table 19c. Final Model Output for TFC-HR
(Continued – See Table 19b)

Compound Name	P-Flux	M-Flux	R-Flux	F-Flux
Methionine	**17.45**	**5.07**	**73.18**	**95.70**
methyl Parathion	**3.28**	**22.48**	**67.29**	**93.05**
Methylene Bromide	6.94	34.66	77.58	119.18
Methylene Chloride	39.50	19.71	44.93	104.15
methyl-tert-butyl Ether (MTBE)	21.96	8.90	76.90	107.76
Monobromobenzene	23.31	107.52	-54.30	76.53
N-Dimethylamine	**35.24**	**7.62**	**62.76**	**105.62**
Nitrilotriacetic Acid	3.27	5.57	78.56	87.39
Nitrobenzene	**0.34**	**100.87**	**-2.19**	**99.02**
N-nitroso dimethyl amine (NDMA)	**74.72**	**20.80**	**2.72**	**98.24**
N-nitrosomorpholine	17.18	28.14	30.68	76.00
Norethindrone	0.36	48.40	68.08	116.85
Norfloxacin	3.75	16.06	83.01	102.82
N-triacetic Acid	2.48	3.55	76.47	82.50
Octachloro-4-7-methanotetrahydroindane	4.71	49.51	70.66	124.88
Paraxanthine	5.69	13.90	58.57	78.16
Perchloric Acid	7.16	1.98	99.37	108.51
Phenanthrene	**0.51**	**88.47**	**5.46**	**94.45**
Phenol	**32.48**	**61.87**	**-1.19**	**93.15**
Phenylalanine	16.24	3.15	90.21	109.59
Phthalic Anhydride	**8.20**	**3.06**	**88.36**	**99.62**
Progesterone	**0.17**	**26.30**	**69.81**	**96.28**
Pyrene	1.29	87.34	-1.56	87.07
Salbutamol	14.32	8.40	80.01	102.73
Serine	7.00	5.68	80.18	92.87
Sulfachlorpyridazine	0.80	41.79	81.89	124.48
Sulfadimethoxine	1.19	12.36	85.35	98.89
Sulfamerazine	0.54	9.60	83.61	93.75
Sulfamethazine	0.80	9.80	86.30	96.90
Sulfathiazole	0.66	10.41	71.33	82.41
t Butyl Alcohol	**19.14**	**8.47**	**66.84**	**94.46**
Terramycin	2.26	23.38	80.83	106.47
tert amyl methyl Ether	7.73	9.28	76.61	93.62
Testosterone	**0.33**	**14.39**	**85.55**	**100.27**
Tetracycline	**2.98**	**15.89**	**83.45**	**102.32**
Thio-N-methyl-carbamoyl-oxy-methylester	8.26	18.42	80.19	106.88
Threonine	**8.68**	**5.22**	**84.04**	**97.94**
Toluene	**7.12**	**93.08**	**-1.25**	**98.95**
Tributyl Tin	0.08	2.31	98.08	100.47
Trichloroacetic Acid	**28.16**	**6.18**	**67.17**	**101.51**
Triclosan	18.33	32.78	61.95	113.06
triphenyl Phosphate	0.15	17.48	99.44	117.07
Urea	**72.31**	**1.76**	**7.26**	**81.33**
Valine	**9.41**	**6.05**	**82.94**	**98.40**

Table 20a. Final Model Output for CA
The predicted values represent a 25% noise-band criteria. Bolded compounds represent surrogates used to build the models

Compound Name	P-Flux	M-Flux	R-Flux	F-Flux
1,1,2,2 Tetrachloroethane	32.88	64.71	5.31	102.89
1,1,2,2, Tetrachloroethylene (PCE)	**30.91**	**66.34**	**6.04**	**103.29**
1,2 Dichlorobenzene	13.09	86.00	-0.73	98.36
1,2,4 Trimethylbenzene	24.52	96.41	1.94	122.87
1,3,5 Trimethylbenzene	17.79	98.96	3.46	120.22
1,4 Dichlorobenzene	6.32	90.95	-0.57	96.71
1,4 Dichlorophenoxyacetic Acid	**43.90**	**6.40**	**46.61**	**96.91**
17a Estradiol	**3.03**	**97.45**	**0.84**	**101.32**
2,2 bis-p-Chlorophenyl 1,1,1 Trichloroethane	2.44	98.53	-2.07	98.90
2,3 Naphthalenedicarboxylic Acid	8.98	85.75	0.62	95.35
2,3,4,5,6 Pentachlorophenol	**2.06**	**97.69**	**0.35**	**100.10**
2,4 Dichloro-4'-nitrodiphenyl Ether	2.79	98.01	-1.18	99.62
2,4 Dinitrotoluene	**7.90**	**93.28**	**0.47**	**101.64**
2,6 bis-1,1 Dimethylethyl 2,5 Cyclohexadiene 1,4 dione	4.93	98.87	6.33	110.13
2,6 bis-1,1 Dimethylethyl Phenol	9.66	98.33	0.88	108.87
2,6 di-tert-butyl-p-Cresol	7.26	98.49	2.08	107.83
2-chloro-2'-6'-diethyl-N-methoxymethyl-acetanilide (Alachlor)	**5.73**	**86.29**	**4.95**	**96.97**
3-amino-1H-1,2,4 Triazole	77.12	54.36	9.79	90.23
4 Nonylphenol	**0.54**	**98.57**	**1.88**	**100.99**
4,6 Dichlorophenol	**2.18**	**97.54**	**-0.80**	**98.91**
4-amino-6-tert-butyl-3-methylthio-as-triazin-5,4H-one	50.52	62.28	0.23	113.03
Acetaminophen	88.96	28.10	0.76	117.82
Alanine	**58.64**	**8.33**	**40.05**	**107.01**
Aldicarbsulfone	73.16	31.81	12.56	117.53
Aldrin	14.72	93.59	2.07	110.38
alpha-naphthyl-N-Methylcarbamate	4.59	98.04	9.85	112.48
Androsterone	3.95	87.95	0.55	92.45
Anthracene	0.45	99.66	0.97	101.08
Asparagine	**66.08**	**0.64**	**42.86**	**109.59**
Aspartic Acid	**35.62**	**9.24**	**61.70**	**106.55**
Benzene	**57.21**	**44.79**	**1.48**	**103.48**
benzo-a-Pyrene	0.23	99.40	4.16	103.79
beta Sitostanol n Hydrate	**0.53**	**24.04**	**75.84**	**100.42**
bis-2-Ethylhexyl-adipate	5.10	97.77	0.87	103.74
Bisphenol	**0.84**	**97.96**	**0.21**	**99.01**
Butylated-Hydroxyanisole	11.79	98.90	2.30	113.00
Caffeine	**70.35**	**11.46**	**15.14**	**96.96**
Carbadox	2.17	82.21	1.58	85.96
Chloralhydrate	38.42	51.35	1.57	91.34
Chlorpyrifos	**3.32**	**20.11**	**-0.19**	**100.76**
Cholesterol	**0.27**	**21.54**	**70.30**	**90.68**

Table 20b. Final Model Output for CA
(Continued – See Table 20a)

Compound Name	P-Flux	M-Flux	R-Flux	F-Flux
Cimetidine	**62.08**	**24.20**	**22.86**	**106.48**
Ciprofloxacin	**34.38**	**98.23**	**24.76**	**83.35**
Codeine	**55.86**	**27.10**	**10.66**	**93.62**
Cymene	12.32	99.49	1.63	113.44
Cysteine	**42.90**	**6.61**	**42.02**	**91.54**
Diazinon	7.65	97.52	-1.34	103.83
Dibromoacetonitrile	58.43	33.98	16.00	108.42
Dichloroacetic Acid	**44.11**	**5.87**	**37.16**	**87.13**
Dichlorodifluoromethane	2.57	95.58	1.75	99.90
Dichlorodiphenyldichloroethylene	7.58	98.63	13.22	119.43
Diethylphthalate	**15.81**	**82.97**	**0.22**	**99.00**
Diethylstilbestrol	**0.28**	**99.37**	**0.43**	**100.08**
Diltiazem	5.25	95.30	-0.32	100.22
Dipropylthiocarbamic Acid-s-ethylester	13.74	89.44	7.33	110.51
di-sec-Octylphthalate	2.59	98.78	9.08	110.44
Diuron	30.36	69.47	7.30	107.12
d--n-Butylphthalate	0.36	69.10	12.77	82.23
d--n-Octylphthalate	0.24	87.88	22.22	110.34
Doxycycline	**17.04**	**29.48**	**53.97**	**100.49**
Enalaprilat	79.49	4.62	6.42	90.52
Endosulfansulfate	7.82	97.87	5.86	111.55
Enrofloxacin	13.30	43.41	28.45	85.16
Equilenin	1.42	97.55	4.97	103.95
Equilin	1.63	87.53	0.13	89.29
Erythromycin	**29.37**	**6.06**	**70.00**	**105.43**
Estriol	1.15	87.31	3.31	91.76
Estrone	**2.56**	**97.30**	**-0.39**	**99.47**
Ethylbenzene	**25.86**	**68.70**	**1.42**	**95.98**
Ethylenediaminetetraacetic Acid (EDTA)	**47.11**	**7.05**	**45.09**	**99.26**
Fluoranthrene	0.36	99.43	1.48	101.27
Fluoxetine	1.35	97.92	-1.93	97.34
Fonofos	5.03	97.71	0.44	103.17
Glycine	**62.73**	**9.95**	**38.56**	**111.24**
Hexachlorobenzene	2.74	99.67	-0.85	101.55
Histidine	**44.17**	**8.06**	**44.55**	**96.78**
Ibuprofen	**57.58**	**23.00**	**22.96**	**103.54**
Leucine	60.64	2.21	37.79	100.64
Lincomycin	51.04	23.24	12.59	86.86
Lindane	**1.53**	**98.80**	**-0.22**	**100.11**
Lysine	**53.44**	**9.55**	**27.34**	**90.34**

Table 20c. Final Model Output for CA
(Continued – See Table 20b)

Compound Name	P-Flux	M-Flux	R-Flux	F-Flux
Mestranol	1.68	98.14	0.24	100.07
Metformin	69.85	32.89	2.30	105.04
Methionine	**48.80**	**8.93**	**39.66**	**97.40**
methyl Parathion	**1.86**	**97.86**	**-0.10**	**99.61**
Metribuzin	50.49	62.26	0.22	112.97
N N diethyl 3 methylbenzamide	25.38	91.94	0.29	117.61
N-Dimethylamine	**55.85**	**12.92**	**10.38**	**79.16**
Nitrilotriacetic Acid	50.70	4.55	49.24	104.49
Nitrobenzene	**35.98**	**63.65**	**0.80**	**100.43**
Nitrosodiethylamine	57.49	19.87	8.70	86.07
N-nitroso dimethyl amine (NDMA)	**90.16**	**3.67**	**3.67**	**97.50**
N-nitrosomorpholine	29.62	33.98	9.73	73.33
N-nitrosopiperidine	39.06	20.47	12.29	71.81
Norfloxacin	34.01	67.82	11.89	113.71
N-triacetic Acid	66.99	4.26	33.92	105.17
o-Cresol	23.12	93.78	0.05	116.96
Paraxanthine	53.15	13.62	16.16	82.93
Paroxetine	1.39	98.99	0.49	100.88
p-Dichlorobenzene	6.32	90.95	-0.57	96.71
Phenanthrene	**0.50**	**99.65**	**0.97**	**101.12**
Phenol	**71.96**	**31.30**	**-0.34**	**102.93**
Phthalic Anhydride	**28.58**	**5.34**	**64.35**	**98.27**
Progesterone	**1.68**	**98.63**	**-0.28**	**100.03**
Pyrene	0.33	99.68	1.71	101.72
Salbutamol	75.08	31.51	3.65	110.25
Saxitoxin	39.84	54.89	7.91	102.64
Sulfamerazine	70.15	7.32	0.68	78.15
Sulfamethazine	49.20	22.93	2.80	74.93
t Butyl Alcohol	**86.51**	**3.69**	**12.52**	**102.72**
Terbufos	20.24	99.14	4.87	124.25
Testosterone	**19.64**	**55.06**	**2.77**	**77.46**
Tetracycline	**37.95**	**15.49**	**57.31**	**110.75**
Threonine	**49.43**	**7.53**	**35.08**	**92.04**
Toluene	**46.90**	**48.83**	**2.04**	**97.76**
Trichloroacetic Acid	**55.91**	**4.60**	**39.79**	**100.31**
Trimethoprim	12.12	66.48	41.94	120.54
triphenyl Phosphate	0.50	98.14	-1.50	97.13
tris 2 Chloroethyl Phosphate	2.23	96.31	1.67	100.20
Urea	**91.95**	**4.59**	**28.21**	**124.75**
Valine	**61.69**	**4.93**	**34.09**	**100.71**

Table 21a. Final Model Output for "Universal" PA
The predicted values represent a 25% noise-band criteria. Bolded compounds represent surrogates used to build the models

Compound Name	P-Flux	M-Flux	R-Flux	F-Flux
1,1 Dichloropropanone	3.57	23.46	57.76	84.78
1,1,2,2 Tetrachloroethane	0.12	95.55	1.14	96.81
1,1,2,2, Tetrachloroethylene (PCE)	**0.12**	**95.55**	**-3.28**	**92.39**
1,2 Dichlorobenzene	1.61	102.05	16.70	120.36
1,2 Dimethylbenzene	3.20	91.92	-8.47	86.65
1,2,4 Trimethylbenzene	6.31	100.40	-8.54	98.17
1,3,5 Trimethylbenzene	1.57	101.77	-8.54	94.80
1,4 Dichlorophenoxyacetic Acid	**7.33**	**7.65**	**80.77**	**95.74**
17a Estradiol	**0.58**	**88.30**	**24.93**	**113.81**
2,2 bis-p-Chlorophenyl 1,1 Dichloroethane	0.68	12.84	88.53	102.04
2,2 bis-p-Chlorophenyl 1,1,1 Trichloroethane	0.29	13.06	79.91	93.27
2,2 bis-p-Methoxyphenyl 1,1,1 Trichloroethane	0.33	7.82	93.66	101.80
2,2,2 Trichloro 1,1-bis-4-chlorophenyl Ethanol	0.75	36.48	79.90	117.12
2,3 Naphthalenedicarboxylic Acid	1.87	5.08	72.27	79.22
2,3,4,5,6 Pentachlorophenol	**1.72**	**55.61**	**39.53**	**96.86**
2,3,5,6 Tetrachloroterephthalic Acid	10.70	26.45	75.96	113.10
2,4 Dichloro-4'-nitrodiphenyl Ether	0.43	60.86	43.74	105.04
2,4 Dinitrotoluene	**2.76**	**98.89**	**-2.48**	**99.17**
2,4,5 Trichlorophenoxyacetic Acid	1.83	14.09	73.24	89.17
2,6 Naphthalenedicarboxylic Acid	1.67	12.48	72.32	86.47
2-chloro-2'-6'-diethyl-N-methoxymethyl-acetanilide (Alachlor)	**1.51**	**14.15**	**85.37**	**101.03**
3 Hydroxycarbofuran	2.19	97.55	80.60	90.45
4 Nonylphenol	**0.45**	**33.54**	**68.02**	**102.00**
4,6 Dichlorophenol	**3.30**	**97.88**	**-3.38**	**97.80**
6-chloro-N-ethyl-N'-isopropyl-1,3,5 Triazine-2,4-diamine	4.80	82.34	-9.79	77.34
Acetochlor	11.77	12.76	67.96	92.49
Alanine	**16.43**	**4.40**	**80.97**	**101.80**
Aldicarbsulfone	38.37	9.21	72.46	120.03
Aldrin	0.72	23.30	74.38	98.41
alpha-naphthyl-N-Methylcarbamate	11.43	48.93	60.69	121.05
Androsterone	0.39	33.46	43.83	77.69
Anthracene	0.42	95.91	5.91	102.23
Asparagine	**12.98**	**3.78**	**79.02**	**95.78**
Aspartic Acid	**13.22**	**5.04**	**80.64**	**98.89**
Atrazine	4.18	83.95	-7.85	80.28
Benzene	**20.79**	**74.11**	**8.13**	**103.03**
benzo-a-Pyrene	0.19	84.70	6.04	90.93
benzo-e-1,3,2 Dioxathiepin-3-oxide	14.62	2.98	64.78	82.38
beta Sitostanol n Hydrate	**0.54**	**18.84**	**70.10**	**89.47**
beta-Estradiol	0.29	88.77	26.86	115.92
Bisphenol	**1.18**	**21.31**	**74.46**	**96.94**
Bromochloroacetic Acid	2.81	11.65	62.45	76.91
Bromochloroacetonitrile	11.12	34.88	69.12	115.12
Bromodichloromethane	32.11	52.01	31.09	115.21
Bromoform	24.67	66.32	5.54	96.52
Caffeine	**20.08**	**16.70**	**64.92**	**101.70**
Chloralhydrate	9.47	6.21	71.50	87.18
Chloroform	36.59	39.01	33.19	108.79
Chlorpyrifos	**0.71**	**19.07**	**62.81**	**104.99**
Cholesterol	**0.21**	**25.86**	**85.63**	**104.91**
Cimetidine	**9.39**	**11.68**	**67.54**	**102.79**
Ciprofloxacin	**6.24**	**50.80**	**80.62**	**98.53**

Table 21b. Final Model Output for "Universal" PA
(Continued – See Table 21a)

Compound Name	P-Flux	M-Flux	R-Flux	F-Flux
Codeine	**11.13**	**28.03**	**61.67**	**100.83**
Cylindrospermopsin	2.96	15.48	84.32	102.77
Cymene	1.64	93.46	-10.39	84.72
Cysteine	**9.99**	**6.06**	**82.35**	**98.39**
Dibromoacetatic Acid	5.28	4.32	69.17	78.77
Dibromoacetonitrile	4.49	42.01	69.65	116.15
Dibromochloromethane	12.15	61.68	29.28	103.11
Dichloroacetic Acid	**23.83**	**7.46**	**66.72**	**98.01**
Dichloroacetonitrile	3.17	25.19	71.90	100.26
Dichloropropane	11.06	27.63	56.84	95.53
Dieldrin	0.86	9.21	91.26	101.33
Diethylphthalate	**4.88**	**32.62**	**61.30**	**98.79**
Diethylstilbestrol	**0.14**	**27.74**	**69.13**	**97.00**
Digoxigenin	1.80	2.70	72.19	76.69
Digoxin	3.26	28.42	79.32	111.00
Diltiazem	7.77	12.15	75.54	95.46
Disulfoton	1.81	13.67	85.98	101.47
Diuron	12.47	16.17	70.19	98.84
d--n-Butylphthalate	2.58	19.39	80.70	102.67
Doxycycline	**5.08**	**14.48**	**78.59**	**98.15**
Enalaprilat	8.74	1.90	83.14	93.78
Endosulfansulfate	0.73	59.18	46.75	106.65
Enrofloxacin	2.60	4.55	74.79	81.95
Equilenin	0.41	79.33	0.77	80.50
Erythromycin	**3.33**	**9.15**	**88.25**	**100.73**
Estriol	3.35	27.98	87.63	118.96
Estrone	**0.42**	**77.69**	**32.56**	**110.67**
Ethylbenzene	**2.61**	**95.58**	**-4.95**	**93.24**
Ethylenediaminetetraacetic Acid (EDTA)	**8.77**	**3.56**	**85.89**	**98.22**
ethyl-tert-Butyl Ether	46.45	63.46	-0.39	109.52
exo-Dimethanonaphthalene	7.28	24.45	88.09	119.83
Fluoranthrene	0.28	99.17	7.01	106.45
Fluoxetine	0.56	9.98	77.75	88.29
Fonofos	1.43	3.64	85.06	90.14
Glycine	**33.98**	**3.93**	**86.59**	**124.50**
Hexachlorobutadiene	0.21	103.90	-3.00	101.11
Hexachlorocyclohexane	7.29	98.91	-4.50	101.70
Histidine	**14.13**	**6.98**	**78.75**	**99.86**
Ibuprofen	**5.07**	**9.92**	**82.17**	**97.15**
Leucine	16.80	8.40	86.31	111.51
Lincomycin	7.41	14.33	85.48	107.22
Lindane	**1.51**	**49.52**	**47.32**	**98.35**
Linuron	4.93	29.94	65.54	100.41
Lysine	**10.41**	**3.88**	**84.69**	**98.99**
Mestranol	0.89	7.39	81.69	89.97
Methionine	**12.22**	**6.01**	**75.75**	**93.97**
methyl Parathion	**1.45**	**20.55**	**78.87**	**100.88**
Methylene Chloride	31.93	59.43	23.26	114.63
methyl-tert-butyl Ether (MTBE)	48.05	50.92	-0.47	98.50
Metolachlor	27.61	21.75	61.32	110.69

Table 21c. Final Model Output for "Universal" PA
(Continued – See Table 21b)

Compound Name	P-Flux	M-Flux	R-Flux	F-Flux
N N diethyl 3 methylbenzamide	37.29	6.06	48.87	92.21
N-Dimethylamine	**35.30**	**14.10**	**51.93**	**101.33**
Nitrilotriacetic Acid	11.20	6.53	88.64	106.37
Nitrobenzene	**0.37**	**97.53**	**-6.95**	**90.95**
Nitrosodibutylamine	34.40	64.15	-9.03	89.52
N-nitroso dimethyl amine (NDMA)	**67.55**	**12.02**	**3.63**	**83.20**
N-nitrosodi-n-butylamine	29.66	59.69	-3.09	86.25
N-nitrosopyrrolidine	25.28	4.74	83.64	113.66
Norethindrone	0.28	23.12	63.34	86.75
Norfloxacin	7.62	12.85	83.52	103.99
N-triacetic Acid	14.58	6.07	82.21	102.85
o-Cresol	5.87	82.85	3.55	92.26
Octachloro-4-7-methanotetrahydroindane	0.39	48.15	75.90	124.44
Octachloroepoxide	0.77	28.00	78.59	107.36
Paraxanthine	12.22	15.03	56.47	83.71
p-Cresol	15.07	76.90	-0.29	91.69
Perchloric Acid	12.02	10.77	60.07	82.87
Phenanthrene	**0.47**	**94.79**	**7.52**	**102.77**
Phenol	**31.55**	**65.52**	**3.93**	**101.00**
Phenylalanine	5.84	1.62	86.01	93.47
Phthalic Anhydride	**7.53**	**2.90**	**89.95**	**100.38**
Pramitol	10.61	87.08	-10.85	86.84
Progesterone	**0.21**	**28.97**	**70.12**	**99.29**
Pyrene	0.33	90.93	10.05	101.31
Ranitidine	12.61	34.88	69.39	116.89
s-1-Methyl-5-3-Pyridinyl-2-Pyrrolidinone	1.55	36.32	38.95	76.82
Salbutamol	23.10	3.29	85.57	111.95
Saxitoxin	5.28	8.52	86.56	100.37
Serine	15.56	3.13	77.26	95.95
Sulfachlorpyridazine	1.48	9.09	82.49	93.05
Sulfadimethoxine	1.52	10.30	85.40	97.22
Sulfamerazine	1.64	5.60	84.19	91.43
Sulfamethazine	1.77	5.99	85.23	93.00
Sulfamethizole	4.18	6.24	86.92	97.34
Sulfamethoxazole	1.43	8.86	81.01	91.30
Sulfathiazole	2.94	8.99	84.23	96.17
t Butyl Alcohol	**20.79**	**7.08**	**71.30**	**99.17**
Terbacil	6.98	5.90	69.12	82.00
Terramycin	3.76	27.89	83.81	115.47
tert amyl methyl Ether	21.30	66.97	-0.77	87.49
Testosterone	**1.04**	**20.57**	**75.39**	**97.01**
Tetracycline	**3.40**	**14.16**	**83.29**	**100.85**
Thio-N-methyl-carbamoyl-oxy-methylester	15.94	19.09	74.25	109.29
Threonine	**10.38**	**4.86**	**82.90**	**98.14**
Toluene	**5.76**	**90.38**	**-4.88**	**91.26**
Trichloroacetic Acid	**22.09**	**5.51**	**73.92**	**101.52**
Trimethoprim	2.13	87.68	2.16	91.97
triphenyl Phosphate	0.33	17.03	74.74	92.10
Urea	**75.25**	**2.21**	**4.50**	**81.95**
Valine	**16.93**	**6.39**	**76.44**	**99.76**

Table 22a. Estimated Percent Rejection based on mass of compound passing through the membrane (P-Flux) and on mass of compound not interacting with the membrane (R-Flux). P-Flux represents the classical method of determining rejection, which does not take into account association with the membrane. Bolded compounds represent surrogates used to build the models. Blank spaces indicate model failure.

	BW-30		ESPA-2		LFC-1		TFC-HR		"Univ" PA		CA	
Compound Name	**P-Flux**	**R-Flux**	**P-Flux**	**R-Flux**	**P-Flux**	**R-Flux**	**P-Flux**	**R-Flux**	**P-Flux**	**R-Flux**	**P-Flux**	**R-Flux**
1,1 Dichloropropanone			85.18	33.24	80.32	61.57	84.66	58.21	96.43	57.76		
1,1,2 Trichloroethene (TCE)	95.96	21.20	80.43	11.14	93.46	34.08						
1,1,2,2 Tetrachloroethane	99.91	0.00	99.68	-33.49	99.89	16.02	99.91	0.12	99.88	1.14	67.12	5.31
1,1,2,2, Tetrachloroethylene (PCE)	**99.91**	**0.00**	**99.71**	**-2.36**	**99.89**	**-2.58**	**99.92**	**-2.44**	**99.88**	**-3.28**	**69.09**	**6.04**
1,2 Dichlorobenzene	98.77	2.00	93.76	-1.78					98.39	16.70	86.91	-0.73
1,2 Dimethylbenzene	96.04	0.00	97.02	-5.39	98.54	-19.89			96.80	-8.47		
1,2,4 Trimethylbenzene	99.88	0.00	99.14	-6.13	98.96	-16.39			93.69	-8.54	75.48	1.94
1,3,5 Trimethylbenzene	99.00	0.00	98.37	-5.02	99.76	-19.54	99.90	-7.06	98.43	-8.54	82.21	3.46
1,4 Dichlorobenzene	98.07	0.52	94.62	-4.85							93.68	-0.57
1,4 Dichlorophenoxyacetic Acid	**88.88**	**81.08**	**85.36**	**66.00**	**95.48**	**90.28**	**94.96**	**83.49**	**92.67**	**80.77**	**56.10**	**46.61**
17a Estradiol	**99.82**	**29.32**	**98.16**	**15.35**	**99.11**	**32.61**	**99.63**	**16.91**	**99.42**	**24.93**	**96.97**	**0.84**
2,2 bis-p-Chlorophenyl 1,1 Dichloroethane	99.49	71.86							99.32	88.53		
2,2 bis-p-Chlorophenyl 1,1,1 Trichloroethane	96.74	72.46					99.52	77.47	99.71	79.91	97.56	-2.07
2,2 bis-p-Methoxyphenyl 1,1,1 Trichloroethane	90.36	72.19					98.80	98.03	99.67	93.66		
2,2,2 Trichloro 1,1-bis-4-chlorophenyl Ethanol	99.15	71.60							99.25	79.90		
2,3 Naphthalenedicarboxylic Acid	84.35	90.42	97.07	79.80	88.75	81.66	97.48	78.47	98.13	72.27	91.02	0.62
2,3,4,5,6 Pentachlorophenol	**99.63**	**53.52**	**97.40**	**52.89**	**99.18**	**37.65**	**94.26**	**23.23**	**98.28**	**39.53**	**97.94**	**0.35**
2,3,5,6 Tetrachloroterephthalic Acid	99.08	68.40	96.76	75.26	86.47	99.68			89.30	75.96		
2,4 Dichloro-4'-nitrodiphenyl Ether	89.46	75.16							99.57	43.74	97.21	-1.18
2,4 Dinitrophenol					97.54	44.18	89.90	36.53				
2,4 Dinitrotoluene	**95.94**	**8.41**	**96.56**	**3.88**	**98.11**	**1.75**	**98.04**	**1.68**	**97.24**	**-2.48**	**92.10**	**0.47**
2,4,5 Trichlorophenoxyacetic Acid	93.43	73.24	89.87	56.28	96.73	82.31	90.67	74.91	98.17	73.24		
2,6 bis-1,1 Dimethylethyl 2,5 Cyclohexadiene 1,4 dione	77.52	54.10									95.07	6.33
2,6 bis-1,1 Dimethylethyl Phenol	99.58	70.31					99.91	52.45			90.34	0.88
2,6 Dinitrotoluene												
2,6 di-tert-butyl-p-Cresol	98.16	74.91					99.88	40.35			92.74	2.08
2,6 Naphthalenedicarboxylic Acid			97.80	74.88	96.11	82.51	96.81	76.20	98.33	72.32		
2-chloro-2'-6'-diethyl-N-methoxymethyl-acetanilide (Alachl	**99.56**	**94.03**	**97.45**	**77.40**			**97.35**	**77.77**	**98.49**	**85.37**	**94.27**	**4.95**
3 Hydroxycarbofuran	99.23	94.98										
3,4,5,6,7,8,8a-Heptachlorodicyclopentadiene	99.70	19.81			96.25	55.84	99.82	47.92			76.45	28.83
3-amino-1H-1,2,4 Triazole	93.03	81.25	69.84	49.65	76.40	0.29	87.65	1.20	95.40	24.45		
4 Nonylphenol	**99.75**	**63.88**	**99.87**	**78.85**	**99.63**	**76.99**	**99.78**	**26.83**	**99.55**	**68.02**	**99.46**	**1.88**
4,6 Dichlorophenol	**92.37**	**0.00**	**96.69**	**0.07**	**98.28**	**6.22**	**97.82**	**4.68**	**96.70**	**-3.38**	**97.82**	**-0.80**
4-amino-6-tert-butyl-3-methylthio-as-triazin-5,4H-one			79.12	70.65							49.48	0.23
5-methyl-1H-Benzotriazole	93.71	33.56							72.13	-12.38		

Table 22b. Estimated Percent Rejection based on mass of compound passing through the membrane (P-Flux) and on mass of compound not interacting with the membrane (R-Flux).
(Continued – See Table 22a)

Compound Name	BW-30		ESPA-2		LFC-1		TFC-HR		"Univ" PA		CA	
	P-Flux	R-Flux	P-Flux	R-Flux	P-Flux	R-Flux	P-Flux	R-Flux	P-Flux	R-Flux	P-Flux	R-Flux
6-chloro-N-ethyl-N'-isopropyl-1,3,5 Triazine-2,4-diamine									95.20	-9.79		
Acetaminophen	93.56	3.34					78.98	31.71			11.04	0.76
Acetochlor			91.91	80.83					88.23	67.96		
Alanine	**87.26**	**79.84**	**85.04**	**76.28**	**84.89**	**76.08**	**90.27**	**82.22**	**83.57**	**80.97**	**41.36**	**40.05**
Aldicarbsulfone	78.37	86.28	97.26	69.22	87.46	75.89	98.58	77.50	61.63	72.46	26.84	12.56
Aldrin					99.02	67.59	91.99	84.69	99.28	74.38	85.28	2.07
alpha-naphthyl-N-Methylcarbamate	91.86	81.67	99.16	77.57					88.57	60.69	95.41	9.85
Anatoxin a												
Androsterone	99.76	95.88							99.61	43.83	96.05	0.55
Anthracene	99.91	12.48	99.55	14.71	99.45	-10.69	99.51	16.93	99.58	5.91	99.55	0.97
Asparagine	**90.53**	**91.74**	**77.83**	**73.00**	**87.94**	**83.17**	**65.09**	**64.01**	**87.02**	**79.02**	**33.92**	**42.86**
Aspartic Acid	**85.68**	**82.57**	**81.18**	**76.75**	**91.69**	**87.17**	**88.00**	**80.79**	**86.78**	**80.64**	**64.38**	**61.70**
Atrazine									95.82	-7.85		
Benzene	**75.03**	**0.00**	**69.28**	**-2.55**	**83.79**	**12.98**	**77.79**	**2.46**	**79.21**	**8.13**	**42.79**	**1.48**
benzo-a-Pyrene			99.99	18.06			99.37	58.99	99.81	6.04	99.77	4.16
benzo-e-1,3,2 Dioxathiepin-3-oxide	95.55	94.70	81.26	81.43	99.89	81.18	90.83	83.96	85.38	64.78		
beta Sitostanol n Hydrate	**99.55**	**73.77**	**99.53**	**59.95**	**99.69**	**85.52**	**99.60**	**74.20**	**99.46**	**70.10**	**99.47**	**75.84**
beta-Estradiol	99.76	33.22	98.01	30.65			99.62	17.25	99.71	26.86		
bis-2-Ethylhexyl-adipate	46.62	0.00	96.45	79.05							94.90	0.87
Bisphenol	**97.31**	**65.81**	**98.00**	**69.88**	**99.04**	**84.03**	**99.76**	**74.45**	**98.82**	**74.46**	**99.16**	**0.21**
Bromochloroacetic Acid	94.74	87.76					90.03	69.30	97.19	62.45		
Bromochloroacetonitrile			75.35	32.48	53.56	67.87	73.96	74.57	88.88	69.12		
Bromochloromethane	10.19	15.85	88.57	63.48			78.83	62.77				
Bromodichloromethane					94.61	72.32	81.45	59.89	67.89	31.09		
Bromoform							99.72	51.00	75.33	5.54		
Bromomethane			82.59	49.51	86.14	75.90	80.30	52.96				
Butylated-Hydroxyanisole			99.75	31.89			99.81	39.50			88.21	2.30
Caffeine	**82.39**	**69.59**	**80.36**	**59.49**	**82.99**	**72.39**	**82.80**	**68.49**	**79.92**	**64.92**	**29.65**	**15.14**
Carbadox					98.13	73.90	90.29	71.49			97.83	1.58
Chloralhydrate	99.47	71.24	93.03	89.52					90.53	71.50	61.58	1.57
Chloroform					88.92	56.31	73.82	56.20	63.41	33.19		
Chlorotetracycline	99.54	86.21			99.04	100.87						
Chlorpyrifos	**99.20**	**71.33**	**99.29**	**43.86**	**98.88**	**76.80**	**99.25**	**46.84**	**99.29**	**62.81**	**96.68**	**-0.19**
Cholesterol	**99.91**	**87.46**	**99.97**	**76.24**	**99.76**	**87.83**	**99.66**	**88.03**	**99.79**	**85.63**	**99.73**	**70.30**
Cimetidine	**92.20**	**79.85**	**83.79**	**44.47**	**95.22**	**63.65**	**86.46**	**62.29**	**90.61**	**67.54**	**37.92**	**22.86**
Ciprofloxacin												
cis-Chlordane	99.31	86.35	98.28	103.47	98.98	46.42	98.06	-54.30	99.42	79.64	91.73	48.52
Codeine	**92.85**	**77.34**	**84.12**	**36.50**	**89.15**	**46.74**	**92.61**	**76.11**	**88.87**	**61.67**	**44.14**	**10.66**
Cyclotrimethylenetrinitramine							29.83	-54.30				
Cylindrospermopsin	93.37	91.02			90.89	84.36	87.00	73.06	97.04	84.32		
Cymene	99.32	0.00	99.76	14.69	99.22	26.58	99.92	35.94	98.36	-10.39	87.68	1.63
Cysteine	**83.80**	**76.79**	**91.64**	**83.09**	**84.67**	**80.05**	**92.25**	**86.50**	**90.01**	**82.35**	**57.10**	**42.02**

Table 22c. Estimated Percent Rejection based on mass of compound passing through the membrane (P-Flux) and on mass of compound not interacting with the membrane (R-Flux).
(Continued – See Table 22b)

Compound Name	BW-30		ESPA-2		LFC-1		TFC-HR		"Univ" PA		CA	
	P-Flux	R-Flux	P-Flux	R-Flux	P-Flux	R-Flux	P-Flux	R-Flux	P-Flux	R-Flux	P-Flux	R-Flux
Diazinon	95.60	96.52									92.35	-1.34
Dibromoacetatic Acid	98.28	78.09	67.24	66.79	82.00	80.90	96.85	80.56	94.72	69.17		
Dibromoacetonitrile	90.43	0.00					90.90	75.88	95.51	69.65	41.57	16.00
Dibromochloromethane							92.47	67.86	87.85	29.28		
Dibromochloropropane	99.57	0.00			98.80	50.91						
Dichloroacetic Acid	**85.35**	**75.43**	**69.44**	**58.63**	**73.25**	**75.94**	**79.33**	**67.59**	**76.17**	**66.72**	**55.89**	**37.16**
Dichloroacetonitrile			80.85	39.77	91.79	71.71			96.83	71.90		
Dichlorodifluoromethane							78.28	61.43			97.43	1.75
Dichlorodiphenyldichloroethylene	97.45	79.24	99.39	78.66			83.37	36.15			92.42	13.22
Dichloropropane			95.98	33.88	91.24	66.38	84.99	76.99	88.94	56.84		
Dieldrin	99.96	94.96							99.14	91.26		
Diethylphthalate	**94.24**	**59.64**	**94.09**	**63.20**	**94.50**	**64.57**	**98.58**	**62.42**	**95.12**	**61.30**	**84.19**	**0.22**
Diethylstilbestrol	**99.90**	**67.32**	**99.85**	**81.93**	**99.85**	**80.44**	**99.85**	**50.95**	**99.86**	**69.13**	**99.72**	**0.43**
Digoxigenin	99.09	81.64	98.65	89.12			99.43	58.85	98.20	72.19		
Digoxin	96.00	73.73							96.74	79.32		
Diltiazem			92.65	72.69			99.72	73.85	92.23	75.54	94.75	-0.32
Dipropylthiocarbamic Acid-s-ethylester			94.32	91.28	97.15	87.52					86.26	7.33
di-sec-Octylphthalate			98.46	70.20			99.82	82.66			97.41	9.08
Disulfoton	99.81	96.58			98.91	93.07	99.78	103.16	98.19	85.98		
Diuron	36.22	2.64	96.04	60.35					87.53	70.19	69.64	7.30
d--n-Butylphthalate	99.60	67.47	96.30	71.57					97.42	80.70	99.64	12.77
d--n-Octylphthalate			99.94	74.83			99.96	93.84			99.76	22.22
Doxycycline	**95.86**	**85.33**	**95.91**	**82.58**	**94.26**	**79.40**	**91.42**	**77.12**	**94.92**	**78.59**	**82.96**	**53.97**
Enalaprilat	99.56	92.11			99.12	74.00	99.67	76.88	91.26	83.14	20.51	6.42
Endosulfansulfate	99.94	93.66							99.27	46.75	92.18	5.86
Enrofloxacin	96.82	89.40	97.39	69.09	96.62	54.77	91.25	81.74	97.40	74.79	86.70	28.45
Equilenin	99.77	42.95			99.16	56.24			99.59	0.77	98.58	4.97
Equilin					99.76	27.29					98.37	0.13
Erythromycin	**96.28**	**91.16**	**95.76**	**82.74**	**97.22**	**90.00**	**97.46**	**87.94**	**96.67**	**88.25**	**70.63**	**70.00**
Estriol	99.97	94.26	91.62	26.36					96.65	87.63	98.85	3.31
Estrone	**99.41**	**28.69**	**99.72**	**1.39**	**99.10**	**18.65**	**99.80**	**-1.54**	**99.58**	**32.56**	**97.44**	**-0.39**
Ethylbenzene	**95.50**	**0.00**	**97.37**	**-2.72**	**98.05**	**-2.06**	**97.17**	**-4.96**	**97.39**	**-4.95**	**74.14**	**1.42**
Ethylenediaminetetraacetic Acid (EDTA)	**94.91**	**91.11**	**86.31**	**74.29**	**92.79**	**92.16**	**88.70**	**88.17**	**91.23**	**85.89**	**52.89**	**45.09**
ethyl-tert-Butyl Ether							81.34	84.91	53.55	-0.39		
exo-Dimethanonaphthalene							98.73	57.89	92.72	88.09		
Fluoranthrene	99.92	19.06	99.85	13.32			98.15	-0.87	99.72	7.01	99.64	1.48
Fluoxetine	99.63	90.00					95.48	66.67	99.44	77.75	98.65	-1.93
Fonofos	99.78	72.71	99.84	108.88			99.89	75.24	98.57	85.06	94.97	0.44
Gemfibrozil	85.94	72.36	93.79	83.44	98.39	94.10	95.83	84.61				
Glycine	**93.88**	**87.92**	**74.78**	**79.11**	**73.40**	**76.65**	**97.32**	**87.17**	**66.02**	**86.59**	**37.27**	**38.56**
Hexachlorobenzene			99.99	18.07							97.26	-0.85
Hexachlorobutadiene	89.59	39.32			93.10	69.69			99.79	-3.00		

Table 22d. Estimated Percent Rejection based on mass of compound passing through the membrane (P-Flux) and on mass of compound not interacting with the membrane (R-Flux).
(Continued – See Table 22c)

Compound Name	BW-30		ESPA-2		LFC-1		TFC-HR		"Univ" PA		CA	
	P-Flux	R-Flux	P-Flux	R-Flux	P-Flux	R-Flux	P-Flux	R-Flux	P-Flux	R-Flux	P-Flux	R-Flux
Hexachlorocyclohexane							99.60	10.65	92.71	-4.50		
Hexachloropentadiene												
Histidine	**84.39**	**76.70**	**87.00**	**77.22**	**80.74**	**75.48**	**90.36**	**83.38**	**85.87**	**78.75**	**55.83**	**44.55**
Ibuprofen	**84.17**	**65.88**	**95.49**	**82.48**	**94.75**	**85.14**	**96.09**	**86.27**	**94.93**	**82.17**	**42.42**	**22.96**
Leucine			95.47	77.42			93.46	94.32	83.20	86.31	39.36	37.79
Lincomycin	96.87	91.88			99.89	87.68	99.03	98.72	92.59	85.48	48.96	12.59
Lindane	**98.07**	**24.78**	**97.66**	**40.32**	**98.91**	**61.22**	**99.00**	**35.69**	**98.49**	**47.32**	**98.47**	**-0.22**
Linuron	57.93	26.34			98.00	78.01			95.07	65.54		
Lysine	**86.12**	**82.97**	**85.25**	**81.25**	**94.15**	**91.00**	**83.15**	**84.53**	**89.59**	**84.69**	**46.56**	**27.34**
Mestranol	99.82	83.41	99.18	106.34					99.11	81.69	98.32	0.24
Metformin							36.18	13.44			30.15	2.30
Methionine	**74.61**	**64.32**	**83.05**	**55.26**	**89.44**	**84.79**	**82.55**	**73.18**	**87.78**	**75.75**	**51.20**	**39.66**
methyl Parathion	**98.81**	**86.03**	**98.46**	**69.41**	**98.86**	**75.01**	**96.72**	**67.29**	**98.55**	**78.87**	**98.14**	**-0.10**
Methylene Bromide			93.22	45.07	79.85	70.36	93.06	77.58				
Methylene Chloride					85.09	70.67	60.50	44.93	68.07	23.26		
methyl-tert-butyl Ether (MTBE)							78.04	76.90	51.95	-0.47		
Metolachlor									72.39	61.32		
Metribuzin			79.13	70.58							49.51	0.22
Microcystin LR	86.57	79.75			96.92	105.68						
Molinate	75.37	31.17	98.69	71.99								
Monobromobenzene	98.53	0.00	93.76	11.34			76.69	-54.30				
N N diethyl 3 methylbenzamide									62.71	48.87	74.62	0.29
N-Dimethylamine			**65.06**	**42.84**	**71.24**	**39.43**	**64.76**	**62.76**	**64.70**	**51.93**	**44.15**	**10.38**
Nitrilotriacetic Acid					96.56	102.92	96.73	78.56	88.80	88.64	49.30	49.24
Nitrobenzene	**99.61**	**0.00**	**99.53**	**-3.05**	**99.71**	**-2.69**	**99.66**	**-2.19**	**99.63**	**-6.95**	**64.02**	**0.80**
Nitrosodibutylamine	87.49	1.88	97.27	63.27					65.60	-9.03		
Nitrosodiethylamine											42.51	8.70
N-nitroso dimethyl amine (NDMA)			**28.03**	**6.45**	**19.63**	**18.60**	**25.28**	**2.72**	**32.45**	**3.63**	**9.84**	**3.67**
N-nitrosodi-n-butylamine			96.19	59.18					70.34	-3.09		
N-nitrosodi-n-propylamine												
N-nitrosomorpholine							82.82	30.68				
N-nitrosopiperidine												
N-nitrosopyrrolidine									74.72	83.64		
Norethindrone	99.90	25.64			99.83	63.79	99.64	68.08	99.72	63.34		
Norfloxacin	98.13	92.71	93.61	67.80	91.62	51.13	96.25	83.01	92.38	83.52	65.99	11.89
N-triacetic Acid	72.70	85.39			99.57	96.32	97.52	76.47	85.42	82.21	33.01	33.92
o-Cresol	88.82	13.24	94.30	10.57	85.52	-0.03			94.13	3.55	76.88	0.05
Octachloro-4-7-methanotetrahydroindane	99.93	91.90					95.29	70.66	99.61	75.90		
Octachloroepoxide	99.58	86.70							99.23	78.59		
Paraxanthine	77.67	79.02	82.82	60.94	89.63	77.01	94.31	58.57	87.78	56.47	46.85	16.16
Paroxetine	99.36	83.20			99.36	78.53					98.61	0.49

Table 22e. Estimated Percent Rejection based on mass of compound passing through the membrane (P-Flux) and on mass of compound not interacting with the membrane (R-Flux).
(Continued – See Table 22d)

Compound Name	BW-30		ESPA-2		LFC-1		TFC-HR		"Univ" PA		CA	
	P-Flux	R-Flux	P-Flux	R-Flux	P-Flux	R-Flux	P-Flux	R-Flux	P-Flux	R-Flux	P-Flux	R-Flux
p-Cresol	97.32	8.39	95.08	7.43	65.13	-3.43			84.93	-0.29		
p-Dichlorobenzene	98.00	0.52	94.62	-4.85							93.68	-0.57
Perchloric Acid	88.65	74.43					92.84	99.37	87.98	60.07		
Phenanthrene	**99.73**	**12.63**	**99.45**	**14.04**	**99.28**	**-4.09**	**99.49**	**5.46**	**99.53**	**7.52**	**99.50**	**0.97**
Phenol	**66.54**	**2.68**	**72.11**	**10.55**	**60.46**	**-1.45**	**67.52**	**-1.19**	**68.45**	**3.93**	**28.04**	**-0.34**
Phthalic Anhydride	**94.42**	**91.30**	**92.92**	**90.53**	**94.41**	**90.03**	**91.80**	**88.36**	**92.47**	**89.95**	**71.42**	**64.35**
Progesterone	**99.94**	**77.15**	**99.79**	**65.15**	**99.99**	**80.95**	**99.83**	**69.81**	**99.79**	**70.12**	**98.32**	**-0.28**
Pyrene	99.86	18.31	99.73	22.23	99.43	-26.66	98.71	-1.56	99.67	10.05	99.67	1.71
Ranitidine									87.39	69.39		
s-1-Methyl-5-3-Pyridinyl-2-Pyrrolidinone			96.04	62.09					98.45	38.95		
Salbutamol			89.16	68.81			85.68	80.01	76.90	85.57	24.92	3.65
Saxitoxin	96.68	92.84	91.75	65.29	97.91	82.08			94.72	86.56	60.16	7.91
Serine	71.77	85.65	78.14	85.84	65.78	80.40	93.00	80.18	84.44	77.26		
Simazine												
Sulfachlorpyridazine	98.15	79.70	97.89	70.01			99.20	81.89	98.52	82.49		
Sulfadimethoxine	95.88	83.37	97.11	58.41	96.58	62.32	98.81	85.35	98.48	85.40		
Sulfamerazine	99.42	84.60	98.63	74.61			99.46	83.61	98.36	84.19	29.85	0.68
Sulfamethazine	97.72	82.96	97.40	77.32	97.65	48.85	99.20	86.30	98.23	85.23		
Sulfamethizole	97.64	88.97			84.76	84.93			95.82	86.92		
Sulfamethoxazole	97.48	82.42	98.65	73.11	93.60	60.94			98.57	81.01		
Sulfathiazole	98.75	82.91	97.58	74.96	95.44	80.74	99.34	71.33	97.06	84.23		
t Butyl Alcohol	**80.37**	**78.13**	**82.11**	**79.67**	**77.68**	**66.91**	**80.86**	**66.84**	**79.21**	**71.30**	**13.49**	**12.52**
Terbacil					98.44	65.34			93.02	69.12		
Terbufos	97.42	74.10	98.60	73.79	99.37	70.40					79.76	4.87
Terramycin	95.67	86.59	91.05	74.69	95.42	80.61	97.74	80.83	96.24	83.81		
tert amyl methyl Ether	99.35	0.00					92.27	76.61	78.70	-0.77		
Testosterone	**99.13**	**87.55**	**97.69**	**70.40**	**98.23**	**61.03**	**99.67**	**85.55**	**98.96**	**75.39**	**80.36**	**2.77**
Tetracycline	**96.68**	**86.62**	**94.18**	**75.41**	**96.67**	**78.49**	**97.02**	**83.45**	**96.60**	**83.29**	**62.05**	**57.31**
Thio-N-methyl-carbamoyl-oxy-methylester			81.25	66.30	98.45	75.62	91.74	80.19	84.06	74.25		
Threonine	**90.99**	**83.13**	**88.41**	**83.70**	**88.14**	**80.51**	**91.32**	**84.04**	**89.62**	**82.90**	**50.57**	**35.08**
Toluene	**98.59**	**0.00**	**93.40**	**7.43**	**80.49**	**0.23**	**92.88**	**-1.25**	**94.24**	**-4.88**	**53.10**	**2.04**
Tributyl Tin	99.85	54.28			99.22	96.50	99.92	98.08				
Trichloroacetic Acid	**77.20**	**63.68**	**79.80**	**71.78**	**87.35**	**82.86**	**71.84**	**67.17**	**77.91**	**73.92**	**44.09**	**39.79**
Triclosan			99.00	72.65			81.67	61.95				
Trimethoprim	92.64	95.68	94.43	56.41					97.87	2.16	87.88	41.94
triphenyl Phosphate	98.04	91.86	99.22	90.90			99.85	99.44	99.67	74.74	99.50	-1.50
tris 2 Chloroethyl Phosphate	95.95	95.96	98.76	53.03	97.48	92.71					97.77	1.67
Tylosin	92.25	97.15	94.55	72.09	99.29	68.20						
Urea	**3.68**	**4.12**	**15.48**	**5.69**	**14.67**	**4.38**	**27.69**	**7.26**	**24.75**	**4.50**	**8.05**	**28.21**
Valine	**78.61**	**70.71**	**82.84**	**79.31**	**87.71**	**83.59**	**90.59**	**82.94**	**83.07**	**76.44**	**38.31**	**34.09**

Table 23. Comparison between predicted rejection and reported values.
Generally, rejection of compounds predicted by the ANN models were in accord with results obtained from the literature. Bolded compounds indicate surrogate compounds used in the study.

Test Compounds	Percent Rejection by P-Flux						References
	BW-30	ESPA-2	LFC-1	TFC-HR	"Univ" PA	CA	
1-2 Dichlorobenzene	98.77	93.76	99.84	91.63	98.39	86.91	70-92% (PA) DOW-Filmtec
2,3,4,5,6 Pentachlorophenol	99.63	97.40	99.18	94.26	98.28	97.94	>86% (PA) DOW-Filmtec; >95% (PA) Ozaki et al.
2,4 Dinitrophenol	33.56	94.71	97.54	89.90	97.73	92.63	~95% (PA) Ozaki et al.
Bromodichloromethane	45.93	81.58	94.61	81.45	67.89	8.31	79% (PA) DOW-Filmtec
Caffeine	82.39	80.40	82.99	82.80	79.92	29.65	92% (PA) Reinhard et al.
Ciprofloxacin	98.49	88.33	92.03	95.11	93.76	65.62	>91% WBMWD
Dieldrin	99.96	99.18	98.59	78.91	99.14	83.15	95.4% (CA) Chian et al.
Estrone	99.41	99.72	99.10	99.80	99.58	97.44	93-98% Schafer et al.
Gemfibrozil	85.94	93.79	98.39	95.83	69.07	91.43	>99% WBMWD
Glycine	93.88	74.78	73.40	97.32	66.02	37.27	78% (PA) DOW-Filmtec
Ibuprofen	84.17	95.49	94.75	96.09	94.93	41.30	>89% WBMWD
Lindane	98.07	97.66	98.91	99.00	98.49	98.47	99.5% (CA) Chian et al.
Methyl parathion	98.81	98.46	98.86	96.72	98.55	98.14	99.6% (CA) Chian et al.
Phenol	66.54	72.11	60.46	67.52	68.45	28.04	65% (PA) DOW-Filmtec; 67-85% (PA) Koyama et al.
Sulfamethoxazole	97.48	98.65	93.60	99.26	98.57	86.36	>90% WBMWD
t butyl alcohol	80.37	82.11	77.68	80.86	79.21	13.49	81-83% (PA) Koyama et al.; 87% (PA) Dickson et al.
Toluene	98.59	93.40	80.49	92.88	94.24	53.10	84-94% (PA) Schutte et al.
Urea	3.68	15.48	14.67	27.69	24.75	8.05	30% (PA) Ozaki et al.

WBMWD = West Basin Municipal Water District
PA = Polyamide
CA = Cellulose Acetate

Table 24. Compounds that 75% or more of the PA Models Fail to Predict Compounds that failed or didn't model well were identified and it is suggested to use them to build future models.

Compounds 75%+ of the PA Models Failed to Predict		
QSAR Cluster	**Compound Name**	**Notes**
1	Cyclotrimethylenetrinitramine	Carcinogen
1	Dichlorodifluoromethane	Refrigerant Gas
1	Metformin	Pharmaceutical
1	Nitrosodiethylamine	Carcinogen
1	N-nitrosomorpholine	Carcinogen
1	N-nitrosopiperidine	Carcinogen
1	N-nitrosopyrrolidine	Carcinogen
1	s-1-Methyl-5-3-Pyridinyl-2-Pyrrolidinone	
2	3,4,5,6,7,8,8a-Heptachlorodicyclopentadiene	Endocrine Disruptor
2	5-methyl-1H-Benzotriazole	Antioxidant-Wastewater Product
2	Bromoform	Disinfection Byproduct
2	Dibromochloromethane	Disinfection Byproduct
2	exo-Dimethanonaphthalene	Endocrine Disruptor
3	2,4 Dichloro-4'-nitrodiphenyl Ether	Endocrine Disruptor
4	Androsterone	Pharmaceutical
4	Equilin	Pharmaceutical
5	2,2 bis-p-Chlorophenyl 1,1,1 Trichloroethane	Endocrine Disruptor
5	2,2-bis-p-Chlorophenyl 1,1 Dichloroethane	Endocrine Disruptor
7	2,6 bis-1,1 Dimethylethyl 2,5 Cyclohexadiene 1,4 dione	
7	ethyl-tert-Butyl Ether	Fuel Oxygenate-Carcinogen
7	methyl-tert-butyl Ether (MTBE)	Fuel Hydrocarbon-Carcinogen
8	2,6 Dinitrotoluene	Ammuntion/Explosives/Foams Manuf
9	4-amino-6-tert-butyl-3-methylthio-as-triazin-5,4H-one	Endocrine Disruptor
9	Acetochlor	Herbicide
9	Atrazine	Carcinogen
9	Metolachlor	Pesticide
9	Metribuzin	Pesticide
9	N N diethyl 3 methylbenzamide	Insecticide
9	N-nitrosodi-n-butylamine	Carcinogen
9	N-nitrosodi-n-propylamine	Carcinogen
9	Pramitol	Herbicide
9	Simazine	Carcinogen
9	Terbacil	Herbicide
10	Diazinon	Pesticide
10	Endosulfansulfate	Pesticide
11	cis-Chlordane	Pesticide
11	Dieldrin	Pesticide
11	Hexachloropentadiene	Endocrine Disruptor
11	Octachloroepoxide	Endocrine Disruptor
12	benzo-a-Pyrene	Polycyclic Aromatic Hydrocarbon
13	Hexachlorobenzene	Endocrine Disruptor
13	Hexachlorocyclohexane	Carcinogen
16	Ranitidine	Pharmaceutical
17	Digoxin	Pharmaceutical
	Anatoxin a	Marine Toxin

Table 25. Conditions used for MD simulations of NDMA and TCE transport.

Parameter	Value	Comment
Temperature	300°K	27°C
Time Step Size	1 fs	0.001 ps (data analysis at 0.01 ps intervals)
Simulation Duration	200 ps	0.2 ns
Boundary Conditions	Yes	cubic, 30Å per side
System Density	1.19 g/cc	membrane + water + solute
Water Content	18.96 Wt%	TIP3P water models added randomly
Membrane Charge	-24	-1.0 for each free COO- group
Membrane Mass	15398 amu	1724 atoms
Total Monomers	116	MPD + TMC
Crosslink Probability	1.0	all possible crosslinks formed
Number of Crosslinks	14	28 crosslink bonds
COO-/Amide Bond Ratio	0.186	experimental ratios from IR ~0.2-0.5
Number Solute Molecules	1	either NDMA or TCE
Solute Concentration	0.062 M	concentration in membrane

Table 26. Modeled compound diffusivities and flux calculation results.

	Diffusion Coefficient, Membrane System (cm^2/s)	Diffusion Coefficient, Pure Water System (cm^2/s)	Partition Coefficient (K_A) from Experiment (OCWD data)	Flux - Expt. (M/cm^2-s)	Flux - Model (M/cm^2-s)	Rejection - Expt.	Rejection - Model
NDMA	7.25E-06	7.82E-06	2.10E+01	6.70E-12	6.08E-08	0.44	NC**
TCE	1.92E-06	7.82E-06	5.06E+02	1.54E-14	8.73E-07	0.99	NC
Water	1.62E-05	1.56E-05	NA	2-20E-05	9.83E-05*	NA	NA

***Corresponds to 37.4 gallons/ft^2/day**
****NC = not calculated**

Table 27. Summary of NDMA and TCE interactions with pure water. No membrane present (data from 200 ps simulations)

.

	NDMA	SD	N		TCE	SD	N
Ave. Shell Water Count	4.34	1.10	200		2.06	0.66	200
Ave. Distance To Shell Water (Å)	3.73	0.09	200		3.52	0.16	200
Ave. H-Bonded Water Count	1.59	1.00	200		0.00	0.00	200

Appendix 1

Definitions of ANN Model Inputs

1. QSAR Molecular Descriptors used in modeling (* *Indicates inclusion in one or more of the final ANN models*)

General 3D Descriptors: These molecular descriptors describe the 3D properties of the entire molecule.

ABSQ* - The sum of the absolute value of the charges on each atom of a molecule, expressed as electrons.

Dipole - The dipole moment of the molecule expressed in Debyes.

MaxHp - The largest positive charge on a hydrogen atom in the molecule.

MaxNeg* – The largest negative charge over the atoms in the molecule.

MaxQp* – The largest positive charge over the atoms in the molecule.

Ovality* – The ovality of the molecule, expressed as the ratio of the surface of the molecule to that of a perfect sphere (larger values indicate increasingly elongated molecules.

Polarizability – Molecular polarizability calculated on the base of the additive approach. Polarizability is the relative tendency of the electron cloud of the molecule to be distorted from its normal shape by the presence of a nearby external electric field.

Surface* – The surface area of the molecule.

2D Descriptors – These descriptors quantify properties such as bond properties, shape, information content, connectivity topological information and other properties.

Molecular Connectivity Chi Indices – A chi index is a weighted count of values computed for a function of the delta values of the constituent atoms in a given type of subgraph (portion of the molecular skeleton - delta values refer to the count of neighboring atoms bonded to an atom in a hydrogen-suppressed molecule and also corresponds to the count of sigma electrons contributed by that atom to bonded, non-hydrogen atoms). There are two classes of chi indices. *Simple chi indices*, in which all atoms are treated as carbon atoms and *valence chi indices*, in which the value for heteroatoms (non-carbon atoms) are computed differently than for the values of carbon atoms according to their electron characteristics. Chi indices have two attributes, *order* (the number of bonds in the molecule fragment being described) and type (the type of molecular fragment). There are four characteristic types – path (p), cluster (c), pathcluster (pc) and chain (ring) (ch). The molecular connectivity chi indices represent molecular structure by encoding significant features of whole molecules. Five general categories of molecular information are encoded by these indices: *degree of branching* (low order indices 0 – 2), *variable branching patterns* (high order path chi indices 3 – 10), *position and influence of heteroatoms* (valence chi indices), *patterns of adjacency* (chi cluster and path/cluster indices) and *degree of cyclicity* (chi chain indices).

x1 – Simple 1st order chi index – 2 atom simple path index, encodes degree of molecular branching.
xp4 – 4th order path chi index – 5 atom index, encodes variable branching patterns.
xc3 – 3rd order cluster chi index – 4 atom index, encodes patterns of molecular adjacency.
xpc4* – 4th order path/cluster chi index – 5 atom index, encodes patterns of adjacency.
xv1* – 1st order valence chi index – 2 atom index, encodes degree of branching, sensitive to nature of different atom types.
xvp4 – 4th order valence path chi index – 5 atom index, encodes variable branching patterns, sensitive to variations in atom types.
xvp7 – 7th order valence path chi index – 8 atom index, encodes variable branching patterns, sensitive to atom types.
xvp10 – 10th order valence path chi index – 11 atom index, encodes variable branching patterns, sensitive to atom types.
xvc3 – 3rd order valence cluster chi index – 4 atom index, encodes patterns of adjacency, sensitive to atom types.
xvpc4* – 4th order valence path/cluster chi index – 5 atom index, encodes patterns of adjacency, sensitive to atom types.
xvch6 – 6th order valence chain chi index – 7 atom index, encodes degree of cyclicity, sensitive to atom types.

Subgraph count indices – These indices are based on a count of a particular type of molecular feature such as a path, cluster, path/cluster or ring (chain). These descriptors are useful in characterizing the molecular skeleton.
nxp5* – the number of paths in the molecule with 5 edges
nxc3 – the number of 3-way clusters in the molecule
nxch6* – the number of 6-membered rings in the molecule.

3D Descriptors for Comparative Molecular Moment Analysis (CoMMA) – CoMMA descriptors provide a succinct representation of the 3D distribution of molecular mass, shape and charge.
Ix -Principal Moment of Inertia along X-Axis - Measure of the difficulty accelerating the molecule along its X-axis.
Iy* - Principal Moment of Inertia along Y-Axis - Measure of difficulty accellerating molecule along its Y-axis.
Py* - Component of Dipole Moment along Inertial Y-Axis - Magnitude of charge separation along the molecule's Y-axis.
Pz* - Component of Dipole Moment along Inertial Z-Axis - Magnitude of charge separation along the molecule's Z-axis.
P* - Magnitude of Dipole Moment - Magnitude of charge separation across entire molecule.
Q* - Magnitude of Principal Quadripole Moment - High order multipole moment of charge distribution.

Dx - Displacement between Center of Mass and Center of Dipole Moment along X-Axis - Difference between center of mass in the X-axis and point along X-axis where charge is zero.
Dy - Displacement between Center of Mass and Center of Dipole Moment along Y-Axis - Difference between center of mass in the Y-axis and point along Y-axis where charge is zero.
Dz - Displacement between Center of Mass and Center of Dipole Moment along Z-Axis - Difference between center of mass in the Z-axis and point along Z-axis where charge is zero.
Qxx - The xx Component of Second Rank Tensor Translated so Origin Coincides With Center of Dipole.
Qyy - The yy Component of Second Rank Tensor Translated so Origin Coincides With Center of Dipole.

Total Topological Descriptors - These are descriptors related to the geometrical structure of molecules (including the geometry of electron distribution about the molecule).

W - Weiner Index - The number of bonds between all pairs of atoms (based on shortest path around the molecule).
Pf - Platt f Index - Total sum of degrees of edges in the molecular graph; the degree of an edge in the number of adjacent edges.
sumdelI* - Sum of Delta Intrinsic States of atoms - Sum of degree of perturbation of the intrinsic state of all atoms in the molecule caused by the presence of the adjacent atoms.
tets2 - Total Electrotopological Index - Sum of E-States values of all atoms in the molecule. E-State is the sum of the intrinsic state of an atom (group) plus the sum of the perturbations of the intrinsic state caused by all the other atoms in the molecule.
totop - Total Topological Index – The total topological index, based on molecular connectivity formalism.
Wt* - Total Weiner Number - Same as W, but pairs of atoms are counted with respect to all paths in the molecule, not just the shortest path. This makes Wt > W for cyclic molecules.
nclass - # Symmetry Classes in Molecule - Number of classes of topologically similar molecular vertices.

Traditional Kappa Shape Indices – Kappa shape indices represent a method of molecular structure quantification in which attributes of molecular shape are encoded into three indices derived from counts of one, two and three bond fragments.

k0 – Kappa 0 – Encodes the number of vertex symmetry classes in the molecule; the value decreases with increasing molecular symmetry.
k1* - Kappa 1 – Encodes the degree of cyclicity in the molecule; the value decreases as the degree of cyclicity increases. Long, straight chain molecules have the highest value.
k2* - Kappa 2 – Encodes the degree of central branching in the molecule; the value decreases as the degree of central branching increases.

k3* - Kappa 3 – Encodes the degree of separated branching in the molecule. (far it is between branches along the molecular backbone); the index increases as the degree of branch separation increases (as the distance between branch points increases along the molecular backbone).

Other 2D Descriptors

LogP* - The octanol/water partition coefficient. A measure of hydrophobicity, this represents the log of the ratio of the solubility of the molecule in octanol over the solubility in water. The index increases as molecules become more hydrophobic and decreases as they become more hydrophilic.

LD50 - The mouse oral LD50 for the molecule, a measure of toxicity.

Atom Type E-State Descriptors – These descriptors describe the electronic environment (the accessibility of the electrons) of each atom in the molecule that arise due to a combination of the intrinsic properties of the of the atom and the influence of the neighboring atoms in the molecule. These descriptors parameterize such properties as hydrogen bonds, molecular polarity, etc. Atom type and group type E-state descriptors are computed for a number of atoms and functional groups. Large E-state values may indicate the molecule is more apt to participate in intermolecular interactions.

SsCH3* - Describes the sum of the E-state values for all -CH3 groups in the molecule.

SssCH2 - Describes the sum of the E-state values for all –CH2- groups in the molecule.

SaaCH* - Describes the sum of the E-state values for all aromatic carbon-hydride (=CH-) groups in the molecule (the aromatic ring CH).

SdssC* - Describes the sum of the E-state values for all =C< carbon in molecule.

SdO* - Describes the sum of E-state values for all =O oxygen in the molecule.

SsCl – Describes the sum of E-state values for all –Cl chlorine in the molecule.

Hydrogen Atom Type E-State Descriptors – These descriptors describe the sum of the hydrogen E-states (electron accessibility at the hydrogen atoms) for all polar or non-polar hydride groups of a given type in the molecule. These descriptors relate to such molecular properties as hydrogen bonding. As with E-state descriptors, large values indicate an increased ability of the molecule to participate in intermolecular interactions.

SssOH – Sum of the hydrogen E-states for the –OH groups in the molecule.

Shother – Sum of the hydrogen E-states for non-polar hydrogens (CH hydrogen) in the molecule

Hmax – The largest atom hydrogen E-state in the molecule – the largest polarity on a hydrogen atom in the molecule (also correlates with partial charge).

Gmax* - The largest atom E-state in the molecule (the most electronegative atom in the molecule).

Hmin* - The smallest atom hydrogen E-state in the molecule.

Gmin* - The smallest atom E-state in the molecule (also, the most electrophilic atom in the molecule).

Information Indices – These molecular descriptors are related to the information content of the molecule, and are derived from information theory.

si - Shannon Information Index – A measure of molecular complexity accounting for both diversity and concentration of features.

IC - Information Content - Based on the total number of molecular vertices, hydride groups or non-polar hydrogen atoms.

R - Molecular Redundancy – A measure of structural repetition within the molecule (is highest in highly internally symmetrical molecules like benzene and lowest in internally diverse molecules such as tetracycline).

idc - Bonchev-Trinajsti Information Content – Index is based on 2-path counts. Value increases with increasing molecular complexity.

idcbar* - Bonchev-Trinajsti Mean Information Content – Index is based on 2-path counts. Index increases with molecular complexity.

Molecular Properties – These descriptors include some fundamental properties of the entire molecule.

fw* – Formula weight – the molecular weight of the molecule in Daltons.

nelem – Number of elements – The total number of different elements in the molecule.

nrings – Number of rings – The number of rings in the molecule (also known as the cyclomatic number).

ncirc – Number of circuits – The total number of all cycles in the molecule. Includes ring structures as well as path circuits. Example: biphenyl = 2, but naphthalene = 3 because in addition to the aromatic rings, a circuit can be made about the periphery of the naphthalene molecule.

phia - Kappa Flexibility Index (# Bonds in normal graph for alkanes) – Inversely proportional to molecular complexity; increases with homolgation and decreases with increased branching or cyclicity.

knotp - Difference Between Chi cluster-3 and chi path/cluster-4 – Decreases with increasing molecular complexity.

numHBa* – The number of hydrogen bond acceptors in the molecule.

SHHbd – The number of hydrogen bond donors in the molecule.

Qs* – Specific Molecular and Group Polarity Descriptor – This descriptor is inversely proportional to molecular polarity and hydrophibicity.

Qsv* – Average Molecular and Group Polarity Descriptor – This descriptor is inversely proportional to molecular polarity and hydrophibicity.

2. Polyamide (PA) reverse osmosis membrane properties used as inputs in development of the "Universal" PA model.

Contact Angle (degrees) – The air bubble contact angle of the membrane, measured as the outside angle between the membrane surface and a line tangential to an air bubble trapped against the membrane surface (in 17 MOhm deionized water at 24^{o}C). The contact angle represents a measure of surface hydrophibicity; the smaller the angle, the greater the surface hydrophibicity.

COO^-/Amide I Ratio - A unitless relative index of membrane cross-link frequency derived from attenuated total internal reflection Fourier transform infra-red (ATR-FTIR) spectroscopic measurements based on the ratio of the absorption at 1415 cm^{-1} corresponding to the presence of free carboxylate groups and the absorption 1665 cm^{-1} corresponding to the amide I bonds in the membrane. The larger the ration, the less cross-linked the membrane.

COO^-/Amide II Ratio - A unitless relative index of membrane cross-link frequency derived from ATR-FTIR spectroscopic measurements based on the ratio of the absorption at 1415 cm^{-1} corresponding to the presence of free carboxylate groups and the absorption at 1542 cm^{-1} corresponding to the amide II bonds in the membrane. The larger the ration, the less cross-linked the membrane.

OH^-/Amide I Ratio - A unitless relative index of membrane cross-link frequency derived from ATR-FTIR spectroscopic measurements based on the ratio of the absorption at 3400 cm^{-1} corresponding to the presence of hydroxyl groups and the absorption at 1665 cm^{-1} corresponding to the amide I bonds in the membrane. The larger the ratio, the less cross-linked the membrane.

Polyamide Thickness – A unitless relative index derived from ATR-FTIR spectroscopic measurements based on the ratio of the strength of the 1665 cm^{-1} amide I absorption band of the polyamide layer and the 874 cm^{-1} absorption band of the polysulfone membrane support layer. The greater the ratio, the thicker the polyamide layer.

Roughness (nm) – A direct measurement by atomic force microscopy (AFM) of the rugosity of the membrane surface defined as the standard deviation of the height of features on the membrane, expressed in nanometers. The roughness of the membrane may reflect subtle differences in internal physicochemical properties. Interactions of nanoparticles with membrane surfaces are often positively related to surface roughness.

Specific Water Flux (GFD/PSI) – Measurement of the membrane water flux per unit water pressure. Many membrane properties are represented by the specific water flux, including membrane density and intrinsic porosity, hydraulic conductivity, hydrogen bonding, charge interactions and many others.

Zeta Potential (mV, pH 7) – The Zeta potential of the membrane, in millivolts. Zeta , was determined at pH 7.0 at 20^oC in 1000 mg/L NaCl using measurement of streaming potential obtained with a streaming potential analyzer (ZetaCAD, CAD Instrumentation, Les Essarts Le Roi, France) and applying the Helmholtz-Smoluchowski equation:

$$\zeta = \frac{\Delta U_s}{\Delta P}\frac{\mu}{\varepsilon\varepsilon_0}\frac{L}{A}\frac{1}{R}$$

where ζ is the zeta potential; U_s is the streaming potential; P is the applied pressure, $\Delta U_s/\Delta P$ is the slope of the streaming potential versus applied pressure curve; μ is the dynamic viscosity of the solution; ε is the permittivity of the test solution; ε_0 is the permittivity of free space; L is the channel length of the membrane test cell; A is the test cell channel cross-sectional area; and R is the test cell channel resistance.

Zeta Potential Slope (pH 5-7) - This is rate of change of the Zeta potential as the pH is shifted from 5 to 7. This index is inversely proportional to the ease with which membrane protons may be introduced or removed as a function of pH; the more negative the index, the more easily the membrane may be protonated or deprotonated.

Appendix 2

Structures and QSAR Molecular Descriptors of the Surrogate Molecules Used for Modeling Compound Interactions with Reverse Osmosis Membranes

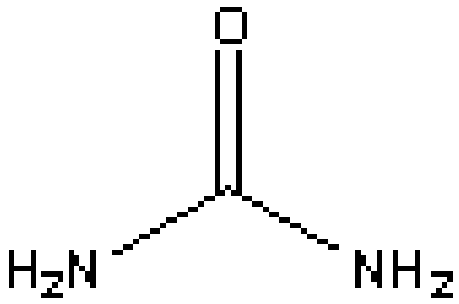

Urea

ABSQ	MaxNeg	MaxQp	Ovality	Surface	xpc4	xv1	xvpc4	nxp5	nxch6
2.0688	-0.4507	0.2383	1.2151	86.1161	0.0000	0.7815	0.0000	0.0000	0.0000
Iy	Py	Pz	P	Q	sumdell	Wt	k1	k2	k3
48.1178	0.9057	0.0000	0.9057	2.0820	3.1667	9.0000	4.0000	1.3333	0.0000
LogP	SsCH3	SaaCH	SdssC	SdO	Gmax	Hmin	Gmin	idcbar	fw
-1.8420	0.0000	0.0000	-0.8333	9.0000	9.0000	1.5514	-0.8333	1.0000	60.0556
numHBa	Qs	Qsv							
3.0000	0.4224	0.4400							

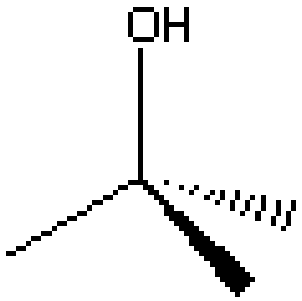

t Butyl Alcohol

ABSQ	MaxNeg	MaxQp	Ovality	Surface	xpc4	xv1	xvpc4	nxp5	nxch6
0.8702	-0.3118	0.1834	1.2193	82.6823	0.0000	1.0233	0.0000	0.0000	0.0000
Iy	Py	Pz	P	Q	sumdeII	Wt	k1	k2	k3
53.6047	0.1875	0.0000	0.1951	0.6462	1.6944	4.0000	3.0000	2.0000	0.0000
LogP	SsCH3	SaaCH	SdssC	SdO	Gmax	Hmin	Gmin	idcbar	fw
-0.0314	1.6806	0.0000	0.0000	0.0000	7.5694	0.3833	0.2500	0.9183	46.0690
numHBa	Qs	Qsv							
1.0000	0.5485	0.7618							

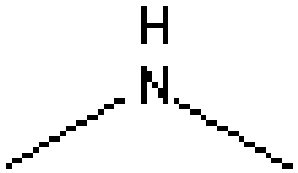

N-dimethylamine

ABSQ	MaxNeg	MaxQp	Ovality	Surface	xpc4	xv1	xvpc4	nxp5	nxch6
1.1210	-0.3578	0.2604	1.3094	112.1383	0.4082	1.2770	0.0816	0.0000	0.0000
Iy	Py	Pz	P	Q	sumdeII	Wt	k1	k2	k3
114.3784	0.0749	0.0000	0.6665	0.7723	2.6528	18.0000	5.0000	2.2500	4.0000
LogP	SsCH3	SaaCH	SdssC	SdO	Gmax	Hmin	Gmin	idcbar	fw
-0.2035	3.1528	0.0000	0.0000	9.1806	9.1806	0.5934	1.1944	1.5219	74.0824
numHBa	Qs	Qsv							
3.0000	0.8626	0.6614							

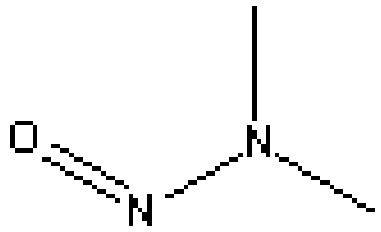

N-Nitroso Dimethylamine (NDMA)

ABSQ	MaxNeg	MaxQp	Ovality	Surface	xpc4	xv1	xvpc4	nxp5	nxch6
0.9623	-0.2788	0.0604	1.2497	102.4022	0.4082	1.2770	0.0816	0.0000	0.0000
Iy	Py	Pz	P	Q	sumdeII	Wt	k1	k2	k3
123.8753	0.2195	0.0001	1.0488	1.2847	2.6528	18.0000	5.0000	2.2500	4.0000
LogP	SsCH3	SaaCH	SdssC	SdO	Gmax	Hmin	Gmin	idcbar	fw
-0.2035	3.1528	0.0000	0.0000	9.1806	9.1806	0.5934	1.1944	1.5219	74.0824
numHBa	Qs	Qsv							
3.0000	0.8626	0.6614							

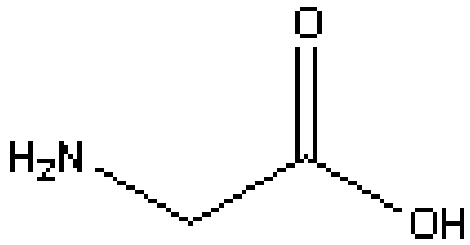

Glycine

ABSQ	MaxNeg	MaxQp	Ovality	Surface	xpc4	xv1	xvpc4	nxp5	nxch6
1.6402	-0.3897	0.3436	1.2919	105.8707	0.4082	1.1895	0.0373	0.0000	0.0000
Iy	Py	Pz	P	Q	sumdeII	Wt	k1	k2	k3
130.0206	0.0537	0.0000	0.4736	0.3324	4.8773	18.0000	5.0000	2.2500	4.0000
LogP	SsCH3	SaaCH	SdssC	SdO	Gmax	Hmin	Gmin	idcbar	fw
-2.6129	0.0000	0.0000	-0.9676	9.2431	9.2431	0.7819	-0.9676	1.5219	75.0672
numHBa	Qs	Qsv							
3.0000	0.5430	0.4163							

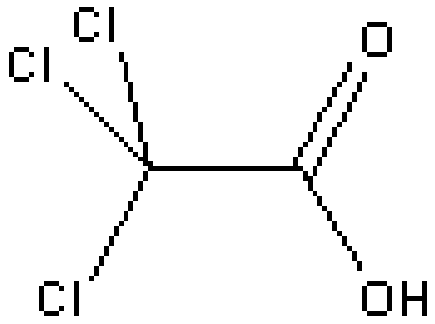

Trichloroacetic Acid

ABSQ	MaxNeg	MaxQp	Ovality	Surface	xpc4	xv1	xvpc4	nxp5	nxch6
1.4882	-0.2795	0.3350	1.2436	109.0973	2.5981	2.3786	0.9802	0.0000	0.0000
ly	**Py**	**Pz**	**P**	**Q**	**sumdell**	**Wt**	**k1**	**k2**	**k3**
369.6898	0.3927	0.0000	0.5364	0.5998	7.6551	42.0000	7.0000	1.8519	2.6667
LogP	**SsCH3**	**SaaCH**	**SdssC**	**SdO**	**Gmax**	**Hmin**	**Gmin**	**idcbar**	**fw**
1.0930	0.0000	0.0000	-1.4606	9.6250	9.6250	2.6583	-2.1667	1.5567	163.3877
numHBa	**Qs**	**Qsv**							
5.0000	0.7726	0.4435							

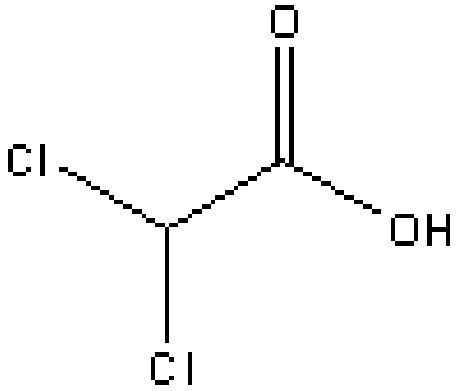

Dichloroacetic Acid

ABSQ	MaxNeg	MaxQp	Ovality	Surface	xpc4	xv1	xvpc4	nxp5	nxch6
1.4396	-0.3014	0.3345	1.2345	107.6139	1.3333	2.0257	0.4370	0.0000	0.0000
Iy	**Py**	**Pz**	**P**	**Q**	**sumdeII**	**Wt**	**k1**	**k2**	**k3**
226.5332	0.3679	0.1487	0.5628	0.3662	6.2886	29.0000	6.0000	2.2222	3.0000
LogP	**SsCH3**	**SaaCH**	**SdssC**	**SdO**	**Gmax**	**Hmin**	**Gmin**	**idcbar**	**fw**
0.3708	0.0000	0.0000	-1.2099	9.4352	9.4352	1.0402	-1.2870	1.5656	128.9427
numHBa	**Qs**	**Qsv**							
4.0000	0.6545	0.4242							

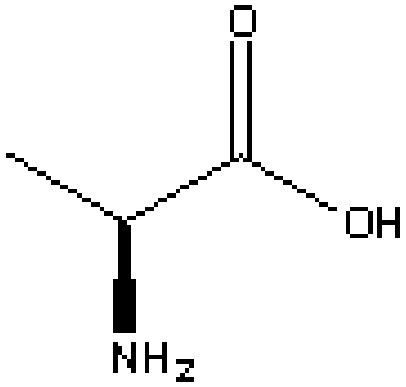

Alanine

ABSQ	MaxNeg	MaxQp	Ovality	Surface	xpc4	xv1	xvpc4	nxp5	nxch6
1.8023	-0.3998	0.3431	1.3117	122.2123	1.3333	1.6271	0.2257	0.0000	0.0000
Iy	Py	Pz	P	Q	sumdell	Wt	k1	k2	k3
171.8076	0.3392	0.1935	0.5073	0.3040	5.9861	29.0000	6.0000	2.2222	3.0000
LogP	SsCH3	SaaCH	SdssC	SdO	Gmax	Hmin	Gmin	idcbar	fw
-2.3284	1.4190	0.0000	-0.9630	9.5741	9.5741	0.5434	-0.9630	1.5656	89.0941
numHBa	Qs	Qsv							
3.0000	0.7934	0.5142							

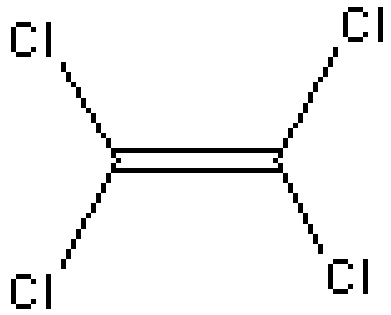

1,1,2,2 Tetrachloroethylene

ABSQ	MaxNeg	MaxQp	Ovality	Surface	xpc4	xv1	xvpc4	nxp5	nxch6
1.1008	-0.2752	0.1376	1.3233	143.6209	1.3333	2.5178	1.4579	0.0000	0.0000
Iy	**Py**	**Pz**	**P**	**Q**	**sumdeII**	**Wt**	**k1**	**k2**	**k3**
353.5459	0.0000	0.0000	0.0000	1.1329	3.5309	29.0000	6.0000	2.2222	3.0000
LogP	**SsCH3**	**SaaCH**	**SdssC**	**SdO**	**Gmax**	**Hmin**	**Gmin**	**idcbar**	**fw**
3.3964	0.0000	0.0000	-0.1975	0.0000	4.9938	0.0000	-0.0988	1.5656	165.8340
numHBa	**Qs**	**Qsv**							
4.0000	0.9817	0.6363							

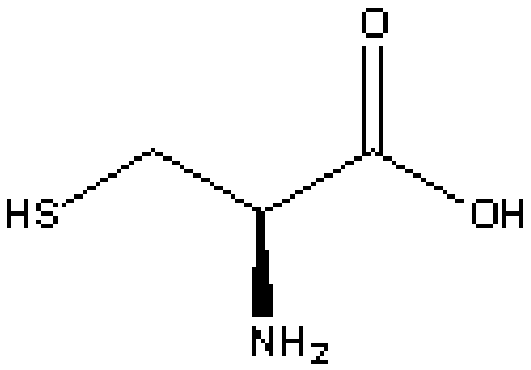

Cysteine

ABSQ	MaxNeg	MaxQp	Ovality	Surface	xpc4	xv1	xvpc4	nxp5	nxch6
1.8902	-0.3693	0.3405	1.3337	131.8441	1.2761	2.4067	0.3266	0.0000	0.0000
Iy	Py	Pz	P	Q	sumdell	Wt	k1	k2	k3
356.3286	0.4084	0.1650	0.4639	0.7559	7.0091	46.0000	7.0000	3.0612	2.6667
LogP	SsCH3	SaaCH	SdssC	SdO	Gmax	Hmin	Gmin	idcbar	fw
-2.1330	0.0000	0.0000	-1.0046	9.7564	9.7564	0.7045	-1.0046	1.8842	121.1601
numHBa	Qs	Qsv							
3.0000	0.9754	0.5143							

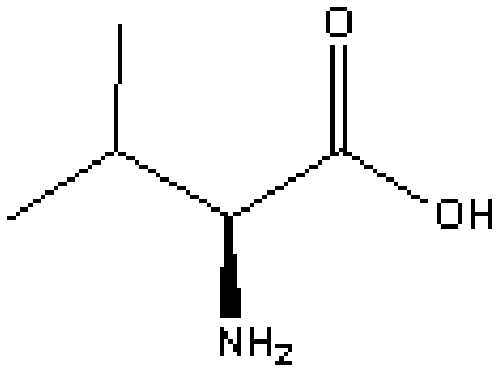

Valine

ABSQ	MaxNeg	MaxQp	Ovality	Surface	xpc4	xv1	xvpc4	nxp5	nxch6
2.1810	-0.3839	0.3404	1.3733	147.1524	1.8214	2.5378	0.6947	0.0000	0.0000
Iy	Py	Pz	P	Q	sumdeII	Wt	k1	k2	k3
334.4675	0.2137	0.1685	0.5063	0.0934	7.4700	65.0000	8.0000	3.1111	2.8125
LogP	SsCH3	SaaCH	SdssC	SdO	Gmax	Hmin	Gmin	idcbar	fw
-1.6909	3.5531	0.0000	-0.9306	10.0157	10.0157	0.4723	-0.9306	1.9438	117.1478
numHBa	Qs	Qsv							
3.0000	1.3961	0.6544							

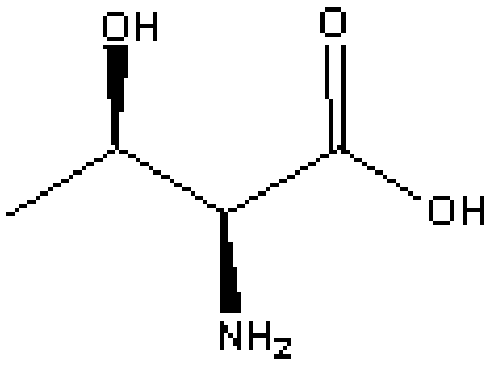

Threonine

ABSQ	MaxNeg	MaxQp	Ovality	Surface	xpc4	xv1	xvpc4	nxp5	nxch6
2.4695	-0.3804	0.3381	1.3550	139.1301	1.8214	2.2186	0.4430	0.0000	0.0000
Iy	Py	Pz	P	Q	sumdeII	Wt	k1	k2	k3
330.7648	0.0731	0.2824	0.4321	0.5552	9.2889	65.0000	8.0000	3.1111	2.8125
LogP	SsCH3	SaaCH	SdssC	SdO	Gmax	Hmin	Gmin	idcbar	fw
-2.7039	1.3321	0.0000	-1.1806	9.8557	9.8557	0.5834	-1.1806	1.9438	119.1204
numHBa	Qs	Qsv							
4.0000	1.0413	0.4881							

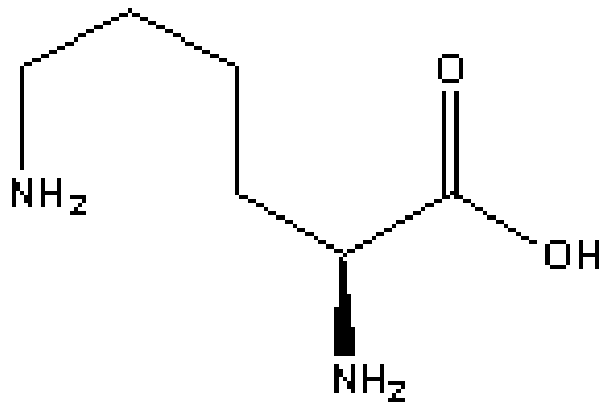

Lysine

ABSQ	MaxNeg	MaxQp	Ovality	Surface	xpc4	xv1	xvpc4	nxp5	nxch6
2.7808	-0.3300	0.2614	1.5190	198.2787	1.2071	3.3662	0.2518	5.0000	0.0000
Iy	Py	Pz	P	Q	sumdeII	Wt	k1	k2	k3
1187.2531	0.0914	0.5505	0.5782	1.1690	8.5844	143.0000	10.0000	5.7600	5.5309
LogP	SsCH3	SaaCH	SdssC	SdO	Gmax	Hmin	Gmin	idcbar	fw
-3.3935	0.0000	0.0000	-0.9333	10.1372	10.1372	0.5321	-0.9333	2.6608	146.1894
numHBa	Qs	Qsv							
4.0000	1.8519	0.6173							

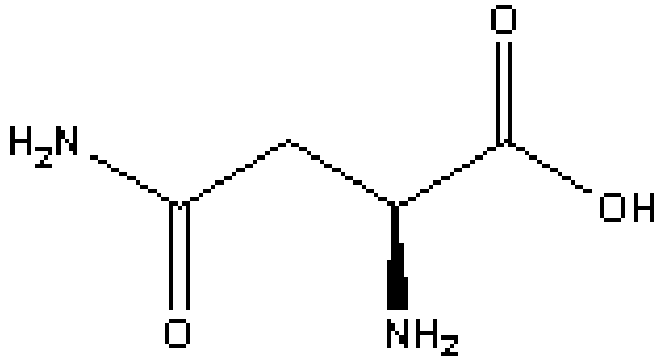

Asparagine

ABSQ	MaxNeg	MaxQp	Ovality	Surface	xpc4	xv1	xvpc4	nxp5	nxch6
3.3170	-0.4237	0.2621	1.4623	175.5508	1.4122	2.3043	0.2756	4.0000	0.0000
Iy	Py	Pz	P	Q	sumdeII	Wt	k1	k2	k3
551.9764	0.4996	0.0595	0.5835	1.5535	10.8249	96.0000	9.0000	3.9200	4.5000
LogP	SsCH3	SaaCH	SdssC	SdO	Gmax	Hmin	Gmin	idcbar	fw
-3.2338	0.0000	0.0000	-1.9179	19.8950	9.9931	0.8948	-1.2141	2.2608	132.1191
numHBa	Qs	Qsv							
5.0000	1.0755	0.4315							

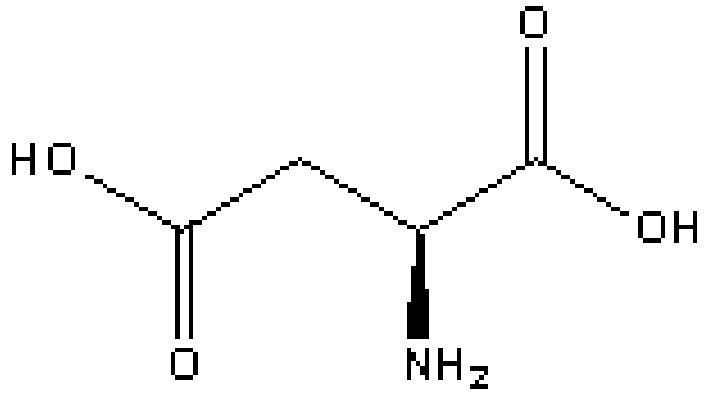

Aspartic Acid

ABSQ	MaxNeg	MaxQp	Ovality	Surface	xpc4	xv1	xvpc4	nxp5	nxch6
3.1448	-0.3271	0.2626	1.4108	158.6067	1.4122	2.2393	0.2647	4.0000	0.0000
Iy	**Py**	**Pz**	**P**	**Q**	**sumdeII**	**Wt**	**k1**	**k2**	**k3**
585.1631	0.1482	0.2765	0.3165	2.3017	11.4988	96.0000	9.0000	3.9200	4.5000
LogP	**SsCH3**	**SaaCH**	**SdssC**	**SdO**	**Gmax**	**Hmin**	**Gmin**	**idcbar**	**fw**
-2.5518	0.0000	0.0000	-2.4979	19.6173	9.8464	0.9503	-1.2941	2.2608	133.1039
numHBa	**Qs**	**Qsv**							
5.0000	0.9598	0.3851							

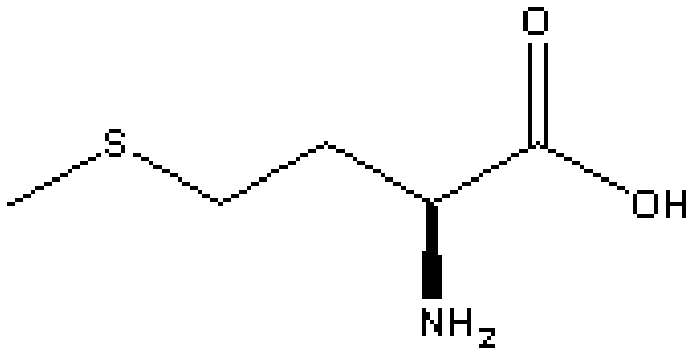

Methionine

ABSQ	MaxNeg	MaxQp	Ovality	Surface	xpc4	xv1	xvpc4	nxp5	nxch6
2.2816	-0.3254	0.2614	1.4852	185.9375	1.2071	3.7686	0.2518	4.0000	0.0000
Iy	**Py**	**Pz**	**P**	**Q**	**sumdeII**	**Wt**	**k1**	**k2**	**k3**
1008.2385	0.2751	0.5057	0.6133	1.7373	7.4537	102.0000	9.0000	4.8395	4.5000
LogP	**SsCH3**	**SaaCH**	**SdssC**	**SdO**	**Gmax**	**Hmin**	**Gmin**	**idcbar**	**fw**
-1.5630	1.9252	0.0000	-0.9129	10.0709	10.0709	0.4899	-0.9129	2.4438	149.2138
numHBa	**Qs**	**Qsv**							
4.0000	1.7062	0.6495							

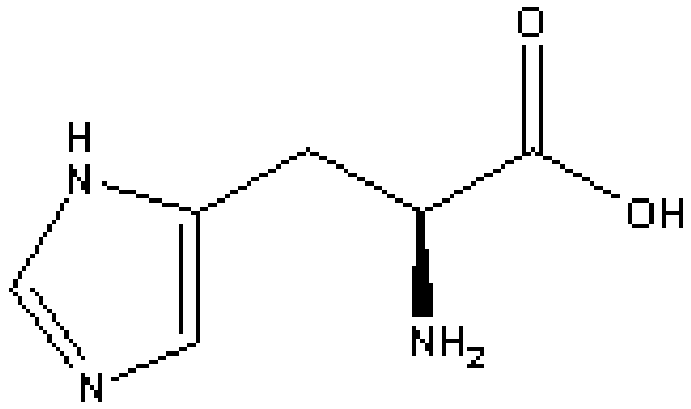

Histidine

ABSQ	MaxNeg	MaxQp	Ovality	Surface	xpc4	xv1	xvpc4	nxp5	nxch6
2.9463	-0.3254	0.2619	1.4658	192.9965	1.5830	3.1553	0.3909	12.0000	0.0000
Iy	**Py**	**Pz**	**P**	**Q**	**sumdeII**	**Wt**	**k1**	**k2**	**k3**
921.0010	0.2561	0.0406	0.3223	4.2728	9.3994	352.0000	9.0909	4.1327	2.8444
LogP	**SsCH3**	**SaaCH**	**SdssC**	**SdO**	**Gmax**	**Hmin**	**Gmin**	**idcbar**	**fw**
-2.4299	0.0000	3.0483	-1.0004	10.2662	10.2662	0.8712	-1.0004	2.4982	155.1564
numHBa	**Qs**	**Qsv**							
4.0000	1.9843	0.5330							

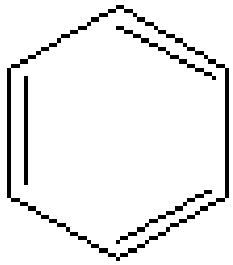

Benzene

ABSQ	MaxNeg	MaxQp	Ovality	Surface	xpc4	xv1	xvpc4	nxp5	nxch6
1.2254	-0.1025	0.1021	1.2646	133.7207	0.0000	2.0000	0.0000	6.0000	1.0000
Iy	Py	Pz	P	Q	sumdeII	Wt	k1	k2	k3
88.4166	0.0000	0.0000	0.0000	1.3002	0.0000	90.0000	4.1667	2.2222	1.3333
LogP	SsCH3	SaaCH	SdssC	SdO	Gmax	Hmin	Gmin	idcbar	fw
1.9516	0.0000	12.0000	0.0000	0.0000	2.0000	1.0531	2.0000	1.5219	78.1136
numHBa	Qs	Qsv							
0.0000	2.2500	0.9375							

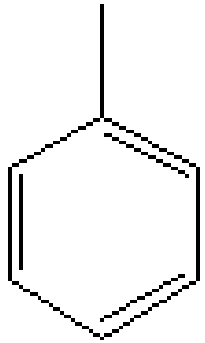

Toluene

ABSQ	MaxNeg	MaxQp	Ovality	Surface	xpc4	xv1	xvpc4	nxp5	nxch6
1.3028	-0.1090	0.1052	1.3300	154.5761	0.4082	2.4107	0.1925	8.0000	1.0000
Iy	Py	Pz	P	Q	sumdeII	Wt	k1	k2	k3
197.2618	0.0017	0.0000	0.0529	1.4244	0.3449	131.0000	5.1429	2.3438	1.5000
LogP	SsCH3	SaaCH	SdssC	SdO	Gmax	Hmin	Gmin	idcbar	fw
2.6571	2.0833	10.2616	0.0000	0.0000	2.0833	0.4868	1.3218	1.7608	92.1405
numHBa	Qs	Qsv							
0.0000	2.8421	1.1117							

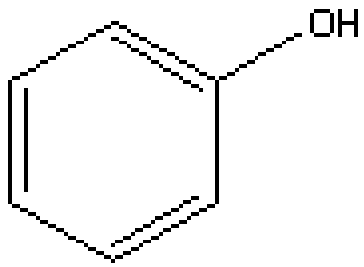

Phenol

ABSQ	MaxNeg	MaxQp	Ovality	Surface	xpc4	xv1	xvpc4	nxp5	nxch6
1.6683	-0.2276	0.1962	1.3246	149.2555	0.4082	2.1343	0.0861	8.0000	1.0000
Iy	**Py**	**Pz**	**P**	**Q**	**sumdeII**	**Wt**	**k1**	**k2**	**k3**
191.5561	0.0921	0.0000	0.1106	2.5196	2.8938	131.0000	5.1429	2.3438	1.5000
LogP	**SsCH3**	**SaaCH**	**SdssC**	**SdO**	**Gmax**	**Hmin**	**Gmin**	**idcbar**	**fw**
1.2356	0.0000	8.7127	0.0000	0.0000	8.6322	1.1011	0.3218	1.7608	94.1130
numHBa	**Qs**	**Qsv**							
1.0000	1.7008	0.6653							

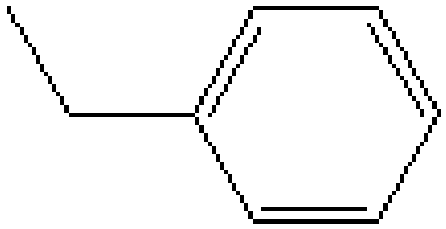

Ethylbenzene

ABSQ	MaxNeg	MaxQp	Ovality	Surface	xpc4	xv1	xvpc4	nxp5	nxch6
1.5028	-0.1117	0.1095	1.4038	176.7742	0.4928	2.9713	0.2539	10.0000	1.0000
Iy	Py	Pz	P	Q	sumdeII	Wt	k1	k2	k3
339.1219	0.0082	0.0000	0.0719	1.7560	0.6589	184.0000	6.1250	3.1111	1.8000
LogP	SsCH3	SaaCH	SdssC	SdO	Gmax	Hmin	Gmin	idcbar	fw
3.1435	2.1620	10.4552	0.0000	0.0000	2.1620	0.4047	1.1397	2.0597	106.1674
numHBa	Qs	Qsv							
0.0000	3.4315	1.1617							

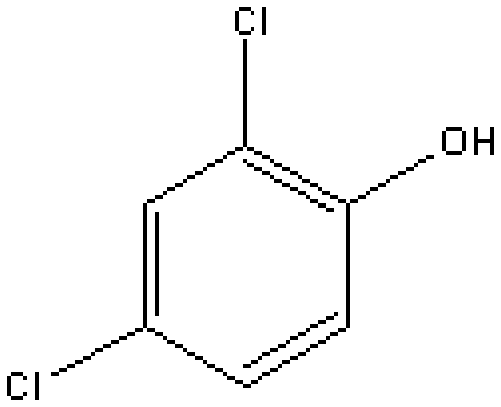

4,6 Dichlorophenol

ABSQ	MaxNeg	MaxQp	Ovality	Surface	xpc4	xv1	xvpc4	nxp5	nxch6
1.6713	-0.2176	0.2041	1.3835	183.1283	1.4783	3.0955	0.6008	14.0000	1.0000
Iy	Py	Pz	P	Q	sumdeII	Wt	k1	k2	k3
675.1678	0.0302	0.0000	0.0327	2.6672	6.3046	243.0000	7.1111	2.7222	1.7041
LogP	SsCH3	SaaCH	SdssC	SdO	Gmax	Hmin	Gmin	idcbar	fw
2.8589	0.0000	4.5058	0.0000	0.0000	8.8531	1.2591	0.0565	2.0375	163.0032
numHBa	Qs	Qsv							
3.0000	1.8462	0.6268							

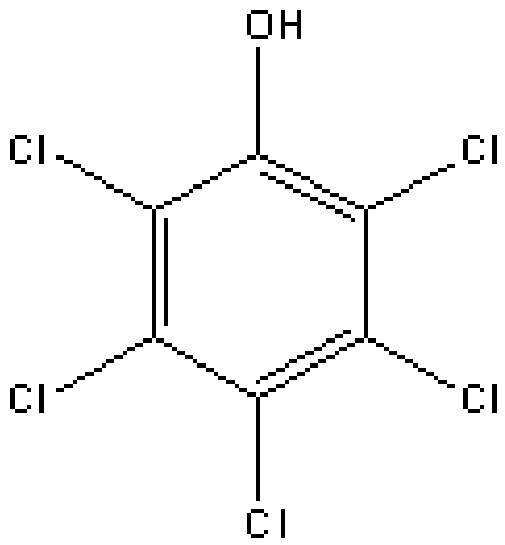

2,3,4,5,6 Pentachlorophenol

ABSQ	MaxNeg	MaxQp	Ovality	Surface	xpc4	xv1	xvpc4	nxp5	nxch6
1.9400	-0.2120	0.2078	1.4810	230.9885	3.6427	4.5583	2.3038	24.0000	1.0000
Iy	**Py**	**Pz**	**P**	**Q**	**sumdeII**	**Wt**	**k1**	**k2**	**k3**
1081.9465	0.0544	0.0000	0.0830	4.4959	10.9893	486.0000	10.0833	3.3951	1.5625
LogP	**SsCH3**	**SaaCH**	**SdssC**	**SdO**	**Gmax**	**Hmin**	**Gmin**	**idcbar**	**fw**
4.9449	0.0000	0.0000	0.0000	0.0000	9.2010	2.6885	-0.3632	2.1339	266.3383
numHBa	**Qs**	**Qsv**							
6.0000	2.1552	0.5987							

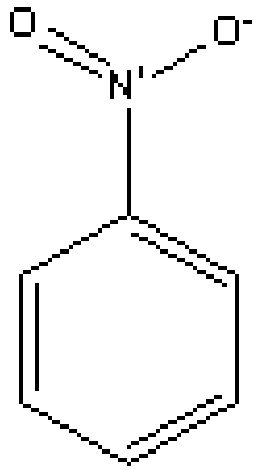

Nitrobenzene

ABSQ	MaxNeg	MaxQp	Ovality	Surface	xpc4	xv1	xvpc4	nxp5	nxch6
2.7005	-0.4222	0.5951	1.4377	183.7826	1.0404	2.5169	0.1970	12.0000	1.0000
ly	Py	Pz	P	Q	sumdell	Wt	k1	k2	k3
437.7393	0.0286	0.0000	0.5942	1.1659	5.8751	239.0000	7.1111	3.2397	2.0000
LogP	SsCH3	SaaCH	SdssC	SdO	Gmax	Hmin	Gmin	idcbar	fw
1.4691	0.0000	8.1666	0.0000	10.1176	10.1176	1.1547	-0.1667	2.1499	124.1191
numHBa	Qs	Qsv							
3.0000	1.6137	0.5146							

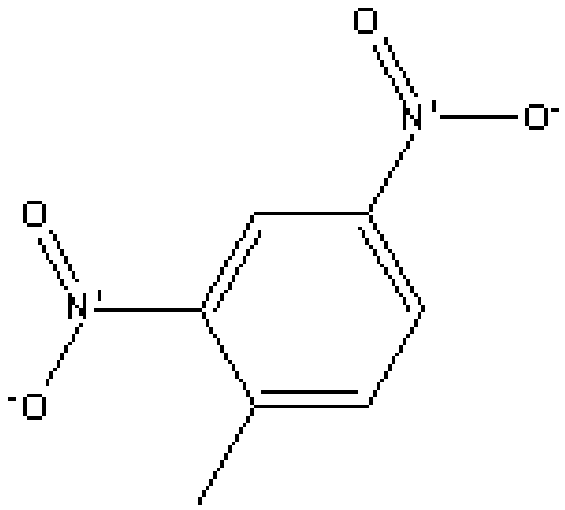

2,4 Dinitrotoluene

ABSQ	MaxNeg	MaxQp	Ovality	Surface	xpc4	xv1	xvpc4	nxp5	nxch6
5.0709	-0.5651	0.7838	1.5199	231.2349	2.4994	3.4504	0.6557	26.0000	1.0000
ly	**Py**	**Pz**	**P**	**Q**	**sumdeII**	**Wt**	**k1**	**k2**	**k3**
1000.4230	0.0792	0.0493	0.1519	0.7408	13.1531	611.0000	11.0769	4.4815	2.7211
LogP	**SsCH3**	**SaaCH**	**SdssC**	**SdO**	**Gmax**	**Hmin**	**Gmin**	**idcbar**	**fw**
1.5672	1.5900	3.8448	0.0000	20.9126	10.5111	0.7100	-0.3825	2.4961	184.1515
numHBa	**Qs**	**Qsv**							
6.0000	1.9346	0.4674							

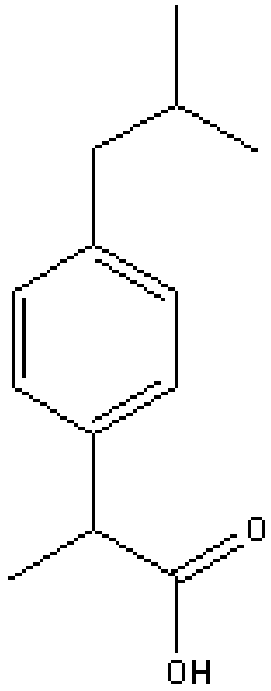

Ibuprofen

ABSQ	MaxNeg	MaxQp	Ovality	Surface	xpc4	xv1	xvpc4	nxp5	nxch6
3.4563	-0.3994	0.3780	1.4646	231.4523	2.3237	5.3203	1.0329	26.0000	1.0000
Iy	Py	Pz	P	Q	sumdeII	Wt	k1	k2	k3
1910.8380	0.4130	0.1644	0.5162	1.4364	8.9442	905.0000	13.0667	5.9150	4.1653
LogP	SsCH3	SaaCH	SdssC	SdO	Gmax	Hmin	Gmin	idcbar	fw
3.7567	6.0569	7.8716	-0.7717	10.7624	10.7624	0.4304	-0.7717	2.9862	206.2847
numHBa	Qs	Qsv							
2.0000	4.1570	0.8468							

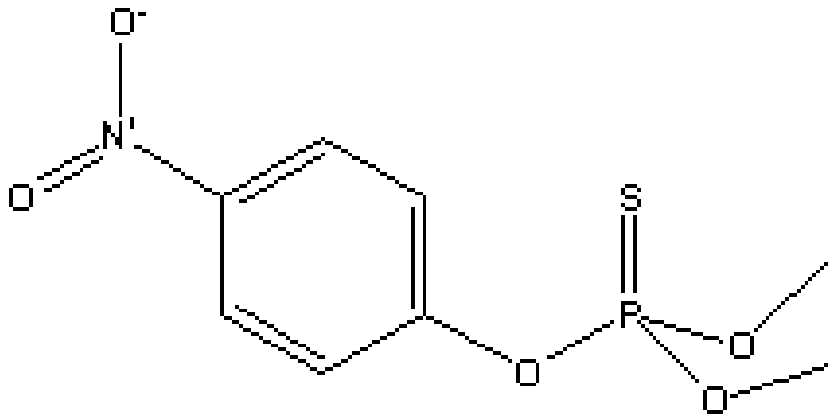

Methyl Parathion

ABSQ	MaxNeg	MaxQp	Ovality	Surface	xpc4	xv1	xvpc4	nxp5	nxch6
7.8037	-0.6714	1.8239	1.6067	273.6969	3.1755	6.7345	1.9643	28.0000	1.0000
Iy	Py	Pz	P	Q	sumdeII	Wt	k1	k2	k3
2651.7883	0.1304	0.5221	0.6457	9.9741	13.9112	1029.0000	14.0625	6.0744	4.0768
LogP	SsCH3	SaaCH	SdssC	SdO	Gmax	Hmin	Gmin	idcbar	fw
2.2530	2.7892	5.7279	0.0000	10.5226	10.5226	0.8433	-2.7628	3.0079	264.2188
numHBa	Qs	Qsv							
7.0000	3.2115	0.6142							

4 - Nonylphenol

ABSQ	MaxNeg	MaxQp	Ovality	Surface	xpc4	xv1	xvpc4	nxp5	nxch6
3.3373	-0.2271	0.1956	1.7495	337.1841	0.8413	6.6056	0.3055	23.0000	1.0000
Iy	**Py**	**Pz**	**P**	**Q**	**sumdeII**	**Wt**	**k1**	**k2**	**k3**
5120.7363	0.0529	0.0000	0.1665	3.2246	4.5156	1178.0000	14.0625	9.0741	7.0582
LogP	**SsCH3**	**SaaCH**	**SdssC**	**SdO**	**Gmax**	**Hmin**	**Gmin**	**idcbar**	**fw**
6.0608	2.2548	7.5893	0.0000	0.0000	9.1487	0.3349	0.3642	3.4482	220.3549
numHBa	**Qs**	**Qsv**							
1.0000	6.4319	1.0887							

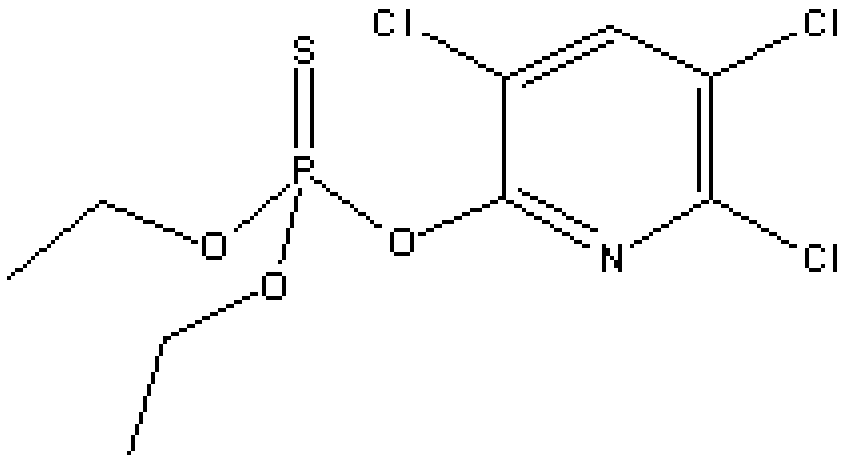

Clorpyrifos

ABSQ	MaxNeg	MaxQp	Ovality	Surface	xpc4	xv1	xvpc4	nxp5	nxch6
6.4551	-0.6716	1.8678	1.6867	298.2288	3.3582	8.7074	2.2281	38.0000	1.0000
Iy	**Py**	**Pz**	**P**	**Q**	**sumdeII**	**Wt**	**k1**	**k2**	**k3**
2999.8074	0.7388	0.0000	0.7394	1.5261	14.9426	1335.0000	16.0556	6.9632	4.5660
LogP	**SsCH3**	**SaaCH**	**SdssC**	**SdO**	**Gmax**	**Hmin**	**Gmin**	**idcbar**	**fw**
4.7570	3.5701	1.4220	0.0000	0.0000	5.9377	0.6322	-2.9185	2.9677	350.5900
numHBa	**Qs**	**Qsv**							
8.0000	4.4586	0.7655							

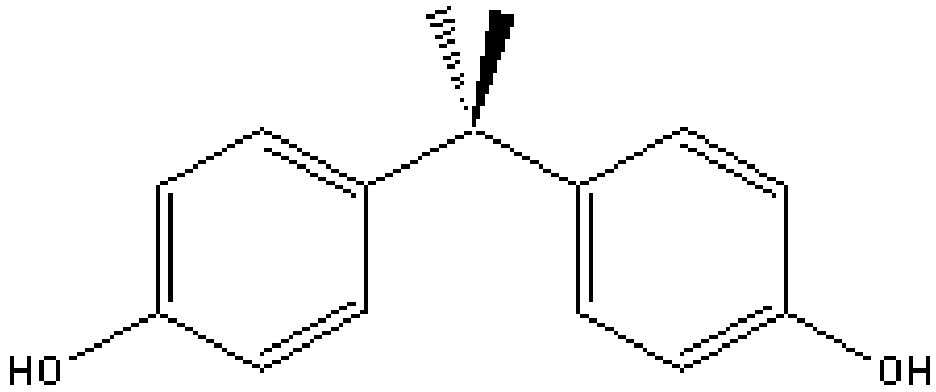

Bisphenol A

ABSQ	MaxNeg	MaxQp	Ovality	Surface	xpc4	xv1	xvpc4	nxp5	nxch6
3.7346	-0.2257	0.1963	1.5936	296.2599	3.7281	5.5899	1.9360	44.0000	2.0000
Iy	Py	Pz	P	Q	sumdeII	Wt	k1	k2	k3
2245.0769	0.1135	0.0000	0.1298	1.6861	9.0630	1950.0000	13.4321	5.3254	3.0625
LogP	SsCH3	SaaCH	SdssC	SdO	Gmax	Hmin	Gmin	idcbar	fw
3.6500	4.2337	14.4432	0.0000	0.0000	9.2963	0.6307	-0.1514	2.9637	228.2908
numHBa	Qs	Qsv							
2.0000	4.8217	0.8029							

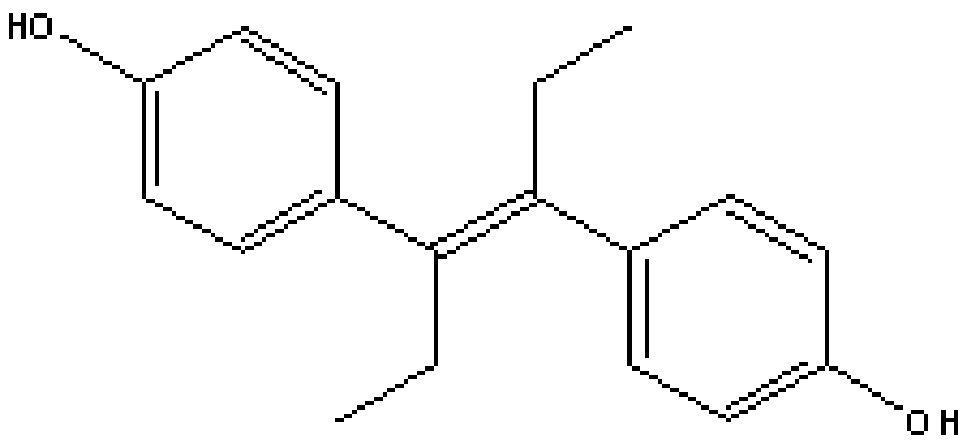

Diethylstilbestrol

ABSQ	MaxNeg	MaxQp	Ovality	Surface	xpc4	xv1	xvpc4	nxp5	nxch6
4.1083	-0.2197	0.1958	1.7229	378.1116	2.7227	6.9613	1.1601	53.0000	2.0000
Iy	**Py**	**Pz**	**P**	**Q**	**sumdeII**	**Wt**	**k1**	**k2**	**k3**
3323.4529	0.1687	0.0000	0.1801	3.0729	9.3131	2638.0000	16.3719	7.8520	4.2500
LogP	**SsCH3**	**SaaCH**	**SdssC**	**SdO**	**Gmax**	**Hmin**	**Gmin**	**idcbar**	**fw**
3.9051	4.2743	14.6640	2.5522	0.0000	9.4107	0.5420	0.2842	3.1174	268.3556
numHBa	**Qs**	**Qsv**							
2.0000	6.1235	0.8420							

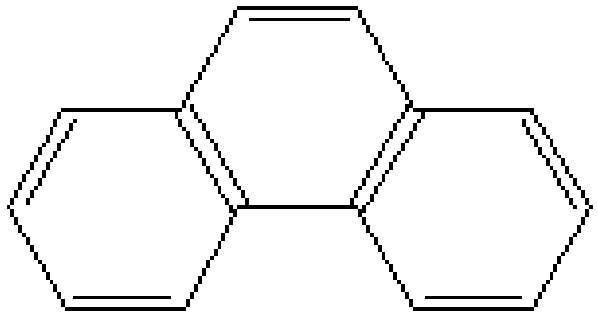

Phenanthrene

ABSQ	MaxNeg	MaxQp	Ovality	Surface	xpc4	xv1	xvpc4	nxp5	nxch6
2.1113	-0.1014	0.1108	1.4586	251.9400	1.8265	4.8154	0.7775	55.0000	3.0000
Iy	**Py**	**Pz**	**P**	**Q**	**sumdeII**	**Wt**	**k1**	**k2**	**k3**
903.6428	0.0095	0.0000	0.0095	3.6724	1.3670	3511.0000	9.2422	3.8678	1.6483
LogP	**SsCH3**	**SaaCH**	**SdssC**	**SdO**	**Gmax**	**Hmin**	**Gmin**	**idcbar**	**fw**
4.6080	0.0000	21.3670	0.0000	0.0000	2.1782	1.1676	1.3113	2.4920	178.2334
numHBa	**Qs**	**Qsv**							
0.0000	5.6044	0.9055							

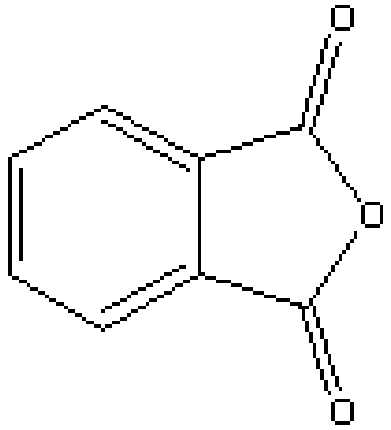

Phthalic Anhydride

ABSQ	MaxNeg	MaxQp	Ovality	Surface	xpc4	xv1	xvpc4	nxp5	nxch6
2.6157	-0.2819	0.4169	1.3867	186.6669	1.8843	3.1438	0.4881	31.0000	1.0000
Iy	Py	Pz	P	Q	sumdeII	Wt	k1	k2	k3
440.7403	0.0001	0.0000	1.0915	0.0243	9.8379	874.0000	7.6389	2.8028	1.2098
LogP	SsCH3	SaaCH	SdssC	SdO	Gmax	Hmin	Gmin	idcbar	fw
1.3456	0.0000	6.5303	-1.1007	21.6657	10.8329	1.2455	-0.5504	2.1152	148.1180
numHBa	Qs	Qsv							
3.0000	1.9685	0.4745							

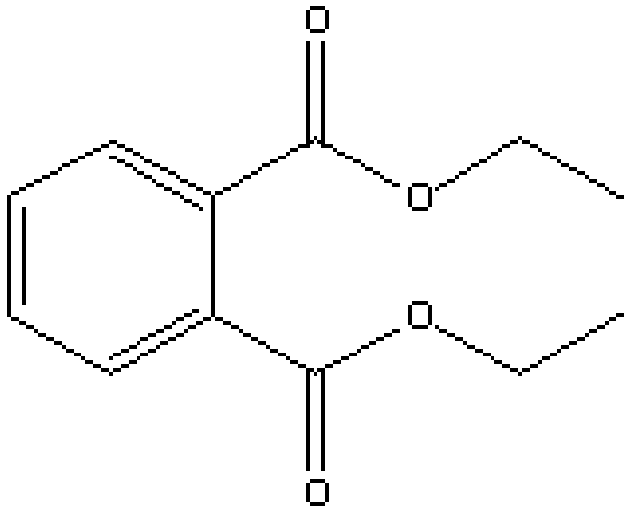

Diethylphthalate

ABSQ	MaxNeg	MaxQp	Ovality	Surface	xpc4	xv1	xvpc4	nxp5	nxch6
3.8160	-0.4001	0.4072	1.6739	304.4620	1.9455	5.1354	0.5054	32.0000	1.0000
Iy	Py	Pz	P	Q	sumdell	Wt	k1	k2	k3
1063.6456	0.3112	0.0000	0.6795	4.6372	13.8608	1084.0000	14.0625	7.3500	4.0768
LogP	SsCH3	SaaCH	SdssC	SdO	Gmax	Hmin	Gmin	idcbar	fw
2.6343	3.4263	6.4429	-1.0164	23.0884	11.5442	0.5929	-0.5082	2.8537	222.2408
numHBa	Qs	Qsv							
4.0000	3.5625	0.6494							

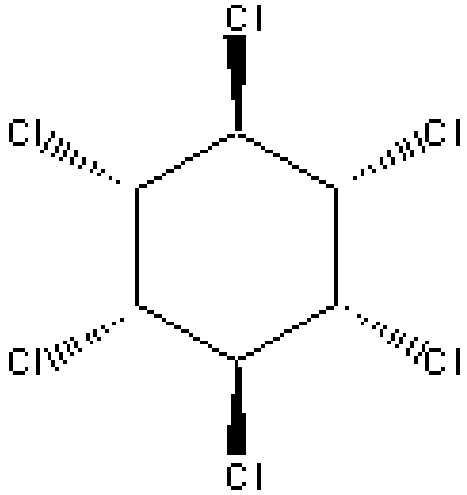

Lindane

ABSQ	MaxNeg	MaxQp	Ovality	Surface	xpc4	xv1	xvpc4	nxp5	nxch6
1.3832	-0.1215	0.1260	1.3847	188.1796	3.6427	5.9279	4.4811	24.0000	1.0000
Iy	Py	Pz	P	Q	sumdeII	Wt	k1	k2	k3
1161.5708	0.1611	0.0920	0.1855	0.1916	10.6204	486.0000	10.0833	3.3951	1.5625
LogP	SsCH3	SaaCH	SdssC	SdO	Gmax	Hmin	Gmin	idcbar	fw
3.5566	0.0000	0.0000	0.0000	0.0000	5.8812	0.9092	-0.4367	2.1339	290.8316
numHBa	Qs	Qsv							
6.0000	2.6989	0.7497							

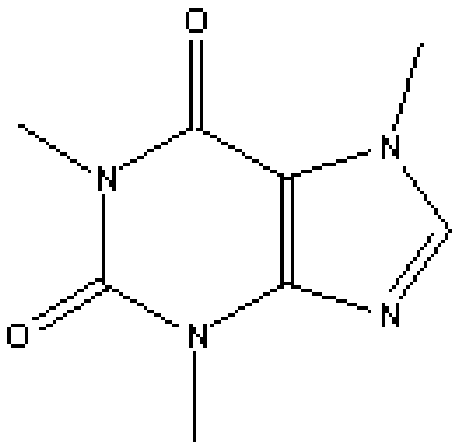

Caffeine

ABSQ	MaxNeg	MaxQp	Ovality	Surface	xpc4	xv1	xvpc4	nxp5	nxch6
3.7109	-0.4136	0.3720	1.5417	247.7542	3.7053	4.1079	1.1570	47.0000	1.0000
Iy	**Py**	**Pz**	**P**	**Q**	**sumdeII**	**Wt**	**k1**	**k2**	**k3**
737.9059	0.1687	0.0906	0.7400	0.4252	11.5069	1538.0000	10.5156	3.5388	1.4545
LogP	**SsCH3**	**SaaCH**	**SdssC**	**SdO**	**Gmax**	**Hmin**	**Gmin**	**idcbar**	**fw**
-0.5099	4.7732	1.5194	-0.6766	23.1613	11.6720	0.7578	-0.3600	2.2940	194.1930
numHBa	**Qs**	**Qsv**							
5.0000	3.0853	0.6559							

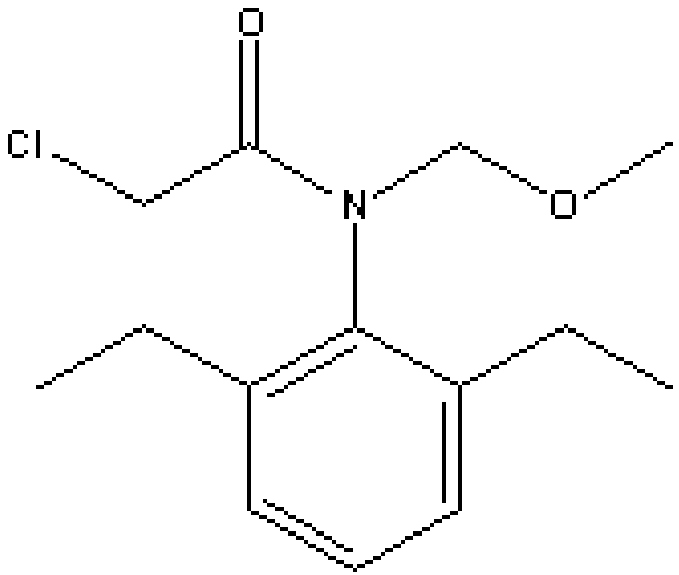

2-chloro-2'-6'-diethyl-N-methoxymethyl-acetanilide (Alachlor)

ABSQ	MaxNeg	MaxQp	Ovality	Surface	xpc4	xv1	xvpc4	nxp5	nxch6
3.2615	-0.2860	0.2630	1.5516	291.5823	2.4350	6.6852	1.0770	45.0000	1.0000
Iy	Py	Pz	P	Q	sumdell	Wt	k1	k2	k3
1733.9794	0.0377	0.4024	0.4135	1.2547	10.5848	1348.0000	16.0556	8.2268	3.9958
LogP	SsCH3	SaaCH	SdssC	SdO	Gmax	Hmin	Gmin	idcbar	fw
2.9333	5.7337	6.1058	-0.1304	11.9527	11.9527	0.5353	-0.1304	2.6952	269.7713
numHBa	Qs	Qsv							
4.0000	5.4512	0.8973							

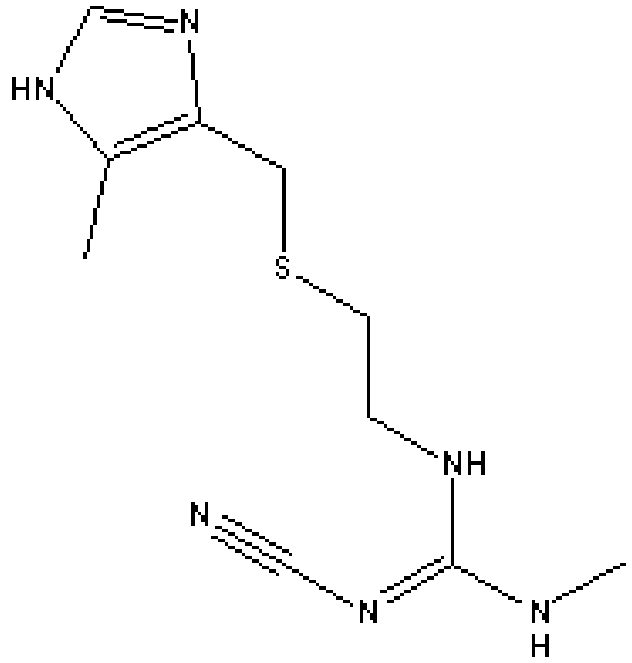

Cimetidine

ABSQ	MaxNeg	MaxQp	Ovality	Surface	xpc4	xv1	xvpc4	nxp5	nxch6
3.0799	-0.2586	0.3129	1.7141	314.0870	1.5130	6.1484	0.5879	19.0000	0.0000
Iy	Py	Pz	P	Q	sumdeII	Wt	k1	k2	k3
4073.7322	0.4029	0.1934	0.7591	10.2766	7.4392	1226	15.0588	9	5.9282
LogP	SsCH3	SaaCH	SdssC	SdO	Gmax	Hmin	Gmin	idcbar	fw
0.646	3.7393	1.7105	0.5038	0	8.3916	0.6245	0.5038	3.3449	252.3432
numHBa	Qs	Qsv							
6	4.9502	0.8136							

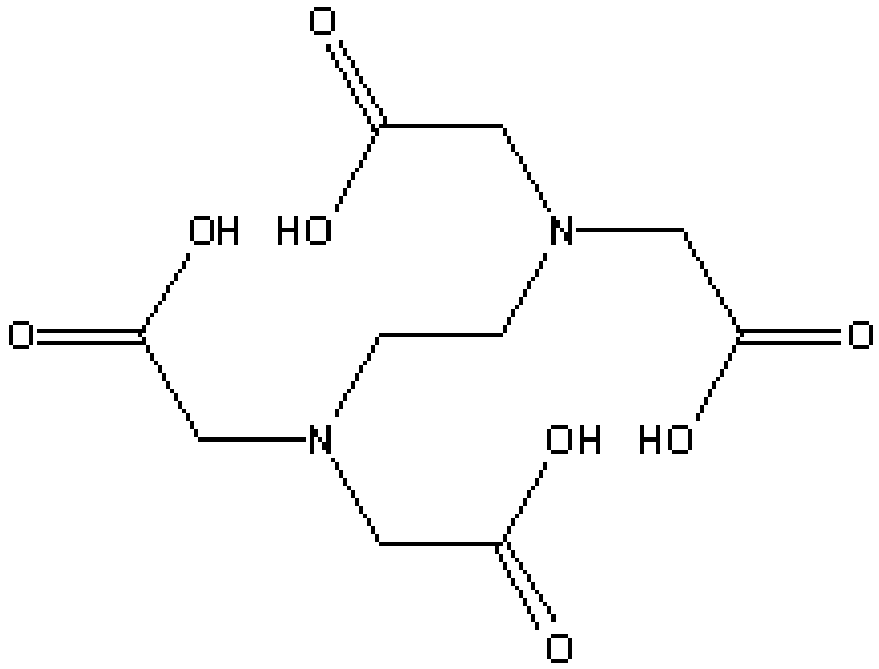

Ethylenediaminetetraacetic Acid

ABSQ	MaxNeg	MaxQp	Ovality	Surface	xpc4	xv1	xvpc4	nxp5	nxch6
6.6799	-0.3979	0.3655	1.6594	317.7363	1.7029	5.2398	0.5227	24.0000	0.0000
Iy	Py	Pz	P	Q	sumdeII	Wt	k1	k2	k3
3381.7441	0.0017	0.7572	0.7572	9.8344	26.5053	910.0000	20.0000	10.6875	12.4898
LogP	SsCH3	SaaCH	SdssC	SdO	Gmax	Hmin	Gmin	idcbar	fw
-2.9415	0.0000	0.0000	-5.1151	42.0844	10.5211	1.1567	-1.2788	3.1503	290.2298
numHBa	Qs	Qsv							
10.0000	2.4998	0.4062							

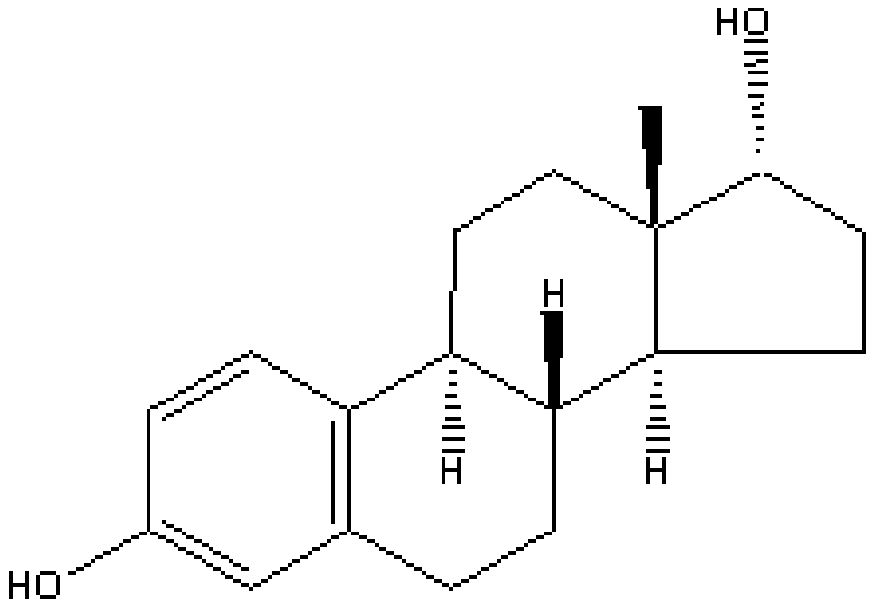

17 a Estradiol

ABSQ	MaxNeg	MaxQp	Ovality	Surface	xpc4	xv1	xvpc4	nxp5	nxch6
3.8151	-0.3052	0.1949	1.4357	226.2367	3.5726	7.7366	2.4643	90.0000	3.0000
Iy	Py	Pz	P	Q	sumdell	Wt	k1	k2	k3
2622.6062	0.1989	0.1080	0.3222	3.0584	10.0301	13763.0000	12.7190	4.7769	2.0000
LogP	SsCH3	SaaCH	SdssC	SdO	Gmax	Hmin	Gmin	idcbar	fw
3.4696	0.0000	5.9495	0.0000	0.0000	10.1132	0.5784	-0.0350	2.9420	258.3605
numHBa	Qs	Qsv							
2.0000	6.8009	0.8635							

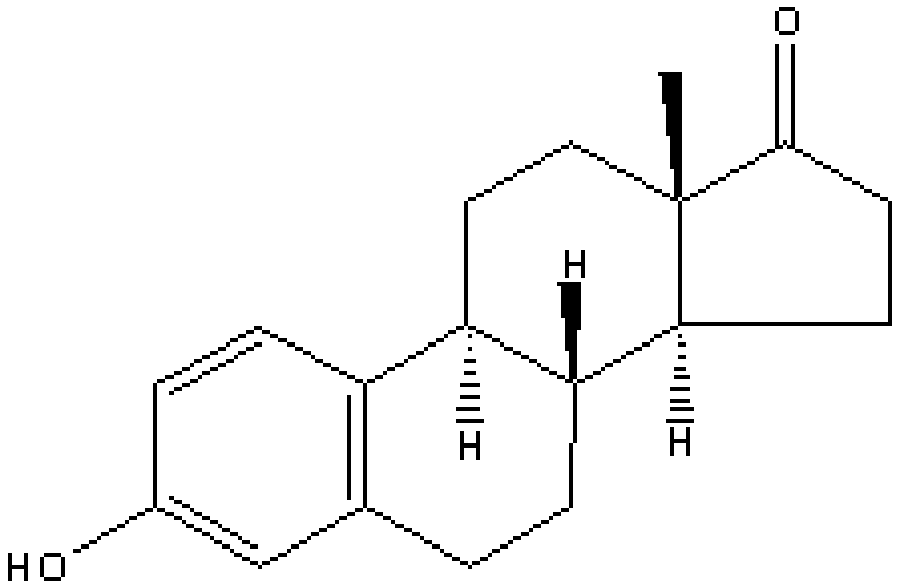

Estrone

ABSQ	MaxNeg	MaxQp	Ovality	Surface	xpc4	xv1	xvpc4	nxp5	nxch6
4.1119	-0.3024	0.2905	1.5212	292.9848	5.0919	7.9452	3.4729	97.0000	3.0000
ly	**Py**	**Pz**	**P**	**Q**	**sumdeII**	**Wt**	**k1**	**k2**	**k3**
2765.3069	0.4227	0.0913	0.4833	1.2049	12.0300	15139.0000	13.6484	4.7500	1.9608
LogP	**SsCH3**	**SaaCH**	**SdssC**	**SdO**	**Gmax**	**Hmin**	**Gmin**	**idcbar**	**fw**
3.6617	2.2178	5.8977	0.5115	12.2620	12.2620	0.5691	-0.0322	2.9579	270.3715
numHBa	**Qs**	**Qsv**							
2.0000	6.8488	0.8668							

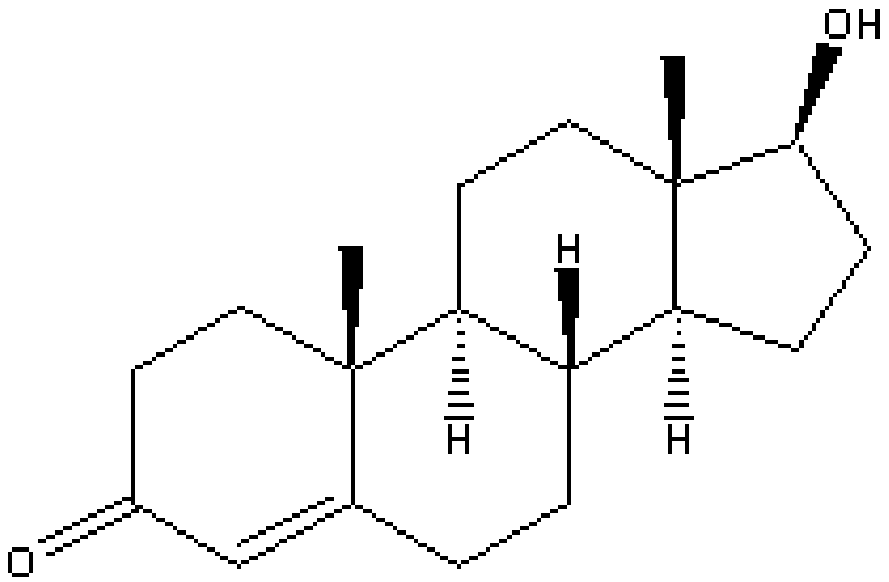

Testosterone

ABSQ	MaxNeg	MaxQp	Ovality	Surface	xpc4	xv1	xvpc4	nxp5	nxch6
4.1977	-0.3194	0.3163	1.4550	185.2442	3.5726	8.1516	2.7452	90.0000	3.0000
Iy	Py	Pz	P	Q	sumdeII	Wt	k1	k2	k3
2680.8655	0.0469	0.0522	0.6833	1.2642	10.4973	13763.0000	12.7190	4.7769	2.0000
LogP	SsCH3	SaaCH	SdssC	SdO	Gmax	Hmin	Gmin	idcbar	fw
2.6015	0.0000	0.0000	1.8233	11.5941	11.5941	0.5594	-0.0178	2.9420	260.3763
numHBa	Qs	Qsv							
2.0000	6.9197	0.8785							

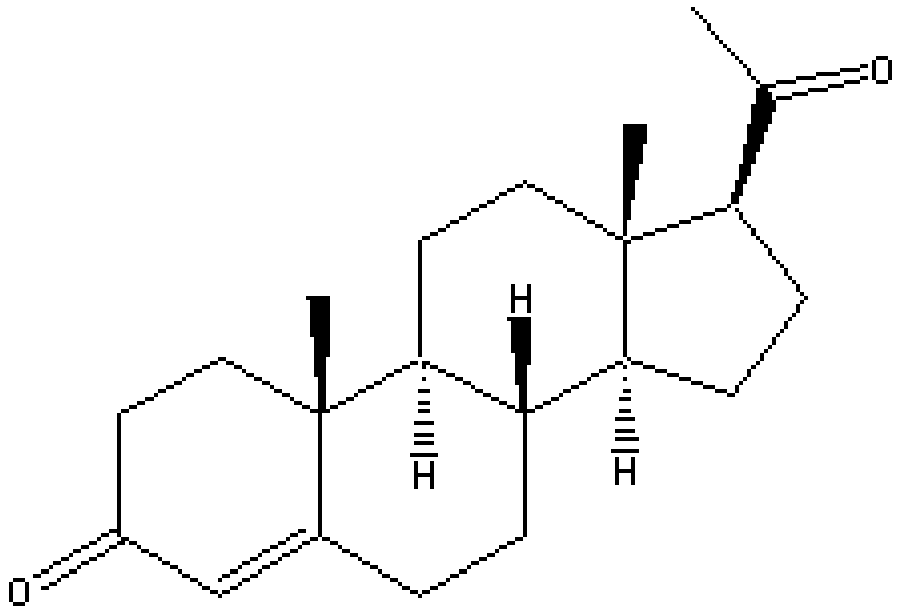

Progesterone

ABSQ	MaxNeg	MaxQp	Ovality	Surface	xpc4	xv1	xvpc4	nxp5	nxch6
4.7039	-0.3173	0.3155	1.5482	294.9027	4.0170	8.8862	3.0945	98.0000	3.0000
Iy	Py	Pz	P	Q	sumdeII	Wt	k1	k2	k3
3542.6272	0.1935	0.4017	0.5362	12.7234	11.9352	17841.0000	14.5833	5.5710	2.3965
LogP	SsCH3	SaaCH	SdssC	SdO	Gmax	Hmin	Gmin	idcbar	fw
2.7916	1.7992	0.0000	2.2487	23.5431	11.8785	0.5785	0.3527	3.1115	286.4142
numHBa	Qs	Qsv							
2.0000	7.5130	0.8944							

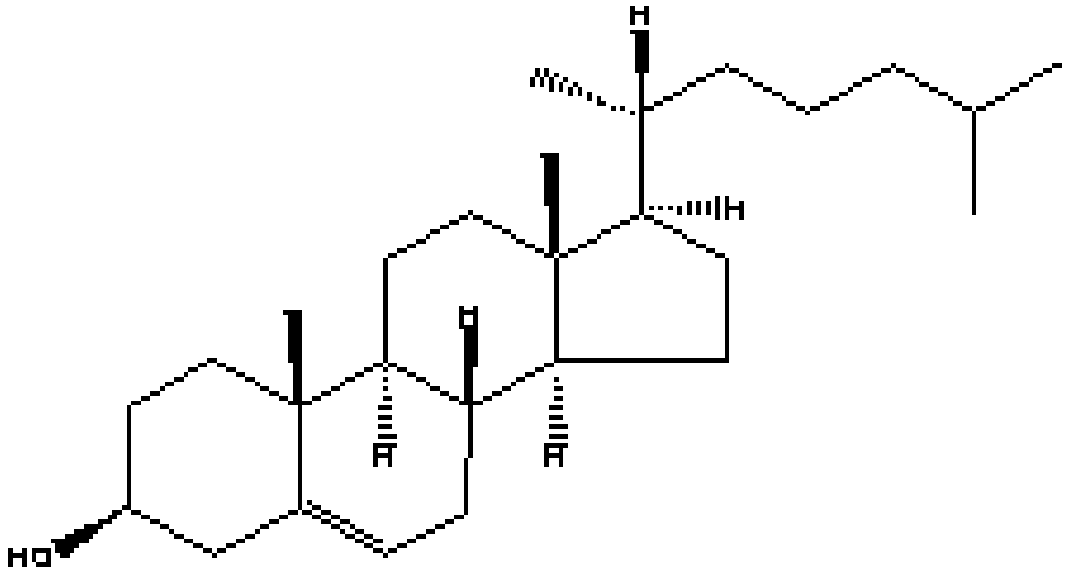

Cholesterol

ABSQ	MaxNeg	MaxQp	Ovality	Surface	xpc4	xv1	xvpc4	nxp5	nxch6
5.1725	-0.3091	0.1852	1.6324	366.9083	3.8018	11.7428	3.6830	102.0000	3.0000
Iy	Py	Pz	P	Q	sumdeII	Wt	k1	k2	k3
7507.9116	0.1026	0.0517	0.2109	0.7824	7.6142	28571.0000	18.3673	7.9350	3.8400
LogP	SsCH3	SaaCH	SdssC	SdO	Gmax	Hmin	Gmin	idcbar	fw
7.1009	4.7328	0.0000	1.6613	0.0000	10.0320	0.1403	-0.0351	3.5795	345.5889
numHBa	Qs	Qsv							
1.0000	13.2866	1.3287							

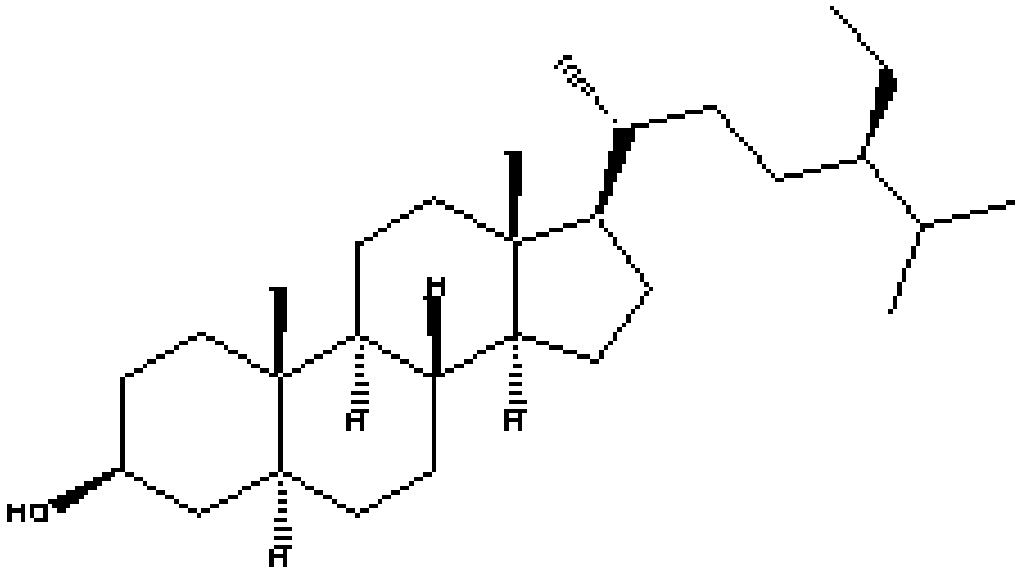

beta Sitostanol-n-hydrate

ABSQ	MaxNeg	MaxQp	Ovality	Surface	xpc4	xv1	xvpc4	nxp5	nxch6
5.5836	-0.3127	0.1859	1.6526	370.1698	4.6023	12.7606	4.3974	104.0000	3.0000
Iy	**Py**	**Pz**	**P**	**Q**	**sumdeII**	**Wt**	**k1**	**k2**	**k3**
7152.4863	0.0637	0.1380	0.2319	0.6953	6.8588	33956.0000	20.2800	8.7885	4.1600
LogP	**SsCH3**	**SaaCH**	**SdssC**	**SdO**	**Gmax**	**Hmin**	**Gmin**	**idcbar**	**fw**
7.5768	7.2236	0.0000	0.0000	0.0000	10.1025	0.3646	0.0211	3.6533	374.6506
numHBa	**Qs**	**Qsv**							
1.0000	14.8095	1.4051							

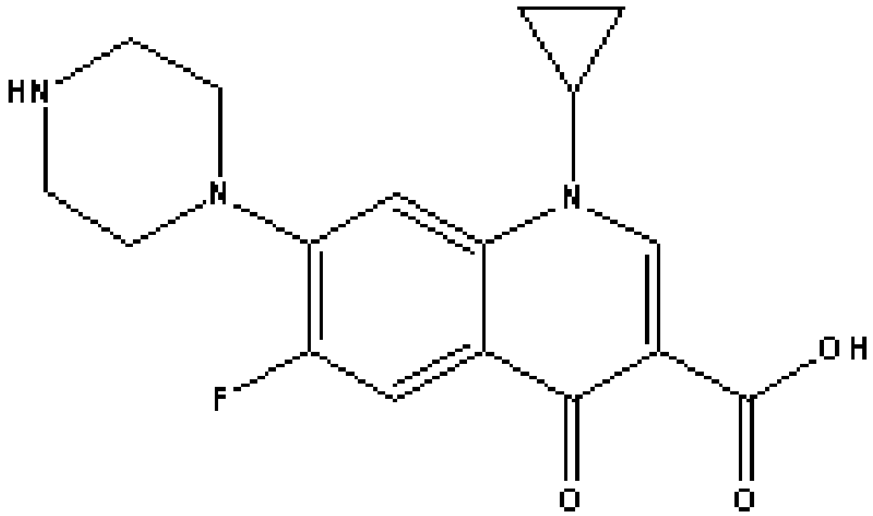

Ciprofloxacin

ABSQ	MaxNeg	MaxQp	Ovality	Surface	xpc4	xv1	xvpc4	nxp5	nxch6
5.6687	-0.3800	0.4588	1.5852	311.2392	4.4359	8.1339	1.5796	101.0000	3.0000
Iy	Py	Pz	P	Q	sumdeII	Wt	k1	k2	k3
3400.7456	1.2467	0.1828	1.4960	3.8252	23.6997	11660.0000	17.4156	6.9575	3.4856
LogP	SsCH3	SaaCH	SdssC	SdO	Gmax	Hmin	Gmin	idcbar	fw
-0.5653	0.0000	2.8906	-2.2021	23.7581	14.6077	0.6899	-1.2751	3.1701	331.3466
numHBa	Qs	Qsv							
7.0000	5.3576	0.5736							

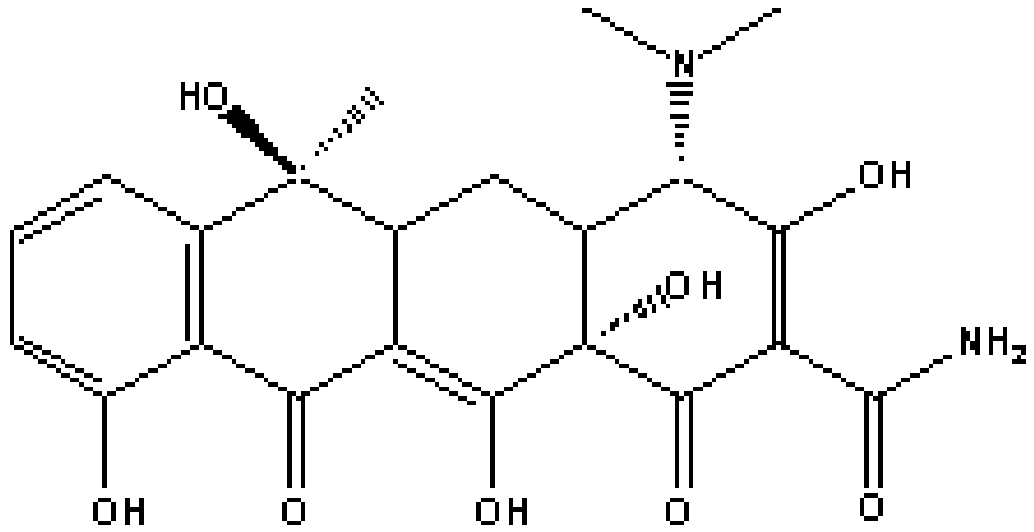

Tetracycline

ABSQ	MaxNeg	MaxQp	Ovality	Surface	xpc4	xv1	xvpc4	nxp5	nxch6
8.5480	-0.4552	0.4188	1.6843	399.9212	9.0664	9.5882	3.5123	168.0000	4.0000
Iy	Py	Pz	P	Q	sumdeII	Wt	k1	k2	k3
5550.8569	0.5439	0.1154	0.7765	7.7079	47.3737	42500	24.1349	8.3405	3.3333
LogP	SsCH3	SaaCH	SdssC	SdO	Gmax	Hmin	Gmin	idcbar	fw
-0.3782	3.0591	4.1574	-6.4174	38.1444	13.1715	0.8141	-2.7275	3.1951	430.4143
numHBa	Qs	Qsv							
10	5.6223	0.5351							

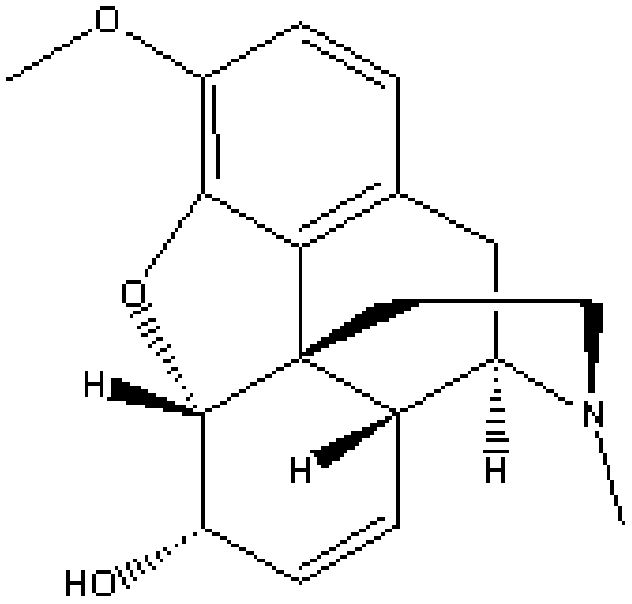

Codeine

ABSQ	MaxNeg	MaxQp	Ovality	Surface	xpc4	xv1	xvpc4	nxp5	nxch6
3.7291	-0.2989	0.1963	1.4480	243.4733	5.5732	8.1021	3.3159	162.0000	4.0000
Iy	**Py**	**Pz**	**P**	**Q**	**sumdeII**	**Wt**	**k1**	**k2**	**k3**
1856.4359	0.1326	0.0280	0.4259	1.9912	13.6669	40612.0000	14.3521	4.7619	1.6436
LogP	**SsCH3**	**SaaCH**	**SdssC**	**SdO**	**Gmax**	**Hmin**	**Gmin**	**idcbar**	**fw**
1.5614	3.9071	4.2046	0.0000	0.0000	10.5542	0.6335	-0.5386	2.7299	299.3696
numHBa	**Qs**	**Qsv**							
4.0000	7.9154	0.8824							

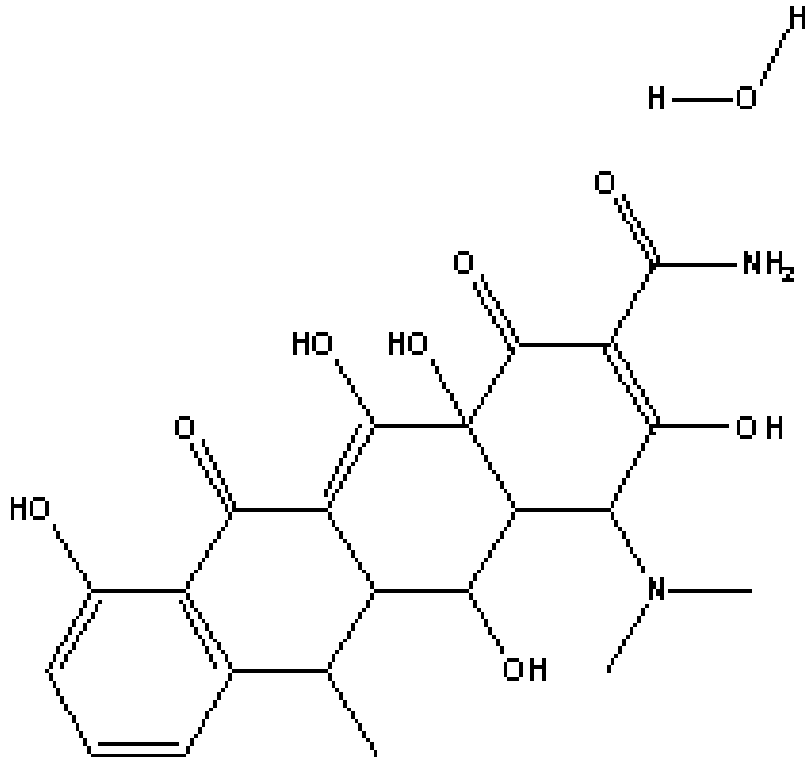

Doxycycline

ABSQ	MaxNeg	MaxQp	Ovality	Surface	xpc4	xv1	xvpc4	nxp5	nxch6
8.3023	-0.3723	0.3991	1.7216	422.4388	9.4271	10.0157	3.9079	182.0000	4.0000
Iy	**Py**	**Pz**	**P**	**Q**	**sumdeII**	**Wt**	**k1**	**k2**	**k3**
5809.5972	1.3701	0.6225	1.5197	4.7566	49.0391	45143	25.1037	8.5873	3.3704
LogP	**SsCH3**	**SaaCH**	**SdssC**	**SdO**	**Gmax**	**Hmin**	**Gmin**	**idcbar**	**fw**
0.6689	4.6519	4.438	-6.6737	38.446	13.317	0.8165	-2.8948	3.1767	444.4412
numHBa	**Qs**	**Qsv**							
10	5.9729	0.5578							

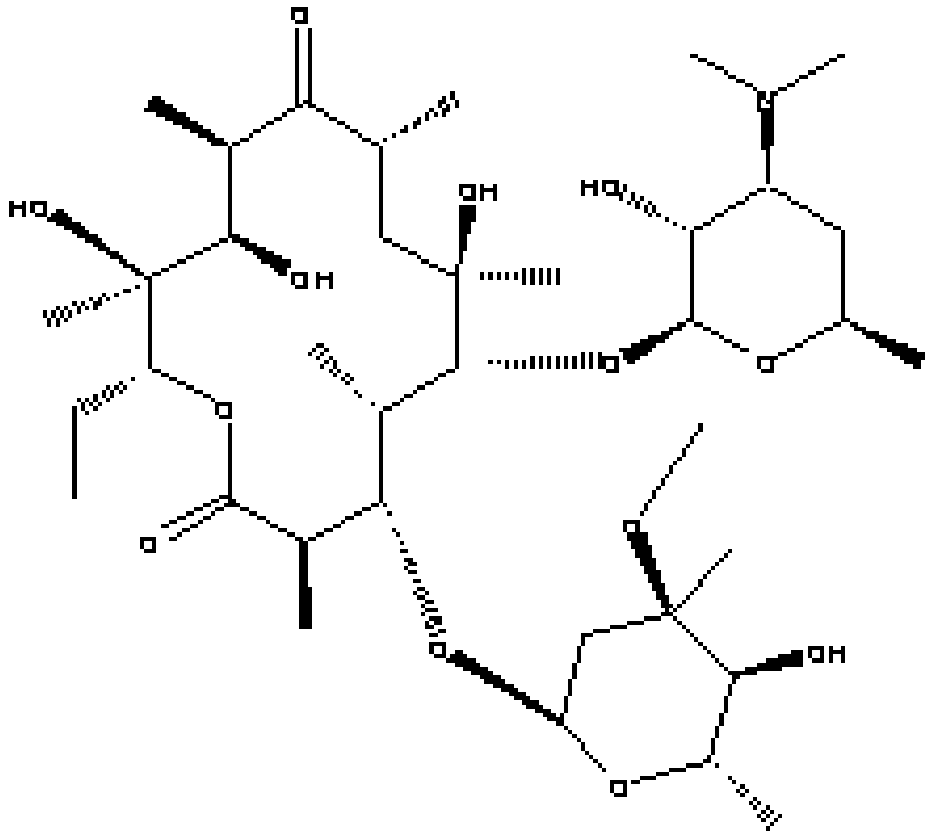

Erythromycin

ABSQ	MaxNeg	MaxQp	Ovality	Surface	xpc4	xv1	xvpc4	nxp5	nxch6
11.3255	-0.3412	0.3587	1.6139	351.6028	6.8221	12.6401	2.1928	94.0000	2.0000
Iy	**Py**	**Pz**	**P**	**Q**	**sumdeII**	**Wt**	**k1**	**k2**	**k3**
6838.5083	0.5434	0.1510	0.8247	2.9768	58.3048	27758.0000	32.5137	15.2908	9.8097
LogP	**SsCH3**	**SaaCH**	**SdssC**	**SdO**	**Gmax**	**Hmin**	**Gmin**	**idcbar**	**fw**
-2.9301	0.0000	0.0000	-1.3692	24.8209	12.5329	0.8824	-1.7761	3.5862	554.5457
numHBa	**Qs**	**Qsv**							
15.0000	6.8278	0.5122							

Appendix 3.

All Compound QSAR Molecular Descriptors and Molecular Properties

			General 3D Desecriptors								Molecular Connectivity Chi Indices										
			Sum of Absolute Values of Charges on Each Atom in Molecule	Molecule Dipole Moment (Debyes)	The Largest + Charge on a H Atom	The Largest - Charge Over Atoms in Molecule	The Largest + Charge Over Atoms in Molecule	Ratio of Surface of Molecule to Surface of Perfect Sphere with Same Volume	Molecular Polarizability (by additive approach)	Molecule Surface Area	Chi Low Order	Chi Path	Chi Cluster	Chi Path Cluster	Chi Low Order Valence	Chi Valence Path	Chi Valence Path	Chi Valence Path	Chi Valence Cluster	Chi Valence Path Cluster	Chi Valence Chain
Notes	**QSAR Cluster**	**Compound Name**	**ABSQ**	**Dipole**	**MaxHp**	**MaxNeg**	**MaxQp**	**Ovality**	**Polarizability**	**Surface**	**x1**	**xp4**	**xc3**	**xpc4**	**xv1**	**xvp4**	**xvp7**	**xvp10**	**xvc3**	**xvpc4**	**xvch6**
DBP	1	1,1 Dichloropropanone	1.2522	1.4552	0.1108	-0.2867	0.2640	1.2585	6.1780	117.6005	2.6427	0.0000	0.6667	1.3333	2.3021	0.0000	0.0000	0.0000	0.4890	0.7899	0.0000
AH	2	1,2,4 Trimethylbenzene	1.4769	0.3775	0.1070	-0.1063	0.1070	1.4175	4.6440	192.4606	4.1984	1.8168	0.7601	1.4783	3.2380	0.8913	0.0241	0.0000	0.4553	0.7904	0.0241
	2	1,2 Dichlorobenzene	1.2723	0.4202	0.1182	-0.1355	0.1182	1.3524	6.1780	168.8331	3.8045	1.5017	0.4714	1.1381	2.9612	0.7108	0.0357	0.0000	0.3273	0.7491	0.0278
AH	2	1, 2 Dimethylbenzene	1.4075	0.6766	0.1037	-0.1040	0.1037	1.3619	3.8700	171.7717	3.8045	1.5017	0.4714	1.1381	2.8273	0.6627	0.0278	0.0000	0.2887	0.6220	0.0278
AH	2	1,3,5 Trimethylbenzene	1.4575	0.0001	0.1080	-0.1122	0.1080	1.4391	4.6440	195.5892	4.1815	2.3493	0.8660	1.0000	3.2321	1.2024	0.0000	0.0000	0.5000	0.5000	0.0241
P	2	1,4 Dichlorobenzene	1.2409	0.0000	0.1193	-0.1286	0.1193	1.3680	6.1780	172.2792	3.7877	1.4267	0.5774	0.8165	2.9553	0.6815	0.0000	0.0000	0.3780	0.4364	0.0278
S,ED	3	1,4 Dichlorophenoxyacetic Acid	2.8674	2.2450	0.2265	-0.3974	0.3728	1.5564	6.9520	248.0090	6.0922	2.7044	1.0993	1.6491	4.1460	1.1948	0.0826	0.0034	0.4761	0.6496	0.0241
S,HO,ES	4	17a Estradiol	3.8151	1.7495	0.1949	-0.3062	0.1949	1.4357	8.5140	226.2367	9.2372	7.0361	1.3715	3.5726	7.7366	5.1932	2.1115	0.5373	0.8914	2.4643	0.1213
ED	5	2,2,2 Trichloro 1,1-bis-4-chlorophenyl Ethanol	3.1546	0.9549	0.2100	-0.2849	0.2539	1.4584	10.4280	243.7398	7.9980	4.3415	1.7767	3.7281	6.0672	2.0121	0.3358	0.0499	0.9958	1.7249	0.0556
ED	5	2,2 bis-p-Chlorophenyl 1,1,1 Trichloroethane	2.4951	0.2474	0.1223	-0.1183	0.1223	1.4716	15.0580	269.7674	8.8760	5.0891	2.3729	3.2079	7.3435	2.8888	0.8786	0.0577	2.4850	2.3767	0.0556
ED	5	2,2-bis-p-Chlorophenyl 1,1 Dichloroethane	2.5337	0.5778	0.1248	-0.1233	0.1248	1.4805	13.1300	252.4810	8.5754	4.8151	1.3551	2.5942	6.9966	2.6575	0.7546	0.0577	1.0823	1.6760	0.0556
ED	5	2,2 bis-p-Methoxyphenyl 1,1,1 Trichloroethane	3.1958	0.6544	0.1226	-0.1870	0.1226	1.5741	12.7500	296.6425	9.9520	5.7103	2.2038	3.3770	7.4343	2.9191	0.6844	0.0394	2.2431	2.2335	0.0556
S,ED	3	2,3,4,5,6 Pentachlorophenol	1.9400	0.5494	0.2078	-0.2120	0.2078	1.4810	11.9620	230.9885	5.4641	2.8729	1.1547	3.6427	4.5583	1.7217	0.0962	0.0000	0.7646	2.3038	0.0156
	3	2,3,5,6 Tetrachlorotorophthalic Acid	3.9604	2.4526	0.2339	0.3834	0.4248	1.5756	10.0340	280.3667	7.2855	4.7882	1.6587	4.0184	5.1232	2.1832	0.1858	0.0000	0.7832	2.1000	0.0156
	3	2,3 Naphthalenedicarboxylic Acid	3.9198	5.7085	0.2305	-0.4125	0.4128	1.5418	3.0960	273.8519	7.5922	4.4869	1.2722	2.8069	4.5875	1.5942	0.3015	0.0154	0.4023	0.8215	0.0486
ED	3	2,4,5 Trichlorophenoxyacetic Acid	2.9655	2.9384	0.2321	-0.3566	0.3682	1.5792	8.8800	265.9502	6.5029	2.9031	1.2820	2.3336	4.6296	1.3458	0.1331	0.0029	0.6145	1.1653	0.0208
ED	3	2,4 Dichloro-4'-nitrodiphenyl Ether	4.6702	3.5254	0.2446	-0.5731	0.7875	1.6641	7.7260	327.6079	8.5586	4.5970	1.3952	2.7858	5.7077	1.7737	0.2285	0.0331	0.5950	0.9206	0.0518
	3	2,4 Dinirophenol	5.0975	2.4025	0.2477	-0.5470	0.8022	1.5697	2.3220	238.4767	6.0197	2.9255	1.2051	2.4994	3.1740	0.7840	0.0559	0.0000	0.2853	0.4922	0.0241
S	6	2,4 Dinitrotoluene	5.0709	0.9473	0.2491	-0.5651	0.7838	1.5199	3.0960	231.2349	6.0197	2.9255	1.2051	2.4994	3.4504	0.9229	0.0618	0.0000	0.3651	0.6557	0.0241
	7	2,6 bis-1,1 Dimethylethyl 2,5 Cyclohexadiene 1,4 dione	3.6959	1.4333	0.1362	-0.2888	0.3481	1.5977	7.7400	269.3009	7.0317	3.9574	3.4489	4.2377	5.5629	1.7166	0.2402	0.0000	2.7634	2.4303	0.0208
	7	2,6 bis-1,1 Dimethylethyl Phenol	3.0583	0.8611	0.2115	-0.2471	0.2115	1.5675	8.5140	259.4433	6.6379	3.8073	3.1602	3.9349	5.4676	1.7539	0.2273	0.0000	2.7002	2.3895	0.0241
	7	2,6 di-tert-butyl-p-Cresol	3.0960	0.8436	0.2110	-0.2466	0.2110	1.6095	9.2880	280.4217	7.0317	3.9574	3.4489	4.2377	5.8783	1.9222	0.3051	0.0000	2.8669	2.5450	0.0208
	8	2,6 Dinitrotoluene	5.0097	0.4997	0.2455	-0.5565	0.7527	1.4638	3.0960	211.7636	6.0366	3.3135	1.1313	2.5168	3.4564	1.0261	0.0748	0.0000	0.3357	0.7227	0.0241
	3	2,6 Naphthalenedicarboxylic Acid	4.0955	3.4293	0.2308	-0.3987	0.4268	1.5496	3.0960	274.4657	7.5754	4.1727	1.3333	2.9372	4.5815	1.5118	0.3135	0.0179	0.4246	0.7996	0.0481
S,ED	9	2-chloro-2'6'-diethyl-N-methoxymethyl-acetanilide (Alachlor)	3.2615	1.3239	0.1148	-0.2860	0.2630	1.5516	10.0550	291.5823	8.6886	4.5562	0.8162	2.4350	6.6852	2.1686	0.3542	0.0234	0.4036	1.0770	0.0241
ED	2	3,4,5,6,7,8,8a-Heptachlorodicyclopentadiene	2.0296	0.1554	0.1165	-0.1538	0.1165	1.2932	4.6440	140.6393	4.9495	4.0184	0.6055	1.7832	4.2997	2.9729	0.5814	0.0000	0.5194	1.4063	0.0370
ED	1	3-amino-1H-1,2,4 Triazole	1.6505	0.5266	0.1632	-0.3622	0.2975	1.2838	1.5480	119.1838	2.8938	1.1299	0.2887	0.4082	1.5064	0.2189	0.0000	0.0000	0.0577	0.0622	0.0000
	9	3-Hydroxycarbofuran	3.4429	0.5374	0.1926	-0.3101	0.1926	1.5688	6.5790	261.4002	7.9535	4.6814	1.9447	3.9983	5.4996	1.8148	0.3423	0.0220	1.0585	1.5043	0.0241
S	3	4,6 Dichlorophenol	1.6713	0.1767	0.2041	-0.2176	0.2041	1.3835	6.1780	183.1283	4.1984	1.8168	0.7601	1.4783	3.0955	0.8898	0.0122	0.0000	0.4172	0.6008	0.0241
ED	9	4-amino-6-tert-butyl-3-methylthio-as-triazin-5,4H-one	2.7381	4.8678	0.0849	-0.3610	0.2690	1.5563	5.4180	249.2121	6.3752	3.5127	2.0354	3.3942	5.1477	1.3159	0.2677	0.0000	1.5222	1.4671	0.0112
S,ED	4	4 Nonylphenol	3.3373	0.8263	0.1956	-0.2271	0.1956	1.7495	9.2880	337.1841	7.8257	3.0079	0.4928	0.8413	6.6056	1.9488	0.4560	0.1028	0.1924	0.3055	0.0278
	2	5-methyl-1H-Benzotriazole	1.5853	2.0832	0.1227	-0.1796	0.1980	1.3920	2.7090	184.0322	4.8602	2.9372	0.6220	1.2920	3.1352	0.9517	0.0921	0.0000	0.3034	0.4581	0.0241
ED	9	6-chloro-N-ethyl-N'-isopropyl-1,3,5 Triazine-2,4-diamine	2.6358	2.7856	0.0852	-0.2675	0.1403	1.5747	7.7330	258.5230	6.6134	3.4012	1.1052	1.3026	4.9126	1.0701	0.1214	0.0051	0.5021	0.4220	0.0112
PhAC	3	Acetaminophen	2.6564	3.8095	0.1963	-0.3835	0.2358	1.4848	3.4830	216.8366	5.1815	2.2315	0.9010	1.0505	3.2491	0.7480	0.0740	0.0000	0.2599	0.2750	0.0278
H	9	Acetochlor	3.4156	1.9221	0.1098	-0.3159	0.2762	1.4585	10.0550	254.8176	8.6506	4.3983	0.8853	2.4295	6.7120	2.0515	0.3436	0.0219	0.4459	1.0558	0.0241
S,AA	1	Alanine	1.8023	3.2266	0.2273	-0.3998	0.3431	1.3117	2.7090	122.2123	2.6427	0.0000	0.6667	1.3333	1.6271	0.0000	0.0000	0.0000	0.2194	0.2257	0.0000
	10	Aldicarbsulfone	7.2031	3.6040	0.1127	-0.8228	2.1580	1.4814	5.4180	202.2197	6.2045	1.4716	2.4958	4.8338	5.7248	0.5770	0.0957	0.0000	2.4560	4.4542	0.0000
	11	Aldrin	2.6416	1.9721	0.1223	-0.2151	0.1802	1.4147	16.9860	216.9138	8.2757	8.2146	2.6865	9.0285	8.0455	7.6143	2.5617	0.3463	2.7569	9.4843	0.0579
ED	9	alpha-naphthyl-N-Methylcarbamate	2.9444	2.8661	0.1701	-0.3953	0.3498	1.5676	4.2570	277.9931	7.3089	4.0478	0.7581	1.8144	4.6837	1.4356	0.2544	0.0168	0.2561	0.5716	0.0518
HO	4	Androsterone	4.2277	3.1465	0.1868	-0.3117	0.2693	1.4885	10.0620	273.5769	9.2372	7.0361	1.3715	3.5726	8.4455	6.2499	2.8629	0.8833	1.0413	2.9165	0.1792
PAH	12	Anthracene	2.0967	0.0000	0.1081	-0.0999	0.1081	1.4810	3.8700	256.8265	6.9327	4.5879	0.6667	1.7991	4.8094	1.8826	0.4421	0.0523	0.3333	0.7440	0.0764
	9	Atrazine	2.6618	2.6146	0.0843	-0.2690	0.1411	1.5386	7.7330	245.3636	6.6134	3.4012	1.1052	1.3026	4.9126	1.0701	0.1214	0.0051	0.5021	0.4220	0.0112
S,AH	13	Benzene	1.2254	0.0001	0.1021	-0.1025	0.1021	1.2646	2.3220	133.7207	3.0000	1.0607	0.0000	0.0000	2.0000	0.3849	0.0000	0.0000	0.0000	0.0000	0.0370
S,PAH	12	benzo-a-Pyrene	2.5484	0.0670	0.1110	-0.1005	0.1110	1.5863	4.6440	338.2936	9.9158	8.1390	1.1611	3.4533	6.9701	3.4895	1.2095	0.3035	0.6027	1.5150	0.1115
ED	1	benzo-e-1,3,2 Dioxathiepin-3-oxide	2.6012	2.8033	0.1294	-0.3291	0.4690	1.2249	3.0960	131.1733	5.3433	4.2896	0.8942	2.0813	3.9003	2.2903	0.3167	0.0000	0.4633	1.0571	0.0370
HO,ES	4	beta-Estradiol	3.8254	1.0974	0.1950	-0.3033	0.1950	1.3748	8.5140	173.6102	9.2372	7.0361	1.3715	3.5726	7.7366	5.1932	2.1115	0.5373	0.8914	2.4643	0.1213
S	4	beta Sitostanol n Hydrate	5.5836	1.0965	0.1859	-0.3127	0.1859	1.6526	17.8020	370.1698	13.0797	8.8756	1.8024	4.6023	12.7606	8.6161	4.1168	1.6702	1.6428	4.3974	0.1792
	14	bis-2-Ethylhexyl-adipate	6.2122	4.1627	0.0867	-0.3741	0.3721	1.6554	16.2540	357.3068	12.5656	4.4055	0.9856	1.8021	10.8789	2.9008	0.4280	0.0908	0.5261	1.0303	0.0000
S,ED	5	Bisphenol	3.7346	0.6802	0.1963	-0.2257	0.1963	1.5936	6.1920	296.2599	7.9980	4.3415	1.7767	3.7281	5.5899	1.9229	0.2930	0.0238	1.0657	1.9360	0.0556
DBP	1	Bromochloroacetic Acid	1.5379	2.9764	0.2059	-0.2971	0.3390	1.2212	6.1020	113.5931	2.6427	0.0000	0.6667	1.3333	2.5050	0.0000	0.0000	0.0000	0.6956	0.7132	0.0000
DBP	1	Bromochloroacetonitrile	0.4821	1.8951	0.1183	-0.1980	0.1183	1.2294	5.7150	111.4349	2.2701	0.0000	0.4082	0.4082	2.3008	0.0000	0.0000	0.0000	0.6429	0.2875	0.0000
DBP	2	Bromochloromethane	0.3765	1.7001	0.0830	-0.0966	0.0830	1.1969	6.1020	93.7706	1.4142	0.0000	0.0000	0.0000	2.1905	0.0000	0.0000	0.0000	0.0000	0.0000	0.0000
DBP	2	Bromodichloromethane	0.4598	1.5141	0.1157	-0.1586	0.1157	1.2159	8.0300	105.3554	1.7321	0.0000	0.5774	0.0000	2.4432	0.0000	0.0000	0.0000	1.4579	0.0000	0.0000
DBP	2	Bromoform	0.3320	0.4481	0.1378	-0.1660	0.1378	1.1896	9.4260	113.5365	1.7321	0.0000	0.5774	0.0000	3.4017	0.0000	0.0000	0.0000	4.3736	0.0000	0.0000
DBP	2	Bromomethane	0.3384	1.3608	0.0564	-0.1153	0.0564	1.1206	4.1740	72.7908	1.0000	0.0000	0.0000	0.0000	1.9640	0.0000	0.0000	0.0000	0.0000	0.0000	0.0000
	9	Butylated-Hydroxyanisole	2.5075	0.9093	0.1941	-0.2269	0.1941	1.5329	6.1920	238.3722	5.9477	2.9870	1.9237	2.6526	4.3240	1.2428	0.1312	0.0000	1.4548	1.3827	0.0241
S	1	Caffeine	3.7109	4.1937	0.1677	-0.4136	0.3720	1.5417	3.8700	247.7542	6.5366	4.4818	1.2527	3.7053	4.1079	1.4712	0.1738	0.0032	0.5451	1.1570	0.0125
AB	9	Carbadox	4.3950	3.2600	0.1689	-0.3990	0.3592	1.7243	4.6440	342.4852	9.1302	5.0775	1.1557	2.9170	5.2820	1.5104	0.2624	0.0268	0.3530	0.7343	0.0422
DBP	1	Chloralhydrate	1.5394	1.4417	0.1954	-0.3069	0.2050	1.2911	8.1060	121.3857	2.9434	0.0000	1.6547	2.5981	2.5059	0.0000	0.0000	0.0000	1.9001	1.1923	0.0000
DBP	2	Chloroform	0.3062	0.3096	0.1045	-0.1531	0.1045	1.2136	7.3320	98.3076	1.7321	0.0000	0.5774	0.0000	1.9640	0.0000	0.0000	0.0000	0.8417	0.0000	0.0000
AB	15	Chlorotetracycline	9.6871	2.5250	0.2887	-0.4539	0.4203	1.6725	9.6680	405.4038	15.1832	12.6898	4.1396	10.5911	9.9594	5.6003	1.8628	0.4320	1.8224	4.1500	0.0892
S	4	Cholesterol	5.1725	1.0133	0.1852	-0.3091	0.1852	1.6324	15.8670	366.9083	12.1310	8.1836	1.7107	3.8018	11.7428	7.9416	4.0306	1.5531	1.5758	3.6830	0.1751
S,PhAC	9	Cimetidine	3.0799	3.0871	0.1651	-0.2586	0.3129	1.7141	6.1920	314.0870	8.2744	3.6282	0.6065	1.5130	6.1484	1.8762	0.3741	0.0629	0.2600	0.5879	0.0000
S,AB,PhAC	16	Ciprofloxacin	5.6687	5.1323	0.2243	-0.3800	0.4588	1.5852	7.2620	311.2392	11.5586	7.6872	1.7752	4.4359	8.1339	3.2393	0.8939	0.1592	0.7401	1.5796	0.0929
P	11	cis-Chlordane	2.3594	1.1668	0.1187	-0.2299	0.1891	1.4458	20.8420	228.9608	8.1139	7.3428	2.8029	9.3645	8.3548	7.4605	2.2939	0.1650	2.9918	10.2446	0.0208

			General 3D Descriptors								Molecular Connectivity Chi Indices										
			Sum of Absolute Values of Charges on Each Atom in Molecule	Molecule Dipole Moment (Debyes)	The Largest + Charge on a H Atom	The Largest - Charge Over Atoms in Molecule	The Largest + Charge Over Atoms in Molecule	Ratio of Surface of Molecule to Surface of Perfect Sphere with Same Volume	Molecular Polarizability (by additive approach)	Molecule Surface Area	Chi Low Order	Chi Path	Chi Cluster	Chi Path Cluster	Chi Low Order Valence	Chi Valence Path	Chi Valence Path	Chi Valence Path	Chi Valence Cluster	Chi Valence Path Cluster	Chi Valence Chain
Notes	**QSAR Cluster**	**Compound Name**	**ABSQ**	**Dipole**	**MaxHp**	**MaxNeg**	**MaxQp**	**Ovality**	**Polarizability**	**Surface**	**x1**	**xp4**	**xc3**	**xpc4**	**xv1**	**xvp4**	**xvp7**	**xvp10**	**xvc3**	**xvpc4**	**xvch6**
S,P	10	Clorpyrifos	6.4551	4.7264	0.1310	-0.6716	1.8678	1.6867	12.7400	298.2288	8.4148	4.4071	1.8005	3.3582	8.7074	3.5945	0.5583	0.0289	1.4126	2.2281	0.0161
S	4	Codeine	3.7291	1.8531	0.1963	-0.2989	0.1963	1.4480	8.1270	243.4733	10.6639	9.3533	1.8586	5.5732	8.1021	5.3887	2.4198	0.6175	1.2181	3.3159	0.1196
	1	Cyclotrimethylenetrinitramine	6.3531	1.5702	0.2364	-0.4988	0.6284	1.4855	3.4830	207.8020	6.9136	3.0883	1.5000	2.9916	3.6451	1.0241	0.1185	0.0000	0.4095	0.6799	0.0316
	2	Cymene	1.7335	0.0486	0.1073	-0.1114	0.1073	1.4345	5.4180	196.3139	4.6984	1.9525	0.7887	1.4487	3.7647	0.9514	0.0641	0.0000	0.5516	0.8293	0.0278
S,AA	1	Cysteine	1.8902	2.6086	0.2316	-0.3693	0.3405	1.3337	2.7090	131.8441	3.1807	0.4714	0.5690	1.2761	2.4067	0.2343	0.0000	0.0000	0.1706	0.3266	0.0000
	6	d--n-Butylphthalate	5.0445	0.7557	0.1424	-0.4075	0.4204	1.8092	9.2880	396.8090	10.1126	4.9683	0.9543	2.3548	7.5521	1.8771	0.3297	0.0405	0.3623	0.7629	0.0241
	14	d--n-Octylphthalate	6.5129	0.5348	0.1376	-0.4025	0.4149	2.0430	14.7060	551.2847	13.7019	5.8762	0.7436	1.9455	11.1354	3.0891	0.6284	0.1269	0.2277	0.5054	0.0278
	14	di-sec-Octylphthalate	6.4377	1.5096	0.1190	-0.3642	0.4217	1.8450	14.7060	472.1701	13.5656	6.1174	1.1518	2.9311	10.9991	3.1779	0.4680	0.0940	0.6359	1.3690	0.0278
P	10	Diazinon	7.0624	1.1088	0.1449	-0.7010	1.8537	1.6908	9.6650	337.1485	8.8980	4.7468	1.9196	3.0161	8.8972	3.3841	0.5172	0.0347	1.4411	1.9071	0.0144
DBP	1	Dibromoacetatic Acid	1.4494	2.6724	0.2037	-0.2902	0.3454	1.2203	6.8000	117.7078	2.6427	0.0000	0.6667	1.3333	2.9842	0.0000	0.0000	0.0000	0.1662	1.1595	0.0000
DBP	1	Dibromoacetonitrile	0.3881	1.8011	0.1289	-0.1874	0.1289	1.2196	6.4130	116.6013	2.2701	0.0000	0.4082	0.4082	2.7801	0.0000	0.0000	0.0000	1.1135	0.4980	0.0000
DBP	2	Dibromochloromethane	0.4693	1.0640	0.1264	-0.1637	0.1264	1.2020	8.7280	109.2071	1.7321	0.0000	0.5774	0.0000	2.9224	0.0000	0.0000	0.0000	2.5251	0.0000	0.0000
DBP	2	Dibromochloropropane	0.9196	2.1624	0.1206	-0.1135	0.1206	1.2943	10.2760	147.2590	2.8081	0.2887	0.2887	0.5774	4.2486	1.1135	0.0000	0.0000	0.3273	1.2857	0.0000
S	1	Dichloroacetic Acid	1.4396	3.0592	0.2052	-0.3014	0.3345	1.2345	5.4040	107.6139	2.6427	0.0000	0.6667	1.3333	2.0257	0.0000	0.0000	0.0000	0.4239	0.4370	0.0000
	1	Dichloroacetonitrile	0.4096	2.2167	0.1077	-0.2048	0.1077	1.2356	5.0170	106.4089	2.2701	0.0000	0.4082	0.4082	1.8216	0.0000	0.0000	0.0000	0.3712	0.1660	0.0000
	1	Dichlorodifluoromethane	0.4325	1.5256	0.0000	-0.1081	0.1530	1.2456	5.2220	93.4665	2.0000	0.0000	2.0000	0.0000	1.5119	0.0000	0.0000	0.0000	0.6479	0.0000	0.0000
	3	Dichlorodiphenyldichloroethylene	3.4746	7.2886	0.2342	-0.4445	0.4707	1.6642	12.3560	349.5894	8.5754	4.8151	1.3551	2.5942	6.6605	2.3064	0.5992	0.0499	0.9286	1.4031	0.0556
	1	Dichloropropane	1.2292	1.8625	0.1149	-0.2745	0.2596	1.2622	6.1780	115.8423	2.6427	0.0000	0.6667	1.3333	2.3021	0.0000	0.0000	0.0000	0.4890	0.7899	0.0000
P	11	Dieldrin	2.6966	2.1813	0.1262	-0.2355	0.1923	1.3651	16.9860	211.9359	8.7757	8.9188	2.8975	9.5229	8.5169	8.3437	3.3841	0.6328	2.9140	9.8880	0.0899
S	9	Diethylphthalate	3.8160	3.7562	0.1337	-0.4001	0.4072	1.6739	5.4180	304.4620	7.7019	3.9401	0.7436	1.9455	5.1354	1.2568	0.1687	0.0073	0.2277	0.5054	0.0278
S,ES	5	Diethylstilbestrol	4.1083	0.8650	0.1958	-0.2197	0.1958	1.7229	7.7400	378.1116	9.6514	5.3994	1.1828	2.7227	6.9613	2.5087	0.4257	0.0235	0.4925	1.1601	0.0556
	4	Digoxigenin	6.7255	4.2846	0.2035	-0.3249	0.3974	1.4984	13.1580	292.4600	13.1982	10.7365	3.3048	9.2261	11.1563	8.3667	3.7050	1.2310	2.4368	6.8653	0.1411
PhAC	17	Digoxin	13.6446	5.5591	0.2067	-0.3198	0.3912	2.0006	24.7680	633.5723	26.0107	19.8272	5.7114	14.8105	20.9409	12.7623	5.0475	1.7669	3.5974	9.1282	0.2373
PhAC	16	Diltiazem	5.7624	4.1388	0.1250	-0.3543	0.3753	1.7602	10.0620	415.8889	13.9011	8.2176	2.0907	4.2525	10.1366	4.2918	1.5594	0.3476	1.1580	2.2276	0.0556
	9	Dipropylthiocarbamic Acid-s-ethylester	2.3537	3.1916	0.0783	-0.1821	0.1085	1.7144	7.3530	284.1748	5.7567	2.1460	0.4024	1.0202	5.4618	1.5381	0.1677	0.0000	0.2086	0.5277	0.0000
P	10	Disulfoton	6.0262	2.5361	0.1082	-0.6304	1.5909	1.6585	8.8910	292.7476	6.6820	2.5607	0.9268	1.4357	9.6103	5.7590	1.8331	0.0000	1.9340	2.9029	0.0000
H	9	Diuron	2.5275	4.1252	0.1745	-0.3853	0.2254	1.5982	8.5000	278.4868	6.5029	2.6711	1.2446	2.6641	4.6941	1.1073	0.1817	0.0000	0.6799	1.1851	0.0241
S,AB	15	Doxycycline	8.3023	6.9853	0.2432	-0.3723	0.3991	1.7216	9.2880	422.4388	14.8667	12.5325	3.3896	9.4271	10.0157	5.5823	1.8507	0.4143	1.6616	3.9079	0.0898
PhAC	16	Enalaprilat	6.2730	3.5126	0.2297	-0.3945	0.3780	1.7213	9.2880	379.3154	11.8968	6.2611	1.7378	3.9924	8.4591	3.1428	0.5311	0.0851	0.7049	1.4334	0.0321
	10	Endosulfansulfate	7.5961	4.9166	0.1099	-0.8650	2.4571	1.4594	16.2120	245.1395	8.9997	7.4151	3.6035	9.6122	8.9562	6.7656	2.2616	0.3148	2.8613	9.3526	0.0208
	16	Enrofloxacin	6.0562	8.0286	0.2245	-0.3797	0.4583	1.5431	8.8100	289.8369	12.4904	8.1495	1.9794	4.9287	9.0826	3.6386	1.0773	0.2097	0.8982	1.9614	0.0870
	4	Equilenin	3.7600	2.2135	0.1963	-0.3047	0.2851	1.5179	6.9660	302.0155	9.5932	7.3506	1.8783	5.0919	7.3727	4.2749	1.4239	0.3141	1.2033	2.9617	0.0810
	4	Equilin	3.9704	1.9724	0.1959	-0.3044	0.2827	1.5044	7.7400	275.7459	9.5932	7.3506	1.8783	5.0919	7.6445	4.7320	1.7271	0.3983	1.2597	3.1527	0.0952
S,AB	16	Erythromycin	11.3255	1.1394	0.2214	-0.3412	0.3587	1.6139	14.7060	351.6028	17.9385	9.7800	3.1180	6.8221	12.6401	4.4180	1.1325	0.3073	1.2587	2.1928	0.0714
ES,HO	6	Estriol	4.4001	0.5287	0.1955	-0.3138	0.1955	1.5214	9.2880	297.5412	10.0039	7.6997	2.0766	5.5575	8.1842	5.5563	2.2106	0.5472	1.5044	3.7759	0.1138
S,ES,HO	4	Estrone	4.1119	2.8523	0.1954	-0.3024	0.2905	1.5212	8.5140	292.9848	9.5932	7.3506	1.8783	5.0919	7.9452	5.3398	2.1097	0.5075	1.3312	3.4729	0.1138
	7	ethyl-tert-Butyl Ether	1.5821	0.9862	0.0537	-0.2621	0.1035	1.4361	5.4180	148.2493	3.0607	0.7500	1.5607	0.7500	2.6999	0.4330	0.0000	0.0000	1.1124	0.4330	0.0000
S,AH	2	Ethylbenzene	1.5028	0.4384	0.1095	-0.1117	0.1095	1.4038	3.8700	176.7742	3.9319	1.5954	0.2041	0.4928	2.9713	0.7137	0.0454	0.0000	0.1179	0.2539	0.0321
S	18	Ethylenediaminetetraacetic Acid (EDTA)	6.6799	0.0328	0.2270	-0.3979	0.3655	1.6594	5.4180	317.7363	9.2013	3.8019	2.0412	1.7029	5.2398	1.2061	0.1474	0.0000	0.5164	0.5227	0.0000
ED	2	exo-Dimethanonaphthalene	2.4127	2.0091	0.1182	-0.2427	0.1182	1.3137	5.4180	167.5950	6.4327	6.2626	1.0999	2.9971	5.7711	5.1738	1.9730	0.2851	0.9237	2.4882	0.1061
PAH	12	Fluoranthrene	2.0834	0.1820	0.1074	-0.1058	0.1074	1.5214	3.8700	281.3071	7.9495	6.4127	0.8221	2.6186	5.5654	2.7427	0.8043	0.1368	0.4345	1.1639	0.0759
PhAC	9	Fluoxetine	4.2679	4.6030	0.1288	-0.2262	0.4083	1.6446	7.8540	333.7897	10.5034	5.3102	2.0478	3.1896	7.0393	2.1235	0.4287	0.0580	0.4651	0.8475	0.0599
P	9	Fonofos	4.1854	2.3357	0.1055	-0.4511	0.8177	1.5225	8.1170	249.0252	6.6996	3.1149	1.1309	1.9368	8.9989	5.3962	0.9447	0.0295	2.9775	4.8884	0.0321
PhAC	9	Gemfibrozil	4.0817	3.4503	0.2269	-0.3930	0.3796	1.6538	8.5140	310.4698	8.3262	3.3283	2.0302	4.0834	6.2621	1.6660	0.2505	0.0358	1.3727	1.7091	0.0241
S,AA	1	Glycine	1.6402	3.2077	0.2337	-0.3897	0.3436	1.2919	1.9350	105.8707	2.2701	0.0000	0.4082	0.4082	1.1895	0.0000	0.0000	0.0000	0.0645	0.0373	0.0000
ED	13	Hexachlorobenzene	1.6030	0.0000	0.0000	-0.1336	0.1336	1.4839	13.8900	236.5462	5.4641	2.8729	1.1547	3.6427	4.9017	2.0022	0.1205	0.0000	0.8504	2.7790	0.0156
	13	Hexachlorobutadiene	2.2402	4.1354	0.0000	-0.4336	0.3986	1.4603	13.8900	217.7766	4.4641	1.2142	1.0516	2.4285	4.1517	0.9263	0.0000	0.0000	0.9263	2.1564	0.0000
	13	Hexachlorocyclohexane	1.1533	0.0001	0.0493	-0.0961	0.0493	1.2485	4.6440	123.5611	3.0000	1.0607	0.0000	0.0000	3.0000	1.0607	0.0000	0.0000	0.0000	0.0000	0.1250
ED	11	Hexachloropentadiene	2.5517	0.0000	0.1410	-0.2130	0.1410	1.4574	29.3280	272.3328	9.4142	8.3525	5.2678	17.5156	10.2176	9.7473	2.6107	0.1774	6.2294	21.8410	0.0000
S,PhAC	9	Ibuprofen	3.4563	1.9928	0.2256	-0.3994	0.3780	1.4646	6.9660	231.4523	7.0029	3.1607	1.3048	2.3237	5.3203	1.5664	0.3397	0.0000	0.8194	1.0329	0.0278
AA	1	Leucine	2.4187	3.0333	0.2293	-0.3852	0.3409	1.4053	5.0310	167.5290	4.0366	1.0157	0.9773	1.4122	3.0209	0.6087	0.0000	0.0000	0.5788	0.4723	0.0000
AB	16	Lincomycin	6.3343	2.9596	0.2002	-0.3386	0.2002	1.4337	13.1580	248.3711	12.7048	7.5766	2.1611	5.4820	10.6478	4.6750	1.0759	0.1666	1.2633	2.6656	0.0262
S,L	13	Lindane	1.3832	0.8369	0.1260	-0.1215	0.1260	1.3847	16.2120	188.1796	5.4641	2.8729	1.1547	3.6427	5.9279	3.3814	0.2857	0.0000	1.3093	4.4811	0.0370
H	9	Linuron	2.6241	4.4781	0.1838	-0.3836	0.2103	1.5979	7.7260	272.7617	6.6302	3.0528	0.9642	1.8583	4.4384	1.1213	0.1459	0.0049	0.4617	0.9143	0.0241
ES,PhAC	4	Mestranol	4.5978	1.6548	0.1963	-0.2934	0.2511	1.5861	10.0620	335.8868	11.0211	8.2635	2.2527	6.7108	8.8921	5.9388	2.4773	0.6791	1.5549	4.3596	0.1138
	1	Metformin	1.4058	2.3308	0.0978	-0.2193	0.0978	1.3996	4.2570	170.9456	4.0366	1.0157	0.9773	1.4122	2.4067	0.2394	0.0000	0.0000	0.3517	0.3994	0.0000
	2	Methylene Bromide	0.3629	1.4615	0.0907	-0.0860	0.0907	1.1771	6.8000	99.3067	1.4142	0.0000	0.0000	0.0000	2.7775	0.0000	0.0000	0.0000	0.0000	0.0000	0.0000
	2	Methylene Chloride	0.2989	0.8746	0.0747	-0.1062	0.0747	1.2026	5.4040	85.9501	1.4142	0.0000	0.0000	0.0000	1.6036	0.0000	0.0000	0.0000	0.0000	0.0000	0.0000
S,P	8	methyl Parathion	7.8037	2.9946	0.2458	-0.6714	1.8239	1.6067	5.7950	273.6969	7.5041	3.2946	1.6309	3.1755	6.7345	1.8489	0.3521	0.0000	1.0963	1.9643	0.0278
	9	Metolachlor	3.4524	3.8251	0.1111	-0.3651	0.2510	1.4946	10.8290	267.7177	9.0613	4.9610	1.0960	2.8453	7.0521	2.4495	0.3464	0.0258	0.6140	1.3445	0.0241
	9	Metribuzin	2.7377	4.8653	0.0849	-0.3608	0.2691	1.5554	5.4180	249.1451	6.3752	3.5127	2.0354	3.3942	5.1477	1.3159	0.2677	0.0000	1.5222	1.4671	0.0112
H	9	Molinate	2.4683	0.9447	0.0843	-0.3649	0.1866	1.3861	6.5790	172.3937	5.8425	2.5710	0.4024	1.0202	5.5476	1.9571	0.3745	0.0419	0.2086	0.5277	0.0000
	2	Monobromobenzene	1.1295	1.4467	0.1229	-0.1086	0.1229	1.3299	4.9480	161.6071	3.3938	1.3067	0.2887	0.4082	2.8927	0.7199	0.0000	0.0000	0.3273	0.3780	0.0321
	7	methyl-tert-butyl Ether (MTBE)	1.3360	1.0211	0.0532	-0.2602	0.0984	1.3820	4.6440	127.3996	2.5607	0.0000	1.5607	1.0607	2.1124	0.0000	0.0000	0.0000	1.1124	0.6124	0.0000
S	1	N-Dimethylamine	1.1210	3.4821	0.0525	-0.3578	0.2604	1.3094	2.3220	112.1383	2.2701	0.0000	0.4082	0.4082	1.2770	0.0000	0.0000	0.0000	0.2000	0.0816	0.0000

			General 3D Descriptors								Molecular Connectivity Chi Indices											
			Sum of Absolute Values of Charges on Each Atom in Molecule	Molecule Dipole Moment (Debyes)	The Largest + Charge on a H Atom	The Largest - Charge Over Atoms in Molecule	The Largest + Charge Over Atoms in Molecule	Ratio of Surface of Molecule to Surface of Perfect Sphere with Same Volume	Molecular Polarizability (by additive approach)	Molecule Surface Area	Chi Low Order	Chi Path	Chi Cluster	Chi Path Cluster	Chi Low Order Valence	Chi Valence Path	Chi Valence Path	Chi Valence Path	Chi Valence Cluster	Chi Valence Path Cluster	Chi Valence Chain
Notes	**QSAR Cluster**	**Compound Name**	**ABSQ**	**Dipole**	**MaxHp**	**MaxNeg**	**MaxQp**	**Ovality**	**Polarizability**	**Surface**	**x1**	**xp4**	**xc3**	**xpc4**	**xv1**	**xvp4**	**xvp7**	**xvp10**	**xvc3**	**xvpc4**	**xvch6**
	9	N-nitrosodi-n-butylamine	2.3792	3.6467	0.0722	-0.3619	0.2633	1.6463	6.9660	244.9514	5.3461	1.5382	0.2041	0.4928	4.4292	0.8747	0.1118	0.0000	0.1000	0.1822	0.0000
	9	N-nitrosodi-n-propylamine	1.9750	3.8005	0.0697	-0.3626	0.2634	1.5147	5.4180	194.1534	4.3461	1.3691	0.2041	0.4928	3.4292	0.7097	0.0000	0.0000	0.1000	0.1822	0.0000
	1	N-nitrosomorpholine	1.7300	2.0994	0.0886	-0.3278	0.2644	1.3276	3.0960	142.0898	3.9319	1.5954	0.2041	0.4928	2.5924	0.6354	0.0167	0.0000	0.1000	0.1822	0.0456
	1	N-nitrosopiperidine	1.7787	2.6801	0.0812	-0.3340	0.2620	1.2651	3.8700	130.8193	3.9319	1.5954	0.2041	0.4928	3.0150	0.9589	0.0289	0.0000	0.1000	0.1822	0.0791
	1	N-nitrosopyrrolidine	1.5141	3.4225	0.0668	-0.3450	0.2626	1.2776	3.0960	129.9703	3.4319	1.4186	0.2041	0.4928	2.5150	0.7821	0.0000	0.0000	0.1000	0.1822	0.0000
	18	N-triacetic Acid	4.5666	3.8360	0.2349	-0.3745	0.3769	1.3901	3.4830	181.2289	5.9136	2.2887	1.4289	1.0607	3.2925	0.7416	0.0000	0.0000	0.3518	0.3238	0.0000
	9	Nitrosodibutylamine	2.3555	4.2283	0.0726	-0.3674	0.2692	1.6280	6.9660	242.2445	5.3461	1.5382	0.2041	0.4928	4.4292	0.8747	0.1118	0.0000	0.1000	0.1822	0.0000
	18	Nitrilotriacetic Acid	4.3754	2.8957	0.2197	-0.3364	0.3533	1.3926	3.4830	182.4949	5.9136	2.2887	1.4289	1.0607	3.2925	0.7416	0.0000	0.0000	0.3518	0.3238	0.0000
	1	Nitrosodiethylamine	1.5936	3.9311	0.0597	-0.3588	0.2487	1.4346	3.8700	155.0135	3.3461	0.8660	0.2041	0.6124	2.4292	0.3391	0.0000	0.0000	0.1000	0.2408	0.0000
S	3	Nitrobenzene	2.7005	3.7349	0.1634	-0.4222	0.5951	1.4377	2.3220	183.7826	4.3045	1.8008	0.5000	1.0404	2.5169	0.5555	0.0245	0.0000	0.1154	0.1970	0.0321
	4	Norethindrone	3.6752	3.2176	0.1252	-0.3165	0.3167	1.4772	9.2880	258.9969	8.8265	6.7097	1.1663	3.0673	8.0601	5.8025	2.5211	0.7173	0.8940	2.5746	0.1453
AB	16	Norfloxacin	4.9962	9.7322	0.2239	-0.3815	0.4604	1.6382	7.2620	345.7708	11.0241	7.2715	1.6392	4.2706	7.5825	2.9614	0.7380	0.1345	0.6278	1.4612	0.0929
	9	N N diethyl 3 methylbenzamide	2.8615	4.3934	0.1316	-0.4039	0.2948	1.5995	6.5790	280.4504	6.6851	3.3757	0.8145	1.9883	5.0458	1.4715	0.1772	0.0000	0.4074	0.7830	0.0278
	1	o-Cresol	1.7221	0.2385	0.1969	-0.2275	0.1969	1.3792	3.0960	168.9442	3.8045	1.5017	0.4714	1.1381	2.5510	0.5634	0.0124	0.0000	0.2089	0.3703	0.0278
ED	11	Octachloro-4-7-methanotetrahydroindane	2.4462	1.7315	0.1195	-0.2281	0.1941	1.4714	20.8420	252.8330	8.1139	7.3428	2.8029	9.3645	8.3548	7.4605	2.2939	0.1650	2.9918	10.2446	0.0208
ED	11	Octachloroepoxide	2.3894	1.8330	0.1367	-0.2294	0.1918	1.4012	20.0680	221.4726	8.5592	8.0992	3.3304	10.3912	8.4678	7.6582	2.6360	0.2582	3.2660	10.7165	0.0435
	1	p-Cresol	1.7155	0.7196	0.1957	-0.2276	0.1957	1.3781	3.0960	169.1012	3.7877	1.4267	0.5774	0.8165	2.5450	0.5448	0.0000	0.0000	0.2412	0.2785	0.0278
	2	p-Dichlorobenzene	1.2409	0.0000	0.1193	-0.1286	0.1193	1.3676	6.1780	172.2792	3.7877	1.4267	0.5774	0.8165	2.9553	0.6815	0.0000	0.0000	0.3780	0.4364	0.0278
	1	Paraxanthine	3.6064	3.6934	0.1678	-0.4090	0.3780	1.4792	3.0960	221.7401	6.1091	4.1099	1.1341	3.0332	3.7135	1.2101	0.1510	0.0013	0.4440	0.8950	0.0140
	9	Paroxetine	4.6453	1.7327	0.1308	-0.2560	0.2000	1.4775	9.1970	270.0124	12.1287	7.7216	2.0182	4.0451	8.7806	3.7145	0.9025	0.1709	1.0320	1.9037	0.1108
	19	Perchloric Acid	7.7742	5.2744	0.2648	-1.2104	3.6223	1.2951	2.7020	90.1319	2.0000	0.0000	2.0000	0.0000	1.8958	0.0000	0.0000	0.0000	0.3307	0.0000	0.0000
S	12	Phenanthrene	2.1113	0.0648	0.1108	-0.1014	0.1108	1.4586	3.8700	251.9400	6.9495	4.7450	0.6055	1.8265	4.8154	1.9548	0.4424	0.0523	0.3110	0.7775	0.0764
S	1	Phenol	1.6683	0.5325	0.1962	-0.2276	0.1962	1.3246	2.3220	149.2555	3.3938	1.3067	0.2887	0.4082	2.1343	0.4280	0.0000	0.0000	0.0745	0.0861	0.0321
S	3	Phthalic Anhydride	2.6157	5.8931	0.1246	-0.2619	0.4169	1.3867	1.5480	186.6669	5.2877	3.5373	0.7436	1.8843	3.1438	1.0333	0.1081	0.0000	0.2277	0.4881	0.0278
	9	Pramitol	3.3801	2.6903	0.1026	-0.3244	0.2254	1.5964	7.3530	276.0571	7.5072	3.7545	1.4289	1.6183	5.3408	1.0933	0.1931	0.0083	0.7182	0.5281	0.0112
S,HO	8	Progesterone	4.7039	2.0951	0.1249	-0.3173	0.3155	1.5482	10.0620	294.9027	10.1479	7.6185	1.6052	4.0170	8.8862	6.3434	2.8619	0.8853	1.0991	3.0945	0.1453
PAH	12	Pyrene	2.0986	0.0000	0.1056	-0.0996	0.1056	1.4848	3.8700	274.6119	7.9327	6.2846	0.8889	2.5977	5.5594	2.6696	0.8025	0.1564	0.4583	1.1319	0.0898
PhAC	16	Ranitidine	5.4776	3.3267	0.2430	-0.5810	0.8672	1.5514	8.9010	247.6150	10.0072	4.5196	1.4289	1.7243	7.5197	2.2331	0.5608	0.1027	0.6022	0.6424	0.0000
	1	s-1-Methyl-5-3-Pyridinyl-2-Pyrrolidinone	2.5363	4.3589	0.1237	-0.3462	0.2582	1.3540	4.6440	182.7268	6.2877	3.6304	0.7309	2.0673	4.4440	1.7674	0.2334	0.0149	0.3812	0.9638	0.0248
	9	Salbutamol	4.1158	1.2226	0.2027	-0.3145	0.2027	1.5334	8.1270	260.0958	7.8315	3.4339	2.3654	2.7960	5.6901	1.4601	0.2442	0.0251	1.6041	1.2175	0.0241
AA	1	Serine	2.2133	3.8333	0.2297	-0.3754	0.3493	1.3125	2.7090	121.3651	3.1807	0.4714	0.5690	1.2761	1.7742	0.0781	0.0000	0.0000	0.1706	0.2212	0.0000
	9	Simazine	2.5982	4.3555	0.0956	-0.3141	0.1284	1.6185	6.9590	261.0195	6.2575	3.1861	0.6969	1.0934	4.5299	0.9845	0.1080	0.0031	0.2134	0.2841	0.0112
AB	19	Sulfachlorpyridazine	7.2544	7.8895	0.1236	-0.8080	2.3219	1.6430	5.7980	310.8341	8.4712	4.4855	1.9763	3.2275	6.7096	2.3112	0.4980	0.0538	0.9654	1.4933	0.0444
AB	19	Sulfadimethoxine	8.3161	5.9963	0.1393	-0.8064	2.3211	1.7823	5.4180	370.5638	9.9410	5.4885	2.0959	3.6460	7.2813	2.4877	0.5390	0.0700	0.9126	1.5288	0.0422
AB	19	Sulfamerazine	7.3945	4.8665	0.1300	-0.8137	2.3119	1.7038	4.6440	325.5358	8.4712	4.6974	1.9763	3.1636	6.6358	2.2751	0.4353	0.0598	0.9336	1.4523	0.0444
S,AB	19	Sulfamethazine	7.5538	4.7125	0.1306	-0.8135	2.3103	1.7482	5.4180	347.5558	8.8650	5.2325	2.2650	3.4330	7.0566	2.5416	0.4737	0.0748	1.0627	1.5675	0.0422
AB, PhAC	19	Sulfamethizole	7.1287	6.8722	0.1199	-0.8088	2.3158	1.6847	3.4830	308.6381	7.9712	4.4626	1.9763	3.1636	6.5813	2.6729	0.5225	0.0641	1.0100	1.5854	0.0278
AB	19	Sulfamethoxazole	7.0869	6.1852	0.1437	-0.8236	2.3100	1.5538	4.2570	296.3359	7.9712	4.4626	1.9763	3.1636	6.2724	2.2418	0.4162	0.0474	0.9369	1.4474	0.0278
AB	19	Sulfathiazole	7.4764	6.3320	0.1560	-0.8172	2.3028	1.6433	3.4830	295.2863	7.5773	4.1667	1.6876	2.8193	6.5426	2.7134	0.5306	0.0606	0.8731	1.4803	0.0278
H	9	Terbacil	3.3065	3.0941	0.1082	-0.3942	0.3275	1.5642	7.3460	246.5316	6.2479	3.9534	2.3186	3.6456	4.6460	1.3630	0.1175	0.0000	1.5847	1.7293	0.0140
P	10	Terbufos	5.9078	2.0821	0.1203	-0.6965	1.5570	1.6366	9.6650	275.1683	6.8284	2.6276	2.4874	2.1857	9.6835	6.6846	1.2324	0.0000	4.0250	4.0279	0.0000
	15	Terramycin	9.2497	6.8841	0.2743	-0.4629	0.4227	1.6365	8.5140	385.7108	14.8667	12.5325	3.3896	9.4271	9.6965	5.2482	1.6911	0.3920	1.5694	3.6101	0.0898
	7	tert amyl methyl Ether	1.5661	0.9071	0.0625	-0.2620	0.0981	1.3233	5.4180	136.7417	3.1213	0.2500	1.2071	1.7071	2.6730	0.1443	0.0000	0.0000	0.8464	1.1350	0.0000
S,HO	4	Testosterone	4.1977	2.7872	0.1856	-0.3194	0.3163	1.4550	9.2880	285.2442	9.2372	7.0361	1.3715	3.5726	8.1516	5.8081	2.5299	0.7144	0.9688	2.7452	0.1453
S	13	1,1,2,2 Tetrachloroethane	0.8995	0.0306	0.0000	-0.2249	0.1134	1.3351	9.2600	142.4223	2.6427	0.0000	0.6667	1.3333	2.5178	0.0000	0.0000	0.0000	0.6429	1.4579	0.0000
S	13	1,1,2,2, Tetrachloroethylene (PCE)	1.1008	0.0000	0.0000	-0.2752	0.1376	1.3233	9.2600	143.6209	2.6427	0.0000	0.6667	1.3333	2.5178	0.0000	0.0000	0.0000	0.6429	1.4579	0.0000
S,AB	15	Tetracycline.hin	8.5480	4.6612	0.2756	-0.4552	0.4188	1.6843	8.5140	399.9212	14.4392	11.8893	3.2437	9.0664	9.5882	5.2052	1.7522	0.4333	1.5266	3.5123	0.0952
ED	6	Thio-N-methyl-carbamoyl-oxy-methylester	2.2458	1.0045	0.0889	-0.4074	0.3244	1.5293	3.0960	205.4974	4.6259	1.1052	0.8165	0.5774	3.2903	0.4880	0.0731	0.0000	0.2619	0.1852	0.0000
S,AA	1	Threonine	2.4695	2.8308	0.2299	-0.3804	0.3381	1.3550	3.4830	139.1301	3.5534	0.7698	0.8591	1.8214	2.2186	0.2063	0.0000	0.0000	0.2980	0.4430	0.0000
S,AH	2	Toluene	1.3028	0.3389	0.1052	-0.1090	0.1052	1.3300	3.0960	154.5761	3.3938	1.3067	0.2887	0.4082	2.4107	0.5344	0.0000	0.0000	0.1667	0.1925	0.0321
ES	20	Tributyl Tin	2.9043	0.3249	0.0645	-0.1558	0.0754	1.6571	-111111.0000	306.5492	6.3461	1.9114	0.2041	0.4330	13.3372	12.8221	2.9047	0.0000	1.3693	2.9047	0.0000
S,DBP	3	Trichloroacetic Acid	1.4882	2.8918	0.2050	-0.2795	0.3350	1.2436	7.3320	109.0973	2.9434	0.0000	1.6547	2.5981	2.3786	0.0000	0.0000	0.0000	1.7389	0.9802	0.0000
	2	1,1,2 Trichloroethene (TCE)	0.9360	0.1971	0.1361	-0.2614	0.1361	1.2997	7.3320	127.3657	2.2701	0.0000	0.4082	0.4082	2.0772	0.0000	0.0000	0.0000	0.3712	0.4208	0.0000
AM	3	Triclosan	2.9634	2.2182	0.2063	-0.2168	0.2063	1.6281	9.6540	315.0919	8.0586	4.5454	1.3821	2.6776	5.8088	1.8667	0.2168	0.0423	0.7240	1.0344	0.0481
AB	9	Trimethoprim	3.4040	0.6983	0.1296	-0.2829	0.1309	1.5583	6.9660	279.7229	10.0832	5.9914	1.3646	3.1673	6.2440	2.0278	0.3960	0.0479	0.5111	0.9908	0.0353
S	10	triphenyl Phosphate	8.5722	1.1242	0.1272	-0.8418	2.1850	1.6524	7.3430	312.5922	11.2349	6.5146	1.5391	2.3444	8.5353	3.1388	0.7163	0.1242	0.5693	0.9204	0.0962
	10	tris 2 Chloroethyl Phosphate	6.3188	0.4330	0.0740	-0.8665	2.1774	1.6503	13.1270	268.7487	6.6820	2.1857	0.9268	1.4357	6.9623	2.2732	0.3803	0.0000	0.3651	0.5809	0.0000
AB	17	Tylosin	14.5026	3.3645	0.2175	-0.3833	0.3869	1.9631	25.1550	640.9055	27.6827	16.3464	4.1417	9.0643	20.1098	7.9529	1.9476	0.4787	2.1123	4.0527	0.1034
	1	t Butyl Alcohol	0.8702	1.0835	0.1834	-0.3118	0.1834	1.2193	2.3220	82.6823	1.4142	0.0000	0.0000	0.0000	1.0233	0.0000	0.0000	0.0000	0.0000	0.0000	0.0000
S,AA	1	Valine.hin	2.1810	2.9748	0.2292	-0.3839	0.3404	1.3733	4.2570	147.1524	3.5534	0.7698	0.8591	1.8214	2.5378	0.2852	0.0000	0.0000	0.4823	0.6947	0.0000
S, AA		Asparagine	3.3170	3.3723	0.2290	-0.4237	0.2621	1.4623	3.0960	175.5508	4.0366	1.0157	0.9773	1.4122	2.3043	0.3041	0.0000	0.0000	0.2539	0.2756	0.0000
S, AA		Aspartic Acid	3.1448	0.8208	0.2290	-0.3271	0.2626	1.4108	2.7090	158.6067	4.0366	1.0157	0.9773	1.4122	2.2393	0.2754	0.0000	0.0000	0.2351	0.2647	0.0000
S, AA		Histidine	2.9463	1.8041	0.2290	-0.3254	0.2619	1.4658	3.4830	192.9965	5.1984	2.0440	0.7732	1.5830	3.1553	0.7206	0.0571	0.0000	0.2726	0.3909	0.0000
S, AA		Lysine	2.7808	2.0149	0.2290	-0.3300	0.2614	1.5190	5.4180	198.2787	4.6807	1.0496	0.5690	1.2071	3.3662	0.6321	0.0356	0.0000	0.1706	0.2518	0.0000

			General 3D Desecriptors								Molecular Connectivity Chi Indices										
			Sum of Absolute Values of Charges on Each Atom in Molecule	Molecule Dipole Moment (Debyes)	The Largest + Charge on a H Atom	The Largest - Charge Over Atoms in Molecule	The Largest + Charge Over Atoms in Molecule	Ratio of Surface of Molecule to Surface of Perfect Sphere with Same Volume	Molecular Polarizability (by additive approach)	Molecule Surface Area	Chi Low Order	Chi Path	Chi Cluster	Chi Path Cluster	Chi Low Order Valence	Chi Valence Path	Chi Valence Path	Chi Valence Path	Chi Valence Cluster	Chi Valence Path Cluster	Chi Valence Chain
Notes	**QSAR Cluster**	**Compound Name**	**ABSQ**	**Dipole**	**MaxHp**	**MaxNeg**	**MaxQp**	**Ovality**	**Polarizability**	**Surface**	**x1**	**xp4**	**xc3**	**xpc4**	**xv1**	**xvp4**	**xvp7**	**xvp10**	**xvc3**	**xvpc4**	**xvch6**
S, AA		Methionine	2.2816	2.7133	0.2290	-0.3254	0.2614	1.4852	4.2570	185.9375	4.1807	0.8594	0.5690	1.2071	3.7686	0.7595	0.0000	0.0000	0.1706	0.2518	0.0000
S, DBP		N-nitroso dimethyl amine (NDMA)	0.9623	5.9261	0.0601	-0.2788	0.0604	1.2497	2.3220	102.4022	2.2701	0.0000	0.4082	0.4082	1.2770	0.0000	0.0000	0.0000	0.2000	0.0816	0.0000
S, AA		Phenylalanine	2.5762	2.2097	0.2290	-0.3254	0.2617	1.4553	4.2570	204.5864	5.6984	2.2208	0.7732	1.5830	3.7222	0.9553	0.1087	0.0000	0.2884	0.4316	0.0321
S		Urea	2.0688	3.4975	0.2005	-0.4507	0.2383	1.2151	1.5480	86.1161	1.7321	0.0000	0.5774	0.0000	0.7815	0.0000	0.0000	0.0000	0.0680	0.0000	0.0000
Marine Toxin		Anatoxin a	1.7445	0.9316	0.1231	-0.4196	0.1231	1.3725	5.8050	183.0999	5.7709	3.5203	0.8402	1.8237	4.7418	2.2634	0.6087	0.0169	0.4318	0.9232	0.0000
Marine Toxin		Cylindrospermopsin	4.7769	9.3090	0.3035	-0.4008	0.3035	1.3755	7.7400	224.2284	12.6469	9.2825	3.3600	6.0375	10.1675	5.6238	2.0632	0.4943	1.6755	3.7142	0.0767
Marine Toxin		Microcystin LR	16.3975	11.7305	0.2325	-0.4456	0.2773	1.8486	26.3160	643.2284	32.0160	15.1134	5.3466	10.3666	22.2091	6.7673	1.5379	0.3042	2.2869	3.6602	0.0321
Marine Toxin		Saxitoxin	5.4481	0.6742	0.2301	-0.3751	0.3089	1.5786	7.3530	284.3227	9.7765	7.2459	2.6974	5.7422	6.4848	3.3896	0.8106	0.0958	1.0011	2.3045	0.0186

Legend:
S = Surrogate
PhAC = Pharmaceutically Active Compound
ED = Endocrine Disruptor
ES = Estrogenicity
HO = Hormone
P = Pesticide
H = Herbicide
AHC = Aromatic Hydrocarbon
PHA = Polyaromatic Hydrocarbon
AB = Antibiotic
AM = Antimicrobial
AA = Amino Acid
DBP = Disinfection Byproduct

			Subgraph Count Indices			3D Descriptors for Comparitive Molecular Moment Analysis (CoMMA)											Total Topological Descriptors						
			# Paths = Length 5	#3-Way Clusters	#6-Member Rings	Principal Moment of Inertia along X-Axis	Principal Moment of Inertia along Y-Axis	Component of Dipole Moment along Inerial Y-Axis	Component of Dipole Moment along Inertial Z-Axis	Magnitude of Dipole Moment	Magnitude of Principal Quadripole Moment	Displacement between Center of Mass and Center of Dipole Moment along X-Axis	Displacement between Center of Mass and Center of Dipole Moment along Y-Axis	Displacement between Center of Mass and Center of Dipole Moment along Z-Axis	The xx Component of Second Rank Tensor Translated so Origin Coincides With Center of Dipole	The yy Component of Second Rank Tensor Translated so Origin Coincides With Center of Dipole	Weiner Index	Platt f Index	Sum of Delta Intrinsic States of atoms	Total Electrotopological Index	Total Topological Index	Total Weiner Number	#Symmetry Classes in Molecule
Notes	**QSAR Cluster**	**Compound Name**	**nxp5**	**nxc3**	**nxch6**	**Ix**	**Iy**	**Py**	**Pz**	**P**	**Q**	**Dx**	**Dy**	**Dz**	**Qxx**	**Qyy**	**W**	**Pf**	**sumdell**	**tets2**	**totop**	**Wt**	**nclass**
DBP	1	1,1 Dichloropropanone	0.0000	2.0000	0.0000	197.5835	231.5178	0.3648	0.0681	0.3940	0.6319	2.3277	0.1767	0.0211	-0.1123	-0.0847	29	12	5.3164	2.853	21.111	29	5
AH	2	1,2,4 Trimethylbenzene	14.0000	3.0000	1.0000	174.1057	383.6151	0.0379	0.0000	0.0579	2.1658	3.3289	1.2628	0.0000	1.9125	1.1989	84	24	0.8947	9.501	40.1992	243	9
	2	1,2 Dichlorobenzene	10.0000	2.0000	1.0000	253.0619	349.4085	0.0000	0.0000	0.0783	2.1746	4.4775	0.0000	0.0000	0.6253	2.1746	60	20	3.2877	6.6071	34.8411	182	4
AH	2	1, 2 Dimethylbenzene	10.0000	2.0000	1.0000	162.5852	228.9608	0.0000	0.0000	0.0996	2.2382	4.3562	0.0001	0.0000	0.0092	2.2382	60	20	0.5972	8.2406	35.5862	182	4
AH	2	1,3,5 Trimethylbenzene	12.0000	3.0000	1.0000	285.1384	285.1399	0.0000	0.0000	0.0000	1.7446	0.0004	0.0008	0.0001	1.7440	1.7446	84	24	0.9375	9.4784	40.1261	243	3
P	2	1,4 Dichlorobenzene	12.0000	2.0000	1.0000	89.5007	741.3848	0.0000	0.0000	0.0000	1.9429	0.0001	0.0001	0.0000	1.1701	1.9429	62	20	3.3653	6.8616	34.736	182	3
S,ED	3	1,4 Dichlorophenoxyacetic Acid	23.0000	4.0000	1.0000	347.0912	1806.9476	0.0747	0.0000	0.3979	2.9487	2.4621	0.7481	0.0001	0.1041	2.8447	266	34	11.336	10.2616	74.3295	640	13
S,HO,ES	4	17a Estradiol	90.0000	8.0000	3.0000	483.0354	2622.6062	0.1989	0.1080	0.3222	3.0584	0.3347	0.4496	0.4895	0.7747	1.8231	641	66	10.0301	28.9229	143.4427	13763	19
ED	5	2,2,2 Trichloro 1,1-bis-4-chlorophenyl Ethanol	44.0000	8.0000	2.0000	961.3065	2876.2126	0.2472	0.0706	0.3097	1.6517	0.2467	3.9486	0.1195	-0.6459	-0.5994	516	52	11.9158	20.4609	97.6767	1950	8
ED	5	2,2 bis-p-Chlorophenyl 1,1,1 Trichloroethane	52.0000	9.0000	2.0000	1769.1957	3180.7339	0.1310	0.0562	0.1425	1.6394	0.0016	8.3120	0.4460	-1.6394	0.2548	678	58	11.7926	23.2637	100.0329	2296	8
ED	5	2,2-bis-p-Chlorophenyl 1,1 Dichloroethane	48.0000	6.0000	2.0000	1391.9965	3033.0776	0.0525	0.0852	0.1314	0.9617	3.3612	5.3133	4.2759	-0.4518	0.8008	603	52	9.6678	18.4771	94.9077	2135	8
ED	5	2,2 bis-p-Methoxyphenyl 1,1,1 Trichloroethane	56.0000	9.0000	2.0000	1793.2950	2955.1260	0.2049	0.0186	0.2065	7.1467	3.3374	5.9029	0.5731	2.7111	0.0958	932	62	11.993	28.113	122.7448	3114	9
S,ED	3	2,3,4,5,6 Pentachlorophenol	24.0000	6.0000	1.0000	853.2334	1081.9465	0.0544	0.0000	0.0830	4.4959	4.1988	0.5944	0.0000	2.3958	2.4573	174	36	10.9893	2.3312	59.5122	486	8
	3	2,3,5,6 Tetrachloroterephthalic Acid	40.0000	8.0000	1.0000	1179.4177	1451.2129	0.4567	0.0000	0.4567	0.2469	0.0000	3.3538	0.0000	-0.2469	0.0000	390	48	20.658	15.8643	102.1085	998	6
	3	2,3 Naphthalenedicarboxylic Acid	52.0000	6.0000	2.0000	514.9874	1333.3635	0.4691	0.0000	0.8941	3.2870	0.4908	0.8518	0.0000	0.9049	2.3821	406	48	15.0568	17.6572	119.0799	2258	8
ED	3	2,4,5 Trichlorophenoxyacetic Acid	28.0000	5.0000	1.0000	651.6973	2040.2909	0.3737	0.0000	0.4528	4.0481	2.9178	0.5569	0.0000	2.7582	1.2900	318	38	13.0987	9.407	79.3716	769	14
ED	3	2,4 Dichloro-4'-nitrodiphenyl Ether	44.0000	6.0000	2.0000	426.0353	3986.5217	0.2497	0.0000	0.7283	5.4453	2.6047	0.5518	0.0000	0.6401	4.8052	667	52	13.455	15.7719	119.3589	2719	16
	3	2,4 Dinirophenol	26.0000	5.0000	1.0000	400.3216	956.7458	0.4069	0.0000	0.4095	4.0852	1.1625	3.8892	0.0000	-4.0350	-0.0501	240	36	15.5798	9.6111	94.6981	611	13
S	6	2,4 Dinitrotoluene	26.0000	5.0000	1.0000	368.1762	1000.4230	0.0792	0.0493	0.1519	0.7408	11.7987	14.3628	1.2083	-0.2582	0.0826	240	36	13.1531	6.8581	89.0354	611	13
	7	2,6 bis-1,1 Dimethylethyl 2,5 Cyclohexadiene 1,4 dione	40.0000	12.0000	1.0000	639.7651	1301.2711	0.2271	0.0000	0.2272	3.1563	0.7124	6.6314	0.0000	3.1527	0.0036	392	52	12.7314	6.8118	88.2304	986	8
	7	2,6 bis-1,1 Dimethylethyl Phenol	30.0000	11.0000	1.0000	452.3190	1275.4045	0.0060	0.0000	0.1630	1.9534	3.9497	1.7469	0.0006	0.0026	1.9507	334	48	6.988	7.9458	74.2529	843	7
	7	2,6 di-tert-butyl-p-Cresol	40.0000	12.0000	1.0000	669.4944	1278.6190	0.0534	0.0000	0.1721	2.7313	2.9579	1.3034	0.0004	0.2628	2.4685	392	52	7.4209	9.6516	80.0306	986	8
	8	2,6 Dinitrotoluene	24.0000	5.0000	1.0000	330.7554	989.5244	0.0606	0.2049	0.2159	8.2348	3.2096	4.7764	0.8568	-7.1287	6.9813	234	36	13.275	6.317	89.3581	611	8
	3	2,6 Naphthalenedicarboxylic Acid	48.0000	6.0000	2.0000	269.1767	2195.3699	0.4975	0.0000	0.5049	2.9673	0.3198	3.0225	0.0000	-2.8813	-0.0859	442	48	14.6327	16.5695	118.2036	2351	8
S,ED	9	2-chloro-2'-6'-diethyl-N-methoxymethyl-acetanilide (Alachlor)	45.0000	5.0000	1.0000	1187.9919	1733.9794	0.0377	0.4024	0.4135	1.2547	3.8897	0.1971	3.5958	-1.1914	1.2297	569	46	10.5848	15.4532	97.2637	1348	14
ED	2	3,4,5,6,7,8,8a-Heptachlorodicyclopentadiene	40.0000	4.0000	1.0000	175.2914	372.6687	0.0241	0.0177	0.0329	1.0993	0.7238	1.0446	0.2109	-0.0283	1.0727	98	36	1.9046	15.5293	59.279	1260	10
ED	1	3-amino-1H-1,2,4 Triazole	2.0000	1.0000	0.0000	53.4575	139.6305	0.0676	0.0000	0.1020	1.4636	14.3552	6.8393	0.0000	0.6420	0.8217	26	14	2.4873	5.2228	36.332	79	6
	9	3-Hydroxycarbofuran	56.0000	9.0000	1.0000	706.9651	1506.9421	0.0542	0.0858	0.1201	2.1241	2.4230	1.9426	4.0969	-0.4597	1.3842	491	54	11.6495	21.1297	117.2513	2574	16
S	3	4,6 Dichlorophenol	14.0000	3.0000	1.0000	233.9300	675.1678	0.0302	0.0000	0.0327	2.6672	2.0931	1.4932	0.0000	2.1220	0.9058	84	24	6.3046	4.6118	44.8678	243	9
ED	9	4-amino-6-tert-butyl-3-methylthio-as-triazin-5,4H-one	28.0000	8.0000	1.0000	431.2530	1351.9285	0.1719	0.0023	0.7349	0.8932	2.1584	1.4868	0.0144	0.0489	0.8442	284	42	10.1625	11.1524	80.8534	718	12
S,ED	4	4 Nonylphenol	23.0000	2.0000	1.0000	176.1078	5120.7363	0.0529	0.0000	0.1665	3.2246	3.0539	0.3056	0.0000	0.3258	2.8988	594	36	4.5156	13.9255	68.4255	1178	14
	2	5-methyl-1H-Benzotriazole	25.0000	3.0000	1.0000	143.9608	481.5730	0.3650	0.0000	0.4099	4.4073	1.3938	0.0896	0.0000	3.4951	0.9122	108	30	2.6274	14.8753	66.0886	694	10
ED	9	6-chloro-N-ethyl-N'-isopropyl-1,3,5 Triazine-2,4-diamine	26.0000	4.0000	1.0000	883.4859	1118.0472	0.1021	0.0258	0.5729	4.4622	0.4543	0.6060	0.0873	0.1215	4.2836	319	36	7.0386	11.6577	77.3698	779	13
PhAC	3	Acetaminophen	18.0000	3.0000	1.0000	152.5966	908.2939	0.3694	0.0001	0.5617	1.7401	3.2604	1.8107	0.0002	0.7527	0.9874	166	28	7.7581	7.0842	63.8125	409	9
H	9	Acetochlor	42.0000	5.0000	1.0000	1190.4967	1693.2067	0.1545	0.2551	0.3406	2.9295	0.5223	3.8927	0.7843	2.1415	-2.2464	585	46	10.7392	14.8585	96.52	1320	18
S,AA	1	Alanine	0.0000	2.0000	0.0000	98.0152	171.8076	0.3392	0.1935	0.5073	0.3040	0.1744	0.9717	0.6108	0.1544	0.1022	29	12	5.9861	4.2264	29.514	29	6
	10	Aldicarbsulfone	9.0000	9.0000	0.0000	360.2875	2090.1462	0.1999	0.8774	0.9689	3.7802	0.7341	1.2620	0.6077	1.4973	-2.1776	337	38	16.1347	18.0201	71.0307	337	12
	11	Aldrin	140.0000	18.0000	2.0000	1688.4248	1839.3016	0.0000	0.2040	0.3057	0.2269	2.1463	0.0000	0.0953	0.1010	-0.2269	448	78	16.4982	25.5662	144.0941	8979	10
ED	9	alpha-naphthyl-N-Methylcarbamate	42.0000	4.0000	2.0000	397.9063	1382.2261	0.4147	0.0317	0.4242	4.8028	4.5834	1.0046	0.4400	4.6137	0.1621	362	42	7.6097	19.4915	100.6146	1970	15
HO	4	Androsterone	90.0000	8.0000	3.0000	529.2229	2615.9258	0.4061	0.1996	0.5607	3.5785	3.2209	0.2202	0.6699	-1.3097	1.2103	641	66	10.1346	25.2299	131.9599	13763	19
PAH	12	Anthracene	54.0000	4.0000	3.0000	235.5132	1116.0750	0.0000	0.0000	0.0000	3.8336	0.0002	0.0001	0.0000	3.8336	3.0830	279	44	1.4215	27.3469	98.0885	3516	4
	9	Atrazine	26.0000	4.0000	1.0000	753.9598	1160.7399	0.0803	0.0190	0.5564	3.9882	0.5302	0.2076	0.1099	0.0869	3.7017	319	36	7.0386	11.6577	77.3698	779	13
S,AH	13	Benzene	6.0000	0.0000	1.0000	88.4162	88.4166	0.0000	0.0000	0.0000	1.3002	0.0000	0.0005	0.0000	1.3002	1.3002	27	12	0	5.8967	26.845	90	1
S,PAH	12	benzo-a-Pyrene	122.0000	8.0000	5.0000	594.7486	1958.3552	0.0112	0.0000	0.0119	5.6569	0.7776	1.8037	0.0000	5.6563	4.7428	680	72	2.5126	72.8462	218.3313	34134	20
ED	1	benzo-e-1,3,2 Dioxathiepin-3-oxide	48.0000	5.0000	1.0000	211.6938	475.9140	0.0000	0.3300	0.9252	0.6445	1.1632	0.0000	0.2629	0.0820	-0.6445	132	40	8.5881	8.4501	85.7549	1595	7
HO,ES	4	beta-Estradiol	90.0000	8.0000	3.0000	488.8848	2670.9702	0.2243	0.1304	0.3113	3.8280	0.8674	0.5333	1.0815	-0.1062	1.8399	641	66	10.0301	28.9229	143.4427	13763	19
S	4	beta Sitostanol n Hydrate	104.0000	10.0000	3.0000	1275.5083	7152.4863	0.0637	0.1380	0.2319	0.6953	6.2038	2.4688	1.9456	0.2977	-0.4647	2003	86	6.8588	46.3748	167.8418	33956	26
	14	bis-2-Ethylhexyl-adipate	29.0000	4.0000	0.0000	2468.2520	6874.4795	0.6588	0.4969	0.8334	5.2899	0.9434	1.1138	0.4140	-1.3759	1.1796	2351	56	16.1955	13.7482	110.0352	2351	13
S,ED	5	Bisphenol	44.0000	8.0000	2.0000	416.8336	2245.0769	0.1135	0.0000	0.1298	1.6861	6.3586	10.4827	0.0001	1.2883	0.3978	516	52	9.063	15.937	104.1583	1950	7
DBP	1	Bromochloroacetic Acid	0.0000	2.0000	0.0000	221.6212	310.6979	0.1261	0.3309	0.5127	1.1898	2.2188	0.4677	0.4035	-0.5173	1.1107	29	12	6.1184	4.8176	25.372	29	6
DBP	1	Bromochloroacetonitrile	0.0000	1.0000	0.0000	164.2567	248.6100	0.2923	0.1924	0.3500	0.6736	0.9534	0.1917	0.5779	-0.5862	0.1770	18	8	3.413	2.8975	16.836	18	5
DBP	2	Bromochloromethane	0.0000	0.0000	0.0000	20.6488	208.3103	0.1743	0.0000	0.2509	0.0742	0.1808	0.6878	0.0001	-0.0358	-0.0384	4	2	1.1165	0.9362	3.611	4	3
DBP	2	Bromodichloromethane	0.0000	1.0000	0.0000	151.5457	244.9822	0.0000	0.0942	0.2287	0.0373	0.3658	0.0000	0.3857	-0.0063	0.0373	9	6	2.0455	1.617	6.1225	9	3
DBP	2	Bromoform	0.0000	1.0000	0.0000	334.4268	334.4281	0.0000	0.1252	0.1252	0.0000	0.0000	0.0000	1.4588	0.0000	0.0000	9	6	1.0625	1.1466	4.6347	9	2
DBP	2	Bromomethane	0.0000	0.0000	0.0000	3.2357	53.5663	0.0000	0.0000	0.2833	0.0000	0.7322	0.0000	0.0000	0.0000	0.0000	1	0	0.1875	0.5769	1.3866	1	2
	9	Butylated-Hydroxyanisole	26.0000	7.0000	1.0000	372.6790	963.4121	0.1208	0.0000	0.1806	2.4221	4.1384	1.7772	0.0001	1.0838	1.3383	234	38	6.9695	9.525	69.5988	599	11
S	1	Caffeine	47.0000	7.0000	1.0000	496.9071	737.9059	0.1687	0.0906	0.7400	0.4252	1.2125	0.0425	0.7064	0.0259	0.0511	258	46	11.5069	14.1235	107.2062	1538	14
AB	9	Carbadox	53.0000	6.0000	2.0000	668.8977	3014.8047	0.4703	0.3429	0.6432	3.3811	0.0779	2.8393	0.7027	0.9162	-1.5489	748	54	15.4812	20.2649	143.0295	3544	19
DBP	1	Chloralhydrate	0.0000	5.0000	0.0000	321.6766	369.7343	0.0000	0.3390	0.3485	0.2993	2.3121	0.0002	1.1097	0.2833	-0.2993	42	18	7.1898	9.4134	26.9267	42	4
DBP	2	Chloroform	0.0000	1.0000	0.0000	150.3323	150.3327	0.0000	0.0865	0.0865	0.0659	0.0000	0.0000	0.8168	-0.0330	-0.0330	9	6	2.0833	2.2863	6.8856	9	2
AB	15	Chlorotetracycline	187.0000	23.0000	4.0000	2196.0491	6692.6729	0.1816	0.1563	0.4955	2.2036	0.9427	1.0061	1.9117	-0.5148	-0.1048	2546	120	57.41	93.0289	373.2905	49545	32
S	4	Cholesterol	102.0000	9.0000	3.0000	1206.4767	7507.9116	0.1026	0.0517	0.2109	0.7824	4.0630	3.1186	2.4332	-0.1605	0.1863	1611	80	7.6142	37.2946	157.8669	28571	24
S,PhAC	9	Cimetidine	19.0000	3.0000	0.0000	459.3784	4073.7322	0.4029	0.1934	0.7591	10.2766	0.3722	6.4360	1.6658	3.4549	5.0033	664	40	7.4392	17.5016	88.308	1226	17
S,AB,PhAC	16	Ciprofloxacin	101.0000	10.0000	3.0000	1247.6976	3400.7456	1.2467	0.1828	1.4960	3.8252	1.6957	0.2677	0.3649	2.1429	0.4326	1234	80	23.6997	29.2032	204.2236	11660	21
P	11	cis-Chlordane	119.0000	18.0000	1.0000	1763.2012	2632.9268	0.1912	0.1502	0.2485	3.4602	1.6981	1.7454	1.9663	-3.2467	1.0676	459	74	18.9957	23.9516	116.2086	4960	17

			Subgraph Count Indices			3D Descriptors for Comparitive Molecular Moment Analysis (CoMMA)											Total Topological Descriptors						
			# Paths = Length 5	# 3-Way Clusters	# 6-Member Rings	Principal Moment of Inertia along X-Axis	Principal Moment of Inertia along Y-Axis	Component of Dipole Moment along Inertial Y-Axis	Component of Dipole Moment along Inertial Z-Axis	Magnitude of Dipole Moment	Magnitude of Principal Quadrupole Moment	Displacement between Center of Mass and Center of Dipole Moment along X-Axis	Displacement between Center of Mass and Center of Dipole Moment along Y-Axis	Displacement between Center of Mass and Center of Dipole Moment along Z-Axis	The xx Component of Second Rank Tensor Translated so Origin Coincides With Center of Dipole	The yy Component of Second Rank Tensor Translated so Origin Coincides With Center of Dipole	Weiner Index	Platt f Index	Sum of Delta Intrinsic States of atoms	Total Electrotopological Index	Total Topological Index	Total Weiner Number	#Symmetry Classes in Molecule
Notes	**QSAR Cluster**	**Compound Name**	**nxp5**	**nxc3**	**nxch6**	**Ix**	**Iy**	**Py**	**Pz**	**P**	**Q**	**Dx**	**Dy**	**Dz**	**Qxx**	**Qyy**	**W**	**Pf**	**sumdell**	**tets2**	**totop**	**Wt**	**nclass**
S,P	10	Clorpyrifos	38.0000	8.0000	1.0000	1518.1132	2999.8074	0.7388	0.0000	0.7394	1.5261	4.6849	0.3488	0.0002	1.5235	0.0026	612	50	14.9426	16.8671	88.98	1335	15
S	4	Codeine	162.0000	13.0000	4.0000	1098.8831	1856.4359	0.1326	0.0280	0.4259	1.9912	1.3790	0.6457	1.3475	-0.0104	-0.8460	824	84	13.6669	51.9242	257.2345	40612	22
	1	Cyclotrimethylenetrinitramine	36.0000	6.0000	1.0000	752.8083	1056.5775	0.2225	0.3144	0.3983	4.5311	2.8437	0.5626	0.9685	2.3376	-0.7017	354	42	19.6862	11.53	113.5973	879	5
	2	Cymene	16.0000	3.0000	1.0000	154.9662	678.4987	0.0014	0.0052	0.0090	2.1604	0.5363	0.0939	0.5093	2.1476	0.8839	120	26	1.3507	10.1796	43.7442	314	7
S,AA	1	Cysteine	0.0000	2.0000	0.0000	175.4139	356.3286	0.4084	0.1650	0.4639	0.7559	0.8296	0.0067	1.3423	-0.4863	-0.0855	46	14	7.0091	4.55	32.2913	46	7
	6	d--n-Butylphthalate	43.0000	5.0000	1.0000	1100.5322	2746.7280	0.0779	0.0015	0.1164	2.1638	22.1178	11.7457	0.1862	0.9682	1.1917	1008	52	16.2657	15.6343	120.1898	2311	21
	14	d--n-Octylphthalate	46.0000	4.0000	1.0000	1671.9385	7992.7358	0.0004	0.0000	0.0997	1.4895	27.8305	0.1355	0.0000	0.0426	-1.5321	2724	64	17.1603	21.5504	142.1806	5678	14
	14	di-sec-Octylphthalate	52.0000	6.0000	1.0000	2796.2358	4354.4878	0.0487	0.6528	0.6792	3.0955	3.2693	2.2479	3.0550	-0.9933	1.1776	2388	68	19.0335	20.8551	146.798	5086	14
P	10	Diazinon	38.0000	8.0000	1.0000	1103.8807	2576.4204	0.2393	0.4411	0.5033	4.4044	1.8389	2.8485	5.0048	4.2908	-3.2732	720	52	12.6747	25.2782	97.7242	1574	15
DBP	1	Dibromoacetatic Acid	0.0000	2.0000	0.0000	304.3811	368.6839	0.3635	0.3015	0.5434	0.4616	0.1731	2.1314	0.3658	0.3350	-0.1787	29	12	5.6458	3.9863	24.5112	29	5
DBP	1	Dibromoacetonitrile	0.0000	1.0000	0.0000	214.0618	327.4244	0.1846	0.2306	0.2953	0.0186	0.0000	1.1127	0.9870	-0.0186	0.0114	18	8	2.8553	2.1839	16.0163	18	4
DBP	2	Dibromochloromethane	0.0000	1.0000	0.0000	198.6092	325.1898	0.2379	0.1034	0.2594	0.6766	0.0000	0.6279	0.2632	-0.6766	0.1075	9	6	1.7052	0.695	5.3722	9	3
DBP	2	Dibromochloropropane	0.0000	1.0000	0.0000	179.4238	1251.4248	0.1413	0.3201	0.3499	1.7037	0.0002	0.3587	1.6079	-1.7037	1.4258	31	10	2.6242	2.1652	11.4816	31	4
S	1	Dichloroacetic Acid	0.0000	2.0000	0.0000	189.0297	226.5332	0.3679	0.1487	0.5628	0.3662	1.5534	0.4211	0.2318	0.0683	0.2074	29	12	6.2886	5.6651	26.2455	29	5
	1	Dichloroacetonitrile	0.0000	1.0000	0.0000	152.4555	164.7694	0.0000	0.1675	0.3369	0.0431	0.7224	0.0000	0.5692	0.0106	-0.0431	18	8	3.6682	3.4733	17.6685	18	4
	1	Dichlorodifluoromethane	0.0000	4.0000	0.0000	134.4577	191.9879	0.2460	0.0000	0.2460	0.5667	0.0000	0.4082	0.0000	0.5667	0.0000	16	12	6.534	8.5341	25.119	16	3
	3	Dichlorodiphenyldichloroethylene	48.0000	6.0000	2.0000	1280.8843	3487.6978	0.3160	0.0065	1.1027	6.8677	0.6585	2.5868	0.0193	0.5638	6.3036	603	52	8.7409	19.5922	99.1232	2135	8
	1	Dichloropropane	0.0000	2.0000	0.0000	197.9101	254.1833	0.0171	0.2879	0.3476	0.4121	2.6216	0.0089	0.2555	0.2829	-0.4111	29	12	5.3164	2.853	21.111	29	5
P	11	Dieldrin	170.0000	20.0000	3.0000	1488.0356	2106.7551	0.0000	0.2432	0.4509	3.0115	1.5309	0.0002	1.7608	-0.8761	3.0115	520	88	18.1387	28.0848	188.1703	16825	11
S	9	Diethylphthalate	32.0000	4.0000	1.0000	897.8379	1063.6456	0.3112	0.0000	0.6795	4.6372	0.8407	1.1919	0.0000	0.9728	3.6644	446	40	13.8608	11.4836	98.497	1084	8
S,ES	5	Diethylstilbestrol	53.0000	6.0000	2.0000	610.5297	3323.4529	0.1687	0.0000	0.1801	3.0729	2.4434	9.8461	0.0015	2.6983	0.3746	814	56	9.3131	22.4167	120.2587	2638	8
	4	Digoxigenin	155.0000	20.0000	3.0000	1524.4807	4672.1011	0.9691	0.0265	1.1322	3.8467	3.2298	1.9600	0.2711	-0.9510	-0.4468	1758	106	26.5112	29.8648	257.2982	47322	28
PhAC	17	Digoxin	254.0000	32.0000	6.0000	3736.1450	46810.1953	0.2335	0.6347	1.2375	8.3915	4.5320	4.1496	4.2806	1.6881	-7.8721	14940	196	62.0251	129.0286	738.0654	1102711	55
PhAC	16	Diltiazem	102.0000	10.0000	2.0000	2243.2332	5308.1333	0.4493	0.7077	0.8486	5.5423	0.7530	2.4261	3.4882	5.1318	-3.4655	2077	86	20.184	42.6024	209.8006	15257	26
	9	Dipropylthiocarbamic Acid-s-ethylester	10.0000	2.0000	0.0000	621.2010	1670.3262	0.4305	0.0183	0.4731	1.8623	1.9907	0.5615	0.1480	1.5374	0.3054	220	24	5.8737	6.7061	43.5127	220	9
P	10	Disulfoton	11.0000	4.0000	0.0000	869.1507	2469.6440	0.0504	0.4514	0.5523	0.6530	3.1085	0.8119	3.4507	0.0586	-0.1664	356	30	7.4827	14.1139	39.6569	356	11
H	9	Diuron	25.0000	5.0000	1.0000	366.5488	2273.0137	0.5000	0.0546	0.6143	2.1421	3.5796	0.6075	0.3263	1.3979	0.7154	321	38	9.1986	10.5854	74.4993	742	13
S,AB	15	Doxycycline	182.0000	20.0000	4.0000	1897.5870	5809.5972	1.3701	0.6225	1.5197	4.7566	1.3871	0.2931	0.8402	3.4462	-0.8811	2336	114	49.0391	78.8016	346.9281	45143	31
PhAC	16	Enalaprilat	53.0000	8.0000	1.0000	976.4327	7068.4800	0.3988	0.3996	0.5692	6.3094	7.4079	3.6096	0.4011	1.5014	0.0272	1634	70	25.0982	25.8139	154.2482	4515	23
	10	Endosulfansulfate	113.0000	20.0000	1.0000	1760.8430	3130.1804	0.0003	0.3056	0.7311	3.2483	3.6836	0.0049	0.8654	-0.5675	3.2483	641	80	27.9742	38.1273	143.5446	7152	11
	16	Enrofloxacin	107.0000	11.0000	3.0000	1341.2472	4550.1855	1.1578	0.1841	1.5523	3.9554	1.8424	0.1969	0.3442	1.9495	0.9433	1601	86	24.0281	33.287	218.664	15088	23
	4	Equilenin	97.0000	11.0000	3.0000	518.4125	2753.6050	0.2682	0.0478	0.3804	2.2816	4.1341	2.4228	0.2564	1.1336	1.1120	724	72	12.0253	32.9735	169.3107	15139	20
	4	Equilin	97.0000	11.0000	3.0000	529.5236	2815.1526	0.3130	0.0871	0.4429	0.9400	3.8525	2.1211	2.1850	-0.4852	-0.4148	724	72	12.3981	30.2271	163.0387	15139	20
S,AB	16	Erythromycin	94.0000	14.0000	2.0000	5743.3848	6838.5083	0.5434	0.1510	0.8247	2.9768	2.5782	0.8953	1.9971	-1.3815	-1.3874	4495	112	58.3048	61.0072	274.0955	27758	38
ES,HO	6	Estriol	105.0000	12.0000	3.0000	596.3016	3248.3037	0.0839	0.0109	0.0869	1.3227	10.6112	11.1028	5.3375	-0.6521	0.5829	826	76	15.2199	29.9883	168.6355	17097	21
S,ES,HO	4	Estrone	97.0000	11.0000	3.0000	534.9425	2765.3069	0.4227	0.0913	0.4833	1.2049	3.7137	2.1862	0.3638	-0.8321	-0.0394	724	72	12.03	27.928	157.0097	15139	20
	7	ethyl-tert-Butyl Ether	0.0000	4.0000	0.0000	123.6765	323.9455	0.1543	0.0000	0.1640	0.8859	0.1324	1.2083	0.0000	0.7843	0.1016	46	16	2.5851	2.285	23.0115	46	5
S,AH	2	Ethylbenzene	10.0000	1.0000	1.0000	105.0760	339.1219	0.0082	0.0000	0.0719	1.7560	3.4506	0.5147	0.0000	0.6778	1.7469	64	18	0.6589	8.0864	34.8843	184	6
S	18	Ethylenediaminetetraacetic Acid (EDTA)	24.0000	6.0000	0.0000	965.7805	3381.7441	0.0017	0.7572	0.7572	9.8344	0.0464	0.0258	2.7943	-3.8376	3.8375	910	48	26.5053	19.3982	126.124	910	6
ED	2	exo-Dimethanonaphthalene	100.0000	8.0000	3.0000	251.2859	721.5801	0.0000	0.1925	0.4409	0.2145	3.0045	0.0001	0.2534	-0.0409	0.2145	197	58	3.6968	31.4137	117.2015	7387	8
PAH	12	Fluoranthrene	89.0000	6.0000	3.0000	490.5517	1018.0054	0.0004	0.0003	0.0268	4.2097	3.7969	0.0555	0.0786	3.9221	4.2091	364	56	1.7561	43.3264	142.2573	9577	9
PhAC	9	Fluoxetine	51.0000	8.0000	2.0000	1099.0315	4462.7490	0.0123	0.0277	0.8053	3.6028	1.4147	0.1535	0.5082	-0.0015	-1.8125	1148	62	19.4468	31.1108	146.65	3540	16
P	9	Fonofos	22.0000	5.0000	1.0000	657.3520	2136.4878	0.2170	0.1687	0.3618	3.3432	2.8969	0.3768	0.3484	1.5784	0.9025	316	36	5.8676	17.5272	52.2776	672	12
PhAC	9	Gemfibrozil	28.0000	8.0000	1.0000	588.9100	3430.4558	0.5339	0.1111	0.5514	1.3969	3.4628	0.3314	0.3572	1.0625	-0.0741	705	50	11.4611	17.4617	94.4339	1474	17
S,AA	1	Glycine	0.0000	1.0000	0.0000	49.3825	130.0206	0.0537	0.0000	0.4736	0.3324	0.5804	1.5492	0.0000	0.0043	0.3281	18	8	4.8773	2.9246	25.738	18	5
ED	13	Hexachlorobenzene	24.0000	6.0000	1.0000	1072.1543	1072.1582	0.0000	0.0000	0.0000	2.9940	0.0000	0.0000	0.0000	2.9940	2.9934	174	36	9.3459	3.0535	53.4637	486	2
	13	Hexachlorobutadiene	4.0000	4.0000	0.0000	625.8945	1177.5597	0.5198	0.0008	0.6114	7.0918	1.5659	2.7966	0.0062	5.1260	1.9668	121	24	7.1473	2.5257	32.4079	121	4
	13	Hexachlorocyclohexane	6.0000	0.0000	1.0000	116.1301	116.1303	0.0000	0.0000	0.0000	0.1032	0.0000	0.0000	0.0000	0.1032	0.1032	27	12	0	4.4225	17.8967	90	1
ED	11	Hexachloropentadiene	136.0000	32.0000	0.0000	2890.8179	3039.8105	0.0000	0.0000	0.0000	1.9229	0.0000	0.0000	0.0000	0.5310	-2.2832	748	100	28.5309	70.617	144.358	7136	7
S,PhAC	9	Ibuprofen	26.0000	5.0000	1.0000	389.8374	1910.8380	0.4130	0.1644	0.5162	1.4364	2.2086	1.7350	0.2002	0.8558	-0.1993	404	40	8.9442	14.1797	77.7241	905	12
AA	1	Leucine	4.0000	3.0000	0.0000	220.0124	484.0496	0.3859	0.1485	0.4898	0.1383	0.7624	0.4403	1.4614	0.0419	-0.0378	96	20	7.8176	5.397	39.7607	96	8
AB	16	Lincomycin	76.0000	11.0000	1.0000	1945.6948	5827.0620	0.0111	0.4092	0.6842	2.2759	1.7837	0.3624	0.9274	0.4716	-1.2352	1843	80	29.7742	34.4304	163.0578	6105	27
S,L	13	Lindane	24.0000	6.0000	1.0000	1122.0149	1161.5708	0.1611	0.0920	0.1855	0.1916	0.0001	0.4138	0.3969	0.1916	-0.0471	174	36	10.6204	7.6982	42.2244	486	2
H	9	Linuron	24.0000	4.0000	1.0000	383.5900	2233.0730	0.5332	0.2028	0.7090	2.8191	3.6404	0.0726	0.0675	1.5254	1.0391	332	36	10.1158	11.9266	79.3263	760	14
ES,PhAC	4	Mestranol	110.0000	14.0000	3.0000	687.7363	4071.4277	0.2856	0.0787	0.2982	4.0105	1.3323	0.4811	2.3124	1.7164	0.1117	1092	82	12.9696	42.0271	186.1342	21644	23
	1	Metformin	4.0000	3.0000	0.0000	163.4338	573.2252	0.4084	0.1024	0.4212	1.6517	1.1030	0.5472	0.0708	1.5769	-0.0989	96	20	5.6116	3.9925	43.9859	96	8
	2	Methylene Bromide	0.0000	0.0000	0.0000	27.1097	316.1404	0.2357	0.0000	0.2357	0.5045	0.0000	1.0330	0.0002	-0.5045	0.0000	4	2	0.625	1.0426	2.9355	4	2
	2	Methylene Chloride	0.0000	0.0000	0.0000	17.1701	144.9819	0.1410	0.0000	0.1410	0.3107	0.0003	0.8465	0.0002	-0.3107	0.0000	4	2	1.3056	0.6635	4.2976	4	2
S,P	8	methyl Parathion	28.0000	7.0000	1.0000	549.9229	2651.7883	0.1304	0.5221	0.6457	9.9741	0.9739	0.8364	0.1355	-4.4813	7.9341	473	44	13.9112	18.8058	92.1611	1029	12
	9	Metolachlor	47.0000	6.0000	1.0000	1520.0126	1804.9882	0.5098	0.1081	0.5648	3.5537	1.5960	2.1752	0.2083	-0.9889	-0.6407	656	50	11.3147	14.5158	101.6364	1455	19
	9	Metribuzin	28.0000	8.0000	1.0000	431.2857	1352.1702	0.1719	0.0006	0.7344	0.8950	2.1604	1.4871	0.0162	0.0491	0.8460	284	42	10.1625	11.1524	80.8534	718	12
H	9	Molinate	17.0000	2.0000	0.0000	303.6676	1201.1111	0.5113	0.0360	0.5411	2.8112	0.2335	1.7149	0.3447	2.3439	0.2999	206	28	5.5262	8.7479	49.4389	533	9
	2	Monobromobenzene	8.0000	1.0000	1.0000	89.5084	496.0972	0.0000	0.0000	0.2277	2.4141	1.5387	0.0000	0.0000	0.0000	2.4141	42	16	0.8228	6.8957	29.7124	131	5
	7	methyl-tert-butyl Ether (MTBE)	0.0000	4.0000	0.0000	115.5357	184.9442	0.1684	0.0000	0.1723	0.7802	0.4719	1.3391	0.0000	0.7448	0.0354	28	14	2.0833	1.7411	19.5633	28	4
S	1	N-Dimethylamine	0.0000	1.0000	0.0000	58.2644	114.3784	0.0749	0.0000	0.6665	0.7723	0.6142	0.1225	0.0000	0.0098	0.7625	18	8	2.6528	3.4908	23.6049	18	4

			Subgraph Count Indices			3D Descriptors for Comparitive Molecular Moment Analysis (CoMMA)											Total Topological Descriptors						
			# Paths = Length 5	#3-Way Clusters	#6-Member Rings	Principal Moment of Inertia along X-Axis	Principal Moment of Inertia along Y-Axis	Component of Dipole Moment along Inerial Y-Axis	Component of Dipole Moment along Inertial Z-Axis	Magnitude of Dipole Moment	Magnitude of Principal Quadripole Moment	Displacement between Center of Mass and Center of Dipole Moment along X-Axis	Displacement between Center of Mass and Center of Dipole Moment along Y-Axis	Displacement between Center of Mass and Center of Dipole Moment along Z-Axis	The xx Component of Second Rank Tensor Translated so Origin Coincides With Center of Dipole	The yy Component of Second Rank Tensor Translated so Origin Coincides With Center of Dipole	Weiner Index	Platt f Index	Sum of Delta Intrinsic States of atoms	Total Electrotopological Index	Total Topological Index	Total Weiner Number	# Symmetry Classes in Molecule
Notes	**QSAR Cluster**	**Compound Name**	**nxp5**	**nxc3**	**nxch6**	**Ix**	**Iy**	**Py**	**Pz**	**P**	**Q**	**Dx**	**Dy**	**Dz**	**Qxx**	**Qyy**	**W**	**Pf**	**sumdell**	**tets2**	**totop**	**Wt**	**nclass**
	9	N-nitrosodi-n-butylamine	8.0000	1.0000	0.0000	363.3437	1093.8734	0.3835	0.0001	0.6767	1.3530	0.2337	1.8434	0.0003	0.4346	0.9184	188	20	5.0501	7.8482	43.6381	188	7
	9	N-nitrosodi-n-propylamine	4.0000	1.0000	0.0000	247.2324	557.6726	0.3825	0.0001	0.6709	1.2283	0.3401	1.4645	0.0001	0.3992	0.8291	102	16	4.6017	6.2688	37.1351	102	6
	1	N-nitrosomorpholine	10.0000	1.0000	1.0000	131.4587	307.1545	0.2888	0.1143	0.4416	0.9978	2.8608	1.6836	0.4341	-0.3662	0.1021	64	18	5.4704	6.7221	44.6678	184	6
	1	N-nitrosopiperidine	10.0000	1.0000	1.0000	140.7075	304.3040	0.2502	0.1495	0.6085	0.8430	1.4323	0.0578	0.3224	0.0505	0.6961	64	18	4.059	7.0152	39.0946	184	6
	1	N-nitrosopyrrolidine	4.0000	1.0000	0.0000	84.7174	254.7965	0.2421	0.0352	0.6757	0.9677	1.1079	0.0937	0.1551	0.1216	0.8433	43	16	3.815	6.0656	35.5828	118	5
	18	N-triacetic Acid	12.0000	4.0000	0.0000	574.9562	819.2914	0.1712	0.6211	0.6597	9.0561	0.9097	0.8427	2.2507	-6.6072	5.7729	270	30	17.4113	12.0416	80.1925	270	5
	9	Nitrosodibutylamine	8.0000	1.0000	0.0000	178.4437	1433.6268	0.5193	0.0000	0.6252	1.6557	0.3359	1.5831	0.0000	1.1422	0.5135	188	20	5.0501	7.8482	43.6381	188	7
	18	Nitrilotriacetic Acid	12.0000	4.0000	0.0000	490.9178	930.1865	0.4124	0.3342	0.5309	12.0856	0.2705	0.9628	0.7440	-12.0738	4.7923	270	30	17.4113	12.0416	80.1925	270	5
	1	Nitrosodiethylamine	0.0000	1.0000	0.0000	131.4826	255.7314	0.1864	0.0000	0.7300	1.0925	1.1005	0.0294	0.0000	0.0712	1.0213	48	12	3.9139	4.751	30.5371	48	5
S	3	Nitrobenzene	12.0000	2.0000	1.0000	144.2756	437.7393	0.0286	0.0000	0.5942	1.1659	0.3510	0.2534	0.0000	0.0027	1.1632	88	22	5.8751	5.8196	54.2658	239	7
	4	Norethindrone	84.0000	7.0000	3.0000	512.8732	2099.5930	0.0713	0.1889	0.7147	1.5430	3.3582	0.1000	0.4617	-0.0935	1.5275	548	62	6.3208	32.0582	122.5658	11907	18
AB	16	Norfloxacin	90.0000	9.0000	3.0000	940.8177	3890.8025	1.2142	0.0420	1.4461	4.4340	1.7148	0.2742	0.6070	2.2909	0.8363	1116	72	22.859	26.2574	186.0679	8930	21
	9	N N diethyl 3 methylbenzamide	24.0000	4.0000	1.0000	402.9850	1269.1726	0.6635	0.0002	0.6638	4.8746	1.0397	0.7105	0.0013	4.8698	0.0048	307	36	6.5538	11.1844	72.1016	692	12
	1	o-Cresol	10.0000	2.0000	1.0000	158.4998	225.9372	0.0214	0.0000	0.0496	2.4556	0.8048	2.1791	0.0003	0.4280	2.4525	60	20	3.3961	6.3317	40.9664	182	8
ED	11	Octachloro-4-7-methanotetrahydroindane	119.0000	18.0000	1.0000	1667.4930	2522.9360	0.0322	0.2266	0.3415	2.5587	1.0201	0.0724	0.3208	-0.7137	1.1259	459	74	18.9957	23.9516	116.2086	4960	17
ED	11	Octachloroepoxide	154.0000	22.0000	2.0000	1591.0120	2629.8701	0.1025	0.0834	0.3332	1.8165	0.7313	1.3173	5.8835	-0.0657	1.5440	523	86	21.3997	37.3876	159.2402	9245	18
	1	p-Cresol	12.0000	2.0000	1.0000	93.4081	340.6002	0.0892	0.0000	0.1411	2.8961	0.3497	0.2541	0.0000	1.1561	1.7401	62	20	3.3348	6.4005	40.798	182	6
	2	p-Dichlorobenzene	12.0000	2.0000	1.0000	89.5007	741.3849	0.0000	0.0000	0.0000	1.9430	0.0000	0.0003	0.0000	1.1700	1.9430	62	20	3.3653	6.8616	34.736	182	3
	1	Paraxanthine	40.0000	6.0000	1.0000	357.9181	718.6223	0.1320	0.0306	0.7596	5.0161	1.1567	0.5867	0.3961	-0.0159	-0.4662	215	42	11.2598	12.8589	99.9327	1301	13
	9	Paroxetine	84.0000	10.0000	3.0000	1702.0732	4007.1782	0.2176	0.1238	0.2716	1.0661	4.0570	4.1046	4.0164	0.6701	0.1358	1567	80	16.4539	34.4927	185.5464	16747	23
	19	Perchloric Acid	0.0000	4.0000	0.0000	91.8061	155.4283	0.0002	0.1862	1.0904	0.2605	1.6678	0.0008	0.3187	0.0076	-0.2605	16	12	6.0556	10.7124	27.8557	16	3
S	12	Phenanthrene	55.0000	4.0000	3.0000	315.1087	903.6428	0.0095	0.0000	0.0095	3.6724	0.0003	1.0449	0.0000	3.6724	3.2518	271	44	1.367	27.5177	98.7403	3511	7
S	1	Phenol	8.0000	1.0000	1.0000	90.2208	191.5561	0.0921	0.0000	0.1106	2.5196	1.6527	2.0502	0.0000	1.7456	0.7740	42	16	2.8938	5.3877	36.3488	131	5
S	3	Phthalic Anhydride	31.0000	4.0000	1.0000	273.1031	440.7403	0.0001	0.0000	1.0915	0.0243	0.2813	0.0002	0.0000	0.0000	-0.0243	137	34	9.8379	10.9868	83.3043	874	6
	9	Pramitol	32.0000	5.0000	1.0000	1025.9146	1192.6646	0.2081	0.0235	0.5209	4.9043	0.3591	0.8071	0.4342	0.7577	4.1164	458	42	7.7403	14.5264	93.428	1096	9
S,HO	8	Progesterone	98.0000	9.0000	3.0000	601.1573	3542.6272	0.1935	0.4017	0.5362	12.7234	5.0363	3.1239	4.0635	-8.6865	8.5976	867	72	11.9352	32.2041	154.4724	17841	21
PAH	12	Pyrene	88.0000	6.0000	4.0000	498.9910	909.9629	0.0000	0.0000	0.0000	4.2760	0.0003	0.0000	0.0000	4.2760	3.8967	362	56	1.858	44.3387	143.2875	10677	5
PhAC	16	Ranitidine	29.0000	5.0000	0.0000	814.4919	7432.7734	0.2253	0.1261	0.5957	1.5489	3.5895	1.1889	1.3134	0.1439	1.3250	1227	52	11.5487	19.4301	111.8423	2326	20
	1	s-1-Methyl-5-3-Pyridinyl-2-Pyrrolidinone	31.0000	4.0000	1.0000	305.9994	969.8868	0.3618	0.3416	0.6633	1.1519	1.5443	0.9352	0.2284	0.0623	0.7303	238	38	6.9022	12.8848	78.9081	1114	13
	9	Salbutamol	33.0000	8.0000	1.0000	550.5433	2758.9746	0.4537	0.1220	0.4731	0.6181	2.1827	0.1684	1.4280	0.4389	0.0011	560	48	13.5232	9.3152	92.1717	1225	15
AA	1	Serine	0.0000	2.0000	0.0000	160.6930	230.3558	0.3831	0.2868	0.6407	0.4543	0.0392	0.5782	0.9087	-0.2259	0.1621	46	14	8.04	5.742	37.715	46	7
	9	Simazine	24.0000	3.0000	1.0000	911.6400	951.4818	0.0019	0.0000	0.6846	5.9225	0.2132	0.0008	0.0000	0.0000	5.9224	260	32	6.4596	11.2833	72.7431	649	8
AB	19	Sulfachlorpyridazine	44.0000	8.0000	2.0000	398.0069	3950.2231	0.8718	0.0000	1.4926	7.8554	3.0893	0.6951	0.0001	2.6797	5.1757	638	54	17.5082	20.2948	110.8163	2278	15
AB	19	Sulfadimethoxine	54.0000	9.0000	2.0000	868.7017	4023.4807	0.8275	0.0012	1.1598	8.9985	3.2769	0.0339	0.0514	4.5813	4.4171	956	62	20.4638	19.5989	139.6848	3465	18
AB	19	Sulfamerazine	43.0000	8.0000	2.0000	454.4897	2925.5393	0.4695	0.0020	0.9025	6.0298	4.3822	0.4872	0.0734	1.6321	4.3977	627	54	16.7142	20.8806	111.3576	2278	15
S,AB	19	Sulfamethazine	46.0000	9.0000	2.0000	606.2046	3230.9436	0.6129	0.0044	0.9092	8.2613	4.3119	0.6487	0.0518	3.7546	4.5064	722	58	17.4454	22.1522	117.3798	2637	13
AB, PhAC	19	Sulfamethizole	38.0000	8.0000	1.0000	457.7110	3049.0801	1.1599	0.0104	1.4106	12.5755	1.5586	1.2884	0.0662	8.5030	4.0717	535	52	16.9957	19.2156	103.3761	1867	14
AB	19	Sulfamethoxazole	38.0000	8.0000	1.0000	505.6649	2667.8994	1.0653	0.0911	1.3456	5.8631	1.6744	1.3985	0.1039	3.6121	2.1845	535	52	16.4671	20.9475	106.8783	1867	14
AB	19	Sulfathiazole	34.0000	7.0000	1.0000	407.2141	2520.7915	0.2612	0.0027	1.0821	2.9895	3.1330	0.8280	0.0688	0.1741	2.8129	448	48	14.9691	20.6599	91.9879	1547	13
H	9	Terbacil	29.0000	9.0000	1.0000	497.7588	1103.9886	0.3249	0.0017	0.5358	2.6202	3.8358	0.8909	0.0066	-0.9635	-1.6567	269	44	13.3797	9.3085	82.7077	704	12
P	10	Terbufos	12.0000	8.0000	0.0000	763.9087	3009.0227	0.1579	0.3668	0.4017	7.5966	2.9101	1.8425	5.5571	7.2046	-5.9689	412	38	8.2453	14.2734	43.5656	412	10
	15	Terramycin	182.0000	20.0000	4.0000	2022.7040	5167.8428	0.7042	0.1922	1.1228	5.9263	1.1756	0.4928	2.1209	2.3557	3.3857	2336	114	52.8031	85.7196	353.7815	45143	31
	7	tert amyl methyl Ether	0.0000	4.0000	0.0000	150.4944	256.9858	0.1138	0.1042	0.2008	0.8682	1.0391	0.8363	0.5752	0.3194	0.3067	44	16	2.4583	2.6372	23.0088	44	6
S,HO	4	Testosterone	90.0000	8.0000	3.0000	496.7452	2680.8655	0.0469	0.0522	0.6833	1.2642	3.6005	1.6371	2.0594	0.0060	1.0511	641	66	10.4973	25.7543	136.9225	13763	19
S	13	1,1,2,2 Tetrachloroethane	0.0000	2.0000	0.0000	281.8305	356.6922	0.0000	0.0000	0.0048	0.9234	0.1341	0.0007	0.0020	0.8350	0.9232	29	12	3.5309	1.365	15.6442	29	2
S	13	1,1,2,2, Tetrachloroethylene (PCE)	0.0000	2.0000	0.0000	285.2621	353.5459	0.0000	0.0000	0.0000	1.1329	0.0000	0.0000	0.0000	1.0558	1.1329	29	12	3.5309	1.365	15.6442	29	2
S,AB	15	Tetracycline.hin	168.0000	19.0000	4.0000	1835.5490	5550.8569	0.5439	0.1154	0.7765	7.7079	0.3768	0.6782	0.5798	1.6742	3.3616	2196	110	47.3737	67.0063	332.0904	42500	30
ED	6	Thio-N-methyl-carbamoyl-oxy-methylester	5.0000	2.0000	0.0000	123.9382	1556.9707	0.0665	0.0713	0.2154	3.8880	0.3144	15.9845	1.1867	0.6842	1.2268	151	20	9.6407	5.9185	45.917	151	10
S,AA	1	Threonine	0.0000	3.0000	0.0000	175.0438	330.7648	0.0731	0.2824	0.4321	0.5552	0.9131	1.5025	0.5720	-0.0377	0.2711	65	18	9.2689	7.3162	41.7452	65	8
S,AH	2	Toluene	8.0000	1.0000	1.0000	91.5973	197.2618	0.0017	0.0000	0.0529	1.4244	2.8357	0.1137	0.0000	1.1294	1.4244	42	16	0.3449	7.0195	31.0674	131	5
ES	20	Tributyl Tin	12.0000	1.0000	0.0000	811.8245	2052.7202	0.0172	0.1101	0.1129	0.5045	0.1249	0.6906	2.5729	0.4793	-0.4856	300	24	2.287	9.4577	29.0179	300	5
S,DBP	3	Trichloroacetic Acid	0.0000	5.0000	0.0000	325.4921	369.6898	0.3927	0.0000	0.5364	0.5998	1.6157	0.5231	0.0000	0.3215	0.2783	42	18	7.6551	9.1761	29.8323	42	5
	2	1,1,2 Trichloroethene (TCE)	0.0000	1.0000	0.0000	121.3447	321.5974	0.0278	0.0000	0.0297	0.9529	0.3085	0.5743	0.0000	0.9457	0.5795	18	8	2.5741	1.549	12.5193	18	4
AM	3	Triclosan	44.0000	6.0000	2.0000	526.6010	3548.6460	0.1678	0.0000	0.3377	5.5322	1.5053	0.0313	0.0000	1.3663	4.1659	536	50	12.2245	13.4909	105.0623	2316	17
AB	9	Trimethoprim	58.0000	7.0000	2.0000	867.3920	3155.9792	0.1542	0.0447	0.2534	6.4013	2.9334	3.9386	5.6716	2.5673	3.0991	946	60	12.4926	22.8866	145.7629	3874	17
S	10	triphenyl Phosphate	60.0000	7.0000	3.0000	1155.8573	3284.4592	0.1415	0.1420	0.3040	2.7781	5.6246	1.5418	2.9560	1.0698	-1.5135	1204	66	15.4141	41.5819	146.304	4564	7
	10	tris 2 Chloroethyl Phosphate	15.0000	4.0000	0.0000	1419.3313	2667.4719	0.0168	0.1689	0.1703	0.8988	0.0560	0.5150	2.0825	-0.8793	0.8744	343	30	14.4328	12.852	54.6633	343	6
AB	17	Tylosin	159.0000	20.0000	3.0000	6188.8774	29610.6445	0.3922	0.4435	0.7200	15.1762	5.6615	6.5149	2.0463	10.1466	-5.0111	15462	168	71.984	73.5171	431.5438	120355	57
	1	t Butyl Alcohol	0.0000	0.0000	0.0000	14.3856	53.6047	0.1875	0.0000	0.1951	0.6462	0.7491	0.5508	0.0000	0.5971	0.0491	4	2	1.6944	0.6694	9.3835	4	3
S,AA	1	Valine.hin	0.0000	3.0000	0.0000	176.4189	334.4675	0.2137	0.1685	0.5063	0.0934	0.5946	0.4168	1.4129	0.0111	-0.0678	65	18	7.4700	4.1072	36.6983	65	7
S, AA		Asparagine	4.0000	3.0000	0.0000	137.3298	551.9764	0.4996	0.0595	0.5835	1.5535	4.0141	0.2460	0.3615	-0.7419	-0.0968	96.0000	20.0000	10.8249	7.3501	50.1692	96.0000	9.0000
S, AA		Aspartic Acid	4.0000	3.0000	0.0000	142.3582	585.1631	0.1482	0.2765	0.3165	2.3017	1.2191	1.2166	0.8703	1.0395	-1.0433	96.0000	20.0000	11.4988	8.8317	52.6341	96.0000	9.0000
S, AA		Histidine	12.0000	3.0000	0.0000	157.6205	921.0010	0.2561	0.0406	0.3223	4.2728	2.0779	0.8392	1.3137	-0.9813	0.2499	165.0000	28.0000	9.3994	10.4433	65.1158	352.0000	11.0000
S, AA		Lysine	5.0000	2.0000	0.0000	145.4799	1187.2531	0.0914	0.5505	0.5782	1.1690	0.4095	0.4472	0.5756	-1.0445	1.0613	143.0000	20.0000	8.5844	6.1935	44.9297	143.0000	10.0000

			Subgraph Count Indices			3D Descriptors for Comparitive Molecular Moment Analysis (CoMMA)											Total Topological Descriptors						
			# Paths = Length 5	#3-Way Clusters	#6-Member Rings	Principal Moment of Inertia along X-Axis	Principal Moment of Inertia along Y-Axis	Component of Dipole Moment along Inerial Y-Axis	Component of Dipole Moment along Inertial Z-Axis	Magnitude of Dipole Moment	Magnitude of Principal Quadripole Moment	Displacement between Center of Mass and Center of Dipole Moment along X-Axis	Displacement between Center of Mass and Center of Dipole Moment along Y-Axis	Displacement between Center of Mass and Center of Dipole Moment along Z-Axis	The xx Component of Second Rank Tensor Translated so Origin Coincides With Center of Dipole	The yy Component of Second Rank Tensor Translated so Origin Coincides With Center of Dipole	Weiner Index	Platt f Index	Sum of Delta Intrinsic States of atoms	Total Electrotopological Index	Total Topological Index	Total Weiner Number	# Symmetry Classes in Molecule
Notes	**QSAR Cluster**	**Compound Name**	**nxp5**	**nxc3**	**nxch6**	**Ix**	**Iy**	**Py**	**Pz**	**P**	**Q**	**Dx**	**Dy**	**Dz**	**Qxx**	**Qyy**	**W**	**Pf**	**sumdell**	**tets2**	**totop**	**Wt**	**nclass**
S, AA		Methionine	4.0000	2.0000	0.0000	147.9831	1008.2385	0.2751	0.5057	0.6133	1.7373	0.1180	0.7577	0.8671	0.5294	-0.9194	102.0000	18.0000	7.4537	5.8340	37.7209	102.0000	9.0000
S, DBP		N-nitroso dimethyl amine (NDMA)	0.0000	1.0000	0.0000	57.0324	123.8753	0.2195	0.0001	1.0488	1.2847	0.2609	0.0675	0.0010	0.0563	1.2284	18.0000	8.0000	2.6528	3.4908	23.6049	18.0000	4.0000
S, AA		Phenylalanine	18.0000	3.0000	1.0000	203.2934	1101.3171	0.3270	0.1876	0.4635	1.2560	1.3601	0.9247	0.3205	0.5976	0.4446	212.0000	30.0000	8.5541	11.4686	65.9145	486.0000	10.0000
S		Urea	0.0000	1.0000	0.0000	43.0044	48.1178	0.9057	0.0000	0.9057	2.0820	0.0211	0.3311	0.0000	2.0817	0.0003	9.0000	6.0000	3.1667	2.6046	20.2482	9.0000	3.0000
Marine Toxin		Anatoxin a	30.0000	4.0000	0.0000	286.8275	711.8845	0.6868	0.6015	1.1011	1.7030	1.3408	0.4059	0.6417	0.7660	0.4272	177.0000	36.0000	6.5704	10.7436	65.7271	1066.0000	12.0000
Marine Toxin		Cylindrospermopsin	116.0000	15.0000	3.0000	1889.4125	4420.8535	1.3528	0.3198	1.4183	10.5558	0.8512	0.3369	0.8044	4.1351	0.7903	1748.0000	94.0000	35.5885	43.1226	239.1495	26067.0000	26.0000
Marine Toxin		Microcystin LR	135.0000	22.0000	1.0000	14388.4570	18163.1172	1.1651	1.2165	1.7972	19.1394	1.5971	2.8222	2.9181	-0.9204	-6.1703	22868.0000	184.0000	88.6029	84.7113	443.3233	84061.0000	66.0000
Marine Toxin		Saxitoxin	103.0000	14.0000	1.0000	1044.1387	2174.7734	0.0118	0.0707	0.2045	4.4033	17.9893	14.7684	3.9878	0.1837	-2.6765	805.0000	74.0000	26.3172	28.9214	184.6335	7898.0000	20.0000

Legend:

S = Surrogate
PhAC = Pharmaceutically Active Compound
ED = Endocrine Disruptor
ES = Estrogenicity
HO = Hormone
P = Pesticide
H = Herbicide
AHC = Aromatic Hydrocarbon
PHA = Polyaromatic Hydrocarbon
AB = Antibiotic
AM = Antimicrobial
AA = Amino Acid
DBP = Disinfection Byproduct

			Traditional Kappa Shape Indices				Other 2D Descriptors		Atom Type E-State Descriptors							H Atom Type E-State Descriptors					
			Kappa Zero	Kappa 1	Kappa 2	Kappa 3	Octanol/Water Partition Coefficient	Mouse Oral LD50	-CH3 Group	-CH2- Group	=CH- Aromatic Carbon	=C< Double Bonded Carbon	=O Double Bonded Oxygen	-Cl Chloride Group	-OH Polar H Atom	CH Sum of Hydrogen E-States on Non-Polar H Groups	Largest Atom Hydrogen Aton E-State in Molecule	Largest Atom E-State Value in Molecule	Smallest Hydrogen Atom Hydrogen E-State Value in Molecule	Smallest Atom E-State Value in Molecule
Notes	**QSAR Cluster**	**Compound Name**	**k0**	**k1**	**k2**	**k3**	**LogP**	**LD50**	**SsCH3**	**SssCH2**	**SaaCH**	**SdssC**	**SdO**	**SsCl**	**SHsOH**	**SHother**	**Hmax**	**Gmax**	**Hmin**	**Gmin**
DBP	1	1,1 Dichloropropanone	4.0668	6	2.2222	3	1.0723	3.6658	1.338	0	0	-0.2099	9.8796	10.0571	0	0.6042	0.9291	9.8796	0.6042	-0.8426
AH	2	1,2,4 Trimethylbenzene	8.5882	7.1111	2.7222	1.7041	3.7399	6.4346	6.3924	0	6.5023	0	0	0	0	4.8186	1.1101	2.2037	0.5003	1.3455
	2	1,2 Dichlorobenzene	4.8165	6.125	2.52	1.4876	3.089	1.2872	0	0	7.1907	0	0	11.1535	0	4.6911	1.2036	5.5767	1.142	0.6057
AH	2	1, 2 Dimethylbenzene	4.8165	6.125	2.52	1.4876	3.2193	9.3453	4.2407	0	8.3565	0	0	0	0	5.3214	1.0878	2.1204	0.4992	1.3681
AH	2	1,3,5 Trimethylbenzene	4.2941	7.1111	2.7222	2	3.5907	4.1226	6.375	0	6.5625	0	0	0	0	4.825	1.1056	2.1875	0.5027	1.3542
P	2	1,4 Dichlorobenzene	3.6124	6.125	2.52	1.8	2.9825	1.2514	0	0	7.0154	0	0	11.106	0	4.8143	1.2036	5.553	1.2036	0.717
S,ED	3	1,4 Dichlorophenoxyacetic Acid	14.4813	11.0769	5.0242	3.7037	2.3947	0.9048	0	-0.4153	4.5819	-1.05	10.1567	11.3339	2.6676	5.2419	2.6676	10.1567	1.114	-1.05
S,HO,ES	4	17a Estradiol	24.2963	12.719	4.7769	2	3.4696	1.3158	0	6.9947	5.9495	0	0	0	4.951	11.1689	2.5391	10.1132	0.5784	-0.035
ED	5	2,2,2 Trichloro 1,1-bis-4-chlorophenyl Ethanol	14.295	13.4321	5.3254	3.0625	4.991	6.0191	0	0	13.4607	0	0	17.7338	2.6912	10.7768	2.6912	10.3182	1.3237	-1.5742
ED	5	2,2 bis-p-Chlorophenyl 1,1,1 Trichloroethane	16.2423	15.39	6.1855	3.9862	6.14	4.1311	0	0	14.4989	0	0	30.1001	0	11.8768	1.3579	6.1127	1.1605	-1.4567
ED	5	2,2-bis-p-Chlorophenyl 1,1 Dichloroethane	15.3702	14.41	6.4379	3.75	5.4662	4.0655	0	0	15.037	0	0	23.9424	0	11.5456	1.3232	6.0919	1.0282	-0.5349
ED	5	2,2 bis-p-Methoxyphenyl 1,1,1 Trichloroethane	19.1105	17.3554	7.513	4.4875	5.4739	3.1326	3.232	0	14.9916	0	0	18.5518	0	13.7411	1.3944	6.1839	0.7344	-1.4552
S,ED	3	2,3,4,5,6 Pentachlorophenol	10.5419	10.0833	3.3951	1.5625	4.9449	6.1448	0	0	0	0	0	27.9041	2.6885	0	2.6885	9.201	2.6885	-0.3632
	3	2,3,5,6 Tetrachloroterephthalic Acid	12.0412	14.0625	5.1042	2.4883	4.3035	12.9638	0	0	0	-2.8968	21.5892	22.382	5.5928	0	2.7964	10.7946	2.7964	-1.4484
	3	2,3 Naphthalenedicarboxylic Acid	14.4494	12.4567	5.1042	2.6514	2.9169	0.4544	0	0	9.7836	-2.4664	21.8131	0	5.5157	8.2192	2.7579	10.9066	1.2469	-1.2332
ED	3	2,4,5 Trichlorophenoxyacetic Acid	16.0458	12.0714	5.1856	3.5918	3.0464	0.6765	0	-0.4745	2.7617	-1.0906	10.2087	17.0674	2.6812	4.0827	2.6812	10.2087	1.1381	-1.0906
ED	3	2,4 Dichloro-4'-nitrodiphenyl Ether	21.3908	14.41	6.4379	3.9958	4.4291	2.5762	0	0	10.8014	0	10.6022	11.721	2.7609	10.1045	2.7609	10.6022	1.3626	-0.2232
	3	2,4 Dinirophenol	14.4813	11.0769	4.4815	2.7211	1.2262	1.5124	0	0	2.9004	0	20.6709	0	8.3113	4.574	2.8124	10.3511	1.4731	-0.6088
S	6	2,4 Dinitrotoluene	14.4813	11.0769	4.4815	2.7211	1.5672	0.237	1.59	0	3.8448	0	20.9126	0	5.5409	5.0479	2.7724	10.5111	0.71	-0.3825
	7	2,6 bis-1,1 Dimethylethyl 2,5 Cyclohexadiene 1,4 dione	12.7908	14.0625	4.3491	3.25	3.6807	0.346	11.7239	0	2.9396	0	23.8934	0	0	6.1701	1.3893	12.2756	0.5653	-0.2803
	7	2,6 bis-1,1 Dimethylethyl Phenol	11.1663	13.0667	4.1076	2.9822	4.7709	0.0002	12.7172	0	6.0377	0	0	0	2.5598	6.6891	2.5598	10.26	0.515	-0.0086
	7	2,6 di-tert-butyl-p-Cresol	12.7908	14.0625	4.3491	3.25	5.1767	0.0002	14.8844	0	4.1757	0	0	0	2.5653	6.1622	2.5653	10.3845	0.5206	-0.0178
	8	2,6 Dinitrotoluene	11.471	11.0769	4.4815	2.4793	1.5842	0.0002	1.4374	0	4.0323	0	21.0221	0	5.5448	4.9682	2.7724	10.5111	0.7862	-0.3588
	3	2,6 Naphthalenedicarboxylic Acid	14.4494	12.4567	5.1042	2.8311	3.26	3.5984	0	0	9.1485	-1.9922	21.4513	0	5.3966	8.5493	2.6983	10.7257	1.4031	-0.9961
S,ED	9	2-chloro-2'-6'-diethyl-N-methoxymethyl-acetanilide (Alachlor)	20.1867	16.0556	8.2268	3.9958	2.9333	1.1989	5.7337	1.9425	6.1058	-0.1304	11.9527	5.6767	0	8.0689	1.2721	11.9527	0.5353	-0.1304
ED	2	3,4,5,6,7,8,8a-Heptachlorodicyclopentadiene	10	5.625	1.7778	0.6145	3.1526	0.0002	0	2.8153	0	0	0	0	0	7.3562	1.0003	2.4433	0.5031	0.9248
ED	1	3-amino-1H-1,2,4 Triazole	4.6689	4.1667	1.6327	0.9796	-0.8808	12.9108	0	0	1.4259	0	0	0	0	1.3118	1.7493	5.0243	1.3118	0.287
	9	3-Hydroxycarbofuran	20.3156	13.4321	4.9383	2.56	2.1138	0.0002	5.4105	0	5.4487	0.4317	0	0	2.5899	8.3678	2.5899	10.1063	0.647	-0.6492
S	3	4,6 Dichlorophenol	8.5882	7.1111	2.7222	1.7041	2.8589	2.5348	0	0	4.5058	0	0	11.0009	2.565	3.8746	2.565	8.8531	1.2591	0.0565
ED	9	4-amino-6-tert-butyl-3-methylthio-as-triazin-5,4H-one	14.6144	12.0714	4.2449	2.5344	2.0309	3.0648	7.4951	0	0	0.5256	11.7172	0	0	2.477	1.7641	11.7172	0.6042	-0.3312
S,ED	4	4 Nonylphenol	18.0618	14.0625	9.0741	7.0582	6.0608	1.0106	2.2548	10.6371	7.5893	0	0	0	2.5092	8.9707	2.5092	9.1487	0.3349	0.3642
	2	5-methyl-1H-Benzotriazole	10	6.6942	2.56	1.241	1.8822	2.8438	2.0358	0	6.0056	0	0	0	0	4.3119	1.8354	3.874	0.5706	0.9306
ED	9	6-chloro-N-ethyl-N'-isopropyl-1,3,5 Triazine-2,4-diamine	15.4437	12.0714	5.7778	4.3878	2.5926	2.6739	5.9747	0.7514	0	0	0	5.727	0	3.0553	1.7846	5.727	0.5163	0.1936
PhAC	3	Acetaminophen	10.2512	9.0909	4.1327	3.2653	0.4933	0.2745	1.4374	0	6.3095	-0.1151	10.5245	0	2.5412	5.8566	2.5412	10.5245	0.6684	-0.1151
H	9	Acetochlor	22.5949	16.0556	8.2268	4.2667	2.8728	0.4979	5.9714	1.6519	6.0272	-0.1304	11.9527	5.6767	0	8.0619	1.2697	11.9527	0.5337	-0.1304
S,AA	1	Alanine	4.6689	6	2.2222	3	-2.3284	9.5633	1.419	0	0	-0.963	9.5741	0	2.5521	1.3753	2.5521	9.5741	0.5434	-0.963
	10	Aldicarbsulfone	14.8417	14	5.1856	4.8889	-0.3102	1.3245	5.3716	0	0	-0.7449	32.8526	0	0	4.5012	1.8051	11.1509	0.6963	-3.268
	11	Aldrin	17.7784	11.7959	2.8613	0.8554	5.4712	2.4672	0	1.0382	0	0.6538	0	39.2112	0	6.4975	1.1493	6.762	0.6791	-1.3655
ED	9	alpha-naphthyl-N-Methylcarbamate	17.6414	11.4844	5.3651	2.7654	2.5439	3.8018	1.5352	0	13.3839	-0.4525	11.0916	0	0	9.7067	1.7932	11.0916	0.6878	-0.4525
HO	4	Androsterone	24.2963	12.719	4.7769	2	2.771	0.0002	0	10.5191	0	0.5737	11.9757	0	2.3844	9.9165	2.3844	11.9757	0.5499	-0.0257
PAH	12	Anthracene	8.219	9.2422	3.8678	1.76	4.6703	0.9473	0	0	21.4215	0	0	0	0	12.1921	1.3016	2.2407	1.1676	1.3113
	9	Atrazine	15.4437	12.0714	5.7778	4.3878	2.5926	2.6739	5.9747	0.7514	0	0	0	5.727	0	3.0553	1.7846	5.727	0.5163	0.1936
S,AH	13	Benzene	0	4.1667	2.2222	1.3333	1.9516	7.1333	0	0	12	0	0	0	0	6.3187	1.0531	2	1.0531	2
S,PAH	12	benzo-a-Pyrene	26.0206	12.5347	4.75	1.8208	6.2238	1.4694	0	0	26.5126	0	0	0	0	15.5967	1.3843	2.3091	1.212	1.3179
ED	1	benzo-e-1,3,2 Dioxathiepin-3-oxide	9.0471	6.5089	2.025	0.761	0.8582	1.136	0	1.0998	0	-0.4876	10.7033	0	0	6.4945	1.1229	10.7033	0.6527	-0.4876
HO,ES	4	beta-Estradiol	24.2963	12.719	4.7769	2	3.4696	1.3158	0	6.9947	5.9495	0	0	0	4.951	11.1689	2.5391	10.1132	0.5784	-0.035
S	4	beta Sitostanol n Hydrate	38.0448	20.28	8.7885	4.16	7.5768	0.0002	7.2236	18.5164	0	0	0	0	2.3793	13.7449	2.3793	10.1025	0.3646	0.0211
	14	bis-2-Ethylhexyl-adipate	28.9625	26	18.3673	15.7527	5.249	1.8223	8.6438	12.3309	0	-0.2798	23.5955	0	0	12.1014	0.8542	11.7978	0.3864	-0.1399
S,ED	5	Bisphenol	13.6929	13.4321	5.3254	3.0625	3.65	4.596	4.2337	0	14.4432	0	0	0	5.0985	11.6237	2.5492	9.2963	0.6307	-0.1514
DBP	1	Bromochloroacetic Acid	4.6689	6	2.2222	3	0.5787	4.473	0	0	0	-1.0586	9.5203	4.9298	2.5859	0	2.5859	9.5203	0.9673	-1.0586
DBP	1	Bromochloroacetonitrile	3.4948	5	2.25	4	0.8435	18.2101	0	0	0	0	0	5.0177	0	0	0.8687	7.7147	0.8687	-0.5255
DBP	2	Bromochloromethane	1.4314	3	2	0	1.1345	3.7022	0	0.5347	0	0	0	4.9151	0	0	0.5604	4.9151	0.5604	0.5347
DBP	2	Bromodichloromethane	1.8062	4	1.3333	0	1.8088	0.0651	0	0	0	0	0	9.9136	0	0	0.7771	4.9568	0.7771	-0.4097
DBP	2	Bromoform	0.9769	4	1.3333	0	2.5818	3.3975	0	0	0	0	0	0	0	0.6313	0.6313	3.1042	0.6313	0.2708
DBP	2	Bromomethane	0.6021	2	0	0	0.9308	9.0527	1.8125	0	0	0	0	0	0	0.3438	0.3438	2.9375	0.3438	1.8125
	9	Butylated-Hydroxyanisole	13.0499	11.0769	4.0222	2.7211	3.285	3.4046	7.7949	0	5.291	0	0	0	2.5607	6.2391	2.5607	9.6105	0.5346	-0.0569
S	1	Caffeine	16.0458	10.5156	3.5388	1.4545	-0.5099	1.8751	4.7732	0	1.5194	-0.6766	23.1613	0	0	3.8635	1.4644	11.672	0.7578	-0.36
AB	9	Carbadox	24.2963	15.39	7.1358	3.7616	2.7764	0.0002	1.2032	0	7.9285	-0.7376	10.7953	0	5.5775	9.5933	2.8078	10.7953	0.8226	-0.7376
DBP	1	Chloralhydrate	3.8823	7	1.8519	2.6667	-0.594	2.892	0	0	0	0	0	14.6968	5.1361	1.1389	2.568	8.0486	1.1389	-1.9722
DBP	2	Chloroform	0.9769	4	1.3333	0	1.7631	1.7353	0	0	0	0	0	14.4167	0	0	0.85	4.8056	0.85	-0.75
AB	15	Chlorotetracycline	49.5089	26.0741	8.5422	3.4778	-0.6262	0.3332	1.2141	-0.5792	2.3111	-8.4947	38.1416	6.1833	20.5295	9.7993	3.0232	13.3085	0.9678	-3.1029
S	4	Cholesterol	34.3464	18.3673	7.935	3.84	7.1009	0.5541	4.7328	16.8637	0	1.6613	0	0	2.3981	12.2978	2.3981	10.032	0.1403	-0.0351
S,PhAC	9	Cimetidine	20.9176	15.0588	9	5.9282	0.646	1.2464	3.7393	2.5786	1.7105	0.5038	0	0	0	5.0398	1.7827	8.3916	0.6245	0.5038
S,AB,PhAC	16	Ciprofloxacin	31.3189	17.4156	6.9575	3.4856	-0.5653	0.0002	0	4.8443	2.8906	-2.2021	23.7581	0	2.7954	10.4877	2.7954	14.6077	0.6899	-1.2751
P	11	cis-Chlordane	21.9928	13.005	3.179	0.999	5.5601	5.7275	0	0.5555	0	0.3937	0	51.0059	0	2.7931	1.0151	6.6189	0.8051	-1.5032

			Traditional Kappa Shape Indices				Other 2D Descriptors		Atom Type E-State Descriptors						H Atom Type E-State Descriptors						
			Kappa Zero	Kappa 1	Kappa 2	Kappa 3	Octanol/Water Partition Coefficient	Mouse Oral LD50	-CH3 Group	-CH2- Group	=CH- Aromatic Carbon	+C< Double Bonded Carbon	=O Double Bonded Oxygen	-Cl Chloride Group	-OH Polar H Atom	CH Sum of Hydrogen E-States on Non-Polar H Groups	Largest Atom Hydrogen Aton E-State in Molecule	Largest Atom E-State Value in Molecule	Smallest Hydrogen Atom Hydrogen E-State Value in Molecule	Smallest Atom E-State Value in Molecule
Notes	**QSAR Cluster**	**Compound Name**	**k0**	**k1**	**k2**	**k3**	**LogP**	**LD50**	**SsCH3**	**SssCH2**	**SaaCH**	**SdssC**	**SdO**	**SsCl**	**SHsOH**	**SHother**	**Hmax**	**Gmax**	**Hmin**	**Gmin**
S,P	10	Clorpyrifos	20.7887	16.0556	6.9632	4.566	4.757	1.1394	3.5701	0.7147	1.422	0	0	17.487	0	4.6242	1.5206	5.9377	0.6322	-2.9185
S	4	Codeine	29.5333	14.3521	4.7619	1.6436	1.5614	2.8616	3.9071	3.1323	4.2046	0	0	0	2.5934	13.3279	2.5934	10.5542	0.6335	-0.5386
	1	Cyclotrimethylenetrinitramine	10.4846	13.0667	5.3651	3.5	0.4574	3.8492	0	-1.3204	0	0	31.4266	0	8.5425	3.6798	2.8475	10.4755	1.2266	-0.6189
	2	Cymene	8.1938	8.1	3.4083	2.2857	4.0344	3.9626	6.5411	0	8.713	0	0	0	0	6.3883	1.1128	2.213	0.4311	0.6533
S,AA	1	Cysteine	5.9157	7	3.0612	2.6667	-2.133	0.0002	0	0.1898	0	-1.0046	9.7564	0	2.5779	1.6081	2.5779	9.7564	0.7045	-1.0046
	6	d--n-Butylphthalate	27.7666	19.0476	10.6805	6.3281	4.0998	5.2335	5.8417	4.2672	5.1443	-0.918	24.2625	0	0	10.0006	1.4469	12.1656	0.453	-0.4633
	14	d--n-Octylphthalate	32.0916	26.0357	17.8242	12.3448	7.4094	1.0208	4.3846	14.4179	6.7436	-0.8876	24.7036	0	0	14.6785	1.4526	12.3518	0.3755	-0.4438
	14	di-sec-Octylphthalate	32.0916	26.0357	15.7889	10.0535	7.0589	2.8884	8.5439	9.4021	6.7741	-0.8879	25.1396	0	0	15.3272	1.4598	12.5698	0.4114	-0.444
P	10	Diazinon	21.8881	17.0526	7.6953	5.4792	4.1634	0.1905	9.6599	0.8857	1.741	0	0	0	0	7.2636	1.5038	5.6848	0.593	-2.7681
DBP	1	Dibromoacetatic Acid	4.0668	6	2.2222	3	0.9501	0.4183	0	0	0	-0.9074	9.6053	0	2.5677	0.8944	2.5677	9.6053	0.8944	-0.9074
DBP	1	Dibromoacetonitrile	2.8928	5	2.25	4	0.7944	15.028	0	0	0	0	0	0	0	0.7958	0.7958	7.7998	0.7958	-0.1852
DBP	2	Dibromochloromethane	1.8062	4	1.3333	0	1.9851	3.4141	0	0	0	0	0	5.108	0	0	0.7042	5.108	0.7042	-0.0694
DBP	2	Dibromochloropropane	3.4648	6	3.2	3	2.2958	0.4743	0	1.7218	0	0	0	5.5559	0	1.0964	0.6444	5.5559	0.5482	0.2407
S	1	Dichloroacetic Acid	4.0668	6	2.2222	3	0.3708	1.1399	0	0	0	-1.2099	9.4352	9.5571	2.6042	0	2.6042	9.4352	1.0402	-1.287
	1	Dichloroacetonitrile	2.8928	5	2.25	4	0.8046	6.4523	0	0	0	0	0	9.733	0	0	0.9416	7.6296	0.9416	-0.8657
	1	Dichlorodifluoromethane	2.2907	5	1	0	1.8859	11.0957	0	0	0	0	0	7.9244	0	0	0	10.5517	0	-3.5556
	3	Dichlorodiphenyldichloroethylene	15.3702	14.41	6.4379	3.75	5.9304	2.5425	0	0	14.6689	0.9642	0	23.6695	0	10.7575	1.3666	5.9715	1.3228	0.208
	1	Dichloropropane	4.0668	6	2.2222	3	1.0723	3.6658	1.338	0	0	-0.2099	9.8796	10.0571	0	0.6042	0.9291	9.8796	0.6042	-0.8426
P	11	Dieldrin	19.4798	11.6371	2.687	0.8192	4.5917	2.0702	0	1.0613	0	0.6423	0	39.5238	0	6.1413	0.9743	6.8242	0.6985	-1.3747
S	9	Diethylphthalate	14.4494	14.0625	7.35	4.0768	2.6343	6.3305	3.4263	0.5476	6.4429	-1.0164	23.0884	0	0	8.3516	1.4261	11.5442	0.5929	-0.5082
S,ES	5	Diethylstilbestrol	17.5918	16.3719	7.852	4.25	3.9051	2.1689	4.2743	1.8508	14.664	2.5522	0	0	5.1209	13.1096	2.5604	9.4107	0.542	0.2842
	4	Digoxigenin	40.5204	19.9336	6.4977	2.5758	1.2516	3.9451	4.3946	7.1929	0	0.6459	11.646	0	7.6005	14.6466	2.5988	12.1269	0.5781	-0.9062
PhAC	17	Digoxin	95.7199	41.7222	15.794	7.3445	0.7587	0.6543	9.6477	7.0774	0	0.5686	11.9442	0	15.9055	36.5456	2.6988	12.5684	0.6712	-1.0125
PhAC	16	Diltiazem	40.6034	23.6587	11.0395	6.0357	2.7064	0.0002	6.879	1.2096	15.3568	-0.6794	25.4176	0	0	18.9744	1.4738	13.5553	0.6438	-0.9162
	9	Dipropylthiocarbamic Acid-s-ethylester	11.144	12	7.6389	5.3254	2.9963	2.9549	6.22	4.7859	0	0.2372	11.412	0	0	4.3456	0.6844	11.412	0.417	0.2372
P	10	Disulfoton	14.2396	14	8.32	7.04	3.2099	0.8262	6.0827	4.5958	0	0	0	0	0	5.092	0.7929	5.5075	0.4246	-2.0229
H	9	Diuron	15.4437	12.0714	5.1856	3.5918	2.6942	0.129	3.3192	0	4.9267	-0.2052	11.2472	11.5047	0	5.4332	1.9219	11.2472	0.6742	-0.2052
S,AB	15	Doxycycline	47.5627	25.1037	8.5873	3.3704	0.6689	0.0002	4.6519	0	4.438	-6.6737	38.446	0	14.3892	13.4752	2.9804	13.317	0.8165	-2.8948
PhAC	16	Enalaprilat	33.7444	21.3018	10.3641	6.2823	-1.3444	0.8267	1.5814	2.3949	9.5324	-2.4032	35.2112	0	5.4313	14.461	2.7237	12.4997	0.7235	-1.0215
	10	Endosulfansulfate	20.6021	14.9174	3.8475	1.4329	3.7277	1.471	0	-0.5981	0	0.0092	22.7848	37.9555	0	4.7825	1.1981	11.3924	1.1931	-4.1142
	16	Enrofloxacin	34.9831	19.3222	7.788	3.9382	0.9588	6.0561	2.1117	6.0854	2.9327	-2.1896	23.9048	0	2.7976	11.7776	2.7976	14.7935	0.4963	-1.2718
	4	Equilenin	26.0206	13.6484	4.75	1.9608	4.1514	0.8917	2.1498	3.6526	9.8637	0.4435	12.2153	0	2.5747	11.104	2.5747	12.2153	0.6117	-0.1413
	4	Equilin	26.0206	13.6484	4.75	1.9608	3.259	0.6402	2.177	4.7741	5.7851	1.9733	12.2347	0	2.5577	11.0643	2.5577	12.2347	0.5947	-0.1004
S,AB	16	Erythromycin	60.0318	32.5137	15.2908	9.8097	-2.9301	4.6725	0	-2.1911	0	-1.3692	24.8209	0	21.7407	25.5161	2.7672	12.5329	0.8824	-1.7761
ES,HO	6	Estriol	27.7666	14.5833	5	2.0663	2.5465	1.1373	2.1678	4.9239	5.8026	0	0	0	7.5384	12.1133	2.551	10.391	0.5737	-0.5651
S,ES,HO	4	Estrone	26.0206	13.6484	4.75	1.9608	3.6617	0.4741	2.2178	6.3435	5.8977	0.5115	12.262	0	2.5457	10.7409	2.5457	12.262	0.5691	-0.0322
	7	ethyl-tert-Butyl Ether	4.4843	7	2.3438	6	1.6904	5.6462	8.1615	0.809	0	0	0	0	0	2.3744	0.6097	5.2292	0.4198	0.0503
S,AH	2	Ethylbenzene	6.0206	6.125	3.1111	1.8	3.1435	0.755	2.162	1.1397	10.4552	0	0	0	0	6.3311	1.0878	2.162	0.4047	1.1397
S	18	Ethylenediaminetetraacetic Acid (EDTA)	15.1835	20	10.6875	12.4898	-2.9415	0.2165	0	-2.4572	0	-5.1151	42.0844	0	10.9172	7.7992	2.7293	10.5211	1.1567	-1.2788
ED	2	exo-Dimethanonaphthalene	11.471	6.4775	1.7265	0.5671	2.3722	0.7529	0	3.0011	0	0	0	0	0	8.3556	1.0171	5.7729	0.5268	0.7213
PAH	12	Fluoranthrene	15.0515	9.9723	3.75	1.378	5.5373	1.3437	0	0	21.7561	0	0	0	0	12.4972	1.2845	2.2199	1.2003	1.3391
PhAC	9	Fluoxetine	25.6937	18.3403	8.7409	5.8642	3.9717	3.275	1.8474	1.4739	14.4329	0	0	0	0	15.7694	1.5506	12.5645	0.5775	-4.3299
P	9	Fonofos	14.8417	12.0714	5.7778	3.96	3.8241	0.1474	4.1706	1.7707	10.3394	0	0	0	0	9.4844	1.4974	5.7486	0.5097	-1.8531
PhAC	9	Gemfibrozil	21.9928	16.0556	6.9632	5.2675	3.683	0.0002	7.5241	1.9175	6.0965	-0.7553	10.9432	0	2.6059	8.441	2.6059	10.9432	0.5859	-0.7553
S,AA	1	Glycine	3.4948	5	2.25	4	-2.6129	13.4471	0	-0.2778	0	-0.9676	9.2431	0	2.5396	0.7819	2.5396	9.2431	0.7819	-0.9676
ED	13	Hexachlorobenzene	3.6124	10.0833	3.3951	1.5625	5.7266	5.0681	0	0	0	0	0	34.0126	0	0	0	5.6688	0	0.109
	13	Hexachlorobutadiene	5.7856	10	4	3.1111	5.1078	5.2561	0	0	0	-0.4806	0	31.814	0	0	0	5.4182	0	-0.1755
	13	Hexachlorocyclohexane	0	4.1667	2.2222	1.3333	3.4015	8.5194	0	9	0	0	0	0	0	2.1417	0.3569	1.5	0.3569	1.5
ED	11	Hexachloropentadiene	18.0942	16.8438	3.36	1.0771	6.6384	1.7308	0	-0.3276	0	0	0	77.3651	0	2.0854	1.0427	6.5228	1.0427	-1.975
S,PhAC	9	Ibuprofen	15.8352	13.0667	5.915	4.1663	3.7567	0.9563	6.0569	1.0434	7.8716	-0.7717	10.7624	0	2.6162	8.5851	2.6162	10.7624	0.4304	-0.7717
AA	1	Leucine	7.9861	9	3.92	4.5	-1.1675	2.952	3.8944	0.5509	0	-0.9132	10.1098	0	2.5712	2.9202	2.5712	10.1098	0.4266	-0.9132
AB	16	Lincomycin	38.6468	23.2806	10.1563	5.3314	0.2907	5.6887	7.2551	3.7483	0	-0.223	12.8485	0	10.6261	15.3648	2.695	12.8485	0.4325	-1.419
S,L	13	Lindane	3.6124	10.0833	3.3951	1.5625	3.5566	0.8197	0	0	0	0	0	35.287	0	0	0.9092	5.8812	0.9092	-0.4367
H	9	Linuron	16.0458	12.0714	5.7778	3.96	2.5995	0.1581	1.3417	0	4.7588	-0.4807	10.9854	11.4328	0	4.9186	2.0031	10.9854	0.7618	-0.4807
ES,PhAC	4	Mestranol	31.3197	16.4675	5.7716	2.2893	3.9322	0.0002	3.9751	6.3469	6.5865	0	0	0	2.5473	11.7729	2.5473	10.9556	0.5991	-0.9
	1	Metformin	7.9861	9	3.92	4.5	-1.6917	0.2039	3.3855	0	0	-0.1007	0	0	0	1.2284	2.0872	7.0678	0.6142	-0.2142
	2	Methylene Bromide	0.8293	3	2	0	1.6592	6.0053	0	0.875	0	0	0	0	0	0.4875	0.4875	3.0625	0.4875	0.875
	2	Methylene Chloride	0.8293	3	2	0	1.33	0.9342	0	0.1944	0	0	0	9.5278	0	0	0.6333	4.7639	0.6333	0.1944
S,P	8	methyl Parathion	16.8577	14.0625	6.0744	4.0768	2.253	0.8226	2.7892	0	5.7279	0	10.5226	0	2.7632	7.6322	2.7632	10.5226	0.8433	-2.7628
	9	Metolachlor	24.2963	17.0526	8.3232	4.2314	3.1827	0.2304	7.7117	1.3417	6.0842	-0.0878	12.1875	5.7567	0	8.9027	1.2678	12.1875	0.533	-0.0878
	9	Metribuzin	14.6144	12.0714	4.2449	2.5344	2.0309	3.0648	7.4951	0	0	0.5256	11.7172	0	0	2.477	1.7641	11.7172	0.6042	-0.3312
H	9	Molinate	11.144	10.0833	5.6122	3.5156	2.462	2.6641	2.0282	7.8196	0	0.2772	11.4398	0	0	4.5311	0.6889	11.4398	0.4613	0.2772
	2	Monobromobenzene	4.7116	5.1429	2.3438	1.5	2.5436	7.1734	0	0	9.9712	0	0	0	0	5.4883	1.117	3.3112	1.0761	1.1343
	7	methyl-tert-butyl Ether (MTBE)	3.2375	6	1.6327	5.3333	1.1639	1.668	7.7708	0	0	0	0	0	0	1.8806	0.5597	4.9375	0.4403	0.0417

			Traditional Kappa Shape Indices				Other 2D Descriptors		Atom Type E-State Descriptors						H Atom Type E-State Descriptors					
			Kappa Zero	Kappa 1	Kappa 2	Kappa 3	Octanol/Water Partition Coefficient	Mouse Oral LD50	-CH3 Group	-CH2- Group	=CH- Aromatic Carbon	+C< Double Bonded Carbon	=O Double Bonded Oxygen	-Cl Chloride Group	-OH Polar H Atom	CH Sum of Hydrogen E-States on Non-Polar H Groups	Largest Atom Hydrogen Aton E-State in Molecule	Largest Atom E-State Value in Molecule	Smallest Hydrogen Atom Hydrogen E-State Value in Molecule	Smallest Atom E-State Value in Molecule
Notes	**QSAR Cluster**	**Compound Name**	**kΦ**	**k1**	**k2**	**k3**	**LogP**	**LD50**	**SsCH3**	**SssCH2**	**SaaCH**	**SdssC**	**SdO**	**SsCl**	**SHsOH**	**SHother**	**Hmax**	**Gmax**	**Hmin**	**Gmin**
S	1	N-Dimethylamine	2.8928	5	2.25	4	-0.2035	2.9634	3.1528	0	0	0	9.1806	0	0	1.1868	0.5934	9.1806	0.5934	1.1944
	9	N-nitrosodi-n-butylamine	9.0471	11	8.1	6.4	2.6636	1.7191	4.2278	6.0151	0	0	10.1927	0	0	4.2013	0.7042	10.1927	0.3839	0.8194
	9	N-nitrosodi-n-propylamine	6.782	9	6.125	4.5	1.606	2.8116	4.0711	3.5617	0	0	9.9608	0	0	3.2384	0.6861	9.9608	0.4119	0.789
	1	N-nitrosomorpholine	6.0206	6.125	3.1111	1.8	-0.6311	15.7085	0	2.5461	0	0	9.7803	0	0	3.1382	0.7892	9.7803	0.7799	0.6307
	1	N-nitrosopiperidine	6.0206	6.125	3.1111	1.8	0.488	13.3346	0	5.2465	0	0	9.8358	0	0	2.8825	0.6781	9.8358	0.4665	0.8646
	1	N-nitrosopyrrolidine	4.7116	5.1429	2.3438	1.1852	0.0238	17.6023	0	3.9906	0	0	9.6831	0	0	2.366	0.6656	9.6831	0.5174	0.8646
	18	N-triacetic Acid	8.7558	13	6.4533	8.3333	-2.3798	1.4675	0	-1.7958	0	-3.7847	30.4355	0	8.0662	3.2839	2.6887	10.1452	1.0946	-1.2616
	9	Nitrosodibutylamine	9.0471	11	8.1	6.4	2.6636	1.7191	4.2278	6.0151	0	0	10.1927	0	0	4.2013	0.7042	10.1927	0.3839	0.8194
	18	Nitrilotriacetic Acid	8.7558	13	6.4533	8.3333	-2.3798	1.4675	0	-1.7958	0	-3.7847	30.4355	0	8.0662	3.2839	2.6887	10.1452	1.0946	-1.2616
	1	Nitrosodiethylamine	4.7116	7	4.1667	2.6667	0.6799	12.2763	3.7875	1.4167	0	0	9.6431	0	0	2.2431	0.6559	9.6431	0.4657	0.7083
S	3	Nitrobenzene	7.3841	7.1111	3.2397	2	1.4691	2.5481	0	0	8.1666	0	10.1176	0	2.6909	6.1535	2.6909	10.1176	1.1547	-0.1667
	4	Norethindrone	22.5949	11.7959	4.5286	1.8963	3.66	0.8831	0	12.0865	0	1.9289	11.5842	0	0	9.2418	1.2318	11.5842	0.448	0.3975
AB	16	Norfloxacin	30.1156	17.8112	7.4861	3.52	-0.6469	0.3954	1.8506	3.4104	2.8057	-2.2895	23.504	0	2.7913	9.6605	2.7913	14.4949	0.6399	-1.3003
	9	N N diethyl 3 methylbenzamide	14.8417	12.0714	5.7778	3.2727	2.492	5.2405	5.9935	1.5343	7.7216	0.1238	11.8851	0	0	7.9222	1.2868	11.8851	0.5059	0.1238
	1	o-Cresol	7.2247	6.125	2.52	1.4876	1.7598	16.453	1.8704	0	7.252	0	0	0	2.4992	5.1608	2.4992	8.9193	0.5617	0.3681
ED	11	Octachloro-4-7-methanotetrahydroindane	21.9928	13.005	3.179	0.999	5.5601	5.7275	0	0.5555	0	0.3937	0	51.0059	0	2.7931	1.0151	6.6189	0.8051	-1.5032
ED	11	Octachloroepoxide	23.6943	12.719	2.8134	0.8889	5.3848	3.6013	0	0	0	0.2932	0	51.3335	0	3.3015	1.1063	6.6534	1.0901	-1.5794
	1	p-Cresol	6.0206	6.125	2.52	1.8	1.7107	9.4101	1.9856	0	7.0926	0	0	0	2.4923	5.2187	2.4923	8.7567	0.5201	0.3293
	2	p-Dichlorobenzene	3.6124	6.125	2.52	1.8	2.9825	1.2514	0	0	7.0154	0	0	11.106	0	4.8143	1.2036	5.553	1.2036	0.717
	1	Paraxanthine	14.4813	9.551	3.2925	1.4269	-0.4647	4.769	3.1276	0	1.4881	-0.7825	22.6344	0	0	3.0273	1.9979	11.5131	0.7523	-0.448
	9	Paroxetine	33.7444	18.3673	7.935	4.2959	3.8385	1.7015	2.0259	3.7891	12.7652	0	0	0	0	16.6106	1.5833	13.2242	0.7086	-0.5027
	19	Perchloric Acid	2.0635	5	1	0	-0.5746	5.9106	0	0	0	0	25.8125	0	2.9	0	2.9	8.6042	2.9	-4.6944
S	12	Phenanthrene	11.8314	9.2422	3.8678	1.6483	4.608	0.6594	0	0	21.367	0	0	0	0	12.1743	1.254	2.1782	1.1676	1.3113
S	1	Phenol	4.7116	5.1429	2.3438	1.5	1.2356	11.5349	0	0	8.7127	0	0	0	2.4867	5.7303	2.4867	8.6322	1.1011	0.3218
S	3	Phthalic Anhydride	8.445	7.6389	2.8028	1.2098	1.3456	9.7996	0	0	6.5303	-1.1007	21.6657	0	0	5.2008	1.3549	10.8329	1.2455	-0.5504
	9	Pramitol	14.4494	14.0625	6.6667	5.2645	2.801	7.7672	9.614	0	0	0	0	0	0	4.5313	1.8076	5.0164	0.5485	0.263
S,HO	8	Progesterone	27.7666	14.5833	5.571	2.3965	2.7916	0.0331	1.7992	9.2487	0	2.2487	23.5431	0	0	11.0864	1.2539	11.8785	0.5785	0.3527
PAH	12	Pyrene	10.8371	9.9723	3.75	1.4444	5.0576	0.7981	0	0	21.858	0	0	0	0	12.6058	1.2845	2.2124	1.2138	1.335
PhAC	16	Ranitidine	27.1645	19.0476	10.6805	8.8889	-0.1325	2.2684	5.6809	3.1391	3.9993	0.4716	10.4604	0	2.7289	9.3616	2.7289	10.4604	0.5893	-0.235
	1	s-1-Methyl-5-3-Pyridinyl-2-Pyrrolidinone	14.4813	9.551	4.0222	1.92	0.6545	8.6504	1.8542	1.5804	7.5127	0.2304	11.2633	0	0	8.0866	1.3309	11.2633	0.675	0.2304
	9	Salbutamol	19.4863	15.0588	6.25	5.0176	0.8454	8.6604	6.0705	0.1927	4.759	0	0	0	7.657	8.3497	2.6008	9.9689	0.503	-0.6527
AA	1	Serine	5.9157	7	3.0612	2.6667	-2.9815	12.5787	0	-0.5046	0	-1.1782	9.6453	0	5.0502	1.8087	2.6001	9.6453	0.8434	-1.1782
	9	Simazine	11.471	11.0769	5.6719	3.7037	2.0295	4.7522	3.9258	1.5117	0	0	0	5.6793	0	2.4414	1.7624	5.6793	0.5139	0.1962
AB	19	Sulfachlorpyridazine	20.7887	14.41	5.9698	3.9958	1.1139	7.0814	0	0	8.6724	0	23.8902	5.5526	0	8.6271	2.1944	11.9451	1.3785	-3.6941
AB	19	Sulfadimethoxine	25.9604	17.3554	7.513	4.7334	0.8485	3.6108	2.7709	0	7.1284	0	24.4363	0	0	9.1772	2.2662	12.2182	0.8464	-3.787
AB	19	Sulfamerazine	20.7887	14.41	5.9698	3.9958	0.3512	7.1158	1.7527	0	9.058	0	23.9845	0	0	9.1419	2.2027	11.9923	0.7059	-3.6774
S,AB	19	Sulfamethazine	20.684	15.39	6.1855	4.2314	0.7216	7.2649	3.547	0	7.6761	0	24.2071	0	0	8.4766	2.2107	12.1036	0.7139	-3.6942
AB, PhAC	19	Sulfamethizole	19.1115	13.4321	5.3254	3.4844	-0.8124	6.5117	0	0	5.8156	0	23.7366	0	0	5.6949	2.202	11.8683	1.3768	-3.67
AB	19	Sulfamethoxazole	19.1115	13.4321	5.3254	3.4844	0.826	6.6147	1.6746	0	7.3703	0	23.7771	0	0	7.8764	2.176	11.8885	0.7269	-3.6448
AB	19	Sulfathiazole	17.4597	12.4567	5.1042	3.25	0.4246	4.8062	0	0	9.2041	0	23.6512	0	0	8.3178	2.1427	11.8256	1.3278	-3.5576
H	9	Terbacil	14.6144	12.0714	3.8678	2.3432	1.377	0.0002	6.9147	0	0	-0.3968	23.1766	5.7574	0	2.6059	1.9129	11.6681	0.6311	-0.5675
P	10	Terbufos	14.4038	15	6.554	7.875	4.1719	0.1059	10.5043	2.1902	0	0	0	0	0	4.9978	0.8408	5.5379	0.4886	-2.0762
	15	Terramycin	47.5627	25.1037	8.5873	3.3704	-0.7719	0.0002	2.8502	0	3.9169	-7.5188	38.2323	0	17.3373	13.3115	3.0008	13.2059	0.8475	-3.0059
	7	tert amyl methyl Ether	5.3136	7	2.3438	2.6667	1.9108	9.7463	8.0069	1.0729	0	0	0	0	0	2.3438	0.5677	5.0868	0.3802	0.0833
S,HO	4	Testosterone	24.2963	12.719	4.7769	2	2.6015	0.798	0	9.0941	0	1.8233	11.5941	0	2.4019	10.2935	2.4019	11.5941	0.5594	-0.0178
S	13	1,1,2,2 Tetrachloroethane	1.6586	6	2.2222	3	3.3964	4.8495	0	0	0	-0.1975	0	19.9753	0	0	0	4.9938	0	-0.0988
S	13	1,1,2,2, Tetrachloroethylene (PCE)	1.6586	6	2.2222	3	3.3964	4.8495	0	0	0	-0.1975	0	19.9753	0	0	0	4.9938	0	-0.0988
S,AB	15	Tetracycline.hin	45.6302	24.1349	8.3405	3.3333	-0.3782	0.0002	3.0591	-0.178	4.1574	-6.4174	38.1444	0	14.2991	12.4516	2.9528	13.1715	0.8141	-2.7275
ED	6	Thio-N-methyl-carbamoyl-oxy-methylester	10	10	5.76	9.1429	-1.0323	0.4649	0	0.2985	0	-1.3181	19.982	0	0	1.7774	1.7702	10.0698	0.8534	-0.8533
S,AA	1	Threonine	7.2247	8	3.1111	2.8125	-2.7039	14.5894	1.3321	0	0	-1.1806	9.8557	0	5.0804	2.4643	2.6081	9.8557	0.5834	-1.1806
S,AH	2	Toluene	4.7116	5.1429	2.3438	1.5	2.6571	1.6903	2.0833	0	10.2616	0	0	0	0	5.8298	1.0753	2.0833	0.4868	1.3218
ES	20	Tributyl Tin	8.7558	13	10.0833	8.3333	5.839	0.3124	7.0076	13.9525	0	0	0	0	0	5.0845	0.4782	2.3359	0.3232	-0.9668
S,DBP	3	Trichloroacetic Acid	4.4843	7	1.8519	2.6667	1.093	15.9031	0	0	0	-1.4606	9.625	14.3981	2.6583	0	2.6583	9.625	2.6583	-2.1667
	2	1,1,2 Trichloroethene (TCE)	2.8928	5	2.25	4	2.2918	1.3853	0	0	0	0.0895	0	14.8241	0	0	1.2217	4.9568	1.2217	0.0895
AM	3	Triclosan	20.9176	13.4321	5.76	3.4844	5.5234	8.0591	0	0	9.3925	0	0	17.424	2.6932	8.5022	2.6932	9.6196	1.3627	-0.0523
AB	9	Trimethoprim	25.3584	17.3554	8.0222	4.2604	1.2574	8.5683	4.7037	0.5306	5.3285	0	0	0	0	8.0185	1.7305	5.8481	0.8169	0.1538
S	10	triphenyl Phosphate	17.6878	17.8112	8.9091	5.7857	3.9735	2.7531	0	0	26.3572	0	13.0547	0	0	20.4668	1.4609	13.0547	1.2501	-3.885
	10	tris 2 Chloroethyl Phosphate	10.3203	14	8.32	7.04	1.6486	1.3801	0	0.8806	0	0	11.6473	16.0989	0	2.9519	0.984	11.6473	0.8198	-3.5222
AB	17	Tylosin	101.6768	50.6428	25.3333	15.0651	3.0484	1.3477	10.021	-0.1868	0	-0.2085	38.6009	0	13.545	43.9344	2.8246	13.4474	0.7147	-1.3059
	1	t Butyl Alcohol	1.4314	3	2	0	-0.0314	4.0689	1.6806	0.25	0	0	0	0	2.2722	0.9333	2.2722	7.5694	0.3833	0.25
S,AA	1	Valine.hin	6.6227	8	3.1111	2.8125	-1.6909	2.9433	3.5531	0	0	-0.9306	10.0157	0	2.5681	2.4644	2.5681	10.0157	0.4723	-0.9306
S, AA		Asparagine	8.5882	9.0000	3.9200	4.5000	-3.2338	4.3518	0.0000	-0.3102	0.0000	-1.9179	19.8950	0.0000	2.6298	1.9111	2.6298	9.9931	0.8948	-1.2141
S, AA		Aspartic Acid	8.5882	9.0000	3.9200	4.5000	-2.5518	0.3236	0.0000	-0.5324	0.0000	-2.4979	19.6173	0.0000	5.2716	1.9979	2.6437	9.8464	0.9503	-1.2941
S, AA		Histidine	11.4553	9.0909	4.1327	2.8444	-2.4299	6.3564	0.0000	0.2870	3.0483	-1.0004	10.2662	0.0000	2.6306	4.5321	2.6306	10.2662	0.8712	-1.0004
S, AA		Lysine	10.0000	10.0000	5.7600	5.5309	-3.3935	3.1412	0.0000	2.7677	0.0000	-0.9333	10.1372	0.0000	2.5807	3.2022	2.5807	10.1372	0.5321	-0.9333

			Traditional Kappa Shape Indices				Other 2D Descriptors		Atom Type E-State Descriptors						H Atom Type E-State Descriptors						
			Kappa Zero	Kappa 1	Kappa 2	Kappa 3	Octanol/Water Partition Coefficient	Mouse Oral LD50	-CH3 Group	-CH2- Group	=CH- Aromatic Carbon	+C< Double Bonded Carbon	=O Double Bonded Oxygen	-Cl Chloride Group	-OH Polar H Atom	CH Sum of Hydrogen E-States on Non-Polar H Groups	Largest Atom Hydrogen Aton E-State in Molecule	Largest Atom E-State Value in Molecule	Smallest Hydrogen Atom Hydrogen E-State Value in Molecule	Smallest Atom E-State Value in Molecule
Notes	**QSAR Cluster**	**Compound Name**	**k0**	**k1**	**k2**	**k3**	**LogP**	**LD50**	**SsCH3**	**SssCH2**	**SaaCH**	**SdssC**	**SdO**	**SsCl**	**SHsOH**	**SHother**	**Hmax**	**Gmax**	**Hmin**	**Gmin**
S, AA		Methionine	8.5882	9.0000	4.8395	4.5000	-1.5630	3.2189	1.9252	1.3650	0.0000	-0.9129	10.0709	0.0000	2.5821	2.7032	2.5821	10.0709	0.4899	-0.9129
S, DBP		N-nitroso dimethyl amine (NDMA)	2.8928	5.0000	2.2500	4.0000	-0.2035	2.9634	3.1528	0.0000	0.0000	0.0000	9.1806	0.0000	0.0000	1.1868	0.5934	9.1806	0.5934	1.1944
S, AA		Phenylalanine	11.7461	10.0833	4.8889	3.5156	-1.0067	10.0996	0.0000	0.3851	9.3425	-0.9594	10.3786	0.0000	2.6205	7.6826	2.6205	10.3786	0.8302	-0.9594
S		Urea	1.8062	4.0000	1.3333	0.0000	-1.8420	20.4706	0.0000	0.0000	0.0000	-0.8333	9.0000	0.0000	0.0000	0.0000	1.5514	9.0000	1.5514	-0.8333
Marine Toxin		Anatoxin a	12.9502	8.5917	3.3951	1.7013	1.0476	0.0002	1.6728	4.6684	0.0000	1.2686	11.2311	0.0000	0.0000	5.5435	1.5514	11.2311	0.5447	0.2454
Marine Toxin		Cylindrospermopsin	38.0448	20.2800	7.3563	3.7732	0.0915	0.0002	1.7775	0.8726	0.0000	-1.3303	46.5771	0.0000	5.5989	12.3228	2.8445	11.8070	0.7210	-4.2149
Marine Toxin		Microcystin LR	123.4065	64.1151	34.4816	25.6816	1.2531	0.0002	9.4862	-1.1658	9.7265	-9.3128	118.9162	0.0000	5.8030	38.7195	2.9150	14.1833	0.6657	-1.8431
Marine Toxin		Saxitoxin	27.1645	15.8790	5.2739	2.3069	-3.4871	3.6895	0.0000	0.3048	0.0000	-0.5151	10.7924	0.0000	5.4685	5.4350	2.7342	10.7924	0.9441	-2.0660

Legend:
S = Surrogate
PhAC = Pharmaceutically Active Compound
ED = Endocrine Disruptor
ES = Estrogenicity
HO = Hormone
P = Pesticide
H = Herbicide
AHC = Aromatic Hydrocarbon
PHA = Polyaromatic Hydrocarbon
AB = Antibiotic
AM = Antimicrobial
AA = Amino Acid
DBP = Disinfection Byproduct

			Information Indices					Molecular Properties										
			Shannon Information Index	Information Content	Molecular Redundancy	Bonchev-Trinajsti Information Content	Bonchev-Trinajsti Mean Information Content	Formula Weight (Daltons)	# Elements in Molecule	# Rings in Molecular Graph	# Graph Circuits	Kappa Flexibility Index (# Bonds in normal graph for alkanes)	Difference Between Chi cluster-3 and chi path/cluster-4	# H-Bond Acceptors	-XH Hydrogen Bond Donor	Molecular & Group Polarity Index - Specific Polarity Descriptor	Molecular & Group Polarity Index - Average Polarity Descriptor
Notes	**QSAR Cluster**	**Compound Name**	**si**	**IC**	**R**	**idc**	**idcbar**	**fw**	**nelem**	**nrings**	**ncirc**	**phia**	**knotp**	**numHBa**	**SHHBd**	**Qs**	**Qsv**
DBP	1	1,1 Dichloropropanone	0.6778	4.0668	0.129	23.4839	1.5656	126.9702	4	0	0	2.5287	-0.6667	3	0	0.939	0.6086
AH	2	1,2,4 Trimethylbenzene	0.9542	8.5882	0	73.3491	2.0375	120.1943	2	1	1	1.5635	-0.7182	0	0	4.064	1.3798
	2	1,2 Dichlorobenzene	0.6021	4.8165	0.3333	51.3867	1.8352	147.0038	3	1	1	1.765	-0.6667	2	0	2.1198	0.7729
AH	2	1, 2 Dimethylbenzene	0.6021	4.8165	0.3333	51.3867	1.8352	106.1674	2	1	1	1.3354	-0.6667	0	0	3.448	1.2571
AH	2	1,3,5 Trimethylbenzene	0.4771	4.2941	0.5	70.5293	1.9591	120.1943	2	1	1	1.5635	-0.134	0	0	4.064	1.3798
P	2	1,4 Dichlorobenzene	0.4515	3.6124	0.5	55.7352	1.9905	147.0038	3	1	1	1.765	-0.2391	2	0	2.1198	0.7729
S,ED	3	1,4 Dichlorophenoxyacetic Acid	1.1139	14.4813	0	216.7275	2.7786	221.0398	4	1	1	3.6866	-0.5498	5	2.6676	2.3281	0.5395
S,HO,ES	4	17a Estradiol	1.2788	24.2963	0	503.0751	2.942	258.3605	3	4	10	2.7128	-2.2011	2	4.951	6.8009	0.8635
ED	5	2,2,2 Trichloro 1,1-bis-4-chlorophenyl Ethanol	0.8409	14.295	0.3166	403.0623	2.9637	287.5728	4	2	2	3.6434	-1.9514	4	2.6912	4.3038	0.7167
ED	5	2,2 bis-p-Chlorophenyl 1,1,1 Trichloroethane	0.8549	16.2423	0.3315	507.7382	2.9692	354.4904	3	2	2	4.9182	-0.8349	5	0	5.1474	0.7813
ED	5	2,2-bis-p-Chlorophenyl 1,1 Dichloroethane	0.8539	15.3702	0.3198	456.4711	2.9835	320.0454	3	2	2	4.8007	-1.2391	4	0	5.1977	0.8021
ED	5	2,2 bis-p-Methoxyphenyl 1,1,1 Trichloroethane	0.91	19.1105	0.3117	671.3328	3.1968	345.6529	4	2	2	5.5273	-1.1731	5	0	6.1501	0.8338
S,ED	3	2,3,4,5,6 Pentachlorophenol	0.6785	10.5419	0.186	140.8387	2.1339	266.3383	4	1	1	3.3791	-2.488	6	2.6885	2.1552	0.5987
	3	2,3,5,6 Tetrachloroterephthalic Acid	0.7526	12.0412	0.375	304.697	2.5391	303.9135	4	1	1	4.1745	-2.3597	8	5.5928	2.1942	0.4571
	3	2,3 Naphthalenedicarboxylic Acid	0.9031	14.4494	0.25	318.8191	2.6568	216.1931	3	2	3	2.5172	-1.5347	4	5.5157	2.7778	0.4883
ED	3	2,4,5 Trichlorophenoxyacetic Acid	1.1461	16.0458	0	254.8386	2.8004	255.4849	4	1	1	4.1617	-1.0516	6	2.6812	2.4404	0.5396
ED	3	2,4 Dichloro-4'-nitrodiphenyl Ether	1.1884	21.3908	0.0533	491.3204	3.2112	285.1064	5	2	2	4.0592	-1.3906	6	2.7609	3.7699	0.5818
	3	2,4 Dinirophenol	1.1139	14.4813	0	194.6963	2.4961	186.124	4	1	1	2.6565	-1.2943	7	8.3113	1.6194	0.3913
S	6	2,4 Dinitrotoluene	1.1139	14.4813	0	194.6963	2.4961	184.1515	4	1	1	2.6868	-1.2943	6	5.5409	1.9346	0.4674
	7	2,6 bis-1,1 Dimethylethyl 2,5 Cyclohexadiene 1,4 dione	0.7994	12.7908	0.3361	301.1827	2.5099	220.3116	3	1	1	2.9698	-0.7888	2	0	4.478	0.9548
	7	2,6 bis-1,1 Dimethylethyl Phenol	0.7444	11.1663	0.367	262.655	2.5015	206.3281	3	1	1	2.972	-0.7747	1	2.5598	5.6689	1.2703
	7	2,6 di-tert-butyl-p-Cresol	0.7994	12.7908	0.3361	301.1827	2.5099	220.3549	3	1	1	3.2163	-0.7888	1	2.5653	6.2447	1.3315
	8	2,6 Dinitrotoluene	0.8824	11.471	0.2079	190.3864	2.4409	184.1515	4	1	1	2.6868	-1.3855	6	5.5448	1.9346	0.4674
	3	2,6 Naphthalenedicarboxylic Acid	0.9031	14.4494	0.25	350.0713	2.9173	216.1931	3	2	3	2.5172	-1.6039	4	5.3966	2.7778	0.4883
S,ED	9	2-chloro-2'-6'-diethyl-N-methoxymethyl-acetanilide (Alachlor)	1.1215	20.1867	0.1066	412.3653	2.6952	269.7713	5	1	1	6.3296	-1.6188	4	0	5.4512	0.8973
ED	2	3,4,5,6,7,8,8a-Heptachlorodicyclopentadiene	1	10	0	84.2263	1.8717	132.2053	2	3	6	0.8032	-1.1777	0	0	5.3728	1.1641
ED	1	3-amino-1H-1,2,4 Triazole	0.7782	4.6689	0	21.4421	1.4295	84.0806	3	1	1	0.6643	-0.1196	3	3.3448	1.2856	0.5952
	9	3-Hydroxycarbofuran	1.195	20.3156	0.0288	382.8193	2.8148	235.2829	4	2	3	3.0542	-2.0536	4	4.3006	4.9232	0.8482
S	3	4,6 Dichlorophenol	0.9542	8.5882	0	73.3491	2.0375	163.0032	4	1	1	1.9585	-0.7182	3	2.565	1.8462	0.6268
ED	9	4-amino-6-tert-butyl-3-methylthio-as-triazin-5,4H-one	1.0439	14.6144	0.0892	232.2173	2.5518	214.2914	5	1	1	3.0814	-1.3587	6	1.7641	3.6758	0.8557
S,ED	4	4 Nonylphenol	1.1289	18.0618	0.0625	413.7851	3.4482	220.3549	3	1	1	6.9091	-0.3485	1	2.5092	6.4319	1.0887
	2	5-methyl-1H-Benzotriazole	1	10	0	94.9128	2.1092	133.1527	3	2	3	1.0464	-0.67	2	1.8354	3.245	0.8112
ED	9	6-chloro-N-ethyl-N'-isopropyl-1,3,5 Triazine-2,4-diamine	1.1031	15.4437	0.0375	252.854	2.7786	215.6857	4	1	1	4.1858	-0.1975	6	3.5511	4.2896	0.9119
PhAC	3	Acetaminophen	0.9319	10.2512	0.1051	142.2997	2.5873	151.165	4	1	1	2.3554	-0.1494	3	4.3571	2.2763	0.6114
H	9	Acetochlor	1.2553	22.5949	0	428.67	2.8018	269.7713	5	1	1	6.3296	-1.5442	4	0	5.4512	0.8973
S,AA	1	Alanine	0.7782	4.6689	0	23.4839	1.5656	89.0941	4	0	0	1.7638	-0.6667	3	4.0399	0.7934	0.5142
	10	Aldicarbsulfone	1.0601	14.8417	0.075	260.0822	2.858	222.2652	5	0	0	4.366	-2.338	6	1.8051	2.4313	0.6151
	11	Aldrin	0.9877	17.7784	0.2132	362.6816	2.3051	364.9135	3	4	10	2.3978	-6.342	6	0	5.0476	0.8082
ED	9	alpha-naphthyl-N-Methylcarbamate	1.1761	17.6414	0	288.8997	2.7514	201.2248	4	2	3	2.759	-1.0563	3	1.7932	4.0386	0.703
HO	4	Androsterone	1.2788	24.2963	0	503.0751	2.942	262.3922	3	4	10	2.983	-2.2011	2	2.3844	7.2307	0.918
PAH	12	Anthracene	0.5871	8.219	0.4878	233.8311	2.5696	178.2334	2	3	6	1.5387	-1.1324	0	0	5.6044	0.9055
	9	Atrazine	1.1031	15.4437	0.0375	252.854	2.7786	215.6857	4	1	1	4.1858	-0.1975	6	3.5511	4.2896	0.9119
S,AH	13	Benzene	0	0	1	22.8289	1.5219	78.1136	2	1	1	0.913	0	0	0	2.25	0.9375
S,PAH	12	benzo-a-Pyrene	1.301	26.0206	0	532.37	2.8019	252.3153	2	5	22	1.7814	-2.2923	0	0	8.227	0.8913
ED	1	benzo-e-1,3,2 Dioxathiepin-3-oxide	0.8225	9.0471	0.2102	116.0046	2.1092	152.1497	3	3	6	0.9316	-1.1871	3	0	2.7856	0.5947
HO,ES	4	beta-Estradiol	1.2788	24.2963	0	503.0751	2.942	258.3605	3	4	10	2.7128	-2.2011	2	4.951	6.8009	0.8635
S	4	beta Sitostanol n Hydrate	1.4091	38.0448	0.0156	1282.3051	3.6533	374.6506	3	4	10	6.5697	-2.7999	1	2.3793	14.8095	1.4051
	14	bis-2-Ethylhexyl-adipate	1.1139	28.9625	0.2127	1303.5807	4.011	370.5731	3	0	0	17.16	-0.8165	4	0	8.9099	1.0105
S,ED	5	Bisphenol	0.8055	13.6929	0.3454	403.0623	2.9637	228.2908	3	2	2	3.0068	-1.9514	2	5.0985	4.8217	0.8029
DBP	1	Bromochloroacetic Acid	0.7782	4.6689	0	23.4839	1.5656	173.3937	5	0	0	2.7225	-0.6667	3	2.5859	0.7347	0.4762
DBP	1	Bromochloroacetonitrile	0.699	3.4948	0	15.2193	1.5219	154.3936	5	0	0	2.6245	0	2	0	0.7924	0.6075
DBP	2	Bromochloromethane	0.4771	1.4314	0	2.7549	0.9183	129.3839	4	0	0	3.481	0	1	0	0.7081	0.9834
DBP	2	Bromodichloromethane	0.4515	1.8062	0.25	6	1	163.8289	4	0	0	2.9175	0.5774	2	0	0.7749	0.8071
DBP	2	Bromoform	0.2442	0.9769	0.5944	6	1	252.7309	3	0	0	3.6247	0.5774	0	0	1.2776	1.3308
DBP	2	Bromomethane	0.301	0.6021	0	0	0	94.9388	3	0	0	0	0	0	0	0.7091	1.7729
	9	Butylated-Hydroxyanisole	1.0038	13.0499	0.0988	191.2537	2.452	180.2468	3	1	1	2.7371	-0.7289	2	2.5607	4.0576	0.9954
S	1	Caffeine	1.1461	16.0458	0	208.757	2.294	194.193	4	2	3	1.8449	-2.4526	5	0	3.0853	0.6559
AB	9	Carbadox	1.2788	24.2963	0	546.0276	3.1931	264.2407	4	2	3	4.1183	-1.7613	8	7.6863	3.8393	0.5584
DBP	1	Chloralhydrate	0.5546	3.8823	0.3437	32.6898	1.5567	165.4036	4	0	0	2.643	-0.9434	5	5.1361	0.851	0.4885
DBP	2	Chloroform	0.2442	0.9769	0.5944	6	1	119.3779	3	0	0	2.5913	0.5774	3	0	0.6282	0.6544
AB	15	Chlorotetracycline	1.5003	49.5089	0.012	1698.5786	3.217	482.8313	5	4	10	5.2747	-6.4515	13	22.4745	5.1911	0.4787
S	4	Cholesterol	1.3739	34.3464	0.0172	1073.8627	3.5795	345.5889	3	4	10	5.6042	-2.0911	1	2.3981	13.2866	1.3287
S,PhAC	9	Cimetidine	1.2304	20.9176	0	454.9008	3.3449	252.3432	4	1	1	6.5031	-0.9065	6	5.2001	4.9502	0.8136
S,AB,PhAC	16	Ciprofloxacin	1.305	31.3189	0.0545	874.9444	3.1701	331.3466	5	4	5	3.8037	-2.6607	7	4.3563	5.3576	0.5736
P	11	cis-Chlordane	1.2218	21.9928	0.0266	361.2422	2.3611	409.7816	3	3	6	3.3899	-6.5615	8	0	4.3259	0.7594

			Information Indices					Molecular Properties									
			Shannon Information Index	Information Content	Molecular Redundancy	Bonchev-Trinajsti Information Content	Bonchev-Trinajsti Mean Information Content	Formula Weight (Daltons)	# Elements in Molecule	# Rings in Molecular Graph	# Graph Circuits	Kappa Flexibility Index (# Bonds in normal graph for alkanes)	Difference Between Chi cluster-3 and chi path/cluster-4	# H-Bond Acceptors	-XH Hydrogen Bond Donor	Molecular & Group Polarity Index - Specific Polarity Descriptor	Molecular & Group Polarity Index - Average Polarity Descriptor
Notes	QSAR Cluster	Compound Name	si	IC	R	idc	idcbar	fw	nelem	nrings	ncirc	phia	knotp	numHBa	SHHBd	Qs	Qsv
S,P	10	Clorpyrifos	1.1549	20.7887	0.0799	454.062	2.9677	350.59	7	1	1	6.7925	-1.5577	8	0	4.4586	0.7655
S	4	Codeine	1.3424	29.5333	0	630.5984	2.7299	299.3696	4	5	24	2.5335	-3.7146	4	2.5934	7.9154	0.8824
	1	Cyclotrimethylenetrinitramine	0.699	10.4846	0.4057	268.7782	2.5598	225.1411	4	1	1	3.8004	-1.4916	12	8.5425	1.7896	0.3778
	2	Cymene	0.8194	8.1938	0.1806	105.49	2.3442	134.2212	2	1	1	2.1029	-0.66	0	0	4.5918	1.3776
S,AA	1	Cysteine	0.8451	5.9157	0	39.5676	1.8842	121.1601	5	0	0	2.8198	-0.7071	3	5.445	0.9754	0.5143
	6	d--n-Butylphthalate	1.3222	27.7666	0	698.2791	3.3251	292.3752	3	1	1	7.8661	-1.4005	4	0	5.7734	0.7964
	14	d--n-Octylphthalate	1.1461	32.0916	0.208	1523.7106	4.031	390.5633	3	1	1	14.3918	-1.2019	4	0	9.2308	0.9027
	14	di-sec-Octylphthalate	1.1461	32.0916	0.208	1425.6028	3.7714	390.5633	3	1	1	12.674	-1.7793	4	0	9.1701	0.9357
P	10	Diazinon	1.152	21.8881	0.0991	519.2375	3.0365	304.3501	6	1	1	6.4968	-1.0966	6	0	6.1687	0.9932
DBP	1	Dibromoacetatic Acid	0.6778	4.0668	0.129	23.4839	1.5656	217.8447	4	0	0	2.9785	-0.6667	2	2.5677	0.8307	0.5384
DBP	1	Dibromoacetonitrile	0.5786	2.8928	0.1723	15.2193	1.5219	198.8446	4	0	0	2.9154	0	1	0	0.9393	0.7201
DBP	2	Dibromochloromethane	0.4515	1.8062	0.25	6	1	208.2799	4	0	0	3.2619	0.5774	1	0	0.9796	1.0204
DBP	2	Dibromochloropropane	0.5775	3.4648	0.2579	27.3841	1.8256	236.3337	4	0	0	5.3288	-0.2887	1	0	1.9131	1.1514
S	1	Dichloroacetic Acid	0.6778	4.0668	0.129	23.4839	1.5656	128.9427	4	0	0	2.4783	-0.6667	4	2.6042	0.6545	0.4242
	1	Dichloroacetonitrile	0.5786	2.8928	0.1723	15.2193	1.5219	109.9426	4	0	0	2.3481	0	3	0	0.6774	0.5193
	1	Dichlorodifluoromethane	0.4581	2.2907	0.3445	9.7095	0.971	120.9138	3	0	0	1.3783	2	4	0	0.3564	0.3059
	3	Dichlorodiphenyldichloroethylene	0.8539	15.3702	0.3198	456.4711	2.9835	318.0295	3	2	2	4.579	-1.2391	4	0	5.0357	0.7771
	1	Dichloropropane	0.6778	4.0668	0.129	23.4839	1.5656	126.9702	4	0	0	2.5287	-0.6667	3	0	0.939	0.6086
P	11	Dieldrin	1.0253	19.4798	0.1982	409.9452	2.3973	380.9129	4	5	15	2.179	-6.6254	7	0	5.3029	0.7743
S	9	Diethylphthalate	0.9031	14.4494	0.25	342.4436	2.8537	222.2408	3	1	1	4.8218	-1.2019	4	0	3.5625	0.6494
S,ES	5	Diethylstilbestrol	0.8796	17.5918	0.3239	592.2969	3.1174	268.3556	3	2	2	4.72	-1.5399	2	5.1209	6.1235	0.842
	4	Digoxigenin	1.4472	40.5204	0	1238.1384	3.2755	390.52	3	5	11	4.2097	-5.9214	5	7.6005	8.455	0.8111
PhAC	17	Digoxin	1.7404	95.7199	0	6726.6787	4.5297	780.9507	3	8	14	11.2146	-9.0991	14	15.9055	15.4449	0.7542
PhAC	16	Diltiazem	1.4001	40.6034	0.0426	1356.4204	3.3409	414.5254	5	3	4	7.2095	-2.1617	7	0	8.5262	0.8026
	9	Dipropylthiocarbamic Acid-s-ethylester	0.9287	11.144	0.1395	174.8164	2.6487	189.322	5	0	0	7.6072	-0.6179	3	0	4.1893	1.1152
P	10	Disulfoton	1.0171	14.2396	0.1126	272.059	2.9897	274.4094	5	0	0	10.3538	-0.5089	5	0	5.4366	1.2193
H	9	Diuron	1.1031	15.4437	0.0375	256.0247	2.8135	233.0972	5	1	1	3.8921	-1.4195	5	1.9219	3.3551	0.7418
S,AB	15	Doxycycline	1.4863	47.5627	0.0125	1575.6627	3.1767	444.4412	4	4	10	5.1033	-6.0375	10	16.2941	5.9729	0.5578
PhAC	16	Enalaprilat	1.3498	33.7444	0.0345	1051.7019	3.5057	348.399	4	2	2	6.9506	-2.2546	7	7.3503	5.3462	0.6059
	10	Endosulfansulfate	1.0301	20.6021	0.2082	498.3915	2.6231	422.9282	5	3	6	3.6133	-6.0087	10	0	3.6738	0.574
	16	Enrofloxacin	1.3455	34.9831	0.0491	1095.0878	3.3695	359.4004	5	4	5	4.4794	-2.9494	7	2.7976	6.2501	0.6318
	4	Equilenin	1.301	26.0206	0	561.9974	2.9579	266.3397	3	4	10	2.3723	-3.2136	2	2.5747	6.335	0.8018
	4	Equilin	1.301	26.0206	0	561.9974	2.9579	268.3556	3	4	10	2.4965	-3.2136	2	2.5577	6.5844	0.8333
S,AB	16	Erythromycin	1.5798	60.0318	0	2521.1025	3.5862	554.5457	3	3	3	11.9219	-3.704	15	21.7407	6.8278	0.5122
ES,HO	6	Estriol	1.3222	27.7666	0	630.9919	3.0047	288.3867	3	4	10	2.9748	-3.4809	3	7.5384	6.5329	0.8117
S,ES,HO	4	Estrone	1.301	26.0206	0	561.9974	2.9579	270.3715	3	4	10	2.6247	-3.2136	2	2.5457	6.8488	0.8668
	7	ethyl-tert-Butyl Ether	0.6406	4.4843	0.242	39.974	1.9035	102.1766	3	0	0	2.3009	0.8107	1	0	2.956	1.5961
S,AH	2	Ethylbenzene	0.7526	6.0206	0.1667	57.6702	2.0597	106.1674	2	1	1	1.6801	-0.2887	0	0	3.4315	1.1617
S	18	Ethylenediaminetetraacetic Acid (EDTA)	0.7592	15.1835	0.4165	598.556	3.1503	290.2298	4	0	0	8.3104	0.3384	10	10.9172	2.4998	0.4062
ED	2	exo-Dimethanonaphthalene	0.8824	11.471	0.2079	169.3608	2.1713	174.2426	3	5	15	0.7798	-1.8972	1	0	6.8526	1.0475
PAH	12	Fluoranthrene	0.9407	15.0515	0.2188	293.777	2.4481	202.2554	2	4	12	1.3861	-1.7965	0	0	6.5422	0.8944
PhAC	9	Fluoxetine	1.1679	25.6937	0.13	773.6435	3.3491	309.3312	5	2	2	5.5746	-1.1418	5	1.5458	4.4945	0.563
P	9	Fonofos	1.0601	14.8417	0.075	251.1224	2.7596	248.3501	5	1	1	5.1767	-0.8059	2	1.4974	5.5538	1.1511
PhAC	9	Gemfibrozil	1.2218	21.9928	0.0266	491.135	3.21	250.3379	3	1	1	5.053	-2.0532	3	2.6059	5.1161	0.8783
S,AA	1	Glycine	0.699	3.4948	0	15.2193	1.5219	75.0672	4	0	0	1.7153	0	3	4.0052	0.543	0.4163
ED	13	Hexachlorobenzene	0.301	3.6124	0.7211	140.8387	2.1339	284.784	2	1	1	3.6758	-2.488	6	0	2.3964	0.6657
	13	Hexachlorobutadiene	0.5786	5.7856	0.4214	100.565	2.2348	260.762	2	0	0	5.5775	-1.3769	6	0	1.7655	0.6474
	13	Hexachlorocyclohexane	0	0	1	22.8289	1.5219	84.1613	2	1	1	1.5432	0	0	0	4	1.6667
ED	11	Hexachloropentadiene	0.8225	18.0942	0.3873	554.437	2.4002	549.5778	3	3	6	4.337	-12.2478	12	0	4.609	0.7301
S,PhAC	9	Ibuprofen	1.0557	15.8352	0.1024	313.5526	2.9862	206.2847	3	1	1	4.0363	-1.0188	2	2.6162	4.157	0.8468
AA	1	Leucine	0.8873	7.9861	0.0701	81.3882	2.2608	131.1747	4	0	0	3.4208	-0.4349	3	4.0875	1.7437	0.6996
AB	16	Lincomycin	1.4314	38.6468	0	1205.7446	3.4352	406.5438	5	2	2	8.5066	-3.3208	9	12.6337	6.7065	0.7436
S,L	13	Lindane	0.301	3.6124	0.7211	140.8387	2.1339	290.8316	3	1	1	4.4359	-2.488	6	0	2.6989	0.7497
H	9	Linuron	1.1461	16.0458	0	264.2419	2.9038	235.0697	5	1	1	4.313	-0.8941	6	3.983	2.9703	0.6314
ES,PhAC	4	Mestranol	1.3617	31.3197	0	805.6551	3.1844	310.4362	3	4	10	3.3775	-4.4581	2	2.5473	8.5628	0.978
	1	Metformin	0.8873	7.9861	0.0701	81.3882	2.2608	129.1648	3	0	0	3.0011	-0.4349	5	7.5782	1.8813	0.7548
	2	Methylene Bromide	0.2764	0.8293	0.4206	2.7549	0.9183	173.8349	3	0	0	3.9072	0	0	0	1.0102	1.4031
	2	Methylene Chloride	0.2764	0.8293	0.4206	2.7549	0.9183	84.9329	3	0	0	3.0788	0	2	0	0.5237	0.7273
S,P	8	methyl Parathion	1.0536	16.8577	0.125	360.9513	3.0079	264.2188	6	1	1	4.818	-1.5446	7	2.7632	3.2115	0.6142
	9	Metolachlor	1.2788	24.2963	0	475.206	2.779	283.7982	5	1	1	6.4889	-1.7493	4	0	5.9242	0.9436
	9	Metribuzin	1.0439	14.6144	0.0892	232.2173	2.5518	214.2914	5	1	1	3.0814	-1.3587	6	1.7641	3.6758	0.8557
H	9	Molinate	0.9287	11.144	0.1395	171.3882	2.5968	187.3061	5	1	1	4.6926	-0.6179	3	0	4.3008	0.9956
	2	Monobromobenzene	0.6731	4.7116	0.2035	36.9775	1.7608	157.0097	3	1	1	1.4712	-0.1196	0	0	2.554	0.999
	7	methyl-tert-butyl Ether (MTBE)	0.5396	3.2375	0.3066	22.5873	1.5058	88.1497	3	0	0	1.595	0.5	1	0	2.3806	1.5843

			Information Indices					Molecular Properties									
			Shannon Information Index	Information Content	Molecular Redundancy	Bonchev-Trinajsti Information Content	Bonchev-Trinajsti Mean Information Content	Formula Weight (Daltons)	# Elements in Molecule	# Rings in Molecular Graph	# Graph Circuits	Kappa Flexibility Index (# Bonds in normal graph for alkanes)	Difference Between Chi cluster-3 and chi path/cluster-4	# H-Bond Acceptors	-X-H Hydrogen Bond Donor	Molecular & Group Polarity Index - Specific Polarity Descriptor	Molecular & Group Polarity Index - Average Polarity Descriptor
Notes	**QSAR Cluster**	**Compound Name**	**si**	**IC**	**R**	**idc**	**idcbar**	**fw**	**nelem**	**nrings**	**ncirc**	**phia**	**knotp**	**numHBa**	**SHHBd**	**Qs**	**Qsv**
S	1	N-Dimethylamine	0.5786	2.8928	0.1723	15.2193	1.5219	74.0824	4	0	0	1.6789	0	3	0	0.8626	0.6614
	9	N-nitrosodi-n-butylamine	0.8225	9.0471	0.2102	152.178	2.7669	158.2437	4	0	0	7.358	-0.2887	3	0	3.4525	0.9749
	9	N-nitrosodi-n-propylamine	0.7536	6.782	0.2103	86.4658	2.4018	130.19	4	0	0	5.414	-0.2887	3	0	2.4824	0.8939
	1	N-nitrosomorpholine	0.7526	6.0206	0.1667	57.6702	2.0597	116.1197	4	1	1	1.9339	-0.2887	4	0	1.7076	0.5781
	1	N-nitrosopiperidine	0.7526	6.0206	0.1667	57.6702	2.0597	114.1472	4	1	1	1.9693	-0.2887	3	0	2.0758	0.7028
	1	N-nitrosopyrrolidine	0.6731	4.7116	0.2035	38.6872	1.8375	100.1203	4	1	1	1.3618	-0.2887	3	0	1.6384	0.6409
	18	N-triacetic Acid	0.6735	8.7558	0.3954	200.9765	2.5766	191.1406	4	0	0	5.0024	0.3682	7	8.0662	1.4469	0.3781
	9	Nitrosodibutylamine	0.8225	9.0471	0.2102	152.178	2.7669	158.2437	4	0	0	7.358	-0.2887	3	0	3.4525	0.9749
	18	Nitrilotriacetic Acid	0.6735	8.7558	0.3954	200.9765	2.5766	191.1406	4	0	0	5.0024	0.3682	7	8.0662	1.4469	0.3781
	1	Nitrosodiethylamine	0.6731	4.7116	0.2035	40.9545	1.9502	102.1362	4	0	0	3.5048	-0.4082	3	0	1.6062	0.7922
S	3	Nitrobenzene	0.8205	7.3841	0.1402	77.3953	2.1499	124.1191	4	1	1	1.6704	-0.5404	3	2.6909	1.6137	0.5146
	4	Norethindrone	1.2553	22.5949	0	436.6919	2.8542	244.377	3	4	10	2.6347	-1.9009	1	0	8.0776	1.0388
AB	16	Norfloxacin	1.3094	30.1156	0.0384	800.8793	3.1655	319.3356	5	3	4	4.3595	-2.6315	7	4.3502	4.9384	0.5835
	9	N N diethyl 3 methylbenzamide	1.0601	14.8417	0.075	244.1175	2.6826	191.2731	4	1	1	3.8352	-1.1739	2	0	4.555	0.9683
	1	o-Cresol	0.9031	7.2247	0	51.3867	1.8352	108.1399	3	1	1	1.3084	-0.6667	1	2.4992	2.1688	0.7907
ED	11	Octachloro-4-7-methanotetrahydroindane	1.2218	21.9928	0.0266	361.2422	2.3611	409.7816	3	3	6	3.3899	-6.5615	8	0	4.3259	0.7594
ED	11	Octachloroepoxide	1.2471	23.6943	0.0248	408.6678	2.3899	423.7651	4	4	10	2.7462	-7.0608	9	0	4.3944	0.7101
	1	p-Cresol	0.7526	6.0206	0.1667	55.7352	1.9905	108.1399	3	1	1	1.3084	-0.2391	1	2.4923	2.1688	0.7907
	2	p-Dichlorobenzene	0.4515	3.6124	0.5	55.7352	1.9905	147.0038	3	1	1	1.765	-0.2391	2	0	2.1198	0.7729
	1	Paraxanthine	1.1139	14.4813	0	178.3679	2.2868	180.1661	4	2	3	1.6212	-1.8991	5	1.9979	2.6486	0.5877
	9	Paroxetine	1.3498	33.7444	0.0345	1037.5355	3.4585	344.4059	5	4	5	4.648	-2.0269	5	1.5833	7.673	0.7545
	19	Perchloric Acid	0.4127	2.0635	0.4096	9.7095	0.971	100.4585	3	0	0	0.7467	2	5	2.9	0.2944	0.2527
S	12	Phenanthrene	0.8451	11.8314	0.2627	226.775	2.492	178.2334	2	3	6	1.5387	-1.221	0	0	5.6044	0.9055
S	1	Phenol	0.6731	4.7116	0.2035	36.9775	1.7608	94.113	3	1	1	1.0889	-0.1196	1	2.4867	1.7008	0.6653
S	3	Phthalic Anhydride	0.7677	8.445	0.2628	116.3357	2.1152	148.118	3	2	3	1.1355	-1.1407	3	0	1.9685	0.4745
	9	Pramitol	0.9031	14.4494	0.25	345.3488	2.8779	225.2938	4	1	1	4.7242	-0.1895	6	3.6152	5.3131	1.0031
S,HO	8	Progesterone	1.3222	27.7666	0	653.4138	3.1115	286.4142	3	4	10	3.312	-2.4118	2	0	7.513	0.8944
PAH	12	Pyrene	0.6773	10.8371	0.4375	294.9615	2.458	202.2554	2	4	14	1.3861	-1.7089	0	0	6.5422	0.8944
PhAC	16	Ranitidine	1.2936	27.1645	0.0217	769.6064	3.6648	315.4166	5	1	1	8.6197	-0.2954	8	6.2527	5.7734	0.7964
	1	s-1-Methyl-5-3-Pyridinyl-2-Pyrrolidinone	1.1139	14.4813	0	198.9124	2.5502	176.2181	4	2	2	2.1029	-1.3364	3	0	3.8084	0.7699
	9	Salbutamol	1.1463	19.4863	0.0684	415.6839	3.0565	239.3146	4	1	1	4.6509	-0.4306	4	9.2608	4.2946	0.7895
AA	1	Serine	0.8451	5.9157	0	39.5676	1.8842	105.0935	4	0	0	2.506	-0.7071	4	6.613	0.7883	0.4156
	9	Simazine	0.8824	11.471	0.2079	211.3786	2.71	201.6588	4	1	1	4.009	-0.3965	6	3.5248	3.8211	0.8479
AB	19	Sulfachlorpyridazine	1.1549	20.7887	0.0799	479.0649	3.1311	284.726	6	2	2	3.5753	-1.2512	7	3.8144	3.6115	0.5643
AB	19	Sulfadimethoxine	1.2362	25.9604	0.065	677.8299	3.2278	310.3336	5	2	2	4.6019	-1.5501	8	3.902	4.5074	0.6111
AB	19	Sulfamerazine	1.1549	20.7887	0.0799	470.7816	3.077	264.3079	5	2	2	3.3715	-1.1873	6	3.8195	3.9355	0.6149
S,AB	19	Sulfamethazine	1.0886	20.684	0.1487	532.0729	3.1115	278.3347	5	2	2	3.6077	-1.168	6	3.8291	4.3635	0.6623
AB, PhAC	19	Sulfamethizole	1.1242	19.1115	0.0863	410.9225	3.0215	271.3238	5	2	2	3.2637	-1.1873	8	5.5411	3.3461	0.5572
AB	19	Sulfamethoxazole	1.1242	19.1115	0.0863	410.9225	3.0215	253.2816	5	2	2	3.0731	-1.1873	6	3.7904	3.5403	0.5895
AB	19	Sulfathiazole	1.0912	17.4597	0.0938	351.1327	2.9261	255.3214	5	2	2	3.1041	-1.1317	6	3.7504	3.3872	0.5816
H	9	Terbacil	1.0439	14.6144	0.0892	215.7634	2.371	216.6674	5	1	1	2.8057	-1.327	5	1.9129	3.092	0.746
P	10	Terbufos	0.9603	14.4038	0.1835	307.1499	2.9252	288.4363	5	0	0	8.2087	0.3018	5	0	5.8955	1.321
	15	Terramycin	1.4863	47.5627	0.0125	1575.6627	3.1767	446.4137	4	4	10	5.0801	-6.0375	11	19.2523	5.4932	0.513
	7	tert amyl methyl Ether	0.7591	5.3136	0.1018	37.2191	1.7723	102.1766	3	0	0	2.3009	-0.5	1	0	2.956	1.5961
S,HO	4	Testosterone	1.2788	24.2963	0	503.0751	2.942	260.3763	3	4	10	2.8376	-2.2011	2	2.4019	6.9197	0.8785
S	13	1,1,2,2 Tetrachloroethane	0.2764	1.6586	0.6448	23.4839	1.5656	165.834	2	0	0	3.4217	-0.6667	4	0	0.9817	0.6363
S	13	1,1,2,2, Tetrachloroethylene (PCE)	0.2764	1.6586	0.6448	23.4839	1.5656	165.834	2	0	0	3.4217	-0.6667	4	0	0.9817	0.6363
S,AB	15	Tetracycline.hin	1.4719	45.6302	0.013	1485.7296	3.1951	430.4143	4	4	10	4.869	-5.8227	10	16.1953	5.6223	0.5351
ED	6	Thio-N-methyl-carbamoyl-oxy-methylester	1	10	0	122.6139	2.7248	164.1851	5	0	0	4.949	0.2391	5	4.9958	1.4802	0.4934
S,AA	1	Threonine	0.9031	7.2247	0	54.4251	1.9438	119.1204	4	0	0	2.6047	-0.9622	4	6.6557	1.0413	0.4881
S,AH	2	Toluene	0.6731	4.7116	0.2035	36.9775	1.7608	92.1405	2	1	1	1.116	-0.1196	0	0	2.8421	1.1117
ES	20	Tributyl Tin	0.6735	8.7558	0.3954	226.3696	2.9022	291.0643	3	0	0	11.6044	-0.2289	0	0	8.808	2.0413
S,DBP	3	Trichloroacetic Acid	0.6406	4.4843	0.242	32.6898	1.5567	163.3877	4	0	0	2.3343	-0.9434	5	2.6583	0.7726	0.4435
	2	1,1,2 Trichloroethene (TCE)	0.5786	2.8928	0.1723	15.2193	1.5219	131.3889	3	0	0	3.1718	0	3	0	0.8626	0.6614
AM	3	Triclosan	1.2304	20.9176	0	410.168	3.0159	289.5454	4	2	2	3.9183	-1.2955	5	2.6932	3.986	0.6551
AB	9	Trimethoprim	1.2075	25.3584	0.0867	671.5027	3.1976	290.3219	4	2	2	4.9435	-1.8027	7	3.4393	5.8698	0.7875
S	10	triphenyl Phosphate	0.769	17.6878	0.4353	804.7723	3.1809	326.2885	4	3	3	5.0081	-0.8053	4	0	6.3763	0.6805
	10	tris 2 Chloroethyl Phosphate	0.7372	10.3203	0.3568	260.8962	2.867	285.4916	5	0	0	9.8693	-0.5089	7	0	2.8379	0.6365
AB	17	Tylosin	1.753	101.6768	0.0059	7189.6089	4.3494	831.9526	4	4	4	19.9002	-4.9226	18	13.545	14.0508	0.6822
	1	t Butyl Alcohol	0.4771	1.4314	0	2.7549	0.9183	46.069	3	0	0	1.9339	0	1	2.2722	0.5485	0.7618
S,AA	1	Valine.hin	0.827831984	6.62266016	0.083333001	54.42512894	1.943755031	117.1478424	4	0	0	2.647735119	-0.962249994	3	4.080931187	1.396121025	0.654431999
S, AA		Asparagine	0.9542	8.5882	0.0000	81.3882	2.2608	132.1191	4.0000	0.0000	0.0000	3.0011	-0.4349	5.0000	5.8597	1.0755	0.4315
S, AA		Aspartic Acid	0.9542	8.5882	0.0000	81.3882	2.2608	133.1039	4.0000	0.0000	0.0000	3.0011	-0.4349	5.0000	6.8936	0.9598	0.3851
S, AA		Histidine	1.0414	11.4553	0.0000	137.3988	2.4982	155.1564	4.0000	1.0000	1.0000	2.4768	-0.8099	4.0000	5.9663	1.9843	0.5330
S, AA		Lysine	1.0000	10.0000	0.0000	119.7360	2.6608	146.1894	4.0000	0.0000	0.0000	5.1034	-0.6381	4.0000	5.4720	1.8519	0.6173

			Information Indices					Molecular Properties									
			Shannon Information Index	Information Content	Molecular Redundancy	Bonchev-Trinajsti Information Content	Bonchev-Trinajsti Mean Information Content	Formula Weight (Daltons)	# Elements in Molecule	# Rings in Molecular Graph	# Graph Circuits	Kappa Flexibility Index (# Bonds in normal graph for alkanes)	Difference Between Chi cluster-3 and chi pathcluster-4	# H-Bond Acceptors	-XH Hydrogen Bond Donor	Molecular & Group Polarity Index - Specific Polarity Descriptor	Molecular & Group Polarity Index - Average Polarity Descriptor
Notes	**QSAR Cluster**	**Compound Name**	**si**	**IC**	**R**	**idc**	**idcbar**	**fw**	**nelem**	**nrings**	**ncirc**	**phia**	**knotp**	**numHBa**	**SHHBd**	**Qs**	**Qsv**
S, AA		Methionine	0.9542	8.5882	0.0000	87.9783	2.4438	149.2138	5.0000	0.0000	0.0000	4.7529	-0.6381	4.0000	4.1137	1.7062	0.6495
S, DBP		N-nitroso dimethyl amine (NDMA)	0.5786	2.8928	0.1723	15.2193	1.5219	74.0824	4.0000	0.0000	0.0000	1.6789	0.0000	3.0000	0.0000	0.8626	0.6614
S, AA		Phenylalanine	0.9788	11.7461	0.0930	174.6330	2.6460	165.1918	4.0000	1.0000	1.0000	2.9619	-0.8099	3.0000	4.2066	2.4872	0.6045
S		Urea	0.4515	1.8062	0.2500	6.0000	1.0000	60.0556	4.0000	0.0000	0.0000	0.8760	0.5774	3.0000	3.1028	0.4224	0.4400
Marine Toxin		Anatoxin a	1.0792	12.9502	0.0000	147.1435	2.2294	165.2352	4.0000	2.0000	3.0000	2.0094	-0.9835	2.0000	1.5514	4.0600	0.8928
Marine Toxin		Cylindrospermopsin	1.4091	38.0448	0.0156	1172.8683	3.3415	398.4197	5.0000	4.0000	8.0000	4.4414	-2.6775	11.0000	9.7180	5.1427	0.5276
Marine Toxin		Microcystin LR	1.8148	123.4065	0.0097	9841.6240	4.3203	953.1057	4.0000	2.0000	2.0000	26.1172	-5.0200	22.0000	24.9213	14.5839	0.6360
Marine Toxin		Saxitoxin	1.2936	27.1645	0.0217	602.0011	2.8667	301.3054	4.0000	3.0000	6.0000	3.3800	-3.0447	11.0000	16.5708	4.2283	0.5793

Legend:
S = Surrogate
PhAC = Pharmaceutically Active Compound
ED = Endocrine Disruptor
ES = Estrogenicity
HO = Hormone
P = Pesticide
H = Herbicide
AHC = Aromatic Hydrocarbon
PHA = Polyaromatic Hydrocarbon
AB = Antibiotic
AM = Antimicrobial
AA = Amino Acid
DBP = Disinfection Byproduct

Appendix 4

General Instructions for Operating QSAR Descriptor ANN Models Describing Compound Interactions with RO Membranes

Introduction:

The models described in this study have been embedded as macros in Excel workbooks on a CD-ROM, and as such are being made available for experimentation. There are six workbooks altogether; one each for CA and four PA membranes used in the study, and one for the "Universal" PA model. In order to operate these models, the user must have Excel 2000 or later installed, and macros enabled.

Each of the workbooks consists of two sheets. The first spreadsheet is for data I/O, and is where the user enters information regarding the specific molecule being tested, its salient QSAR molecular descriptors, and information regarding operating conditions that will be used to predict membrane performance based on the results of this study (due to the complexity of parameters involved with field performance, these specific predictions may vary from a specific field site; however, they may be used in a comparative sense to examine the behavior of a series of compounds relative to each other). The second sheet is a graphic representation of the interaction of the compound with the membrane, and plots relative solute flux (P-flux) against membrane association flux (M-Flux). This diagram provides the user with a visual representation of the predicted interaction of the compound with the membrane.

Entering Data in the data spreadsheet:

The used inputs information required by the model by filling in the ***gray boxes***. Care should be taken to ***only*** modify the values in these boxes and not to change the

RO Membrane Organic Compound Interaction Prediction Model

Orange County Water District

Membrane Type: Polyamide RO
ID: BW-30

Model Inputs:

Water Flux:	12	GFD	0.340	L/m^2*min
Solute Compound ID:	Estrone			
		Mass Units		
[Feed]:	9	uMoles	/liter	

	QSARs					
	Ovality	xvpc4	Py	LogP	SsCH3	numHBa
P-Flux QSARs:	1.5212	3.4729	0.4227	3.6617	2.2178	2.0000

	P	LogP	Gmax	Gmin
M-Flux QSARs:	0.4833	3.6617	12.2620	-0.0322

	Pz	Wt	LogP	Gmin
R-Flux QSARs:	0.0911	15139.00	3.6617	-0.0322

values or formulae in any of the other cells in the sheet, or the model will not work correctly.

Limitations to the range of values for the QSAR molecular descriptors:

The QSAR molecular descriptors used in the models must be constrained within the limits used to train the artificial neural networks. If values outside thee limits are used, predictability of the models may be severely compromised. These limits, for all the models, are shown below:

	ABSQ	MaxNeg	MaxQp	Ovality	Surface	xpc4	xv1	xvpc4
Minimum	0.870199	-0.67159	0.060379	1.215067	82.68226	0	0.781474	0
Maximum	11.3255	-0.10137	1.867779	1.749453	422.4388	9.427053	12.76057	4.481088
	nxp5	**nxch6**	**Iy**	**Py**	**Pz**	**P**	**Q**	**sumdelI**
Minimum	0	0	48.11783	0	0	0	0.0243	0
Maximum	182	4	7507.912	1.370073	0.757215	1.519661	12.72342	58.3048
	Wt	**k1**	**k2**	**k3**	**LogP**	**SsCH3**	**SaaCH**	**SdssC**
Minimum	4	3	1.333333	0	-3.39353	0	0	-6.6737
Maximum	45143	32.5137	15.2908	12.4898	7.5768	7.2236	21.367	2.5522
	SdO	**Gmax**	**Hmin**	**Gmin**	**idcbar**	**fw**	**numHBa**	**Qs**
Minimum	0	2	0	-2.9185	0.9183	46.069	0	0.4224
Maximum	42.0844	14.6077	2.6885	2	3.6533	554.5457	15	14.8095
	Qsv							
Minimum	0.385122							
Maximum	1.4051							

Model Output:

As data are entered, the embedded macros will determine the predicted relative P, M and R Fluxes for the compound being evaluated, and will display them on the sheet (below).

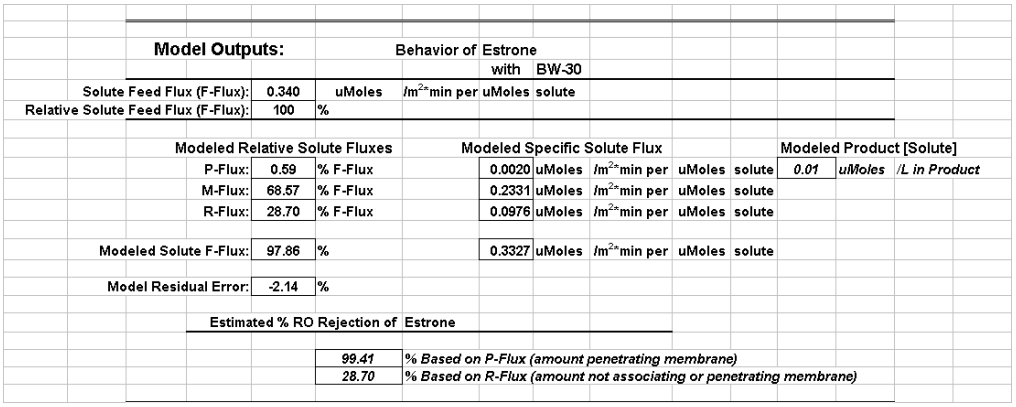

Explanation of Output Data:

The **solute feed flux** represents the estimated actual specific feed flux (actual F-Flux) of the solute (in micromoles of solute/m^2 membrane*min per micromolar solute concentration in the feed the feed) to the membrane based on user-defined values of solute concentration and membrane water flux. The **relative solute feed flux** (F-Flux) is, by definition, always defined as 100 (% of the feed flux).

The modeled relative solute fluxes represent the predicted values from the ANN models describing the relative **P-Flux** (the proportion of the mass interacting with the membrane that passes into the product), the relative **M-Flux** (the proportion of the solute interacting with the membrane that remains bound on or in the membrane) and the relative **R-Flux** (the proportion of the solute that fails to interact with the membrane and remains unassociated in the feed). For each of these fluxes, the spreadsheet calculates **specific P, M and R solute fluxes** (in micromoles/m^2*min per micromolar solute in the feed) using the relative flux data and user-specified values for feed solute concentration and water flux. The spreadsheed also estimates the **modeled concentration of solute in the product**, in micromoles/liter.

The **modeled solute F-Flux** represents a "virtual mass balance" obtained by summing the values of the relative P, M and R-Fluxes. Theoretically, the sum of these relative fluxes should total 100 (the value of the relative F-Flux). The **model residual error** represents the difference between the theoretical relative F-Flux and the value obtained from summation of the modeled flux outputs. This value reflects the deviation of the membrane models from an ideal response, and may be used as an evaluation criterion to determine whether or not the models have provided a reasonable prediction of the various solute-membrane interactions.

Estimated Percent rejection of the solute by the membrane is estimated based on two criteria. The **percent rejection based on the relative solute P-Flux** represents rejection calculated based on the P-Flux. This is the "traditional" expression of RO membrane rejection, determined by the mass of solute passing through the membrane into the product. This value represents the sum of two compound-membrane interactions; the ability of the membrane to act as a mechanical shield against the compound and the removal of the compound by binding on or in the membrane. This, a high percent rejection determined by P-Flux may be due to strong rejection at the membrane surface or strong interaction of the compound with the membrane. However, the **percent rejection based on the relative solute R-Flux** only describes rejection at the membrane surface, in which the membrane acts as a mechanical shield. This result is significant, because compounds exhibiting a high rejection by this criterion are likely to be excluded from the RO product for extended periods of time, whereas, those compounds that are principally removed by interactions with the membrane may, in time as the membrane saturates, begin to break through significantly into the product.

Evaluating Model Results:

The **Modeled Solute F-Flux** should approach 100% if all models are working correctly. A practical **model residual error** is +/-25. (a 25% model noise band). Values outside this range should be treated with suspicion, as this indicates a significant failure

of the “virtual mass balance” technique. Furthermore, instances where solute rejection evaluated by the P-Flux significantly less than that evaluated by the R-Flux should be treated with suspicion, as in order for this to occur the M-Flux needs to be seriously below zero.

Because these results are predicted, it is possible to have relative fluxes in excess of 100 or less than zero. Within error, this is acceptable; however, a value far outside these limits should be treated with suspicion.